

ABSTRACT

Luminescent Supramolecular Silver(I) Coordination Complexes of Pyridyl-substituted Phosphinites, Phosphonites and Amines

Rodney P. Feazell

Mentor: Kevin K. Klausmeyer, Ph.D.

Interest in the design and synthesis of supramolecular metal-organic coordination polymers has increased exponentially in the last decade. This attraction comes along with advances in crystallographic instrumentation that has made the collection and processing of crystal data sets faster and more automated than ever. As a result, our understanding of the intra- and intermolecular forces that exist within the confines of the crystalline lattice is at a historic high. In this work we use several new bi- and tridentate pyridyl-substituted phosphinite ligands as well as a series of isomeric aminomethylpyridines to construct discrete, one-, two, and three-dimensional metal-organic coordination architectures with salts of the silver(I) cation. These complexes were then analyzed and discussed in terms of the variables (metal/ligand ratio, anion, temperature, solvent) and forces (donor-metal bonding, hydrogen-bonding, π -stacking, dispersion forces) that cause the structural motifs that are observed. The luminescence of these complexes was also studied and was seen to be variable with changes in structure and metal environment.

Luminescent Supramolecular Silver(I)
Coordination Complexes of
Pyridyl-substituted Phosphinites,
Phosphonites and Amines

by

Rodney P. Feazell, B.S.

A Dissertation

Approved by the Department of Chemistry and Biochemistry



Marianna A. Busch, Ph.D., Chairperson

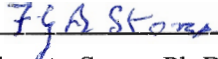
Submitted to the Graduate Faculty of
Baylor University in Partial Fulfillment of the
Requirements for the Degree
of

Doctor of Philosophy

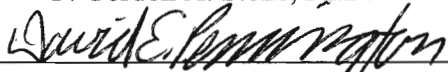
Approved by the Dissertation Committee



Kevin K. Klausmeyer, Ph.D., Chairperson



F. Gordon A. Stone, Ph.D.



David E. Pennington, Ph.D.

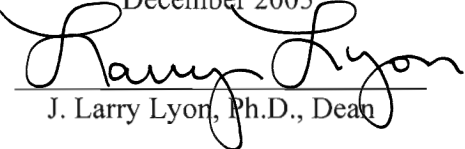


Darrin J. Bellert, Ph.D.



Stephen I. Dworkin, Ph.D.

Accepted by the Graduate School
December 2005



J. Larry Lyon, Ph.D., Dean

Copyright © 2005 Rodney P. Feazell

All rights reserved

TABLE OF CONTENTS

LIST OF FIGURES	vii
LIST OF SCHEMES	xiii
LIST OF TABLES	xiv
LIST OF ABBREVIATIONS	xix
ACKNOWLEDGMENTS	xxii
CHAPTER ONE General Introduction	1
Coordination Polymers by Definition	2
Ligand Constraints	7
Applications	8
Host-Guest Properties / Catalysis	8
Luminescence	9
Conductivity	10
CHAPTER TWO Two, Three, and Four Coordinate Ag(I) Coordination Polymers Formed by the Novel Phosphinite, PPh ₂ (3-OCH ₂ py)	12
Introduction	12
Results and Discussion	13
Synthesis and NMR Spectroscopy	13
X-ray Crystal Structures	19
Luminescence Properties	26
Conclusions	28
Experimental	29
General Considerations	29
Preparations	29
Crystallography	31
CHAPTER THREE Anion Dependent Silver(I) Coordination Polymers of the Tridentate Pyridylphosphonite: PPh(3-OCH ₂ C ₅ H ₄ N) ₂	33

	Introduction	33
	Results and Discussion	34
	Synthesis and NMR Spectroscopy	34
	X-ray Crystal Structures	40
	Luminescence Properties	52
	Conclusions	54
	Experimental	54
	General Considerations	54
	Preparations	55
	Crystallography	57
CHAPTER FOUR	Variability in the Structures of Luminescent Silver(I) 2-aminomethylpyridine Complexes: Effect of Ligand Ratio, Anion, Hydrogen bonding, and π -stacking	60
	Introduction	60
	Results and Discussion	62
	Synthesis and NMR Spectroscopy	62
	X-ray Crystallography	65
	Luminescence Properties	81
	Conclusions	83
	Experimental	84
	General Considerations	84
	Preparations	84
	Crystallography	87
CHAPTER FIVE	Silver(I) 3-aminomethylpyridine Complexes Part 1: Effect of Ligand Ratio, π -stacking and Temperature with a Non-interacting Anion	90
	Introduction	90
	Results and Discussion	91
	Synthesis and NMR Spectroscopy	91
	X-ray Crystallography	94
	Luminescence Properties	108
	Conclusions	109
	Experimental	110
	General Procedures	110

	General Synthesis	110
	Preparations	111
	Crystallography	112
CHAPTER SIX	Silver(I) 3-aminomethylpyridine Complexes Part 2: Effect of Ligand Ratio, Hydrogen bonding and π -stacking with an Interacting Anion	115
	Introduction	115
	Results and Discussion	116
	Synthesis	116
	X-ray Crystal Structures	119
	Luminescence Properties	135
	Conclusions	136
	Experimental	137
	General Procedures	137
	General Synthesis	137
	Preparations	138
	Crystallography	140
CHAPTER SEVEN	Variability in the Structures of [4-(aminomethyl)pyridine] silver(I) Complexes through effects of Ligand Ratio, Anion, Hydrogen Bonding, and π -Stacking	143
	Introduction	143
	Results and Discussion	145
	Synthesis	145
	X-ray Crystal Structures	145
	Luminescence Properties	162
	Conclusions	163
	Experimental	163
	General Procedures	163
	General Preparations	164
	Preparations	164
	Crystallography	167
CHAPTER EIGHT	Summary	169

APPENDIX A	General Considerations	171
	Synthetic procedures	171
	Spectroscopic Characterization	171
	Procedures for X-ray Crystal Structure Determinations	172
	Crystal Preparation	172
	Data Collection	172
	Data Reduction	173
	Structure Solution and Refinement	173
APPENDIX B	Crystallographic Data	175
REFERENCES		273

LIST OF FIGURES

1.1	Bis-(BDA) Mn ^{II} polymers. L = MeOH.	4
1.2	a) The silver(I)-bound 1-phenyl-3-pyridine-3-yl-urea hydrogen bonding to a central PF ₆ ⁻ anion. b) a stick diagram of (a), shown two molecules deep. c) the linear growth of this polymer as an anion-centered rod.	5
1.3	A view of the extended network that is formed by linking 1-D polymers with S···S interactions. M = Cd ^{II} , Co ^{II} , or Zn ^{II} .	6
1.4	Common bidentate ligands used in the construction of coordination networks.	7
1.5	Generic 4,4'-bipy / Zn / RO ₂ ⁻ polymer. The emission spectrum is shown for R = 4-sulfoisothalic acid.	8
1.6	Structural diagram of [Cd(NO ₃) ₂ (4,4'-bipy) ₂] _n . Eq. 1 shows the cyanosilation of an aldehyde by that this complex catalyzes.	9
2.1	Molecular diagram of the cationic polymer of 2.2 with the unique portion and important symmetry generated atoms labeled. Ellipsoids are drawn at the 50% probability level.	20
2.2	Molecular diagram of the unique portion of 2.3 . Ellipsoids are drawn at the 30% probability level. Hydrogen atoms and all but the bound oxygen of the terminal triflates have been removed for clarity.	22
2.3	Ball and stick diagram of 2.3 showing the hexasilver-containing rings. Triflate oxygens bound to Ag are labeled. Phenyl rings and hydrogen atoms are removed for clarity.	23
2.4	Molecular diagram of 2.4 with the unique portion and important symmetry generated atoms labeled. Ellipsoids are drawn at the 30% probability level. Hydrogen atoms have been removed for clarity.	25
2.5	Ball and stick diagram of the ring formed by 2.1 and Ag, which is linked by tfa ⁻ ions to form an infinite chain. Phenyl groups and hydrogen atoms have been removed for clarity.	26

2.6	Normalized excitation and emission spectra of compounds 2.1–2.4 taken in acetonitrile glasses at 1×10^{-4} M concentration at 77 K. $\text{——} = \text{PCP-31AgBF}_4$, $\text{— — —} = \text{PCP-31AgOTf}$, $\text{.....} = \text{PCP-31Agtfa}$, $\text{— . . .} = \text{PCP-31}$.	27
3.1	Molecular diagram of the unique portion of the PCP-32AgOTf polymer. Ellipsoids are drawn at the 30% probability level.	42
3.2	A view of the one-dimensional chain of 3.2 . Hydrogen atoms and the non-coordinating portion of the triflates have been removed for clarity.	43
3.3	Molecular diagram of the cationic unique portion of the polymer of 3.3 . The partial spiral of the pyridyl linkages through the linear chain is apparent. Ellipsoids are drawn at the 50% probability level. Hydrogen atoms have been removed for clarity.	45
3.4	A view of the chain of 3.3 perpetuated in one dimension. The partial spiral of the pyridyl linkages can be seen to abruptly restart at the end of the unique portion. Hydrogen atoms have been removed for clarity	46
3.5	A view down the <i>a</i> -axis of how the two-dimensional sheets of 3.3 stack together encompassing the BF_4^- anions. Hydrogen atoms have been removed for clarity.	46
3.6	Molecular diagram of the unique portion of 3.4 . Ellipsoids are drawn at the 30% probability level. As shown, N4 is seen to be non-coordinating. All other pyridyl donors are metal bound.	48
3.7	Packing structure of complex 3.4 showing the three-dimensional growth of the polymer. hydrogen atoms, trifluoromethyls, and all but the <i>ipso</i> portion of the phenyl rings have been removed for clarity.	49
3.8	Coordination environment of Ag1 in the polymer of 3.4 . Ellipsoids are drawn at the 50% probability level.	51
3.9	Coordination environment of Ag2 in the polymer of 3.4 . Ellipsoids are drawn at the 50% probability level.	52
3.10	Normalized excitation and emission spectra of compounds 3.1–3.4 taken in acetonitrile glasses at 1×10^{-4} M concentration at 77 K. $\text{——} = \text{PCP-32Ag(tfa)}$, $\text{— — —} = \text{PCP-32AgOTf}$, $\text{.....} = \text{PCP-32AgBF}_4$, $\text{— . . .} = \text{PCP-32}$.	53
4.1	Molecular structure of one of the unique cationic monomers of 4.1 . Ellipsoids are drawn at the 50% probability level.	66

4.2	Molecular structure of one of the unique metal dimers of 4.2 showing how H–bonding to the anions hold the “sandwich” together. Ellipsoids are drawn at the 50% probability level. All hydrogens except for those on the amine nitrogens have been removed for clarity.	68
4.3	Molecular structure of the monopositive cation in 4.3 . Ellipsoids are drawn at the 50% probability level. All hydrogens except for those on the amine nitrogens have been removed for clarity.	71
4.4	A view of the cationic complex of 4.4 . Ellipsoids are drawn at the 50% probability level.	74
4.5	A view of the cationic complex of 4.5 . Ellipsoids are drawn at the 50% probability level.	76
4.6	A view of the unique portion of the polymer of 4.6 with the coordination environment about silver shown complete. Ellipsoids are drawn at the 50% probability level.	78
4.7	A view of the 1-D polymer of 4.6 showing the intrapolymeric H–bonding.	79
4.8	Molecular diagram of the unique portion of 4.7 with the coordination environment about silver shown complete. Ellipsoids are drawn at the 50% probability level.	80
4.9	A view of the helical 1–D polymer formed by compound 4.7 showing the intrapolymeric H–bonding.	81
4.10	Normalized excitation and emission spectra of compounds 4.1,4.3,4.6 and 4.7 taken in acetonitrile glasses at 1×10^{-4} M concentration at 77 K. $\text{—} = \text{Ag(2-amp)OTf}$, $\text{— — —} = \text{Ag(2-amp)(tfa)}$, $\cdots\cdots\cdots = \text{Ag(2-amp)}_2\text{BF}_4$, $\text{— - - -} = \text{Ag}_2\text{(2-amp)}_3(\text{OTf})_2$.	82
5.1	Thermal ellipsoid plot of the unique portion of the cationic polymer 5.1.1 . The disordered amine and silver have been omitted for clarity. Ellipsoids are drawn at the 50 % probability level.	96
5.2	Extended ball-and-stick view of the cationic polymeric structure of 5.1.1 . Hydrogen atoms and disorder have been removed for clarity.	97
5.3	Thermal ellipsoid plot of the cationic portion of 5.1.2 . Ellipsoids are drawn at the 50 % probability level. All hydrogen atoms except for those on the amines have been removed for clarity.	99

5.4	Thermal ellipsoid of the unique portion of the cationic polymer of 5.2 with the silver coordination environments shown complete. Ellipsoids are drawn at the 50 % probability level. The disorder of N3 has been removed for clarity.	100
5.5	A view of the extended two-dimensional network of 5.2 . H atoms, anions and disorder have been removed for clarity.	102
5.6	A view of the two-dimensional network of 5.3.1 . Hydrogen atoms and anions have been removed for clarity.	103
5.7	Thermal ellipsoid plot of the unique cationic portion of 5.3.1 . Ellipsoids are drawn at the 50 % probability level.	104
5.8	A view of the extended polymer of 5.3.2 . Hydrogen atoms have been removed for clarity.	105
5.9	Thermal ellipsoid plot of the unique portion of the cationic polymer 5.3.2 . Ellipsoids are drawn at the 50 % probability level.	106
5.10	Thermal ellipsoid of the cationic structure of 5.4 . Hydrogen atoms have been removed for clarity. The symmetry equivalent portion is shown dashed.	107
5.11	Representative Luminescence spectra of the 3-amp AgBF ₄ compounds taken in acetonitrile glasses at 1 X 10 ⁻⁴ M concentration at 77 K. $\text{—} = \text{Ag(3-amp)BF}_4$, $\text{— — —} = \text{Ag}_2(\text{3-amp})_3(\text{BF}_4)_2$, $\text{.....} = \text{Ag(3-amp)}_2\text{BF}_4$	109
6.1	A view of the charge separated polymers of 6.1 . Only the bound oxygens are shown and all H atoms except for those of the amines have been removed for clarity.	120
6.2	Thermal ellipsoid view of the unique portion of compound 6.1 . The fluorine atoms and all hydrogens except for those on the amines have been removed for clarity. Ellipsoids are drawn at the 50 % probability level.	121
6.3	Thermal ellipsoid plot of the unique portion of the polymer 6.2 . Ellipsoids are drawn at the 50% probability level.	123
6.4	Expanded view of the 2-Dimensional growth of the cationic polymer of 6.2 .	124
6.5	A view of the 2-dimensional cationic network of 6.3 . All H atoms except for those on the amines have been removed for clarity.	126

6.6	Thermal ellipsoid plot of the unique portion of 6.3 . Ellipsoids are drawn at the 50 % probability level.	127
6.7	Thermal ellipsoid plot of the unique portion of the 3-dimensional polymer of 6.4 . Ellipsoids are drawn at the 50 % probability level.	128
6.8	An extended view of the 3-dimensional cationic network of 6.4 . All hydrogen atoms except for those on the amines have been omitted for clarity.	130
6.9	Thermal ellipsoid plot of the tetrametallic ring of 6.5 showing the H–bonding of the tfa ⁻ anions to the amine hydrogens. The symmetry generated portion of the structure is shown dashed. All other hydrogens and anions have been removed for clarity. Ellipsoids are drawn at the 50 % probability level.	131
6.10	An extended view of the cationic polymer of Ag ₄ units formed by the metal–metal interactions of 6.5 . Anions and H–atoms have been removed for clarity.	133
6.11	Thermal ellipsoid plot of the two different cationic parts of 6.6 with the unique portion labeled. Symmetry generated atoms are shown dashed. Anions and all hydrogen atoms except for those on the amines have been removed for clarity. Ellipsoids are drawn at the 50 % probability level.	134
6.12	Normalized excitation and emission spectra of representative 3-amp Ag(I) compounds taken in acetonitrile glasses at 1 X 10 ⁻⁴ M concentration at 77 K. ————— = Ag(3-amp) ₂ OTf, - - - = Ag(3-amp)(tfa), = Ag ₂ (3-amp)(BF ₄) ₂ (2,2'-bipy) ₂ , - · - - · = Ag(3-amp)(OTf).	136
7.1	Molecular diagram of the cationic polymer 7.1 . Ellipsoids are drawn at the 50% probability level.	150
7.2	50% thermal ellipsoid representation of the parallel polymers of 7.2 . Hydrogen atoms have been removed for clarity. Inset is a view down the length of the polymers showing the different approaches of the anions.	151
7.3	A view of the cationic chain of 7.3 . Ellipsoids are drawn at the 30% probability level. All hydrogen atoms except for those on the amines have been removed for clarity.	153
7.4	A view of the cationic “box-in-box” structure of 7.4 . All hydrogen atoms except for those on the amines have been removed for clarity.	154

7.5	Thermal ellipsoid plot of the unique cationic portion of 7.4 . Ellipsoids are drawn at the 50% probability level.	155
7.6	An extended view of the cationic “box-in-box” network of 7.5 . All hydrogen atoms except for those on the amines have been removed for clarity.	157
7.7	Molecular diagram of the unique portion of the cationic polymer of 7.5 . Ellipsoids are drawn at the 50% probability level.	158
7.8	Molecular diagram of the bimetallic monomer of 7.6.2 . Ellipsoids are drawn at the 50% probability level. All hydrogen atoms except for those on the amine have been removed for clarity.	160
7.9	Ball and stick diagram showing the polymeric nature of 7.6.2 . Anions and hydrogen atoms have been removed for clarity.	161
7.10	Normalized excitation and emission spectra of representative 3-amp Ag(I) compounds taken in acetonitrile glasses at 1×10^{-4} M concentration at 77 K. _____ = $\text{Ag(4-amp)}_2\text{OTf}$, - - - = Ag(4-amp)(OTf) , = $\text{Ag(4-amp)}_2(\text{BF}_4)$, - - - . = $\text{Ag(4-amp)}_2(\text{tfa})$.	162

LIST OF SCHEMES

1.1	The defining characteristics of the simplest possible one-, two-, and three-dimensional coordination polymers. Terminal ends are linked to equivalent units. D = (typically) N or O.	2
1.2	Diagram of the common extended metal-organic motifs seen in coordination chemistry.	3
2.1	General Synthetic Scheme for the carbinol-substituted phosphine coordination complexes of the silver(I) salts. In a, X = BF ₄ ⁻ or tfa ⁻ and in b, X = OTf ⁻ .	14
3.1	Binding modes of PCP-32 with silver(I) salts.	40
4.1	The binding modes that are seen with the 2-aminomethylpyridine ligand in the silver(I) structures described herein.	61
7.1	Typical coordination modes of amp ligands with silver(I) salts.	144

LIST OF TABLES

2.1	Analytical and Physical Data	15
2.2	Hydrogen-1 and Phosphorus-31 NMR Data	16
2.3	Selected Bond Lengths (Å), Angles (°), Torsion Angles(°), and Important Distances for PCP-31AgBF₄ (2.2)	20
2.4	Selected Bond Lengths (Å), Angles (°), Torsion Angles(°), and Important Distances for PCP-31AgOTf (2.3)	22
2.5	Selected Bond Lengths (Å), Angles (°), Torsion Angles(°), and Important Distances for PCP-31Agtaf (2.4)	25
2.6	Luminescent Spectral Data for compounds 2.1–2.4 , at 77 K and 1×10^{-4} M in CH ₃ CN	27
2.7	Crystallographic Data for 2.2 , 2.3 and 2.4	32
3.1	Analytical and Physical Data	36
3.2	Hydrogen-1 and Phosphorus-31 NMR Data	37
3.3	Selected Bond Lengths (Å), Angles (°), and Important Distances for 3.2	42
3.4	Selected Bond Lengths (Å), Angles (°), and Important Distances for 3.3	45
3.5	Selected Bond Lengths (Å), Angles (°), and Important Distances for 3.4	48
3.6	Luminescent Spectral Data for compounds 3.1–3.4 , at 77 K and 1×10^{-4} M in CH ₃ CN	54
3.7	Crystallographic Data for 3.2 , 3.3 and 3.4	58
4.1	Analytical and Physical Data	63
4.2	Hydrogen-1 NMR Data	64
4.3	Selected bond lengths (Å), angles (deg), and important distances for Ag(2-amp) ₂ BF ₄ , (4.1)	66

4.4	Selected bond lengths (Å), angles (deg), and important distances for Ag(2-amp) ₂ tfa, (4.2)	68
4.5	Selected bond lengths (Å), angles (deg), and important distances for Ag ₂ (2-amp) ₃ (OTf) ₂ , (4.3)	71
4.6	Selected bond lengths (Å), angles (deg), and important distances for Ag ₂ (2-amp) ₃ (BF ₄) ₂ , (4.4)	74
4.7	Selected bond lengths (Å), angles (deg), and important distances for Ag ₂ 2,2'-bpy ₂ (2-amp)(BF ₄) ₂ , (4.5)	76
4.8	Selected bond lengths (Å), angles (deg), and important distances for Ag(2-amp)OTf, (4.6)	78
4.9	Selected bond lengths (Å), angles (deg), and important distances for Ag(2-amp)(tfa) (4.7)	80
4.10	Luminescent Spectral Data for 2-amp and compounds 4.1–4.7 , at 77 K and 1 × 10 ⁻⁴ M in CH ₃ CN	82
4.11	Crystallographic Data for compounds 4.1 to 4.7	88
5.1	Analytical and Physical Data	92
5.2	Hydrogen-1 NMR Data	93
5.3	Selected bond lengths (Å), angles (°), and important distances for Poly(Ag[3-amp]BF ₄) (5.1.1)	96
5.4	Selected bond lengths (Å), angles (°), and important distances for Poly(Ag[3-amp]BF ₄) (5.1.2)	99
5.5	Selected bond lengths (Å), angles (°), and important distances for Ag ₂ (3-amp) ₃ (BF ₄) ₂ (5.2)	100
5.6	Selected bond lengths (Å), angles (°), and important distances for Ag(3-amp) ₂ BF ₄ (5.3.1)	104
5.7	Selected bond lengths (Å), angles (°), and important distances for Ag(3-amp) ₂ BF ₄ (5.3.2)	106
5.8	Selected bond lengths (Å), angles (°), and important distances for Ag ₂ (2,2'-bipy) ₂ -μ-(3-amp)(BF ₄) ₂ (5.4)	107

5.9	Luminescent Spectral Data for 3-amp and the compounds 5.1.1–5.4 , at 77 K and 1×10^{-4} M in CH ₃ CN	109
5.10	Crystallographic Data for compounds 5.1.1 to 5.4	113
6.1	Analytical and Physical Data	117
6.2	Hydrogen-1 NMR Data	118
6.3	Selected bond lengths (Å), angles (°), and important distances for Ag(3-amp)tfa (6.1)	121
6.4	Selected bond lengths (Å), angles (°), and important distances for Ag(3-amp)OTf (6.2)	123
6.5	Selected bond lengths (Å), angles (°), and important distances for Ag(3-amp) ₂ tfa (6.3)	127
6.6	Selected bond lengths (Å), angles (°), and important distances for Ag(3-amp) ₂ OTf (6.4)	128
6.7	Selected bond lengths (Å), angles (°), and important distances for Ag ₂ (2,2'-bipy) ₂ -μ-(3-amp)(tfa) ₂ (6.5)	131
6.8	Selected bond lengths (Å), angles (°), and important distances for Ag ₂ (2,2'-bipy) ₂ -μ-(3-amp)(OTf) ₂ (6.6)	134
6.9	Luminescent Spectral Data for compounds 6.1–6.6 , at 77 K and 1×10^{-4} M in CH ₃ CN	136
6.10	Crystallographic Data for compounds 6.1 to 6.6	141
7.1	Analytical and Physical Data	146
7.2	Hydrogen-1 NMR Data	147
7.3	Selected bond lengths (Å), angles (°), and important distances for Ag(4-amp)OTf (7.1)	150
7.4	Selected bond lengths (Å), angles (°), and important distances for Ag(4-amp)tfa (7.2)	151
7.5	Selected bond lengths (Å), angles (°), and important distances for Ag(4-amp) ₂ tfa (7.3)	153

7.6	Selected bond lengths (Å), angles (°), and important distances for Ag(4-amp) ₂ (OTf) (7.4)	155
7.7	Selected bond lengths (Å), angles (°), and important distances for Ag(4-amp) ₂ BF ₄ (7.5)	158
7.8	Selected bond lengths (Å), angles (°), and important distances for Ag ₂ (5,5'-bis methyl-2,2'-bpy) ₂ (4-amp)(BF ₄) ₂ (7.6.2)	160
7.9	Luminescent Spectral Data for compounds 7.1–7.6.2 , at 77 K and 1×10^{-4} M in CH ₃ CN	162
7.10	Crystallographic Data for compounds 7.1 to 7.6.2	168
B.1	Experimental and statistical crystal data for 2.2	175
B.2	Experimental and statistical crystal data for 2.3	177
B.3	Experimental and statistical crystal data for 2.4	183
B.4	Experimental and statistical crystal data for 3.2	186
B.5	Experimental and statistical crystal data for 3.3	195
B.6	Experimental and statistical crystal data for 3.4	201
B.7	Experimental and statistical crystal data for 4.1	206
B.8	Experimental and statistical crystal data for 4.2	209
B.9	Experimental and statistical crystal data for 4.3	215
B.10	Experimental and statistical crystal data for 4.4	217
B.11	Experimental and statistical crystal data for 4.5	220
B.12	Experimental and statistical crystal data for 4.6	223
B.13	Experimental and statistical crystal data for 4.7	224
B.14	Experimental and statistical crystal data for 5.1.1	226
B.15	Experimental and statistical crystal data for 5.1.2	229
B.16	Experimental and statistical crystal data for 5.2	232

B.17	Experimental and statistical crystal data for 5.3.1	235
B.18	Experimental and statistical crystal data for 5.3.2	237
B.19	Experimental and statistical crystal data for 5.4	239
B.20	Experimental and statistical crystal data for 6.1	241
B.21	Experimental and statistical crystal data for 6.2	245
B.22	Experimental and statistical crystal data for 6.3	247
B.23	Experimental and statistical crystal data for 6.4	249
B.24	Experimental and statistical crystal data for 6.5	251
B.25	Experimental and statistical crystal data for 6.6	254
B.26	Experimental and statistical crystal data for 7.1	259
B.27	Experimental and statistical crystal data for 7.2	261
B.28	Experimental and statistical crystal data for 7.3	263
B.29	Experimental and statistical crystal data for 7.4	264
B.30	Experimental and statistical crystal data for 7.5	266
B.31	Experimental and statistical crystal data for 7.6.2	268

LIST OF ABBREVIATIONS

General Abbreviations and Symbols

CCD	charge coupled device
MOF	metal-organic framework
R, R'	H, alkyl, aryl
L, L'	ligand
M, M'	metal
D, D'	donor atom
BDA	6,6'-dicarboxylate-2,2'-dihydroxy-1,1'-binaphthylene
AgPF ₆	silver hexafluorophosphate
Agtfa	silver trifluoroacetate
AgOTf	silver trifluoromethanesulfonate (triflate)
AgBF ₄	silver tetrafluoroborate
4,4'-bipy	4,4'-bipyridyl
2,2'-bipy	2,2'-bipyridyl
LED	light emitting device
OLED	organic light emitting device
NLO	non-linear optics
py	pyridyl
PCP-31	diphenylphosphino-3-pyridylcarbinol
PCP-32	phenylphosphino-bis(3-pyridylcarbinol)
2-amp	2-aminomethylpyridine

3-amp	3-aminomethylpyridine
3-amp	3-aminomethylpyridine

Spectroscopy

NMR	nuclear magnetic resonance
δ	chemical shift
ppm	parts per million
J	coupling constant
Hz	hertz
MHz	megahertz
s	singlet
d	doublet
dd	doublet of doublets
t	triplet
q	quartet
m	multiplet

Crystallography

$K\alpha$	maxima in the X-ray emission spectrum ($MoK\alpha 1 = 0.71073\text{\AA}$)
λ	monochromated X-ray wavelength taken as weighted average of $K\alpha$ emission
$\theta, \chi, \phi, \omega$	angles variable of the X-ray diffraction experiment
h, k, l	Miller indices, reciprocals of the fractional intercepts which a particular plane makes with a crystallographic axis

a, b, c	lattice parameters defining unit cell dimensions
α, β, γ	lattice parameters defining unit cell angles
D_{calcd}	calculated density
$F(000)$	represents total number of electrons per unit cell
GooF	Goodness-of-fit: the error in the weighting scheme that provides an indication of the agreement between observed and calculated structure factors
$R1$	conventional agreement factor based on refinement of F data
$wR2$	weighted agreement factor based on refinement of all F^2 data
R_{int}	agreement factor between observed and averaged intensities
μ	linear absorption coefficient
V	volume of the unit cell
Z	number of molecules per unit cell
$2\theta_{\text{max}}$	maximum value of 2θ collected in a crystallographic experiment
e.s.d.	estimated standard deviation

ACKNOWLEDGMENTS

I thank God for allowing me to see that things are not always as they seem, for showing me that even the dreariest path may have the most spectacular destination, and for blessing me with all the gifts that life has to offer.

I thank Kevin Klausmeyer for being a most supportive advisor and a good friend. Under his direction I have gained the knowledge and confidence in myself and in my science to stand proudly as equals with those who preceded me.

I thank the Robert A. Welch Foundation for financial support.

I thank my colleagues in the Department of Chemistry at Baylor University, in particular Cody Carson, Dr. Thomas McGrath, Dr. Bruce Hodson and Dr. Andreas Franken for stimulating conversation on topics ranging from the photophysical properties of bipyridyl ruthenium complexes to the eating habits of the Loch Ness Monster. Without them the process might have been unbearable.

I thank my parents, my sister, Rita, Bernardo, Jeannette, Kaki, Abuela Mery and the rest of my family for their unwavering love and support no matter how many times my life changed direction (this was more than once). They would have been just as proud had I ended up flipping burgers as long as I did my best.

And finally I thank Monica. My best friend, my harshest critic, my strongest competitor, my life partner and my Loving Wife. God Himself must have carried this woman to me, there is no other explanation. She completes me . . . and for this I am grateful.

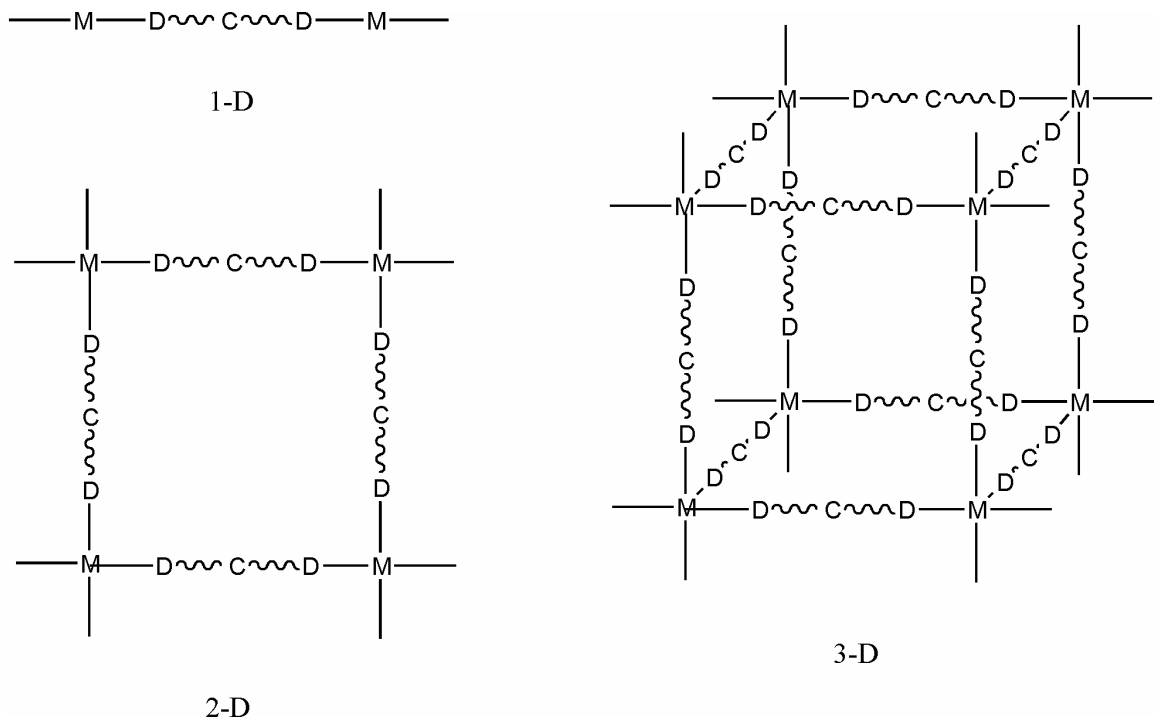
CHAPTER ONE

General Introduction

Knowledge of single-crystal X-ray diffraction developed some eight decades ago and has been an active research topic since shortly after the discovery of X-ray radiation. However, the subjects of supramolecular design and crystal engineering have only seen rapid growth in the last ten years of this era.¹⁻⁴ This sudden surge in investigation can be accounted for as the result of a combination of two important scientific achievements; first and foremost was the development of a microprocessor with sufficient computational power to manage the tremendous amount of data that is unavoidably compiled in the collection of a crystal's reflection data set. This, coupled with the incorporation of the CCD (charge-coupled device) area detector in the mid-nineties reduced the time necessary for the collection of a complete data set from days or weeks to mere hours. This has allowed for X-ray crystallography to take a commanding position as the principal technique for the absolute structural determination of molecular arrangements. As a result, studies now abound on the intra- and intermolecular forces that are present within the crystalline confines of any pure substance. This ever-increasing collection of knowledge has allowed for the rational design and synthesis of countless coordination architectures which display interesting and useful properties.⁵⁻⁹ What follows is a brief overview of the current state of knowledge in the area of supramolecular coordination chemistry, emphasizing those achievements made with infinitely extended coordination networks.

Coordination Polymers by Definition

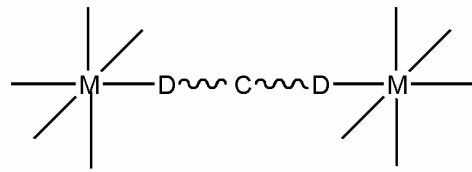
Coordination polymers, also referred to as metal-organic frameworks (MOFs), are ligand-bound metal complexes that extend “infinitely” in one-, two-, or three-dimensions through covalent ligand-donor to metal interactions as shown in Scheme 1.1.¹⁰ Strictly



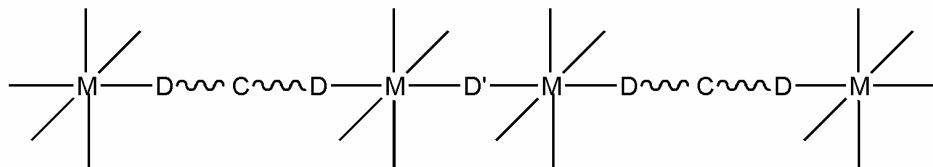
Scheme 1.1. The defining characteristics of the simplest possible one-, two-, and three-dimensional coordination polymers. Terminal ends are linked to equivalent units. D = (typically) N or O.

speaking, in order to have a true coordination polymer, a bridging ligand must have at least one carbon atom in the backbone of that polymer as seen perpetuated in at least one dimension.¹¹ Also, in that same dimension, the polymer must be bridged solely by this organic ligand. This definition separates the coordination polymers from other types of similar extended metal-ligand (be it organic or inorganic) networks, examples of which are shown in Scheme 1.2. Contained within this excluded group are the polymers based

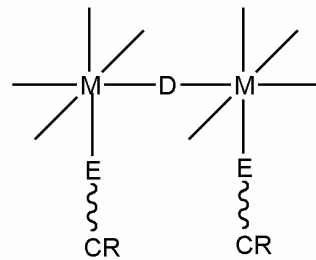
a) true coordination polymer



b) organic-inorganic hybrid materials

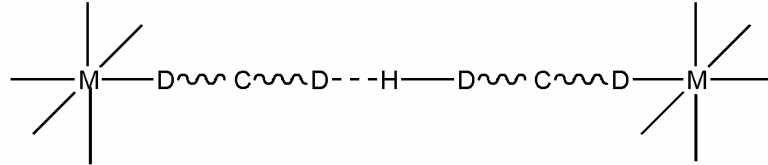


(bridging organic and inorganic ligands)



(bridging inorganic and terminal organic ligands)

c) hydrogen-bonded networks



Scheme 1.2. Diagram of the common extended metal-organic motifs seen in coordination chemistry.

on metals bridged by the inorganic heads of organic oxides (RO^-), phosphonates (RPO_3^{2-}) or sulfonates (RSO_3^-) or of the strictly inorganic bridging ligands such as X^- , CN^- , N_3^- , PO_4^{3-} , or SO_4^{2-} .^{12,13} Also rejected from the coordination polymer definition are

those of the extended hydrogen-bonded networks and those complexes which contain organic bridging ligands that do not continue infinitely in any one dimension but are separated by inorganic spacers (Scheme 1.2, part b and c).^{12,14,15}

Besides the covalent donor-metal bonds that form the basis of the extended metal/ligand framework there are a number of weaker secondary interactions including π -stacking, hydrogen-bonding, solvent effects and anion interactions that must be taken into consideration when examining the overall structural conformation of these complexes.¹⁶⁻

²² Quite often, these features are engineered into coordination networks in attempts to construct predetermined (designed) architectures.²³⁻²⁵ A recent example of this is given by Lin, et al.²⁶ in which the neutral 6,6'-dicyano-2,2'-dihydroxy-1,1'-binaphthalene ligand was functionalized into an anionic (-2) 6,6'-dicarboxylate (BDA) via oxidation of

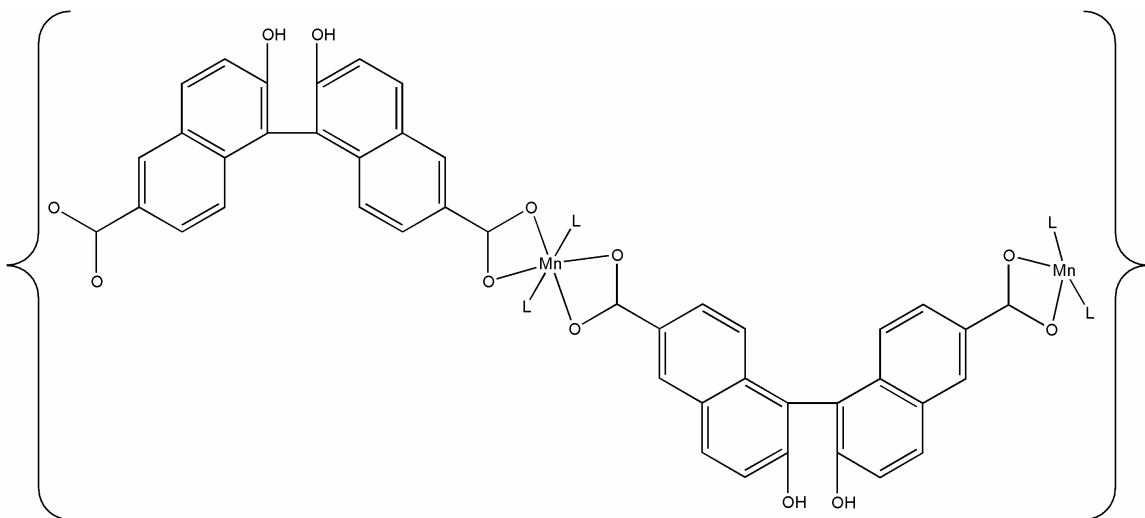


Figure 1.1. bis-(BDA) Mn^{II} polymers. L = MeOH.

the cyano groups. This was then bound to Mn²⁺ constructing charge neutral linear zig-zag coordination polymers shown in Figure 1.1. In addition to balancing the charge of

the metal centers, the carboxylates are seen to be hydrogen bound to the hydroxyl groups of neighboring polymers constructing an overall two-dimensional network motif.

In a similar example, Barboiu and coworkers²⁷ demonstrate how the secondary interactions of hydrogen-bonding and π -stacking can be used to construct supramolecular pipes with AgPF_6 . Once coordinated to a metal, the hydrogen-bonding of Barbouï's urea-based ligand to a typically innocent PF_6^- anion causes the construction of an anion-centered "flower" as shown in Figure 1.2. These monomers are then stacked one on top of another into rods held together by π - π interactions.

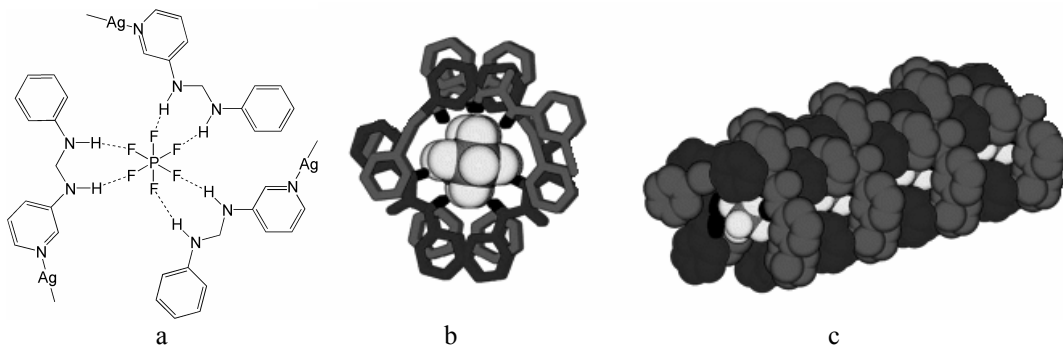


Figure 1.2. a) The silver(I)-bound 1-phenyl-3-pyridine-3-yl-urea hydrogen bonding to a central PF_6^- anion. b) a stick diagram of (a), shown two molecules deep. c) the linear growth of this polymer as an anion-centered rod.

Still other secondary interactions have been used in creative techniques to modify the supramolecular structure of coordination polymers. The ligand 1,3-di(4-pyridyl)propane has been used to construct numerous extended coordination networks and even some discrete, ligand-bridged dimetallic clusters with many different d-block metals.²⁸⁻³⁰ However, the ethane based ligand itself is limited in the interpolymeric interactions in which it can involve itself. In attempts to increase the dimensionality that this ligand has and further study the effects of non-covalent interactions on macromolecular topologies Bu and associates replaced carbon atoms in the backbone of

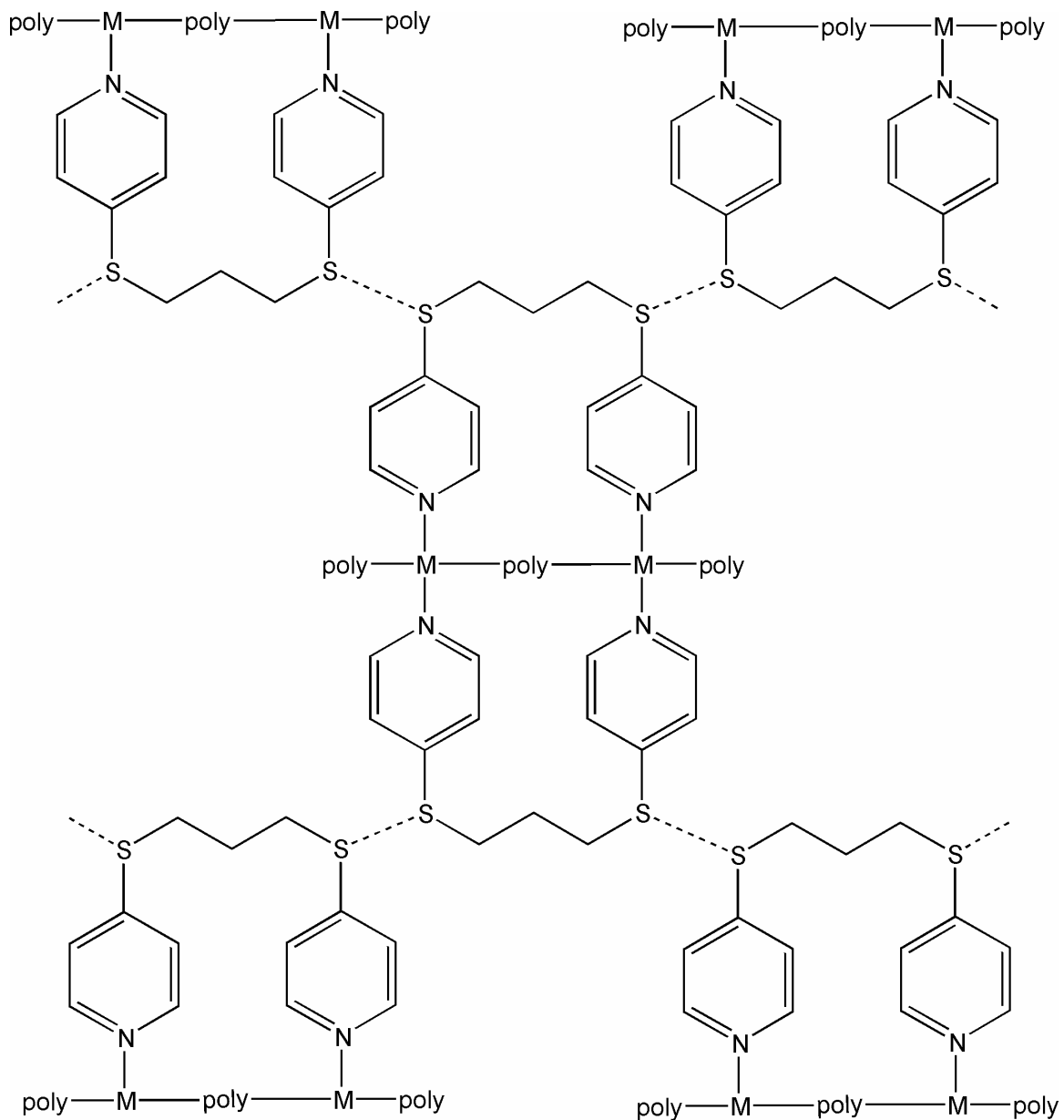


Figure 1.3. A view of the extended network that is formed by linking 1-D polymers with S···S interactions. M = Cd^{II}, Co^{II}, or Zn^{II}.

the 1,3-di(4-pyridyl)propane ligand with sulfur atoms, Figure 1.3.³¹ The resulting structures displayed a primary polymer similar to the hydrocarbon ligand. However, secondary S···S interactions gave an added degree of dimensionality to the complexes, creating several new two and three dimensional networks.

Ligand Constraints

Ligands that are used in the construction of extended coordination networks must bridge between two or more metal ions and are therefore necessarily multidentate.³²⁻³⁵ Unidentate alkoxides, thiolates, etc. may bridge μ_{2-3} , but these linkages typically are seen to form small metal clusters or are used in conjunction with larger organic ligands in the formation of polymeric species.³⁶⁻³⁹ Several common neutral and anionic bidentate ligands used in the synthesis of coordination polymers are shown in Figure 1.4. Ligands are chosen for specific applications based on factors such as rigidity, conjugation, conformation, charge and donor atom.⁴⁰ Each ligand imparts specific characteristics

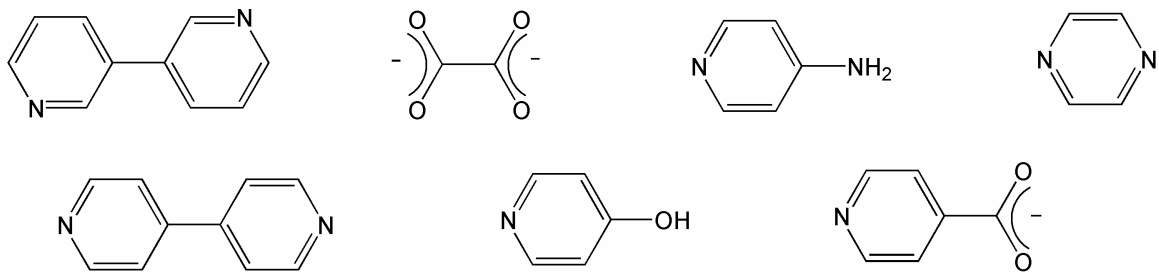


Figure 1.4. Common bidentate ligands used in the construction of coordination networks.

to the polymer of which it is a part and can be used in conjunction with chosen metals to design materials which have desirable characteristics.⁴¹⁻⁵¹ The 4,4'-bipyridyl (4,4'-bipy and its derivatives) ligand, for instance, is one of the most applied linkages for construction of coordination networks due to its predictable binding modes and conformations. These bipy ligands have been used to build one-dimensional chains and ladders, two-dimensional sheets, and three-dimensional scaffolds.⁵²⁻⁵⁵ The complete conjugation of the aromatic ligand also allows for at least partial electronic communication between the opposing metal centers. As a result, the 4,4'-bipy ligand has

been used numerous times in the construction of coordination polymers and networks that are to be studied for specific electronic and luminescent characteristics.⁵⁶⁻⁵⁹ A recent study by Tao and coworkers outlined the use of 4,4'-bipy as a coligand in the assembly of several luminescent extended Zn^{II} networks similar to that shown in Figure 1.5.⁵⁸ They were able to tune the structures and the emission maxima of their polymers by altering the R group of the bridging acid.

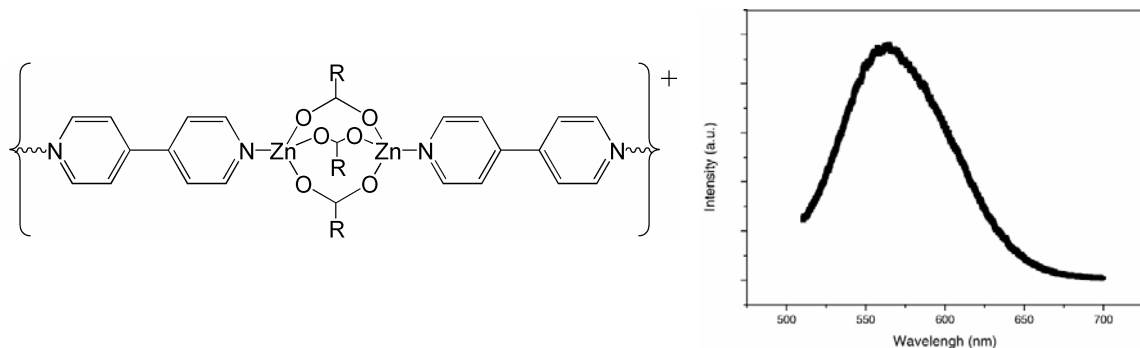


Figure 1.5. Generic 4,4'-bipy / Zn / RO₂⁻ polymer. The emission spectrum is shown for R = 4-sulfoisothalic acid.

Applications

Host-Guest properties / Catalysis

A common goal of many studies of supramolecular coordination networks is the acquisition of new microporous materials that might have zeolitic properties.^{60,61} These porous coordination polymers would have uses in size selective absorption, molecular recognition and gas storage, as well as others. However, as a group, metal-organic coordination polymers tend to be less stable than their inorganic oxide counterparts due to the more labile nature of the metal-ligand bond.⁶² This imposes inherent limitations on their usefulness in the aforementioned areas. Despite these shortcomings, designed porous coordination networks have found application under specialized circumstances

such as size- or shape-specific catalysis.¹¹ Fujita, et al. have reported on the ability of the simple porous network structure made of Cd(NO₃)₂ and 4,4'-bipy to catalyze the cyanosilylation of aldehydes according to Equation 1 (Figure 1.6).⁶³ The structure is

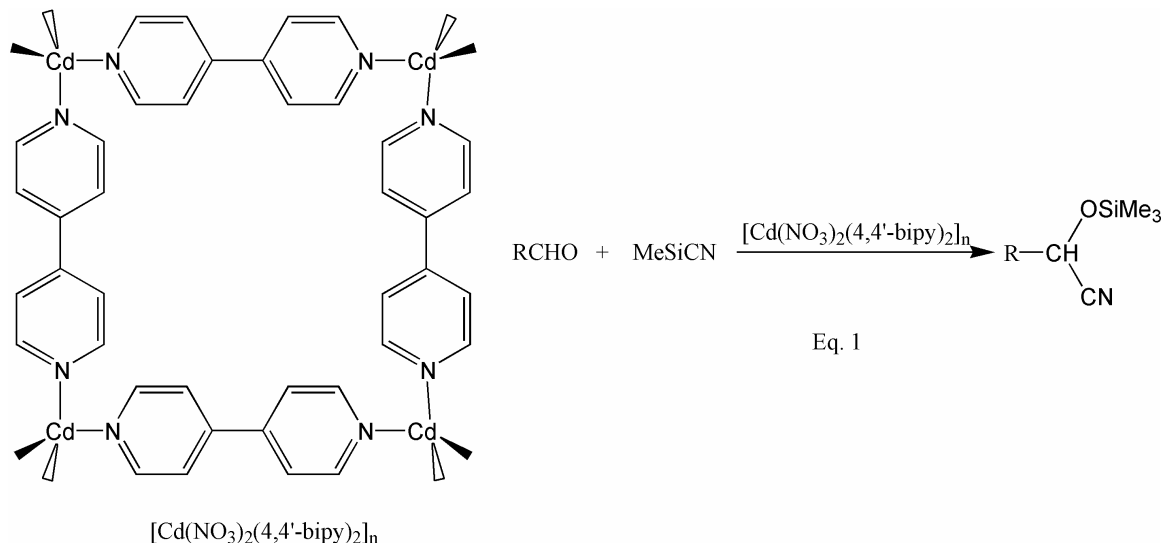


Figure 1.6. Structural diagram of $[Cd(NO_3)_2(4,4'\text{-bipy})_2]_n$. Eq. 1 shows the cyanosilation of an aldehyde that this complex catalyzes.

built into a grid of bipy-walled squares which are presumed to hold the reactants in suitable proximity and position to facilitate the reaction. Cyanosilation of aldehydes typically does not proceed in the absence of a homogeneous Lewis acid catalyst.⁶⁴

Luminescence

The use of coordination polymers as potential new light-emitting devices (LEDs) is of great interest due to the seemingly endless possibilities of ligand / metal combinations.^{58,65-71} A major advantage that these new metal-organic hybrid LEDs have over the traditional organic light-emitting device (OLED) is that they tend to have a much greater thermal stability.⁷¹ This translates into a wider range of applications as well as a

longer lifetime. There is also more room for fine tuning of the emission wavelengths via alterations in both metal environment and ligand properties.

Conductivity

Electrical conductivity, or lack thereof, has traditionally been one of the more sought after properties by materials chemists.⁷²⁻⁷⁴ Coordination chemists have now joined in the effort with the realization that coordination polymers possess the ability to be altered as to allow for regulation of their conductivities.⁷⁵ A stacked coordination polymer of the type $[\text{Fe}^{\text{II}}(\text{pc})(\mu\text{-pyz})]_n$ (pc = phthalocyaninato; pyz = pyrazine) was found to have a conductivity on the order of $1 \times 10^{-6} \text{ S cm}^{-1}$. Doping of this same polymer with iodine increases the conductivity to $2 \times 10^{-1} \text{ S cm}^{-1}$.^{76,77} Coordination polymers with Ag–Ag interactions are also seen to display a temperature dependent semiconductivity.^{67,78,79} This electrical activity is thought to stem from the close metal–metal interactions (often less than 3.0 Å) that are along the lines of that seen in metallic silver (2.89 Å).

Other fields that are seeing advancement from the progression of coordination polymers include those of molecular magnetism^{75,80,81}, which holds great promise as a basis for future generations of computers and information technology, and non-linear optics (NLOs).^{82,83} Several reports of coordination polymers displaying NLO properties are already known, though at present their stability in the laser light used to test them is still inferior to the common inorganic metal oxides presently in service.

In the pages that follow a variety of new extended coordination networks are presented based on a series of pyridyl-substituted phosphinites and amines. All of these complexes have been characterized structurally by X-ray diffraction. This work adds to

the current state of knowledge through the description of new ligands and discussions on structural variability by the use of the intra- and inter-molecular interactions of hydrogen-bonding, π -stacking, temperature and solvent effects. Later chapters also outline what has come to be the first comprehensive study of the ratio dependence of structural motifs in a series of silver(I) salts with the isomeric aminomethylpyridine (amp) ligands; work that readily complements the well-explored area of anion-dependent structural variability.

CHAPTER TWO

Two, Three, and Four Coordinate Ag(I) Coordination Polymers Formed by the Novel Phosphinite, PPh₂(3-OCH₂py)

Introduction

Silver-based coordination polymers have received great attention lately.^{3,4,84-92}

This is owed to the rich chemistry that is available to this versatile metal. Silver-phosphine/silver-pyridine complexes have repeatedly demonstrated interesting electronic, medicinal, and structural properties.^{12,93-113} Part of what gives silver the ability to produce such intriguing structural motifs is the ease with which it varies its coordination number, generally from 2 to 4.¹⁰³ Thus far the vast majority of silver coordination polymers employ ligands that are symmetric, very often using some isomer of bipyridine.⁴

Pyridyl-substituted phosphines, which were first reported nearly 60 years ago, have been commonplace and thoroughly explored since their introduction.^{91,104,112-133} They are an interesting family of ligands because they have the potential to display both the harder and softer donating abilities of the nitrogen and phosphorus, respectively, in a single moiety. The majority of reports in this area have been that of the 2-pyridyl phosphines; their chelating, or their bimetallic/ biligand ring forming abilities.¹³¹⁻¹³⁶ Relatively little work has been reported for the 3- and 4-pyridyl phosphines, most likely due to the difficulty with which they are synthesized.^{114,117,129} Using only 2-pyridyl substituents, the arrangement of complexes formed is inherently limited to those discrete structures that can be obtained with the acute angles present. This excludes a vast array

of complexes that could be formed by separating the nitrogen and phosphorus to the point of minimal interaction.

In order to provide an easier entry into new pyridyl containing phosphines and in an attempt to open a new area of coordination polymer chemistry using ligands with different binding functionalities, an $-\text{OCH}_2-$ “spacer” has been inserted between the P and 3-pyridyl components, thereby achieving the goal of P-N isolation with added benefit of inherent flexibility in the P-N distance. From this, several new coordination compounds of silver that have been prepared with a novel pyridylcarbinol substituted phosphine ligand, **PCP-31**, are now reported. The **PCP-nm** naming convention that we have adopted allows for ease in discussion of this and similar pyridylmethylphosphinites, as there are many substitutions that can be made and systematic nomenclature can be cumbersome. As such, **PCP** indicates the PyridylCarbinol class of Phosphorus ligands, where **n** is the position of substitution on the pyridyl ring and **m** is the number of carbinol substitutions on the phosphorus. This work has recently been published.¹⁴⁷

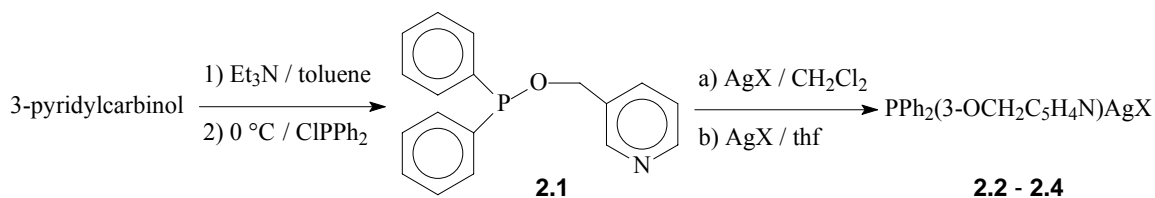
Results and Discussion

Synthesis and NMR Spectroscopy

Compound **2.1 (PCP-31)** is made by the S_{N}^2 type substitution of a chlorophosphine with an alkoxy-pyridine in a modified version of the phenol-derived analog reported by Bedford and Welch.¹³⁷ Deprotonation of the carbinol to make the $^-$ $\text{OCH}_2\text{C}_5\text{H}_4\text{N}$ nucleophile is facile in toluene with the base triethylamine. Great care must be taken in the synthesis of **2.1** as a result of the observation that in the intermediate stages of reaction, all reaction components are extremely sensitive to factors such as

temperature, light, addition rate, concentration, and solvent. High temperatures, rapid or extremely slow addition rate, and ion-stabilizing solvents, such as THF, tend to favor the production of the well known phosphorus-phosphine oxide by-product $\text{PPh}_2\text{P}(\text{O})\text{Ph}_2$.¹³⁸ Exposure to light at any stage of the synthesis leads to the accelerated formation of the yellow decomposition product. Once isolated, **2.1** is stable to moisture but unstable to air, heat, or light. Decomposition can be slowed, though not completely halted, by keeping it shielded from light and refrigerated under an inert atmosphere. ^1H and ^{31}P NMR spectra of **2.1** were obtained in CDCl_3 and demonstrate the very pronounced 3-bond coupling of phosphorus to the phenyl and methylene protons. A defined phosphorus septet is found centered at $\delta = 116.3$, which is in the region expected for aromatic substituted phosphinites.

The silver compounds **2.2-2.4** were synthesized by reaction with simple silver salts under ambient conditions in an inert atmosphere as outlined in Scheme 2.1. These were characterized by the analytical data given in Tables 2.1 and 2.2. Upon coordination, all of the silver compounds reported herein are white powders that noticeably decompose within several hours upon exposure to light. Solutions of the metal compounds **2.2-2.4** in organic solvents undergo reduction of the silver to precipitate metallic silver and an oily



Scheme 2.1. General Synthetic Scheme for the carbinol-substituted phosphine coordination complexes of the silver(I) salts. In a, $\text{X} = \text{BF}_4^-$ or tfa^- and in b, $\text{X} = \text{OTf}^-$.

Table 2.1. Analytical and Physical Data

	compound ^a	yield (%)	analytical (%) ^b		
			C	H	N
2.1	Ph ₂ P(3-OCH ₂ C ₅ H ₄ N)	81			
2.2	<i>poly</i> -[Ph ₂ P(3-OCH ₂ C ₅ H ₄ N)AgBF ₄]	91	45.1 (44.3)	3.4 (3.3)	3.1 (2.9)
2.3	<i>poly</i> -[Ph ₂ P(3-OCH ₂ C ₅ H ₄ N)AgOTf]	92	40.9 (41.4)	2.8 (2.9)	2.7 (2.6)
2.4	<i>poly</i> -[Ph ₂ P(3-OCH ₂ C ₅ H ₄ N)Agtfa]	98	46.7 (46.7)	3.1 (3.1)	2.9 (2.7)

^a All compounds are white or off white solids except for **2.1**, which is a colorless oil. ^b Calculated values are given in parenthesis.

Table 2.2. Hydrogen-1 and Phosphorus-31 NMR Data

	$^1\text{H}/\delta^{\text{a}}$	$^{31}\text{P}/\delta^{\text{b}}$
2.1	4.93 d, 2H $J(\text{PH}) = 9.10\text{Hz}$; 7.28 m, 1H; 7.39 m, 6H; 7.53 m, 4H; 7.68 dt, 1H; 8.56 d, 1H; 8.63 s, 1H.	116.29 m, $J(\text{PH}) = 8.14\text{Hz}$
2.2	5.05 d, 2H; 7.37 m, 7H; 7.58 t, 4H; 7.78 d, 1H; 8.43 d, 1H; 8.69 s, 1H.	111.905 dd, $J(^{107}\text{Ag-P}) = 790.13\text{Hz}$, $J(^{109}\text{Ag-P}) = 685.16\text{Hz}$
2.3	5.07 d, 2H; 7.34 m, 7H; 7.57 t, 4H; 7.86 d, 1H; 8.46 d, 1H; 8.66 s, 1H.	112.113 dd, $J(^{107}\text{Ag-P}) = 788.67\text{ Hz}$, $J(^{109}\text{Ag-P}) = 688.08\text{ Hz}$
2.4	5.05 d, 2H; 7.43 m, 7H; 7.58 t, 4H; 7.83 d, 1H; 8.51 d, 1H; 8.59 s, 1H.	117.54 d, $J(\text{Ag-P}) = 518.96\text{ Hz}$

^a ^1H NMR spectra of **2.1** and **2.4** were recorded in CD_3Cl at 298 K; ^1H NMR spectra of **2.2** and **2.3** were recorded in CD_3CN at 298 K. ^b ^{31}P NMR spectrum of **2.1** was recorded in CD_3Cl at 298 K; ^{31}P NMR spectra of **2.2** and **2.3** were recorded in CD_3CN at 238 K; ^{31}P spectrum of **2.4** was recorded in CD_3Cl at 219 K.

black phosphorus by-product. Compounds **2.2-2.4** appear to be stable indefinitely in the solid state when kept in the absence of light and refrigerated under inert atmosphere.

Compound **2.2** is the most robust of the coordination complexes presented. Though it still suffers from decomposition in solution, under similar conditions as **2.3** and **2.4**, it is at a notably slower rate; the rapid rate of decomposition of **2.3** and **2.4** may be due to having a counterion bound to the silver which makes reduction of the metal more facile. Compound **2.2** is prepared from the mixing of 1 equivalent AgBF₄ in CH₂Cl₂ with a solution of **2.1**. The 2-coordinate coordination polymer is collected as a white solid by removal of the CH₂Cl₂ under vacuum after less than five minutes of reaction. The precipitation of metallic silver from solutions of **2.2** is at such a rate that after 24 hours layered in a crystallization tube at 5 °C, there is only a slightly dark appearance to the tube; whereas under similar conditions, compounds **2.3** and **2.4** would have released the majority of their solute as a black precipitate. ³¹P spectra of **2.2** were recorded in CD₃CN down to 238 K. At room temperature, ³¹P spectra show a doublet of broad peaks centered at 114.0, owing to the silver-phosphorus coupling. This indicates at least some degree of coordination of the ligand to silver in room temperature solutions, though the process does appear to be dynamic on the NMR timescale. Slowing the dissociation of the Ag-P bond by lowering the temperature, causes the doublet peaks to sharpen and move slightly upfield, and eventually to split revealing the coupling of the separate isotopes of Ag.

A solution of Ag triflate in THF added to a single equivalent of **2.1** in THF yields the mixed coordination complex **2.3** as a white powder upon drying. Stirring for a period of time longer than a few minutes, however, results in a precipitate of metallic silver from an unknown redox reaction. Saturated CH₂Cl₂ solutions of **2.3** turn dark and form a

brown precipitate within hours, but still manage to grow X-ray quality crystals over several days when layered with diethyl ether at 5°C. ^{31}P NMR spectra of this compound were obtained using CDCl_3 and were collected to 238 K. Again, some degree of coordination of phosphorus to silver is seen at room temperature, though dissociation is rapid. Cooling the sample to 238 K, the isotopic coupling of silver can be observed to form a doublet of doublets that is centered slightly upfield of the original doublets 114.6 ppm position.

All attempts to synthesize the coordination compound **2.4** using the ligand **2.1** and completely dissolved silver trifluoroacetate were unsuccessful; the result of such reactions consistently being brown solutions with a rapid precipitation of silver in the flask. It was found that the most productive route to compound **2.4** was to allow the ligand **2.1** to solubilize the silver trifluoroacetate directly into solution from its solid state. The dissolved ligand, upon addition to a CH_2Cl_2 suspension of the silver salt, immediately draws the silver salt into solution. Following several minutes of vigorous stirring, the slightly soluble complex **2.4**, precipitates from solution. The precipitate is collected and washed with several aliquots of CH_2Cl_2 . The product is a white solid that noticeably decomposes in solution within minutes at room temperature. Single crystals of **2.4** were grown with some difficulty from saturated solutions of CH_2Cl_2 , layered with diethyl ether at 5°C. ^1H and ^{31}P NMR spectra were obtained in CDCl_3 by keeping the sample in an ice bath until injection into the spectrometer. ^{31}P spectra were recorded to 219 K. The ^{31}P spectrum of **2.4** indicates a P-Ag bond that is considerably more labile than those of compounds **2.2** and **2.3**, with the room temperature resonance showing no

sign of Ag coupling. A single peak is observed at 116.9 ppm that, upon cooling to 219 K, first broadens, then splits to form a doublet centered at 117.5 ppm.

X-ray Crystal Structures

The coordination of the silver centers in each of the compounds **2.2-2.4** are notably different. We were able to achieve compounds demonstrating each of the common coordination numbers of silver, 2, 3 and 4, by changing only the counterion in each case. Variations in coordination have also been observed by changing the crystallization solvent; for instance, a different structural isomer of compound **3**, obtained by crystallization from THF, has been observed that contains only 3-coordinate silver centers. The crystal structure data for this isomer is of very poor quality and is therefore not included in this report; efforts are continuing to crystallize the compound from THF. As the coordination number about the silver center increases there is a concomitant increase in the Ag-N and Ag-P bond lengths; all of these bond lengths fall well within the expected ranges.^{86,88} For compounds **2.2-2.4** varying only the anion between the structures, we can see the N-Ag-P bond angle increase from 133.4° in **2.4**, to nearly linear with a 167.3° angle in the two coordinate BF_4^- complex, **2.2**. All compounds have the one structural feature in common in that the phosphinite ligand coordinates head-to-tail, P-Ag-N, rather than in a head to head fashion that would form different P-Ag-P and N-Ag-N localities in the polymer. In each of the structures the phosphinite ligand is able to adopt different conformations in the polymer. The P-N distance across the ligand varies from 5.33 Å to 6.11 Å; this ability to adapt the distance between the bonding moieties in the ligand allows the Ag-Ag distances bridged by the same ligand to vary from 5.93 Å to 9.26 Å.

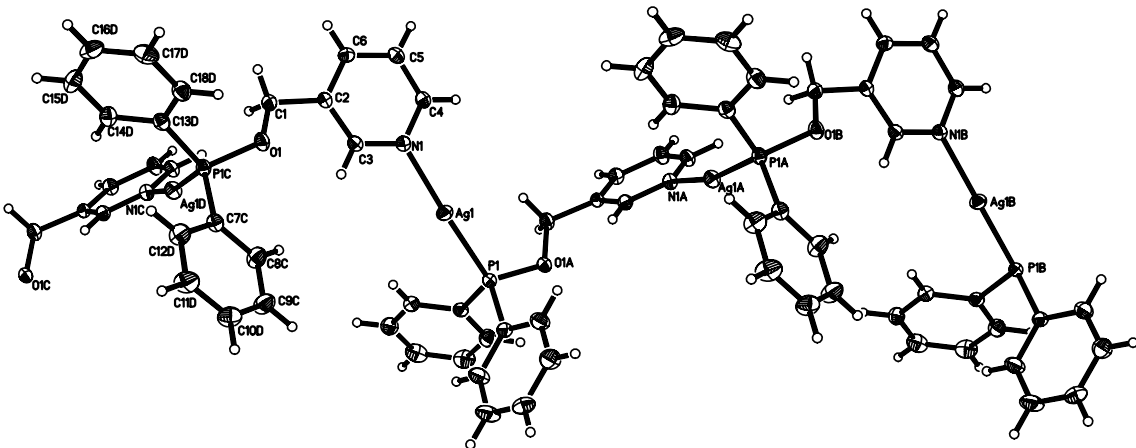


Figure 2.1. Molecular diagram of the cationic polymer of **2.2** with the unique portion and important symmetry generated atoms labeled. Ellipsoids are drawn at the 50% probability level.

Table 2.3. Selected Bond Lengths (\AA), Angles ($^\circ$), Torsion Angles($^\circ$), and Important Distances for **PCP-31AgBF₄** (**2.2**)^a

Ag(1)-N(1)	2.1711(14)	Ag(1)-P(1)	2.3543(5)
Ag(1)-Ag(1)#1	7.1914(9)	Ag(1)#2-F(2)	2.7850(11)
P(1)#1-N(1)	5.5691(15)	P(1)#1-C2	3.8830(15)
N(1)-Ag(1)-P(2)	167.28(4)	P1#1-O1-C1-C2	-155.05(10)

^a Symmetry transformations used to generate equivalent atoms: #1 = x, -y+2, z+1/2, #2 = x, y-1, z

Compound **2.2** makes use of the non-coordinating BF₄ anion to display nearly exclusive ligand-metal interactions. A thermal ellipsoid plot of the one dimensional polymeric structure of zigzag chains of **2.2** is presented in Figure 2.1 and selected bond lengths and angles are in Table 2.3. Without a coordinating counterion, the silver centers take on a near-linear geometry with respect to the head-to-tail linking by **2.1**. The N-Ag-P angle is slightly off linear at 167.3°; the distortion from 180° is likely caused by the long-range interaction of the BF₄⁻ with the Ag⁺. The shortest contact is Ag1-F2 with a

distance of 2.785(1)Å, slightly longer than the sum of the van der Waals radii for the ions. The Ag-P bond length is 2.3543(5)Å, and the N-Ag distance is 2.171(1)Å. All other bond lengths and angles fall well within expected ranges. The Ag-Ag distance across the bridging ligand is 7.1914(9)Å. One and a half molecules of CH₂Cl₂ are present per asymmetric unit.

The X-ray crystal structure of compound **2.3** reveals the triflate anion playing an integral part in deciding the geometry of the silver ions. A thermal ellipsoid plot is shown in Figure 2.2 and selected bond lengths and angles are given in Table 2.4. The asymmetric unit of **2.3** contains 4 unique silver centers, which upon further inspection reveals a cross-linked polymer structure. Cross-linking is achieved by bridging of Ag2 and Ag3 through a triflate (S2). Each phosphinite ligand acts as a bridge that connects two silver cations as in **2.2**. Ag1, Ag3 and Ag4 each have a terminal triflate bound through a single sulfonate oxygen. The triflate bound to Ag2 also forms a bridge to Ag3, resulting in 4 coordination about Ag3. The other three silvers display a distorted trigonal arrangement resulting from the single anion and two ligands coordinating to each giving an O, P, N environment. The cross-linked polymer structure contains repeating 6 Ag containing rings as shown in Figure 2.3. The Ag-Ag distances range from 4.806(1)Å in the triflate bridged atoms, Ag2 and Ag3, to the more than doubled distance of 10.678(3)Å in the diagonal silvers, Ag1 and Ag3. While not bridged by triflate, the Ag1-Ag4 distance is only 4.460(1), probably as a result of packing or a pseudo π-stacking interaction of the pyridine rings. The Ag-N bonds range from 2.217(7) to 2.255(7)Å, slightly longer than that observed in **2.2**, and the Ag-P bonds average 2.34Å, nearly the same as in **2.2**. The intra-ligand P-N distances range from 5.933(7)Å for P1-N1 to

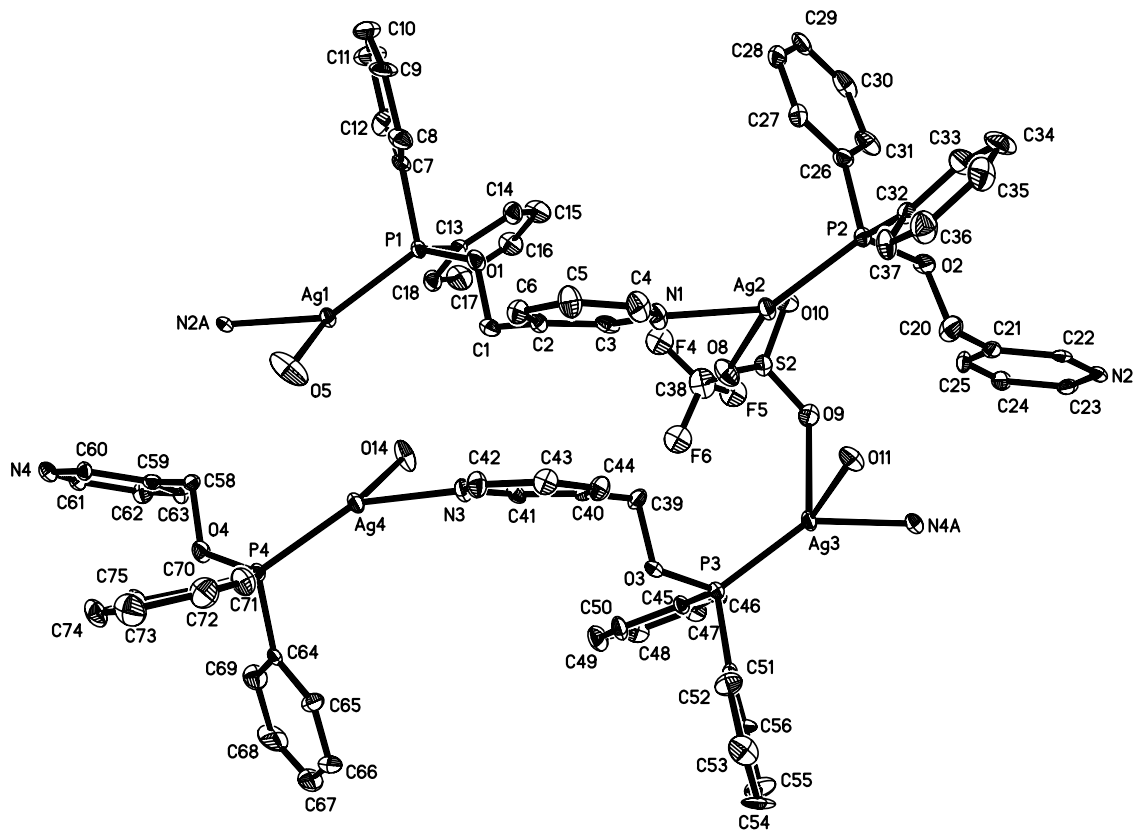


Figure 2.2. Molecular diagram of the unique portion of **2.3**. Ellipsoids are drawn at the 30% probability level. Hydrogen atoms and all but the bound oxygen of the terminal triflates have been removed for clarity.

Table 2.4. Selected Bond Lengths (\AA), Angles ($^\circ$), Torsion Angles($^\circ$), and Important Distances for PCP-31AgOTf (**2.3**)^a

Ag(1)-N(2) ^{#1}	2.232(7)	Ag(1)-P(1)	2.334(2)
Ag(1)-O(5)	2.494(8)	Ag(2)-N(1)	2.217(7)
Ag(2)-P(2)	2.341(2)	Ag(2)-O(8)	2.470(7)
Ag(3)-N(4) ^{#2}	2.255(7)	Ag(3)-P(3)	2.355(2)
Ag(3)-O(11)	2.490(6)	Ag(3)-O(9)	2.524(7)
Ag(4)-N(3)	2.241(7)	Ag(4)-P(4)	2.359(2)
Ag(4)-O(14)	2.515(6)	Ag(1)-Ag(2)	9.1646(23)
Ag(1)-Ag(3)	10.6784(29)	Ag(1)-Ag(4)	4.4604(13)
Ag(2)-Ag(3)	4.8058(13)	Ag(2)-Ag(4)	8.9123(18)
Ag(3)-Ag(4)	9.2645(23)	P(1)-N(1)	5.933(7)
P(2)-N(2)	6.119(7)	P(3)-N(3)	5.979(7)

Table 2.4. Continued

P(4)-N(4)	6.014(7)	P(1)-C(2)	3.902(8)
P(2)-C(21)	3.866(9)	P(3)-C(40)	3.891(8)
P(4)-C(59)	3.865(8)		
N(2)#1-Ag(1)-O(6)	86.5(3)	P(1)-Ag(1)-O(6)	119.44(19)
N(1)-Ag(2)-P(2)	145.5(2)	N(1)-Ag(2)-O(8)	83.8(3)
P(2)-Ag(2)-O(8)	119.93(16)	N(4)#2-Ag(3)-P(3)	140.15(19)
N(4)#2-Ag(3)-O(11)	86.7(2)	P(3)-Ag(3)-O(11)	119.94(15)
N(4)#2-Ag(3)-O(9)	82.3(2)	P(3)-Ag(3)-O(9)	124.08(16)
O(11)-Ag(3)-O(9)	88.2(2)	N(3)-Ag(4)-P(4)	146.9(2)
N(3)-Ag(4)-O(14)	83.3(2)	P(4)-Ag(4)-O(14)	119.87(15)
N(2)#1-Ag(1)-P(1)	142.75(17)	P(2)-O(2)-C(20)-C(21)	166.74(64)
P(3)-O(3)-C(39)-C(40)	-169.61(53)	P(4)-O(4)-C(58)-C(59)	167.34(53)
P(1)-O(1)-C(1)-C(2)	-169.39(54)		

^a Symmetry transformations used to generate equivalent atoms: #1 = x+1,y,z;#2 = x-1,y,z.

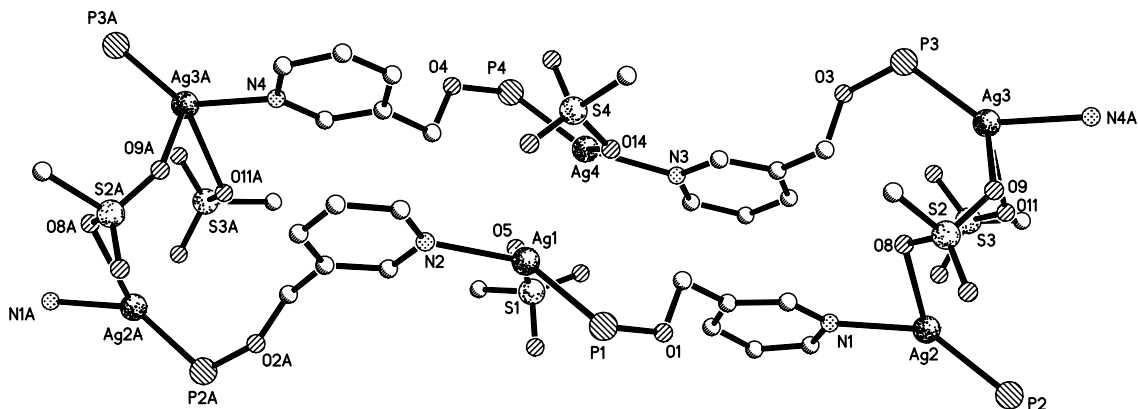


Figure 2.3. Ball and stick diagram of **2.3** showing the hexasilver-containing rings. Triflate oxygens bound to Ag are labeled. Phenyl rings and hydrogen atoms are removed for clarity.

6.119(7) Å for P2-N2, about 0.4 Å longer than that observed in **2.2**. This observation helps to account for the much longer Ag-Ag distances across the same ligand which range from 9.164(2), for Ag1-Ag2 to 9.265(2), for Ag3-Ag4. The N-Ag-O bond angles around the Ag centers range from 82.3° to 86.5°, the P-Ag-O angles for Ag1, Ag2 and

Ag4, are all near the ideal trigonal planar angle of 120°, ranging from 119.4(1)° to 119.9(2)°; the exception is the P-Ag-O angle for Ag3 which is a bit wider at 124.1(2)°. The N-Ag-P angle is consistently the widest in the structure from 140.1(2)° for Ag3 to 146.9(2)° for Ag4. For the three coordinate Ag centers the sum of the angles averages 349°, showing the distortion from trigonal planar geometry. The polymer chains are continued to the next unit by the pendent N2 and N4 pyridine rings. The fluorine atoms of the triflate groups are highly disordered about the C-S axis; due to this disorder they were refined isotropically and each group was restrained to have the same C-F bond lengths, angles and thermal parameters. There are two molecules of CH₂Cl₂ solvent in the lattice one of which (C78) is disordered, this carbon was refined isotropically.

The crystal structure of compound **2.4** reveals a diamond-like binuclear silver center with each Ag bridged by two trifluoroacetate ions. There are two independent Ag centers in the structure with only minor differences between the two. A thermal ellipsoid plot of one of the independent units is shown in Figure 2.4 and selected bond lengths and angles are given in Table 2.5. Each silver has near tetrahedral geometry with a Ag1-Ag1A distance of 3.8686(9)Å and slightly longer for Ag2-Ag2A at 3.9404(9)Å. Each Ag is also bound by two ligands with opposing ends facing each other in a head to tail fashion. The pendent ends of the ligands bound to the Ag⁺ then bind another Ag⁺ making a ring as shown in Figure 2.5. The Ag-Ag distance across this ring is 6.068(1)Å for Ag1-Ag1B and 5.937(1)Å for Ag2-Ag2B. Therefore for **2.4**, the coordination polymer formed is not by linking through the phosphinite ligand, but through the trifluoroacetate bridged Ag⁺ centers. The coordination about the Ag ions in **2.4** is the most electron rich of those presented here being ligated by two O's, an N and a P. The Ag-N bonds of **2.4** reflect the

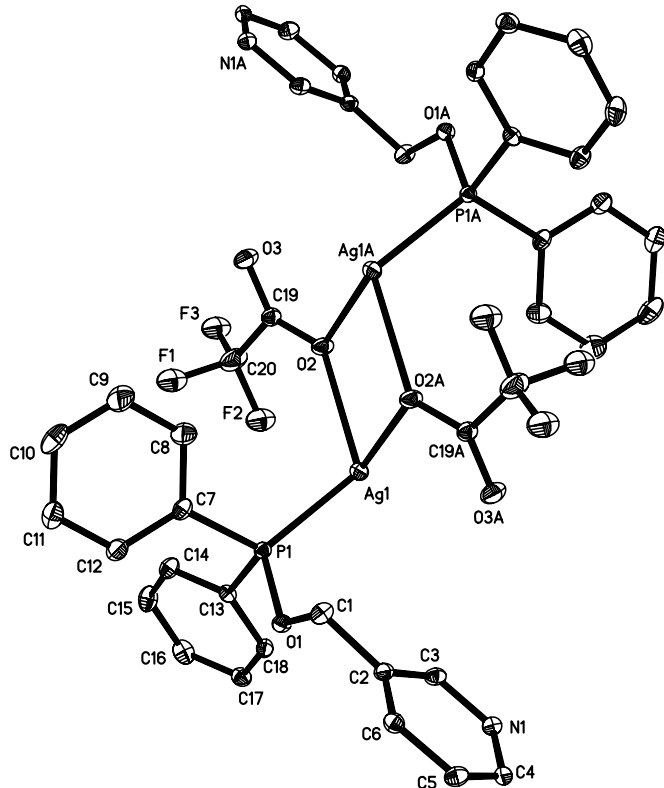


Figure 2.4. Molecular diagram of **2.4** with the unique portion and important symmetry generated atoms labeled. Ellipsoids are drawn at the 30% probability level. Hydrogen atoms have been removed for clarity.

Table 2.5. Selected Bond Lengths (\AA), Angles ($^\circ$), Torsion Angles($^\circ$), and Important Distances for **PCP-31Agtaf (2.4)**^a

Ag(1)-N(1)#1	2.269(4)	Ag(1)-P(1)	2.3556(13)
Ag(1)-O(2)#2	2.375(4)	Ag(1)-O(2)	2.549(4)
Ag(2)-N(2)#3	2.264(5)	Ag(2)-P(2)	2.3681(13)
Ag(2)-O(5)#4	2.419(4)	Ag(2)-O(5)	2.576(4)
Ag(1)-Ag(1)#1	3.8686(9)	Ag(1)-Ag(1)#2	6.0676(11)
Ag(2)-Ag(2)#4	3.9404(9)	Ag(2)-Ag(2)#3	5.9368(11)
P(1)-N(1)	5.370(4)	P(1)-C(2)	3.794(5)
P(2)-N(2)	5.337(4)	P(2)-C(22)	3.784(5)
<hr/>			
N(1)#1-Ag(1)-P(1)	133.36(11)	N(1)#1-Ag(1)-O(2)#2	103.06(15)
P(1)-Ag(1)-O(2)#2	119.72(10)	N(1)#1-Ag(1)-O(2)	91.60(14)
P(1)-Ag(1)-O(2)	114.52(10)	O(2)#2-Ag(1)-O(2)	76.48(13)
N(2)#3-Ag(2)-P(2)	136.26(12)	N(2)#3-Ag(2)-O(5)#4	107.22(15)
P(2)-Ag(2)-O(5)#4	112.73(10)	N(2)#3-Ag(2)-O(5)	92.18(14)
P(2)-Ag(2)-O(5)	113.91(9)	O(5)#4-Ag(2)-O(5)	75.88(14)
P(1)-O(1)-C(1)-C(2)	-136.7(3)	P(2)-O(2)-C(21)-C(22)	-134.4(3)

^a Symmetry transformations used to generate equivalent atoms: #1 = -x,-y+2,-z; #2 = -x,-y+1,-z; #3 = -x+1,-y+2,-z+1; #4 = -x+2,-y+2,-z+1

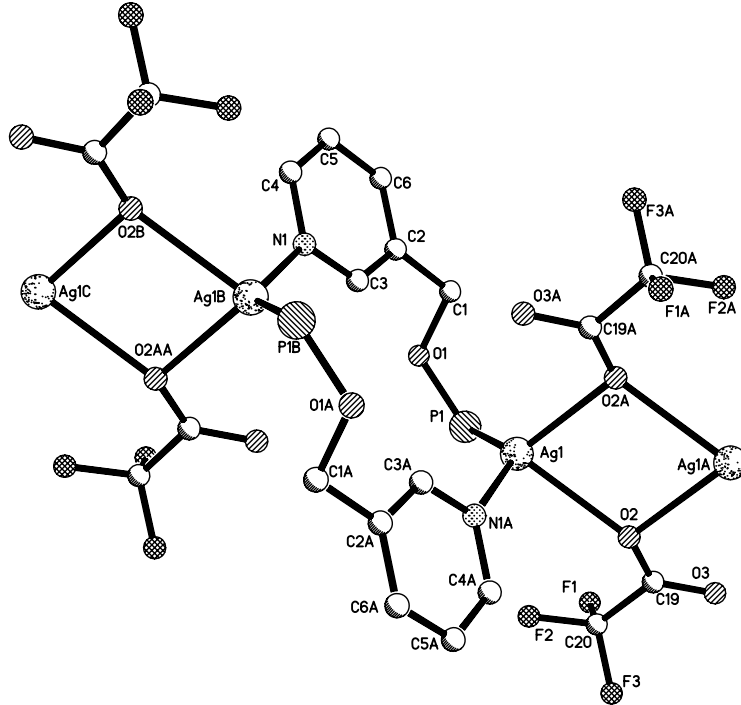


Figure 2.5. Ball and stick diagram of the ring formed by **2.1** and Ag, which is linked by tfa⁻ ions to form an infinite chain. Phenyl groups and hydrogen atoms have been removed for clarity.

effect of increased coordination by lengthening to 2.269(4) Å for Ag1-N1 and 2.264(5) Å for Ag2-N2, nearly a 0.1 Å increase from **2.2**. The Ag-P bond lengths are less impacted being at 2.356(1) for Ag1-P1 and 2.368(1) Å for Ag2-P2. In adopting the conformation for the ring structure the P-N distance displays its shortest distance observed at 5.370(4) Å for P1-N1 and 5.337(4) Å for P2-N2. The P-Ag-N angles are the most acute of the examples presented here being 133.4(1)^o for N1-Ag-P1 and 136.3(1) for N2-Ag2-P2. The fluorine atoms of the trifluoracetate groups are disordered about the C-C axis and were thus restrained to have the same C-F bond lengths and thermal parameters.

Luminescence Properties

Mixed metal-organic hybrid polymers are of considerable interest because of their potential use for the construction of novel light-emitting devices, or LEDs. These

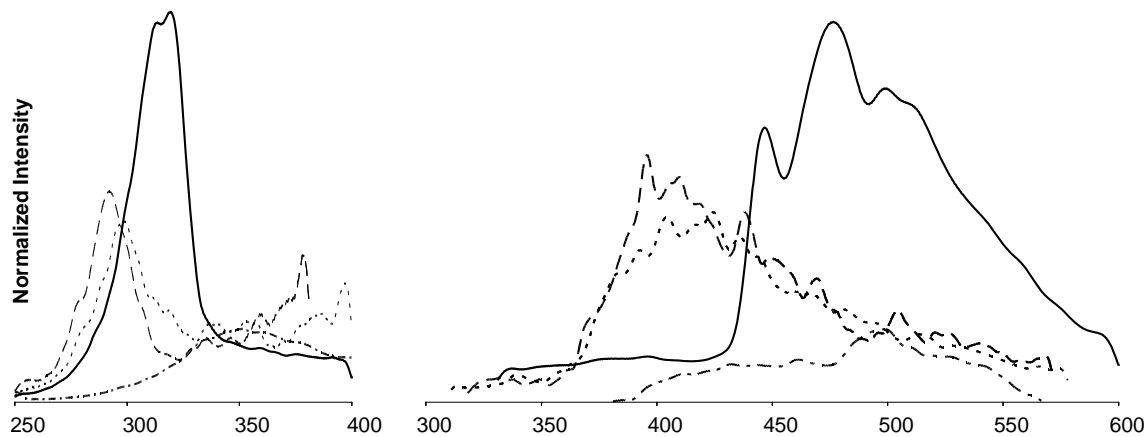


Figure 2.6. Normalized excitation and emission spectra of compounds **2.1–2.4** taken in acetonitrile glasses at 1×10^{-4} M concentration at 77 K. **—** = PCP-31AgBF₄, **— - -** = PCP-31AgOTf, **-----** = PCP-31AgTfa, **- · -** = PCP-31.

Table 2.6. Luminescent Spectral Data for compounds **2.1–2.4**, at 77 K and 1×10^{-4} M in CH₃CN.

Compound	Excitation λ_{\max}	Emission local λ_{\min}
2.1	351	462, 499
2.2	313, 319	447, 477, 501, 512, 593
2.3	292	396, 410, 439, 470, 505
2.4	300	393, 404, 425, 437, 515

materials are seen to have advantages over traditional organic LEDs in that their emission spectra can, in many cases, be tuned by altering the metal environment. This is typically done through changes in ligand, counterion, and oxidation state as well as other methods. We have examined the photoluminescent characteristics of compounds **2.1–2.4** in acetonitrile glasses at low temperatures and have found that the metal complexes exhibit emission curves over a broad area of the visible spectrum as seen in Figure 2.6. The intensities of these emissions are several times greater than that displayed by the free PCP-31 ligand itself, with the BF₄⁻ salt, **2.2**, being the most strongly emissive. The emission spectra of **2.2–2.4** all contain several strong features that are also not as

prevalent in the spectrum of the **2.1**, indicating that these are relics of a metal-based decay likely brought on by ligand-to-metal charge transfer (LMTC). The most intense of the compounds, **2.2**, displays several defining peaks at 447, 477 and 501 nm when excited at its excitation maximum of 351 nm, then decays towards the red end of the spectrum accounting for the light green-yellow color of the luminescent complex. **2.3** and **2.4** display similar excitation maxima at 292 and 300 nm, respectively. This relation is also apparent in the emission curves with both having similar intensities and placement on the electromagnetic (EM) spectrum. **2.3** shows intense emissions at 396, 410 and 439 nm and **2.4** shows high peaks at 393, 404 and 425 nm. A complete tabulation of the spectral features of **2.1-2.4** is presented in Table 2.6.

Conclusions

We have reported the synthesis of a novel pyridyl containing phosphinite which shows the ability to bind silver ions through both the phosphorus and nitrogen moieties. Several new coordination polymers of Ag(I) have been characterized using X-ray crystallography which reveal a structure dependence on the anion used for crystallization. The inherent flexibility of the **PCP-31** ligand is manifested in the wide ranging difference in Ag-Ag distances across the ligand from 5.937(1)Å to 9.265(2)Å. The complexes also demonstrate the wide range of coordination environments that the silver(I) cation can adopt under the simple pressures of anion replacement. What's more, the structures display a large variance from the typical coordination modes of the 2-pyridyl-substituted phosphines by easily constructing several new coordination polymers via outward orientation of the ligand donors.

Experimental

General Considerations

All experiments were carried out under an argon atmosphere, using a Schlenk line and standard Schlenk techniques. All glassware was dried at 120°C for several hours prior to use. All reagents were stored in an inert atmosphere glovebox; solvents were distilled under nitrogen from the appropriate drying agent immediately before use. Triethylamine was purchased from Aldrich and purged with argon before use by bubbling gas through the liquid. 3-pyridyl carbinol was purchased from Aldrich and used as received. Chlorodiphenylphosphine, silver(I) trifluoroacetate, silver(I) triflate, and silver(I) tetrafluoroborate were purchased from Strem Chemicals Inc. and used as received. Celite was purchased from Aldrich and dried at 120°C prior to use. NMR spectra were collected at 298K on a Bruker Spectrospin 300 MHz spectrometer. ¹H and room temp ³¹P were recorded at 300.13 MHz, and 121.49MHz on a Bruker Spectrospin 300MHz Spectrometer. Low temperature ³¹P NMR was recorded at 145.78 MHz on a Bruker Spectrospin 360 MHz Spectrometer. Elemental analyses were performed by Atlantic Microlabs Inc., Norcross, Georgia.

Preparations

Diphenylphoshino-3-pyridylcarbinol, (PPh₂3-OCH₂py), PCP-31 (2.1). In an argon purged addition funnel, 1.3 mL of degassed triethylamine (9.33 mmol) was added via syringe to a stirred solution of 1.00 g 3-pyridylcarbinol (9.16 mmol) in 20 mL toluene at room temperature. The solution was then cooled to 0°C and wrapped with aluminum foil to shield it from light. A solution of 2.02 g (9.16 mmol) chlorodiphenylphosphine in

20 mL toluene was then added dropwise over 10 minutes. The solution was stirred for 1 hour then allowed to warm to room temperature and stirred for an additional hour. The resultant cloudy mixture was reduced to 3/4 its original volume under vacuum and immediately filtered through Celite. The triethylammonium chloride salts were washed with an additional 5 mL of cold toluene to extract any yellow colored compounds remaining. The solvent was removed from the yellow liquid at reduced pressure to leave a pale yellow oil which is the crude diphenylphosphino-3-pyridylcarbinol product in 96% yield. The oil was then extracted several times with hexanes. Drying of the hexane wash in vacuo yielded the clear, colorless oil, **2.1**, in 81% yield (2.18g, 7.44mmol).

poly-[PCP-3I₄AgBF₄] (2.2). To a stirred solution of 0.300 g AgBF₄ (1.54 mmol) in 5mL CH₂Cl₂ was added 0.452 g (1.54 mmol) of **2.1** in 5 mL CH₂Cl₂. The resulting solution remains clear and colorless, and the solvent is removed by vacuum after 5 minutes of stirring. Upon drying, the white powder, **2.2** is reclaimed in 91.2% yield (0.686 g, 1.406 mmol). Crystals of **2.2** were obtained by vapor diffusion of ether into a solution of **2.2** in CH₂Cl₂ at 5°C.

poly-[PCP-3I₄AgOTf] (2.3). To a stirred solution of 0.088 g (0.342 mmol) AgOTf in 10 mL THF was added 0.100 g (0.341 mmol) **2.1** in 5 mL THF. This solution was stirred for 5 minutes, and then the solvent was removed in vacuo to leave a white, fluffy powder, **2.3**, in 91.5% yield (0.172 g, 0.312 mmol). Crystals of **2.3** were grown by slow diffusion of diethyl ether into a solution of **2.3** in CH₂Cl₂ at 5°C.

poly-[PCP-3I₄Agtaf] (2.4). To a stirred suspension of 0.076 g (0.344 mmol) Agtafa in 10 mL CH₂Cl₂ was added 0.100 g (0.341 mmol) **2.1** in 5 mL CH₂Cl₂. The solid Agtafa

dissolved immediately upon introduction of the ligand. After approximately 5 minutes of vigorous stirring, a precipitate formed. The brown-yellow solvent was removed *via* cannula and the solid **2.4** was washed with another 5 mL aliquot of CH₂Cl₂. The residual solvent was then removed in vacuo to leave a white solid, **2.4**, in 97.7% yield (0.172 g, 0.334 mmol). Crystals of **2.4** were obtained by slow diffusion of diethyl ether into a solution of **2.4** in CH₂Cl₂ at 5°C.

Crystallography

A summary of the crystallographic experimental data for **2.2**, **2.3** and **2.4** is shown in Table 2.7. Full tables of bond lengths, angles and other important distances can be found in Appendix B, Tables B.1 to B.3. Crystallographic data were collected on crystals with dimensions 0.29 x 0.28 x 0.25 mm for **2.2**, 0.22 x 0.17 x 0.13 mm for **2.3**, and 0.26 x 0.22 x 0.15 mm for **2.4**. Data for **2.3** and **2.4** were collected at 110K on a SMART 1000 and Bruker Apex diffractometer, respectively. Data for **2.2** was collected on a Bruker X8 Apex at 110K. All structures were solved by direct methods after correction of the data using SADABS.¹³⁹ All data were processed using Bruker AXS SHELXTL software, version 6.10.¹⁴⁰ Unless otherwise noted, all non-hydrogen atoms were refined anisotropically and hydrogen atoms were placed in calculated positions.

Table 2.7. Crystallographic Data for **2.2**, **2.3** and **2.4**

	2.2	2.3	2.4
Formula	C _{19.50} H ₁₉ AgBCl ₃ F ₄ NOP	C ₃₉ H ₃₄ Ag ₂ Cl ₂ F ₆ N ₂ O ₈ P ₂ S ₂	C ₄₀ H ₃₂ Ag ₂ F ₆ N ₂ O ₆ P ₂
Formula weight	615.36	2370.76	1028.36
a (Å)	29.399(5)	17.972(5)	8.9906(14)
b (Å)	11.2041(15)	10.191(3)	9.1032(14)
c (Å)	14.1888(18)	27.936(8)	25.965(4)
α (°)			96.721(2)
β (°)	94.266(9)	115.441(4)	95.492(2)
γ (°)			105.485(2)
V (Å ³)	4660.7(11)	4620(2)	2015.9(5)
Z	8	2	2
space group	C2/c	Pc	P-1
T (K)	110	110	110
λ (Å)	0.71073	0.71073	0.71073
D _{calcd} (g cm ⁻³)	1.754	1.704	1.694
μ (mm ⁻¹)	1.323	1.198	1.127
2θ _{max} , deg	66°	55°	55°
reflns measured	34150	47570	27968
reflns used (R _{int})	8789	18852	8965
Restraints / Parameters	0 / 285	201 / 1106	125 / 546
R1, [I>2σ(I)]	0.0301	0.0624	0.0531
wR ² , [I>2σ(I)]	0.0812	0.1531	0.1260
R(F _o ²), (all data)	0.0402	0.0693	0.0567
R _w (F _o ²), (all data)	0.0834	0.1531	0.1278
GooF on F ²	1.073	1.088	1.105

CHAPTER THREE

Anion Dependent Silver(I) Coordination Polymers of the Tridentate Pyridylphosphonite: PPh(3-OCH₂C₅H₄N)₂

Introduction

The self-assembly of coordination polymers that offer a variety of novel structural, electronic, optical, catalytic and medicinal properties is currently an intense area of study in supramolecular chemistry.^{3,4,7,11,25,141} Specific attention has been given to those structures based upon the coinage metals.^{142,143} In particular, coordination polymers involving the silver (I) ion have made a large contribution to this field due in part to the ease with which it varies its coordination number.^{14,16,18-20,23,33-35,41-45,47,48,65,144-147} The fact that silver (I) can readily vary its coordination number from 2 to 6 by merely changing the size or concentration in solution of a ligating species makes it an appealing candidate for use in deliberately designed or “tailored” polymeric coordination complexes.^{49,148} Other options for controlling structural growth that have proven useful include varying anions to achieve different degrees of interaction or changing the bridging ligand itself to make it more or less rigid.^{92,146}

Silver(I) coordination polymers of pyridyl-substituted phosphines are virtually unknown. This could be owed to the fact that the majority of work done with pyridyl-substituted phosphines has involved 2-pyridyl substitution.^{104-108,110,112,113,118,127,128} The small bite angle associated with the 2-pyridyl substitution inherently limits such a ligand’s ability to bridge and as a result most complexes of the 2-pyridyl-substituted phosphines are small, discrete structures.^{104-108,110,112,113,128} The few reported 3- and 4-

pyridyl-substituted phosphines have been sparsely explored in terms of their coordination chemistry and polymer forming abilities given, at least in part, to the difficulty by which these ligands are synthesized and handled.^{114,117,119,149} With the synthesis of the 3-pyridyl-substituted phosphinite, Ph₂P(3-OCH₂C₅H₄N) or **PCP-31**, we demonstrated that opening the bite angle of these heterobidentate ligands to the point of minimal interaction between the hard and soft binding sites allows the synthesis of some very interesting coordination polymers of various silver(I) salts.¹⁴⁷ As shown in the previous chapter, the flexibility imparted upon the pyridyl phosphinite ligand by the addition of an –OCH₂– spacer, as well as the outwardly oriented binding sites of the meta- and para-nitrogen donors allow for amazing versatility in the coordination modes achievable. We have taken our inquiry of the **PCPs** a step further by adding a second pyridyl substitution, effecting a tridentate pyridyl/phosphine donor ligand, **PCP-32**, and expanding the dimensionality available to the coordination polymers formed by ligation to silver(I) salts of various anions. These polymers display a variety of interesting structural and electronic characteristics. The molecular structures and luminescence properties are discussed herein. The results which appear below have been recently published.¹⁵⁹

Results and Discussion

Synthesis and NMR Spectroscopy

Compound **3.1** is made by a similar procedure as reported for the synthesis of the singly substituted derivative, diphenylphosphino-3-pyridylcarbinol, adjusting for the addition of a second equivalent of carbinol to the phosphine. **PCP-32** is seen to be quite a bit more sensitive to reaction conditions than its singly substituted counterpart, and

decomposes at a more rapid rate in solution at room temperature. After isolation as a colorless oil, **3.1** is found to be readily hydrolyzed, oxidizes in air and decomposes with exposure to heat or light. The thermal instability is such that storage at a temperature of –35 °C is insufficient to halt the degradation of the fluid, colorless oil into a thick, dark-yellow cloudy oil over time. Pure **3.1** can be separated at any point, when necessary, from its decomposition products by extraction into hexanes. The ligand is, however, formed in sufficient purity to allow for further use without the final hexane extraction. ¹H and ³¹P NMR spectra of **3.1** were obtained in CDCl₃ and show the pronounced three-bond coupling of phosphorus to the phenyl and methylene protons; a well-defined phosphorus septet is thus found centered at 159.9 ppm.

The silver compounds **3.2** – **3.4** were made by reaction of **3.1** with silver salts of the respective anions under ambient conditions and inert atmosphere. Analytical data for these compounds are presented in Tables 3.1 and 3.2. Solutions of the three compounds readily decompose to leave metallic silver and an unidentifiable black by-product. However, the powders of each complex have proven themselves to be quite robust, withstanding long exposure to air and room temperatures with little signs of decomposition. They demonstrate a concomitant increase in photostability, defending against signs of decomposition for days upon exposure to light as opposed to hours for the analogous complexes of the mono-substituted PPh₂(3-OCH₂C₅H₄N). This relative increase in solid-state stability could be accredited to the extra dimensionality that the second carbinol substitution imparts on the coordination of the ligand. Compounds **3.2** – **3.4** appear to be stable indefinitely in the solid state if stored in the dark and refrigerated under inert atmosphere. Variable temperature ³¹P NMR spectra were recorded to –35 °C

Table 3.1. Analytical and Physical Data

	compound ^a	yield (%)	analytical (%) ^b		
			C	H	N
3.1	PhP(3-OCH ₂ C ₅ H ₄ N) ₂ , PCP-32	77			
3.2	<i>poly</i> -[PhP(3-OCH ₂ C ₅ H ₄ N) ₂ AgBF ₄]	86	30.7 (30.9)	2.4 (2.3)	3.6 (3.9)
3.3	<i>poly</i> -[PhP(3-OCH ₂ C ₅ H ₄ N) ₂ AgOTf]	93	41.2 (41.7)	3.3 (3.3)	5.3 (5.4)
3.4	<i>poly</i> -[PhP(3-OCH ₂ C ₅ H ₄ N) ₂ Agtfa]	94	35.8 (35.6)	2.4 (2.4)	3.8 (4.0)

^a All compounds are white or off white solids except for **3.1**, which is a colorless oil. ^b Calculated values are given in parenthesis.

Table 3.2. Hydrogen-1 and Phosphorus-31 NMR Data

	$^1\text{H}/\delta^{\text{a}}$	$^{31}\text{P}/\delta^{\text{b}}$
3.1	4.87 d,m, 4 H, $J(\text{PH}) = 8.28$ Hz; 7.34 m, 2 H; 7.48 m, 3 H; 7.681 m, 4 H; 8.59 m, 4 H.	160.4 sep, $J(\text{PH}) = 7.27$ Hz.
3.2	5.11 d,m, 4H; 7.47 m, 2H; 7.65 m, 3H; 7.85 m, 4H; 8.12 m, 4H.	146.4 d, $J(\text{Ag-P}) = 908.2$ Hz.
3.3	5.07 d,m, 4H; 7.45 m, 2H; 7.65 m, 3H; 7.85 m, 4H; 8.48 d, 2H; 8.55 s, 2H.	149.8 d, $J(\text{Ag-P}) = 804.7$ Hz.
3.4	5.12 d,m, 4H; 7.39 m, 2H; 7.59 m, 3H; 7.82 m, 4H; 8.50 d, 2H; 8.59 s 2H.	152.2.

^a ^1H NMR spectrum of **3.1** was recorded in CD_3Cl at 298 K. ^1H NMR spectra of **3.2-3.4** were recorded in CD_3CN at 298 K. ^b ^{31}P NMR spectrum of **3.1** was recorded in CD_3Cl at 298 K. ^{31}P NMR spectra of **3.2-3.4** were recorded in CD_3CN at 238 K.

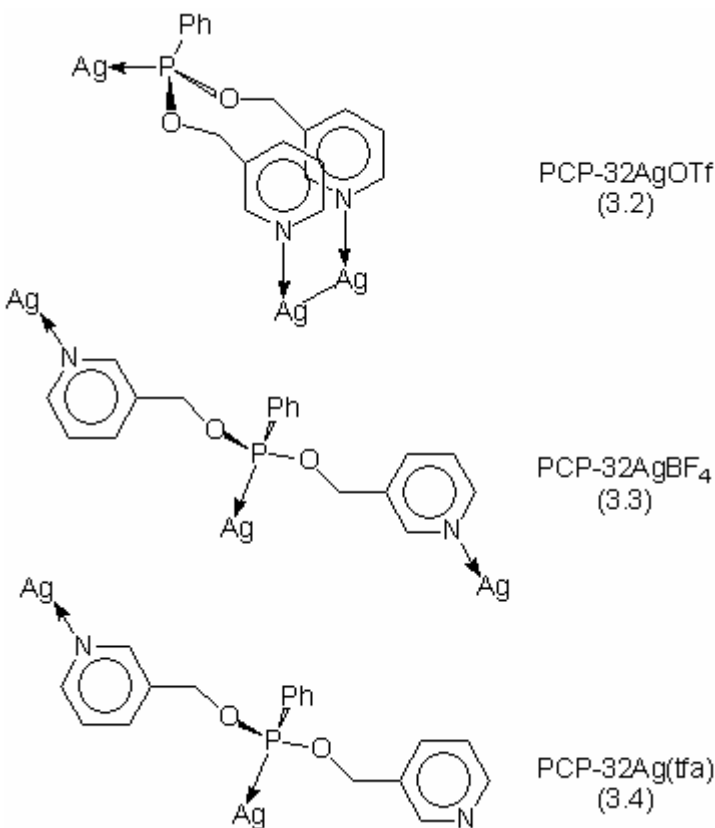
in deuterated acetonitrile. At this temperature the dissociation of the Ag–P bond is slowed to a timescale where significant polymeric character is observed and the various Ag–P couplings can be readily seen.

Compound **3.2** is made by the mixing of two equivalents of AgOTf with a solution of **3.1** in acetonitrile. A light brown color appears almost immediately upon mixing and is indicative of the reactions of **3.1** with the various silver salts. If left stirring at room temperature, this color rapidly grows more intense and eventually becomes cloudy signifying the decomposition of the coordination complex. Drying of the solution in vacuo yields a crude, oily brown powder that is purified with acetonitrile and ether. Upon drying of the precipitate, **3.2** is collected as a white powder. Solutions of **3.2** in various solvents noticeably decompose within minutes at room temperature. However, when dichloromethane solutions layered with ether are kept at 5 °C, they are sufficiently stable to allow the growth of diffraction quality crystals. Over time, oxidation of the ligand in solution results in precipitation of metallic silver. At room temperature, a very broad phosphorus resonance is evident centered at 148.0 ppm in the ^{31}P spectrum, indicating at least some degree of Ag–P coupling in solution. Upon cooling to –35 °C, this broad signal splits into a doublet of very sharp peaks centered slightly upfield at 146.4 ppm.

The coordination polymer, **3.3**, is obtained as an off-white powder by the reaction of AgBF₄ with a solution of one molar equivalent of **3.1** in acetonitrile. Solutions of **3.3** also quickly develop a brown tint but do not undergo the extensive decomposition in such a short time as **3.2**. This increase in stability of the BF₄[–] complex is analogous to the behavior of the Ph₂P(3-OCH₂C₅H₄N)AgBF₄ coordination polymer; the reasoning behind

this has been previously theorized.¹⁴⁷ Tiny, colorless parallelpiped shaped crystals of **3.3** were grown by the slow diffusion of ether into a solution of **3.3** in acetonitrile at 5 °C. Room temperature ^{31}P NMR spectra of **3.3** reveal a shouldered peak, due to Ph–H coupling, centered upfield from the free ligand at 149.0 ppm. The Ag–P coupling is hardly apparent in acetonitrile solution at 23 °C. Upon cooling to –35 °C, a silver–split phosphorus doublet is again noticed, now centered at 149.8 ppm.

Complex **3.4** is seen to be overly prone to decomposition in solution, rapidly precipitating metallic silver and an oily black by-product. To circumvent this difficulty, the ligand was added to a suspension of Ag(tfa) in CH_2Cl_2 , in which **3.4** is only sparingly soluble. In this manner, as the silver salt is drawn into solution by the forming coordination polymer it is immediately precipitated back out of solution, reducing the chance for decomposition. Reaction is apparent from the rapid replacement of the Ag(tfa) granules with a light-brown oily precipitate, along with a slight darkening of solution. Upon purification the compound is reclaimed as a finely divided colorless powder that quickly deposits metallic silver from solutions. Crystals of **3.4** were grown with some difficulty by vapor diffusion of ether into dilute solutions of **3.4** in acetonitrile at 5 °C. Solutions in high concentrations of **3.4** typically resulted in precipitation versus crystallization. ^{31}P NMR spectra of **3.4** show a single broadened phosphorus peak approximately 8 ppm upfield of the free ligand at 152.0 ppm. Lowering the NMR operating temperature to –35 °C shows a slight broadening (~ 1 ppm) of the ^{31}P resonance, though the Ag–P coupling can still not be discerned.



Scheme 3.1. Binding modes of PCP-32 with silver(I) salts.

X-Ray Crystal Structures

The silver coordination environments as well as the twisted conformations of the carbinol portions of the ligand in each of the structures are quite diverse. Silver geometries range from the near linear 172.3(1) $^\circ$ of Ag2 in **3.2** to the distorted tetrahedrons of the silvers in **3.4**. Scheme 3.1 gives a representation of the different binding modes displayed by PCP-32. The two carbinol substitutions of each ligand are, as expected, capable of a variety of rotations and extensions allowing the py-Ag binding of the two “arms”, in relation to one another, to go from nearly parallel in **3.2** to nearly perpendicular in **3.3**. The flexibility of the OCH₂ spacer groups also allow for a broad range of metal–metal distances to be had by the N–bound silvers of the ligand. This

interval spans from the very close Ag–Ag interaction of **3.2** at 3.1918(8) Å to the outstretching reach of 14.015(2) Å in **3.4**. With the 1:2 ratio of P to N in the ligand, a strict head-to-tail type coordination throughout the polymer analogous to those seen in the **PCP-31** structures is difficult to achieve and is therefore not observed in any of the structures. There is instead a mixture of Ag coordination environments within **3.2** and **3.4**, and a repetitive head-to-tail-to-tail motif apparent in **3.3**. All of these structural arrangements are spawned from the varying degrees of interaction that are seen by the different anions. With both of the structures containing oxygen donor anions, at least partial oxide bridging is apparent between some of the silver atoms. Conversely, in the case of BF_4^- , there is no anionic bridge and only a slight M–anion interaction that merely serves to hold the BF_4^- in position in the lattice.

The molecular structure of compound **3.2** contains two distinct silver environments representative of the coordination extremes shown herein. Both a pseudo-2-coordinate and a four-coordinate arrangement are displayed. A thermal ellipsoid plot of the unique portion of this structure is shown in Figure 3.1 and selected bonds and angles are given in Table 3.3. The two unique metal centers are repeated in one dimension, linked by bridging anions, to form the linear coordination polymer as demonstrated in Figure 3.2. Ag1 is bridged via one oxygen atom of each of two separate triflates to an opposing, symmetry equivalent P-bound Ag. The tetrahedron of P and O around Ag1 is completed by a terminal triflate bound to each metal. This effectively imposes a 2– charge on the Ag_2OTf_4 cluster that balances the positive charge levied across the ligand at the N-bound silvers. It is seen that the coordinating triflates are only observed at the phosphorus-bound Ag centers. This enforces a very prominent trans-

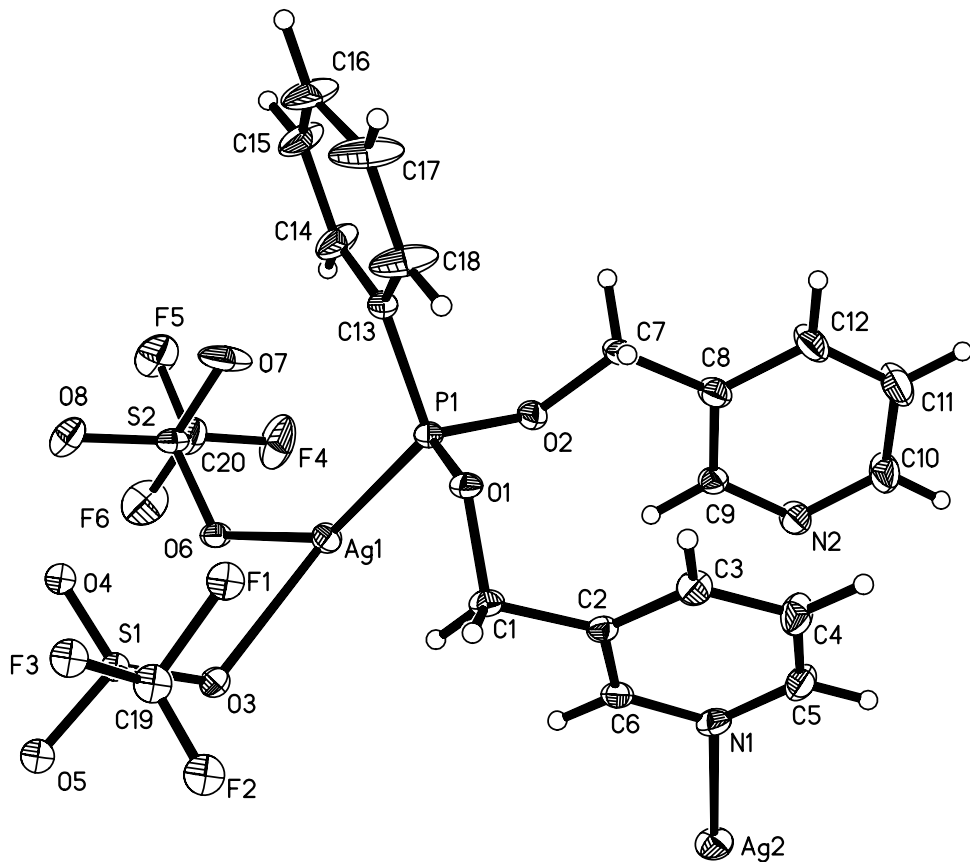


Figure 3.1. Molecular diagram of the unique portion of the **PCP-32AgOTf** polymer, **3.2**. Ellipsoids are drawn at the 30% probability level.

Table 3.3. Selected Bond Lengths (\AA), Angles ($^\circ$), and Important Distances for **3.2^a**

Ag1–O6	2.287(3)	Ag1–P1	2.323(1)
Ag1–O3#1	2.434(3)	Ag1–O3	2.456(3)
Ag2–N2	2.152(4)	Ag2–N1	2.156(3)
Ag2–Ag2#2	3.1918(8)	P1–N1	5.161(3)
P1–N2#2	5.487(4)	N1–N2#2	3.466(5)
Ag1–Ag1#1	3.8137(7)	Ag1–Ag2	6.5088(7)
Ag1–Ag2#2	6.7435(7)		
<hr/>			
O6–Ag1–O3#1	84.0(1)	P1–Ag1–O3#1	122.30(7)
O6–Ag1–O3	82.6(1)	P1–Ag1–O3	122.99(7)
O3#1–Ag1–O3	77.5(1)	N2–Ag2–N1	172.3(1)
N2–Ag2–Ag2#2	112.5(1)	N1–Ag2–Ag2#2	75.2(1)
O6–Ag1–P1	144.84(7)		

^a Symmetry transformations used to generate equivalent atoms: For **2**: #1 = $-x+1, -y, -z+2$; #2 = $-x+1, -y, -z+1$.

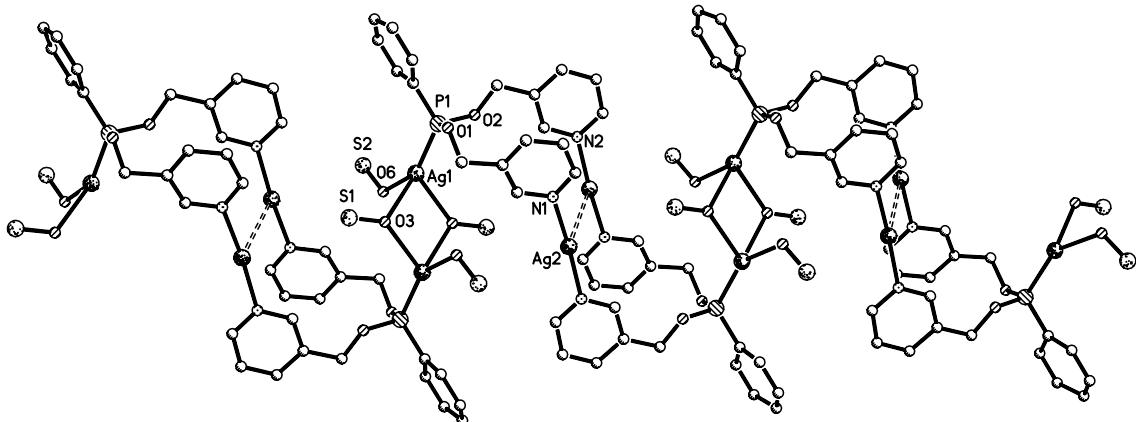


Figure 3.2. A view of the one-dimensional chain of **3.2**. Hydrogen atoms and the non-coordinating portion of the triflates have been removed for clarity.

ligand static charge separation. The two pyridyl rings of each ligand are brought within close proximity of one another at 3.466(5) Å, possibly by slight π – π interactions of the adjacent aromatic rings. The planes of these rings are seen to be nearly parallel though the N2 pyridyl is disordered over two positions as it hinges about the N–Ag bond. This close positioning of pyridyl donors allows for the N-bound silvers to come within 3.1918(8) Å of each other, leading to a respectable Ag–Ag interaction that likely has influence on the luminescence of this species. The average cross-ligand distance observed separating the P– and N–bound silvers is 6.626 Å, from which is given some indication of the amount of charge separation present. Intraligand P–N distances vary slightly from P1–N1 to P1–N2A being given at 5.161(3) and 5.487(4) Å, respectively. The Ag–P bonds display typical values at 2.323(1) Å, while the N–Ag bonds are noticeably short with an average of 2.155 Å. This is undoubtedly due to the charge density present on the N–bound silvers that are not balanced by a closely associated anion. Ag(1)–O distances vary from 2.287(3) to 2.456(3) Å, with the shorter value represented by the terminal bound triflate. Ag1 is in a severely distorted tetrahedral

arrangement, with its oxygen-only face being constricted by the bridging trifluoroacetates and displaying O–Ag–O angles from 77.5(1) $^{\circ}$ to 84.0(1) $^{\circ}$. The O–Ag–P angles are in turn exaggerated from 122.30(7) $^{\circ}$ to 144.84(7) $^{\circ}$. The environment of Ag2 is nearly linear with respect to pyridyl coordination, with an N–Ag–N angle of 172.2(1) $^{\circ}$. This slight distortion results from the movement of the Ag towards its symmetry equivalent which is slightly askew from Ag2. The N–Ag–Ag angles, at 75.2(1) $^{\circ}$ and 112.5(1) $^{\circ}$ show one silver to be oriented slightly above the other.

A thermal ellipsoid plot of the unique portion of **3.3** is shown in Figure 3.3 along with selected bond lengths and angles in Table 3.4. In the structure of **3.3** we see four unique silver centers arranged linearly whose differences arise from a slight twisting of the ligands through the length of the unique portion. However, rather than a fully spiraling polymer only a partial helix is seen to repeat throughout the lattice. This partial spiral is evident in either of the two dimensions in which the polymer is perpetuated and is demonstrated in Figure 3.4. This two dimensional growth of **3.3** gives rise to an infinite pleated sheet structure with anions dispersed throughout the crevices of the layers. A view of how these 2-D layers pack together is shown in Figure 3.5. Opposing the trend of structures **3.2** and **3.4**, all silvers in **3.3** are identical in connectivity, being coordinated by two pyridyl and one phosphorus donor in a doubly distorted trigonal arrangement. The N–Ag–N angles of the pyridyls are all acute from 93.1(2) to 107.3(2) $^{\circ}$, while the other two N–Ag–P angles are increased to values of 124.1(2) to 136.4(2) $^{\circ}$. The second distortion stems from the long distance interaction of a BF_4^- fluorine approaching at an average proximity of 2.786 Å to the metal. As the metal centers are pulled out of their N–N–P coordination planes, a resulting mean perturbation of 0.121 Å is seen. All

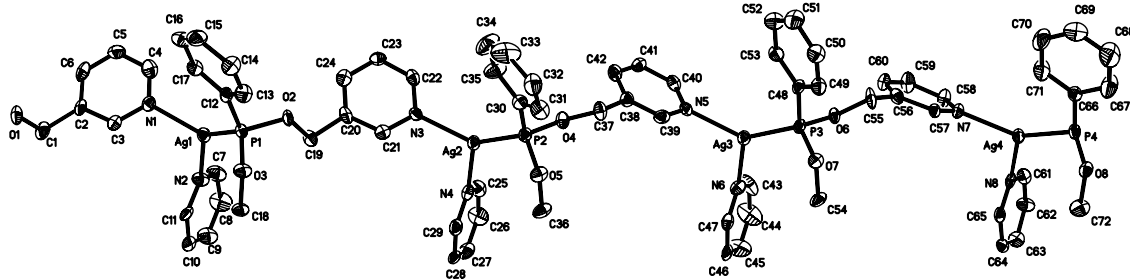


Figure 3.3. Molecular diagram of the cationic unique portion of the polymer of **3.3**. The partial spiral of the pyridyl linkages through the linear chain is apparent. Ellipsoids are drawn at the 50% probability level. Hydrogen atoms have been removed for clarity.

Table 3.4. Selected Bond Lengths (\AA), Angles ($^\circ$), and Important Distances for **3.3**^a

Ag1–N1	2.289(6)	Ag1–N2	2.296(6)
Ag1–P1	2.3363(19)	Ag2–N3	2.274(6)
Ag2–N4	2.318(7)	Ag2–P2	2.348(2)
Ag3–N5	2.265(6)	Ag3–N6	2.285(6)
Ag3–P3	2.362(2)	Ag4–N7	2.268(6)
Ag4–N8	2.295(6)	Ag4–P4	2.352(2)
P1–N3	6.195(6)	P1–N8#4	5.906(7)
N3–N8#4	8.743(8)	P2–N5	6.165(7)
P2–N2#1	5.860(7)	N5–N2#1	8.541(9)
P3–N7	6.145(6)	P3–N4#11	5.999(7)
N7–N4#11	8.444(9)	P4–N1#6	6.061(6)
P4–N6#3	5.956(7)	N1#6–N6#3	8.769(9)
Ag1–Ag2	9.287(1)	Ag1–Ag4#5	9.024(1)
Ag2–Ag4#5	8.648(1)	Ag2–Ag3	9.454(1)
Ag2–Ag1#1	9.099(1)	Ag3–Ag1#1	8.763(1)
Ag3–Ag4	9.597(1)	Ag3–Ag2#2	9.324(1)
Ag4–Ag2#2	8.648(1)	Ag4–Ag1#6	9.263(1)
Ag4–Ag3#4	9.208(1)	Ag1#7–Ag3#4	8.763(1)
Ag1–F16#8	2.90(1)	Ag2–F7#9	2.92(1)
Ag3–F8#10	2.87(2)	Ag4–F15#11	2.73(1)
N(1)–Ag(1)–N(2)	93.1(2)	N(1)–Ag(1)–P(1)	132.4(2)
N(2)–Ag(1)–P(1)	133.1(2)	N(3)–Ag(2)–N(4)	99.4(2)
N(3)–Ag(2)–P(2)	134.4(2)	N(4)–Ag(2)–P(2)	125.6(2)
N(5)–Ag(3)–N(6)	107.3(2)	N(5)–Ag(3)–P(3)	127.8(2)
N(6)–Ag(3)–P(3)	124.1(2)	N(7)–Ag(4)–N(8)	98.3(2)
N(7)–Ag(4)–P(4)	136.4(2)	N(8)–Ag(4)–P(4)	124.4(1)

^a Symmetry transformations used to generate equivalent atoms: #1 = $-x+1, y+1/2, -z+1/2$; #2 = $-x, y+1/2, -z+1/2$; #3 = $-x+1, y-1/2, -z+1/2$; #4 = $-x-1, y+1/2, -z+1/2$; #5 = $-x, y-1/2, -z+1/2$; #6 = $-x-1, y-1/2, -z+1/2$; #8 = $x-2, y-1, z$; #9 = $x-0.5, -y+0.5, -z+1$; #10 = $x-1, y, z-1$; #11 = $-x, y-0.5, -z+0.5$.

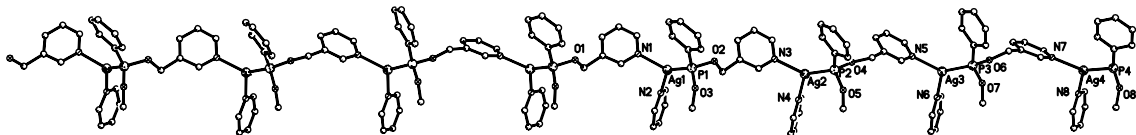


Figure 3.4. A view of the chain of **3.3** perpetuated in one dimension. The partial spiral of the pyridyl linkages can be seen to abruptly restart at the end of the unique portion. Hydrogen atoms have been removed for clarity.

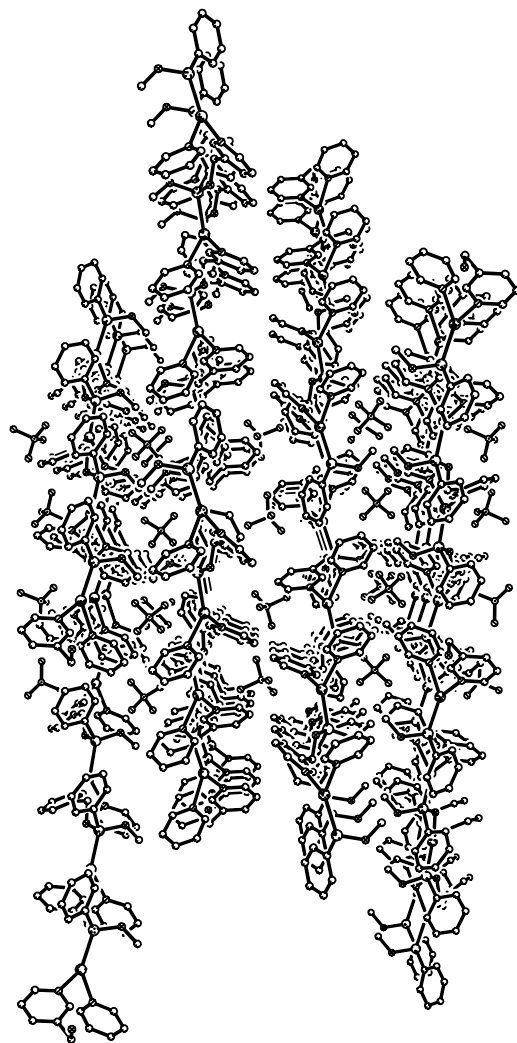


Figure 3.5. A view down the *a*-axis of how the two-dimensional sheets of **3.3** stack together encompassing the BF_4^- anions. Hydrogen atoms have been removed for clarity.

$\text{Ag}-\text{N}$ and $\text{Ag}-\text{P}$ bonds show typical lengths with ranges of 2.265(6) to 2.318(7) Å and 2.336(2) to 2.362(2) Å, respectively. Overall intraligand P–N distances show an increase in length of close to one angstrom from **3.2**. Averages are 5.932 Å on the outstretched

pyridyl arms and 6.142 Å on the collinear pyridyls. This results in an increase in separation of P– and N–bound silvers; the magnitude of this separation depending upon the orientation of the pyridyl extension. Those silvers contained within the collinear backbone of the structure have separations from 9.263(1) to 9.597(1) Å, while those arranged perpendicular have slightly smaller values of 9.024(1) to 9.324(1) Å. This accompanies a substantial increase in cross-ligand metal-metal separation of the N–bound silvers, whose distance in **3.3** averages at 8.7055 Å. **3.3** crystallizes in the noncentrosymmetric space group *P2₁2₁2₁* with a refined Flack parameter of 0.00(2).

Compound **3.4** forms a structurally complicated polymer that displays a variety of interesting attributes. Figure 3.6 shows the molecular structure of the unique portion of **3.4** and Table 3.5 gives selected interatomic distances and angles. The winding 3-D growth of this polymer is displayed in Figure 3.7. Growth occurs in three dimensions due to the bridging actions of both the ligand and the trifluoroacetates. The ligand in this case occupies two separate roles within the structure. In the first instance the phosphonite is tridentate using all three binding sites to coordinate to two different types of metal centers. Using one pyridyl “arm” and the phosphorus, two equivalent silvers, Ag1 and Ag1#1, are bound by two symmetry equivalent ligands in a head-to-tail fashion forming a ring. Each of these silvers are subsequently bridged by two η^1,μ_2 – trifluoroacetates to yet another equivalent metal. The remaining “arm” of the ligand extends from the ring and acts as a bridge to the other unique silver of the polymer, Ag2. It is as a result of this outstretching reach that we see the greatest cross ligand metal–metal distance of the three polymers. The N-bound silvers of these oppositely directed donors are separated by a distance of 14.015(2) Å across the breadth of the ligand. The

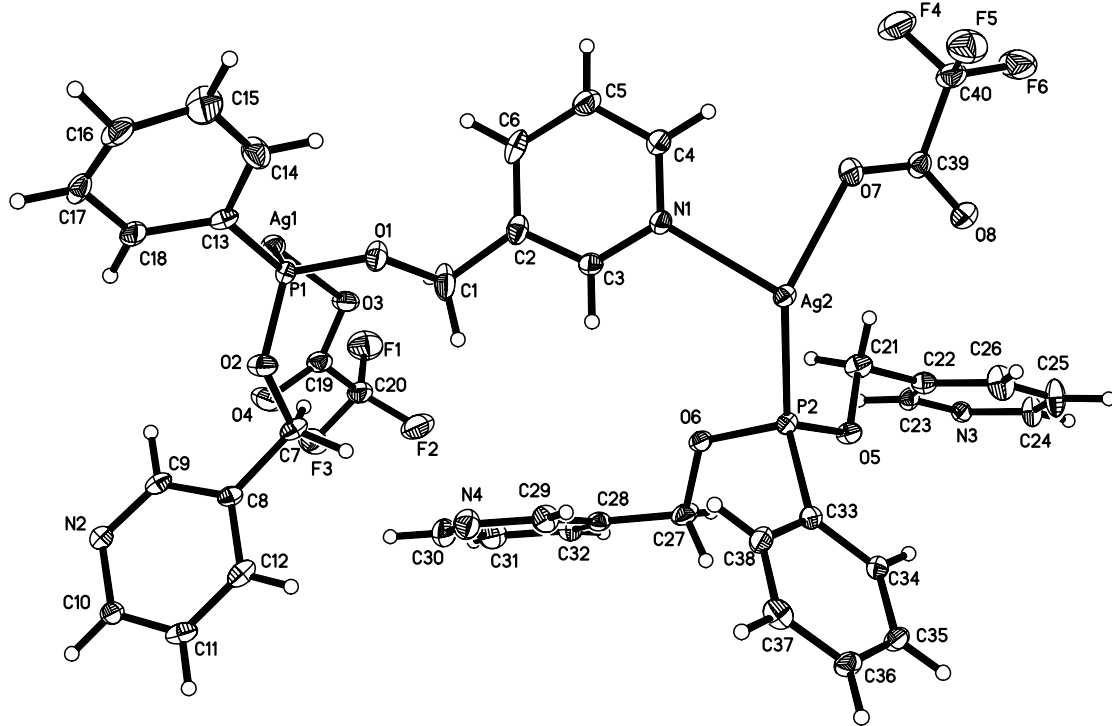


Figure 3.6. Molecular diagram of the unique portion of **3.4**. Ellipsoids are drawn at the 30% probability level. As shown, N4 is seen to be non-coordinating. All other pyridyl donors are metal bound.

Table 3.5. Selected Bond Lengths (\AA), Angles ($^\circ$), and Important Distances for **3.4**^a

Ag1–N2#1	2.297(4)	Ag1–P1	2.357(1)
Ag1–O3	2.386(4)	Ag1–O3#2	2.509(4)
Ag2–N3#3	2.322(4)	Ag2–P2	2.329(1)
Ag2–O7	2.344(4)	Ag2–N1	2.355(4)
P1–N1	6.203(4)	P1–N2	5.520(5)
P2–N3	6.108(4)	P2–N4	5.651(5)
N1–N2	10.774(6)	N3–N4	10.026(6)
Ag1–Ag2	9.112(1)	Ag1–Ag1#1	6.466(1)
Ag1#1–Ag2	14.015(2)	Ag2–Ag2#3	9.227(1)
N(2)#1–Ag(1)–P(1)	132.5(1)	N(2)#1–Ag(1)–O(3)	94.1(1)
P(1)–Ag(1)–O(3)	126.8(1)	N(2)#1–Ag(1)–O(3)#2	87.9(1)
P(1)–Ag(1)–O(3)#2	122.5(1)	O(3)–Ag(1)–O(3)#2	74.4(1)
N(3)#3–Ag(2)–P(2)	125.4(1)	N(3)#3–Ag(2)–O(7)	86.8(1)
P(2)–Ag(2)–O(7)	133.3(1)	N(3)#3–Ag(2)–N(1)	98.2(1)
P(2)–Ag(2)–N(1)	116.3(1)	O(7)–Ag(2)–N(1)	86.4(1)

^a Symmetry transformations used to generate equivalent atoms: #1 = $-x+1, -y+1, -z+1$; #2 = $-x+2, -y+1, -z+1$; #3 = $x-1/2, -y+3/2, z-1/2$

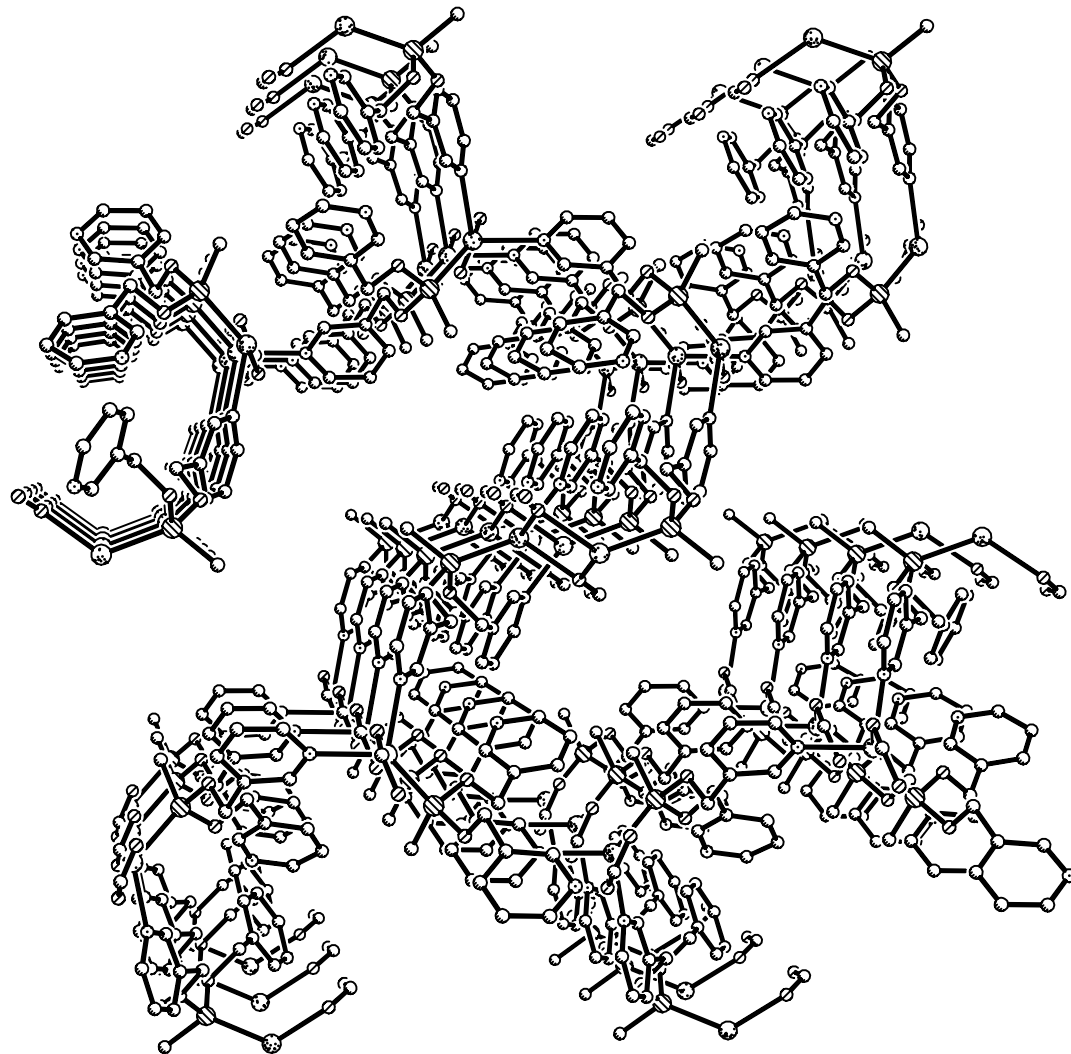


Figure 3.7. Packing structure of complex **3.4** showing the three-dimensional growth of the polymer. hydrogen atoms, trifluoromethyls, and all but the *ipso* portion of the phenyl rings have been removed for clarity.

P-bound to N-bound metal distances across this ligand show separations of 9.112(1) and 6.466(1) Å for Ag1–Ag2 and Ag1–Ag1A, respectively. Ag2 is bound by the phosphorus and nitrogen of two separate, but equivalent, ligands that are in a similar conformation to that of the one P-bound to Ag1 and the pyridyl that bridges to Ag1 to achieve a head-to-tail-to-tail motif. In this case however, the ligands are not involved in ring formation. The attached ligands instead continue off via one pyridyl extension each in two separate

polymeric strands that run parallel to one another. The remaining “arm” of this ligand is a curious feature in that it has a non-coordinating “dangling” pyridyl that sits comfortably within the space between ligands. It is believed that the steric packing that encapsulates this particular pyridyl ring is responsible for its unsaturated coordination state, since even when an excess of Ag(tfa) is used the non-coordinating nitrogen is present in the crystal structure. The similar conformations of the two unique ligands in the structure of **3.4** likewise display similar intraligand N–N distances at 10.774(6) Å for the P1 ligand and 10.026(6) Å for that of P2. Comparable P–N distances are also noticed with each ligand having a short and a long stretch: P1–N2 and P1–N1 separations are 5.520(5) and 6.203(4) Å, respectively, while the analogous P2–N4 and P2–N3 distances are 5.651(5) and 6.108(4) Å. The single cross-ligand metal–metal distance of the P2 ligand is that of the P2 to N3 silvers, which is slightly longer than that of the P1 ligand at 9.227(1) Å. Both silver centers here are in distorted tetrahedral arrangements. The coordination around Ag1 is completed by one each pyridyl and phosphorus donors, as well two bridging trifluoroacetate oxygens and is shown in a close-up view in Figure 3.8. The Ag1–N2#1 bond is only slightly stretched for a Ag–pyridyl distance at 2.297(4) Å while the Ag1–P1 bond is a typical 2.357(2) Å. Bonds to the bridging trifluoroacetates are seen to be inequivalent with Ag1–O3 at 2.386(4) Å, and Ag1–O3#2 at 2.509(4) Å. It is also noticed that the small bridging distance of the η^1,μ_2 –trifluoroacetates constrict the angle they create with the metal to an acute 74.4(1) $^\circ$. As a result, the P1–Ag1–N1 angle has room to spread apart which is apparent with a 132.5(1) $^\circ$ angle. The remaining angles around Ag1 are also distorted from the ideal tetrahedral geometry and have values interspersed between the aforementioned extremes. In the absence of the bridging

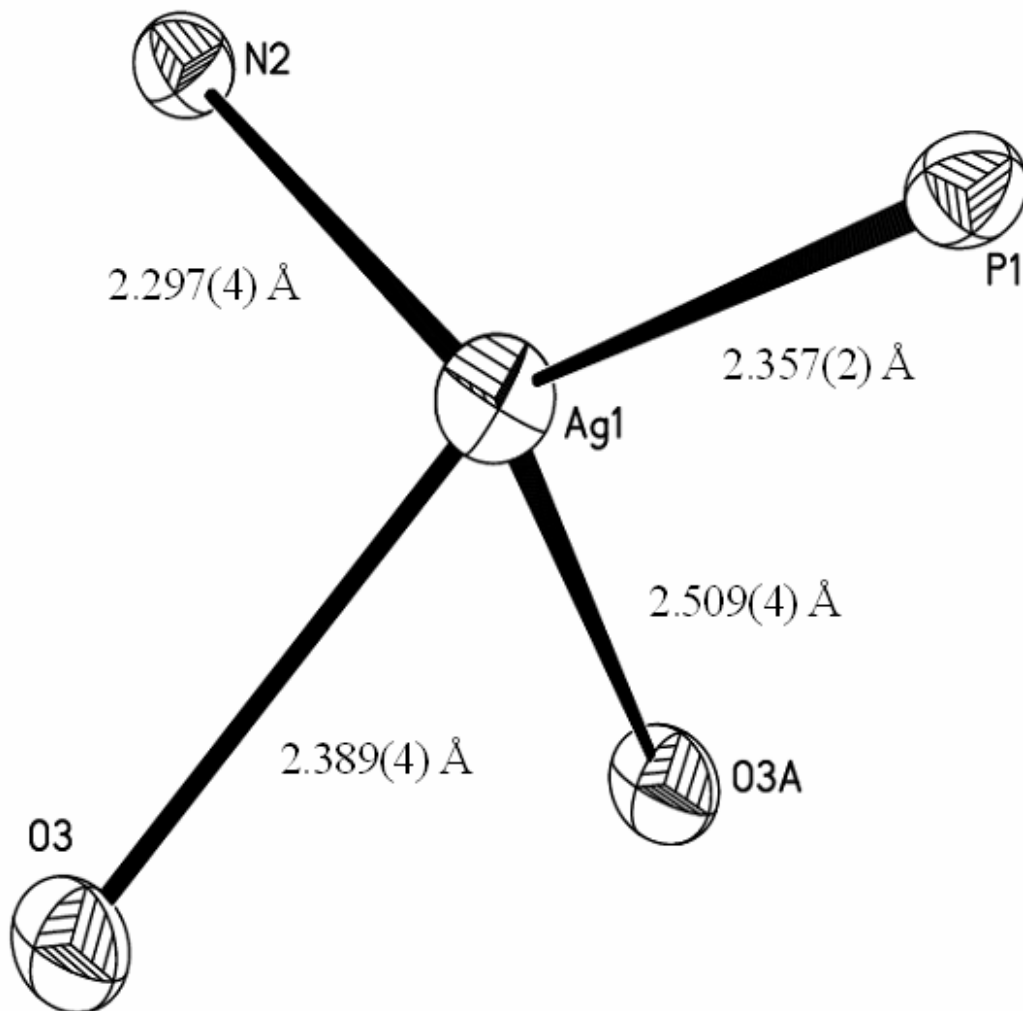


Figure 3.8. Coordination environment of Ag1 in the polymer of **3.4**. Ellipsoids are drawn at the 50% probability level.

trifluoroacetates displayed by Ag1, the distortions of the tetrahedral coordination sphere of Ag2 are not seen to be as severe. The environment of Ag2 is displayed in Figure 3.9 and includes two pyridyl donors, the phosphorus atom P2 and a terminal bound η^1 -trifluoroacetate. The silver-pyridyl linkages in this case are uncommonly lengthy at 2.355(4) and 2.322(4) Å for Ag2–N1 and Ag2–N3#3, while the Ag2–P2 and Ag2–O7 bonds are in the typical range at 2.329(1) and 2.344(4) Å, respectively. The angles about Ag2 however are still shown to be rather extreme from 86.4(1) to 133.3(1) $^\circ$.

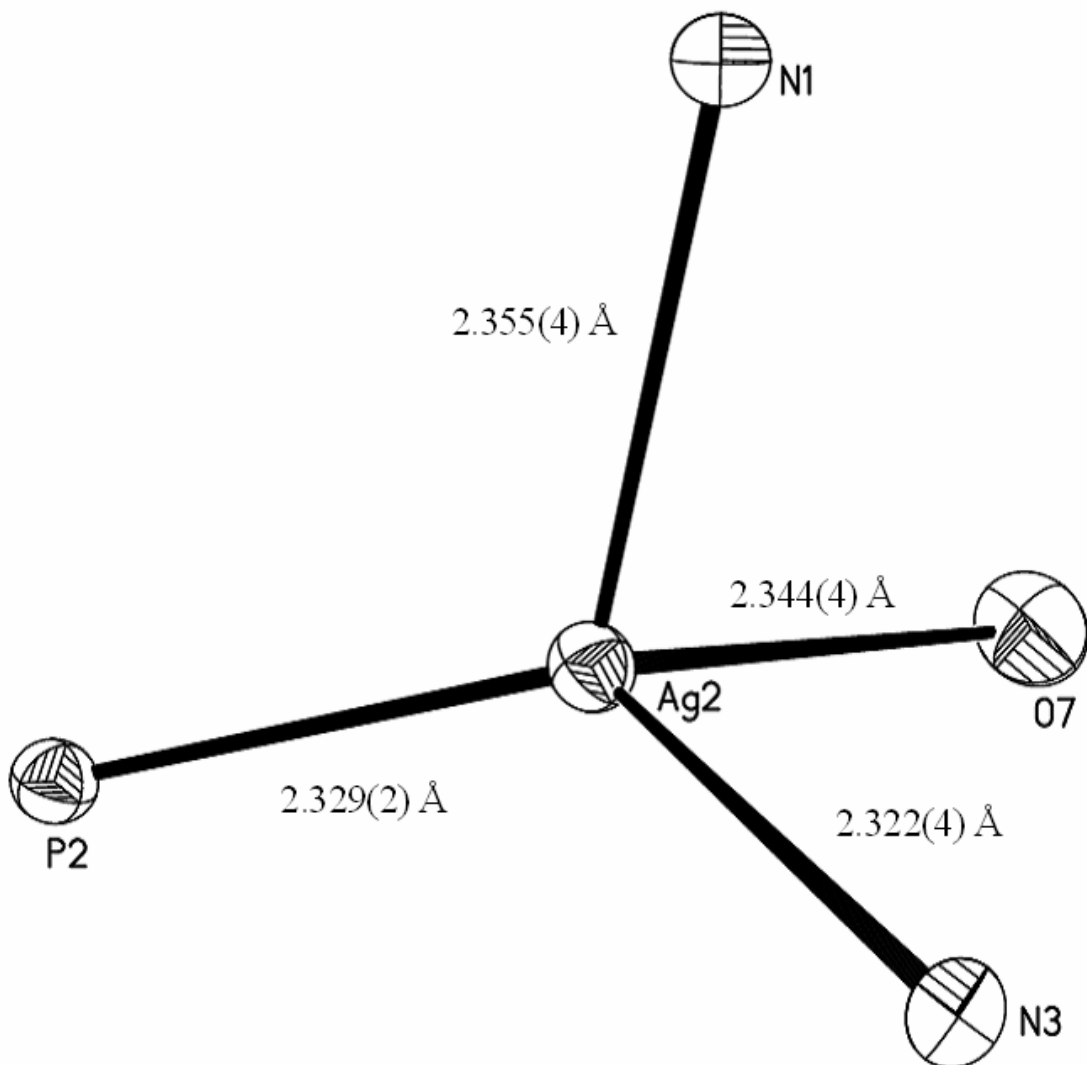


Figure 3.9. Coordination environment of Ag_2 in the polymer of **3.4**. Ellipsoids are drawn at the 50% probability level.

Luminescent Properties

Mixed inorganic–organic coordination polymers have been recently explored as potentials for new “organic” light emitting devices, OLEDs. The advantage of these hybrids over the strictly organic luminescent materials is the ability to tune their absorption and emission by altering the metal environment. This variability stems from either metal-to-ligand or ligand-to-metal charge transfer, which is obviously not an option with the traditional organic LED.¹⁵⁰ All excitation and emission spectra were recorded at

concentrations of 1×10^{-4} M in acetonitrile glasses at 77 K. These spectra are demonstrated in Figure 3.10. The resemblance of the excitation spectra of compounds **3.2–3.4** with that of the free PhP(3-OCH₂C₅H₄N)₂ ligand are suggestive of a ligand based absorption which then decays by means of ligand-to-metal charge transfer. The excitation spectrum of the free ligand **3.1** shows two maxima at 298 and 352 nm. Excitation maxima for **3.2–3.4** are 295, 297 and 305 nm, respectively. Emission spectra for all compounds **3.1–3.4** show multiple maxima, illustrating the complexity of the decay transitions associated with such a complicated system. The ligand itself demonstrates several emission maxima across a wide section of the spectrum. Peaks are seen at 412, 442, 474 and 544 nm. A great deal of free ligand character is seen in the spectrum of **3.3**, which is the weakest emitter of the silver complexes. Peaks are seen at 412, 441, 477 and a shoulder is noticed at ~ 547 nm. This suggests that the emission is mainly a ligand-based one intensified by metal coordination. The emission of the silver triflate complex, **3.2**, is much more intense and covers a broader spectral range than

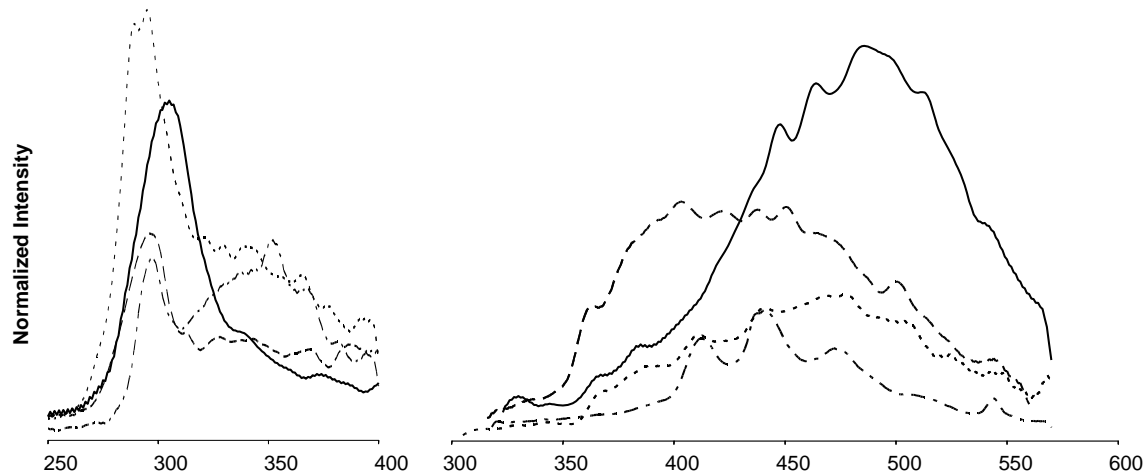


Figure 3.10. Normalized excitation and emission spectra of compounds **3.1–3.4** taken in acetonitrile glasses at 1×10^{-4} M concentration at 77 K. **PCP-32Ag(tfa)**, **PCP-32AgOTf**, **PCP-32AgBF₄**, **PCP-32**.

Table 3.6. Luminescent Spectral Data for compounds **3.1–3.4**, at 77 K and 1×10^{-4} M in CH₃CN.

Compound	Excitation λ_{max}	Emission local λ_{min}
3.1	298, 352	412, 442, 474, 544
3.2	295	363, 404, 423, 438, 452, 501, 547
3.3	297	412, 441, 477, 547
3.4	305	449, 465, 487, 513

either **3.1** or **3.3**. Peaks are displayed at 363, 404, 423, 438, 452 and 501 nm and again a shoulder is noticed at 547nm. The emission spectrum of complex **3.4** is noticeably more intense than the others, as expected from visual observations, and is also slightly red-shifted. The local maxima for this complex are seen at 449, 465, 487 and 513 nm. Full luminescence data are presented in Table 3.6

Conclusions

We have demonstrated in this study the versatility of the phosphonite PhP(3-OCH₂C₅H₄N)₂ in the formation of anion-dependent, luminescent coordination polymers. The flexibility of the pyridyl extensions allowed trans-ligand metal–metal distances to span a range of over 10 Å from 3.1918(8) to 14.015(2) Å. These pyridyl arms were seen to adopt conformations ranging from parallel to perpendicular. The silver coordination environment, dimensionality of the polymers and luminescence characteristics are all seen to be dependent upon the anion present.

Experimental

General Considerations

All experiments were carried out under an argon atmosphere, using a Schlenk line and standard Schlenk techniques. Glassware was dried at 120°C for several hours prior

to use. All reagents were stored in an inert atmosphere glovebox; solvents were distilled under nitrogen from the appropriate drying agent immediately before use. Triethylamine was purchased from Aldrich and purged with argon before use. 3-pyridylcarbinol was purchased from Aldrich and used as received. Dichlorophenylphosphine, silver(I) trifluoroacetate, silver(I) triflate, and silver(I) tetrafluoroborate were purchased from Strem Chemicals Inc. and used as received. Celite was purchased from Aldrich and dried at 120°C prior to use. ^1H and variable temperature ^{31}P NMR were recorded at 360.13 MHz and 145.78 MHz respectively, on a Bruker Spectrospin 360 MHz Spectrometer. Elemental analyses were performed by Atlantic Microlabs Inc., Norcross, Georgia. Excitation and emission spectra were recorded on an Instruments S. A. Inc. model Fluoromax-2 spectrometer, using band pathways of 5 nm for both excitation and emission and are presented uncorrected.

Preparations

Phenylphosphino-bis-3-pyridylcarbinol, PPh(3-OCH₂C₅H₄N)₂, PCP-32 (3.1). In an argon purged addition funnel degassed triethylamine (2.28 mL, 16.36 mmol) was added via syringe to a stirred solution of 3-pyridylcarbinol (1.50 g, 13.75 mmol) in 20 mL toluene at room temperature. The solution was stirred for 15 minutes, then cooled to 0°C and shielded from light with aluminum foil. A solution of dichlorophenylphosphine (1.23 g, 6.87 mmol) in 15 mL toluene was then added over 15 minutes. The solution was stirred for 1 h, and then warmed to room temperature. The resultant, thick cloudy mixture was reduced to $\frac{3}{4}$ of its original volume under vacuum and immediately filtered through Celite and washed with 5 mL of cold toluene. The solvent was removed from

the yellow solution in vacuo to leave the crude product as a pale yellow oil in 95 % yield (2.12 g, 6.26 mmol). The oil was then extracted with 180 mL of hexanes to leave the final product, **3.1**, as a colorless oil in 77% yield (1.71g, 5.28 mmol). ^1H NMR (CDCl_3 , 298 K) δ : 4.87 d,m, 4 H, $J(\text{PH})$ = 8.8 Hz; 7.34 m, 2 H; 7.48 m, 3 H; 7.681 m, 4 H; 8.59 m, 4 H. ^{31}P NMR (CDCl_3 , 298 K) δ : 160.4 sep, $J(\text{PH})$ = 7.3 Hz.

poly-[PCP–32AgOTf] (3.2). To a stirred solution of AgOTf (0.158 g, 0.612 mmol) in 3 mL CH_3CN was added **3.1** (0.100 g, 0.310 mmol) in 3 mL CH_3CN . The resulting solution was stirred for 3 minutes then dried in vacuo to leave a fluffy, off-white solid. The solid was then repeatedly redissolved in a small amount of CH_3CN and precipitated with ether until compound **3.2** was obtained as a white powder in 86 % (0.222 g, 0.263 mmol) yield upon drying. Colorless plates of **3.2** were obtained by slow diffusion of ether into a solution of **3.2** in CH_2Cl_2 at 5 °C. ^1H NMR (CD_3CN , 298 K) δ : 5.11 d,m, 4H; 7.47 m, 2H; 7.65 m, 3H; 7.85 m, 4H; 8.12 m, 4H. ^{31}P NMR (238 K) δ : 146.4 d, $J(\text{Ag–P})$ = 908.2 Hz. Elem anal. Calcd for $\text{C}_{23}\text{H}_{20.5}\text{N}_{2.5}\text{O}_{8.5}\text{PS}_2\text{F}_6\text{Ag}_2$: C, 30.94; H, 2.31; N, 3.92. Found: C, 30.66; H, 2.37; N, 3.61.

poly-[PCP–32AgBF₄] (3.3). To a stirred solution of AgBF₄ (0.120 g, 0.624 mmol) in 3 mL CH_3CN was added **3.1** (0.198 g, 0.611 mmol) in 3 mL CH_3CN . The resulting solution was stirred for 2 minutes then dried in vacuo to leave an off-white powder. This was then dissolved in a small amount of CH_3CN and precipitated with ether, repeating this until compound **3.3** is obtained as a white powder upon drying, in 93 % (0.295 g, 0.574 mmol) yield. Colorless plates of **3.3** were obtained by slow diffusion of ether into a solution of **3.3** in CH_3CN at 5 °C. ^1H NMR (CD_3CN , 298 K) δ : 5.07 d,m,

4H; 7.45 m, 2H; 7.65 m, 3H; 7.85 m, 4H; 8.48 d, 2H; 8.55 s, 2H. ^{31}P NMR (238 K) δ : 149.8 d, $J(\text{Ag-P}) = 804.7$ Hz. Elem anal. Calcd for $\text{C}_{18}\text{H}_{17}\text{N}_2\text{O}_2\text{P}\text{AgBF}_4$: C, 41.66; H, 3.30; N, 5.40. Found: C, 41.15; H, 3.27; N, 5.30.

poly-[PCP-32Ag(tfa)] (3.4). To a stirred suspension of Ag(tfa) (0.136 g, 0.626 mmol) in 5 mL CH_2Cl_2 was added **3.1** (0.100 g, 0.312 mmol) in 5 mL CH_2Cl_2 . This was stirred for 5 minutes until the solid Ag(tfa) was dissolved, after which time a brown oil precipitated. The solution was dried in vacuo to leave a fluffy brown powder. This was then dissolved in a small amount of CH_3CN and precipitated with ether. This was repeated until the off-white powder, **3.4**, was obtained in 94 % (0.223 g, 0.294 mmol) yield. Colorless blocks of **3.4** were obtained by the vapor diffusion of ether into a solution of **3.4** in CH_3CN at 5 °C. ^1H NMR (CD_3CN , 298 K) δ : 5.12 d,m, 4H; 7.39 m, 2H; 7.59 m, 3H; 7.82 m, 4H; 8.50 d, 2H; 8.59 s 2H. ^{31}P NMR (238 K) δ : 152.2. Elem anal. Calcd for $\text{C}_{23.5}\text{H}_{18.75}\text{N}_{2.25}\text{O}_{6.25}\text{P}\text{Ag}_2\text{F}_6$: C, 35.58; H, 2.38; N, 3.97. Found: C, 35.86; H, 2.40; N, 3.78.

Crystallography

A summary of crystallographic experimental data for **3.2**, **3.3** and **3.4** is presented in Table 3.7. Complete listings of interatomic distances and angles can be found in Appendix B, Tables B.4 to B.6. Crystallographic data were collected on crystals with dimensions 0.081 x 0.097 x 0.196 mm for **3.2**, 0.168 x 0.140 x 0.041 mm for **3.3**, and 0.070 x 0.090 x 0.100 mm for **3.4**. Data were collected at 110 K on a Bruker X8 Apex using MoK α radiation ($\lambda = 0.71073$ Å). All structures were solved by direct methods after the correction of the data using SADABS.¹³⁹ All of the data were processed using

Table 3.7. Crystallographic Data for **3.2**, **3.3** and **3.4**

	3.2	3.3	3.4
Formula	C ₂₀ H ₁₇ Ag ₂ F ₆ N ₂ O ₈ PS ₂ ·(CH ₃ CN) _{0.33} ·(CH ₂ Cl ₂) _{0.66}	C ₈₀ H ₈₀ Ag ₄ B ₄ F ₁₆ N ₁₂ O ₈ P ₄	C ₄₀ H ₃₄ Ag ₂ F ₆ N ₄ O ₈ P ₂ ·(C ₄ H ₁₀ O) _{0.5}
Formula weight	914.92	2240.16	1127.45
a (Å)	10.8716(9)	15.565(2)	9.343(1)
b (Å)	11.9998(9)	20.999(3)	31.912(5)
c (Å)	12.170(1)	28.131(4)	15.157(3)
α (°)	94.502(5)		
β (°)	100.834(5)		95.63(1)
γ (°)	93.599(4)		
V (Å ³)	1549.7(2)	9195(2)	4497(1)
Z	2	4	4
space group	<i>P</i> -1	<i>P</i> 2 ₁ 2 ₁ 2 ₁	<i>P</i> 2 ₁ /n
T (K)	110	110	110
D _{calcd} (g cm ⁻³)	1.961	1.618	1.665
μ (mm ⁻¹)	1.671	1.000	1.024
2θ _{max} , deg	62.40	46.52	52.00
reflns measured	20219	67540	38630
reflns used (R _{int})	9442 (0.0400)	13167(0.0836)	8838(0.0809)
Restraints / Parameters	56/431	0/1147	6/601
R1, [I>2σ(I)]	0.0459	0.0464	0.0497
wR ² , [I>2σ(I)]	0.1136	0.1126	0.1073
R(F _o ²), (all data)	0.0755	0.0543	0.0797
R _w (F _o ²), (all data)	0.1281	0.1177	0.1204
GooF on F ²	1.016	1.112	1.027

the Bruker AXS SHELXTL software, version 6.10.¹⁴⁰ Unless otherwise noted, all non-hydrogen atoms were refined anisotropically and hydrogen atoms were placed in calculated positions. The crystal structure of **3.2** contains a disordered solvent position that is occupied in part by a molecule of dichloromethane and in part by a molecule of acetonitrile. The crystal structure of **3.3** contains four solvent molecules of acetonitrile and four noncoordinating BF_4^- anions, two of which are disordered over two positions. Compound **3.4**'s crystal structure contains an ether solvent molecule whose disorder is linked to the disorder of the C32 phenyl ring.

CHAPTER FOUR

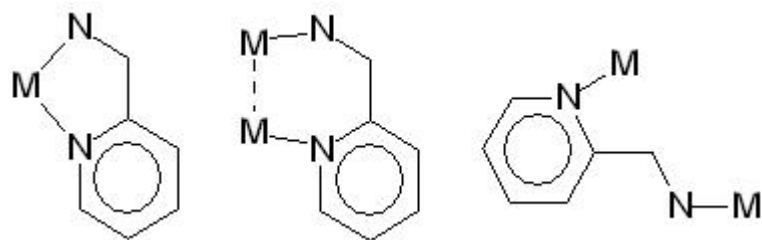
Variability in the Structures of Luminescent Silver(I) 2-aminomethylpyridine Complexes: Effect of Ligand Ratio, Anion, Hydrogen-bonding, and π -stacking

Introduction

Progress in the field of crystal engineering has been greatly complemented by coordination studies of the coinage metals.^{7,11,88,146,151-154} Studies of silver, in particular, have had much to offer. This is due to the flexibility in its coordination sphere and the ease with which it varies coordination number.^{4,25,49,142,148} Many silver coordination architectures are readily obtainable through slight variations in ligand and / or anion and include discrete, small molecules, supramolecular arrays, and 1-, 2-, and 3-dimensional coordination networks.¹⁵⁵⁻¹⁵⁸ Several systematic studies of the structural dependence on anions have been nicely demonstrative of the diversity possible with small changes in counterion properties such as coordinating or hydrogen bonding ability.^{91,92,147,159-161} A related area of this research that has proved lacking however is that concerned with the ligand to metal ratio dependence of these structures.²² To the best of our knowledge, no thorough report has been given that shows the effects of changing the ratio of ligand to metal in bidentate silver(I) systems of various anions. This led us to investigate the changes in the solid state structures of silver(I) 2-aminomethylpyridyl complexes that are caused by altering the ratio of ligand-to-metal in the reaction mixtures. One resulting feature that is of particular interest in these and other silver complexes is the closed shell metal–metal interaction that is very well known to occur in the monovalent group 11 elements.^{1,162-167} While not as broadly represented or studied as the aurophilic attraction

that holds the gold–gold interaction intact, a small surge of recent work has been dedicated to examining the properties of this argentophilic contact.^{15,98,162,168–170} Included in this group are a handful of theoretical studies that put the strength of the interaction along the same intensity as that of a hydrogen bond with an idealized internuclear separation of $3.137 - 3.208\text{\AA}$.^{163,171–173}

Herein we demonstrate that not only can the molecular architecture of silver(I) coordination complexes be altered by changes in the counterion, but they can also be largely affected by the ratio of ligand to metal. The 2-aminomethylpyridine ligand, whose small bite angle imposes a predisposition for chelation, is seen to construct a range of coordination motifs, shown in Scheme 4.1, from simple monomers to coordination



Scheme 4.1. The binding modes that are seen with the 2-aminomethylpyridine ligand in the silver(I) structures described herein.

polymers with various silver(I) salts simply by changing its ratio in solution. The resulting complexes contain a number of interesting structural features and physical properties including several short, sterically unfavored Ag–Ag interactions, bridging 2-amp ligands and a pronounced luminescence. This work has been recently published.¹⁷⁷

Results and Discussion

Synthesis and NMR Spectroscopy

The 2-aminomethylpyridine complexes **4.1–4.7** were all made by the direct reaction of the ligand with silver(I) salts in varying ratios. Characteristic analytical data for these complexes are presented in Tables 4.1 and 4.2. The 1:1 AgBF₄ structure has already been discussed in a previous study.⁹¹ The many intriguing structural features of the complexes presented here are seen to stem directly from the ratio of ligand to metal, with the ratio itself often being influenced by the properties of the anion present. An example of this is the silver triflate complex which we have been unable to force beyond a 3:2 ratio of ligand to metal, while that of the trifluoroacetate has not been isolable at 3:2 but proceeds directly to 2:1. Hydrogen bonding between the amine protons and the anions are a major determining factor in the structure, orientation, and 3-dimensional growth of the complexes.

The ¹H NMR spectra of all the compounds were, as expected, generally similar. Shifts in the amine protons as well as the ortho-N hydrogens on the pyridyl rings are demonstrative of the differences in coordinated silver environments caused by the different anions present. The greatest shifts are seen examining the –NH₂– protons in the presence of silver, ranging from 1.3 to 2.0 ppm downfield of the 1.67 ppm chemical shift of free 2-amp ligand in solution (NMR data for the free ligand is available in supporting information). These shifts are implicative of solution–state complexation. Low temperature NMR spectra of representative compounds collected to –35 °C reveal no dramatic shift in resonances.

Table 4.1. Analytical and Physical Data

	compound ^a	yield (%)	analytical (%) ^b		
			C	H	N
4.1	Ag(2-amp) ₂ BF ₄	92	35.0 (35.0)	3.8 (3.9)	13.3 (13.6)
4.2	Ag(2-amp) ₂ (tfa)	82	38.2 (38.4)	3.6 (3.7)	12.5 (12.8)
4.3	Ag ₂ (2-amp) ₃ (OTf) ₂	76	29.2 (28.9)	2.9 (2.9)	10.0 (10.0)
4.4	Ag ₂ (2-amp) ₃ (BF ₄) ₂	84	30.4 (30.3)	3.3 (3.3)	11.6 (11.7)
4.5	Ag ₂ 2,2'-bpy ₂ (2-amp)(BF ₄) ₂	90	40.7 (40.4)	3.3 (3.3)	11.2 (11.4)
4.6	poly-[Ag(2-amp)OTf]	85	26.2 (25.8)	2.3 (2.4)	8.7 (8.6)
4.7	poly-[Ag(2-amp)(tfa)]	75	29.4 (29.2)	2.4 (2.4)	8.4 (8.5)

^a All compounds are white or off white solids. ^b Calculated values are given in parenthesis.

Table 4.2. Hydrogen-1 NMR Data

	$^1\text{H}/\delta^{\text{a}}$
4.1	2.93 (s, br, 4H, -NH ₂); 4.14 (s, 4H, -CH ₂); 7.28 (m, 2H); 7.739 (t,d, $J_{\text{H-H}_o} = 7.5$ Hz, $J_{\text{H-H}_m} = 1.5$ Hz, 4H); 8.49 (d, $J_{\text{H-H}_o} = 6.0$ Hz, 2H)
4.2	3.47 (s, br, 4H, -NH ₂); 3.83 (s, 4H, -CH ₂); 7.29 (m, 2H); 7.77 (d, $J_{\text{H-H}_o} = 6.0$ Hz , 4H); 8.48 (s, 2H)
4.3	3.32 (s, br, 6H, -NH ₂); 4.11 (s, 6H, -CH ₂); 7.28 (m, 3H); 7.74 (t,d, $J_{\text{H-H}_o} = 7.5$ Hz, $J_{\text{H-H}_m} = 1.5$ Hz, 6H); 8.49 (d, $J_{\text{H-H}_o} = 6.0$ Hz, 3H)
4.4	3.12 (s, br, 6H, -NH ₂); 4.15 (s, 6H, -CH ₂); 7.29 (m, 3H); 7.75 (t,d, $J_{\text{H-H}_o} = 7.4$ Hz, $J_{\text{H-H}_m} = 1.5$ Hz, 6H); 8.50 (s, 3H)
4.5	3.19 (s,br, 2H, -NH ₂); 4.05 (s, 2H, -CH ₂); 7.43 (m, 8H); 7.89 (m, 9H); 7.98 (d, $J_{\text{H-H}_o} = 8.1$ Hz, 2H); 8.36 (d, $J_{\text{H-H}_o} = 4.8$ Hz, 1H)
4.6	3.42 (s, br, 2H, -NH ₂); 4.16 (s, 2H, -CH ₂); 7.25 (m, 1H); 7.77 (t,d, $J_{\text{H-H}_o} = 6.9$ Hz, $J_{\text{H-H}_m} = 1.0$ Hz, 2H); 8.52 (d, $J_{\text{H-H}_o} = 3.6$ Hz, 1H)
4.7	3.68 (s, 2H, -NH ₂); 4.11 (s, 2H, -CH ₂); 7.28 (m, 1H); 7.75 (t,d, $J_{\text{H-H}_o} = 7.5$ Hz, $J_{\text{H-H}_m} = 1.5$ Hz, 2H); 8.53 (d, $J_{\text{H-H}_o} = 6.0$ Hz, 1H)

^a ^1H NMR spectra were recorded in CD₃CN at 298 K.

X-ray Crystallography

The ratio of 2-amp ligand to Ag in the structures of both compounds **4.1** and **4.2** is 2:1. A significant change in both the metal geometries and the ligand to metal bond distances are seen when going from **4.1** to **4.2**, and are the result of differences in interaction of the BF_4^- and tfa^- anions. The structure of **4.2** contains a rather short Ag–Ag interaction¹⁶³ that is obtained at the expense of the relaxed tetrahedral environment of the metal separated structure of **4.1**.

The expansion of the silver coordination environment from linear in a 2-coordinate polymeric setting⁹¹ to near tetrahedral upon the addition of 2 equivalents of the chelating 2-aminomethylpyridyl ligand to produce compound **4.1** was as expected. In the former structure, the only way to achieve the two-coordinate environment necessary to accommodate a 1:1 ratio of 2-amp to AgBF_4 is with an outward twisting of the ligand. In this way the amino and pyridyl donors of separate 2-amp ligands are utilized, linking the linearly coordinated silvers into a one-dimensional coordination polymer. In the latter, the added donors crowd the metal center to the point where donor–metal–donor angle is within range of that easily achieved by the chelating action of the 2-amp ligand creating the distorted tetrahedron that is shown in Figure 4.1. The deformation of the tetrahedral bond angles in this compound is caused by the small bite angle of the coordinated 2-amps which averages 73° . The interligand angles are thus made more obtuse, ranging from $125.9(2)^\circ$ to $133.9(2)^\circ$. BF_4^- ions are held in place in the lattice by H-bonding with the amine protons. The crystal structure of compound **4.1** contains two independent molecules of bis(2-amp) AgBF_4 caused by slight differences in conformation. Amine–Ag and pyridyl–Ag bonds cannot be distinguished from one another in this

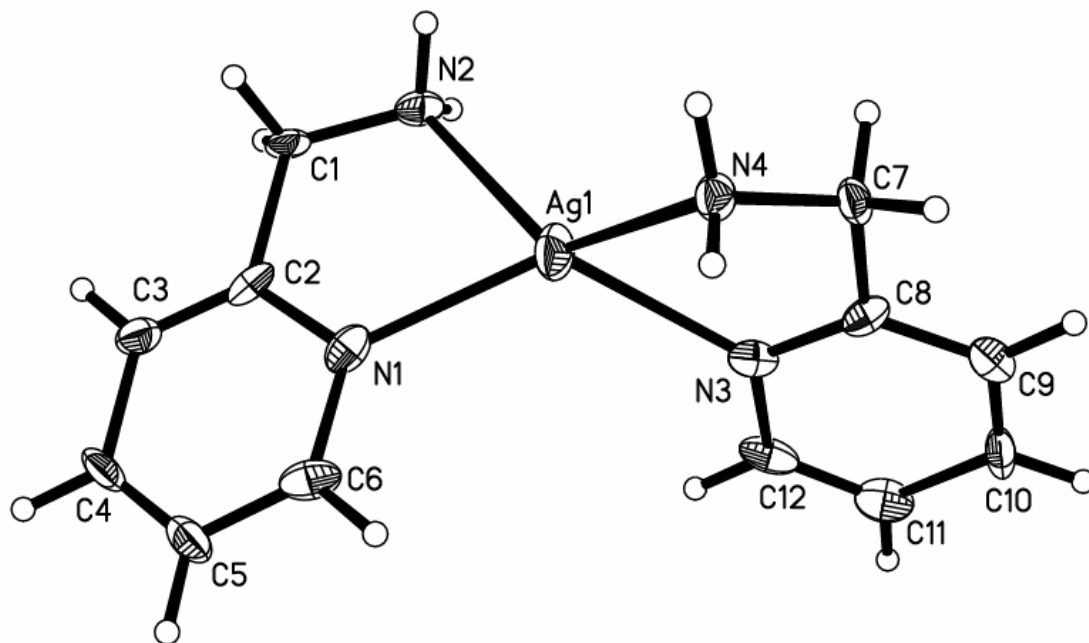


Figure 4.1. Molecular structure of one of the unique cationic monomers of **4.1**. Ellipsoids are drawn at the 50% probability level.

Table 4.3. Selected bond lengths (\AA), angles (deg), and important distances for $\text{Ag}(\text{2-amp})_2\text{BF}_4$, **(4.1)**^a

Ag1–N1	2.262(6)	Ag1–N3	2.319(5)
Ag1–N4	2.336(6)	Ag1–N2	2.371(5)
Ag2–N6	2.293(6)	Ag2–N7	2.310(5)
Ag2–N8	2.322(5)	Ag2–N5	2.368(4)
N1–Ag1–N3	125.6(2)	N1–Ag1–N4	131.9(2)
N3–Ag1–N4	72.5(2)	N1–Ag1–N2	74.61(2)
N3–Ag1–N2	133.9(2)	N4–Ag1–N2	128.3(2)
N6–Ag2–N7	133.4(2)	N6–Ag2–N8	126.5(2)
N7–Ag2–N8	74.4(2)	N6–Ag2–N5	73.3(2)
N7–Ag2–N5	125.9(2)	N8–Ag2–N5	133.3(2)
N2–H···F2 ¹	3.123(7)	N6–H···F7 ⁴	3.146(6)
N2–H···F3 ²	3.068(6)	N6–H···F8 ⁵	3.031(6)
N4–H···F1 ¹	3.049(6)	N8–H···F6 ⁶	3.070(7)
N4–H···F4 ³	3.101(6)	N8–H···F5 ⁵	3.090(7)

^aSymmetry transformations used to generate atoms: #1 = $x-1, y, z+1$; #2 = $x-1, y, z$; #3 = $x, y, z+1$; #4 = $x, y, z-1$; #5 = $x+1, y, z-1$; #6 = $x+1, y, z$

structure by bond lengths alone. Considerable overlap is seen with the amine–Ag distances ranging from 2.293(6) to 2.371(5) Å and the pyridyl–Ag distances ranging from 2.262(6) to 2.368(4) Å. Selected bond lengths and angles for this compound are found in Table 4.3.

The crystal structure of complex **4.2** is shown in Figure 4.2, with selected interatomic parameters in Table 4.4, and is demonstrative of the strong effects that hydrogen bonding and the exchange of anion can have upon the structural characteristics of these compounds. Stoichiometrically identical to **4.1**, the use of the strong H–bond accepting trifluoroacetate results in an unexpected sandwiching of two of the cationic units that were present in **4.1**. The increased propensity of the trifluoroacetate to hydrogen bond enables it to act as a bridge pulling two amine groups of what would be separate units into close proximity of one another. This bridging activity is seen to occur on both sides of a now dimetallic cluster utilizing all four amine groups. The result is that the metal centers are pulled into such proximity to one another as to form a significant metal–to–metal interaction at 3.0077(4) Å. Similar distances are normally found only in complexes where the interacting silvers are being bridged directly by another donor or anion.¹⁷¹ This is a noteworthy interaction seeing as how the tetrahedral environments of the individual metal centers have to undergo considerable distortions in order to achieve a geometry that allows for the contact to occur. The resulting metal–metal interaction hence seems not only to be lightly supported, but even unfavored. The reasoning behind the fact that the complex does not snap apart to become isostructural with **4.1** lies in the fact that the silver(I) ion is extremely flexible in its coordination sphere. In order to accommodate the silver–silver interaction the two metal centers must

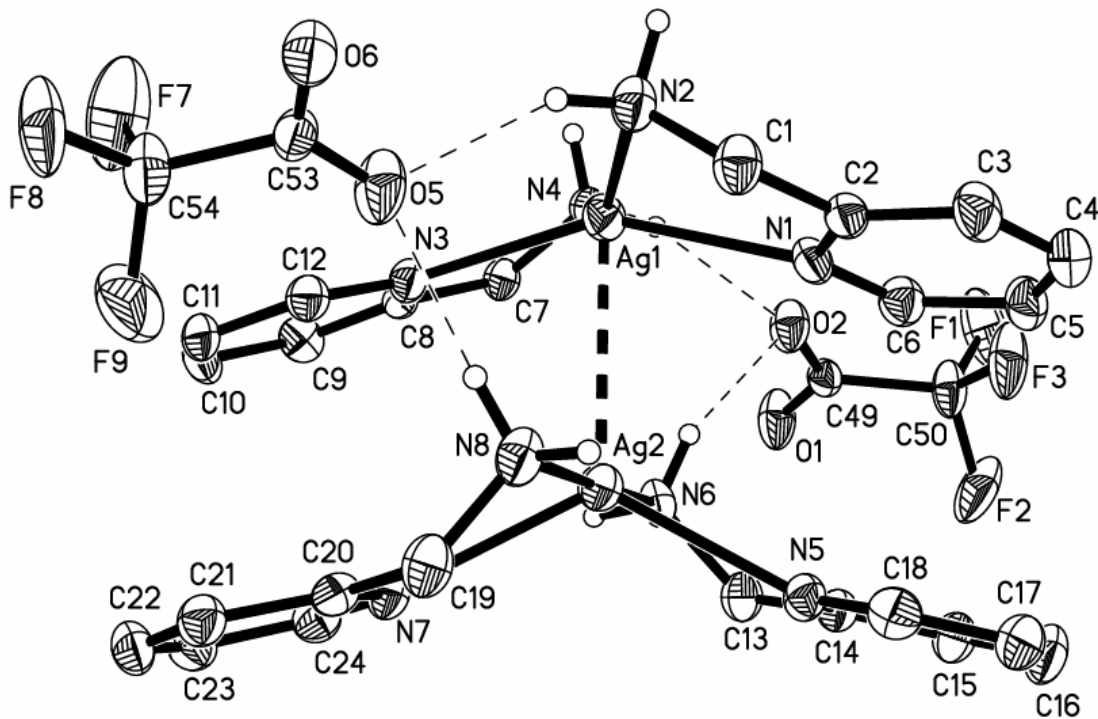


Figure 4.2. Molecular structure of one of the unique metal dimers of **4.2** showing how H-bonding to the anions hold the “sandwich” together. Ellipsoids are drawn at the 50% probability level. All hydrogens except for those on the amine nitrogens have been removed for clarity.

Table 4.4. Selected bond lengths (\AA), angles (deg), and important distances for $\text{Ag}(\text{2-amp})_2\text{Tfa}$, **(4.2)**^a

Ag1–N2	2.309(3)	Ag1–N4	2.326(3)
Ag1–N3	2.402(3)	Ag1–N1	2.418(3)
Ag2–N–8	2.265(3)	Ag2–N6	2.273(3)
Ag2–N5	2.499(3)	Ag2–N7	2.558(3)
Ag3–N10	2.298(3)	Ag3–N12	2.339(3)
Ag3–N11	2.390(3)	Ag3–N9	2.425(3)
Ag4–N16	2.277(3)	Ag4–N14	2.292(3)
Ag4–N13	2.459(3)	Ag4–N15	2.516(3)
Ag1–Ag2	3.0077(4)	Ag3–Ag4	3.0305(4)
N2–Ag1–N4	146.3(1)	N2–Ag1–N3	119.4(1)
N4–Ag1–N3	71.5(1)	N2–Ag1–N1	72.6(1)
N4–Ag1–N1	113.8(1)	N3–Ag1–N1	151.7(1)
N2–Ag1–Ag2	105.64(8)	N4–Ag1–Ag2	107.98(7)
N3–Ag1–Ag2	76.79(7)	N1–Ag1–Ag2	75.17(7)
N8–Ag2–N6	174.6(1)	N8–Ag2–N5	112.8(1)

Table 4.4. Continued

N6–Ag2–N5	72.5(1)	N8–Ag2–N7	71.7(1)
N6–Ag2–N7	106.1(1)	N5–Ag2–N7	124.9(1)
N8–Ag2–Ag1	91.69(8)	N6–Ag2–Ag1	84.96(8)
N5–Ag2–Ag1	116.92(7)	N7–Ag2–Ag1	117.73(7)
N10–Ag3–N12	147.3(1)	N10–Ag3–N11	118.9(1)
N12–Ag3–N11	71.2(1)	N10–Ag3–N9	73.5(1)
N12–Ag3–N9	113.5(1)	N11–Ag3–N9	151.3(1)
N10–Ag3–Ag4	108.08(8)	N12–Ag3–Ag4	104.59(7)
N11–Ag3–Ag4	73.78(7)	N9–Ag3–Ag4	77.76(7)
N16–Ag4–N14	176.1(1)	N16–Ag4–N13	110.8(1)
N14–Ag4–N13	72.7(1)	N16–Ag4–N15	72.7(1)
N14–Ag4–N15	107.0(1)	N13–Ag4–N15	124.3(1)
N16–Ag4–Ag3	90.13(8)	N14–Ag4–Ag3	86.76(8)
N13–Ag4–Ag3	113.12(7)	N15–Ag4–Ag3	122.55(7)
N2–H···O8 ¹	2.993(4)	N10–H···O1	2.905(4)
N2–H···O5 ²	2.945(4)	N10–H···O3	2.988(4)
N4–H···N7 ³	3.380(4)	N12–H···O6	2.949(4)
N4–H···O2	3.087(4)	N12–H···N13 ³	3.144(4)
N6–H···O4 ⁴	2.965(4)	N14–H···O6	3.076(4)
N6–H···O2	3.060(4)	N14–H···O7 ⁶	2.974(4)
N8–H···O8 ⁵	2.965(4)	N16–H···O1	3.049(4)
N8–H···O5 ²	3.060(4)	N16–H···O3 ⁴	2.960(4)

^aSymmetry transformations used to generate atoms: #1 = x, y, z –1; #2 = x, y+1, z–1; #3 = x–1, y, z; #4 = x +1, y, z; #5 = x+1, y, z–1; #6 = x+1, y–1, z

contort into two quite different conformations. The top silver adopts a distorted square-based pyramidal arrangement. For this to occur the N–Ag bond lengths are stretched to suit the new setting with the pyridyl–silver bonds being stretched more, making it now possible to distinguish between the two types of donors based on bond distances.

Amine–silver lengths range from 2.298(3) to 2.339 (3) Å whereas the pyridyl–silver lengths are stretched slightly longer to between 2.390(3) and 2.425(3) Å. The bottom

silver suffers a similar contortion that leaves it in a trigonal bipyramidal setting with both amines occupying the axial positions. Pyridyl donors and the metal–metal interaction hold the equatorial spaces. This distinct difference in coordination sites assists in broadening the division between the lengths of the amine– and pyridyl–silver separations; the axial amine–silver distances range from 2.265(3) to 2.292(3) Å while the equatorial pyridyl–silver distances range from 2.459(3) to 2.558(3) Å. Looking outward from the initial interdimeric H-bonded bridge it is noticed that each oxygen of the trifluoroacetate is used to hold a separate set of these stacked complexes on top of each other such that the anion acts η^2,μ_4 . This effectively constructs a linear chain of dimetallic clusters held together by hydrogen bonds.

The molecular structures of compounds **4.3** and **4.4** offer another example of the marked effect that changes in H–bond accepting ability of the anion has upon the conformation of the molecule. Ratios of ligand to metal in both complexes are 3:2 such that the structural differences again are being caused solely by the anion. The addition of a more strongly interacting anion has the effect of closing the 3:2 structure onto itself.

In **4.3**, the ratio itself of ligand to metal is controlled, or at least limited, by the anion. It is seen that even a 5-fold excess of 2-amp does not force a ratio higher than 3:2 in the crystal structure shown in Figure 4.3. This is accredited to a bifunctional role of the triflate in the molecule: its first function is to act as a coordinating anion to one of the metals, and second is to concomitantly engage in an intramolecular H–bond through a separate oxygen. The addition of more than one equivalent of 2-amp disrupts the linear coordination environment that silver has when the ligand is present in only a single equivalent (as in compound **4.6**). The first $\frac{1}{2}$ an equivalent of ligand that is added past an

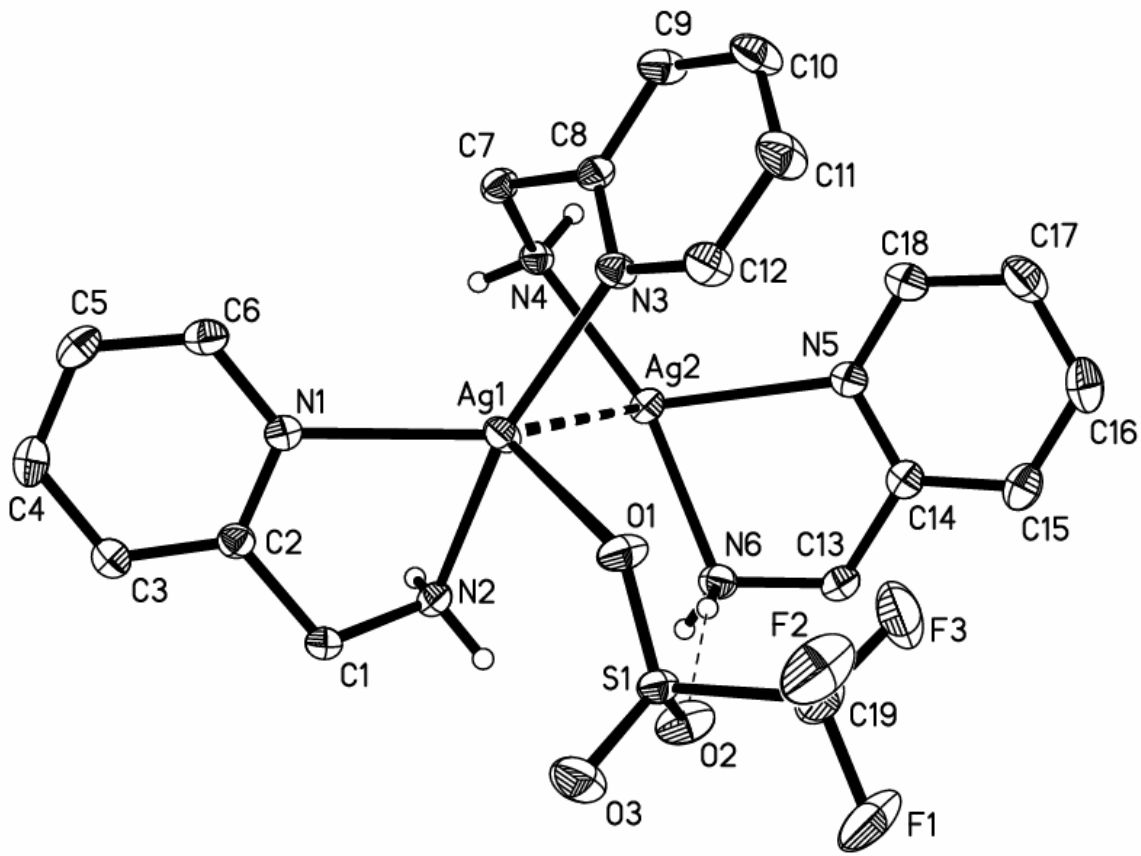


Figure 4.3. Molecular structure of the monopositive cation in **4.3**. Ellipsoids are drawn at the 50% probability level. All hydrogens except for those on the amine nitrogens have been removed for clarity.

Table 4.5. Selected bond lengths (\AA), angles (deg), and important distances for $\text{Ag}_2(2\text{-amp})_3(\text{OTf})_2$, **(4.3)**^a

Ag1–N3	2.211(1)	Ag1–N2	2.277(1)
Ag1–N1	2.396(1)	Ag1–O1	2.591(1)
Ag2–N4	2.199(1)	Ag2–N6	2.236(1)
Ag2–N5	2.403(1)	Ag1–Ag2	2.9137(3)
N3–Ag1–N2	159.77(4)	N3–Ag1–N1	122.35(4)
N2–Ag1–N1	73.09(4)	N3–Ag1–O1	88.42(4)
N2–Ag1–O1	96.65(4)	N1–Ag1–O1	114.76(4)
N3–Ag1–Ag2	74.26(3)	N2–Ag1–Ag2	85.69(3)
N1–Ag1–Ag2	130.76(3)	O1–Ag1–Ag2	111.41(2)
N4–Ag2–N6	165.33(5)	N4–Ag2–N5	119.63(4)
N6–Ag2–N5	74.73(4)	N4–Ag2–Ag1	80.05(4)
N6–Ag2–Ag1	91.03(3)	N5–Ag2–Ag1	115.98(3)
N2–H \cdots O2 ¹	3.1438(17)	N4–H \cdots O4	2.9911(17)
N2–H \cdots O6 ²	3.1422(17)	N6–H \cdots O2	3.0426(18)
N4–H \cdots O5 ²	2.9799(17)	N6–H \cdots O3 ¹	3.0810(18)

^aSymmetry transformations used to generate atoms: #1 = $-x+1, -y, -z$; #2 = $-x+1, -y, -z+1$

initial 1:1 ratio forms a bridge joining two 2-amp chelated silver(I) units. After this point a triflate that binds to one of the metal centers through a single oxygen halts the addition of a full second equivalent of 2-amp ligand to the silvers. In this orientation the triflate is then able to H–bond *via* a second oxygen to the amine protons of the ligand chelating the opposite silver. The effect is similar to that seen in compound **4.2**; H–bonding with the anion holds the N–only bound silver sufficiently close to the anion-bound silver to create a strong metal–metal interaction. However, the geometry of the SO₃ portion of the triflate allows it to be involved in both coordination and H–bonding thus forcing the structural difference with **4.2**. The bridging 2-amp acts as a hinge as the H–bonded anion squeezes the silvers to within 2.9137(3) Å of one another. In this structure there is a notable difference in bond lengths between the two types of ligand present. This should be expected as the stress of the 5-membered ring is relieved in going from a chelating to a more relaxed bridging 6-membered system. The chelated amine–silver distances are 2.277(1) and 2.236(1) Å and the chelated pyridyl–silver distances are 2.396(1) and 2.403(1) Å. The same distances measured for the bridging ligand are noticeably shorter at 2.199(1) and 2.211(1) Å respectively. The coordinating O1 has a bond length to Ag1 of 2.590(1) Å. A selection of bond lengths and angles is presented in Table 4.5. In this structure, as in the last two, intermolecular H–bonding again plays a role in determining the packing of the complex with another 1-D “polymer” being constructed of the bimetallic units held together by H–bonds to the anions. H–bonds to O2 and O3 fashion a sort of dimer, while those to the noncoordinating anions assemble these dimers into a chain.

In the absence of an anion capable of strongly receiving an H–bond the cationic closed structure of compound **4.3** opens to form the flat 3:2 complex, **4.4**. The structure, as shown in Figure 4.4, is an intermediate one that bridges the gap between the polymer formed by 2-amp and AgBF₄ in the 1:1 ratio and the discrete structure of compound **4.1** with its 2:1 ratio, making AgBF₄ the only silver salt studied with which all three of these ratios were able to be achieved. Selected interatomic distances and angles for **4.4** are given in Table 4.6. Without the H–bonding of the anion to hold them together, the metal centers situate themselves widely separated by 5.794(2) Å on opposite sides of the bridging ligand. Each silver is then chelated by another 2-amp creating a nearly planar bimetallic complex. Although twists and rotations about the center bridging ligand are likely to be occurring in solution, stacking of the molecules into sheets, as well as π – π interactions help keep them flat in the solid state. The distance between the planes of the aromatic rings averages around 3.2 Å from one layer to the next in the crystal structure. The BF₄[−] anions can be seen to fit nicely into holes formed by this stacking of molecules and are held in place by weak H–bonds to the amine nitrogens. The chelating amine–silver distances in **4.4** are 2.267(2) and 2.287(2) Å and the pyridyl–silver distances are 2.313(2) and 2.355(2) Å. The bridging amine–silver and pyridyl–silver distances are again seen to be quite a bit shorter at 2.186(2) and 2.185(2) Å. Angles around the silvers are distorted from the ideal 120° trigonal geometry due to the small bite angle of the chelating 2-amp and have values ranging from 74.97(7) to 154.73(8)°. However, deviations of the silvers from their respective three-nitrogen planes are small at 0.054(1) Å for Ag1 and 0.170(1) Å for Ag2, showing that they are still very much in a planar environment.

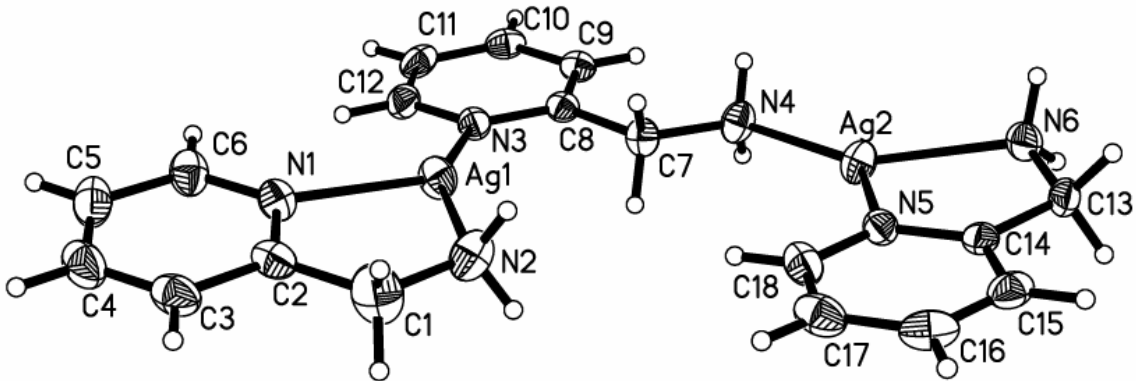


Figure 4.4. A view of the cationic complex of **4.4**. Ellipsoids are drawn at the 50% probability level.

Table 4.6. Selected bond lengths (\AA), angles (deg), and important distances for $\text{Ag}_2(2\text{-amp})_3(\text{BF}_4)_2$, **(4.4)**^a

Ag1–N3	2.185(2)	Ag1–N2	2.267(2)
Ag1–N1	2.355(2)	Ag2–N4	2.186(2)
Ag2–N6	2.287(2)	Ag2–N5	2.313(2)
Ag1–Ag2	5.794(2)		
N3–Ag1–N2		N3–Ag1–N1	
74.86(8)		130.16(7)	
N4–Ag2–N5		N4–Ag2–N6	
135.55(7)		146.26(8)	
N2–H ··· F8A ¹		N6–Ag2–N5	
3.055(16)		74.97(7)	
N2–H ··· F5 ¹		N4–H ··· F4	
3.094(3)		3.112(3)	
N2–H ··· F8 ¹		N4–H ··· F1 ¹	
3.330(4)		2.982(3)	
N2–H ··· F7A		N6–H ··· F4 ²	
2.97(3)		3.133(3)	
N2–H ··· F7		N6–H ··· F1 ²	
3.211(5)		3.384(3)	
		N6–H ··· F2	
		3.000(3)	

^aSymmetry transformations used to generate atoms: #1= x+1, y, z; #2 = -x+2, -y, -z+1

Compound **4.5** was made in an attempt to mimic the structural characteristics of **4.4** using 2,2'-bipyridine as the chelating ligand that caps the ends of the bimetallic structure. The addition of two equivalents of 2,2'-bipyridine to a solution that is 1:2 in 2-amp to AgBF_4 does indeed produce a compound that is stoichiometrically identical to **4.4** (when the bipyridine is substituted for the chelating 2-amps). However, what resulted

was the unexpected hybrid shown in Figure 4.5 that contains features of both **4.3** and **4.4**.

The 2-amp ligand acts as expected in the presence of an excess of AgBF_4 , bridging two separate metal centers. The addition of 2,2'-bipyridine results in two 2,2'-bipyridyl chelated silvers separated by the bridging 2-amp ligand. The connectivity of the structure formed is analogous to that seen in **4.4**. Otherwise, the similarities between this and **4.4** are few. Instead of opening up to make a flat structure, the amine-bound silver twists back around to form an interaction with the pyridyl-bound silver. The resulting hairpin structure bears closer resemblance to the triflate salt in **4.3**. A major difference here is that there are no good H–bond donors on the bipyridyl ligands and no strongly H–bond accepting anion to link the chelating ligands, as in **4.2** and **4.3**. This leaves only the weaker π -stacking forces of the two bipyridyl ligands to account for the conformation of this compound. Selected interatomic distances and angles are shown in Table 4.7. The angle of the bipyridyl planes from one another is a rather obtuse 28.4° and the ring centers are separated by an average of 4.546 \AA . This lends itself to the observation that the argentophilic interaction in these compounds is a highly favored one and the 2-amp ligand bridging two interacting silvers appears to be only slightly higher in energy than the conformation in which the silvers are completely separated. There is also fairly prominent intermolecular π -stacking of the bipyridyl rings both above and below each molecule with the parallel ring planes averaging only 3.316 \AA from one another. The N–Ag distances here are quite short, second only to those seen in the polymer complex **4.6**. The Ag1–pyridyl bond length is $2.150(2)\text{ \AA}$ and the Ag2–amine distance is $2.178(2)\text{ \AA}$. The bipyridyl N–Ag distances are more along the lines of the lengths that have been displayed so far and range from $2.271(1)$ to $2.330(2)\text{ \AA}$.

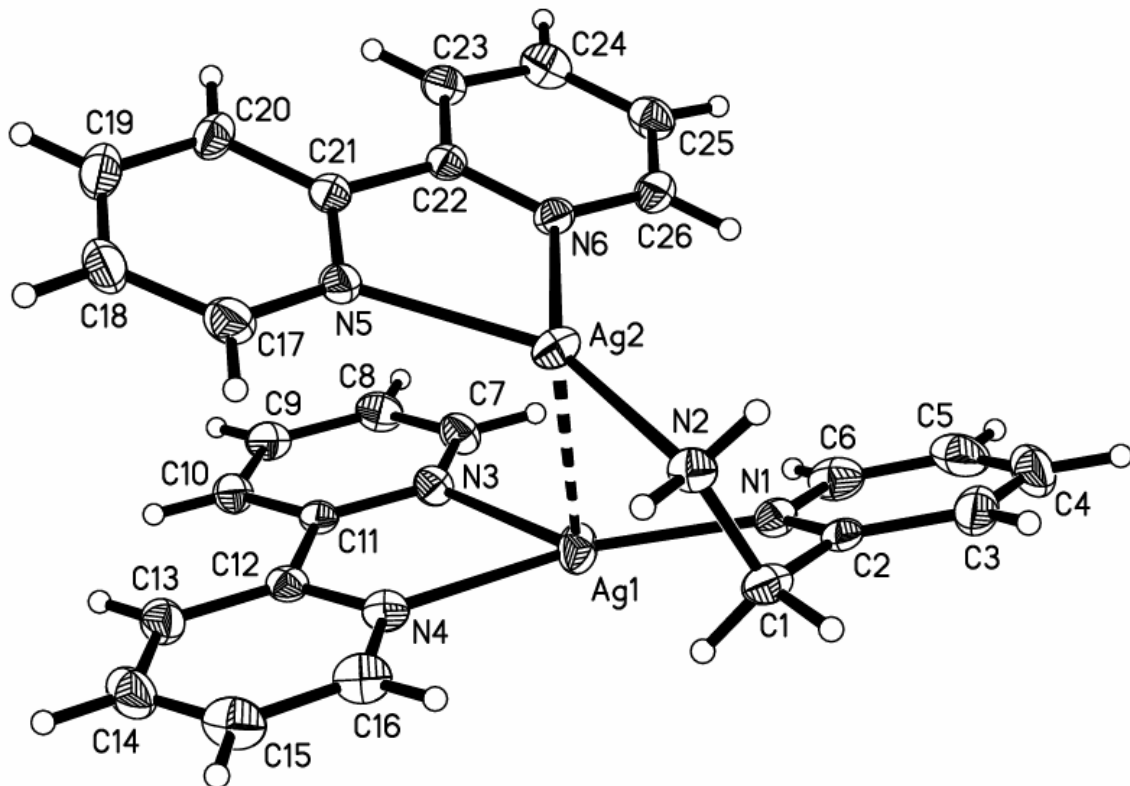


Figure 4.5. A view of the cationic complex of **4.5**. Ellipsoids are drawn at the 50% probability level.

Table 4.7. Selected bond lengths (\AA), angles (deg), and important distances for $\text{Ag}_2\text{2,2}'\text{-bpy}_2(2\text{-amp})(\text{BF}_4)_2$, **(4.5)**^a

Ag1–N1	2.150(2)	Ag1–N3	2.270(1)
Ag1–N4	2.284(2)	Ag2–N2	2.178(2)
Ag2–N6	2.287(2)	Ag2–N5	2.329(2)
Ag1–Ag2	2.8958(3)		
N1–Ag1–N3	136.91(6)	N1–Ag1–N4	148.32(6)
N3–Ag1–N4	73.34(5)	N1–Ag1–Ag2	82.92(4)
N3–Ag1–Ag2	100.56(4)	N4–Ag1–Ag2	81.52(4)
N2–Ag2–N6	142.97(6)	N2–Ag2–N5	145.38(6)
N6–Ag2–N5	71.65(5)	N2–Ag2–Ag1	86.46(4)
N6–Ag2–Ag1	85.99(4)	N5–Ag2–Ag1	99.82(4)
N2–H···F5 ¹	2.977(2)	N2–H···F2 ¹	3.1257(19)
N2–H···F3 ¹	3.099(2)		

^aSymmetry transformations used to generate atoms: #1= x, y+1, z

Compounds **4.6** and **4.7** show the result of the addition of the 2-amp ligand to silver triflate and trifluoroacetate salts in a 1:1 ratio. In the absence of a sufficient amount of strong donor sites to construct at least a 3-coordinate environment around the metal center (in this case N-donors), each silver attempts to adopt its desired linear coordination environment. Since a maximum bite angle of around only 75° is obtainable with the chelating 2-amp, donors from two separate ligands must be used in order to achieve this arrangement. The results are linear zigzag coordination polymers similar to those seen previously with non-coordinating anions.⁹¹ In the case of **4.6** and **4.7**, the anions display an increasing coordination ability resulting in varying degrees of perturbation of the metal centers from their ideal linear geometry. They also allow for H-bonding within the polymer and to adjacent polymers, adding to the dimensionality of the structure.

2-aminomethylpyridine together with one equivalent of silver triflate assembles into a zigzagging 1-dimensional coordination polymer of slightly bent silvers, compound **4.6**. Selected interatomic distances and angles for this compound are given in Table 4.8. The unique portion of the polymer, shown in Figure 4.6, contains one silver bound in near-linear coordination by an amine and its symmetry equivalent pyridyl. The triflate anion is coordinated as well through a stretched bond to O1. When perpetuated, the aminomethylpyridyl backbone of the polymer, shown in Figure 4.7, is seen to be nearly planar both perpendicular to and in the direction of its growth. This is similar to the conformation displayed in compound **4.4** and is likely the result of a combination of ring stacking and hydrogen bonding. The linear chains are stacked one on top of another with each row slightly offset from the previous as to accommodate the anions protruding into

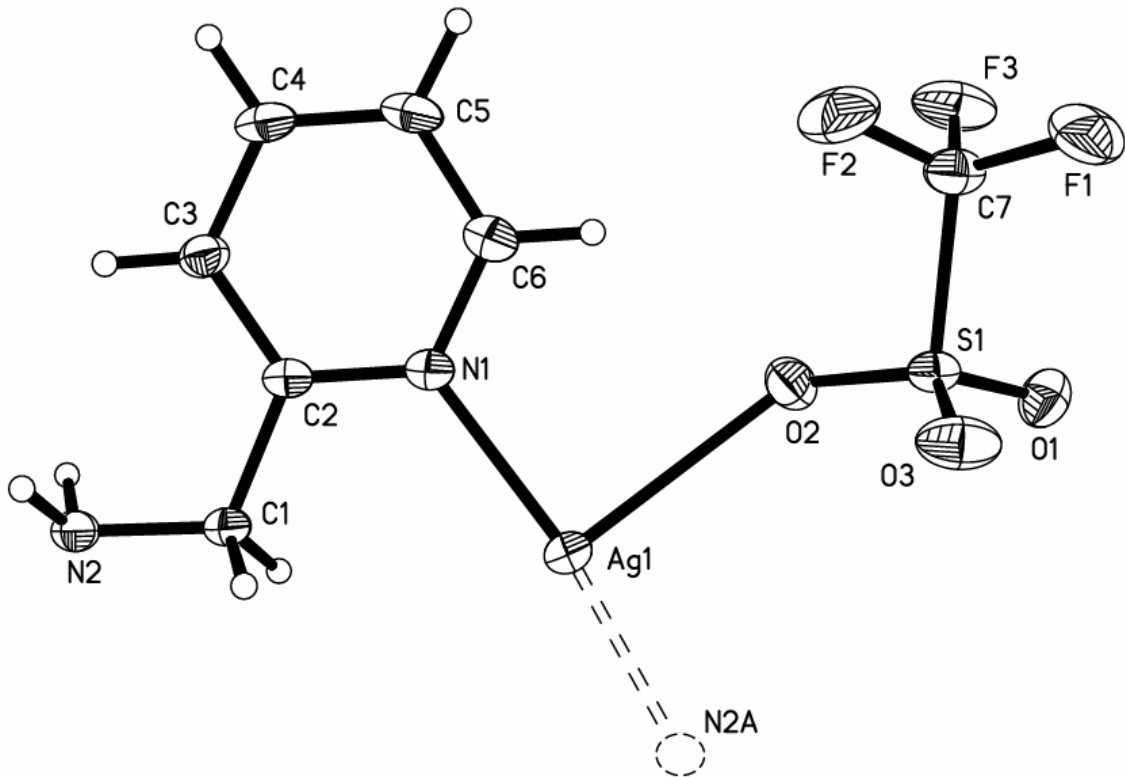


Figure 4.6. A view of the unique portion of the polymer of **4.6** with the coordination environment about silver shown complete. Ellipsoids are drawn at the 50% probability level.

Table 4.8. Selected bond lengths (\AA), angles (deg), and important distances for Ag(2-amp)OTf , **(4.6)**^a

Ag1-N2^1	2.144(2)	Ag1-N1	2.145(2)
Ag1-O2	2.644(2)	Ag1-Ag1^2	5.977(2)
$\text{N2}^1-\text{Ag1-N1}$		171.93(6)	
$\text{N2-H}\cdots\text{O1}^3$	2.913(2)	$\text{N2-H}\cdots\text{O1}^5$	2.993(3)
$\text{N2-H}\cdots\text{O3}^4$	2.967(3)		

^aSymmetry transformations used to generate atoms: #1 = $-x+2, y+1/2, -z+1/2$; #2 = $-x+2, y-1/2, -z+1/2$; #3 = $-x+1, y-1/2, -z+1/2$; #4 = $-x+1, -y+1, -z$; #5 = $-x+1, -y+1, -z+1$

the next layer. The layers are held together throughout the length of the polymers by the interpolymeric hydrogen bonding of each triflate to an amine both above and below the plane in which it is in. The triflates themselves are held in the plane of the polymer by

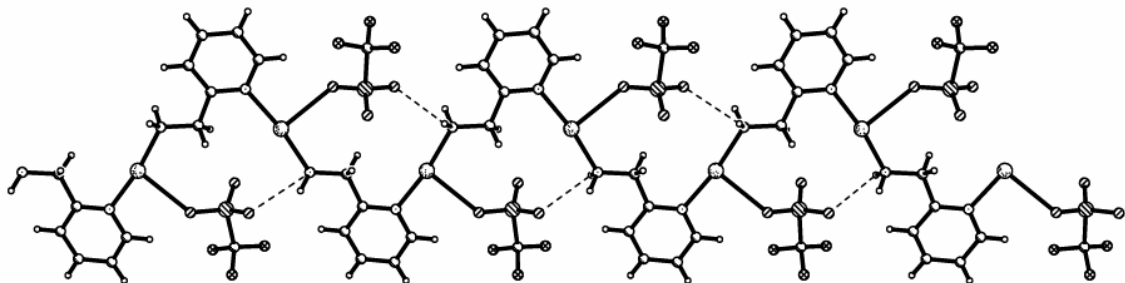


Figure 4.7. A view of the 1-D polymer of **4.6** showing the intrapolymeric H-bonding.

intrapolymeric H-bonding to an amine in the next unit. This also likely assists in keeping the planarity of the polymer. The triflate's O–Ag bond is a weak one at 2.644 Å, which is apparent from the only slight bending of the amine–Ag–pyridyl angle of 171.93(6)°. The N–Ag distances of this polymer are the shortest displayed herein at 2.145(2) Å for the pyridyl–Ag length and 2.144(2) Å for the amine–silver distance.

The unique portion of compound **4.7**, shown in Figure 4.8, again contains a single silver, 2-amp ligand, and anion. Selected bond lengths and angles for **4.7** are given in Table 4.9. It is made apparent here that trifluoroacetate acts as a stronger coordinating anion than triflate when there are insufficient N–donors to saturate the coordination sites of silver. The 1-dimensional coordination polymer backbone of **4.7** that is seen in Figure 4.9 is connectively very similar to that of **4.6**. The more strongly interacting anion, while generally occupying the same spaces in the polymer as those held by triflate in the previous structure, imparts structural features not formerly seen. O1 coordinates strongly to Ag with a bond length of 2.498(2) Å, distorting the pyridyl–Ag–amine angle to 152.96(9)°. This distortion causes the amino nitrogen to be pushed out of its planar position to give the linear polymer an overall helical appearance seen looking down the length of the polymer. With its remaining oxygen atom, the trifluoroacetate extends a

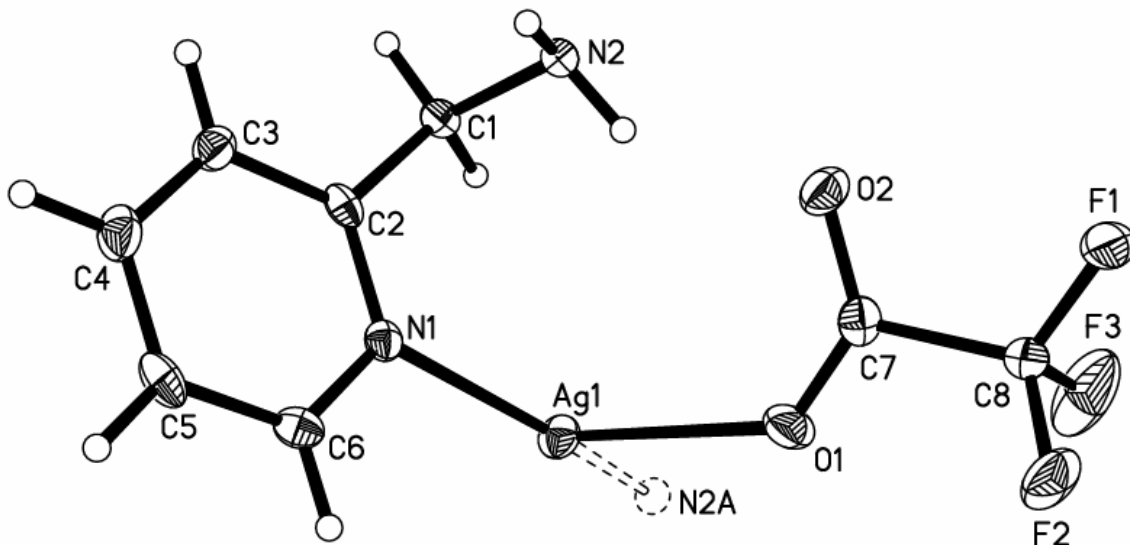


Figure 4.8. Molecular diagram of the unique portion of **4.7** with the coordination environment about silver shown complete. Ellipsoids are drawn at the 50% probability level.

Table 4.9. Selected bond lengths (\AA), angles (deg), and important distances for Ag(2-amp)(tfa) (**4.7**)^a

Ag1-N2^1	2.186(2)	Ag1-N1	2.188(2)
Ag1-O1	2.498(2)	Ag1-Ag1^2	5.437(1)
$\text{N2}^1-\text{Ag1-N1}$	152.96(9)	$\text{N2}^1-\text{Ag1-O1}$	94.27(8)
N1-Ag1-O1	110.63(8)		
$\text{N2}-\text{H}\cdots\text{O2}$	2.922(3)	$\text{N2}-\text{H}\cdots\text{O1}^3$	2.904(3)

^aSymmetry transformations used to generate atoms: #1 = $-x+1, y+1/2, -z+1/2$; #2 = $-x+1, y-1/2, -z+1/2$; #3 = $-x+2, y-1/2, -z+1/2$

bridge both above and, via symmetry equivalent, below the original polymer to link to silvers of adjacent polymers. This stretched interaction at $2.715(2)$ \AA crosslinks the helical polymers into a pseudo 2-dimensional pleated sheet structure. The intrapolymeric H-bonding here serves to help hold the 1-dimensional polymer into its spiraling conformation. The N–Ag bond lengths are quite short in this polymer as they were in

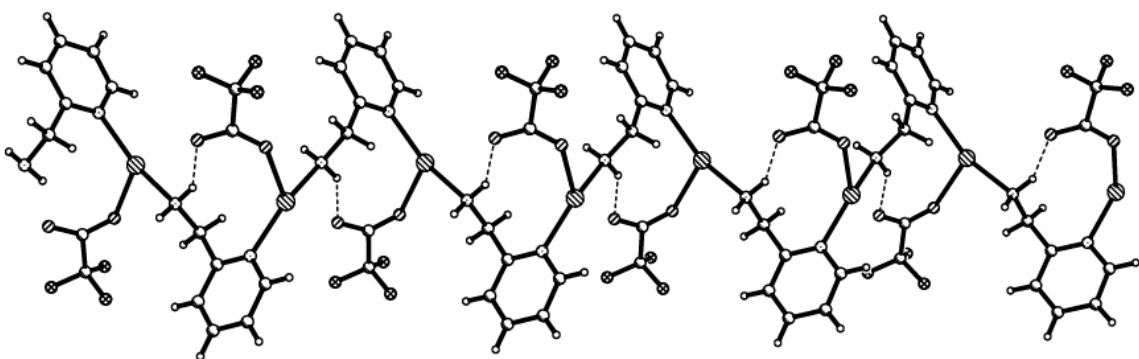


Figure 4.9. A view of the helical 1-D polymer formed by compound **4.7** showing the intrapolymeric H-bonding.

compound **4.6**, though the presence of the more strongly donating anion causes them to lengthen slightly. The pyridyl–Ag distance is 2.188(2) Å and the amine–Ag distance is 2.186(2) Å.

Luminescent Properties

Interest in hybrid inorganic-organic polymers for application as potential new “organic” light emitting devices, OLEDs, has been on a steady upward incline over the past decade. Their versatility comes from the ability to tune their absorption and emission spectra by (typically) facile modifications to the metal environment. Such tuning is not an easy option for the strictly organic LEDs, which often require drastic synthesis and modifications to alter their photoluminescent properties.¹⁵⁰ All excitation and emission spectra were recorded at concentrations of 1×10^{-4} M in acetonitrile glasses as 77 K. The low temperature solution luminescence was collected to give a general representation of what the solid state excitation and emission would be, given that in the 77 K glasses there is substantial complex character (polymeric character in the case of compounds **4.6** and **4.7**).^{153,174,175} Luminescence spectra of representative compounds are displayed in Figure 4.10.

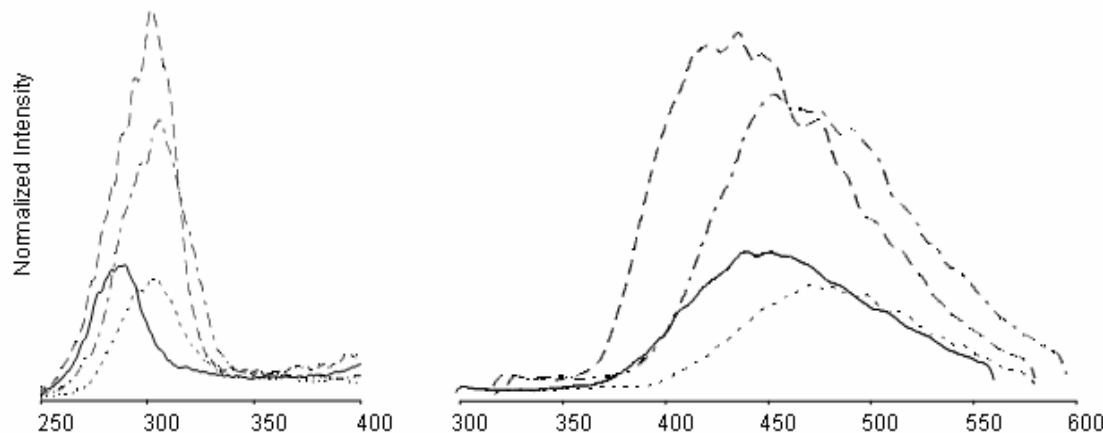


Figure 4.10. Normalized excitation and emission spectra of compounds **4.1**, **4.3**, **4.6** and **4.7** taken in acetonitrile glasses at 1×10^{-4} M concentration at 77 K. — = $\text{Ag}(2\text{-amp})\text{OTf}$, - - - = $\text{Ag}(2\text{-amp})(\text{tfa})$, = $\text{Ag}(2\text{-amp})_2\text{BF}_4$, - · - - = $\text{Ag}_2(2\text{-amp})_3(\text{OTf})_2$.

Table 4.10. Luminescent Spectral Data for 2-amp and compounds **4.1–4.7**, at 77 K and 1×10^{-4} M in CH_3CN .

Compound	Excitation λ_{\max}	Emission local λ_{\min}
2-amp	318	378
4.1	303	472, 483, 500, 516
4.2	303	460, 470, 495
4.3	307	454, 468, 477, 492
4.4	300	446, 454, 462, 475
4.5	369	392, 435
4.6	290	440, 452, 462
4.7	302	422, 437, 449, 476

The resemblance of the excitation spectra of compounds **4.1–4.7** with that of free 2-aminomethylpyridine ligand suggest that the luminescent behavior of these complexes is initiated by a ligand-based absorption followed by ligand-to-metal charge transfer, and then undergoes a metal-based decay. Excitation maxima of all compounds are presented in Table 4.10 along with the local emission maxima. The emission spectra of the various compounds cover a modest range of the spectrum with local maxima spanning

approximately 100 nm. The strongest emissions are seen to be produced by the compounds that have the most interacting anions, OTf and (tfa), and of these the coordination polymer, **4.7**, likely accredited to the extended networks of electronic interaction, shows a stronger emission. It is seen that the most intense luminescence, that of the 1:1 2-ampAg(tfa) polymer, also occurs at the most energetic wavelengths with three strong transitions at 422, 436 and 448 nm. As a general trend, as the intensity of the luminescence drops off, so does the energy of the transitions. The next most intense emission comes from the 3:2 2-ampAgOTf cluster, **4.3**, with its strongest maxima at 453 nm, followed by the silver “sandwich” complex, **4.2**, at 460 nm. The triflate polymer, **4.6**, and the tetrafluoroborate monomers of **4.1** show similar intensity with maxima at 441 and 473 nm, respectively.

Conclusions

We have demonstrated here that a variety of silver(I) complexes can be formed with the bidentate nitrogen ligand, 2-aminomethylpyridine. The complexes, their structures and luminescent characteristics are seen to be highly dependant not only on the hydrogen–bonding and coordinating ability of the anion but also on the ratio of ligand to metal present. The simplicity of the 2-amp ligand made it a desirable prospect for this concentration/ counter ion study that produced molecular structures ranging from simple monomers to folded bimetallic metal–metal interacting species to elaborate multidimensional polymers.

Experimental

General Considerations

All experiments were carried out under an argon atmosphere using a Schlenk line and standard Schlenk techniques. Glassware was dried at 120 °C for several hours prior to use. All reagents except 2,2'-bipyridine, which was stored in a bench top dessicator, were stored in an inert atmosphere glovebox. Acetonitrile and diethyl ether were distilled from calcium hydride and sodium/bezophenone ketyl, respectively, immediately before use. 2-aminomethylpyridine and 2,2'-bipyridine were purchased from Aldrich and used as received. Silver(I) trifluoroacetate, silver(I) trifluoromethanesulfonate, and silver(I) tetrafluoroborate were purchased from Strem Chemicals Inc. and used as received. ¹H NMR spectra were recorded at 300.13 MHz on a Bruker Spectrospin 300 MHz spectrometer. Elemental analyses were performed by Atlantic Microlabs Inc. in Norcross Georgia. Excitation and emission spectra were recorded on an Instruments S. A. Inc. Fluoromax-2 model spectrometer using band pathways of 5 nm for both excitation and emission and are presented uncorrected.

Preparations

General Preparations. General procedures for the synthesis of compounds **4.1-4.4**, **4.6** and **4.7** involve the addition of a 5 mL acetonitrile solution of 2-aminomethylpyridine to a stirred solution of the appropriate silver salt in 5 mL acetonitrile. The mixtures are stirred for 10 minutes then dried in vacuo to leave white to off-white powders. All flasks are shielded from light with aluminum foil to prevent the photodecomposition of the silver compounds. Crystals of compound **4.2** were grown by

slow diffusion of hexanes into a dichloromethane solution at 5 °C. Crystals of compound **4.5** were grown by slow diffusion of ether into a dichloromethane solution at 5 °C. Crystals of all other compounds were obtained by the slow diffusion of ether into acetonitrile solutions at 5 °C. The amount of reagents used, yields, and analytical data are presented in the following paragraphs as well as any modifications to the general synthetic procedure. Percent yields are based upon the amount of silver salt used.

Ag(2-amp)₂BF₄ (**4.1**). This reaction used 2 equivalents of 2-aminomethylpyridine (0.111 g, 1.03 mmol) added to AgBF₄ (0.100 g, 0.514 mmol) to leave a white flaky solid in 92 % (0.190 g, 0.471 mmol) yield upon solvent evaporation. Colorless block shaped crystals were grown from acetonitrile and ether. ¹H NMR (CD₃CN, 298 K) δ: 2.93 (s, br, 4H, -NH₂); 4.14 (s, 4H, -CH₂); 7.28 (m, 2H); 7.739 (t,d, *J*_{H-Ho} = 7.5 Hz, *J*_{H-Hm} = 1.5 Hz, 4H); 8.49 (d, *J*_{H-Ho} = 6.0 Hz, 2H). Anal. Calcd for AgC₁₂H₁₆N₄BF₄: C, 35.07; H, 3.92; N, 13.63. Found: C, 35.03; H, 3.78; N, 13.33.

Ag(2-amp)₂(tfa) (**4.2**). This reaction used 2 equivalents of 2-aminomethylpyridine (0.098 g, 0.906 mmol) added to Ag(tfa) (0.100 g, 0.453 mmol) to leave a light-brown fluffy solid in 82 % (0.162 g, 0.371 mmol) yield upon evaporation of the solvent. Colorless block shaped crystals were grown from dichloromethane and hexanes. ¹H NMR (CD₃CN, 298 K) δ: 3.47 (s, br, 4H, -NH₂); 3.83 (s, 4H, -CH₂); 7.29 (m, 2H); 7.77 (d, *J*_{H-Ho} = 6.0 Hz , 4H); 8.48 (s, 2H). Anal. Calcd for AgC₁₄H₁₆N₄O₂F₃: C, 38.46; H, 3.69; N, 12.82. Found: C, 38.24; H, 3.57; N, 12.54.

Ag₂(2-amp)₃(OTf)₂ (**4.3**). This reaction used 3 equivalents of 2-aminomethylpyridine (0.063 g, 0.577 mmol) added to 2 equivalents of AgOTf

(0.100 g, 0.389 mmol). An oily yellow solid was left upon evaporation of the solvent in vacuo. This was then redissolved in a small amount of CH₃CN and precipitated with ether to leave a fluffy white solid in 76 % (0.123 g, 0.154 mmol) yield upon drying. Colorless block shaped crystals were grown from acetonitrile and ether. ¹H NMR (CD₃CN, 298 K) δ: 3.32 (s, br, 6H, -NH₂); 4.11 (s, 6H, -CH₂); 7.28 (m, 3H); 7.74 (t,d, $J_{\text{H}-\text{H}_o} = 7.5$ Hz, $J_{\text{H}-\text{H}_m} = 1.5$ Hz, 6H); 8.49 (d, $J_{\text{H}-\text{H}_o} = 6.0$ Hz, 3H). Anal. Calcd for Ag₂C₂₀H₂₄N₆O₆F₆S₂: C, 28.86; H, 2.89; N, 10.02. Found: C, 29.29; H, 2.92; N, 10.00.

Ag₂(2-amp)₃(BF₄)₂ (**4.4**). This reaction used 3 equivalents of 2-aminomethylpyridine (0.150 g, 1.39 mmol) added to 2 equivalents AgBF₄ (0.180 g, 0.925 mmol). A white powder was left in 84% yield (0.278 g, 0.398 mmol) upon evaporation of the solvent in vacuo. Colorless block shaped crystals were grown from acetonitrile and ether. ¹H NMR (CD₃CN, 298K) δ: 3.12 (s, br, 6H, -NH₂); 4.15 (s, 6H, -CH₂); 7.29 (m, 3H); 7.75 (t,d, $J_{\text{H}-\text{H}_o} = 7.4$ Hz, $J_{\text{H}-\text{H}_m} = 1.5$ Hz, 6H); 8.50 (s, 3H).

Ag₂2,2'-bpy₂(2-amp)(BF₄)₂ (**4.5**). This reaction used 2-aminomethylpyridine (0.050 g, 0.463 mmol) added to 2 equivalents of AgBF₄ (0.180 g, 0.925 mmol). This solution was stirred for 10 minutes then 2 equivalents of 2,2'-bipyridyl (0.144 g, 0.922 mmol) in 5 mL CH₃CN was added. This was stirred an additional 5 minutes then dried in vacuo to leave an off-white powder in 90 % (0.126 g, 0.221 mmol) yield. Colorless block shaped crystals were grown from dichloromethane and ether. ¹H NMR (CD₃CN, 298 K) δ: 3.19 (s,br, 2H, -NH₂); 4.05 (s, 2H, -CH₂); 7.43 (m, 8H); 7.89 (m, 9H); 7.98 (d, $J_{\text{H}-\text{H}_o} = 8.1$ Hz, 2H); 8.36 (d, $J_{\text{H}-\text{H}_o} = 4.8$ Hz, 1H).

poly-[Ag(2-amp)OTf] (4.6). This reaction used 2-aminomethylpyridine (0.042 g, 0.388 mmol) added to AgOTf (0.100 g, 0.389 mmol) to leave an oily brown solid upon evaporation of the solvent. This solid was then redissolved in a small amount of CH₃CN and precipitated with ether to leave a brown solid in 85 % (0.120 g, 0.334 mmol) yield. Colorless block shaped crystals were grown from acetonitrile and ether. ¹H NMR (CD₃CN, 298 K) δ: 3.42 (s, br, 2H, -NH₂); 4.16 (s, 2H, -CH₂); 7.25 (m, 1H); 7.77 (t,d, *J*_{H-Ho} = 6.9 Hz, *J*_{H-Hm} = 1.0 Hz, 2H); 8.52 (d, *J*_{H-Ho} = 3.6 Hz, 1H). Anal. Calcd for AgC₇H₈N₂O₃SF₃: C, 25.80; H, 2.47; N, 8.56. Found: C, 26.27; H, 2.33; N, 8.77.

poly-[Ag(2-amp)(tfa)] (4.7). This reaction used 2-aminomethylpyridine (0.049 g, 0.453 mmol) added to Ag(tfa) (0.100 g, 0.452 mmol) to leave an off-white powder in 75 % (0.116 g, 0.338 mmol) yield upon evaporation of the solvent. Colorless plates were grown from acetonitrile and ether. ¹H NMR (CD₃CN, 298 K) δ: 3.68 (s, 2H, -NH₂); 4.11 (s, 2H, -CH₂); 7.28 (m, 1H); 7.75 (t,d, *J*_{H-Ho} = 7.5 Hz, *J*_{H-Hm} = 1.5 Hz, 2H); 8.53 (d, *J*_{H-Ho} = 6.0 Hz, 1H). Anal. Calcd for AgC₈H₈N₂O₂F₃: C, 29.20; H, 2.45; N, 8.51. Found: C, 29.38; H, 2.39; N, 8.40.

Crystallography

A summary of the experimental crystallographic data for **4.1** through **4.7** is given in Table 4.11. Full tables of bond lengths and angles can be found in Appendix B, Tables B.7 through B.13. Crystallographic data were collected on crystals with dimensions 0.181 × 0.150 × 0.100 mm for **4.1**, 0.210 × 0.150 × 0.090 mm for **4.2**, 0.279 × 0.216 × 0.202 mm for **4.3**, 0.310 × 0.270 × 0.250 mm for **4.4**, 0.245 × 0.231 × 0.199 mm for **4.5**, 0.167 × 0.143 × 0.094 mm for **4.6**, and 0.240 × 0.150 × 0.080 mm for **4.7**. Crystals of all

Table 4.11. Crystallographic Data for compounds **4.1** to **4.7**

	4.1	4.2	4.3	4.4	4.5	4.6	4.7
formula	$\text{Ag}_2\text{C}_{24}\text{H}_{32}\text{B}_2\text{F}_8\text{N}_8$	$\text{Ag}_4\text{C}_{56}\text{H}_{64}\text{F}_{12}\text{N}_{16}\text{O}_8$	$\text{Ag}_2\text{C}_{20}\text{H}_{24}\text{F}_6\text{O}_6\text{S}_2$	$\text{Ag}_2\text{C}_{18}\text{H}_{24}\text{B}_2\text{F}_8\text{N}_6$	$\text{Ag}_2\text{C}_{26}\text{H}_{24}\text{B}_2\text{F}_8\text{N}_6$	$\text{AgC}_7\text{H}_8\text{F}_3\text{N}_2\text{O}_3\text{S}$	$\text{AgC}_8\text{H}_8\text{F}_3\text{N}_2\text{O}_2$
fw	821.94	1748.71	838.31	713.79	809.87	365.08	329.03
a(Å)	7.8817(5)	7.4205(6)	8.1167(9)	7.112(1)	10.5634(6)	12.982(6)	4.7270(8)
b(Å)	14.0058(8)	13.284(1)	22.930(4)	8.335(2)	13.6804(9)	11.458(4)	9.898(2)
c(Å)	7.2894(4)	18.049(2)	15.625(2)	21.471(4)	19.709(1)	7.709(5)	22.111(4)
α (deg)	106.208(2)	69.342(4)		97.23(3)			
β (deg)	93.211(2)	89.255(4)	97.430(5)	98.51(3)		101.40(3)	
γ (deg)	100.710(3)	80.621(4)		99.10(3)			
V(Å ³)	754.25(8)	1640.8(2)	2883.7(7)	1228.4(4)	2848.3(3)	1124(1)	1034.6(3)
Z	1	1	4	2	4	4	4
space group	P1	P1	P2 ₁ /n	P-1	P2 ₁ 2 ₁ 2 ₁	P2 ₁ /c	P2 ₁ 2 ₁ 2 ₁
T(K)	110(2)	110(2)	110(2)	110(2)	110(2)	110(2)	110(2)
Dcalcd(g cm ⁻³)	1.810	1.770	1.931	1.930	1.889	2.157	2.112
μ (mm ⁻¹)	1.379	1.275	1.588	1.675	1.457	2.017	1.978
2 θ _{max} , deg	28.31	26.43	28.30	28.39	28.29	28.37	26.45
reflns measured	15414	54807	66994	14615	33450	39350	13577
reflns used (R _{int})	5828(0.0267)	12763(0.0401)	7095(0.0308)	5935(0.0226)	7004(0.0291)	2751(0.0310)	2121(0.0626)
restraints/params	7/391	3/865	0/397	10/341	0/397	0/154	0/145
R ₁ , [I > 2σ(I)]	0.0174	0.0274	0.0177	0.0274	0.0174	0.0194	0.0200
wR ² , [I > 2σ(I)]	0.0465	0.0635	0.0432	0.0678	0.0408	0.0491	0.0443
R(F _o ²)(all data)	0.0184	0.0364	0.0226	0.0317	0.0194	0.0232	0.0229
R _w (F _o ²)(all data)	0.0472	0.0675	0.0443	0.0705	0.0412	0.0502	0.0450
GooF on F ²	1.028	1.016	1.063	1.034	1.067	1.067	1.067

compounds were immobilized on a cryoloop by encasing them in Paratone-N® oil then cooling them in a nitrogen coldstream. Data were collected at 110 K on a Bruker X8 Apex. Graphite-monochromated Mo- K_{α} radiation ($\lambda = 0.71073 \text{ \AA}$) was used throughout. All structures were solved by direct methods after processing with SAINT-Plus and correction of the data using SADABS.¹³⁹ All of the data were processed using the Bruker AXS SHELXTL software, version 6.10.¹⁴⁰ All non-hydrogen atoms were refined anisotropically and hydrogen atoms were placed in calculated positions except for the amine hydrogens of compound **4.3**, whose positions were allowed to refine. The crystal structures of compounds **4.1** and **4.2** each contain 2 unique monomers of their respective compounds. The structure of compound **4.4** contains a BF_4^- anion disordered over 2 positions. The anisotropic displacement parameters for the two orientations of the disorder are constrained to be equal and the site occupancies were refined as 0.825(3)/0.173(3) [for B(1/1a), F(1/1a), F(2/2a), F(3/3a), F(4/4a)].

CHAPTER FIVE

Silver(I) 3-aminomethylpyridine Complexes Part 1: Effect of Ligand Ratio, π -stacking and Temperature with a Non-interacting Anion

Introduction

Progress in the area of crystal engineering has many far reaching effects whose importance often greatly surpass the novelty of the basic investigations from whence they came. A few of the more interesting, and potentially profitable, applications that have accepted advancements from the field include catalysis, molecular recognition, molecular sieving and separations.^{10,63,83,176} Much of the usefulness that is obtained from these polymers stems from the ability to control internal features of the structures such as coordination geometry of the metal centers, pore size, and magnetism.^{3,4,7,25,141} During the past few decades numerous examples of designed and constructed coordination architectures that span from discrete macromolecules to multidimensional coordination networks have been demonstrated, most of which were built on the basis of controlling functionality, rigidity, or geometry of the ligand or by using modifications to the counterion or solvent system.^{11,21,49,88,142,146-148,151-154,159,177} Despite the wealth of literature that has been generated describing crystal engineering studies of the aforementioned methods, the equally effective technique of stoichiometry control has been largely overlooked.^{68,69} Only recently have a handful of investigators begun to examine the metal/ligand ratio dependence of structural features with regards to design and growth of supramolecular coordination entities.^{70,71,91,178,179} Recent studies published by Mirkin, et al.⁷⁰ and Dong, et al.⁷¹ both focus on the ratio dependence of metal

complexes of flexible mixed donor ligands and assist in demonstrating the practicality of this seldom used method. The previous chapter reported on the structural modifications that could be had by variations in the ratio of ligand to metal in the reactions of silver(I) complexes of 2-aminomethylpyridine.¹⁵⁹ This is now followed with an inquiry of the meta-substituted 3-aminomethylpyridine ligand.

Herein we describe the dramatic changes that can be brought about in the flexible coordination sphere of the silver(I) cation merely by altering the ratio of the bifunctional 3-aminomethylpyridine ligand. In this study only the tetrafluoroborate salt of silver was used in order to keep counterion interactions to a minimum. As a result, we were able to obtain a number of exceedingly varied structural motifs whose differences stem only from the ratio of ligand to metal in the reactions from which they were produced. As an added feature, two of the ratios were also seen to display a temperature dependent morphology with separate structures of each consistently being obtained when crystallized at temperature differences of only 40 K.

Results and Discussion

Synthesis and NMR Spectroscopy.

The 3-aminomethylpyridyl complexes **5.1.1–5.4** were made by the direct reaction of the ligand with silver(I) tetrafluoroborate and 2,2'-bipyridine in varying ratios. Analytical data for these compounds are presented in Tables 5.1 and 5.2. It is seen that when using the same noncoordinating BF_4^- anion the structural features of the silver(I) complexes made can be varied greatly by changes in ratio of ligand to metal and by

Table 5.1. Analytical and Physical Data

	compound ^a	yield ^b (%)	analytical (%) ^c		
			C	H	N
5.1.1	<i>poly</i> (Ag[3-amp]BF ₄)	91	35.0 (35.0)	3.8 (3.9)	13.3 (13.6)
5.1.2	Ag ₄ (3-amp) ₄ (BF ₄) ₄		verbatim 5.1.1		
5.2	poly-Ag ₂ (3-amp) ₃ (BF ₄) ₂	88	30.4 (30.3)	3.3 (3.3)	11.6 (11.8)
5.3.1	poly-Ag(3-amp) ₂ BF ₄	84	35.2 (35.1)	3.8 (3.9)	13.5 (13.6)
5.3.2	poly-Ag(3-amp) ₂ BF ₄		verbatim 5.3.1		
5.4	Ag ₂ (2,2'-bipy) ₂ -μ-(3-amp)(BF ₄) ₂	92	40.6 (40.3)	3.3 (3.3)	11.2 (11.4)

^a All compounds are white or off white solids. ^b Compounds **5.1.1** and **5.1.2**, as well as **5.3.1** and **5.3.2** were derived from the same reaction and were thus analyzed only once per set. ^c Calculated values are given in parenthesis.

Table 5.2. Hydrogen-1 NMR Data

$^1\text{H}/\delta^{\text{a}}$

5.1.1 3.13 s, br, 8H (-NH₂-); 3.92 s, 8H (-CH₂-); 7.47 q,d, 4H; 7.88 d,t, 8H; 8.41 d,d, 4H

5.1.2 verbatim **5.1.1**

5.2 2.93 s, br, 6H, (-NH₂-); 3.875 s, 6H, (-CH₂-); 7.38 m, 3H; 7.739 d,d, 6H; 8.34 d, 3H

5.3.1 3.20 s, br, 4H, (-NH₂-); 3.90 s, 4H, (-CH₂-); 7.42 m, 2H; 7.86 t,d, 4H; 8.32 d, 2H

5.3.2 verbatim **5.3.1**

5.4 2.48 s,br, 2H, (-NH₂-); 3.79 s, 2H, (-CH₂-); 7.42 m, 8H; 7.89 t, 9H; 8.26 d, 2H; 8.55 d, 1H

^a ^1H NMR spectra were recorded in CD₃CN at 298 K. The spectra of **5.1.1** and **5.1.2** as well as **5.3.1** and **5.3.2** are identical in room temperature solution, as a result each set is reported only once.

changes in crystallization temperature. However, it should be noted that modifications in crystallization method do not cause changes in connectivity, merely in the conformation of the product implying a separate thermodynamic product versus a kinetic one. The synthesis of the 1:1 ratio 3-ampAgBF₄ complex has been previously described by an alternate route in an anion dependent study⁹¹; though in the earlier investigation the researchers were unable to obtain satisfactory samples for study by X-ray diffraction. The five 3-amp only compounds mentioned herein display three different ligand to metal ratios. When in solution, the two 1:1 and the two 2:1 structures are indistinguishable by room temperature ¹H NMR. This is indicative that the two connectively identical structures of each pair lose the structural differences that separate them when dissolved in room temperature solution.

X-ray Crystallography

The silver coordination environments that are seen in structures **5.1.1–5.4** differ greatly from one structure to the next. Geometries of the metal centers range from the near linear 175(1)° of Ag2 in compound **5.1.1** to the distorted tetrahedrons of **5.3.1** and **5.3.2**. Median to these are several structures containing trigonal environments with some displaying very short metal–metal interactions. Interestingly, the silver–silver interactions are only seen to be present on those metals bound by pyridyl donors, even if more crowded. This is likely reasoned to the ease of accessibility that the planar pyridyl rings allow for the metals to come close to one another, as well as the attractive force of the ring π–systems themselves for one another.

Ligand to metal ratios in the structures of **5.1.1** and **5.1.2** are 1:1. The silver environments of both structures are connectively similar with each containing

3-coordinate, pyridyl-only bound silvers as well as linear, amine-only bound silvers. In both cases, the pyridyl-only bound silvers each contain a bound acetonitrile that fills in a third coordination site. Differences between the two structures stem solely from the method of crystallization. Using identical solvent systems, the polymeric conformation of **5.1.1** develops when crystallization is allowed to occur rapidly within several hours at 5 °C. A slower crystallization over several days at –35 °C results in the folded macrocycle of **5.1.2**.

The unique portion of the linear polymer formed by the rapid crystallization of a 1:1 mixture of 3-amp with AgBF₄ is shown in Figure 5.1 along with selected bond lengths and angles in Table 5.3. Each of the amine bound silvers are ½ occupied, keeping a 1:1 ratio with the two 3-amp ligands in the asymmetric unit. Perpetuation of the polymer of **5.1.1** occurs in one dimension as the 3-amp ligands coordinate in a head to head fashion to the metal centers. What results is a zigzagging coordination polymer of two coordinate amine bound silvers and three coordinate pyridyl bound silvers, with the pyridyl only bound silvers being also connected to an acetonitrile molecule. This polymer is then linked to a second, symmetry equivalent one by silver–silver interactions at every pyridyl-only bound silver. This forms the chain-like structure shown in Figure 5.2 that is constructed of alternating circular and oval “links” joined at every other metal center. The more circular links are forced to be so by the coordinated acetonitriles present on every pyridyl-bound metal that protrude into the center of the ring forcing the amine-bound silvers here outward and away from the center of the polymer. The amine-bound silvers of the oval rings have no such steric push and, as a result, are allowed to twist back in towards the center of the polymer. A C2 axis running the length of the

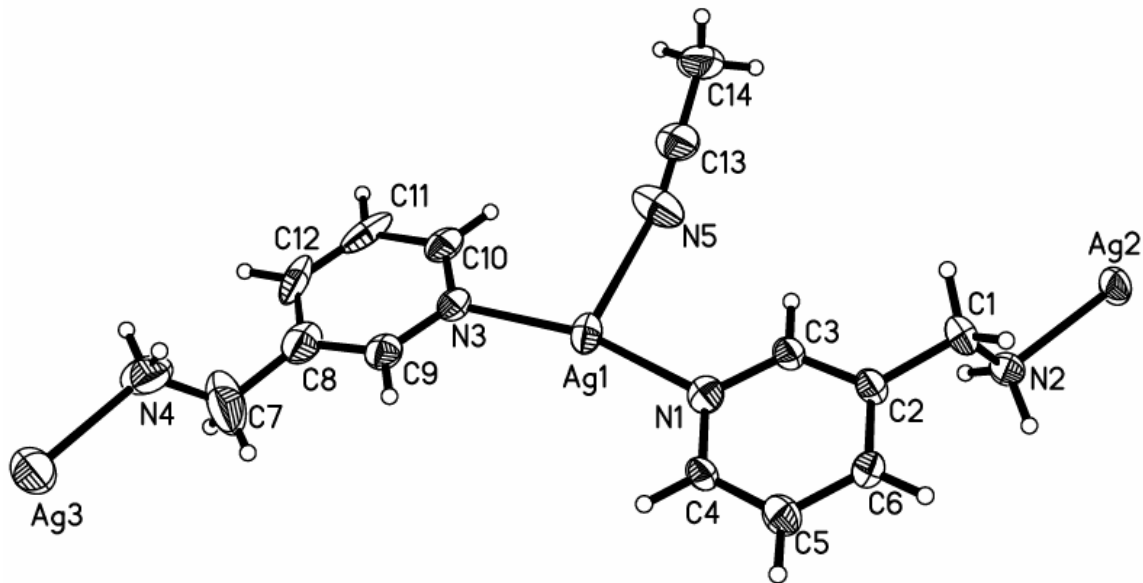


Figure 5.1. Thermal ellipsoid plot of the unique portion of the cationic polymer **5.1.1**. The disordered amine and silver have been omitted for clarity. Ellipsoids are drawn at the 50 % probability level.

Table 5.3. Selected bond lengths (\AA), angles ($^\circ$), and important distances for Poly($\text{Ag}[\text{3-amp}] \text{BF}_4$) (**5.1.1**)^a

Ag1-N1	2.181(7)	Ag1-N3	2.183(7)
Ag1-N5	2.515(9)	Ag1-Ag1#1	3.2896(1)
Ag2-N2	2.146(7)	Ag2-N2#2	2.146(7)
Ag3-N4	2.154(15)	Ag3-N4#3	2.154(1)
<hr/>			
N1-Ag1-N3	164.3(3)	N1-Ag1-N5	99.9(3)
N3-Ag1-N5	95.8(3)	N1-Ag1-Ag1#1	113.25(2)
N3-Ag1-Ag1#1	68.27(2)	N5-Ag1-Ag1#1	82.5(2)
N2-Ag2-N2#2	172.7(4)	N4-Ag3-N4#3	174.9(9)

^aSymmetry transformations used to generate atoms: #1 = $-x+2, y, -z+3$; #2 = $x, -y+3, z$ #3 = $x, -y+2, z$.

polymer relates the two halves. The metal-metal distance contained herein is a bit lengthy at 3.289(1) \AA but appears to be completely unsupported with virtually no π -stacking occurring between the rings of the connected silvers. There does appear to be, however, substantial π -interactions of the metals with the pyridyl rings of the polymer

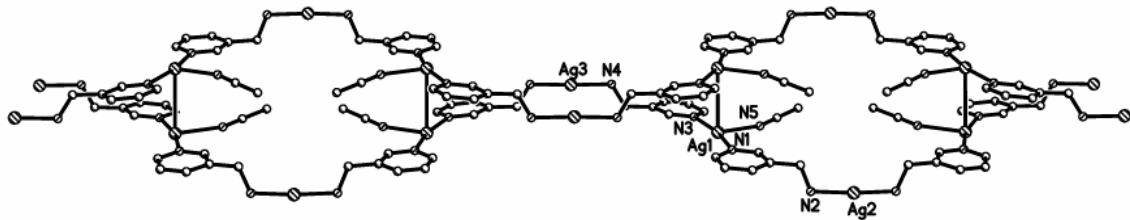


Figure 5.2. Extended ball-and-stick view of the cationic polymeric structure of **5.1.1**. Hydrogen atoms and disorder have been removed for clarity.

strands stacked above and below those silvers that hold the two halves of the polymer chain together. The π cloud of the pyridyl rings approach to within 3.03 Å (Ag–ring atom distances range from 3.031(9) to 4.176(9) Å) from the silvers constructing a pseudo double-metal sandwich arrangement. This is comparable to other known compounds with aromatic Ag– π interactions.^{101,180,181} The stacking of the rings onto the sides of the metal centers effectively flattens out the ligands surrounding Ag1 into a near perfectly planar environment with respect to both the donor-metal geometry and the planes of the two coordinated pyridyl rings themselves. The rings vary from being coplanar by an angle of 7.3(4) $^{\circ}$. The Ag–amine and Ag–pyridyl distances are seen to be nearly identical in this structure with ranges of 2.146(7) to 2.15(1) Å and 2.181(7) to 2.183(7) Å, respectively. The bound acetonitrile has a much longer bond to Ag1 at 2.515(9) Å. This weaker bond helps to account for the fact that this three coordinate silver is quite far from the ideal trigonal geometry with a pyridyl–Ag–pyridyl angle of 164.3(3) $^{\circ}$. The acetonitrile N–Ag–pyridyl angles are 95.8(3) and 99.9(3) $^{\circ}$. The two coordinate silvers are closer to a linear geometry with N–Ag–N angles of 172.7(4) and 174.9(9) $^{\circ}$ for Ag2 and Ag3, respectively. A smaller disordered part of these linear amine bound silvers also contains a coordinated acetonitrile that is oriented away from the center of the polymer.

It is seen that when the 1:1 ratio of 3-amp to AgBF_4 is crystallized at a lower temperature and over a longer period of time the polymeric structure of **5.1.1** is no longer the more favorable one. The structure that instead is formed, **5.1.2**, is a discrete unit that is connectively identical to its polymeric relative. A view of the folded tetramer of **5.1.2** is shown in Figure 5.3 and selected interatomic lengths and angles are given in Table 5.4. The unique portion of **5.1.2** can be thought of as one of the larger links of the chain of compound **5.1.1** truncated on either end with the dangling pyridyl ends tied together to the same silver (as opposed to a silver on an adjacent polymer unit). The macrocycle that results contains four silvers; two each bound head to head and tail to tail by four 3-amp ligands as in the original polymer. However, without the polymeric backbone stretching the ring open, the propensity of the silver to engage in its closed shell metal–metal interaction causes the loop to fold over onto itself allowing the two pyridyl-bound silvers to come to within $3.2543(8)$ Å of one another. Contrary to the metal–metal interaction seen in **5.1.1**, it is apparent that the one occurring between Ag3 and Ag4 has substantially more support by the intramolecular stacking of the π –systems. Intermolecular sandwiching of the silvers by pyridyl rings is not pronounced in this case and is made obvious by the distortions of the rings from the planarity that they displayed in the previous structure. Nitrogen–Ag distances are similar to those displayed in **5.1.1** with the amine–Ag distances again being slightly shorter and ranging from $2.111(6)$ to $2.132(5)$ Å. Pyridyl–Ag distances have lengths of $2.142(5)$ to $2.195(5)$ Å. The coordinated acetonitriles are quite different with respect to their bond strengths to the metals to which they are bound. The $\text{Ag3–N}_{\text{acetonitrile}}$ bond length is quite a bit longer at $2.609(7)$ Å than that of the $\text{Ag4–N}_{\text{acetonitrile}}$ which is $2.374(7)$ Å. Effects of this increase in bond strength

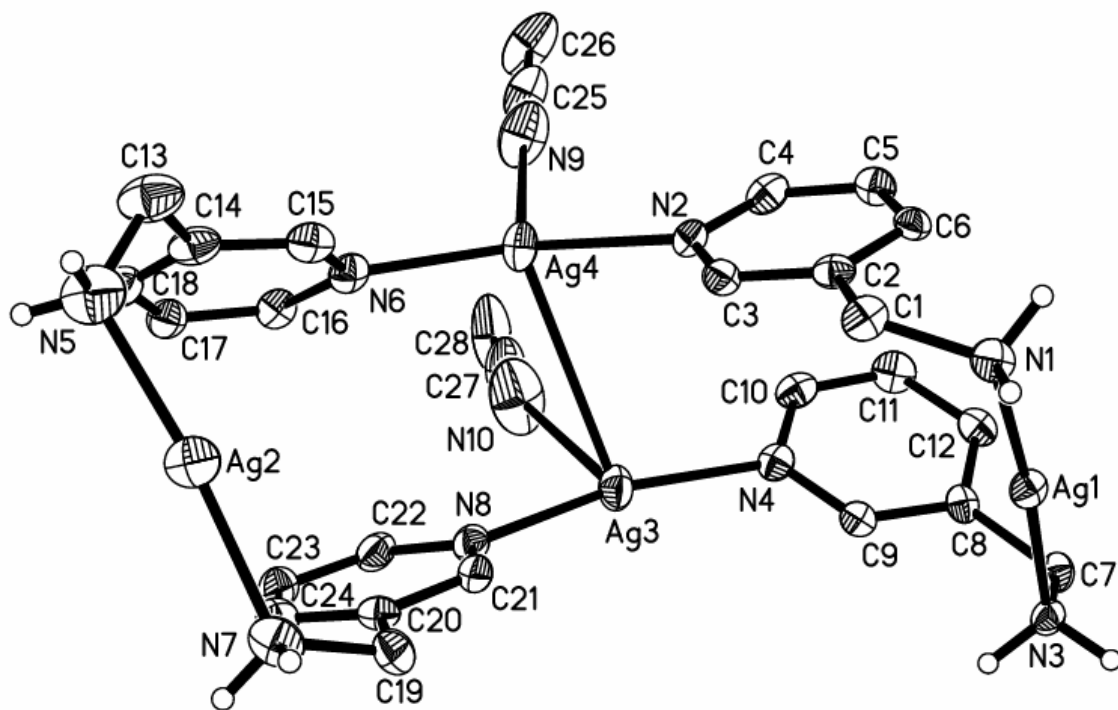


Figure 5.3. Thermal ellipsoid plot of the cationic portion of **5.1.2**. Ellipsoids are drawn at the 50 % probability level. All hydrogen atoms except for those on the amines have been removed for clarity.

Table 5.4. Selected bond lengths (\AA), angles ($^\circ$), and important distances for Poly($\text{Ag}[3\text{-amp}] \text{BF}_4$) (**5.1.2**)^a

Ag1-N1	2.130(5)	Ag1-N3	2.132(5)
Ag2-N5	2.111(6)	Ag2-N7	2.130(6)
Ag3-N8	2.142(5)	Ag3-N4	2.145(5)
Ag3-N10	2.609(7)	Ag3-Ag4	3.2543(8)
Ag4-N2	2.189(5)	Ag4-N6	2.195(5)
Ag4-N9	2.374(7)		
N5-Ag2-N7	174.4(2)	N8-Ag3-N4	163.6(2)
N8-Ag3-N10	94.8(2)	N4-Ag3-N10	101.5(2)
N8-Ag3-Ag4	84.16(1)	N4-Ag3-Ag4	104.97(1)
N10-Ag3-Ag4	62.6(2)	N2-Ag4-N6	143.53(2)
N2-Ag4-N9	102.7(2)	N6-Ag4-N9	109.5(2)
N2-Ag4-Ag3	74.31(13)	N6-Ag4-Ag3	103.89(1)
N9-Ag4-Ag3	118.16(2)	N1-Ag1-N3	174.4(2)

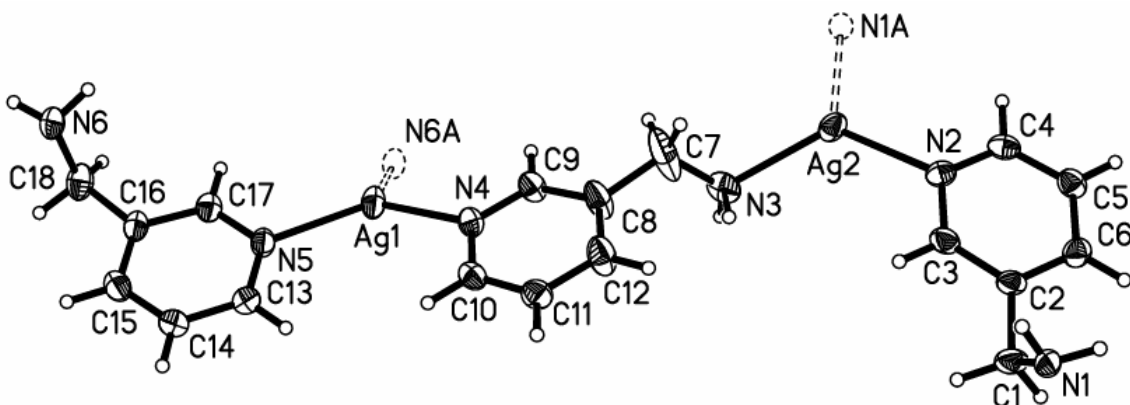


Figure 5.4. Thermal ellipsoid of the unique portion of the cationic polymer of **5.2** with the silver coordination environments shown complete. Ellipsoids are drawn at the 50 % probability level. The disorder of N3 has been removed for clarity.

Table 5.5. Selected bond lengths (\AA), angles ($^\circ$), and important distances for $\text{Ag}_2(3\text{-amp})_3(\text{BF}_4)_2$ (**5.2**)^a

Ag1-N5	2.235(3)	Ag1-N4	2.246(3)
Ag1-N6#1	2.265(3)	Ag2-N3	2.222(4)
Ag2-N1#2	2.246(2)	Ag2-N2	2.262(3)
N5-Ag1-N4	121.84(1)	N5-Ag1-N6#1	119.78(1)
N4-Ag1-N6#1	117.26(1)	N3-Ag2-N1#2	124.0(2)
N3-Ag2-N2	119.5(2)	N1#2-Ag2-N2	116.37(1)

^aSymmetry transformations used to generate atoms: #1 = x+1,y,z; #2 = x,y+1,z

are made apparent when examining the angles of the pyridyl nitrogens with respect to one another; the more constricted angle of N2–Ag4–N6 at 143.5(2) $^\circ$ is seen for Ag4 which has the shorter Ag–N_{acetonitrile} bond. The N4–Ag3–N8 angle is 163.6(2) $^\circ$. The two linearly coordinated silvers have identical N–Ag–N angles of 174.4(2) $^\circ$.

Compound **5.2** is representative of an intermediate structural motif that can be isolated when moving from the 1:1 to 2:1 ratios of 3-amp ligand to metal. When 3-amp and AgBF_4 are mixed in a 3:2 ratio the resulting two-dimensional polymer contains two different three-coordinate silver environments. As shown in Figure 5.4, the coordination

sphere of Ag1 is completed by two pyridyl donors and an amine while that of Ag2 is the opposite with a single pyridyl and two amines bound to the metal center. Selected geometric parameters for this compound are given in Table 5.5. The amp–nitrogen–only environments of the two unique silvers are both very nicely trigonal with acute ranges of N–Ag–N angles from 117.26(9) to 121.82(9) $^{\circ}$ about Ag1 and 117.7(2) to 124.9(2) $^{\circ}$ about Ag2. Both metals also sit well within their respective N–donor planes with only small deviations of 0.103(1) and 0.097(1) Å for Ag1 and Ag2, respectively. The exclusion of solvent acetonitrile from the coordination sphere of the silvers of this and the following structures is demonstrative of the contented nature of the three-coordinate silver to stay as such even in the presence of an excess of weak donors. With two similar, but distinctly different silver environments, the effects of the differences in electron donation of the amines versus the pyridines are barely made apparent. Bond lengths around Ag1 range from 2.236(3) to 2.265(3) Å, the longest of which is to an amine nitrogen. Ag2 is involved in slightly longer bonds from 2.245(2) to 2.289(5) Å, with the lengthiest bond again being with an amine donor. The central 3-amp ligand of Figure 5.4 serves to connect the two unique silver centers of the “planar” portion of the polymer. When the terminal ends of this structure are grown out, it is seen that each of the end amines serves a different purpose in the polymer. The N1 amine bridges to a symmetry equivalent, slightly offset Ag2 to construct a looping one-dimensional saw tooth polymer. The N6 “teeth” of this polymer then reach upward to join the linear sections into the two dimensional pseudocorrogated sheets shown in Figure 5.5. Interestingly, there was not seen to be a temperature dependence upon the conformation of the present structure as was seen in the 1:1 or 2:1 ratios of ligand to metal.

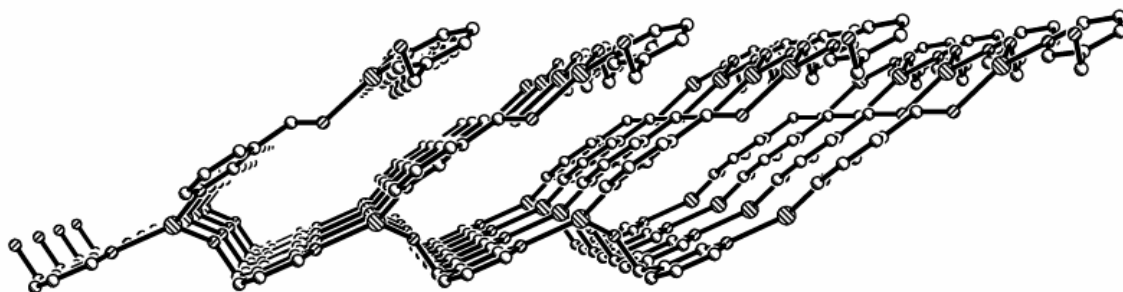


Figure 5.5. A view of the extended two-dimensional network of **5.2**. H atoms, anions and disorder have been removed for clarity.

Compounds **5.3.1** and **5.3.2** again demonstrate the ability of the bifunctional 3-amp ligand to form connectively identical coordination complexes with different topologies that are solely dependent upon the method of crystallization. Both **5.3.1** and **5.3.2** contain 3-amp and AgBF_4 in a 2:1 ratio formed from the combination of its constituents in acetonitrile, followed by recrystallization with ether. However, as was the case with compounds **5.1.1** and **5.1.2**, variances in temperature of the crystallizing solution caused pronounced structural differences in the crystals that are obtained. The results are both polymeric in nature and span one and two dimensions.

Crystallization of a 2:1 mixture of 3-amp and AgBF_4 at 5 °C produces the two-dimensional polymeric sheet of tetrahedral silvers, **5.3.1**, shown in Figure 5.6. As can be seen in the figure, there are two unique 3-amp ligands in the structure that perform separate tasks. One ligand coordinates in a head-to-tail fashion with a symmetry equivalent one to bridge two silvers into a bimetallic rectangular box. A second ligand extends outward to join each of these small units together forming larger rectangles. The resulting box-in-box motif sets two of the smaller units at opposing corners of the larger boxes. The remaining large box corners are occupied by silvers of adjacent polygons to give large hexametallic rectangles. Figure 5.7 shows the two unique ligands bound to

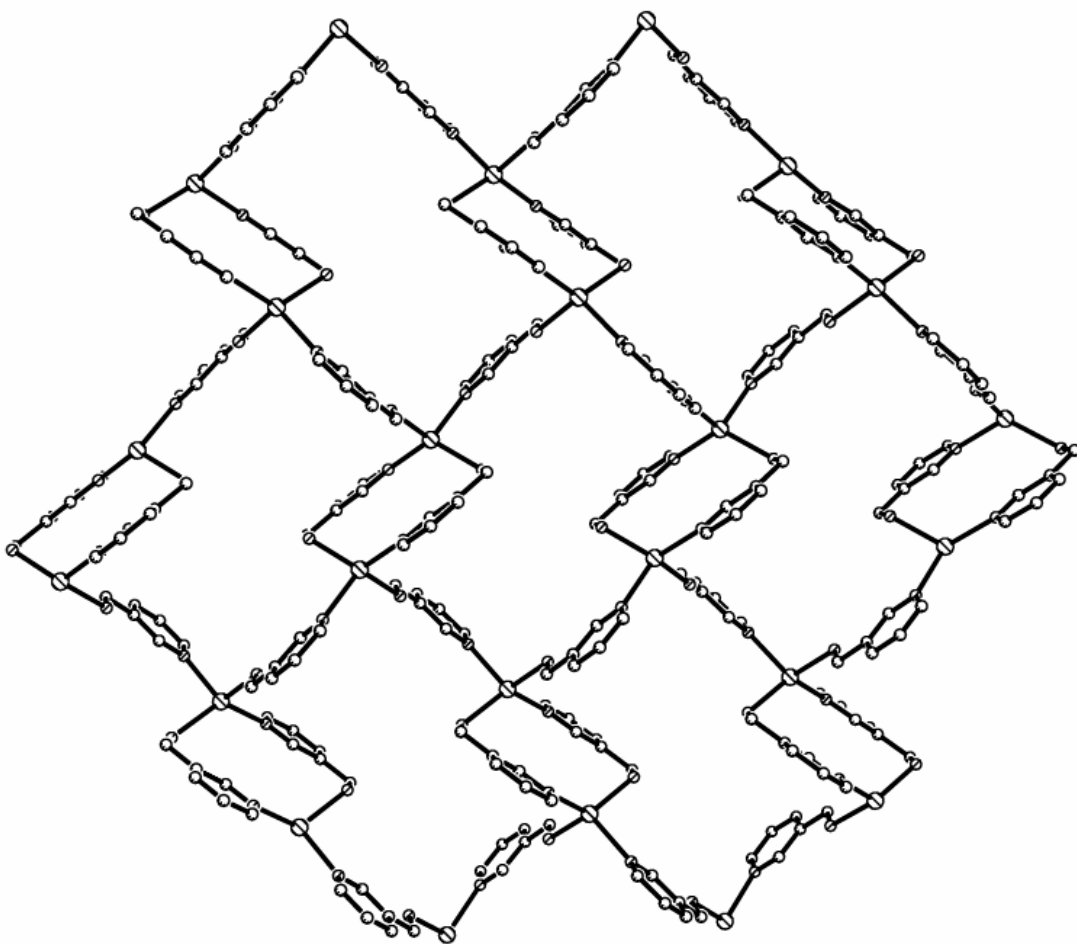


Figure 5.6. A view of the two-dimensional network of **5.3.1**. Hydrogen atoms and anions have been removed for clarity.

Ag1. The planes of the pyridyl rings manage to orient themselves parallel to one another throughout the structure, being concomitantly perpendicular to the growth of the polymer. This effectively forms a honeycomb of alternating cells one ligand thick the breadth of the polymeric sheet. It is within these cells that the BF_4^- “bees” sit, held in place by weak H–bonds to the amine hydrogens. Ligand N–Ag bond lengths lengthen with the increased coordination number with pyridyl–Ag distances of 2.305(1) to 2.377(1) Å and amine–Ag distances of 2.334(2) to 2.357(1) Å. The four donor sites available for each metal center give the silvers of **5.3.1** a slightly distorted tetrahedral

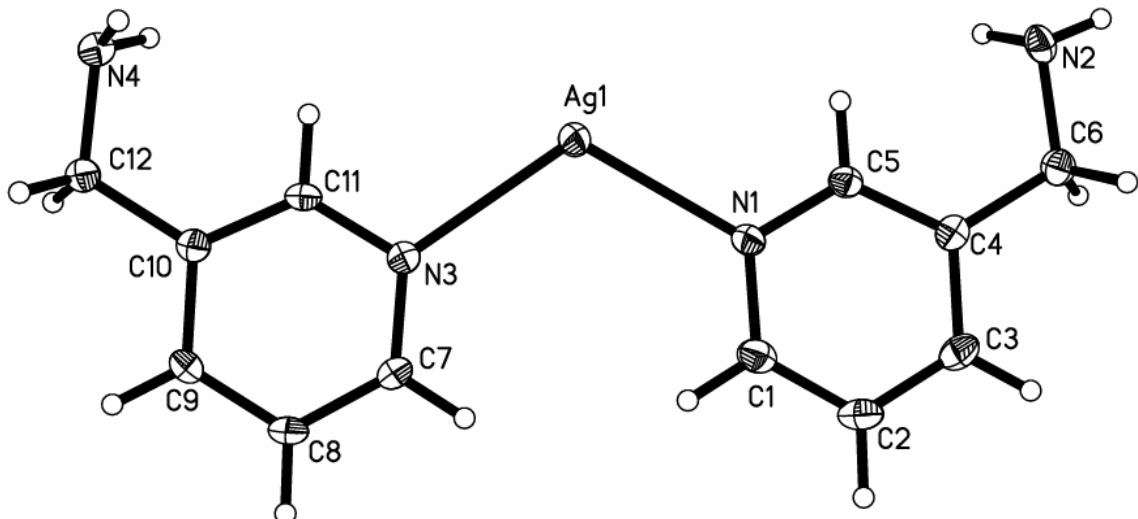


Figure 5.7. Thermal ellipsoid plot of the unique cationic portion of **5.3.1**. Ellipsoids are drawn at the 50 % probability level.

Table 5.6. Selected bond lengths (\AA), angles ($^\circ$), and important distances for $\text{Ag(3-amp)}_2\text{BF}_4$ (**5.3.1**)^a

Ag1-N1	2.3057(1)	Ag1-N2#1	2.3341(2)
Ag1-N4#2	2.3572(1)	Ag1-N3	2.3776(1)
N1-Ag1-N2#1	123.50(6)	N1-Ag1-N4#2	100.71(6)
N2#1-Ag1-N4#2	112.60(6)	N1-Ag1-N3	115.12(5)
N2#1-Ag1-N3	95.97(5)	N4#2-Ag1-N3	108.90(6)

^a Symmetry transformations used to generate equivalent atoms: #1 = $-x, -y+2, -z+1$; #2 = $-x, y+1/2, -z+1/2$.

geometry with N–Ag–N angles ranging from 95.97(5) to 123.50(6) $^\circ$. Selected

interatomic distances and angles for **5.3.1** are given in Table 5.6.

When the solution that produced compound **5.3.1** is allowed to crystallize over a longer period of time at a reduced temperature of -35 $^\circ\text{C}$ the structure that results is a degree of dimensionality less than that seen in **5.3.1**. The connectivity and activity of the ligands and metal of **5.3.2** are similar to that seen in the previous structure; one of the two unique ligands is used to construct a bimetallic head-to-tail ring while the other is used as

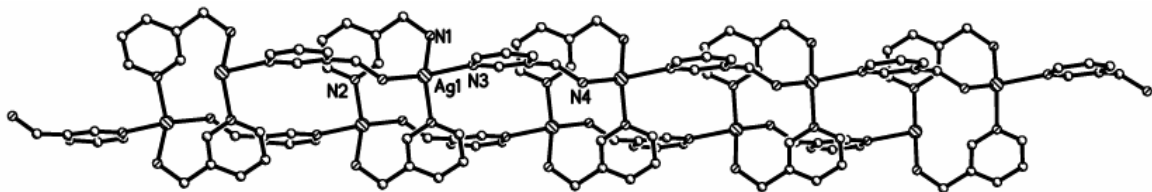


Figure 5.8. A view of the extended polymer of **5.3.2**. Hydrogen atoms have been removed for clarity.

a bridge to adjacent units. However, as seen in Figure 5.8, lower temperatures cause a constriction in the size of the larger ring that is formed by the bridging 3-amps. This smaller, more constrained bridge preferentially grows into a one-dimensional polymer as opposed to the two-dimensional network of **5.3.2**. Viewing the polymer down its long axis reveals that the structure is actually a rectangular tube that is not quite of sufficient volume to contain the anions. The BF_4^- ions instead sit within the spaces formed by the stacking of the polymers on top of one another. Figure 5.9 shows the unique portion of the polymer of **5.3.2** having the same ratio as **5.3.1**. The ligand bonds to silver are the longest displayed herein with distances of 2.438(1) to 2.381(1) Å and 2.307(1) to 2.354(1) Å for the pyridyl–Ag and amine–Ag distances, respectively. The distorted tetrahedral geometry about Ag1 is similar to that of the previous structure. N–Ag–N angles range here from 93.38(5) to 123.01(5)°. Selected bond lengths and angles for 5.3.2 are given in Table 5.7.

When 2,2'-bipyridyl (bipy) is added in at least a 1:1 ratio with silver in solutions of 3-amp and AgBF_4 it effectively stops the formation of the other structural motifs by capping each of the silvers. The polymeric motifs that were typically seen with 1:1 to 2:1 ratios of 3-amp to AgBF_4 are truncated by the chelating bipyridyls such that introduction

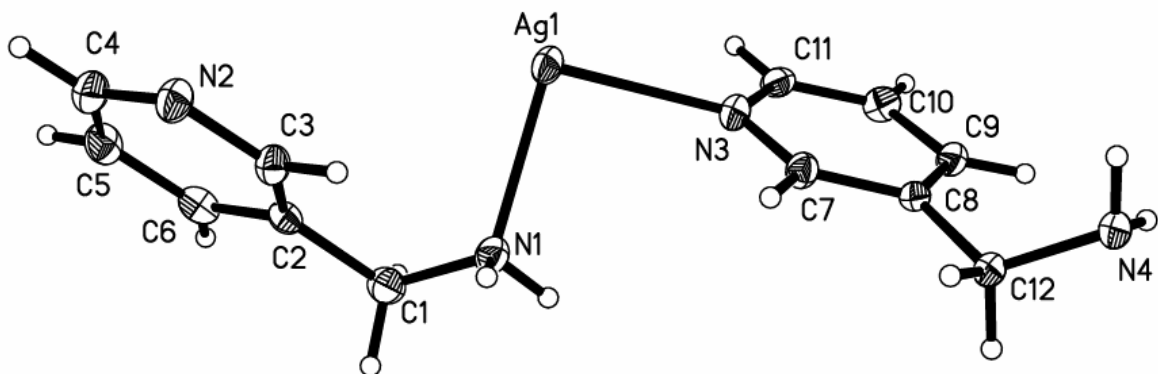


Figure 5.9. Thermal ellipsoid plot of the unique portion of the cationic polymer **5.3.2**. Ellipsoids are drawn at the 50 % probability level.

Table 5.7. Selected bond lengths (\AA), angles ($^\circ$), and important distances for $\text{Ag}(\text{3-amp})_2\text{BF}_4$ (**5.3.2**)^a

Ag1-N4#1	2.3071(1)	Ag1-N2#2	2.3482(1)
Ag1-N1	2.3537(1)	Ag1-N3	2.3807(1)
N4#1-Ag1-N2#2	109.26(5)	N4#1-Ag1-N1	123.01(5)
N2#2-Ag1-N1	108.75(5)	N4#1-Ag1-N3	114.96(5)
N2#2-Ag1-N3	105.53(5)	N1-Ag1-N3	93.38(5)

^a Symmetry transformations used to generate equivalent atoms: #1 = $x-1, y, z$; #2 = $-x+1, -y+2, -z+2$.

of 2,2'-bipy to any of the solutions that produced the previous structures gives rise to the discrete, singly 3-amp bridged structure of **5.4** shown in Figure 5.10. The 1:2:2 ratio of 3-amp to Ag to 2,2'bipy in **5.4** has been shown to be the most favorable structure available and is the one isolatable from the several different ratios of reaction mixtures. The effect is similar to that seen previously where the chelating ability of the 2-amp ligand was used to cap the ends of a would-be polymer.¹⁷⁷ A symmetry equivalent unit is held close together with the first by a silver–silver interaction of 2.9875(4) \AA . This

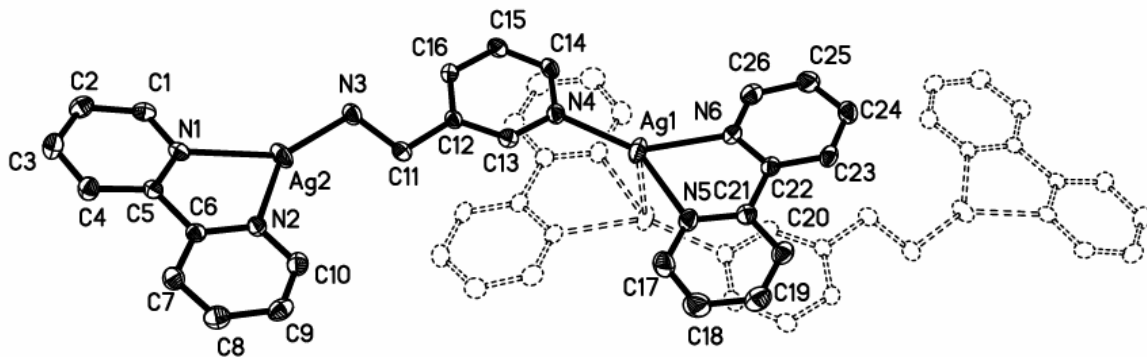


Figure 5.10. Thermal ellipsoid of the cationic structure of **5.4**. Hydrogen atoms have been removed for clarity. The symmetry equivalent portion is shown dashed.

Table 5.8. Selected bond lengths (\AA), angles ($^\circ$), and important distances for $\text{Ag}_2(2,2'\text{-bipy})_2\text{-}\mu\text{-}(3\text{-amp})(\text{BF}_4)_2$ (**5.4**)^a

Ag1-N4	2.1457(2)	Ag1-N5	2.286(2)
Ag1-N6	2.291(2)	Ag1-Ag1#1	2.9875(4)
Ag2-N3	2.1610(2)	Ag2-N2	2.287(2)
Ag2-N1	2.2908(2)		
<hr/>			
N4-Ag1-N6	141.39(7)	N5-Ag1-N6	72.81(7)
N4-Ag1-Ag1#1	98.38(5)	N5-Ag1-Ag1#1	89.30(5)
N6-Ag1-Ag1#1	83.86(5)	N3-Ag2-N2	145.57(7)
N3-Ag2-N1	141.44(7)	N2-Ag2-N1	72.90(7)
N4-Ag1-N5	145.36(8)		

^a Symmetry transformations used to generate equivalent atoms: #1 = $-x, -y+1, -z+2$

relatively short Ag–Ag interaction, which is over 0.3 \AA closer than the others described herein, is held tightly together by the resonance stacking of the three coordinated rings with those on the adjacent silver; an interaction not possible on the opposing amine bound silvers due to the protrusion of the amine hydrogens into the area of space needed for the ring stacking. Each of the Ag environments is nicely planar with respect to its surrounding nitrogens, with the bipy N–Ag–N angle of both being expectedly acute from trigonal at 72.81(7) and 72.90(7) $^\circ$ for Ag1 and Ag2, respectively. The pyridyl–Ag and

amine–Ag distances are of an average length here at 2.287(2) and 2.291(2) Å. Geometric parameters for **5.4** are given in Table 5.8.

Luminescent Properties

The compounds of this chapter were tested for photoluminescent properties as a consequence of a recent surge in interest in the use of supramolecular coordination assemblies as LEDs. Coordination polymers of the type described herein are thought to be superior to traditional organic LEDs (OLEDs) due to the enhanced structural flexibility and electronic characteristics that the d-block metals impart. The maximum excitation wavelengths for compounds **5.1.1-5.4** that are compiled in Table 5.9 are seen to be similar to that of the free 3-amp ligand, all of which are around 300 nm. It is thus surmised that the luminescent properties of these complexes have origins in a ligand based absorption followed by a ligand-to-metal charge transfer and then a metal-based decay. This is supported by the observation that the emission spectra of the metal complexes are quite far removed from that of the ligand with red-shifts of nearly 200 nm in wavelength difference in some cases. Representative spectra of the complexes **5.1.1-5.4** taken in acetonitrile glasses at 77 K are displayed in Figure 5.11. The most intense emission was seen to come from the 2:1 3-ampAgBF₄ polymers, which displays peaks in the emission spectrum at 413, 458, 489 and 546 nm. The next highest intensities come from the 1:1 and 3:2 ratios, in decreasing order. Surprisingly, the luminescence of the 3-ampAgBF₄ complex was actually quenched by the presence of the chelating 2,2'-bipyridyl ligand in compound **5.4**, with the metal complex showing a less intense spectrum than that of the free ligand.

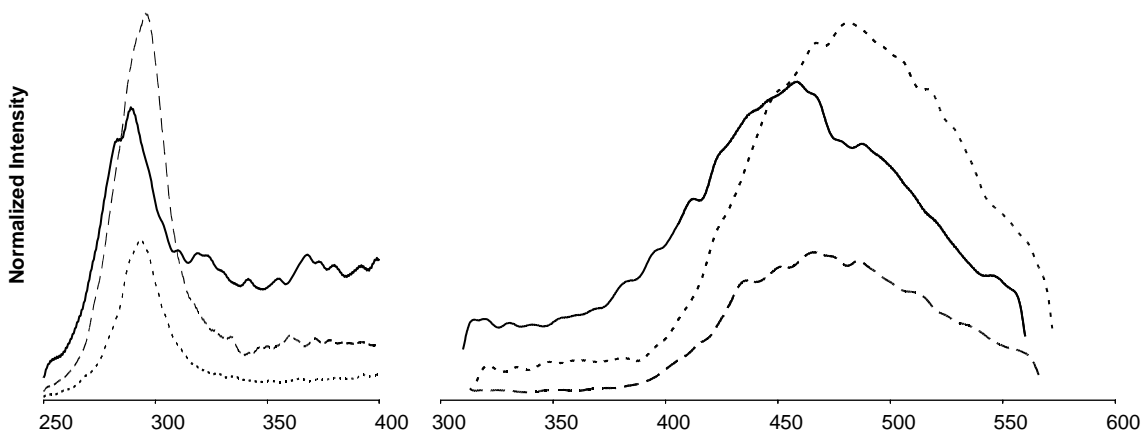


Figure 5.11. Representative Luminescence spectra of the 3-amp AgBF_4 compounds taken in acetonitrile glasses at 1×10^{-4} M concentration at 77 K. — = $\text{Ag}(3\text{-amp})\text{BF}_4$, - - - = $\text{Ag}_2(3\text{-amp})_3(\text{BF}_4)_2$, = $\text{Ag}(3\text{-amp})_2\text{BF}_4$

Table 5.9. Luminescent Spectral Data for 3-amp and the compounds **5.1.1–5.4**, at 77 K and 1×10^{-4} M in CH_3CN .^a

Compound	Excitation λ_{\max}	Emission local λ_{\min}
3-amp	313, 342	347, 365, 391
5.1.1	290	413, 458, 489, 546
5.1.2	verbatim 5.1.1	
5.2	294	436, 452, 456, 487, 513
5.3.1	297	467, 483, 518
5.3.2	verbatim 5.3.1	
5.4	328	399, 461, 505

^a Luminescence spectra were only collected once each on the two sets of structural isomers given that at the same temperature the two compounds would be structurally identical.

Conclusions

This study demonstrates that changes in the ratio of ligand to metal can have significant effects on the structural characteristics of coordination complexes of silver with a noncoordinating anion. The results of this work add to the relatively unexplored area of ratio dependence which complements nicely the well surveyed field of anion

dependent structures of the coinage metals. It was shown herein how several of the common silver structural motifs including discrete structures (**5.1.2** and **5.4**), one dimensional (**5.1.1** and **5.3.2**) and two dimensional polymers (**5.2** and **5.3.1**) can be achieved by changes in stoichiometry. It was also demonstrated how different conformations of the same ratio can be isolated by crystallization at different temperatures obtaining both a kinetic product and a more thermodynamically favored product.

Experimental

General Procedures

All experiments were carried out under an argon atmosphere, using a Schlenk line and standard Schlenk techniques. Glassware was dried at 120°C for several hours prior to use. All reagents were stored in an inert atmosphere glovebox; solvents were distilled under nitrogen from the appropriate drying agent immediately before use. 3-Aminomethylpyridine and 2,2'-bipyridine were purchased from Aldrich and used as received. Silver(I) tetrafluoroborate was purchased from Strem Chemicals Inc. and used as received. ^1H NMR spectra were recorded at 300.13 MHz on a Bruker Spectrospin 300 MHz spectrometer. Elemental analyses were performed by Atlantic Microlabs Inc., Norcross, Georgia.

General Synthesis

General procedures for the synthesis of compounds **5.1.1-5.3.2** involve the addition of a 5 mL acetonitrile solution of 3-aminomethylpyridine to a stirred solution of AgBF_4 in 5 mL acetonitrile. The mixtures are stirred for 10 minutes, then dried in vacuo

to leave white or off-white powders. All flasks are shielded from light with aluminum foil to prevent the photodecomposition of the silver compounds. Crystals of **5.1.1**, **5.2**, **5.3.1** and **5.4** were grown by layering ether over acetonitrile solutions at 5 °C. Crystals of **5.1.2** and **5.3.2** were grown by layering ether over dilute acetonitrile solutions at -35 °C. The amounts of reagents used, yields, and analytical data are presented below as well as any modifications to the general synthetic procedure. Percent yields are based upon the amount of silver salt used.

Preparations

*poly(Ag[3-amp]BF₄) (**5.1.1**) and Ag₄(3-amp)₄(BF₄)₄ (**5.1.2**).* This reaction used 3-aminomethylpyridine (0.052 g, 0.481 mmol) added to AgBF₄ (0.100 g, 0.514 mmol) to leave a white powder in 91 % yield (0.142 g, 0.464 mmol) upon evaporation of the solvent. Colorless plates of **5.1.1** were grown at 5 °C and colorless blocks of **5.1.2** were grown at -35 °C from acetonitrile and ether. ¹H NMR (CD₃CN, 298 K) δ: 3.13 s, br, 8H (-NH₂-); 3.92 s, 8H (-CH₂-); 7.47 q,d, 4H; 7.88 d,t, 8H; 8.41 d,d, 4H.

*poly-Ag₂(3-amp)₃(BF₄)₂ (**5.2**).* This reaction used 3 equivalents of 3-aminomethylpyridine (0.150 g, 1.40 mmol) added to 2 equivalents of AgBF₄ (0.180 g, 0.925 mmol). A clear, colorless oil was left upon evaporation of the solvent. Dissolution of this oil in a small amount of CH₂Cl₂ followed by precipitation with ether leaves a white fluffy solid in 88 % yield (0.290 g, 0.407 mmol) upon isolation of the precipitate. Colorless blocks were grown from acetonitrile and ether. ¹H NMR (CD₃CN, 298 K) δ: 2.93 s, br, 6H, (-NH₂-); 3.875 s, 6H, (-CH₂-); 7.38 m, 3H; 7.739 d,d, 6H; 8.34 d, 3H.

Anal. Calcd for $\text{Ag}_2\text{C}_{18}\text{H}_{24}\text{N}_6\text{B}_2\text{F}_8$: C, 30.29; H, 3.25; N, 11.77. Found: C, 30.39; H, 3.25; N, 11.56.

poly-Ag(3-amp)₂BF₄ (**5.3.1**) and *poly-Ag(3-amp)₂BF₄* (**5.3.2**). This reaction used 2 equivalents of 3-aminomethylpyridine (0.150 g, 1.40 mmol) added to AgBF_4 (0.135 g, 0.694 mmol). Evaporation of the solvent left a white powder in 84% yield (0.239 g, 0.583 mmol). Colorless plates of **5.3.1** were grown at 5 °C and colorless blocks of **5.3.2** were grown at -35 °C from acetonitrile and ether. ¹H NMR (CD₃CN, 298 K) δ: 3.20 s, br, 4H, (-NH₂-); 3.90 s, 4H, (-CH₂-); 7.42 m, 2H; 7.86 t,d, 4H; 8.32 d, 2H. Anal. Calcd for $\text{AgC}_{12}\text{H}_{16}\text{N}_4\text{BF}_4$: C, 35.07; H, 3.92; N, 13.63. Found: C, 35.20; H, 3.84; N, 13.51.

Ag₂(2,2'-bipy)₂-μ-(3-amp)(BF₄)₂ (**5.4**). To a stirred solution of one equivalent of 3-aminomethylpyridine (0.100 g, 0.926 mmol) in 5 mL CH₃CN was added 2 equivalents of AgBF_4 (0.360 g, 1.82 mmol) in 5 mL CH₃CN. This was stirred for 5 minutes then a solution of 2,2'-bipyridine (0.289 g, 1.82 mmol) in 5 mL CH₃CN was added. This mixture was stirred for 10 minutes then the solvent was removed in vacuo to leave a light yellow powder in 92 % yield (0.689 g, 0.848 mmol). Crystallization from acetonitrile and ether formed colorless blocks. ¹H NMR (CD₃CN, 298 K) δ: 2.48 s, br, 2H, (-NH₂-); 3.79 s, 2H, (-CH₂-); 7.42 m, 8H; 7.89 t, 9H; 8.26 d, 2H; 8.55 d, 1H. Anal. Calcd for $\text{Ag}_2\text{C}_{29}\text{H}_{28}\text{N}_7\text{B}_2\text{F}_8$: C, 40.32; H, 3.27; N, 11.35. Found: C, 40.68; H, 3.26; N, 11.20.

Crystallography

A summary of crystallographic experimental data for **5.1.1** through **5.4** is given in Table 5.10. Complete listings of bond lengths and angles can be found in Appendix B, Tables B.14 to B.19. Crystallographic data were collected on crystals with dimensions

Table 5.10. Crystallographic Data for compounds **5.1.1** to **5.4**

	5.1.1	5.1.2	5.2	5.3.1	5.3.2	5.4
Formula	C ₁₄ H ₁₉ Ag ₂ B ₂ F ₈ N ₅ O	C ₂₈ H ₃₈ Ag ₄ B ₄ F ₁₆ N ₁₀	C ₁₈ H ₂₄ Ag ₂ B ₂ F ₈ N ₆	C ₁₂ H ₁₆ AgBF ₄ N ₄	C ₁₂ H ₁₆ AgBF ₄ N ₄	C ₂₆ H ₂₄ Ag ₂ B ₂ F ₈ N ₆
Formula weight	662.68	1293.40	713.79	410.97	410.97	809.87
a (Å)	13.592(2)	7.8143(7)	6.850(1)	15.318(1)	8.6991(4)	7.1224
b (Å)	27.841(3)	25.736(2)	8.409(1)	10.489(1)	14.1060(7)	10.618(1)
c (Å)	13.281(2)	21.193(2)	11.598(1)	18.819(2)	12.9311(7)	19.166(2)
α			110.934(6)			92.490(5)
β (°)	113.100(2)	96.381(2)	97.226(6)		109.607	96.249(5)
γ (°)			96.238(6)			93.248(5)
space group	C2/m	P2 ₁ /c	P1	Pbca	P2 ₁ /c	P-1
D _{calcd} (g cm ⁻³)	1.973	2.028	1.941	1.805	1.826	1.872
μ (mm ⁻¹)	1.781	1.929	1.685	1.375	1.391	1.444
2 θ _{max} (°)	51.36	52.7	53.06	52.9	52.74	56.56
reflns measured	12024	36620	15095	40167	29846	21440
reflns used (R _{int})	4433 (0.0463)	8655 (0.0436)	4220 (0.0259)	3087 (0.0391)	3040 (0.0316)	6988
restraints/param	10/378	6/574	5/329	0/211	0/199	10/443
R1, [I>2σ(I)]	0.0679	0.0530	0.0185	0.0187	0.0155	0.0291
wR ² , [I>2σ(I)]	0.1730	0.1156	0.0476	0.0452	0.0413	0.0638
R(F _o ²), (all data)	0.0980	0.0655	0.0187	0.0274	0.0171	0.0433
R _w (F _o ²), (all data)	0.1959	0.1215	0.0478	0.0471	0.0420	0.0663
GooF on F ²	1.037	1.128	1.060	1.069	1.080	1.075

$0.128 \times 0.091 \times 0.062$ mm for **5.1.1**, $0.091 \times 0.105 \times 0.192$ mm for **5.1.2**, $0.200 \times 0.210 \times 0.350$ mm for **5.2**, $0.046 \times 0.112 \times 0.232$ mm for **5.3.1**, $0.151 \times 0.222 \times 0.232$ mm for **5.3.2** and $0.062 \times 0.169 \times 0.177$ mm for **5.4**. Data were collected at 110 K on a Bruker X8 Apex diffractometer using MoK α radiation ($\lambda = 0.71073$ Å). All structures were solved by direct methods after the correction of the data using SADABS.¹³⁹ All of the data were processed using the Bruker AXS SHELXTL software, version 6.10.¹⁴⁰ Unless otherwise noted, all non-hydrogen atoms were refined anisotropically and hydrogen atoms were placed in calculated positions. The crystal structure of compound **5.1.1** contains two molecules of water, one of which is disordered over two positions. It also contains a disordered amine and silver atom with a 37:63 occupancy ratio. The smaller occupancy disorder contains a coordinated acetonitrile and which is refined isotropically along with the silver and nitrogen. The crystal structures of compounds **5.1.2** and **5.4** both contain BF₄⁻ anions disordered over two positions. One of the amine nitrogens in the structure of compound **5.2** is disordered over two positions.

CHAPTER SIX

Silver(I) 3-aminomethylpyridine Complexes Part 2: Effect of Ligand Ratio, Hydrogen bonding and π -stacking with an Interacting Anion

Introduction

Advances that are being made in the field of crystal engineering have numerous applications including catalysis, molecular recognition, molecular sieving, separations and optics.^{10,63,83,176} A large portion of the knowledge associated with this area can be attributed to coordination studies of the group 11 metals, silver in particular.^{4,7,11,35,49,88,142,148,151-154,159,177} Coordination complexes of silver are known to be alterable via several methods; typically by changes in ligand geometry, rigidity or functionality or by modifications to the counterion or solvent system.^{25,141,147} Despite the wealth of literature that is to be had on methods of forcing variations in coordination complexes the technique of stoichiometry control has gone largely overlooked.^{68,69} Only recently has our group and a few others endeavored to give a comprehensive exploration on the ratio dependence of coordination complexes of variable-coordination metals.^{70,71,91,177-179,182}

Herein we describe the remarkable changes in structure that can be achieved through variances in relative amount of ligand to metal in the presence of the interacting anions OTf^- and tfa^- . Both of these anions have been previously shown to affect the supramolecular growth of coordination complexes of silver through direct interaction with the metal as well as H–bonding when a suitable donor is present. In the present study, both the degree of interaction of the anion with the metal and the degree of

H–bonding existing are themselves controlled by the ratio in which the heterobidentate 3-aminomethylpyridine ligand is present. The coordination sphere of the metal and, as a result, the overall structural growth are seen to be readily altered by the addition of a greater than stoichiometric amount of 3-amp ligand.

Results and Discussion

Synthesis

The 3-aminomethylpyridine complexes **6.1–6.4** are the result of the direct reaction of 3-amp with either of the two silver salts, triflate or trifluoroacetate. All of the compounds synthesized herein are isolable as white or off-white powders that appear to be stable indefinitely when kept shielded from light in a sealed container. In the presence of light compounds **6.1–6.6** tend to photodecompose over time. Analytical data for these compounds are presented in Tables 6.1 and 6.2. The ratios of ligand to metal in the crystal structures are easily controlled by varying the stoichiometry in which the reactants are mixed. Interestingly, the intermediate 3:2 ratio of 3-amp ligand to metal that we have been able to isolate using 2-amp¹⁷⁷ and again with 3-amp¹⁷⁸ and a non-interacting anion has been so far elusive in the current case using a more coordinating anion. Both 1:1 and 2:1 ratios of 3-amp to silver were achieved with AgOTf and Agtfa by reaction in the correct proportions followed by crystallization. The bipyridyl complexes **6.5** and **6.6** were formed by the addition of 2,2'-bipyridine to solutions of 3-amp and the appropriate silver salt. It is interesting to note that when bipyridine is present in a 1:1 ratio with Ag a tetrahedral metal environment seems unfavorable. They are instead all trigonal even with an excess of 3-amp which, when used, must be removed in order to obtain a solid.

Table 6.1. Analytical and Physical Data

	compound ^a	yield (%)	analytical (%) ^b		
			C	H	N
6.1	poly-[Ag(3-amp)tfa]	91	29.4 (29.2)	2.4 (2.5)	8.4 (8.5)
6.2	poly-[Ag(3-amp)OTf]	96	26.2 (25.8)	2.3 (2.5)	8.8 (8.6)
6.3	poly-[Ag(3-amp) ₂ tfa]	73	38.2 (38.4)	3.6 (3.7)	12.5 (12.8)
6.4	poly-[Ag(3-amp) ₂ Otf]	73	33.2 (33.0)	3.2 (3.4)	11.8 (11.8)
6.5	poly-[Ag ₂ (2,2'-bipy) ₂ -μ-(3-amp)(tfa) ₂]	92	40.5 (40.5)	2.8 (2.8)	9.4 (9.3)
6.6	Ag ₂ (2,2'-bipy) ₂ -μ-(3-amp)(OTf) ₂	89	36.0 (36.0)	2.7 (2.6)	9.4 (9.0)

^a All compounds are white or off white solids. ^b Calculated values are given in parenthesis.

Table 6.2. Hydrogen-1 NMR Data

	$^1\text{H}/\delta^{\text{a}}$
6.1	3.19 s, br, 2H, (-NH ₂); 3.89 s, 2H, (-CH ₂); 7.41 m, 1H; 7.83 t,d, 2H; 8.45 d, 1H
6.2	3.00 s, br, 2H, (-NH ₂); 3.87 s, 2H, (-CH ₂); 7.43 m, 1H; 7.81 t,d, 2H; 8.49 m, 1H
6.3	3.27 s, br, 4H, (-NH ₂); 3.85 s, 4H, (-CH ₂); 7.31 m, 2H; 7.78 t,d, 4H; 8.43 d, 2H
6.4	3.02 s, br, 4H, (-NH ₂); 3.89 s, 4H, (-CH ₂); 7.38 m, 2H; 7.78 t,d, 4H; 8.47 d, 2H
6.5	3.91 s,br, 2H, (-NH ₂); 4.75 s, 2H, (-CH ₂); 7.40 m, 8H; 7.89 m, 9H; 8.10 d, 2H; 8.55 d, 1H
6.6	4.22 s,br, 2H, (-NH ₂); 4.82 s, 2H, (-CH ₂); 7.55 m, 8H; 8.05 m, 9H; 8.26 d, 2H; 8.65 d, 1H

a ^1H NMR spectra were recorded in CD₃CN at 298 K.

X-Ray Crystal Structures

The crystal structures of compounds **6.1** to **6.6** contain the silver(I) cation in a variety of settings and with coordination numbers from 2 to 5. This variability in structure and bonding is demonstrative of the effects of two variables that were explored herein: anion dependence and ratio dependence of structural features. The former has been thoroughly explored and is a well documented feature of the coordination chemistry of the group 11 triad while the latter, still in its infancy, has only recently aroused interest and, as a result, is still relatively unknown. It is seen that by using anions with comparable basicity and structure (triflate versus trifluoroacetate) small changes in geometry around the H-bonding oxygen containing portion of the anion can have drastic effects on the dimensionality of the resulting complexes, particularly in the current case where the ligand used has the strongly H-bonding amine functionality. Perhaps even more interesting is the observation that these same types of structural reformations can be had by simply changing the ratio of ligand to metal in the reactions. These alterations are very pronounced in the following silver(I) complexes due to the ease with which it varies its coordination sphere to accept the number of donors present. A feature that is seen to occur with the non-interacting tetrafluoroborate anion but was not observed here is the temperature dependence of morphology caused by lowering the crystallization temperature. In the present case strong H-bonding to the anions likely overwhelms any temperature effects that would be had on the structures.

The structures of compounds **6.1** and **6.2** both contain the ligand 3-amp and a silver(I) salt in a 1:1 ratio. Differences between the two structures stem from the

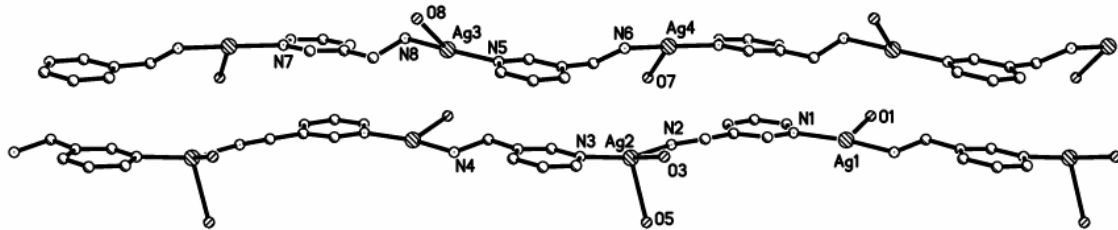


Figure 6.1. A view of the charge separated polymers of **6.1**. Only the bound oxygens are shown and all H atoms except for those of the amines have been removed for clarity.

coordinating ability as well as the H-bonding geometry of the trifluoroacetate anion versus triflate, with the result being either a one- or two-dimensional polymer.

When 3-amp is reacted in a 1:1 ratio with Agtfa the lack of sufficient donors from the ligand to fill out the coordination sphere allows the anion to crowd the metal and coordinate through the oxygen atoms. As a result, the two inequivalent polymers of **6.1**, shown in Figure 6.1, are formed. The 3-amp ligand coordinates in a head-to-tail fashion down the length of both polymers which are differentiated from one another by the degree of interaction of the anions with the silvers contained within each strand. It is seen that one contains three coordinated anions (O1, O3, and O5) for each two silvers of the chain while the adjacent polymer contains only one (O7) per two silvers. Consequently the former polymer has associated with it a negative charge and the latter a positive one. They are then stacked so that two of the cationic strands are adjacent to one another bridged by the single coordinated anion. These are then bordered on either side by the anionic polymers. The unique part of these polymers is shown in Figure 6.2 and geometric parameters are given in Table 6.3. As a general trend on the singly anion-bound silvers (those of the cationic strand and Ag1), the Ag–amine distances are quite similar to the the Ag–pyridyl distances with bond lengths of 2.147(2) to 2.161(2) Å and 2.157(2) to 2.164(2) Å, respectively. For Ag2, which has two closely associated anions,

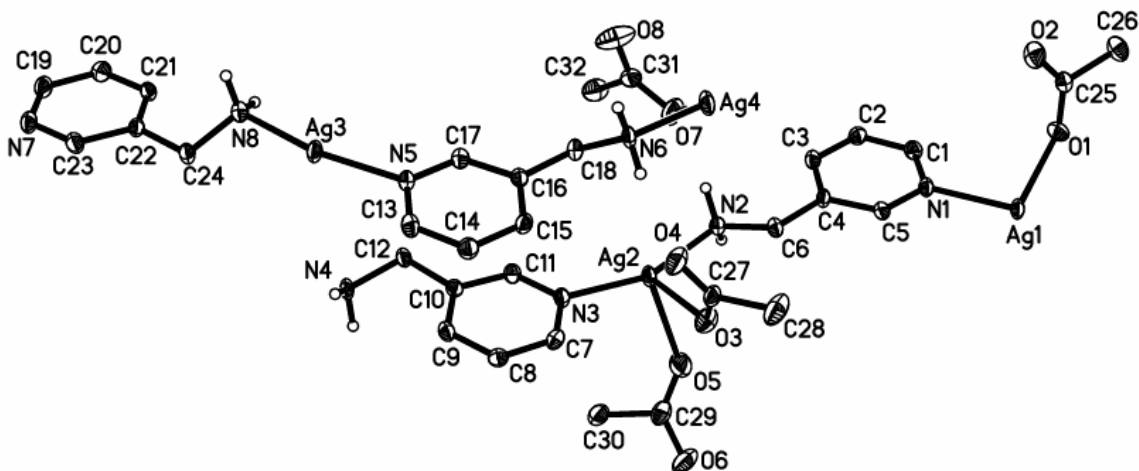


Figure 6.2. Thermal ellipsoid view of the unique portion of compound **6.1**. The fluorine atoms and all hydrogens except for those on the amines have been removed for clarity. Ellipsoids are drawn at the 50 % probability level.

Table 6.3. Selected bond lengths (\AA), angles ($^{\circ}$), and important distances for $\text{Ag}(3\text{-amp})\text{tfa}$ (**6.1**)^a

Ag(1)-N(4)#1	2.147(2)	Ag(1)-N(1)	2.157(2)
Ag(1)-O(1)	2.542(2)	Ag(2)-N(3)	2.165(2)
Ag(2)-N(2)	2.177(2)	Ag(2)-O(5)	2.585(2)
Ag(2)-O(3)	2.595(2)	Ag(3)-N(5)	2.158(2)
Ag(3)-N(8)	2.161(2)	Ag(3)-O(8)#2	2.549(2)
Ag(4)-N(6)	2.153(2)	Ag(4)-N(7)#1	2.164(2)
Ag(4)-O(7)	2.567(2)		
N(4)#1-Ag(1)-N(1)	165.07(9)	N(4)#1-Ag(1)-O(1)	98.49(8)
N(1)-Ag(1)-O(1)	96.42(8)	N(3)-Ag(2)-N(2)	159.12(9)
N(3)-Ag(2)-O(5)	106.28(8)	N(2)-Ag(2)-O(5)	89.35(8)
N(3)-Ag(2)-O(3)	93.01(8)	N(2)-Ag(2)-O(3)	101.03(8)
O(5)-Ag(2)-O(3)	89.54(7)	N(5)-Ag(3)-N(8)	164.27(9)
N(5)-Ag(3)-O(8)#2	101.33(9)	N(8)-Ag(3)-O(8)#2	92.93(9)
N(6)-Ag(4)-N(7)#1	166.19(9)	N(6)-Ag(4)-O(7)	104.56(8)
N(7)#1-Ag(4)-O(7)	87.20(8)		
N(2)-H(2A)...O(1)#5	3.024(3)	N(2)-H(2B)...O(7)	2.870(3)
N(4)-H(4A)...O(6)#6	2.914(3)	N(4)-H(4A)...O(5)#6	3.359(4)
N(4)-H(4B)...O(3)#6	3.001(3)	N(6)-H(6A)...O(4)	2.886(3)
N(6)-H(6B)...O(2)#7	3.126(3)	N(8)-H(8A)...O(4)#3	3.109(3)
N(8)-H(8B)...O(2)#4	2.907(3)		

^a Symmetry transformations used to generate atoms: #1 = $x, y+1, z$; #2 = $x-1/2, -y+1/2, -z$ #3 = $x+1/2, -y+1/2, -z$; #4 = $x, y-1, z$; #5 = $-x+2, y-1/2, -z+1/2$; #6 = $-x+1, y-1/2, -z+1/2$; #7 = $x-1/2, -y+3/2, -z$.

the Ag–N distances are, as expected, slightly above the average lengths at 2.165(2) Å for Ag₂–N₃(pyridyl) and 2.1774(2) Å for Ag₂–N₂(amine). Another result of the close association of two anions with Ag₂ is a greater distortion of its N–Ag–N angle from linear at 159.12(9) °. The remaining 3 unique silvers (Ag1, Ag3, and Ag4) have N–Ag–N angles ranging from 164.27(9) to 166.19(9) °. Hydrogen bonding between the anions and amines also assist in holding the chains together.

Upon changing to the less strongly coordinating triflate anion a 1:1 ratio of 3-amp with Ag(I) still results in the formation of polymers containing two distinctly different types of metal center. However, in this case the differences are not caused by coordinating anions but rather by the preference of the ligand to coordinate in a head-to-head fashion. The unique portion of complex **6.2**, displayed in Figure 6.3 with geometric parameters given in Table 6.4, shows these two coordinatively different silvers; one bound by amines only and the other by pyridyls only but both linearly coordinated by the N-donors. We have demonstrated this type of donor segregation of the aminomethylpyridine ligand in our previous study of non-interacting anions. In a fashion similar to that described in the preceding work, it is seen that the two pyridyl donors of the pyridyl-only bound silvers manage to orient themselves in a nearly coplanar arrangement allowing two metals from adjacent polymers to come close enough to one another to form a closed shell metal–metal interaction. In this instance (more than in the previous) the interaction appears to be supported by interpolymeric π-stacking of the pyridyl rings which helps hold the metals to within 3.1820(4) Å of one another. The effect that this interaction has is to join the would-be isolated polymers into two-dimensional sheets linked at every other silver to a neighboring polymer on either side of

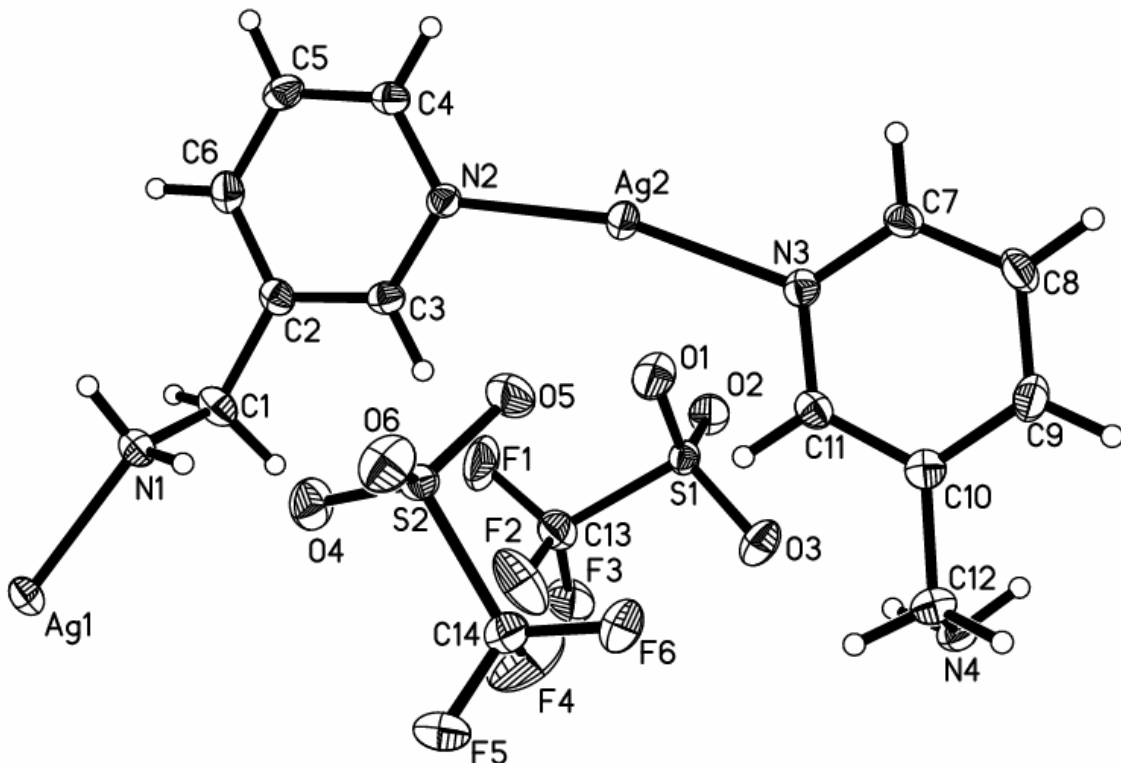


Figure 6.3. Thermal ellipsoid plot of the unique portion of the polymer **6.2**. Ellipsoids are drawn at the 50% probability level.

Table 6.4. Selected bond lengths (\AA), angles ($^\circ$), and important distances for Ag(3-amp)OTf (**6.2**)^a

Ag1-N4#1	2.1235(2)	Ag1-N1	2.1283(2)
Ag2-N2	2.1640(2)	Ag2-N3	2.1675(2)
Ag2-Ag2#2	3.1820(4)		
N4#1-Ag1-N1	177.85(8)	N2-Ag2-N3	165.38(7)
N2-Ag2-Ag2#2	83.98(5)	N3-Ag2-Ag2#2	101.56(5)
N4-H4A...O6	3.144(3)	N4-H4A...O4	3.090(3)
N4-H4B...O3	3.001(3)	N1-H1A...O2#3	3.022(3)
N1-H1B...O4#3	3.010(3)		

^a Symmetry transformations used to generate atoms: #1 = $x-1, -y+3/2, z+1/2$; #2 = $-x, -y+1, -z+1$; #3 = $x-1, y, z$.

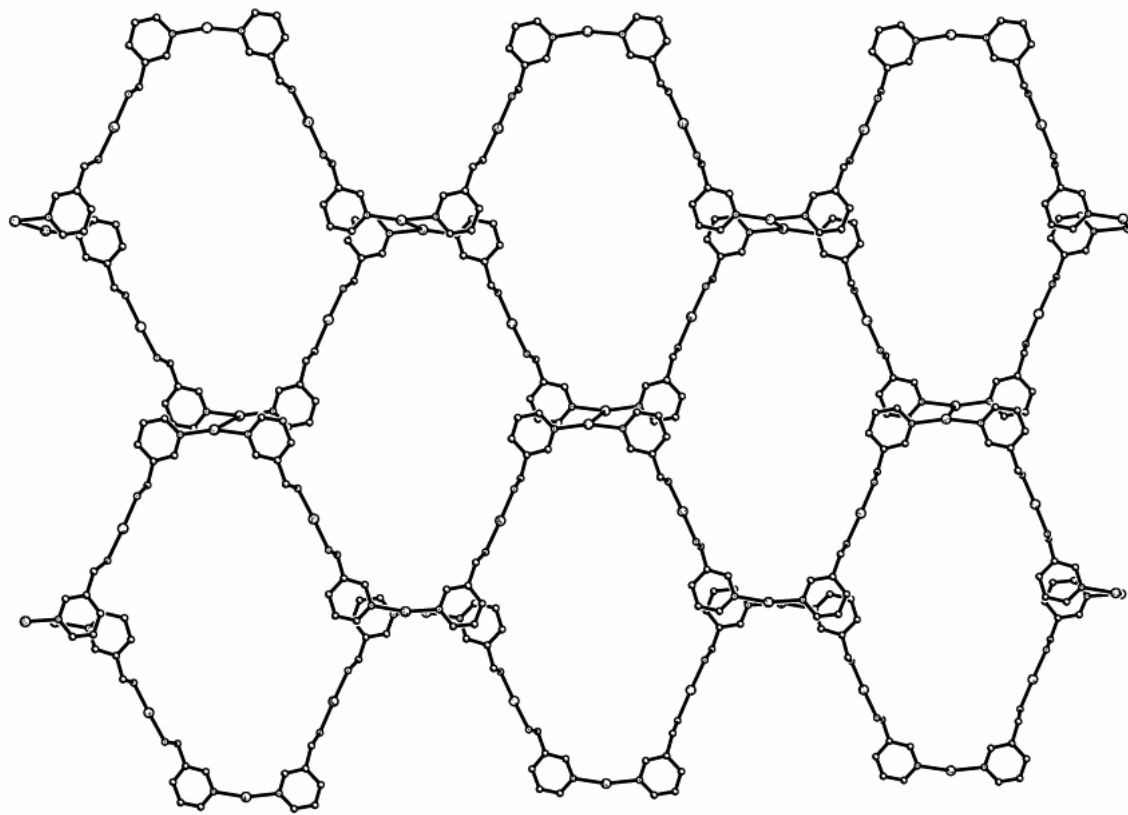


Figure 6.4. Expanded view of the 2-Dimensional growth of the cationic polymer of **6.2**.

the original. As shown in Figure 6.4, the resulting sheets exhibit a staggered array of interlaced hexagons similar to that of a chain-link fence. Adding a third dimension to this structure is the activity of the anion which sits inside the cavities of the fence connecting stacked layers using H-bonds to the amine nitrogens. The $\text{Ag}-\text{N}_{\text{amine}}$ and $\text{Ag}-\text{N}_{\text{pyridyl}}$ bonds distances are quite similar in this case with respective values of 2.123(2) to 2.128(2) Å and 2.164(2) to 2.168(2) Å for the two sets. The $\text{N}-\text{Ag}-\text{N}$ angle of Ag2 is slightly more off-linear at 165.38(7) ° than that of Ag1 due to the distortion of the pyridyl rings away from the $\text{Ag}-\text{Ag}$ interaction. Ag1, which has no such distortion, is very nearly linear in its coordination environment with an $\text{N}-\text{Ag}-\text{N}$ angle of 177.85(8) °.

Compounds **6.3** and **6.4** again contain the anions trifluoroacetate and triflate. However, altering the ratios of ligand to metal from 1:1 to 2:1 has profound effects on the coordination environment of the metal as well as the dimensionality of the coordination polymers that result. The linear charge-separated polymers of **6.1** grow into the square nets of **6.3** while the two-dimensional chain-link fence of **6.2** morphs into the three-dimensional network of **6.4**. It is also interesting to note that the 3-amp Ag complexes of OTf⁻ and tfa⁻ have been as yet unobtainable in the 3:2 ratio that is readily crystallized in the case of the non-interacting anion BF₄⁻.¹⁷⁸

In the presence of more than one equivalent of 3-amp ligand the stronger amine and pyridyl donors readily displace the weakly bound tfa⁻ anions from the metals of **6.1** to form a tetrahedral environment of only N-donors. These 4-coordinate silvers sit at the corners of squares that are then woven into the net of **6.3** shown in Figure 6.5. The walls of the “squares” are constructed of bridging 3-amp ligands that coordinate head-to-tail with the previous ligand when the polymerization is followed in any one direction. The anion, though no longer coordinating, still influences the overall structure of the polymer through H-bonding to the amine nitrogens. Similar in mannerism to the vertical supports in a wall, the tfa⁻ anions sit within the cavities of the polymer bridging two opposing parallel “walls” η^2,μ_2- via H-bonds. The unique cationic portion of this structure is shown in Figure 6.6 and selected bond lengths and angles are given in Table 6.5. In this instance, a much better distinction can be made between the amine–Ag and pyridyl–Ag bonds based upon distance than in the previous cases where all of the N–donor–silver distances were more or less similar. The Ag–amine bonds range in lengths from 2.285(1) to 2.303(1) Å and are slightly shorter than those to pyridyl donors; these have distances

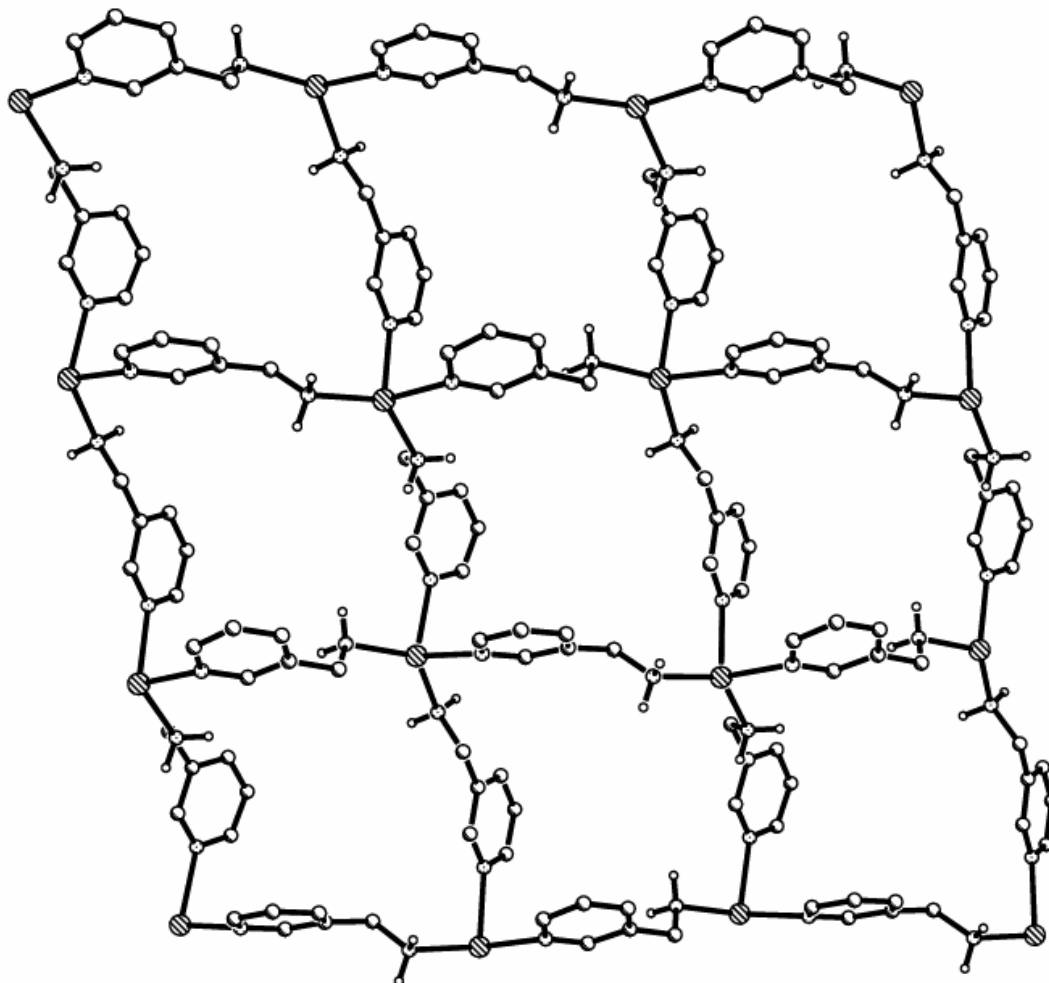


Figure 6.5. A view of the 2-dimensional cationic network of **6.3**. All H atoms except for those on the amines have been removed for clarity.

of 2.376(1) to 2.446(1) Å. The environment of Ag1 is distorted from the ideal tetrahedral geometry by the H-bonded supports of the anions showing a range of N–Ag–N angle from 93.80(4) to 130.93(4) °.

Two equivalents of 3-amp ligand has the same effect of taking a metal from a two coordinate environment to one that is pseudotetrahedral in the case of AgOTf as it did with Agtfa. The four N-donors for each silver surround the metal in a manner so that the unique portion of compound **6.4**, shown in Figure 6.7, is similar in appearance to that of **6.3**. However, H-bonding to the anion again plays a part in determining the overall

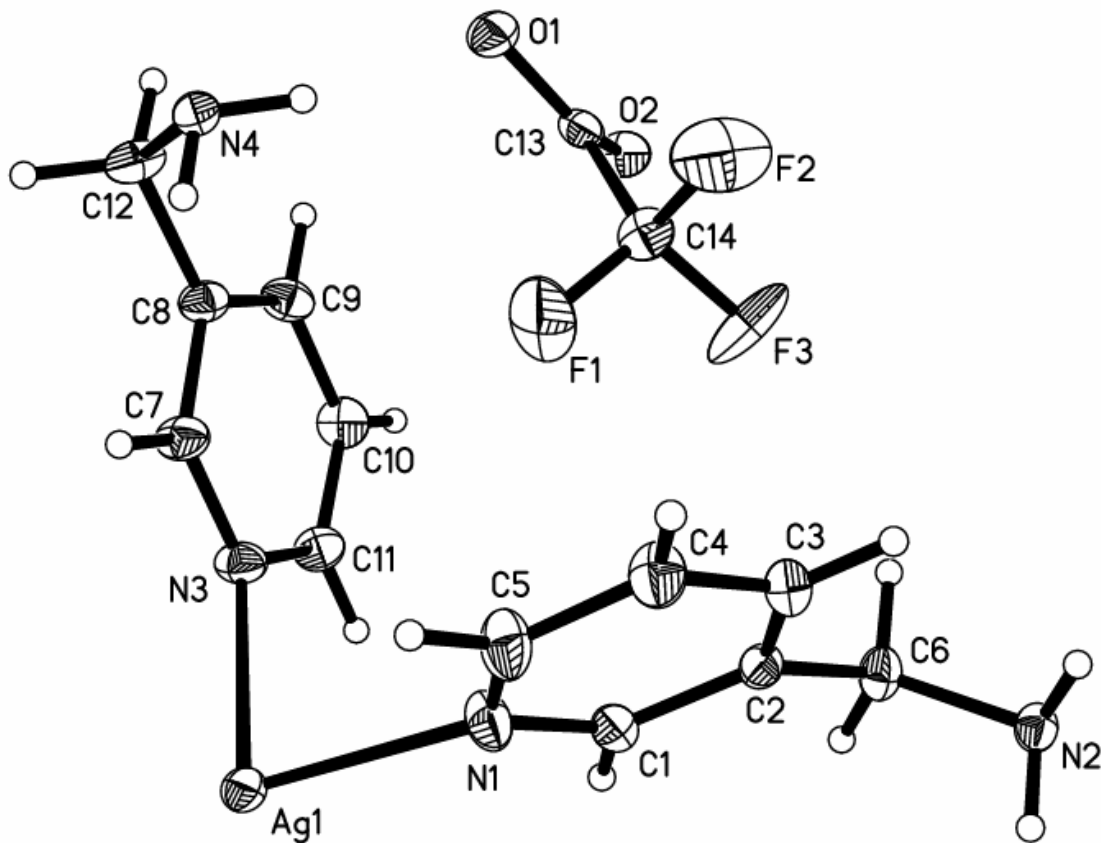


Figure 6.6. Thermal ellipsoid plot of the unique portion of **6.3**. Ellipsoids are drawn at the 50 % probability level.

Table 6.5. Selected bond lengths (\AA), angles ($^{\circ}$), and important distances for $\text{Ag}(\text{3-amp})_2\text{tfa}$ (**6.3**)^a

Ag1-N2\#1	2.2851(1)	Ag1-N4\#2	2.3028(1)
Ag1-N3	2.3765(1)	Ag1-N1	2.4460(1)
N2\#1-Ag1-N4\#2	130.93(4)	N2\#1-Ag1-N3	113.77(4)
N4\#2-Ag1-N3	99.83(4)	N2\#1-Ag1-N1	103.69(4)
N4\#2-Ag1-N1	108.81(4)	N3-Ag1-N1	93.80(4)
N2-H2A...O2\#3	3.0692(1)	N2-H2B...O2\#5	3.0282(1)
N4-H4A...O1\#6	3.1528(1)	N4-H4B...O1\#4	3.1525(1)

^a Symmetry transformations used to generate atoms: #1 = $-x+3/2, y-1/2, -z+1/2$; #2 = $-x+1/2, y-1/2, -z+1/2$; #3 = $-x+3/2, y+1/2, -z+1/2$; #4 = $-x+1/2, y+1/2, -z+1/2$; #5 = $x+1/2, -y+3/2, z+1/2$; #6 = $x, y+1, z$.

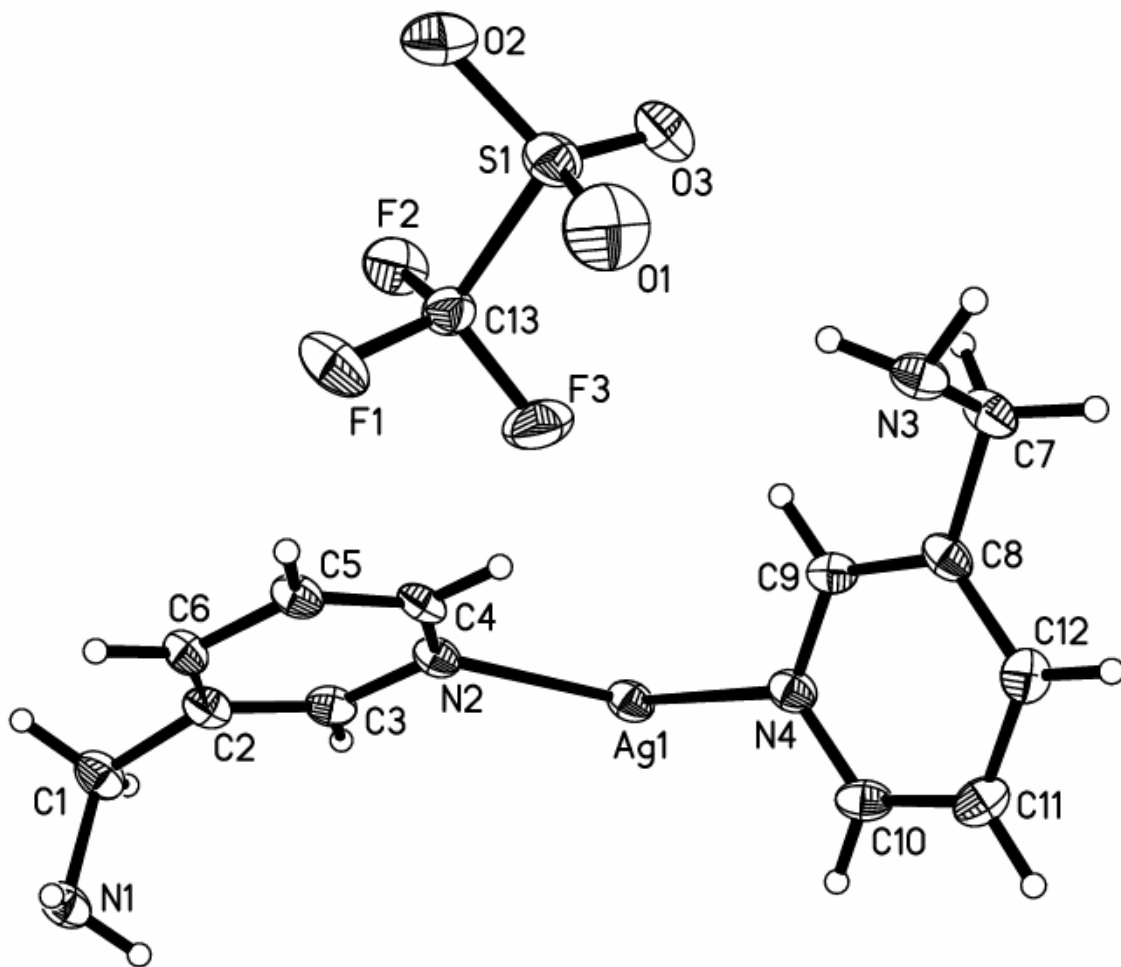


Figure 6.7. Thermal ellipsoid plot of the unique portion of the 3-dimensional polymer of **6.4**. Ellipsoids are drawn at the 50 % probability level.

Table 6.6. Selected bond lengths (\AA), angles ($^{\circ}$), and important distances for $\text{Ag}(\text{3-amp})_2\text{OTf}$ (**6.4**)^a

Ag1-N2	2.3065(2)	Ag1-N3#1	2.3273(2)
Ag1-N4	2.3352(2)	Ag1-N1#2	2.3483(2)
N2-Ag1-N3#1	119.86(7)	N2-Ag1-N4	105.34(6)
N3#1-Ag1-N4	119.58(7)	N2-Ag1-N1#2	104.74(7)
N3#1-Ag1-N1#2	96.63(7)	N4-Ag1-N1#2	108.92(7)
N1-H1A...O2#5	3.076(3)	N1-H1B...O1#3	2.980(3)
N3-H3A...O3#4	3.225(3)	N3-H3B...O2#6	3.318(3)

^a Symmetry transformations used to generate atoms: #1 = $x-1/2, -y+3/2, -z$: #2 = $-x+2, y-1/2, -z+1/2$: #3 = $-x+2, y+1/2, -z+1/2$: #4 = $x+1/2, -y+3/2, -z$: #5 = $x+1, y+1, z$: #6 = $-x+3/2, -y+1, z-1/2$

appearance of the resulting polymer. In this case, the SO_3^- head of the triflate causes the aminomethyl tails of the ligand to twist in opposing directions such that the growth of the complex occurs in three dimensions rather than two. An expanded view of this growth is shown in Figure 6.8. The same type of distortions that were seen in the tetrahedral metal environments of **6.3** are again displayed in **6.4**, though not as severe, with the N–Ag–N angles ranging from 96.63(7) to 119.87(7) °. Likely due to this more relaxed conformation, the Ag–N bonds settle into a position to where they are again more comparable in length. The Ag–amine distances show a range of 2.327(2) to 2.348(2) Å while the Ag–pyridyl distances are 2.307(2) to 2.348(2) Å. Geometric parameters are given in Table 6.6.

Compounds **6.5** and **6.6** result when 2,2'-bipyridine is added to solutions of the 3-amp ligand with either of the previous silver salts. The strong chelating action of the bipy ligand acts as a scissor to truncate the polymers at each metal center. In the resulting structures all of the silvers are three-coordinate with two of the donors being those of the 2,2'-bipy. The planarity of the metal environments is conducive to the formation of the d^{10} metal–metal interaction that is currently the object of much scrutiny from the theoretical community.^{163,171–173} It is interesting to note that the ratio of 3-amp ligand in the present cases is insignificant; provided that there is at least ½ equivalent present to bridge the metal centers, compounds **6.5** and **6.6** will be formed. An excess of 3-amp has been so far unable to force a greater ratio of ligand-to-metal than 1:2 in either structure.

When 2,2'-bipy is added to either of the solutions that produced **6.2** or **6.3** a stoichiometric amount of silver is bound by its chelating bite. It was assumed that as

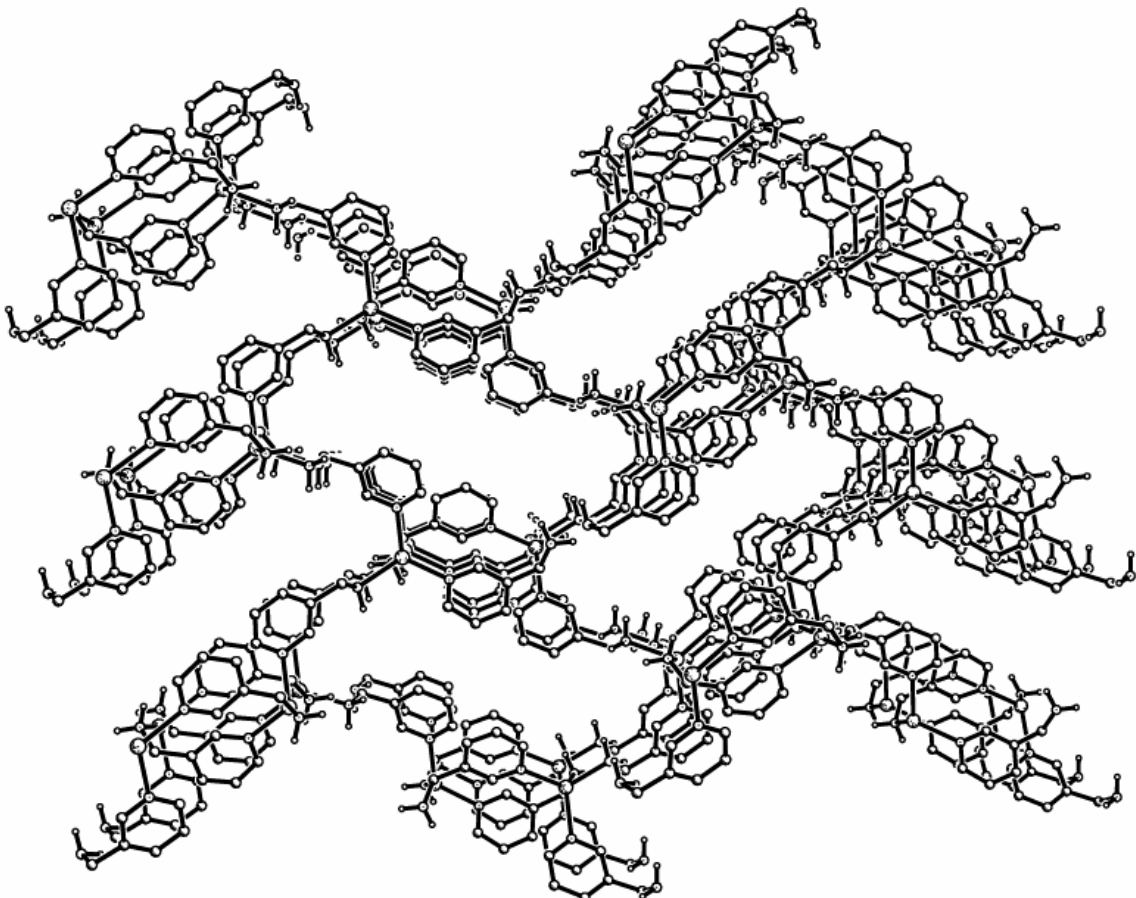


Figure 6.8. An extended view of the 3-dimensional cationic network of **6.4**. All hydrogen atoms except for those on the amines have been omitted for clarity.

long as there is no more than a single equivalent of the 2,2'-bipy present, there should be at least two available binding sites on each metal center from which polymerization by 3-amp can occur. Contrary to this supposition, it was seen that no more than $\frac{1}{2}$ of an equivalent of 3-amp ligand could be incorporated into the structures obtained when the bidentate bipyridine is present. Crystallization of 3-amp with Agtfa and 2,2'-bipy occurs in a 1:2:2 ratio to form compound **6.5** which is seen in Figure 6.9 with selected geometric data shown in Table 6.7. The single 3-amp ligand that is present acts to bridge two metal centers that are themselves capped by the bipyridyl creating two coordinatively unique silvers. This unit is then connected to an identical one via Ag–Ag interactions such that

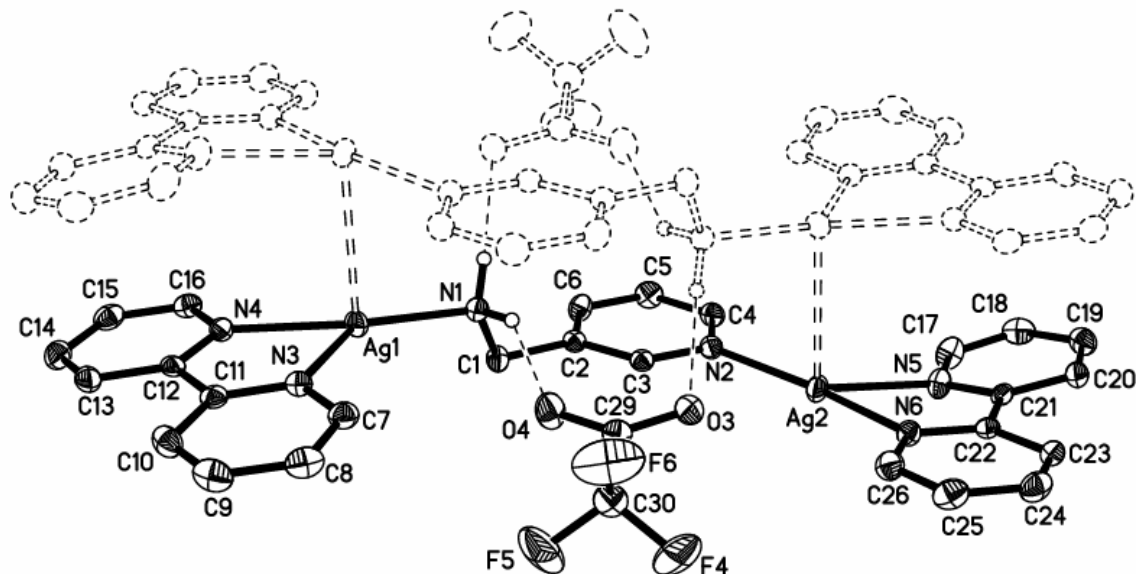


Figure 6.9. Thermal ellipsoid plot of the tetrametallic ring of **6.5** showing the H–bonding of the tfa⁻ anions to the amine hydrogens. The symmetry generated portion of the structure is shown dashed. All other hydrogens and anions have been removed for clarity. Ellipsoids are drawn at the 50 % probability level.

Table 6.7. Selected bond lengths (Å), angles (°), and important distances for Ag₂(2,2'-bipy)₂·μ-(3-amp)(tfa)₂ (**6.5**)^a

Ag1-N1	2.1487(2)	Ag1-N4	2.2552(2)
Ag1-N3	2.3313(2)	Ag1-Ag2#1	3.0583(3)
Ag2-N2	2.1481(2)	Ag2-N6	2.2143(2)
Ag2-N5	2.382(2)	Ag2-Ag1#1	3.0583(3)
Ag2-Ag2#2	3.1615(4)		
N1-Ag1-N4	154.80(7)	N1-Ag1-N3	131.65(7)
N4-Ag1-N3	72.58(7)	N1-Ag1-Ag2#1	95.43(5)
N4-Ag1-Ag2#1	91.29(5)	N3-Ag1-Ag2#1	89.05(4)
N2-Ag2-N6	161.15(7)	N2-Ag2-N5	125.99(7)
N6-Ag2-N5	72.31(7)	N2-Ag2-Ag1#1	83.18(5)
N6-Ag2-Ag1#1	89.56(5)	N5-Ag2-Ag1#1	99.40(5)
N2-Ag2-Ag2#2	113.37(5)	N6-Ag2-Ag2#2	75.15(5)
N5-Ag2-Ag2#2	70.00(5)	Ag1#1-Ag2-Ag2#2	163.358(1)
N1-H1A...O3#3	2.893(3)	N1-H1B...O4#4	2.868(2)

^a Symmetry transformations used to generate atoms: #1 = -x,-y+1,-z+2; #2 = -x+1,-y+1,-z+2; #3 = x-1,y,z+1; #4 = -x+1,-y+1,-z+1.

the two 3-amp bridges are arranged head-to-tail with respect to one another. A tfa⁻ anion sits comfortably in the void on each side of the resulting tetrametallic ring and forms a H–bond bridge through both oxygen atoms to each of the amines. The metal–metal interaction of this loop appears to be supported by the π–stacking of the aromatic bipy rings which assists Ag1 and Ag2A to stay within 3.0583(3) Å of one another. A second Ag–Ag interaction involving Ag2 and its symmetry equivalent joins this cycle to an identical one both above and below the original, effectively constructing a polymer held together by metal–metal interactions that is demonstrated in Figure 6.10. This second interaction is a bit longer than the first at 3.1615(4) Å, likely due to the lack of H–bonding assistance, though they are again assisted by π–stacking of the pyridyl donors. The four silver stacked chain of trigonal metals appears to be an unusually stable configuration of this particular coinage metal and has been demonstrated previously.^{17,66,145,183} Each of the silvers of this structure are in a distorted trigonal geometry caused by the acute bite angle of the bipyridyl ligand. Angles around Ag1 and Ag2 range from 72.31(7) ° on the low end to 161.15(7) °. However, the N–donor environments of both metals are nicely planar with the metal being only removed from the nitrogen plane by a minuscule degree (< 0.04 Å) by attractive interactions with the adjoining metals. The Ag1–amine and Ag2–pyridyl distances are identical here at 2.148(2) Å. However, the Ag–N_{bipy} distances are not as symmetric, ranging from 2.148(2) to 2.382(2) Å.

Due to the same factors that caused the stoichiometric limitations on compound **6.5**, compound **6.6** has only been obtainable in a 1:2:2 ratio of 3-amp ligand with AgOTf and 2,2'-bipy. **6.6** was obtained in an analogous manner to **6.5** by the addition of a single

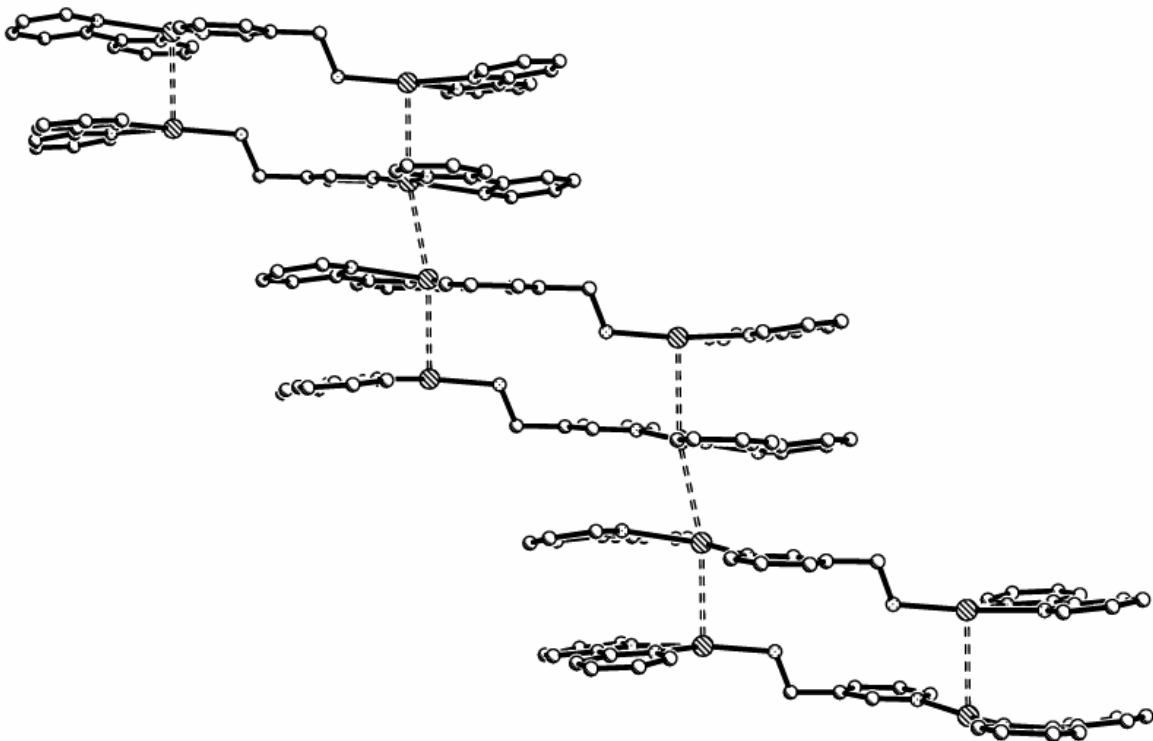


Figure 6.10. An extended view of the cationic polymer of Ag_4 units formed by the metal–metal interactions of **6.5**. Anions and H-atoms have been removed for clarity.

equivalent of 2,2'-bipy to a solution of 3-amp and AgOTf , where again the relative stoichiometries of 3-amp and Ag were irrelevant. A thermal displacement plot of **6.6** is shown in Figure 6.11 and selected bond lengths and angles in Table 6.8. The structure contains two of the 3-amp bridged Ag-bipy units similar to that seen in **6.5**. However, in this case the change in geometry about the hydrogen bonding head of the anion results in the creation of an overall structural motif that is somewhat of a combination of two others that we have described. The first similarity is to that of the previous structure: one of the units, when expanded, is seen to form a tetrametallic ring comparable to that of **6.5**. Here again the anion sits within the space created on either side of the ring drawing the amine groups together through H–bonds. In this case, however, the ring stands alone and is not part of a polymeric network due to the lack of metal–metal interactions extending above

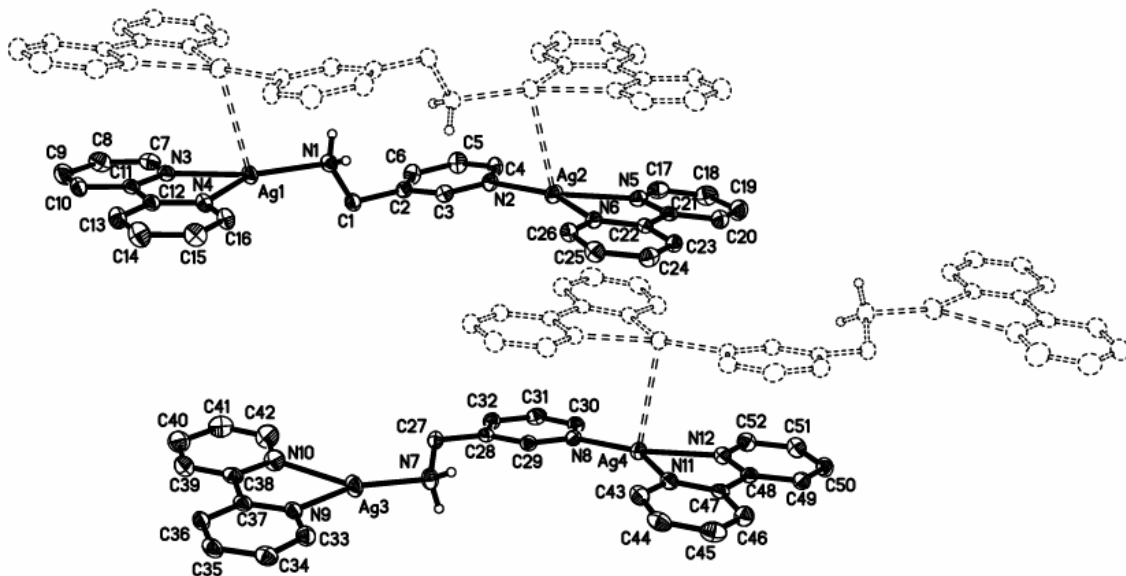


Figure 6.11. Thermal ellipsoid plot of the two different cationic parts of **6.6** with the unique portion labeled. Symmetry generated atoms are shown dashed. Anions and all hydrogen atoms except for those on the amines have been removed for clarity. Ellipsoids are drawn at the 50 % probability level.

Table 6.8. Selected bond lengths (\AA), angles ($^\circ$), and important distances for $\text{Ag}_2(2,2'\text{-bipy})_2\mu\text{-}(3\text{-amp})(\text{OTf})_2$ (**6.6**)^a

Ag1-N1	2.166(2)	Ag1-N3	2.260(2)
Ag1-N4	2.341(2)	Ag1-Ag2#1	3.0846(3)
Ag2-N2	2.141(2)	Ag2-N6	2.221(2)
Ag2-N5	2.357(2)	Ag2-Ag1#1	3.0846(3)
Ag3-N7	2.150(2)	Ag3-N9	2.233(2)
Ag3-N10	2.350(3)	Ag4-N8	2.139(2)
Ag4-N12	2.275(2)	Ag4-N11	2.277(2)
Ag4-Ag4#2	3.0399(4)		
N1-Ag1-N3	155.92(8)	N1-Ag1-N4	131.85(8)
N3-Ag1-N4	72.14(8)	N1-Ag1-Ag2#1	99.96(6)
N3-Ag1-Ag2#1	79.60(6)	N4-Ag1-Ag2#1	81.63(6)
N2-Ag2-N6	153.20(8)	N2-Ag2-N5	132.81(8)
N6-Ag2-N5	73.00(8)	N2-Ag2-Ag1#1	85.77(6)
N6-Ag2-Ag1#1	91.92(6)	N5-Ag2-Ag1#1	109.17(5)
N7-Ag3-N9	152.96(9)	N7-Ag3-N10	134.85(9)
N9-Ag3-N10	72.15(8)	N8-Ag4-N12	142.39(8)
N8-Ag4-N11	143.89(8)	N12-Ag4-N11	73.10(8)
N8-Ag4-Ag4#2	94.98(6)	N12-Ag4-Ag4#2	83.48(6)
N11-Ag4-Ag4#2	96.34(6)		
N1-H1A...O3#1	3.073(3)	N1-H1B...O1	3.061(3)
N7-H7A...O5#3	3.208(3)	N7-H7B...O7	3.034(3)

^a Symmetry transformations used to generate atoms: #1 = $-x+1, -y, -z+2$; #2 = $-x+1, -y+2, -z+1$; #3 = $x-1, y, z$.

the pyridyl bound silvers. The Ag–Ag interactions here are similar in distance to those previously seen at 3.0846(3) Å. The second similarity involves the second unit and bears resemblance to the compound formed by reacting 3-amp with 2,2'-bipy and silver with a non-interacting anion. In the absence of the assistance of the H–bonding bridge across the opposing amines, the 4-silver ring opens and twists 180 ° about the Ag4–Ag4(A) bond. This leaves a spread open conformer held together by the single π–stacking assisted metal–metal interaction which is comparable to those seen in the closed ring at 3.0399(4) Å. H–bonding to the anions here occurs through only a single oxygen and merely serve to hold its place in the lattice. This mixed conformation motif appears to be the most favored in the case of triflate as we have been yet unable to force crystallization of either isolated structure through temperature changes. All of the silvers present are again seen to be in a bipy distorted trigonal environment.

Luminescence Properties

In examining the luminescence properties of **6.1-6.6** it is noticed that the emission bands occur along the same area of the spectrum as those of the 3-ampAgX compounds shown in Figure 6.12 most of the fluorescence occurs in the region centered at approximately 470 nm. The less strongly emitting 1:1 3-ampAgOTf compound is where X is a noncoordinating ligand, though those of the more coordinating ligand tend to be a bit more intense. It can be seen by the emission spectra of representative slightly removed from the others and is centered at around 410 nm. The excitation spectra of all the compounds were also expectedly similar. A full tabulation of all the features of the luminescence spectra of **6.1-6.6** are presented in Table 6.9.

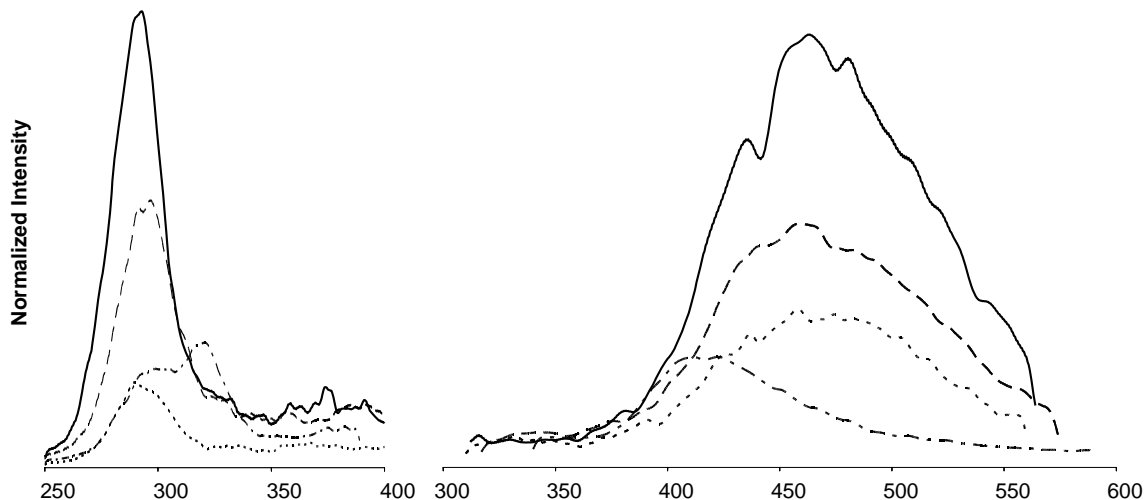


Figure 6.12. Normalized excitation and emission spectra of representative 3-amp Ag(I) compounds taken in acetonitrile glasses at 1×10^{-4} M concentration at 77 K. — = $\text{Ag(3-amp)}_2\text{OTf}$, - - - = $\text{Ag(3-amp)}\text{tfa}$, = $\text{Ag}_2\text{(3-amp)}(\text{BF}_4)_2\text{(2,2'-bipy)}_2$, - · - = $\text{Ag(3-amp)}\text{OTf}$.

Table 6.9. Luminescent Spectral Data for compounds **6.1–6.6**, at 77 K and 1×10^{-4} M in CH_3CN .

Compound	Excitation λ_{\max}	Emission local λ_{\min}
6.1	292, 297	443, 463, 486
6.2	300, 321	383, 422, 423
6.3	297	443, 452, 470, 482, 502
6.4	293	437, 464, 481, 508, 521, 544
6.5	290	428, 437, 459, 476, 505, 518, 535
6.6	335	412, 443, 465

Conclusions

We have demonstrated here that a variety of silver(I) complexes can be formed by using the mixed-donor ligand 3-aminomethylpyridine with silverX, where X = OTf⁻ or tfa⁻, with structural features such as dimensionality of the overall complex, coordination number, and coordination environment being controlled by variations in counterion and ratio of ligand to metal. It is seen that with the highly flexible coordination sphere of the silver(I) cation changes in stoichiometry can be an effective way of manipulating the

structures and properties of the resulting compounds. The results of this work add to the relatively unexplored area of ratio dependence which nicely supplements the thoroughly explored field of anion dependent structures of the coinage metals. It was shown here how the common silver coordination numbers from 2–4 can easily be obtained producing structural motifs ranging from discrete structures to three-dimensional networks.

Experimental

General Procedures

All experiments were carried out under an argon atmosphere, using a Schlenk line and standard Schlenk techniques. Glassware was dried at 120°C for several hours prior to use. All reagents were stored in an inert atmosphere glovebox; solvents were distilled under nitrogen from the appropriate drying agent immediately before use. 3-aminomethylpyridine and 2,2'-bipyridine were purchased from Aldrich and used as received. Silver(I) trifluoroacetate and silver(I) triflate were purchased from Strem Chemicals Inc. and used as received. ^1H NMR spectra were recorded at 300.13 MHz on a Bruker Spectrospin 300 MHz spectrometer. Elemental analyses were performed by Atlantic Microlabs Inc., Norcross, Georgia.

General Synthesis

General procedures for the synthesis of compounds **6.1-6.4** involve the addition of a 5 mL acetonitrile solution of 3-aminomethylpyridine to a stirred solution of the appropriate silver salt in 5 mL of acetonitrile. The mixtures are then stirred for 10 minutes then dried in vacuo to leave white or off-white powders. All flasks are shielded from light with aluminum foil to prevent the photodecomposition of the silver

compounds. Crystals of **6.2**, **6.2**, **6.5** and **6.6** were obtained by the slow diffusion of ether into acetonitrile solutions at 5 °C. Crystals of **6.3** and **6.4** were grown by vapor diffusion of ether into acetonitrile solutions at 5 °C. The amounts of reagents used, yields, and analytical data are presented below as well as any modifications to the general synthetic procedure. Percent yields are based upon the amount of silver salt used.

Preparations

*poly-[Ag(3-amp)tfa] (**6.1**)*. This reaction used 3-aminomethylpyridine (0.150 g, 1.40 mmol) added to Agtfa (0.306 g, 1.40 mmol) to leave a white powder in 91 % yield (0.415 g, 1.26 mmol) upon evaporation of the solvent. Colorless blocks of **6.1** were grown from acetonitrile and ether. ^1H NMR (CD₃CN, 298 K) δ: 3.19 s, br, 2H, (-NH₂); 3.89 s, 2H, (-CH₂); 7.41 m, 1H; 7.83 t,d, 2H; 8.45 d, 1H. Anal. Calcd for AgC₈H₈N₂O₂F₃: C, 29.20; H, 2.45; N, 8.51. Found: C, 29.38; H, 2.39; N, 8.40.

*poly-[Ag(3-amp)OTf] (**6.2**)*. This reaction used 3-aminomethylpyridine (0.075 g, 0.694 mmol) added to AgOTf (0.178 g, 0.693 mmol) to leave a white powder in 96 % yield (0.239 g, 0.674 mmol) upon evaporation of the solvent. Colorless plates of **6.2** were grown from acetonitrile and ether. ^1H NMR (CD₃CN, 298 K) δ: 3.00 s, br, 2H, (-NH₂); 3.87 s, 2H, (-CH₂); 7.43 m, 1H; 7.81 t,d, 2H; 8.49 m, 1H. Anal. Calcd for AgC₇H₈N₂O₃HF₃: C, 25.80; H, 2.47; N, 8.56. Found: C, 26.27; H, 2.33; N, 8.77.

*poly-[Ag(3-amp)₂tfa] (**6.3**)*. In this reaction two equivalents of 3-aminomethylpyridine (0.150 g, 1.40 mmol) were added to Agtfa (0.153 g, 0.693 mmol). Removal of the solvent in vacuo left an oily brown solid. Dissolution of this

solid in 1 mL of acetonitrile followed by precipitation with 15 mL of ether resulted in **6.3** being obtained as a white powder in 73 % yield (0.221 g, 0.514 mmol). Colorless blocks were grown from acetonitrile and ether. ^1H NMR (CD_3CN , 298 K) δ : 3.27 s, br, 4H, (-NH₂); 3.85 s, 4H, (-CH₂); 7.31 m, 2H; 7.78 t,d, 4H; 8.43 d, 2H. Anal. Calcd for $\text{AgC}_{14}\text{H}_{16}\text{N}_4\text{O}_2\text{F}_3$: C, 38.46; H, 3.69; N, 12.82. Found: C, 38.24; H, 3.57; N, 12.54.

poly-[Ag(3-amp)₂Otf] (6.4). This reaction used 2 equivalents of 3-aminomethylpyridine (0.150 g, 1.40 mmol) added to AgOTf (0.178 g, 0.693 mmol). Removal of the solvent in vacuo leaves a yellow oil. Dissolution of this oil in a small aliquot of ether followed by precipitation with 15 mL of ether leaves **6.4** as a white powder in 73 % yield (0.174 g, 0.508 mmol). Colorless blocks were grown from acetonitrile and ether. ^1H NMR (CD_3CN , 298 K) δ : 3.02 s, br, 4H, (-NH₂); 3.89 s, 4H, (-CH₂); 7.38 m, 2H; 7.78 t,d, 4H; 8.47 d, 2H. Anal. Calcd for $\text{AgC}_{13}\text{H}_{16}\text{N}_4\text{O}_3\text{SF}_3$: C, 33.00; H, 3.41; N, 11.84. Found: C, 33.18; H, 3.24; N, 11.75.

poly-[Ag₂(2,2'-bipy)₂- μ -(3-amp)(tfa)₂] (6.5). A solution of one equivalent of 3-aminomethylpyridine (0.100 g, 0.926 mmol) in 5 mL CH_2Cl_2 was added to a stirred suspension of 2 equivalents of Agtfa (0.408 g, 1.86 mmol) in 5 mL CH_2Cl_2 . This solution was stirred for 10 minutes then 2 equivalents of 2,2'-bipyridine (0.288 g, 1.90 mmol) in 5 mL CH_2Cl_2 were added. This mixture was stirred an additional 10 minutes then dried in vacuo to leave **6.5** as an off-white powder in 92 % (0.725 g, 0.852 mmol) yield. Colorless block shaped crystals were grown from acetonitrile and ether. ^1H NMR (CD_3CN , 298 K) δ : 3.91 s, br, 2H, (-NH₂); 4.75 s, 2H, (-CH₂); 7.40 m, 8H; 7.89 m, 9H;

8.10 d, 2H; 8.55 d, 1H. Anal. Calcd for $\text{Ag}_4\text{C}_{60}\text{H}_{48}\text{N}_{12}\text{O}_8\text{F}_{12}\cdot\text{CH}_2\text{Cl}_2$: C, 40.49; H, 2.79; N, 9.29. Found: C, 40.45; H, 2.82; N, 9.37.

Ag₂(2,2'-bipy)₂-μ-(3-amp)(OTf)₂ (6.6). To a stirred solution of one equivalent of 3-aminomethylpyridine (0.100 g, 0.926 mmol) in 5 mL CH₃CN was added 2 equivalents of AgOTf (0.474 g, 1.84 mmol) in 5 mL CH₃CN. This was stirred for 10 minutes then a solution of 2,2'-bipyridine (0.288g, 1.84 mmol) in 5 mL CH₃CN was added. The mixture was stirred an additional 10 minutes then dried in vacuo to leave a fluffy white powder in 89 % (0.759 g, 0.818 mmol) yield. Colorless prisms were grown from acetonitrile and ether. ¹H NMR (CD₃CN, 298 K) δ: 4.22 s,br, 2H, (-NH₂); 4.82 s, 2H, (-CH₂); 7.55 m, 8H; 8.05 m, 9H; 8.26 d, 2H; 8.65 d, 1H. Anal. Calcd for Ag₂C₂₈H₂₄N₆O₆F₆S₂: C, 35.99; H, 2.59; N, 8.99. Found: C, 35.93; H, 2.72; N, 9.47.

Crystallography

A summary of the experimental crystallographic data for **6.1** to **6.6** is given in Table 6.10. Tables of full bond lengths and angles can be found in Appendix B, Tables B.20 to B.25. Crystallographic data were collected on crystals with dimensions 0.289 × 0.189 × 0.169 mm for **6.1**, 0.140 × 0.090 × 0.060 mm for **6.2**, 0.190 × 0.070 × 0.070 mm for **6.3**, 0.293 × 0.270 × 0.119 mm for **6.4**, 0.195 × 0.172 × 0.140 mm for **6.5** and 0.238 × 0.187 × 0.180 mm for **6.6**. Data were collected at 110 K on a Bruker X8 Apex using MoKα radiation ($λ = 0.71073 \text{ Å}$). All structures were solved by direct methods after the correction of the data using SADABS.¹³⁹ All of the data were processed using the Bruker AXS SHELXTL software, version 6.10.¹⁴⁰ Unless otherwise noted, all non-hydrogen atoms were refined anisotropically and hydrogen atoms were placed in calculated

Table 6.10. Crystallographic Data for compounds **6.1** to **6.6**

	6.1	6.2	6.3	6.4	6.5	6.6
Formula	C ₃₂ H ₃₂ Ag ₄ F ₁₂ N ₈ O ₈	C ₁₄ H ₁₆ Ag ₂ F ₆ N ₄ O ₆ S ₂	C ₁₄ H ₁₆ AgF ₃ N ₄ O ₂	C ₁₃ H ₁₆ AgF ₃ N ₄ O ₃ S	C ₃₂ H ₂₇ Ag ₂ F ₆ N ₇ O ₄	C ₅₆ H ₄₈ Ag ₄ F ₁₂ N ₁₂ O ₁₂ S ₄
Formula weight	1316.14	730.17	437.18	473.23	903.35	1868.78
a (Å)	10.3431(4)	10.255(1)	12.5447(9)	7.5817(8)	11.682(1)	12.552(1)
b (Å)	17.0246(5)	23.941(2)	10.5573(7)	10.478(1)	12.249(1)	14.036(1)
c (Å)	23.3149(8)	9.1244(8)	12.9994(9)	21.663(2)	13.297(1)	19.713(2)
α					78.317(2)	100.968(2)
β (°)		91.743	108.001(2)		64.335(2)	97.572(2)
γ (°)					75.003(2)	102.963(2)
space group	P2 ₁ 2 ₁ 2 ₁	P2 ₁ /c	P2 ₁ /n	P2 ₁ 2 ₁ 2 ₁	P-1	P-1
D _{calcd} (g cm ⁻³)	2.129	2.166	1.773	1.826	1.821	1.900
μ (mm ⁻¹)	1.994	2.025	1.277	1.344	1.272	1.413
2θ _{max} (°)	52.74	52.74	56.74	51.50	56.62	53.02
reflns measured	51253	58756	60463	13609	22035	49261
reflns used (R _{int})	8358 (0.0386)	4576 (0.0404)	4039 (0.0329)	3284 (0.0252)	8117 (0.0318)	13372 (0.0340)
restraints/param	0/577	0/307	19/274	0/226	6/489	0/901
R ₁ , [I > 2σ(I)]	0.0209	0.0204	0.0159	0.0178	0.0277	0.0279
wR ² , [I > 2σ(I)]	0.0490	0.0510	0.0427	0.0433	0.0608	0.0679
R(F _o ²), (all data)	0.0233	0.0258	0.0185	0.0191	0.0399	0.0357
R _w (F _o ²), (all data)	0.0497	0.0532	0.0436	0.0436	0.0663	0.0724
GooF on F ²	1.054	1.061	1.056	1.061	1.020	1.021

positions. The trifluoromethyl portion of the non-coordinated anion of **6.3** is disordered over 3 positions. The structure of **6.5** contains a disordered trifluoroacetate as well as a solvent acetonitrile molecule.

CHAPTER SEVEN

Variability in the Structures of [4-(aminomethyl)pyridine]silver(I) Complexes through effects of Ligand Ratio, Anion, Hydrogen Bonding, and π -Stacking

Introduction

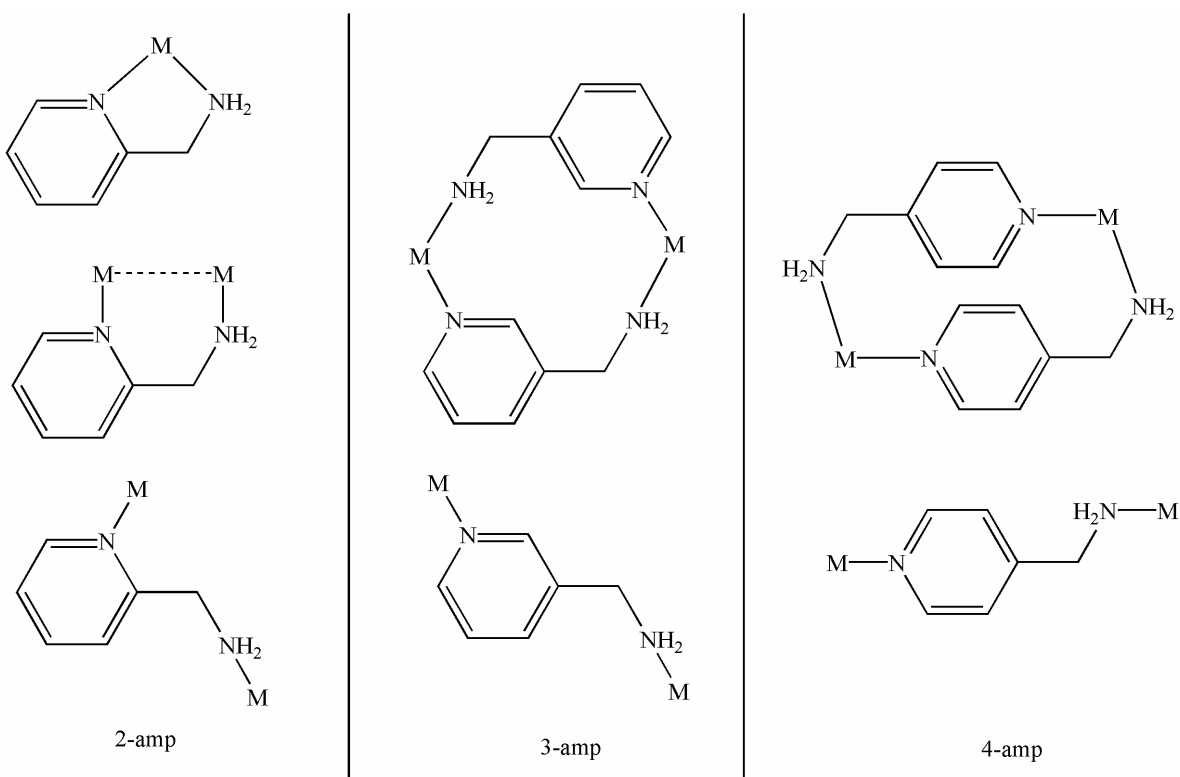
Recent interest in the rational design and construction of novel discrete and polymeric metal-organic coordination complexes has reached a new high due to the realization of their potential for use as functional materials.^{3,8,12,24,26,31,40,50,51,60,61,83,151,184-}

¹⁸⁷ Designed coordination architectures have found application in fields as far spread as catalysis, molecular recognition, sieving, separation and non-linear optics.^{4,7,10,25,63,141,176}

Supramolecular chemists have typically fine tuned the properties of these complexes by using modifications in functionality, rigidity, or geometry of the basis ligand or by changes in solvent or counterion in charged systems.^{11,13,21,31,49,69,88,92,142,146-148,154,159,177-}

^{179,182} Others still have made notable contributions to the field utilizing the non-covalent π -stacking or H-bonding interactions to impart desired characteristics on coordination complexes.^{2,62,188,189} Though a wealth of information is available on crystal engineering studies employing the aforementioned methods the equally effectual practice of stoichiometric control has gone largely unexplored and thus unexploited.^{68,69} Only recently have we and a handful of other researchers taken interest in investigating the effect that ratio dependence can impart upon conformation, dimensionality, and physical properties of supramolecular species.^{70,71,91,177-179}

In several of the previous chapters we have demonstrated that drastic structural modifications can be forced upon coordination complexes through variations in the ratio of ligand to metal; particularly in silver which



Scheme 7.1. Typical coordination modes of amp ligands with silver(I) salts.

has the capacity to readily accept changes in its coordination number and geometry.^{46,154,178,182}

Herein we continue our comprehensive study of the structural effects brought on by changes in ratio of the series of isomeric aminomethylpyridine (amp) ligands shown in Scheme 7.1 with various silver(I) salts. With the factors effecting the structural characteristics of the 2- and 3-ampAgX ($X = \text{BF}_4^-$, tfa^- , or OTf^-) complexes being previously discussed^{177-179,182} we now report on the ratio dependence of 4-ampAgX, with the present account also illustrating the relationship between anion and stoichiometric effects. It is seen that the degree of interaction that the anions (particularly those of oxygen) have with the metal centers as well as the extent of the H-bonding network present is related to the ratio of ligand to metal present in the structure. Also affecting the

overall growth of the complexes is the π -stacking interactions that occur between adjacent pyridyl rings.

Results and Discussion

Synthesis

The 4-aminomethylpyridine complexes **7.1–7.5** were synthesized by the direct reaction of the 4-amp ligand with the appropriate silver(I) salt (OTf^- , tfa^- , or BF_4^-) in varying ratios. All of the compounds containing only 4-amp and silver were isolated as fine white to off-white powders. The 2:1 complex, **7.3**, is the only compound reported herein which shows only sparing solubility in acetonitrile and precipitates in the correct ratio upon formation. As a result, crystallization of **7.3** was achieved with some difficulty from saturated CH_3CN solutions grown over several weeks and the ^1H NMR spectrum are reported in CD_3OD solvent. Compounds **7.6.1** and **7.6.2** were isolated as fine yellow and off-white powders, respectively. Both were formed by the addition of the corresponding bipyridyl ligand to solutions of 4-amp and AgBF_4^- . The formation of **7.6.1** and **7.6.2** was seen to be independent of the ratio of 4-amp to Ag^+ , so long as there was sufficient 4-amp present to bridge each pair of bipy-capped silver ions. 4-amp in excess of $\frac{1}{2}$ equivalent was always isolated in the crude product as uncoordinated ligand. Analytical data for compounds **7.1** to **7.6.2** are presented in Tables 7.1 and 7.2.

X-Ray Crystal Structures

The range of metal coordination environments in the crystal structures of compounds **7.1–7.6.2** is demonstrative of the facility with which the silver(I) cation varies its coordination sphere to accept the number and type of donors required of it.

Table 7.1. Analytical and Physical Data

	compound ^a	yield (%)	analytical (%) ^b		
			C	H	N
7.1	poly-[Ag(4-amp)OTf]	96	26.2 (25.8)	2.3 (2.4)	8.7 (8.6)
7.2	poly-[Ag(4-amp)tfa]	97	29.4 (29.2)	2.4 (2.5)	8.4 (8.5)
7.3	poly-[Ag(4-amp) ₂ tfa]	94	38.2 (38.4)	3.6 (3.7)	12.5 (12.8)
7.4	poly-[Ag(4-amp) ₂ (OTf)]	78	33.2 (33.0)	3.3 (3.4)	11.7 (11.8)
7.5	poly-[Ag(4-amp) ₂ BF ₄]	84	35.0 (35.1)	3.8 (3.9)	13.3 (13.6)
7.6.1	Ag ₂ (2,2'-bipy) ₂ -μ-(4-amp)(BF ₄) ₂	84	40.6 (40.3)	3.2 (3.3)	11.2 (11.3)
7.6.2	poly-[Ag ₂ (5,5'-bis methyl-2,2'-bpy) ₂ (4-amp)(BF ₄) ₂]	89	(41.6)	(3.7)	(9.7)

^a All compounds are white or off white solids. ^b Calculated values are given in parenthesis. Percent compositions were not obtained for **7.6.2** as it was used only as a structural model for compound **7.6.1**.

Table 7.2. Hydrogen-1 NMR Data

	$^1\text{H}/\delta^{\text{a}}$
7.1	3.81 s, br, 2H, (-NH ₂ -); 3.97 s, 2H, (-CH ₂ -); 7.46 m, 2H; 8.43 m, 2H
7.2	3.81 s, br, 2H, (-NH ₂ -); 3.97 s, 2H, (-CH ₂ -); 7.54 m, 2H; 8.43 m, 2H
7.3	4.57 s, br, 2H, (-NH ₂ -); 5.46 s, 2H, (-CH ₂ -); 8.11 m, 2H; 9.07 2H
7.4	3.26 s, br, 4H, (-NH ₂ -); 3.91 s, 24, (-CH ₂ -); 7.36 m, 4H; 8.46 m, 4H
7.5	2.79 s, br, 4H, (-NH ₂ -); 3.89 s, 4H, (-CH ₂ -); 7.36 m, 2H; 8.38 m, 2H
7.6.1	2.17 s, br, 2H, (-NH ₂ -); 3.98 s, 2H, (-CH ₂ -); 8.69 m, 8H; 8.44 m, 9H; 8.08 m, 2H; 7.59 m, 1H
7.6.2	2.39 s, 12H (Me); 2.57 2s, br, 2H (-NH ₂ -); 3.87 s, 2H (-CH ₂ -); 7.33 m, 4H; 7.81 dd, 2H; 8.05 dd, 2H; 8.42 m, 6H

^a ^1H NMR spectra of Compound **7.3** was recorded in CD₃OD at 298 K. All other ^1H NMR spectra were recorded in CD₃CN at 298 K.

Coordination numbers from 2–5 are seen encompassing geometries of linear (**7.1**, **7.2**), T-shaped (**7.2**), trigonal (**7.6.2**), tetrahedral (**7.3–7.5**), and trigonal bipyramidal (**7.6.2**). The conformation of the ligands is seen to be quite sensitive to counterion effects due to the strong H-bonding propensity of the amine donor when oxygen containing anions are present. However, the silver environment seems to be just as susceptible, if not more so, to change when added equivalents of ligand are presented to it. Compounds **7.1** and **7.2** both display a 1:1 ratio of 4-amp ligand to metal with variances between the two arising from the difference in basicity of triflate versus trifluoroacetate. The less strongly interacting tetrafluoroborate 1:1 complex with 4-amp has previously been reported and displays a similar structural motif to those of the first two compounds reported herein.⁹¹ A second equivalent of 4-amp effectively forces the metal center to accept a tetrahedral geometry to receive the two added N-donors present. As a result, compounds **7.3–7.5** all adopt similar 4-coordinate metal environments of two each amine and pyridyl donors. However, the supramolecular structures of these compounds are again quite varied due to the differences in interactions of the anions with the amine protons. Interestingly, the intermediate 3:2 ratio of ligand to metal which we were able to achieve with both 2-amp and 3-amp has been thus far elusive to isolation. This is likely due to the inordinately stable 4-ampAg “box” displayed in Scheme 7.1 that is formed when a 2:1 ratio is achieved. This “box” is constructed of a pair of head-to-tail coordinated 4-amp ligands bound to two symmetry equivalent silvers. In this arrangement the pyridyl π-systems of the opposing ligands are conveniently situated to interact with one another forming an exceptionally sound bimetallic cycle. This “box” is the common unit relating all three 2:1 structures. Compound **7.6.1** consistently produced poor quality crystals and therefore

was modeled by its methylated relative, **7.6.2**, in order to study the solid state structure of the 4-amp bridged bis-[Ag(I)2,2'-bipy] unit.

The 1:1 ratio of ligand to metal in compounds **7.1** and **7.2** causes a 2:1 ratio of N to Ag. This results in both structures adopting a preferred one-dimensional growth due to the propensity of the Ag(I) cation to come to be linear in a two-coordinate environment. Differences between the two structures seem to stem more from the slight differences in coordinating ability of the anions here than in the geometry about the H-bonding head of the anion as was seen in the studies of the other amp isomers.¹⁷⁷⁻¹⁷⁹

A molecular diagram showing the straight line growth of **7.1** is shown in Figure 7.1 and selected bond lengths and angles are shown in Table 7.3. The *para*-substitution of the aminomethyl group on the pyridyl ring allows for a more outward conformation of the ligand in the direction of perpetuation of the structure than was achieved with the 2- or 3-amps. What results is a polymer which is relatively thin in comparison with the bulky helical and zigzag silver(I) polymers constructed using 2- and 3-amp bridges.¹⁷⁷⁻¹⁷⁹ A general planarity of the polymer is also noticed due to the orientation of the methylene-nitrogen bond nearly parallel to the plane of the pyridyl ring. This is given by the C3-C2-C1-N2 torsion angle of only 5.2(3) $^{\circ}$. The triflate anion in this instance acts non-coordinating, preferring to hydrogen bond to the amines rather than link to the metal center, joining the polymers into a pseudo 2-D sheet. Pyridyl-Ag and amine-Ag distances are similar and have typical values at 2.158(2) and 2.164(2) \AA , respectively. The N–Ag–N angle is only slightly off linear at 172.73(7) $^{\circ}$.

The 1:1 ratio of 4-amp to Agtfa produces another one-dimensional coordination polymer, **7.2**. In this instance, however, the structure is actually composed of two unique

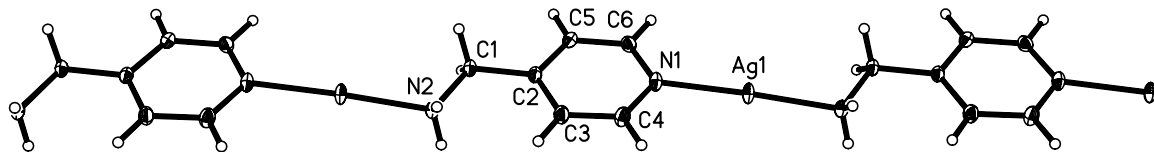


Figure 7.1. Molecular diagram of the cationic polymer **7.1**. Ellipsoids are drawn at the 50% probability level.

Table 7.3. Selected bond lengths (\AA), angles ($^{\circ}$), and important distances for $\text{Ag}(\text{4-amp})\text{OTf}$ (**7.1**)^a

Ag1-N1	2.158(2)	Ag1-N2#1	2.164(2)
N1-Ag1-N2#1	172.73(7)	C2-C3-C6-N2	5.2(3)
N2-H···O1#2	3.134(3)	N2-H···O3#3	2.986(3)

^aSymmetry transformations used to generate equivalent atoms: #1 = x,y,z-1; #2 = -x+1,-y+1,-z+2; #3 = -x,-y+1,-z+2.

polymers running parallel to one another as shown in Figure 7.2. Selected bond lengths and angles for these polymers are given in Table 7.4. The polymer strands are differentiated from each other by the degree of interaction that each strand has with its associated anion. As seen in the diagram, the upper strand has a non-coordinated anion caused by the angle of approach of the tfa^- to the polymer in which the CO_2^- head of the anion is bisected by the plane of that polymer. In the lower strand, the anion approaches from atop the pyridyl plane and is allowed within close enough proximity to bind to the metal centers with a Ag2-O1 bond length of $2.565(2)\text{\AA}$. As a result, both charge neutral and formally positively charged chains are used in the construction of **7.2**. It is also seen that the cationic polymer is more closely related to that of **7.1** than the anion bound polymer in terms of its planarity. In the charged polymer the $-\text{CH}_2-\text{NH}_2-$ bond is again relatively close to planar with the pyridyl rings of the chain, showing an acute C2-C3-C6- N2 torsion angle of $7.4(4)^{\circ}$. Distortions in the opposing polymer likely

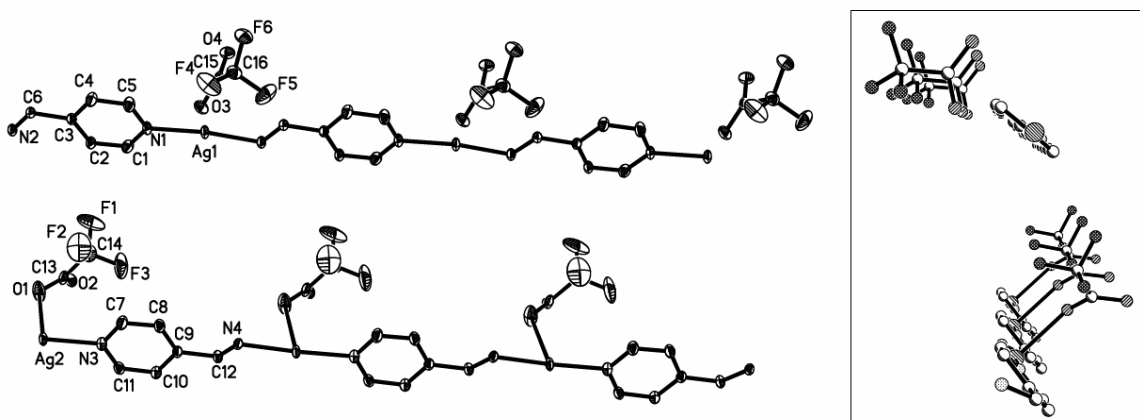


Figure 7.2. 50% thermal ellipsoid representation of the parallel polymers of **7.2**. Hydrogen atoms have been removed for clarity. Inset is a view down the length of the polymers showing the different approaches of the anions.

Table 7.4. Selected bond lengths (\AA), angles ($^\circ$), and important distances for $\text{Ag}(4\text{-amp})\text{tfa}$ (**7.2**)^a

Ag1-N2#1	2.143(2)	Ag1-N1	2.146(2)
Ag2-N3	2.157(2)	Ag2-N4#2	2.173(2)
Ag2-O1	2.565(2)		
		N3-Ag2-O1	103.51(8)
N3-Ag2-N4#2	169.99(9)	C2-C3-C6-N2	7.4(4)
N4#2-Ag2-O1	81.52(8)	N2#1-Ag1-N1	170.68(9)
C8-C9-C12-N4	23.1(4)		
		N2-H \cdots O4#5	2.973(3)
N2-H \cdots O2#4	2.837(3)	N2-H \cdots O3#3	2.859(3)
N4-H \cdots O4#6	2.979(3)		

^aSymmetry transformations used to generate equivalent atoms: #1 = $x+1, y, z$: #2 = $x-1, y, z$: #3 = $-x, -y+1, -z+1$: #4 = $-x, -y+2, -z+1$: #5 = $x, y, z-1$: #6 = $-x+1, -y+1, -z+1$.

caused by the coordinated tfa^- result in the analogous C8-C9-C12-N4 angle being made more obtuse at 23.1(4) $^\circ$. The pyridyl-Ag and amine-Ag bond distances of the neutral polymer are comparable to those seen in **7.1** at 2.157(2) and 2.173(2) \AA , respectively. The same distances in the absence of a closely associated anion are, as expected, slightly shorter at 2.146(2) and 2.143(2) \AA . An interesting observation of the N-Ag-N bond

angles about silvers 1 and 2 sees them nearly identical at 170.68(9) and 169.99(9) $^{\circ}$, respectively. This distortion is implicative of at least partial interaction between the non-coordinating tfa $^{-}$ and the metal center. Hydrogen-bonding to O2 of the coordinated anion and to both oxygens of the non-coordinated anion serve to hold the trifluoroacetates in place as well as acting as a bridge between the parallel polymer strands.

Compounds **7.3-7.5** all display a 2:1 ratio of 4-amp to silver(I) and result from the addition of two equivalents of ligand to the appropriate silver salt. All are based around the bimetallic “box” described previously though these smaller units are connected in different ways to construct the separate structures.

When more than a single equivalent of 4-amp is added to a solution of Agtfa the sparingly soluble compound **7.3** precipitates from the solution. Recrystallization of this solid yields the structure shown in Figure 7.3. Selected geometric parameters for **7.3** are presented in Table 7.5. The unique portion of this structure is labeled in the figure and contains one ligand and one half-occupied silver(I) ion, keeping the correct ratio. When this unique part is grown through an inversion center, the biligand, bimetallic “box” that forms the basis for this and the subsequent two structures can be seen. In the construction of this box the –CH₂–NH₂– bond rotates normal to the pyridyl plane, displaying a C2-C3-C6-N2 torsion angle of 91.6(4) $^{\circ}$ and linking two symmetry equivalent silvers with a cross-box Ag-Ag distance of 6.7848(7) \AA . In this orientation the opposing pyridyl rings are situated directly adjacent to one another such that they achieve a π – π separation of approximately 3.34 \AA . This favorable π –stacking helps account for the preference of the 4-amp AgX compounds to bypass the 3:2 ratio of ligand to metal and proceed directly to the 2:1 structures. The polymerization of **3** occurs in one

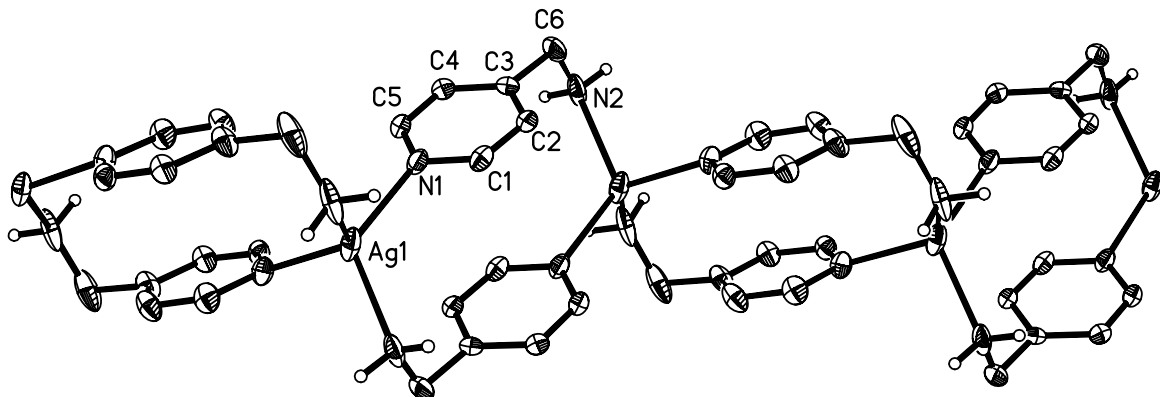


Figure 7.3. A view of the cationic chain of **7.3**. Ellipsoids are drawn at the 30% probability level. All hydrogen atoms except for those on the amines have been removed for clarity.

Table 7.5. Selected bond lengths (\AA), angles ($^\circ$), and important distances for $\text{Ag}(4\text{-amp})_2\text{tfa}$ (**7.3**)^a

Ag1-N2#1	2.321(3)	Ag1-N2#2	2.321(3)
Ag1-N1#3	2.324(3)	Ag1-N1	2.324(3)
N2#1-Ag1-N2#2	100.2(2)	N2#1-Ag1-N1#3	101.3(1)
N2#2-Ag1-N1#3	121.26(9)	N2#1-Ag1-N1	121.26(9)
N2#2-Ag1-N1	101.3(1)	N1#3-Ag1-N1	112.1(1)
C2-C3-C6-N2	91.6(4)		
N2-H···O1#1	3.008(4)	N2-H···O2#4	3.169(3)
Ag1···Ag1#1	6.7848(7)		

^aSymmetry transformations used to generate equivalent atoms: For **3**: #1 = $-x+1/2, -y+1/2, -z+1$; #2 = $x-1/2, -y+1/2, z$; #3 = $-x, y, -z+1$; #4 = $x+1/2, y-1/2, z$.

dimension, forming a linear chain. The back and forth twisting of this chain is assisted by the H-bonding of trifluoroacetates across the face of each link. The chain itself is joined together by the sharing of the two silver occupied corners of each link with the next in line. The metal centers are in slightly distorted tetrahedral environments with N-Ag-N angles ranging from 100.19(2) to 121.26(9) $^\circ$. Ag-N bond lengths display the

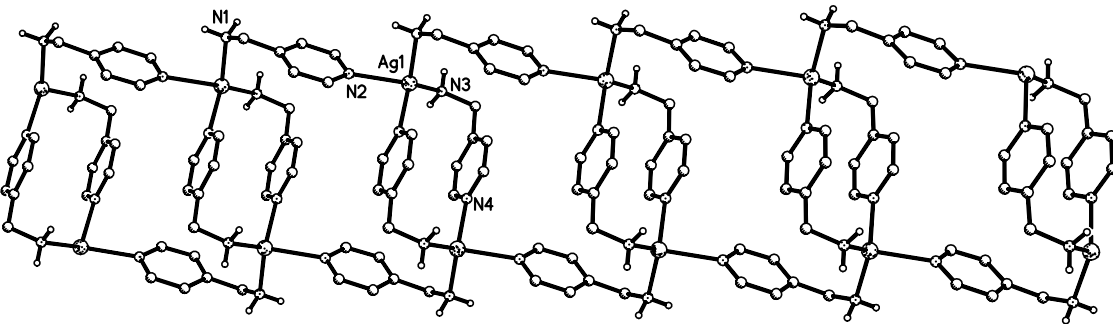


Figure 7.4. A view of the cationic “box-in-box” structure of **7.4**. All hydrogen atoms except for those on the amines have been removed for clarity.

result of this change in coordination number with a corresponding lengthening to $2.324(3)\text{\AA}$ for the Ag-N_{pyridine} distances and $2.321(3)\text{\AA}$ for the Ag-N_{amine} distances.

Compound **7.4** is the consequence of a second equivalent of 4-amp being added to solutions that produced the one-dimensional polymer **7.1**. The resulting linear polymer seen in Figure 7.4 displays a 2:1 ratio of ligand to metal, as well as the small 4-amp box building block reminiscent of the previous structure, **7.3**. The polymer in this case, however, is much bulkier due to the formation of the “box-in-box” network shown. The unique portion of this structure is shown in Figure 7.5 and selected geometric parameters are given in Table 7.6. The C9-C8-C7-N3 torsion angle here is $66.0(2)^\circ$ corresponding to a rotation of the methylene-amine bond away from perpendicular to the pyridyl. This assists in causing a lengthening of the cross-box Ag-Ag distance to $6.9946(4)\text{\AA}$ as well as a concomitant separation of the adjacent pyridyl π -systems to around 3.45\AA . Opposing silver occupied corners of two separate small boxes are subsequently bridged by another 4-amp ligand to construct the box-in-box motif seen in the figure. The open corners of this larger box are occupied by amine nitrogens which have a much greater diagonal distance at $13.577(3)\text{\AA}$. The conformation of this second ligand is different from that of

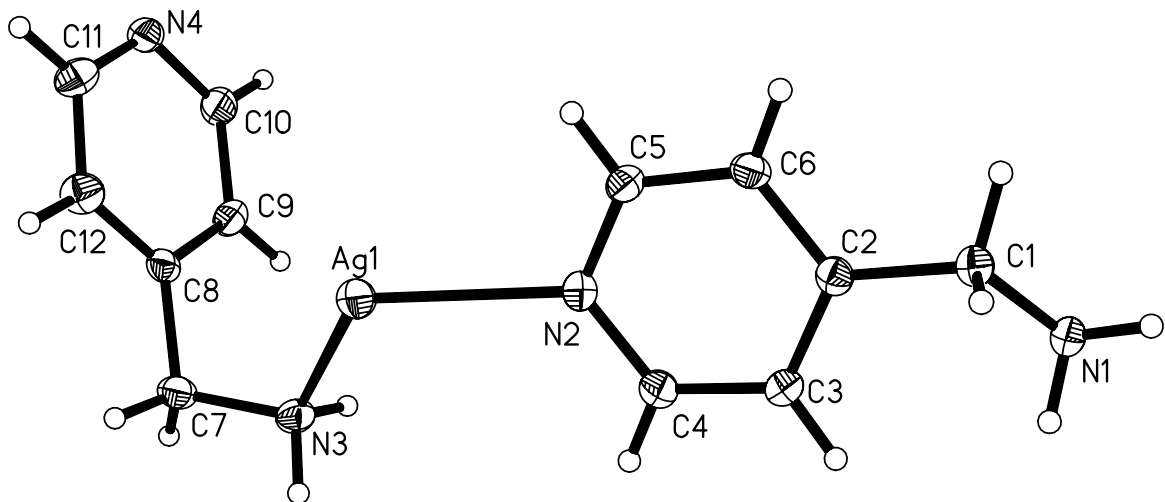


Figure 7.5. Thermal ellipsoid plot of the unique cationic portion of **7.4**. Ellipsoids are drawn at the 50% probability level.

Table. 7.6. Selected bond lengths (\AA), angles ($^\circ$), and important distances for $\text{Ag}(\text{4-amp})_2(\text{OTf})$ (**7.4**)^a

Ag1-N3	2.276(1)	Ag1-N1#1	2.346(1)
Ag1-N4#2	2.391(1)	Ag1-N2	2.431(1)
N3-Ag1-N1#1	119.90(5)	N3-Ag1-N4#2	117.91(5)
N1#1-Ag1-N4#2	109.55(5)	N3-Ag1-N2	118.19(5)
N1#1-Ag1-N2	93.50(4)	N4#2-Ag1-N2	92.07(4)
C9-C8-C7-N3	66.0(2)	C3-C2-C1-N1	39.8(2)
<hr/>			
N1-H···O1#3	3.021(2)	N1-H···O1#4	3.259(2)
N3-H···O(2)#5	3.053(2)	N3-H···O3#6	3.037(2)
Ag1···Ag1#7	6.9946(4)	N1#1···N1#7	13.577(3)

^aSymmetry transformations used to generate equivalent atoms: #1 = $x-1, y, z$; #2 = $-x, -y+1, -z+1$; #3 = $x+1, y, z+1$; #4 = $-x+2, -y+2, -z+1$; #5 = $-x+1, -y+1, -z+1$; #6 = $x, y, z+1$; #7 = $-x, -y+1, -z+1$.

the first as seen by the change in the analogous torsion angle, C3-C2-C1-N1, to a more acute 39.8(2) $^\circ$. A difference in bond lengths are also seen between silver and those ligands that are either involved in the construction of the small box or those that bridge the smaller boxes together, with the intrabox bonds apparently being a bit stronger.

In-box silver-pyridyl and silver-amine distances are 2.391(1) and 2.276(1)Å, respectively, whereas the bridging 4-amp has corresponding distances a bit longer at 2.431(1) and 2.346(1)Å. The tetrahedral environment of the metal center here is also slightly more distorted than in the previous structure with N-Ag-N angles ranging from 92.07(4) to 119.90(5)°. The non-coordinating OTf⁻ anions sit within the cavities formed by the larger box and are held in place by H-bonding to the amine nitrogens.

Keeping with the box-in-box motif is compound **7.5** which is again based upon the symmetric biligand, bimetallic box of the previous two structures. Polymeric growth in this case, however, extends to form a two-dimensional box-in-box network as shown in Figure 7.6. The small box is once more seen to occupy opposite corners of a larger box constructed of linkages formed by an outward facing 4-amp ligand. In the current case the larger box is of much greater size due to the incorporation of two bridging ligands each being used to form the remaining two corners of the box. These corners both terminate with a silver(I) cation; the two metals being separated by a 20.0112(6)Å span. The smaller box sees its shortest Ag-Ag separation discussed herein at 6.5094(3)Å. This is associated with a rotation of the –CH₂–NH₂– bond closer to perpendicular to the pyridyl plane with the C6-C2-C1-N2 torsion angle being 73.0(3)°. Interestingly, the adjacent pyridyl rings in this case are along the same separation as those in the structure of **7.4**, with an approximate division of 3.45Å. The unique portion of **7.5** is displayed in Figure 7.7, with geometric parameters in Table 7.7, and shows the similarities between the conformations of the N1 (small box) ligand and the N3 (bridging) ligand with only a rotation of the methylene-amine vector differentiating the two; the C9-C8-C7-N4 torsion angle is 92.4(3). Silver-pyridyl and silver-amine bond distances of the small box are

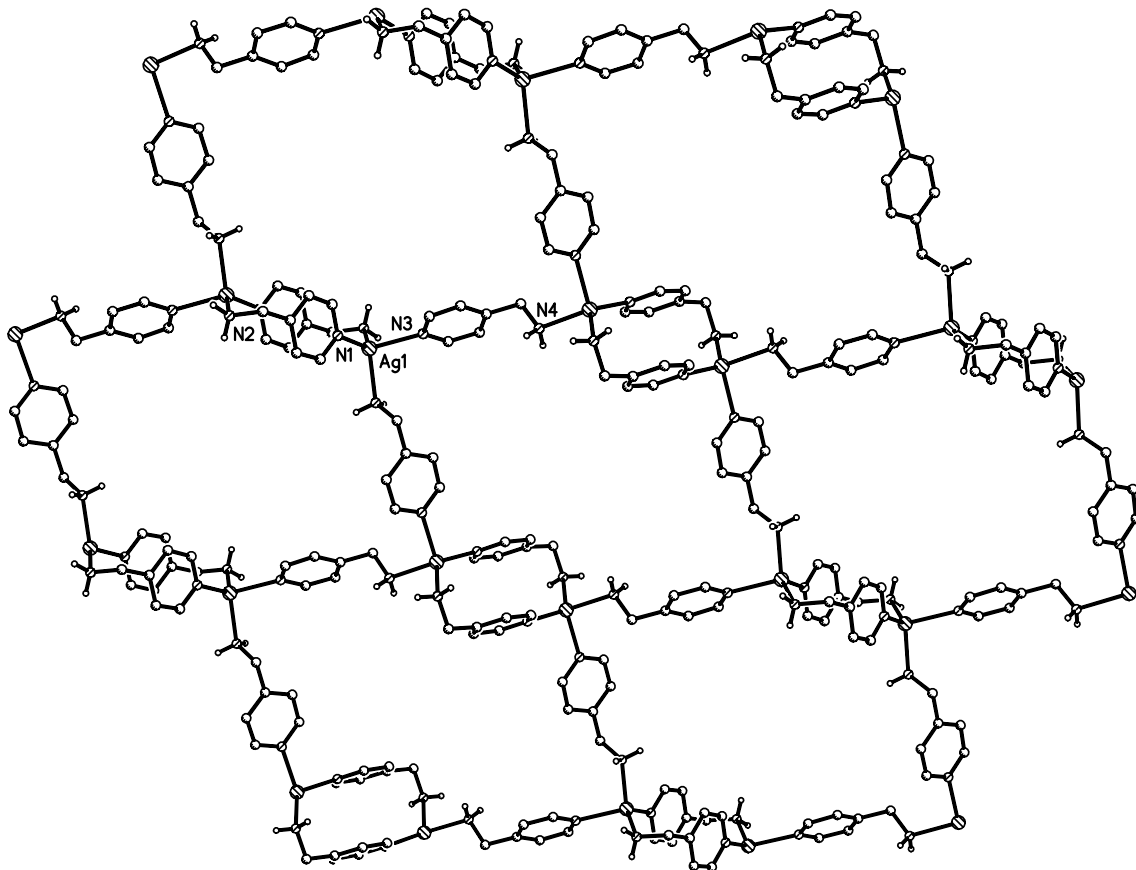


Figure 7.6. An extended view of the cationic “box-in-box” network of **7.5**. All hydrogen atoms except for those on the amines have been removed for clarity.

again seen to be shorter at 2.280(2) and 2.327(2) Å than the open ligand with analogous lengths of 2.380(2) and 2.347(2) Å, respectively. Tetrahedral N-Ag-N angles range from 99.86(7) to 126.6(7)°.

Compound **7.6.1** was synthesized in order to study the effects of adding a strongly chelating ligand on the polymerization of the 4-amp complexes. However, repeated attempts at crystallization consistently produced poor quality crystals from which little could be established. As a result, 5,5'-dimethyl-2,2'-bipyridine was used as a model which was expected to have similar coordination properties and we were able to obtain satisfactory diffraction quality crystals of **7.6.2**.

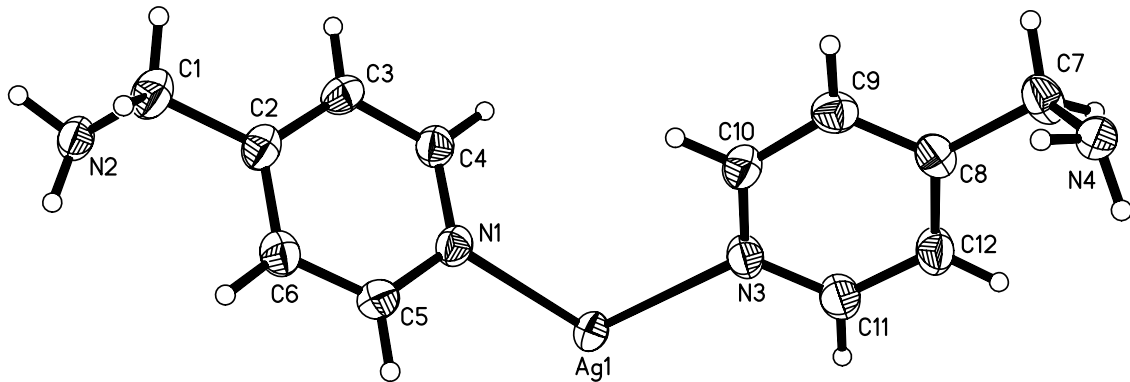


Figure 7.7. Molecular diagram of the unique portion of the cationic polymer of **7.5**. Ellipsoids are drawn at the 50% probability level.

Table 7.7. Selected bond lengths (\AA), angles ($^\circ$), and important distances for $\text{Ag}(\text{4-amp})_2\text{BF}_4$ (**7.5**)^a

Ag1-N1	2.280(2)	Ag1-N2#1	2.327(2)
Ag1-N4#2	2.346(2)	Ag1-N3	2.380(2)
N1-Ag1-N2#1	126.60(7)	N1-Ag1-N4#2	116.96(7)
N2#1-Ag1-N4#2	99.86(7)	N1-Ag1-N3	105.85(6)
N2#1-Ag1-N3	102.97(7)	N4#2-Ag1-N3	101.23(7)
C6-C2-C1-N2	73.0(3)	C9-C8-C7-N4	92.4(3)
<hr/>			
N2-H \cdots F1#3	3.072(3)	N2-H \cdots F4	3.090(2)
N4-H \cdots F4#4	3.156(2)	N4-H \cdots F2#4	3.118(2)
N4-H \cdots F1#5	3.282(3)	Ag1 \cdots Ag1#1	6.5094(3)
Ag1 \cdots Ag1#6	20.0112(6)		

^aSymmetry transformations used to generate equivalent atoms: #1 = $-x+1, -y+1, -z+1$; #2 = $-x+2, y-1/2, -z+1/2$; #3 = $-x+1, -y+1, -z+2$; #4 = $-x+2, -y+1, -z+1$; #5 = $-x+2, y+1/2, -z+3/2$; #6 = $-x+3, -y+1, -z$.

When 5,5'-dimethyl-2,2'-bipyridine is added to solutions of 4-amp with silver(I) BF_4^- , ligand bridged polymerization into the structures seen previously⁹¹ and in **7.5** is impeded. Instead, the bipy-truncated structure shown in Figure 7.8 is formed. Selected bond lengths and angles for this compound are given in Table 7.8. As expected, the chelating bipyridine preferentially binds the silver(I) cation, displacing the monodentate

amine or pyridine of the 4-amp ligand from its coordination sphere to form the bridged bimetallic monomer of **7.6.2**. It is seen that as long as there is sufficient 5,5'-dimethyl-2,2'-bipy present to make a 1:1 ratio of bipy to metal the stoichiometry of 4-amp in the reaction is irrelevant. A bipyridyl complex with a higher ratio of 4-amp to silver than 0.5:1 has been so far elusive, even in the presence of a large excess (~ 4 fold) of the aminomethylpyridine. There are two unique silver(I) environments present in **7.6.2** due to the asymmetric nature of the 4-amp bridge. The amine-bound silver is in a slightly distorted trigonal environment with variance from the ideal 120° angles a result of the small bite angle of the bidentate bipyridyl. Angles around Ag1 range from 72.8(1) to 150.2(1)°. However, the metal cation is only slightly removed from its N₃ plane by 0.033(2)Å. Ag2 sees similar deviations from the ideal with N-Ag-N angles of 73.1(1) to 153.94(1)° and an N₃ plane displacement of 0.042(2)Å. The three aromatic rings bound to Ag2 give the metal a planar surrounding allowing easier access to it than Ag1, which has the amine protons protruding above and below the plane. As a result, the coordination sphere of Ag2 also contains a symmetry equivalent metal situated both directly above and below the plane of the molecule giving the pyridyl-bound silver a metal-capped trigonal bipyramidal environment. The Ag–Ag interactions are typical lengths^{163,171–173} at 3.348(1)Å and appear to be supported by the π-stacking of pyridyl and bipyridyl rings bound to the metals. A particularly unique and interesting feature of this structure that is seen when the molecule is expanded along the direction of the metal–metal interactions, as in Figure 7.9, is that it is actually a linear polymer connected by an infinite metal–metal backbone. This backbone shows only a slight bend at each metal center with a Ag-Ag-Ag angle of 174.85(2)°. Relevant literature and CCDC searches

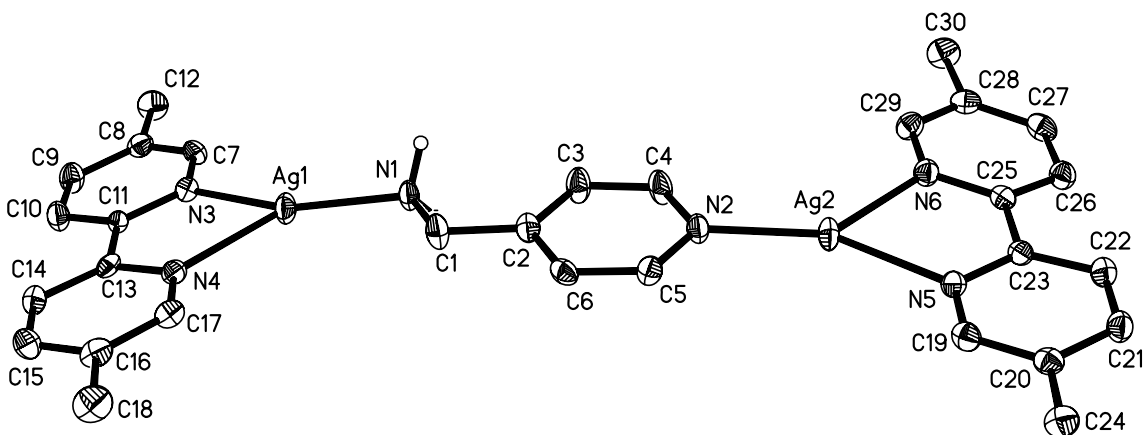


Figure 7.8. Molecular diagram of the bimetallic monomer of **7.6.2**. Ellipsoids are drawn at the 50% probability level. All hydrogen atoms except for those on the amine have been removed for clarity.

Table 7.8. Selected bond lengths (\AA), angles ($^\circ$), and important distances for $\text{Ag}_2(5,5'\text{-bis methyl-}2,2'\text{-bpy})_2(4\text{-amp})(\text{BF}_4)_2$ ^a

Ag1-N1	2.161(3)	Ag1-N3	2.256(3)
Ag1-N4	2.335(3)	Ag2-N2	2.138(3)
Ag2-N5	2.240(3)	Ag2-N6	2.339(3)
Ag2-Ag2#1	3.348(1)	Ag2-Ag2#2	3.348(1)
N1-Ag1-N3	150.2(1)	N1-Ag1-N4	136.7(1)
N3-Ag1-N4	72.8(1)	N2-Ag2-N5	153.9(1)
N2-Ag2-N6	132.8(1)	N5-Ag2-N6	73.1(1)
N2-Ag2-Ag2#1	83.21(8)	N5-Ag2-Ag2#1	104.44(7)
N6-Ag2-Ag2#1	85.93(7)	N2-Ag2-Ag2#2	100.32(8)
N5-Ag2-Ag2#2	74.00(7)	N6-Ag2-Ag2#2	88.93(7)
Ag2#1-Ag2-Ag2#2	174.85(2)	C3-C2-C1-N1	7.4(6)
N1-H···F7#3	2.960(4)	N1-H···F(8)#4	2.978(4)

^aSymmetry transformations used to generate equivalent atoms: #1 = $x, -y + 3/2, z + 1/2$; #2 = $x, -y + 3/2, z - 1/2$; #3 = $-x + 1, -y + 1, -z$; #4 = $-x + 1, -y + 1, -z + 1$.

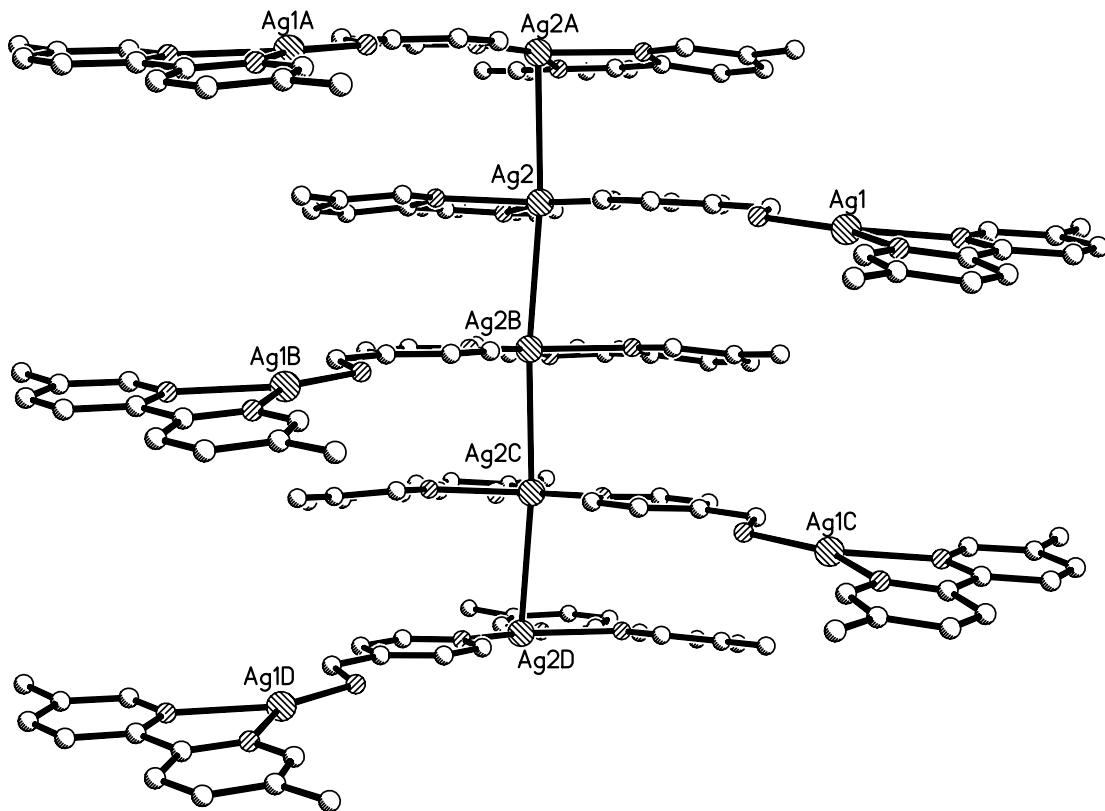


Figure 7.9. Ball and stick diagram showing the polymeric nature of **7.6.2**. Anions and hydrogen atoms have been removed for clarity.

reveal this type of polymerization to be previously unseen, with the only other infinite silver-linked polymers known being held together by bridging ligands.^{17,66} Perpetuation of the polymer sees the molecular axis of each monomer shifted nearly perpendicular to those adjacent to it to give the overall polymer a saw tooth appearance. The C3-C2-C1-N1 torsion angle of the bridging 4-amp ligand has a value similar to that seen in the 1:1 structures at 7.4(6) $^{\circ}$. Ag-pyridyl and Ag-amine distances are also reminiscent of **7.1** and **7.2** at 2.138(3) and 2.161(3) \AA , respectively. Ag-N_{bipy} distances are slightly longer at 2.256(3) and 2.335(3) \AA to Ag1 and 2.240(3) and 2.339(3) \AA to Ag2, which are typical for Ag-N_{bipy} bonds.¹⁷⁷⁻¹⁷⁹ The BF₄⁻ anions here sit in the space formed directly behind the amines in the polymer and are held in place by weak H-bonds.

Luminescence Properties

A representative collection of excitation and emission spectra of the compounds discussed herein is displayed in Figure 7.10. It can be seen by the remarkable resemblance of the features of the spectra that the coordination complexes **7.1-7.5** are not only structurally similar but also electronically similar. This is not completely unexpected seeing as most of the luminescent silver(I) centers are in nearly identical

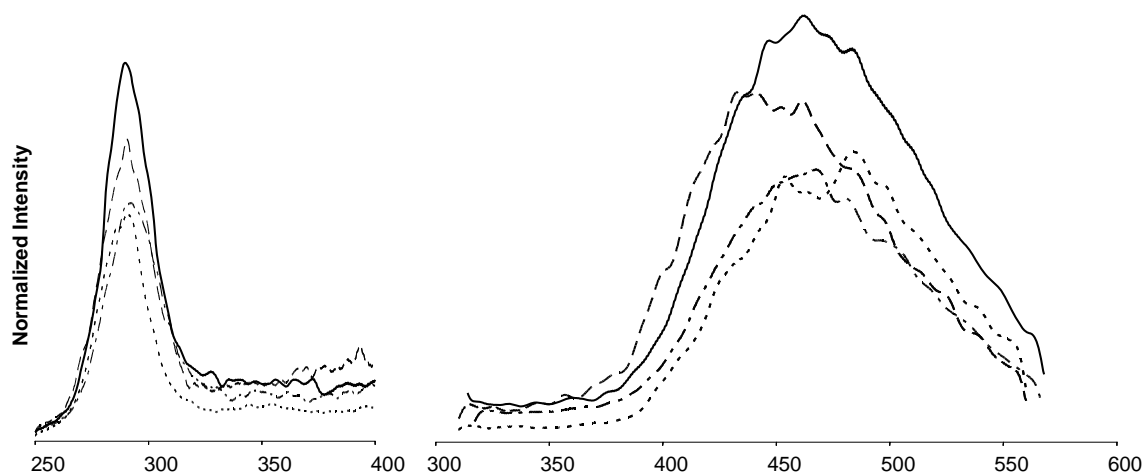


Figure 7.10. Normalized excitation and emission spectra of representative 3-amp Ag(I) compounds taken in acetonitrile glasses at 1×10^{-4} M concentration at 77 K. — = $\text{Ag(4-amp)}_2\text{OTf}$, - - - = $\text{Ag(4-amp)}(\text{OTf})$, = $\text{Ag(4-amp)}_2(\text{BF}_4)$, - · - · = $\text{Ag(4-amp)}_2(\text{tfa})$.

Table 7.9. Luminescent Spectral Data for compounds **7.1-7.6.2**, at 77 K and 1×10^{-4} M in CH_3CN .

Compound	Excitation λ_{\max}	Emission local λ_{\min}
4-amp	375	394
7.1	291	402, 434, 443, 453, 462, 485, 498, 525, 540
7.2	294	437, 449, 456, 467, 484, 499, 556
7.3	298	444, 463, 475, 492,
7.4	290	443, 459, 470, 480
7.5	292	455, 485, 498, 540
7.6.1	364	357, 371, 390
7.6.2	365	341, 350

tetrahedral environments of amine and pyridyl donors. The fluorescence of the complexes **7.6.1** and **7.6.2** is seen to be diminished considerably with respect to the amp-only complexes in the presence of the bipy-based ligands. A full collection of excitation and emission features is presented in Table 7.9.

Conclusions

Herein we have shown how the structures of supramolecular compounds of the ligand 4-aminomethylpyridine with salts of the silver(I) cation are able to be varied not only by the traditional methods such as anion control but also by changes in ratio of ligand to metal. The amine group present on the ligand allowing for H-bonding of the resultant complexes as well as an inclination for the 4-amp ligand to participate in π -stacking interactions also contribute to the overall conformations of the structures presented which display several different one- and two-dimensional motifs. Studies of the amp ligands are to be continued with mixed ligand systems as well as the asymmetric methylpyridine- and bis(methylpyridine)-aminomethylpyridines.

Experimental

General Procedures.

All experiments were carried out under an argon atmosphere, using a Schlenk line and standard Schlenk techniques. Glassware was dried at 120°C for several hours prior to use. All reagents were stored in an inert atmosphere glovebox; solvents were distilled under nitrogen from the appropriate drying agent immediately before use. 4-aminomethylpyridine, 5,5'-dimethyl-2,2'-bipyridine, and 2,2'-bipyridine were purchased from Aldrich and used as received. Silver(I) tetrafluoroborate, silver(I) trifluoroacetate,

and silver(I) trifluoromethanesulfonate were purchased from Strem Chemicals Inc. and used as received. ^1H NMR spectra were recorded at 360.13 MHz on a Bruker Spectrospin 360 MHz spectrometer. Elemental analyses were performed by Atlantic Microlabs Inc., Norcross, Georgia.

General Preparations

General procedures for the synthesis of compounds **7.1-7.6.2** involve the addition of a 5 mL acetonitrile solution of 4-aminomethylpyridine to a stirred solution of the appropriate silver salt in 5 mL acetonitrile. The mixtures are then stirred for 10 minutes then dried in vacuo to leave white or off-white powders. All flasks are shielded from light with aluminum foil to prevent the photodecomposition of the silver compounds. Crystals of compounds **7.2-7.5** were grown by layering ether over acetonitrile solutions at 5 °C. Crystals of compound **7.1** and **7.6.2** were grown by vapor diffusion of ether into acetonitrile solutions at 5 °C. The amounts of reagents used, yields, and analytical data are presented below as well as any modifications to the general synthetic procedure. Percent yields are based upon the amount of silver salt used.

Preparations

*poly-[Ag(4-amp)OTf] (**7.1**)*. This reaction used 4-aminomethylpyridine (0.100 g, 0.924 mmol) added to AgOTf (0.237 g, 0.922 mmol) to leave a white powder in 96 % yield (0.323 g, 0.893 mmol) upon evaporation of the solvent. Colorless plates of **7.1** were grown from acetonitrile and ether. ^1H NMR (CD₃CN, 298 K) δ : 3.81 s, br, 2H, (-NH₂); 3.97 s, 2H, (-CH₂-); 7.46 m, 2H; 8.43 m, 2H. Anal. Calcd for AgC₇H₈N₂O₃SF₃: C, 25.80; H, 2.47; N, 8.56. Found: C, 26.27; H, 2.33; N, 8.77.

poly-[Ag(4-amp)tf_a] (7.2) This reaction used 4-aminomethylpyridine (0.100 g, 0.924 mmol) and Agtfa (0.204 g, 0.925 mmol). Solvent was removed *in vacuo* and the resulting white powder was recovered in 97% yield (0.295 g, 0.897 mmol). Colorless blocks were grown from acetonitrile and ether. ¹H NMR (CD₃CN, 298 K) δ: 3.81 s, br, 2H, (-NH₂-); 3.97 s, 2H, (-CH₂-); 7.54 m, 2H; 8.43 m, 2H. Anal. Calcd for AgC₈H₈N₂O₂F₃: C, 29.20; H, 2.45; N, 8.51. Found: C, 29.38; H, 2.39; N, 8.40.

poly-[Ag(4-amp)₂tf_a] (7.3) The reaction was done in a 2:1 ratio of 4-aminomethylpyridine (0.100 g, 0.924 mmol) to Agtfa (0.102 g, 0.462 mmol). A white precipitate was observed upon addition of the 4-aminomethylpyridine. After the solvent was removed *in vacuo* a white powder was obtained in 94% yield (0.190 g, 0.432 mmol). Colorless blocks were formed by layering ether over an acetonitrile suspension of **7.3** at 5 °C. ¹H NMR (CD₃OD, 298 K) δ: 4.57 s, br, 2H, (-NH₂-); 5.46 s, 2H, (-CH₂-); 8.11 m, 2H; 9.07 2H. Anal. Calcd for AgC₁₄H₁₆N₄O₂F₃: C, 38.46; H, 3.69; N, 12.82. Found: C, 38.24; H, 3.57; N, 12.54

poly-[Ag(4-amp)₂(OTf)] (7.4) This reaction used 2 equivalents of 4-aminomethylpyridine (0.100 g, 0.924 mmol) added to AgOTf (0.118 g, 0.462 mmol). A clear, colorless oil was left upon evaporation of the solvent. The oil was dissolved in a small amount of CH₃CN then precipitated with ether resulting in a white fluffy powder in 78% yield (0.171 g, 0.180 mmol). Colorless blocks were grown from acetonitrile and ether. ¹H NMR (CD₃CN, 298 K) δ: 3.26 s, br, 4H, (-NH₂-); 3.91 s, 24, (-CH₂-); 7.36 m, 4H; 8.46 m, 4H. Anal. Calcd for AgC₁₃H₁₆N₄O₃SF₃: C, 33.00; H, 3.41; N, 11.84. Found: C, 33.18; H, 3.24; N, 11.75.

poly-[Ag(4-amp)₂BF₄] (7.5) This reaction used 2 equivalents of 4-aminomethylpyridine (0.100 g, 0.924 mmol) added to AgBF₄ (.090 g, 0.462 mmol). Upon evaporation of the solvent an off-white powder was isolated in 84% yield (0.160 g, 0.389 mmol). Colorless plates were grown from acetonitrile and ether. ¹H NMR (CD₃CN, 298 K) δ: 2.79 s, br, 4H, (-NH₂-); 3.89 s, 4H, (-CH₂-); 7.36 m, 2H; 8.38 m, 2H. Anal. Calcd for AgC₁₂H₁₆N₄BF₄: C, 35.07; H, 3.92; N, 13.63. Found: C, 35.03; H, 3.78; N, 13.33

Ag₂(2,2'-bipy)₂-μ-(4-amp)(BF₄)₂ (7.6.1). To a stirred solution of one equivalent of 4-aminomethylpyridine (0.100 g, 0.926 mmol) in 5 mL CH₃CN was added 2 equivalents of AgBF₄ (0.360 g, 1.82 mmol) in 5 mL CH₃CN. This was stirred for 5 minutes then a solution of 2,2'-bipyridine (0.289 g, 1.82 mmol) in 5 mL CH₃CN was added. This mixture was stirred for 10 minutes more then the solvent was removed *in vacuo* to leave a light yellow powder in 84% yield (0.631 g, 0.776 mmol). ¹H NMR (CD₃CN, 298 K) δ: 2.17 s, br, 2H, (-NH₂-); 3.98 s, 2H, (-CH₂-); 8.69 m, 8H; 8.44 m, 9H; 8.08 m, 2H; 7.59 m, 1H. Anal. Calcd for Ag₂C₂₉H₂₈N₇B₂F₈: C, 40.32; H, 3.27; N, 11.35. Found: C, 40.68; H, 3.26; N, 11.20.

poly-[Ag₂(5,5'-bis methyl-2,2'-bpy)₂(4-amp)(BF₄)₂] (7.6.2) The procedure for this reaction is the same as that used for the preparation of **7.6.1** and used an equivalent of 4-aminomethylpyridine (0.150 g, 1.39 mmol) added to 2 equivalents of AgBF₄ (0.540 g, 2.77 mmol). After stirring for 5 minutes, 2 equivalents of 5,5'-dimethyl-2,2'-bipyridine was added (0.510 g, 2.77 mmol). After an additional 10 minutes of stirring the solvent was removed *in vacuo* to leave a white powder in 89% yield (1.07g, 1.23mmol).

Colorless blocks were grown from acetonitrile and ether ^1H NMR (CD_3CN , 298K) δ : 2.39 s, 12H (Me); 2.57 2s, br, 2H (-NH₂-); 3.87 s, 2H (-CH₂-); 7.33 m, 4H; 7.81 dd, 2H; 8.05 dd, 2H; 8.42 m, 6H.

Crystallography

A summary of the experimental crystallographic data for **7.1** to **7.6.2** is given in Table 7.10. Full collections of interatomic distances and angles can be found in Appendix B, Tables B.26 to B.31. Crystallographic data were collected on crystals with dimensions $0.171 \times 0.109 \times 0.047$ mm for **7.1**, $0.110 \times 0.100 \times 0.070$ mm for **7.2**, $0.090 \times 0.060 \times 0.060$ mm for **7.3**, $0.249 \times 0.230 \times 0.153$ mm for **7.4**, $0.152 \times 0.114 \times 0.112$ mm for **7.5** and $0.264 \times 0.220 \times 0.189$ mm for **7.6.2**. Data were collected at 110 K on a Bruker X8 Apex using MoK α radiation ($\lambda = 0.71073$ Å). All structures were solved by direct methods after the correction of the data using SADABS.¹³⁹ All of the data were processed using the Bruker AXS SHELXTL software, version 6.10.¹⁴⁰ Unless otherwise noted, all non-hydrogen atoms were refined anisotropically and hydrogen atoms were placed in calculated positions. The structure of **7.1** contains two solvent acetonitrile molecules in the lattice. The trifluoroacetate anion of compound **7.3** is disordered over two positions across a mirror plane. The structure of compound **7.6.2** contains two solvent acetonitrile molecules and a BF_4^- anion which is disordered over three positions. The smaller two occupancies of the disorder are refined as isotropic spheres.

Table 7.10. Crystallographic Data for compounds **7.1** to **7.6.2**

	7.1	7.2	7.3	7.4	7.5	7.6.2
Formula	C ₁₁ H ₁₄ AgF ₃ N ₄ O ₃ S	C ₁₆ H ₁₆ Ag ₂ F ₆ N ₄ O ₄	C ₁₄ H ₁₆ AgF ₃ N ₄ O ₂	C ₁₃ H ₁₆ AgF ₃ N ₄ O ₃ S	C ₁₂ H ₁₆ AgBF ₄ N ₄	C ₃₄ H ₃₈ Ag ₂ B ₂ F ₈ N ₈
Formula weight	447.19	658.07	437.18	473.23	410.97	948.08
a (Å)	6.6871(7)	9.3793(7)	12.4623(14)	7.9279(4)	10.2034(3)	18.76(1)
b (Å)	25.806(2)	10.5770(7)	18.273(2)	10.0058(4)	13.3334(4)	30.12(1)
c (Å)	9.3785(8)	11.6814(8)	7.4106(8)	11.5612(5)	12.3596(4)	6.690(3)
α (°)		95.210(2)		98.964(2)		
β (°)	92.135(3)	91.393(2)	92.986(4)	108.141(2)	103.690(2)	91.96(1)
γ (°)		114.234(2)		95.402(2)		
space group	P2 ₁ /c	P-1	C2/m	P-1	P2 ₁ /c	P2 ₁ /c
D _{calcd} (g cm ⁻³)	1.837	2.082	1.723	1.847	1.671	1.666
μ (mm ⁻¹)	1.424	1.949	1.241	1.359	1.273	1.113
2θ _{max} (°)	32.15	26.35	25.30	25.00	28.27	25.00
reflns measured	26679	15985	7120	29250	21977	29173
reflns used (R _{int})	4711(0.0318)	4258(0.0325)	1572(0.0301)	4113(0.0344)	3961(0.0299)	7788(0.0446)
restraints/param	0/216	0/289	0/133	0/226	0/199	31/528
R1, [I>2σ(I)]	0.0344	0.0248	0.0288	0.0187	0.0255	0.0394
wR ² , [I>2σ(I)]	0.0538	0.0585	0.0624	0.0473	0.0624	0.1039
R(F _o ²), (all data)	0.0493	0.0328	0.0408	0.0199	0.0364	0.0448
R _w (F _o ²), (all data)	0.0578	0.0609	0.0674	0.0477	0.0698	0.1072
GooF on F ²	1.075	1.073	1.012	1.052	1.042	1.078

CHAPTER EIGHT

Summary

The preceding work has described the synthesis and characterization of a series of silver(I) complexes with the novel pyridyl-substituted phosphinite ligands PCP-31 and PCP-32 and the three isomeric aminomethylpyridine ligands, 2-, 3-, and 4-amp. The study has focused on the structural dependence of these complexes on the inter- and intra-molecular strong (covalent) and weak (non-covalent) interactions of metal-ligand bonding, hydrogen-bonding, π -stacking, anion interactions (through hydrogen-bonding, coordination or a combination of both), and temperature effects. In addition, the structural analysis of the silver(I)-amp complexes comprises the first known comprehensive study of stoichiometry control over the supramolecular features of extended coordination networks. This ratio-dependent investigation, in conjunction with the concomitantly discussed anion dependence, relates nicely the two areas which are seen to have equally pronounced effects with regards to forced structural modifications. This inquiry of such a coordinatively versatile metal will no-doubt form a basis for similar ratio studies to follow, extending to the metals with a more defined coordination number and geometry, thus furthering our knowledge and ability to design, construct, and apply these complexes to current and future technologies in which they are required.

APPENDICES

APPENDIX A

General Considerations

The following material describes the general experimental procedures, instrumentation, and software used in the characterization and X-ray crystallographic structure determinations of the compounds discussed herein. Any deviations from these general procedures have been detailed in the Experimental section of the appropriate chapter.

Synthetic Procedures

All experiments were conducted under an atmosphere of either dry nitrogen or high-purity argon using standard Schlenk techniques. Silver(I) salts were purchased from Strem Chemicals, Inc. and all other reagents were purchased from Aldrich Chemical Co. and stored in an inert atmosphere chamber under an atmosphere of high-purity argon. Synthesized ligands and metal complexes were stored under nitrogen in aluminum foil wrapped Schlenk vessels at -35 °C. Solvents were freshly distilled under the appropriate drying agent prior to use.

Spectroscopic Characterization

NMR measurements were recorded on either a Bruker Spectrospin 300 MHz or a Bruker Spectrospin 360 MHz spectrometer and spectra were referenced to residual solvent peaks. Measurements were collected at the following frequencies: ^1H at 300.13 and 360.13 MHz; ^{31}P at 129.49 and 145.78 MHz. All variable temperature ^{31}P spectra

were taken at the higher frequency. Luminescence spectra were recorded on an Instruments S. A. Inc. model Fluoromax-2 spectrometer, using band pathways of 5 nm for both excitation and emission and are presented uncorrected. Low temperature measurements were achieved by inserting an NMR sample tube of a 1×10^{-4} M solution (based on Ag) into a custom designed vacuum cell filled with liquid nitrogen. Spectra were acquired after temperature stabilization of the apparatus.

Procedures for X-ray Crystal Structure Determinations

Crystal Preparation

Suitable diffraction quality crystals were obtained by isolation on a binocular non-polarized microscope in chemically inert Paratone-N® oil. Ideal crystals were perfectly single, optically transparent, and displayed dimensions on the order of 0.15 to 0.25 mm³. The chosen crystal was then immobilized on a polymer-fiber cryoloop in a nitrogen cold stream. The cryoloop was mounted on the goniometer head by means of a magnetic base and centered in the X-ray beam using a digital camera.

Data Collection

Data collection was carried out at 110(2) K to reduce lattice vibrations and prevent sample decomposition on a on a Bruker X8 Apex using MoK α radiation ($\lambda = 0.71073 \text{ \AA}$). Unit cell dimensions were established by indexing reflections collected from a three run matrix set (3 X 12 frames). A data collection strategy was then determined by COSMO that would acquire > 99% of the unique reflections to $\theta \geq 25.00^\circ$ using a combination of ϕ and ω scans.

Data Reduction

All computations were carried out on either an Omnitech or Dell Optiplex GX270 PC using the SHELXTL vs 6.10 or vs 6.3.¹⁴⁰ Data reduction were performed using SAINT-PLUS 7.12A. Raw data were corrected for absorption effects using SADABS.¹³⁹

Structure Solution and Refinement

All structures were solved using direct methods. Typically, positional and anisotropic thermal displacement parameters were refined for all non-hydrogen atoms. Carbon- and nitrogen-bound hydrogens were placed in calculated positions (C–H = 0.96 Å; N–H = 0.93 Å) with fixed isotropic parameters [$U_{\text{iso}}(\text{H}) = 1.2(\text{C})$; $U_{\text{iso}}(\text{H}) = 1.2(\text{N})$].

Structure refinements were made by full-matrix least-squares on all F^2 data. Both conventional indices ($R1$) based on observed F values with $F > 4\sigma F$ and residual indices ($R1$ and $wR2$) are reported. Residual indices and Goodness of fit (Σ_2) were calculated as follows:

$$wR2 = \left[\frac{\sum [w(F_o^2 - F_c^2)^2]}{\sum [w(F_o^2)^2]} \right]^{1/2}$$

$$R1 = \frac{\sum \|F_o\| - \|F_c\|}{\sum \|F_o\|}$$

$$GooF = \sum_2 = \left[\frac{\sum [w(F_o^2 - F_c^2)^2]}{(n - p)} \right]^{1/2}$$

In the equations above $w^{-1} = [\sigma^2(F_o^2) + (a*P)^2 + b*P]$ and $P = [\max(F_o^2, 0) + 2F_c^2] / 3$, n is the number of reflections refined and P is the total number of parameters refined.

APPENDIX B

Crystallographic Data

The following tables are provided to supplement the tables of selected crystallographic parameters presented in the text. Included are statistical data, full bond lengths, full bond angles, torsion angles and hydrogen bonding distances (where appropriate).

Table B.1. Experimental and statistical crystal data for 2.2

Empirical formula	C _{19.50} H ₁₉ AgBCl ₃ F ₄ NP		
Formula weight	615.36		
Temperature	110(2) K		
Wavelength	0.71073 Å		
Crystal system	Monoclinic		
Space group	C2/c		
Unit cell dimensions	a = 29.399(5) Å b = 11.2041(15) Å β = 94.266(9)° c = 14.1888(18) Å 4660.7(11) Å ³ , 8		
Volume, Z	4660.7(11) Å ³ , 8		
Density (calculated)	1.754 Mg/m ³		
Absorption coefficient	1.323 mm ⁻¹		
F(000)	2440		
Crystal size	0.29 x 0.28 x 0.25 mm		
θ range for data collection	1.95 to 33.10°		
Limiting indices	-30 ≤ h ≤ 45, -17 ≤ k ≤ 17, -20 ≤ l ≤ 21		
Reflections collected	34150		
Independent reflections	(R _{int} = 0.0330)		
Completeness to θ = 33.10°	99.2 %		
Absorption correction	Multi-scan (SADABS)		
Refinement method	Full-matrix least-squares on F ²		
Data / restraints / parameters	8789 / 0 / 285		
Goodness-of-fit on F ²	1.073		
Final R indices [I>2σ(I)]	R1 = 0.0301, wR2 = 0.0812		
R indices (all data)	R1 = 0.0402, wR2 = 0.0834		
Largest diff. peak and hole	2.268 and -0.393 eÅ ⁻³		
Bond Lengths (Å)			
Ag(1)-N(1)	2.1711(14)	Ag(1)-P(1)	2.3543(5)
B(1)-F(3)	1.393(2)	B(1)-F(2)	1.3944(19)
B(1)-F(4)	1.398(2)	B(1)-F(1)	1.400(2)
C(1)-O(1)	1.4425(19)	C(1)-C(2)	1.506(2)

Table B.1. Continued

C(2)-C(6)	1.385(2)	C(2)-C(3)	1.391(2)
C(3)-N(1)	1.3424(19)	C(4)-N(1)	1.3509(19)
C(4)-C(5)	1.380(2)	C(5)-C(6)	1.393(2)
C(7)-C(8)	1.398(2)	C(7)-C(12)	1.400(2)
C(7)-P(1)	1.8048(17)	C(8)-C(9)	1.391(2)
C(9)-C(10)	1.383(2)	C(10)-C(11)	1.390(3)
C(11)-C(12)	1.388(2)	C(13)-C(14)	1.388(2)
C(13)-C(18)	1.407(2)	C(13)-P(1)	1.8104(16)
C(14)-C(15)	1.393(2)	C(15)-C(16)	1.388(3)
C(16)-C(17)	1.380(3)	C(17)-C(18)	1.397(3)
C(19)-Cl(2)	1.7627(19)	C(19)-Cl(3)	1.778(2)
C(20)-Cl(1)#1	1.7670(17)	C(20)-Cl(1)	1.7670(17)
O(1)-P(1)#2	1.6322(11)	P(1)-O(1)#3	1.6322(11)
Ag1_\$4 - F1	3.0345 (0.0011)	N1 - P1_\$3	5.5691 (0.0015)
Ag1_\$4 - F2	2.7850 (0.0011)	P1_\$3 - C2	3.8830 (0.0015)
Bond Angles (°)			
N(1)-Ag(1)-P(1)	167.28(4)	F(3)-B(1)-F(2)	110.19(14)
F(3)-B(1)-F(4)	108.75(14)	F(2)-B(1)-F(4)	109.17(13)
F(3)-B(1)-F(1)	109.92(13)	F(2)-B(1)-F(1)	109.04(14)
F(4)-B(1)-F(1)	109.77(14)	O(1)-C(1)-C(2)	109.75(13)
C(6)-C(2)-C(3)	118.05(13)	C(6)-C(2)-C(1)	121.22(14)
C(3)-C(2)-C(1)	120.67(13)	N(1)-C(3)-C(2)	123.11(14)
N(1)-C(4)-C(5)	122.09(14)	C(4)-C(5)-C(6)	119.18(14)
C(2)-C(6)-C(5)	119.27(15)	C(8)-C(7)-C(12)	119.26(15)
C(8)-C(7)-P(1)	119.15(12)	C(12)-C(7)-P(1)	121.32(13)
C(9)-C(8)-C(7)	120.26(16)	C(10)-C(9)-C(8)	119.97(17)
C(9)-C(10)-C(11)	120.39(17)	C(12)-C(11)-C(10)	120.00(16)
C(11)-C(12)-C(7)	120.13(17)	C(14)-C(13)-C(18)	120.03(15)
C(14)-C(13)-P(1)	118.67(12)	C(18)-C(13)-P(1)	121.30(13)
C(13)-C(14)-C(15)	120.02(16)	C(16)-C(15)-C(14)	119.83(17)
C(17)-C(16)-C(15)	120.68(17)	C(16)-C(17)-C(18)	120.16(17)
C(17)-C(18)-C(13)	119.28(17)	Cl(2)-C(19)-Cl(3)	110.46(10)
Cl(1)#1-C(20)-Cl(1)	111.58(15)	C(3)-N(1)-C(4)	118.30(14)
C(3)-N(1)-Ag(1)	121.17(10)	C(4)-N(1)-Ag(1)	120.24(10)
C(1)-O(1)-P(1)#2	116.47(10)	O(1)#3-P(1)-C(7)	100.84(7)
O(1)#3-P(1)-C(13)	106.01(7)	C(7)-P(1)-C(13)	105.46(7)
O(1)#3-P(1)-Ag(1)	112.77(4)	C(7)-P(1)-Ag(1)	114.96(5)
C(13)-P(1)-Ag(1)	115.39(5)		
P1_\$3 - O1 - C1 - C2	-155.05 (0.10)		

Symmetry transformations used to generate equivalent atoms:

#1 -x,y,-z+3/2 #2 x,-y+2,z+1/2 #3 x,-y+2,z-1/2

Table B.2. Experimental and statistical crystal data for 2.3

Empirical formula	C ₇₈ H ₆₈ Ag ₄ C ₁₄ F ₁₂ N ₄ O ₁₆ P ₄ S ₄
Formula weight	2370.73
Temperature	110(2) K
Wavelength	0.71073 Å
Crystal system	Monoclinic
Space group	Pc
Unit cell dimensions	a = 17.972(5) Å α = 90° b = 10.191 Å β = 115.441(4)° c = 27.936 Å γ = 90°
Volume, Z	4620(2) Å ³ , 2
Density (calculated)	1.704 Mg/m ³
Absorption coefficient	1.198 mm ⁻¹
F(000)	2360
Crystal size	0.22 x 0.17 x 0.13 mm
θ range for data collection	2.31 to 26.39°
Limiting indices	-22 ≤ h ≤ 22, -12 ≤ k ≤ 12, -34 ≤ l ≤ 34
Reflections collected	47570
Independent reflections	18852 (R _{int} = 0.0444)
Completeness to θ = 26.39°	99.8 %
Absorption correction	multi-scan (SADABS)
Refinement method	Full-matrix least-squares on F ²
Data / restraints / parameters	18852 / 201 / 1106
Goodness-of-fit on F ²	1.088
Final R indices [I>2σ (I)]	R1 = 0.0624, wR2 = 0.1531
R indices (all data)	R1 = 0.0693, wR2 = 0.1531
Largest diff. peak and hole	2.776 and -0.972 eÅ ⁻³

Bond Lengths (Å)

Ag(1)-N(2)#1	2.231(7)	Ag(1)-P(1)	2.334(2)
Ag(1)-O(5)	2.500(8)	Ag(2)-N(1)	2.217(8)
Ag(2)-P(2)	2.343(2)	Ag(2)-O(8)	2.470(7)
Ag(3)-N(4)#2	2.259(7)	Ag(3)-P(3)	2.356(2)
Ag(3)-O(11)	2.486(7)	Ag(3)-O(9)	2.517(7)
Ag(4)-N(3)	2.241(7)	Ag(4)-P(4)	2.357(2)
Ag(4)-O(14)	2.513(7)	Cl(1)-C(77)	1.729(15)
Cl(2)-C(77)	1.794(14)	S(1)-O(7)	1.356(9)
S(1)-O(5)	1.384(7)	S(1)-O(6)	1.397(11)
S(1)-C(19)	1.812(8)	S(2)-O(9)	1.424(7)
S(2)-O(10)	1.434(7)	S(2)-O(8)	1.437(7)
S(2)-C(38)	1.835(7)	S(3)-O(13)	1.420(6)
S(3)-O(12)	1.428(7)	S(3)-O(11)	1.433(7)
S(3)-C(57)	1.824(9)	S(4)-O(16)	1.404(7)
S(4)-O(14)	1.429(7)	S(4)-O(15)	1.435(7)
S(4)-C(76)	1.825(8)	P(1)-O(1)	1.625(6)
P(1)-C(13)	1.806(9)	P(1)-C(7)	1.821(9)
P(2)-O(2)	1.636(6)	P(2)-C(32)	1.791(9)
P(2)-C(26)	1.798(9)	P(3)-O(3)	1.618(6)
P(3)-C(51)	1.806(8)	P(3)-C(45)	1.820(8)
P(4)-O(4)	1.610(6)	P(4)-C(64)	1.821(8)
P(4)-C(70)	1.831(9)	C(19)-F(1)	1.303(5)
C(19)-F(3)	1.335(5)	C(19)-F(2)	1.378(6)
C(38)-F(4)	1.302(5)	C(38)-F(6)	1.335(5)
C(38)-F(5)	1.379(6)	C(57)-F(9)	1.325(5)

Table B.2. Continued

C(57)-F(7)	1.328(5)	C(57)-F(8)	1.360(7)
C(76)-F(12)	1.322(5)	C(76)-F(10)	1.327(5)
C(76)-F(11)	1.352(7)	O(1)-C(1)	1.439(11)
O(2)-C(20)	1.419(12)	O(3)-C(39)	1.443(10)
O(4)-C(58)	1.446(10)	N(1)-C(3)	1.317(11)
N(1)-C(4)	1.356(13)	N(2)-C(23)	1.306(12)
N(2)-C(22)	1.356(11)	N(2)-Ag(1)#2	2.231(7)
N(3)-C(42)	1.321(12)	N(3)-C(41)	1.348(11)
N(4)-C(60)	1.338(11)	N(4)-C(61)	1.343(11)
N(4)-Ag(3)#1	2.259(7)	C(1)-C(2)	1.519(12)
C(1)-H(1A)	0.9900	C(1)-H(1B)	0.9900
C(2)-C(6)	1.344(14)	C(2)-C(3)	1.387(12)
C(3)-H(3A)	0.9500	C(4)-C(5)	1.353(15)
C(4)-H(4B)	0.9500	C(5)-C(6)	1.410(14)
C(5)-H(5A)	0.9500	C(6)-H(6B)	0.9500
C(7)-C(8)	1.397(13)	C(7)-C(12)	1.409(14)
C(8)-C(9)	1.417(13)	C(8)-H(8A)	0.9500
C(9)-C(10)	1.325(17)	C(9)-H(9A)	0.9500
C(10)-C(11)	1.34(2)	C(10)-H(10B)	0.9500
C(11)-C(12)	1.430(17)	C(11)-H(11A)	0.9500
C(12)-H(12B)	0.9500	C(13)-C(18)	1.387(13)
C(13)-C(14)	1.391(12)	C(14)-C(15)	1.402(14)
C(14)-H(14A)	0.9500	C(15)-C(16)	1.364(15)
C(15)-H(15B)	0.9500	C(16)-C(17)	1.375(15)
C(16)-H(16B)	0.9500	C(17)-C(18)	1.399(15)
C(17)-H(17A)	0.9500	C(18)-H(18A)	0.9500
C(20)-C(21)	1.481(13)	C(20)-H(20A)	0.9900
C(20)-H(20B)	0.9900	C(21)-C(25)	1.367(14)
C(21)-C(22)	1.405(12)	C(22)-H(22A)	0.9500
C(23)-C(24)	1.385(12)	C(23)-H(23A)	0.9500
C(24)-C(25)	1.359(15)	C(24)-H(24A)	0.9500
C(25)-H(25A)	0.9500	C(26)-C(27)	1.360(13)
C(26)-C(31)	1.397(13)	C(27)-C(28)	1.424(13)
C(27)-H(27A)	0.9500	C(28)-C(29)	1.340(18)
C(28)-H(28A)	0.9500	C(29)-C(30)	1.351(17)
C(29)-H(29A)	0.9500	C(30)-C(31)	1.439(14)
C(30)-H(30A)	0.9500	C(31)-H(31A)	0.9500
C(32)-C(37)	1.376(13)	C(32)-C(33)	1.419(13)
C(33)-C(34)	1.382(15)	C(33)-H(33A)	0.9500
C(34)-C(35)	1.388(18)	C(34)-H(34A)	0.9500
C(35)-C(36)	1.396(16)	C(35)-H(35A)	0.9500
C(36)-C(37)	1.401(15)	C(36)-H(36A)	0.9500
C(37)-H(37A)	0.9500	C(39)-C(40)	1.498(12)
C(39)-H(39A)	0.9900	C(39)-H(39B)	0.9900
C(40)-C(44)	1.355(13)	C(40)-C(41)	1.395(12)
C(41)-H(41A)	0.9500	C(42)-C(43)	1.386(13)
C(42)-H(42A)	0.9500	C(43)-C(44)	1.383(14)
C(43)-H(43A)	0.9500	C(44)-H(44A)	0.9500
C(45)-C(46)	1.371(12)	C(45)-C(50)	1.396(11)
C(46)-C(47)	1.379(14)	C(46)-H(46A)	0.9500
C(47)-C(48)	1.366(14)	C(47)-H(47A)	0.9500
C(48)-C(49)	1.393(15)	C(48)-H(48A)	0.9500
C(49)-C(50)	1.347(14)	C(49)-H(49A)	0.9500
C(50)-H(50A)	0.9500	C(51)-C(52)	1.363(13)

Table B.2. Continued

C(51)-C(56)	1.382(13)	C(52)-C(53)	1.391(15)
C(52)-H(52A)	0.9500	C(53)-C(54)	1.394(16)
C(53)-H(53A)	0.9500	C(54)-C(55)	1.403(15)
C(54)-H(54A)	0.9500	C(55)-C(56)	1.328(13)
C(55)-H(55)	0.9500	C(56)-H(56A)	0.9500
C(58)-C(59)	1.475(11)	C(58)-H(58A)	0.9900
C(58)-H(58B)	0.9900	C(59)-C(60)	1.388(12)
C(59)-C(63)	1.411(12)	C(60)-H(60A)	0.9500
C(61)-C(62)	1.403(12)	C(61)-H(61A)	0.9500
C(62)-C(63)	1.359(13)	C(62)-H(62A)	0.9500
C(63)-H(63A)	0.9500	C(64)-C(69)	1.356(13)
C(64)-C(65)	1.422(12)	C(65)-C(66)	1.376(14)
C(65)-H(65A)	0.9500	C(66)-C(67)	1.389(17)
C(66)-H(66A)	0.9500	C(67)-C(68)	1.335(18)
C(67)-H(67A)	0.9500	C(68)-C(69)	1.371(15)
C(68)-H(68A)	0.9500	C(69)-H(69A)	0.9500
C(70)-C(75)	1.380(12)	C(70)-C(71)	1.383(13)
C(71)-C(72)	1.388(15)	C(71)-H(71A)	0.9500
C(72)-C(73)	1.354(17)	C(72)-H(72A)	0.9500
C(73)-C(74)	1.358(17)	C(73)-H(73A)	0.9500
C(74)-C(75)	1.387(14)	C(74)-H(74A)	0.9500
C(75)-H(75A)	0.9500	C(77)-H(77A)	0.9900
C(77)-H(77B)	0.9900	C(78)-Cl(4)	1.72(2)
C(78)-Cl(3)	1.80(2)	C(78)-H(78A)	0.9900
C(78)-H(78B)	0.9900	C(78A)-Cl(4A)	1.73(3)
C(78A)-Cl(3A)	1.80(3)	C(78A)-H(78C)	0.9900
C(78A)-H(78D)	0.9900		

Bond Angles (°)

N(2)#1-Ag(1)-P(1)	142.78(18)	P(1)-Ag(1)-O(5)	119.5(2)
N(2)#1-Ag(1)-O(5)	86.5(3)	N(1)-Ag(2)-O(8)	83.8(3)
N(1)-Ag(2)-P(2)	145.5(2)	N(4)#2-Ag(3)-P(3)	139.95(19)
P(2)-Ag(2)-O(8)	120.15(17)	P(3)-Ag(3)-O(11)	119.94(16)
N(4)#2-Ag(3)-O(11)	86.6(2)	P(3)-Ag(3)-O(9)	124.18(17)
N(4)#2-Ag(3)-O(9)	82.5(2)	N(3)-Ag(4)-P(4)	147.0(2)
O(11)-Ag(3)-O(9)	88.2(2)	P(4)-Ag(4)-O(14)	119.77(16)
N(3)-Ag(4)-O(14)	83.5(2)	O(7)-S(1)-O(6)	113.2(11)
O(7)-S(1)-O(5)	120.0(7)	O(7)-S(1)-C(19)	107.3(5)
O(5)-S(1)-O(6)	107.0(10)	O(6)-S(1)-C(19)	103.2(5)
O(5)-S(1)-C(19)	104.5(4)	O(9)-S(2)-O(8)	112.4(5)
O(9)-S(2)-O(10)	115.3(4)	O(9)-S(2)-C(38)	103.0(4)
O(10)-S(2)-O(8)	115.6(5)	O(8)-S(2)-C(38)	101.3(4)
O(10)-S(2)-C(38)	107.1(4)	O(13)-S(3)-O(11)	116.4(4)
O(13)-S(3)-O(12)	115.0(4)	O(13)-S(3)-C(57)	101.2(4)
O(12)-S(3)-O(11)	112.9(4)	O(11)-S(3)-C(57)	100.3(4)
O(12)-S(3)-C(57)	108.8(5)	O(16)-S(4)-O(15)	116.7(4)
O(16)-S(4)-O(14)	114.5(4)	O(16)-S(4)-C(76)	102.0(4)
O(14)-S(4)-O(15)	113.2(5)	O(15)-S(4)-C(76)	104.0(4)
O(14)-S(4)-C(76)	104.1(4)	O(1)-P(1)-C(7)	98.4(4)
O(1)-P(1)-C(13)	106.0(4)	O(1)-P(1)-Ag(1)	116.7(2)
C(13)-P(1)-C(7)	103.8(4)	C(7)-P(1)-Ag(1)	114.9(3)
C(13)-P(1)-Ag(1)	114.9(3)	O(2)-P(2)-C(26)	101.1(4)
O(2)-P(2)-C(32)	103.7(4)	O(2)-P(2)-Ag(2)	118.3(2)

Table B.2. Continued

C(32)-P(2)-C(26)	104.8(4)	C(26)-P(2)-Ag(2)	114.2(3)
C(32)-P(2)-Ag(2)	113.2(3)	O(3)-P(3)-C(45)	104.9(4)
O(3)-P(3)-C(51)	97.5(3)	O(3)-P(3)-Ag(3)	118.3(2)
C(51)-P(3)-C(45)	104.6(4)	C(45)-P(3)-Ag(3)	113.2(3)
C(51)-P(3)-Ag(3)	116.3(3)	O(4)-P(4)-C(70)	104.9(4)
O(4)-P(4)-C(64)	98.1(4)	O(4)-P(4)-Ag(4)	118.8(2)
C(64)-P(4)-C(70)	104.9(4)	C(70)-P(4)-Ag(4)	113.9(3)
C(64)-P(4)-Ag(4)	114.2(3)	F(1)-C(19)-F(2)	109.2(5)
F(1)-C(19)-F(3)	110.4(5)	F(1)-C(19)-S(1)	118.4(6)
F(3)-C(19)-F(2)	104.5(4)	F(2)-C(19)-S(1)	107.8(6)
F(3)-C(19)-S(1)	105.6(6)	F(4)-C(38)-F(5)	109.2(5)
F(4)-C(38)-F(6)	110.4(5)	F(4)-C(38)-S(2)	116.1(6)
F(6)-C(38)-F(5)	104.4(4)	F(5)-C(38)-S(2)	107.2(5)
F(6)-C(38)-S(2)	108.9(6)	F(9)-C(57)-F(8)	107.5(6)
F(9)-C(57)-F(7)	110.2(7)	F(9)-C(57)-S(3)	105.3(9)
F(7)-C(57)-F(8)	107.5(6)	F(8)-C(57)-S(3)	118.8(10)
F(7)-C(57)-S(3)	107.4(9)	F(12)-C(76)-F(11)	107.8(6)
F(12)-C(76)-F(10)	110.5(6)	F(12)-C(76)-S(4)	108.7(6)
F(10)-C(76)-F(11)	109.4(6)	F(11)-C(76)-S(4)	113.4(6)
F(10)-C(76)-S(4)	107.1(6)	C(20)-O(2)-P(2)	116.3(5)
C(1)-O(1)-P(1)	118.6(5)	C(58)-O(4)-P(4)	119.9(5)
C(39)-O(3)-P(3)	119.8(5)	S(2)-O(8)-Ag(2)	117.3(4)
S(1)-O(5)-Ag(1)	120.7(5)	S(3)-O(11)-Ag(3)	117.7(4)
S(2)-O(9)-Ag(3)	122.8(4)	C(3)-N(1)-C(4)	115.4(8)
S(4)-O(14)-Ag(4)	114.3(4)	C(4)-N(1)-Ag(2)	120.1(6)
C(3)-N(1)-Ag(2)	124.2(7)	C(23)-N(2)-Ag(1)#2	120.3(6)
C(23)-N(2)-C(22)	119.2(8)	C(42)-N(3)-C(41)	118.3(8)
C(22)-N(2)-Ag(1)#2	120.0(6)	C(41)-N(3)-Ag(4)	121.3(6)
C(42)-N(3)-Ag(4)	120.2(6)	C(60)-N(4)-Ag(3)#1	121.6(6)
C(60)-N(4)-C(61)	118.9(7)	O(1)-C(1)-C(2)	106.4(7)
C(61)-N(4)-Ag(3)#1	119.1(5)	C(2)-C(1)-H(1A)	110.5
O(1)-C(1)-H(1A)	110.5	C(2)-C(1)-H(1B)	110.5
O(1)-C(1)-H(1B)	110.5	C(6)-C(2)-C(3)	118.7(8)
H(1A)-C(1)-H(1B)	108.6	C(3)-C(2)-C(1)	118.0(8)
C(6)-C(2)-C(1)	123.0(8)	N(1)-C(3)-H(3A)	117.7
N(1)-C(3)-C(2)	124.5(9)	C(5)-C(4)-N(1)	124.7(9)
C(2)-C(3)-H(3A)	117.7	N(1)-C(4)-H(4B)	117.7
C(5)-C(4)-H(4B)	117.7	C(4)-C(5)-H(5A)	121.2
C(4)-C(5)-C(6)	117.5(10)	C(2)-C(6)-C(5)	119.0(9)
C(6)-C(5)-H(5A)	121.2	C(5)-C(6)-H(6B)	120.5
C(2)-C(6)-H(6B)	120.5	C(8)-C(7)-P(1)	118.2(7)
C(8)-C(7)-C(12)	121.2(9)	C(7)-C(8)-C(9)	116.8(9)
C(12)-C(7)-P(1)	120.5(8)	C(9)-C(8)-H(8A)	121.6
C(7)-C(8)-H(8A)	121.6	C(10)-C(9)-H(9A)	118.2
C(10)-C(9)-C(8)	123.5(11)	C(9)-C(10)-C(11)	119.4(11)
C(8)-C(9)-H(9A)	118.2	C(11)-C(10)-H(10B)	120.3
C(9)-C(10)-H(10B)	120.3	C(10)-C(11)-H(11A)	118.7
C(10)-C(11)-C(12)	122.7(13)	C(7)-C(12)-C(11)	116.3(11)
C(12)-C(11)-H(11A)	118.7	C(11)-C(12)-H(12B)	121.9
C(7)-C(12)-H(12B)	121.9	C(18)-C(13)-P(1)	119.4(7)
C(18)-C(13)-C(14)	119.9(8)	C(13)-C(14)-C(15)	118.9(10)
C(14)-C(13)-P(1)	120.7(7)	C(15)-C(14)-H(14A)	120.6
C(13)-C(14)-H(14A)	120.6	C(16)-C(15)-H(15B)	119.8
C(16)-C(15)-C(14)	120.3(10)	C(15)-C(16)-C(17)	121.6(10)

Table B.2. Continued

C(14)-C(15)-H(15B)	119.8	C(17)-C(16)-H(16B)	119.2
C(15)-C(16)-H(16B)	119.2	C(16)-C(17)-H(17A)	120.7
C(16)-C(17)-C(18)	118.5(9)	C(13)-C(18)-C(17)	120.7(9)
C(18)-C(17)-H(17A)	120.7	C(17)-C(18)-H(18A)	119.7
C(13)-C(18)-H(18A)	119.7	O(2)-C(20)-H(20A)	109.9
O(2)-C(20)-C(21)	108.9(8)	O(2)-C(20)-H(20B)	109.9
C(21)-C(20)-H(20A)	109.9	H(20A)-C(20)-H(20B)	108.3
C(21)-C(20)-H(20B)	109.9	C(25)-C(21)-C(20)	122.6(9)
C(25)-C(21)-C(22)	118.2(8)	N(2)-C(22)-C(21)	120.8(9)
C(22)-C(21)-C(20)	119.2(10)	C(21)-C(22)-H(22A)	119.6
N(2)-C(22)-H(22A)	119.6	N(2)-C(23)-H(23A)	118.6
N(2)-C(23)-C(24)	122.8(9)	C(25)-C(24)-C(23)	118.7(9)
C(24)-C(23)-H(23A)	118.6	C(23)-C(24)-H(24A)	120.6
C(25)-C(24)-H(24A)	120.6	C(24)-C(25)-H(25A)	119.9
C(24)-C(25)-C(21)	120.3(8)	C(27)-C(26)-C(31)	119.8(9)
C(21)-C(25)-H(25A)	119.9	C(31)-C(26)-P(2)	122.6(7)
C(27)-C(26)-P(2)	117.4(7)	C(26)-C(27)-H(27A)	120.3
C(26)-C(27)-C(28)	119.4(10)	C(29)-C(28)-C(27)	121.4(10)
C(28)-C(27)-H(27A)	120.3	C(27)-C(28)-H(28A)	119.3
C(29)-C(28)-H(28A)	119.3	C(28)-C(29)-H(29A)	119.7
C(28)-C(29)-C(30)	120.5(10)	C(29)-C(30)-C(31)	120.0(10)
C(30)-C(29)-H(29A)	119.7	C(31)-C(30)-H(30A)	120.0
C(29)-C(30)-H(30A)	120.0	C(26)-C(31)-H(31A)	120.6
C(26)-C(31)-C(30)	118.9(10)	C(37)-C(32)-C(33)	118.6(8)
C(30)-C(31)-H(31A)	120.6	C(33)-C(32)-P(2)	121.6(7)
C(37)-C(32)-P(2)	119.8(7)	C(34)-C(33)-H(33A)	119.6
C(34)-C(33)-C(32)	120.7(10)	C(33)-C(34)-C(35)	120.6(10)
C(32)-C(33)-H(33A)	119.6	C(35)-C(34)-H(34A)	119.7
C(33)-C(34)-H(34A)	119.7	C(34)-C(35)-H(35A)	120.6
C(34)-C(35)-C(36)	118.8(10)	C(35)-C(36)-C(37)	120.8(11)
C(36)-C(35)-H(35A)	120.6	C(37)-C(36)-H(36A)	119.6
C(35)-C(36)-H(36A)	119.6	C(32)-C(37)-H(37A)	119.8
C(32)-C(37)-C(36)	120.5(9)	O(3)-C(39)-C(40)	106.4(7)
C(36)-C(37)-H(37A)	119.8	C(40)-C(39)-H(39A)	110.4
O(3)-C(39)-H(39A)	110.4	C(40)-C(39)-H(39B)	110.4
O(3)-C(39)-H(39B)	110.4	C(44)-C(40)-C(41)	118.5(8)
H(39A)-C(39)-H(39B)	108.6	C(41)-C(40)-C(39)	118.9(8)
C(44)-C(40)-C(39)	122.7(8)	N(3)-C(41)-H(41A)	119.0
N(3)-C(41)-C(40)	122.0(8)	N(3)-C(42)-C(43)	123.2(8)
C(40)-C(41)-H(41A)	119.0	C(43)-C(42)-H(42A)	118.4
N(3)-C(42)-H(42A)	118.4	C(44)-C(43)-H(43A)	121.1
C(44)-C(43)-C(42)	117.8(9)	C(40)-C(44)-C(43)	120.2(9)
C(42)-C(43)-H(43A)	121.1	C(43)-C(44)-H(44A)	119.9
C(40)-C(44)-H(44A)	119.9	C(46)-C(45)-P(3)	119.1(7)
C(46)-C(45)-C(50)	119.9(8)	C(45)-C(46)-C(47)	119.4(9)
C(50)-C(45)-P(3)	121.0(7)	C(47)-C(46)-H(46A)	120.3
C(45)-C(46)-H(46A)	120.3	C(48)-C(47)-H(47A)	119.5
C(48)-C(47)-C(46)	120.9(8)	C(47)-C(48)-C(49)	119.0(9)
C(46)-C(47)-H(47A)	119.5	C(49)-C(48)-H(48A)	120.5
C(47)-C(48)-H(48A)	120.5	C(50)-C(49)-H(49A)	119.6
C(50)-C(49)-C(48)	120.8(9)	C(49)-C(50)-C(45)	119.8(9)
C(48)-C(49)-H(49A)	119.6	C(45)-C(50)-H(50A)	120.1
C(49)-C(50)-H(50A)	120.1	C(52)-C(51)-P(3)	119.6(7)
C(52)-C(51)-C(56)	117.8(8)	C(51)-C(52)-C(53)	120.2(9)

Table B.2. Continued

C(56)-C(51)-P(3)	122.5(7)	C(53)-C(52)-H(52A)	119.9
C(51)-C(52)-H(52A)	119.9	C(52)-C(53)-H(53A)	120.1
C(52)-C(53)-C(54)	119.8(10)	C(53)-C(54)-C(55)	119.7(10)
C(54)-C(53)-H(53A)	120.1	C(55)-C(54)-H(54A)	120.2
C(53)-C(54)-H(54A)	120.2	C(56)-C(55)-H(55)	121.2
C(56)-C(55)-C(54)	117.5(10)	C(55)-C(56)-C(51)	124.9(10)
C(54)-C(55)-H(55)	121.2	C(51)-C(56)-H(56A)	117.5
C(55)-C(56)-H(56A)	117.5	O(4)-C(58)-H(58A)	110.3
O(4)-C(58)-C(59)	107.3(6)	O(4)-C(58)-H(58B)	110.3
C(59)-C(58)-H(58A)	110.3	H(58A)-C(58)-H(58B)	108.5
C(59)-C(58)-H(58B)	110.3	C(60)-C(59)-C(58)	120.4(8)
C(60)-C(59)-C(63)	117.5(8)	N(4)-C(60)-C(59)	123.2(8)
C(63)-C(59)-C(58)	122.0(8)	C(59)-C(60)-H(60A)	118.4
N(4)-C(60)-H(60A)	118.4	N(4)-C(61)-H(61A)	119.5
N(4)-C(61)-C(62)	121.0(8)	C(63)-C(62)-C(61)	120.1(8)
C(62)-C(61)-H(61A)	119.5	C(61)-C(62)-H(62A)	119.9
C(63)-C(62)-H(62A)	119.9	C(62)-C(63)-H(63A)	120.5
C(62)-C(63)-C(59)	119.1(8)	C(69)-C(64)-C(65)	119.4(8)
C(59)-C(63)-H(63A)	120.5	C(65)-C(64)-P(4)	116.6(6)
C(69)-C(64)-P(4)	124.0(7)	C(66)-C(65)-H(65A)	121.0
C(66)-C(65)-C(64)	118.0(9)	C(65)-C(66)-C(67)	121.0(10)
C(64)-C(65)-H(65A)	121.0	C(67)-C(66)-H(66A)	119.5
C(65)-C(66)-H(66A)	119.5	C(68)-C(67)-H(67A)	120.3
C(68)-C(67)-C(66)	119.3(10)	C(67)-C(68)-C(69)	121.6(11)
C(66)-C(67)-H(67A)	120.3	C(69)-C(68)-H(68A)	119.2
C(67)-C(68)-H(68A)	119.2	C(64)-C(69)-H(69A)	119.8
C(64)-C(69)-C(68)	120.5(11)	C(75)-C(70)-C(71)	120.1(8)
C(68)-C(69)-H(69A)	119.8	C(71)-C(70)-P(4)	119.2(7)
C(75)-C(70)-P(4)	120.8(7)	C(70)-C(71)-H(71A)	120.0
C(70)-C(71)-C(72)	119.9(10)	C(73)-C(72)-C(71)	118.9(12)
C(72)-C(71)-H(71A)	120.0	C(71)-C(72)-H(72A)	120.5
C(73)-C(72)-H(72A)	120.5	C(72)-C(73)-H(73A)	119.0
C(72)-C(73)-C(74)	122.1(11)	C(73)-C(74)-C(75)	119.8(10)
C(74)-C(73)-H(73A)	119.0	C(75)-C(74)-H(74A)	120.1
C(73)-C(74)-H(74A)	120.1	C(70)-C(75)-H(75A)	120.4
C(70)-C(75)-C(74)	119.2(10)	Cl(1)-C(77)-Cl(2)	111.4(8)
C(74)-C(75)-H(75A)	120.4	Cl(2)-C(77)-H(77A)	109.3
Cl(1)-C(77)-H(77A)	109.3	Cl(2)-C(77)-H(77B)	109.3
Cl(1)-C(77)-H(77B)	109.3	Cl(4)-C(78)-Cl(3)	110.2(13)
H(77A)-C(77)-H(77B)	108.0	Cl(3)-C(78)-H(78A)	109.6
Cl(4)-C(78)-H(78A)	109.6	Cl(3)-C(78)-H(78B)	109.6
Cl(4)-C(78)-H(78B)	109.6	Cl(4A)-C(78A)-Cl(3A)	117(3)
H(78A)-C(78)-H(78B)	108.1	Cl(3A)-C(78A)-H(78C)	108.1
Cl(4A)-C(78A)-H(78C)	108.1	Cl(3A)-C(78A)-H(78D)	108.1
Cl(4A)-C(78A)-H(78D)	108.1	H(78C)-C(78A)-H(78D)	107.3

Symmetry transformations used to generate equivalent atoms: #1 x+1,y,z #2 x-1,y,z

Table B.3. Experimental and statistical crystal data for 2.4

Empirical formula	C ₄₀ H ₃₂ Ag ₂ F ₆ N ₂ O ₆ P ₂
Formula weight	1028.36
Temperature	110(2) K
Wavelength	0.71073 Å
Crystal system	Triclinic
Space group	P-1
Unit cell dimensions	a = 8.9906(14) Å α = 96.721(2)° b = 9.1032(14) Å β = 95.492(2)° c = 25.965(4) Å γ = 105.485(2)°
Volume, Z	2015.9(5) Å ³
Density (calculated)	1.694 Mg/m ³
Absorption coefficient	1.127 mm ⁻¹
F(000)	1024
Crystal size	.26 x .22 x .15 mm
θ range for data collection	0.80 to 27.61°
Limiting indices	-11 ≤ h ≤ 11, -11 ≤ k ≤ 11, -33 ≤ l ≤ 33
Reflections collected	27968
Independent reflections	8965 (R _{int} = 0.0358)
Completeness to θ = 27.61°	95.8 %
Absorption correction	multi-scan (SADABS)
Refinement method	Full-matrix least-squares on F ²
Data / restraints / parameters	8965 / 125 / 546
Goodness-of-fit on F ²	1.105
Final R indices [I>2σ(I)]	R1 = 0.0531, wR2 = 0.1260
R indices (all data)	R1 = 0.0567, wR2 = 0.1278
Largest diff. peak and hole	2.177 and -2.382 eÅ ⁻³

Bond Lengths (Å)

Ag(1)-N(1)#1	2.269(4)	Ag(1)-P(1)	2.3556(13)
Ag(1)-O(2)#2	2.375(4)	Ag(1)-O(2)	2.549(4)
Ag(2)-N(2)#3	2.264(5)	Ag(2)-P(2)	2.3681(13)
Ag(2)-O(5)#4	2.419(4)	Ag(2)-O(5)	2.576(4)
P(2)-O(4)	1.643(4)	P(2)-C(27)	1.820(5)
P(2)-C(33)	1.824(5)	P(1)-O(1)	1.634(4)
P(1)-C(7)	1.817(5)	P(1)-C(13)	1.818(5)
O(1)-C(1)	1.459(6)	O(2)-C(19)	1.252(6)
O(2)-Ag(1)#2	2.375(4)	O(3)-C(19)	1.230(7)
O(4)-C(21)	1.459(6)	O(5)-C(39)	1.262(6)
O(5)-Ag(2)#4	2.419(4)	O(6)-C(39)	1.228(7)
N(1)-C(3)	1.347(7)	N(1)-C(4)	1.363(7)
N(1)-Ag(1)#1	2.269(4)	N(2)-C(23)	1.338(6)
N(2)-C(24)	1.355(7)	N(2)-Ag(2)#3	2.264(4)
C(1)-C(2)	1.499(7)	C(1)-H(1B)	0.9700
C(1)-H(1C)	0.9700	C(2)-C(3)	1.397(7)
C(2)-C(6)	1.398(7)	C(3)-H(3A)	0.9300
C(4)-C(5)	1.377(8)	C(4)-H(4A)	0.9300
C(5)-C(6)	1.393(7)	C(5)-H(5A)	0.9300
C(6)-H(6A)	0.9300	C(7)-C(8)	1.397(8)
C(7)-C(12)	1.401(8)	C(8)-C(9)	1.382(9)
C(8)-H(8A)	0.9300	C(9)-C(10)	1.383(10)
C(9)-H(9A)	0.9300	C(10)-C(11)	1.386(9)
C(10)-H(10A)	0.9300	C(11)-C(12)	1.388(8)
C(11)-H(11A)	0.9300	C(12)-H(12A)	0.9300

Table B.3. Continued

C(13)-C(14)	1.397(7)	C(13)-C(18)	1.403(7)
C(14)-C(15)	1.398(8)	C(14)-H(14A)	0.9300
C(15)-C(16)	1.388(9)	C(15)-H(15A)	0.9300
C(16)-C(17)	1.397(8)	C(16)-H(16A)	0.9300
C(17)-C(18)	1.396(7)	C(17)-H(17A)	0.9300
C(18)-H(18A)	0.9300	C(19)-C(20)	1.503(7)
C(21)-C(22)	1.509(7)	C(21)-H(21A)	0.9700
C(21)-H(21B)	0.9700	C(22)-C(26)	1.389(7)
C(22)-C(23)	1.402(7)	C(23)-H(23A)	0.9300
C(24)-C(25)	1.375(8)	C(24)-H(24A)	0.9300
C(25)-C(26)	1.400(8)	C(25)-H(25A)	0.9300
C(26)-H(26A)	0.9300	C(27)-C(28)	1.389(8)
C(27)-C(32)	1.398(7)	C(28)-C(29)	1.396(8)
C(28)-H(28A)	0.9300	C(29)-C(30)	1.385(9)
C(29)-H(29A)	0.9300	C(30)-C(31)	1.384(9)
C(30)-H(30A)	0.9300	C(31)-C(32)	1.393(8)
C(31)-H(31A)	0.9300	C(32)-H(32A)	0.9300
C(33)-C(34)	1.400(7)	C(33)-C(38)	1.403(7)
C(34)-C(35)	1.403(8)	C(34)-H(34A)	0.9300
C(35)-C(36)	1.379(9)	C(35)-H(35A)	0.9300
C(36)-C(37)	1.378(9)	C(36)-H(36A)	0.9300
C(37)-C(38)	1.384(8)	C(37)-H(37A)	0.9300
C(38)-H(38A)	0.9300	C(39)-C(40)	1.538(7)
C(20)-F(3)	1.3390(11)	C(20)-F(2)	1.3391(11)
C(20)-F(1)	1.3417(11)	C(40)-F(6)	1.3397(11)
C(40)-F(5)	1.3400(11)	C(40)-F(4)	1.3406(11)
Ag1-Ag1_1\$1	3.8686(0.0009)	Ag1-Ag1_2\$2	6.0676(0.0011)
Ag1-Ag1_3\$3	24.2214(0.0035)	Ag1-Ag1_4\$4	27.2488(0.0033)
Ag2-Ag2_1\$1	26.0238(0.0033)	Ag2-Ag2_2\$2	27.1730(0.0033)
Ag2-Ag2_3\$3	5.9368(0.0011)	Ag2-Ag2_4\$4	3.9404(0.0009)
P1-N1	5.3704(0.0045)	P2-N2	5.3372(0.0045)
P1-C2	3.7940(0.0050)	P2-C22	3.7845(0.0052)

Bond Angles (°)

N(1)#1-Ag(1)-P(1)	133.36(11)	N(1)#1-Ag(1)-O(2)#2	103.06(15)
P(1)-Ag(1)-O(2)#2	119.72(10)	N(1)#1-Ag(1)-O(2)	91.60(14)
P(1)-Ag(1)-O(2)	114.52(10)	O(2)#2-Ag(1)-O(2)	76.48(13)
N(2)#3-Ag(2)-P(2)	136.26(12)	N(2)#3-Ag(2)-O(5)#4	107.22(15)
P(2)-Ag(2)-O(5)#4	112.73(10)	N(2)#3-Ag(2)-O(5)	92.18(14)
P(2)-Ag(2)-O(5)	113.91(9)	O(5)#4-Ag(2)-O(5)	75.88(14)
O(4)-P(2)-C(27)	97.8(2)	O(4)-P(2)-C(33)	105.2(2)
C(27)-P(2)-C(33)	104.5(2)	O(4)-P(2)-Ag(2)	115.24(14)
C(27)-P(2)-Ag(2)	117.52(17)	C(33)-P(2)-Ag(2)	114.52(17)
O(1)-P(1)-C(7)	105.9(2)	O(1)-P(1)-C(13)	98.6(2)
C(7)-P(1)-C(13)	103.6(2)	O(1)-P(1)-Ag(1)	115.01(14)
C(7)-P(1)-Ag(1)	115.05(18)	C(13)-P(1)-Ag(1)	116.66(16)
C(1)-O(1)-P(1)	116.8(3)	C(19)-O(2)-Ag(1)#2	109.2(3)
C(19)-O(2)-Ag(1)	138.6(3)	Ag(1)#2-O(2)-Ag(1)	103.52(13)
C(21)-O(4)-P(2)	116.6(3)	C(39)-O(5)-Ag(2)#4	108.5(3)
C(39)-O(5)-Ag(2)	135.3(3)	Ag(2)#4-O(5)-Ag(2)	104.12(13)
C(3)-N(1)-C(4)	117.6(4)	C(3)-N(1)-Ag(1)#1	120.4(3)
C(4)-N(1)-Ag(1)#1	121.2(3)	C(23)-N(2)-C(24)	117.9(5)
C(23)-N(2)-Ag(2)#3	120.2(3)	C(24)-N(2)-Ag(2)#3	121.5(3)

Table B.3. Continued

O(1)-C(1)-C(2)	109.5(4)	O(1)-C(1)-H(1B)	109.8
C(2)-C(1)-H(1B)	109.8	O(1)-C(1)-H(1C)	109.8
C(2)-C(1)-H(1C)	109.8	H(1B)-C(1)-H(1C)	108.2
C(3)-C(2)-C(6)	117.6(5)	C(3)-C(2)-C(1)	120.0(4)
C(6)-C(2)-C(1)	122.3(5)	N(1)-C(3)-C(2)	123.6(5)
N(1)-C(3)-H(3A)	118.2	C(2)-C(3)-H(3A)	118.2
N(1)-C(4)-C(5)	122.5(5)	N(1)-C(4)-H(4A)	118.7
C(5)-C(4)-H(4A)	118.7	C(4)-C(5)-C(6)	119.3(5)
C(4)-C(5)-H(5A)	120.3	C(6)-C(5)-H(5A)	120.3
C(5)-C(6)-C(2)	119.3(5)	C(5)-C(6)-H(6A)	120.3
C(2)-C(6)-H(6A)	120.3	C(8)-C(7)-C(12)	119.1(5)
C(8)-C(7)-P(1)	119.1(4)	C(12)-C(7)-P(1)	121.8(4)
C(9)-C(8)-C(7)	120.4(6)	C(9)-C(8)-H(8A)	119.8
C(7)-C(8)-H(8A)	119.8	C(8)-C(9)-C(10)	120.1(6)
C(8)-C(9)-H(9A)	120.0	C(10)-C(9)-H(9A)	120.0
C(9)-C(10)-C(11)	120.4(6)	C(9)-C(10)-H(10A)	119.8
C(11)-C(10)-H(10A)	119.8	C(10)-C(11)-C(12)	119.9(6)
C(10)-C(11)-H(11A)	120.1	C(12)-C(11)-H(11A)	120.1
C(11)-C(12)-C(7)	120.1(6)	C(11)-C(12)-H(12A)	119.9
C(7)-C(12)-H(12A)	119.9	C(14)-C(13)-C(18)	119.3(5)
C(14)-C(13)-P(1)	121.1(4)	C(18)-C(13)-P(1)	119.4(4)
C(13)-C(14)-C(15)	120.2(5)	C(13)-C(14)-H(14A)	119.9
C(15)-C(14)-H(14A)	119.9	C(16)-C(15)-C(14)	120.1(5)
C(16)-C(15)-H(15A)	120.0	C(14)-C(15)-H(15A)	120.0
C(15)-C(16)-C(17)	120.3(5)	C(15)-C(16)-H(16A)	119.8
C(17)-C(16)-H(16A)	119.8	C(18)-C(17)-C(16)	119.6(5)
C(18)-C(17)-H(17A)	120.2	C(16)-C(17)-H(17A)	120.2
C(17)-C(18)-C(13)	120.5(5)	C(17)-C(18)-H(18A)	119.8
C(13)-C(18)-H(18A)	119.8	O(3)-C(19)-O(2)	130.1(5)
O(3)-C(19)-C(20)	114.8(4)	O(2)-C(19)-C(20)	115.0(4)
O(4)-C(21)-C(22)	108.8(4)	O(4)-C(21)-H(21A)	109.9
C(22)-C(21)-H(21A)	109.9	O(4)-C(21)-H(21B)	109.9
C(22)-C(21)-H(21B)	109.9	H(21A)-C(21)-H(21B)	108.3
C(26)-C(22)-C(23)	118.0(5)	C(26)-C(22)-C(21)	122.3(5)
C(23)-C(22)-C(21)	119.7(4)	N(2)-C(23)-C(22)	123.3(5)
N(2)-C(23)-H(23A)	118.4	C(22)-C(23)-H(23A)	118.4
N(2)-C(24)-C(25)	122.8(5)	N(2)-C(24)-H(24A)	118.6
C(25)-C(24)-H(24A)	118.6	C(24)-C(25)-C(26)	119.0(5)
C(24)-C(25)-H(25A)	120.5	C(26)-C(25)-H(25A)	120.5
C(22)-C(26)-C(25)	119.1(5)	C(22)-C(26)-H(26A)	120.5
C(25)-C(26)-H(26A)	120.5	C(28)-C(27)-C(32)	119.0(5)
C(28)-C(27)-P(2)	122.3(4)	C(32)-C(27)-P(2)	118.6(4)
C(27)-C(28)-C(29)	120.6(5)	C(27)-C(28)-H(28A)	119.7
C(29)-C(28)-H(28A)	119.7	C(30)-C(29)-C(28)	120.2(6)
C(30)-C(29)-H(29A)	119.9	C(28)-C(29)-H(29A)	119.9
C(31)-C(30)-C(29)	119.3(5)	C(31)-C(30)-H(30A)	120.3
C(29)-C(30)-H(30A)	120.3	C(30)-C(31)-C(32)	120.9(5)
C(30)-C(31)-H(31A)	119.5	C(32)-C(31)-H(31A)	119.5
C(31)-C(32)-C(27)	119.9(5)	C(31)-C(32)-H(32A)	120.1
C(27)-C(32)-H(32A)	120.1	C(34)-C(33)-C(38)	119.0(5)
C(34)-C(33)-P(2)	118.3(4)	C(38)-C(33)-P(2)	122.7(4)
C(33)-C(34)-C(35)	119.9(5)	C(33)-C(34)-H(34A)	120.1
C(35)-C(34)-H(34A)	120.1	C(36)-C(35)-C(34)	120.1(6)
C(36)-C(35)-H(35A)	119.9	C(34)-C(35)-H(35A)	119.9

Table B.3. Continued

C(37)-C(36)-C(35)	120.0(5)	C(37)-C(36)-H(36A)	120.0
C(35)-C(36)-H(36A)	120.0	C(36)-C(37)-C(38)	120.9(5)
C(36)-C(37)-H(37A)	119.5	C(38)-C(37)-H(37A)	119.5
C(37)-C(38)-C(33)	120.0(5)	C(37)-C(38)-H(38A)	120.0
C(33)-C(38)-H(38A)	120.0	O(6)-C(39)-O(5)	129.9(5)
O(6)-C(39)-C(40)	117.5(5)	O(5)-C(39)-C(40)	112.5(4)
F(3)-C(20)-F(2)	109.9(6)	F(3)-C(20)-F(1)	100.7(5)
F(2)-C(20)-F(1)	99.6(7)	F(3)-C(20)-C(19)	115.8(5)
F(2)-C(20)-C(19)	116.6(7)	F(1)-C(20)-C(19)	111.8(5)
F(6)-C(40)-F(5)	106.9(10)	F(6)-C(40)-F(4)	100.7(8)
F(5)-C(40)-F(4)	100.4(8)	F(6)-C(40)-C(39)	118.6(9)
F(5)-C(40)-C(39)	114.5(7)	F(4)-C(40)-C(39)	113.5(6)
P1 - O1 - C1 - C2	-136.71 (0.36)	P2 - O4 - C21 - C22	-134.47 (0.36)

Symmetry transformations used to generate equivalent atoms: #1 -x,-y+2,-z #2 -x,-y+1,-z #3 -x+1,-y+2,-z+1 #4 -x+2,-y+2,-z+1

Table B.4. Experimental and statistical crystal data for 3.2

Empirical formula	C21.24 H19.27 Ag2 Cl1.61 F5.99 N2.22 O7.99 P S2
Formula weight	914.92
Temperature	110(2) K
Wavelength	0.71073 Å
Crystal system, space group	Triclinic, P-1
Unit cell dimensions	a = 10.8716(9) Å α = 94.502(5) deg. b = 11.9998(9) Å β = 100.834(5) deg. c = 12.1706(10) Å γ = 93.599(4) deg.
Volume	1549.7(2) Å ³
Z, Calculated density	2, 1.961 Mg/m ³
Absorption coefficient	1.671 mm ⁻¹
F(000)	897
Crystal size	0.196 x 0.097 x 0.081 mm
θ range for data collection	2.30 to 31.20 deg.
Limiting indices	-15<=h<=13, -14<=k<=17, -17<=l<=17
Reflections collected / unique	20219 / 9442 [R(int) = 0.0400]
Completeness to θ = 31.20	99.9 %
Absorption correction	Semi-empirical from equivalents
Max. and min. transmission	0.873 and 0.823
Refinement method	Full-matrix least-squares on F ²
Data / restraints / parameters	9442 / 56 / 431
Goodness-of-fit on F ²	1.016
Final R indices [I>2σ(I)]	R1 = 0.0459, wR2 = 0.1136
R indices (all data)	R1 = 0.0755, wR2 = 0.1281
Largest diff. peak and hole	1.618 and -1.251 e.Å ⁻³
Bond Lengths (Å)	
Ag(1)-O(6)	2.287(3)
Ag(1)-O(3)#1	2.434(3)
Ag(2)-N(2)	2.152(4)
Ag(2)-Ag(2)#2	3.1918(8)
Ag(1)-P(1)	2.3230(10)
Ag(1)-O(3)	2.456(3)
Ag(2)-N(1)	2.156(3)
C(1)-O(1)	1.448(4)

Table B.4. Continued

C(1)-C(2)	1.510(5)	C(1)-H(1A)	0.9900
C(1)-H(1B)	0.9900	C(2)-C(6)	1.368(5)
C(2)-C(3)	1.378(5)	C(3)-C(4)	1.373(6)
C(3)-H(3)	0.9500	C(4)-C(5)	1.379(6)
C(4)-H(4)	0.9500	C(5)-N(1)	1.337(6)
C(5)-H(5)	0.9500	C(6)-N(1)	1.352(5)
C(6)-H(6)	0.9500	C(7)-O(2)	1.447(5)
C(7)-C(8)	1.506(6)	C(7)-H(7A)	0.9900
C(7)-H(7B)	0.9900	C(8)-C(9)	1.371(6)
C(8)-C(12A)	1.38(4)	C(8)-C(12)	1.409(8)
C(9)-N(2)	1.351(5)	C(9)-H(9)	0.9500
C(10)-N(2)	1.341(8)	C(10)-C(11)	1.384(9)
C(10)-H(10)	0.9500	C(11)-C(12)	1.383(10)
C(11)-H(11)	0.9500	C(12)-H(12)	0.9500
C(10A)-N(2)	1.35(4)	C(10A)-C(11A)	1.36(5)
C(10A)-H(10A)	0.9500	C(11A)-C(12A)	1.36(5)
C(11A)-H(11A)	0.9500	C(12A)-H(12A)	0.9500
C(13)-C(14)	1.3900	C(13)-C(18)	1.3900
C(13)-P(1)	1.815(3)	C(14)-C(15)	1.3900
C(14)-H(14)	0.9500	C(15)-C(16)	1.3900
C(15)-H(15)	0.9500	C(16)-C(17)	1.3900
C(16)-H(16)	0.9500	C(17)-C(18)	1.3900
C(17)-H(17)	0.9500	C(18)-H(18)	0.9500
C(13A)-C(14A)	1.3900	C(13A)-C(18A)	1.3900
C(13A)-P(1)	1.777(10)	C(14A)-C(15A)	1.3900
C(14A)-H(14A)	0.9500	C(15A)-C(16A)	1.3900
C(15A)-H(15A)	0.9500	C(16A)-C(17A)	1.3900
C(16A)-H(16A)	0.9500	C(17A)-C(18A)	1.3900
C(17A)-H(17A)	0.9500	C(18A)-H(18A)	0.9500
C(20)-F(6)	1.311(6)	C(20)-F(4)	1.314(4)
C(20)-F(5)	1.339(5)	C(20)-S(2)	1.814(4)
C(21)-Cl(1)	1.6742	C(21)-Cl(2)	1.7878
C(21)-H(21A)	0.9900	C(21)-H(21B)	0.9900
Cl(1)-Cl(1A)	0.5889	Cl(1)-Cl(1B)	0.6778
Cl(2)-Cl(2A)	0.5057	Cl(2)-Cl(2B)	0.8715
Cl(2)-N(3)	1.09(3)	C(21A)-Cl(1A)	1.4424
C(21A)-Cl(2A)	2.0169	C(21A)-H(21C)	0.9900
C(21A)-H(21D)	0.9900	Cl(1A)-Cl(1B)	1.2159
Cl(2A)-N(3)	1.06(3)	Cl(2A)-Cl(2B)	1.3623
C(21B)-Cl(2B)	1.5058	C(21B)-Cl(1B)	1.8084
C(21B)-H(21E)	0.9900	C(21B)-H(21F)	0.9900
Cl(2B)-C(23)	1.12(2)	Cl(2B)-N(3)	1.70(3)
C(22)-C(23)	1.85(4)	C(22)-H(22A)	0.9800
C(22)-H(22B)	0.9800	C(22)-H(22C)	0.9800
C(23)-N(3)	0.92(3)	O(1)-P(1)	1.604(3)
O(2)-P(1)#2	1.602(3)	O(3)-S(1)	1.442(6)
O(3)-S(1B)	1.452(5)	O(3)-S(1A)	1.520(10)
O(3)-Ag(1)#1	2.434(3)	O(6)-S(2)	1.456(3)
O(7)-S(2)	1.424(3)	O(8)-S(2)	1.427(3)
P(1)-O(2)#2	1.602(3)	O(4)-O(4A)	0.72(2)
O(4)-S(1A)	1.224(13)	O(4)-S(1)	1.431(9)
O(4)-S(1B)	1.661(9)	O(5)-O(5B)	0.538(10)
O(5)-O(5A)	0.727(19)	O(5)-S(1B)	1.319(9)
O(5)-S(1)	1.452(9)	O(5)-S(1A)	1.669(13)

Table B.4. Continued

S(1)-O(4B)	1.233(11)	S(1)-O(5A)	1.307(16)
S(1)-O(5B)	1.617(11)	S(1)-O(4A)	1.670(19)
S(1)-C(19A)	1.821(17)	S(1)-C(19)	1.830(10)
S(1)-C(19B)	1.868(11)	C(19)-F(1A)	1.085(19)
C(19)-F(2B)	1.263(14)	C(19)-F(3B)	1.287(15)
C(19)-F(2)	1.315(12)	C(19)-F(1)	1.351(15)
C(19)-F(3)	1.362(11)	C(19)-F(3A)	1.48(2)
C(19)-F(1B)	1.566(18)	C(19)-F(2A)	1.66(2)
C(19)-S(1B)	1.736(12)	C(19)-S(1A)	1.784(15)
F(1)-F(1A)	0.85(2)	F(1)-C(19B)	1.141(14)
F(1)-F(2B)	1.697(12)	F(1)-C(19A)	1.74(2)
F(2)-F(2B)	0.524(10)	F(2)-F(2A)	0.840(19)
F(2)-C(19A)	1.118(18)	F(2)-F(1A)	1.34(2)
F(2)-C(19B)	1.453(14)	F(3)-F(3A)	0.666(18)
F(3)-C(19B)	1.390(14)	F(3)-C(19A)	1.44(2)
O(4A)-O(4B)	1.11(2)	O(4A)-S(1A)	1.411(15)
O(4A)-S(1B)	1.876(17)	O(5A)-O(5B)	1.25(2)
O(5A)-S(1B)	1.298(14)	O(5A)-O(4B)	1.41(2)
O(5A)-S(1A)	1.449(14)	S(1A)-O(4B)	1.091(11)
S(1A)-C(19B)	1.793(12)	S(1A)-C(19A)	1.831(14)
S(1A)-O(5B)	1.856(13)	C(19A)-C(19B)	0.64(2)
C(19A)-F(2B)	1.235(18)	C(19A)-F(3B)	1.30(2)
C(19A)-F(2A)	1.299(17)	C(19A)-F(1A)	1.339(18)
C(19A)-F(3A)	1.366(16)	C(19A)-S(1B)	1.679(16)
F(1A)-F(2B)	0.90(2)	F(1A)-C(19B)	0.986(17)
F(1A)-F(1B)	1.30(2)	F(2A)-F(2B)	1.35(2)
F(2A)-C(19B)	1.87(2)	F(3A)-C(19B)	1.602(18)
O(4B)-S(1B)	1.437(8)	O(5B)-S(1B)	1.420(8)
S(1B)-C(19B)	1.800(9)	C(19B)-F(2B)	1.324(11)
C(19B)-F(1B)	1.340(13)	C(19B)-F(3B)	1.354(10)

Bond Angles (°)

O(6)-Ag(1)-P(1)	144.84(7)	O(6)-Ag(1)-O(3)#1	84.01(10)
P(1)-Ag(1)-O(3)#1	122.30(7)	O(6)-Ag(1)-O(3)	82.60(10)
P(1)-Ag(1)-O(3)	122.99(7)	O(3)#1-Ag(1)-O(3)	77.49(10)
N(2)-Ag(2)-N(1)	172.27(14)	N(2)-Ag(2)-Ag(2)#2	112.51(10)
N(1)-Ag(2)-Ag(2)#2	75.21(10)	O(1)-C(1)-C(2)	111.6(3)
O(1)-C(1)-H(1A)	109.3	C(2)-C(1)-H(1A)	109.3
O(1)-C(1)-H(1B)	109.3	C(2)-C(1)-H(1B)	109.3
H(1A)-C(1)-H(1B)	108.0	C(6)-C(2)-C(3)	118.6(4)
C(6)-C(2)-C(1)	119.6(3)	C(3)-C(2)-C(1)	121.7(3)
C(4)-C(3)-C(2)	119.6(4)	C(4)-C(3)-H(3)	120.2
C(2)-C(3)-H(3)	120.2	C(3)-C(4)-C(5)	118.7(4)
C(3)-C(4)-H(4)	120.6	C(5)-C(4)-H(4)	120.6
N(1)-C(5)-C(4)	122.4(4)	N(1)-C(5)-H(5)	118.8
C(4)-C(5)-H(5)	118.8	N(1)-C(6)-C(2)	122.5(4)
N(1)-C(6)-H(6)	118.8	C(2)-C(6)-H(6)	118.8
O(2)-C(7)-C(8)	108.4(3)	O(2)-C(7)-H(7A)	110.0
C(8)-C(7)-H(7A)	110.0	O(2)-C(7)-H(7B)	110.0
C(8)-C(7)-H(7B)	110.0	H(7A)-C(7)-H(7B)	108.4
C(9)-C(8)-C(12A)	116.8(17)	C(9)-C(8)-C(12)	117.6(5)
C(12A)-C(8)-C(12)	29.0(17)	C(9)-C(8)-C(7)	122.1(4)
C(12A)-C(8)-C(7)	116.1(17)	C(12)-C(8)-C(7)	119.9(4)

Table B.4. Continued

N(2)-C(9)-C(8)	123.2(4)	N(2)-C(9)-H(9)	118.4
C(8)-C(9)-H(9)	118.4	N(2)-C(10)-C(11)	122.2(6)
N(2)-C(10)-H(10)	118.9	C(11)-C(10)-H(10)	118.9
C(12)-C(11)-C(10)	118.9(6)	C(12)-C(11)-H(11)	120.5
C(10)-C(11)-H(11)	120.5	C(11)-C(12)-C(8)	119.4(6)
C(11)-C(12)-H(12)	120.3	C(8)-C(12)-H(12)	120.3
N(2)-C(10A)-C(11A)	126(3)	N(2)-C(10A)-H(10A)	117.1
C(11A)-C(10A)-H(10A)	117.1	C(10A)-C(11A)-C(12A)	118(3)
C(10A)-C(11A)-H(11A)	120.9	C(12A)-C(11A)-H(11A)	120.9
C(11A)-C(12A)-C(8)	118(3)	C(11A)-C(12A)-H(12A)	121.1
C(8)-C(12A)-H(12A)	121.1	C(14)-C(13)-C(18)	120.0
C(14)-C(13)-P(1)	117.0(2)	C(18)-C(13)-P(1)	123.0(2)
C(13)-C(14)-C(15)	120.0	C(13)-C(14)-H(14)	120.0
C(15)-C(14)-H(14)	120.0	C(14)-C(15)-C(16)	120.0
C(14)-C(15)-H(15)	120.0	C(16)-C(15)-H(15)	120.0
C(17)-C(16)-C(15)	120.0	C(17)-C(16)-H(16)	120.0
C(15)-C(16)-H(16)	120.0	C(16)-C(17)-C(18)	120.0
C(16)-C(17)-H(17)	120.0	C(18)-C(17)-H(17)	120.0
C(17)-C(18)-C(13)	120.0	C(17)-C(18)-H(18)	120.0
C(13)-C(18)-H(18)	120.0	C(14A)-C(13A)-C(18A)	120.0
C(14A)-C(13A)-P(1)	119.14(17)	C(18A)-C(13A)-P(1)	120.81(16)
C(15A)-C(14A)-C(13A)	120.0	C(15A)-C(14A)-H(14A)	120.0
C(13A)-C(14A)-H(14A)	120.0	C(14A)-C(15A)-C(16A)	120.0
C(14A)-C(15A)-H(15A)	120.0	C(16A)-C(15A)-H(15A)	120.0
C(17A)-C(16A)-C(15A)	120.0	C(17A)-C(16A)-H(16A)	120.0
C(15A)-C(16A)-H(16A)	120.0	C(18A)-C(17A)-C(16A)	120.0
C(18A)-C(17A)-H(17A)	120.0	C(16A)-C(17A)-H(17A)	120.0
C(17A)-C(18A)-C(13A)	120.0	C(17A)-C(18A)-H(18A)	120.0
C(13A)-C(18A)-H(18A)	120.0	F(6)-C(20)-F(4)	108.6(4)
F(6)-C(20)-F(5)	108.2(3)	F(4)-C(20)-F(5)	108.4(4)
F(6)-C(20)-S(2)	110.7(3)	F(4)-C(20)-S(2)	111.8(3)
F(5)-C(20)-S(2)	109.0(3)	Cl(1)-C(21)-Cl(2)	112.3
Cl(1)-C(21)-H(21A)	109.1	Cl(2)-C(21)-H(21A)	109.1
Cl(1)-C(21)-H(21B)	109.1	Cl(2)-C(21)-H(21B)	109.1
H(21A)-C(21)-H(21B)	107.9	Cl(1A)-Cl(1)-Cl(1B)	147.3
Cl(1A)-Cl(1)-C(21)	57.2	Cl(1B)-Cl(1)-C(21)	90.2
Cl(2A)-Cl(2)-Cl(2B)	162.5	Cl(2A)-Cl(2)-N(3)	73.2(14)
Cl(2B)-Cl(2)-N(3)	120.2(14)	Cl(2A)-Cl(2)-C(21)	109.9
Cl(2B)-Cl(2)-C(21)	57.2	N(3)-Cl(2)-C(21)	176.4(14)
Cl(1A)-C(21A)-Cl(2A)	109.0	Cl(1A)-C(21A)-H(21C)	109.9
Cl(2A)-C(21A)-H(21C)	109.9	Cl(1A)-C(21A)-H(21D)	109.9
Cl(2A)-C(21A)-H(21D)	109.9	H(21C)-C(21A)-H(21D)	108.3

Table B.4. Continued

Cl(1)-Cl(1A)-Cl(1B)	17.5	Cl(1)-Cl(1A)-C(21A)	102.8
Cl(1B)-Cl(1A)-C(21A)	85.3	Cl(2)-Cl(2A)-N(3)	79.6(15)
Cl(2)-Cl(2A)-Cl(2B)	11.1	N(3)-Cl(2A)-Cl(2B)	88.4(15)
Cl(2)-Cl(2A)-C(21A)	56.5	N(3)-Cl(2A)-C(21A)	136.0(15)
Cl(2B)-Cl(2A)-C(21A)	48.3	Cl(2B)-C(21B)-Cl(1B)	129.1
Cl(2B)-C(21B)-H(21E)	105.0	Cl(1B)-C(21B)-H(21E)	105.0
Cl(2B)-C(21B)-H(21F)	105.0	Cl(1B)-C(21B)-H(21F)	105.0
H(21E)-C(21B)-H(21F)	105.9	Cl(1)-Cl(1B)-Cl(1A)	15.2
Cl(1)-Cl(1B)-C(21B)	67.8	Cl(1A)-Cl(1B)-C(21B)	52.6
Cl(2)-Cl(2B)-C(23)	7.0(12)	Cl(2)-Cl(2B)-Cl(2A)	6.4
C(23)-Cl(2B)-Cl(2A)	13.4(12)	Cl(2)-Cl(2B)-C(21B)	93.7
C(23)-Cl(2B)-C(21B)	97.5(11)	Cl(2A)-Cl(2B)-C(21B)	89.2
Cl(2)-Cl(2B)-N(3)	33.5(9)	C(23)-Cl(2B)-N(3)	29.9(14)
Cl(2A)-Cl(2B)-N(3)	38.5(9)	C(21B)-Cl(2B)-N(3)	127.2(9)
C(23)-C(22)-H(22A)	109.5	C(23)-C(22)-H(22B)	109.5
H(22A)-C(22)-H(22B)	109.5	C(23)-C(22)-H(22C)	109.5
H(22A)-C(22)-H(22C)	109.5	H(22B)-C(22)-H(22C)	109.5
N(3)-C(23)-Cl(2B)	113(3)	N(3)-C(23)-C(22)	164(3)
Cl(2B)-C(23)-C(22)	51.0(15)	C(23)-N(3)-Cl(2A)	20.6(13)
C(23)-N(3)-Cl(2)	12.4(16)	Cl(2A)-N(3)-Cl(2)	27.2(7)
C(23)-N(3)-Cl(2B)	37.2(17)	Cl(2A)-N(3)-Cl(2B)	53.2(12)
Cl(2)-N(3)-Cl(2B)	26.3(7)	C(5)-N(1)-C(6)	118.1(3)
C(5)-N(1)-Ag(2)	125.2(3)	C(6)-N(1)-Ag(2)	115.6(3)
C(10)-N(2)-C(10A)	29.6(16)	C(10)-N(2)-C(9)	118.6(4)
C(10A)-N(2)-C(9)	111.0(16)	C(10)-N(2)-Ag(2)	120.4(4)
C(10A)-N(2)-Ag(2)	122.8(15)	C(9)-N(2)-Ag(2)	120.8(3)
C(1)-O(1)-P(1)	119.3(2)	C(7)-O(2)-P(1)#2	122.4(2)
S(1)-O(3)-S(1B)	9.7(3)	S(1)-O(3)-S(1A)	9.8(5)
S(1B)-O(3)-S(1A)	18.4(4)	S(1)-O(3)-Ag(1)#1	133.5(3)
S(1B)-O(3)-Ag(1)#1	126.0(3)	S(1A)-O(3)-Ag(1)#1	143.3(4)
S(1)-O(3)-Ag(1)	122.5(4)	S(1B)-O(3)-Ag(1)	131.1(3)
S(1A)-O(3)-Ag(1)	112.9(4)	Ag(1)#1-O(3)-Ag(1)	102.51(10)
S(2)-O(6)-Ag(1)	115.58(15)	O(2)#2-P(1)-O(1)	106.44(15)
O(2)#2-P(1)-C(13A)	106.7(3)	O(1)-P(1)-C(13A)	102.8(2)
O(2)#2-P(1)-C(13)	105.20(19)	O(1)-P(1)-C(13)	98.27(17)
C(13A)-P(1)-C(13)	5.6(2)	O(2)#2-P(1)-Ag(1)	105.83(11)
O(1)-P(1)-Ag(1)	116.40(11)	C(13A)-P(1)-Ag(1)	117.86(18)
C(13)-P(1)-Ag(1)	123.29(13)	O(7)-S(2)-O(8)	116.2(3)
O(7)-S(2)-O(6)	114.03(19)	O(8)-S(2)-O(6)	114.63(19)
O(7)-S(2)-C(20)	105.0(2)	O(8)-S(2)-C(20)	102.28(15)
O(6)-S(2)-C(20)	102.38(18)	O(4A)-O(4)-S(1A)	89.0(15)
O(4A)-O(4)-S(1)	96.1(15)	S(1A)-O(4)-S(1)	7.1(6)
O(4A)-O(4)-S(1B)	95.7(15)	S(1A)-O(4)-S(1B)	7.9(4)
S(1)-O(4)-S(1B)	3.2(3)	O(5B)-O(5)-O(5A)	162(2)
O(5B)-O(5)-S(1B)	89.5(13)	O(5A)-O(5)-S(1B)	72.3(12)
O(5B)-O(5)-S(1)	97.9(13)	O(5A)-O(5)-S(1)	63.9(13)
S(1B)-O(5)-S(1)	8.5(3)	O(5B)-O(5)-S(1A)	101.8(13)
O(5A)-O(5)-S(1A)	60.0(12)	S(1B)-O(5)-S(1A)	12.7(4)
S(1)-O(5)-S(1A)	5.6(5)	O(4B)-S(1)-O(5A)	67.6(12)
O(4B)-S(1)-O(4)	19.4(5)	O(5A)-S(1)-O(4)	86.9(11)
O(4B)-S(1)-O(3)	127.5(6)	O(5A)-S(1)-O(3)	128.4(9)
O(4)-S(1)-O(3)	114.3(5)	O(4B)-S(1)-O(5)	96.7(7)
O(5A)-S(1)-O(5)	30.0(9)	O(4)-S(1)-O(5)	116.1(6)
O(3)-S(1)-O(5)	115.3(6)	O(4B)-S(1)-O(5B)	115.4(7)

Table B.4. Continued

O(5A)-S(1)-O(5B)	49.2(10)	O(4)-S(1)-O(5B)	134.6(6)
O(3)-S(1)-O(5B)	103.9(5)	O(5)-S(1)-O(5B)	19.3(4)
O(4B)-S(1)-O(4A)	41.9(9)	O(5A)-S(1)-O(4A)	107.5(12)
O(4)-S(1)-O(4A)	25.5(7)	O(3)-S(1)-O(4A)	109.5(9)
O(5)-S(1)-O(4A)	133.0(9)	O(5B)-S(1)-O(4A)	146.6(9)
O(4B)-S(1)-C(19A)	117.8(8)	O(5A)-S(1)-C(19A)	108.8(11)
O(4)-S(1)-C(19A)	114.9(8)	O(3)-S(1)-C(19A)	103.6(7)
O(5)-S(1)-C(19A)	89.4(8)	O(5B)-S(1)-C(19A)	76.8(8)
O(4A)-S(1)-C(19A)	93.5(10)	O(4B)-S(1)-C(19)	111.7(7)
O(5A)-S(1)-C(19)	118.4(10)	O(4)-S(1)-C(19)	105.1(6)
O(3)-S(1)-C(19)	101.4(5)	O(5)-S(1)-C(19)	101.8(7)
O(5B)-S(1)-C(19)	89.8(6)	O(4A)-S(1)-C(19)	82.1(9)
C(19A)-S(1)-C(19)	13.0(7)	O(4B)-S(1)-C(19B)	108.6(7)
O(5A)-S(1)-C(19B)	123.5(10)	O(4)-S(1)-C(19B)	100.2(6)
O(3)-S(1)-C(19B)	99.5(4)	O(5)-S(1)-C(19B)	108.6(6)
O(5B)-S(1)-C(19B)	96.7(6)	O(4A)-S(1)-C(19B)	76.4(9)
C(19A)-S(1)-C(19B)	19.9(7)	C(19)-S(1)-C(19B)	6.9(6)
F(1A)-C(19)-F(2B)	44.2(13)	F(1A)-C(19)-F(3B)	103.5(13)
F(2B)-C(19)-F(3B)	109.3(10)	F(1A)-C(19)-F(2)	67.0(14)
F(2B)-C(19)-F(2)	23.4(5)	F(3B)-C(19)-F(2)	102.1(11)
F(1A)-C(19)-F(1)	38.8(13)	F(2B)-C(19)-F(1)	80.9(9)
F(3B)-C(19)-F(1)	106.6(10)	F(2)-C(19)-F(1)	104.2(9)
F(1A)-C(19)-F(3)	108.0(14)	F(2B)-C(19)-F(3)	123.0(10)
F(3B)-C(19)-F(3)	15.4(5)	F(2)-C(19)-F(3)	117.5(11)
F(1)-C(19)-F(3)	100.5(10)	F(1A)-C(19)-F(3A)	118.0(14)
F(2B)-C(19)-F(3A)	111.1(12)	F(3B)-C(19)-F(3A)	18.1(7)
F(2)-C(19)-F(3A)	97.2(11)	F(1)-C(19)-F(3A)	124.6(11)
F(3)-C(19)-F(3A)	26.7(7)	F(1A)-C(19)-F(1B)	55.2(15)
F(2B)-C(19)-F(1B)	97.4(10)	F(3B)-C(19)-F(1B)	102.9(10)
F(2)-C(19)-F(1B)	120.7(10)	F(1)-C(19)-F(1B)	16.6(5)
F(3)-C(19)-F(1B)	93.2(9)	F(3A)-C(19)-F(1B)	119.5(11)
F(1A)-C(19)-F(2A)	96.9(16)	F(2B)-C(19)-F(2A)	52.9(10)
F(3B)-C(19)-F(2A)	96.7(13)	F(2)-C(19)-F(2A)	29.9(7)
F(1)-C(19)-F(2A)	133.1(11)	F(3)-C(19)-F(2A)	110.2(13)
F(3A)-C(19)-F(2A)	84.1(12)	F(1B)-C(19)-F(2A)	148.9(11)
F(1A)-C(19)-S(1B)	137.1(14)	F(2B)-C(19)-S(1B)	119.2(9)
F(3B)-C(19)-S(1B)	118.8(9)	F(2)-C(19)-S(1B)	107.7(9)
F(1)-C(19)-S(1B)	115.6(9)	F(3)-C(19)-S(1B)	111.2(8)
F(3A)-C(19)-S(1B)	104.8(10)	F(1B)-C(19)-S(1B)	105.5(8)
F(2A)-C(19)-S(1B)	85.4(9)	F(1A)-C(19)-S(1A)	133.1(16)
F(2B)-C(19)-S(1A)	129.6(10)	F(3B)-C(19)-S(1A)	116.8(9)
F(2)-C(19)-S(1A)	122.0(10)	F(1)-C(19)-S(1A)	103.7(10)
F(3)-C(19)-S(1A)	105.8(8)	F(3A)-C(19)-S(1A)	106.8(10)
F(1B)-C(19)-S(1A)	91.6(8)	F(2A)-C(19)-S(1A)	101.0(10)
S(1B)-C(19)-S(1A)	15.6(4)	F(1A)-C(19)-S(1)	135.7(15)
F(2B)-C(19)-S(1)	124.2(9)	F(3B)-C(19)-S(1)	118.2(8)
F(2)-C(19)-S(1)	114.4(9)	F(1)-C(19)-S(1)	110.1(9)
F(3)-C(19)-S(1)	108.9(7)	F(3A)-C(19)-S(1)	106.0(10)
F(1B)-C(19)-S(1)	98.9(8)	F(2A)-C(19)-S(1)	92.7(10)
S(1B)-C(19)-S(1)	7.3(3)	S(1A)-C(19)-S(1)	8.3(4)
F(1A)-F(1)-C(19B)	57.2(12)	F(1A)-F(1)-C(19)	53.4(12)
C(19B)-F(1)-C(19)	3.9(8)	F(1A)-F(1)-F(2B)	14.0(13)
C(19B)-F(1)-F(2B)	51.1(6)	C(19)-F(1)-F(2B)	47.3(6)
F(1A)-F(1)-C(19A)	48.5(11)	C(19B)-F(1)-C(19A)	9.1(8)

Table B.4. Continued

C(19)-F(1)-C(19A)	5.2(8)	F(2B)-F(1)-C(19A)	42.1(6)
F(2B)-F(2)-F(2A)	165(2)	F(2B)-F(2)-C(19A)	90.1(17)
F(2A)-F(2)-C(19A)	81.8(14)	F(2B)-F(2)-C(19)	72.8(13)
F(2A)-F(2)-C(19)	98.8(14)	C(19A)-F(2)-C(19)	17.3(11)
F(2B)-F(2)-F(1A)	26.3(13)	F(2A)-F(2)-F(1A)	147.0(15)
C(19A)-F(2)-F(1A)	65.3(12)	C(19)-F(2)-F(1A)	48.3(10)
F(2B)-F(2)-C(19B)	65.4(12)	F(2A)-F(2)-C(19B)	105.9(14)
C(19A)-F(2)-C(19B)	24.7(11)	C(19)-F(2)-C(19B)	7.4(8)
F(1A)-F(2)-C(19B)	41.1(8)	F(3A)-F(3)-C(19)	86.6(15)
F(3A)-F(3)-C(19B)	95.9(15)	C(19)-F(3)-C(19B)	9.4(8)
F(3A)-F(3)-C(19A)	70.0(14)	C(19)-F(3)-C(19A)	16.7(9)
C(19B)-F(3)-C(19A)	26.0(9)	O(4)-O(4A)-O(4B)	18.7(11)
O(4)-O(4A)-S(1A)	60.2(13)	O(4B)-O(4A)-S(1A)	49.5(8)
O(4)-O(4A)-S(1)	58.4(12)	O(4B)-O(4A)-S(1)	47.6(7)
S(1A)-O(4A)-S(1)	1.9(5)	O(4)-O(4A)-S(1B)	61.8(12)
O(4B)-O(4A)-S(1B)	49.9(7)	S(1A)-O(4A)-S(1B)	4.1(4)
S(1)-O(4A)-S(1B)	4.4(3)	O(5)-O(5A)-O(5B)	7.7(9)
O(5)-O(5A)-S(1B)	75.5(15)	O(5B)-O(5A)-S(1B)	67.7(10)
O(5)-O(5A)-S(1)	86.2(16)	O(5B)-O(5A)-S(1)	78.4(11)
S(1B)-O(5A)-S(1)	10.8(4)	O(5)-O(5A)-O(4B)	137.7(17)
O(5B)-O(5A)-O(4B)	130.2(11)	S(1B)-O(5A)-O(4B)	63.8(8)
S(1)-O(5A)-O(4B)	53.7(8)	O(5)-O(5A)-S(1A)	94.3(15)
O(5B)-O(5A)-S(1A)	86.6(10)	S(1B)-O(5A)-S(1A)	19.1(5)
S(1)-O(5A)-S(1A)	9.3(6)	O(4B)-O(5A)-S(1A)	44.8(6)
O(4B)-S(1A)-O(4)	23.5(6)	O(4B)-S(1A)-O(4A)	51.0(12)
O(4)-S(1A)-O(4A)	30.8(9)	O(4B)-S(1A)-O(5A)	66.0(12)
O(4)-S(1A)-O(5A)	89.3(11)	O(4A)-S(1A)-O(5A)	114.9(13)
O(4B)-S(1A)-O(3)	133.0(9)	O(4)-S(1A)-O(3)	122.8(8)
O(4A)-S(1A)-O(3)	120.5(11)	O(5A)-S(1A)-O(3)	112.9(10)
O(4B)-S(1A)-O(5)	91.2(9)	O(4)-S(1A)-O(5)	114.6(9)
O(4A)-S(1A)-O(5)	136.8(12)	O(5A)-S(1A)-O(5)	25.7(8)
O(3)-S(1A)-O(5)	100.0(6)	O(4B)-S(1A)-C(19)	123.9(10)
O(4)-S(1A)-C(19)	118.5(9)	O(4A)-S(1A)-C(19)	91.4(11)
O(5A)-S(1A)-C(19)	113.3(11)	O(3)-S(1A)-C(19)	100.4(6)
O(5)-S(1A)-C(19)	95.6(8)	O(4B)-S(1A)-C(19B)	122.0(9)
O(4)-S(1A)-C(19B)	113.8(8)	O(4A)-S(1A)-C(19B)	85.5(11)
O(5A)-S(1A)-C(19B)	119.7(10)	O(3)-S(1A)-C(19B)	99.8(6)
O(5)-S(1A)-C(19B)	102.8(7)	C(19)-S(1A)-C(19B)	7.2(6)
O(4B)-S(1A)-C(19A)	126.7(10)	O(4)-S(1A)-C(19A)	127.1(10)
O(4A)-S(1A)-C(19A)	102.6(11)	O(5A)-S(1A)-C(19A)	102.0(11)
O(3)-S(1A)-C(19A)	100.0(7)	O(5)-S(1A)-C(19A)	82.8(8)
C(19)-S(1A)-C(19A)	13.1(7)	C(19B)-S(1A)-C(19A)	20.3(7)
O(4B)-S(1A)-O(5B)	107.4(9)	O(4)-S(1A)-O(5B)	130.9(8)
O(4A)-S(1A)-O(5B)	148.9(11)	O(5A)-S(1A)-O(5B)	42.2(9)
O(3)-S(1A)-O(5B)	90.6(6)	O(5)-S(1A)-O(5B)	16.5(3)
C(19)-S(1A)-O(5B)	84.1(7)	C(19B)-S(1A)-O(5B)	91.3(6)
C(19A)-S(1A)-O(5B)	71.0(8)	C(19B)-C(19A)-F(2)	108(2)
C(19B)-C(19A)-F(2B)	83(2)	F(2)-C(19A)-F(2B)	25.1(6)
C(19B)-C(19A)-F(3B)	81.0(19)	F(2)-C(19A)-F(3B)	113.6(14)
F(2B)-C(19A)-F(3B)	110.4(13)	C(19B)-C(19A)-F(2A)	147(2)
F(2)-C(19A)-F(2A)	39.8(10)	F(2B)-C(19A)-F(2A)	64.5(12)
F(3B)-C(19A)-F(2A)	117.4(16)	C(19B)-C(19A)-F(1A)	44.1(17)
F(2)-C(19A)-F(1A)	65.3(14)	F(2B)-C(19A)-F(1A)	40.6(11)
F(3B)-C(19A)-F(1A)	90.2(15)	F(2A)-C(19A)-F(1A)	105.0(15)

Table B.4. Continued

C(19B)-C(19A)-F(3A)	100(2)	F(2)-C(19A)-F(3A)	115.0(14)
F(2B)-C(19A)-F(3A)	121.0(14)	F(3B)-C(19A)-F(3A)	20.3(8)
F(2A)-C(19A)-F(3A)	104.7(15)	F(1A)-C(19A)-F(3A)	109.4(16)
C(19B)-C(19A)-F(3)	72.4(18)	F(2)-C(19A)-F(3)	126.3(14)
F(2B)-C(19A)-F(3)	118.8(14)	F(3B)-C(19A)-F(3)	13.9(6)
F(2A)-C(19A)-F(3)	130.3(15)	F(1A)-C(19A)-F(3)	91.1(14)
F(3A)-C(19A)-F(3)	27.2(8)	C(19B)-C(19A)-S(1B)	90.2(15)
F(2)-C(19A)-S(1B)	123.3(14)	F(2B)-C(19A)-S(1B)	125.4(13)
F(3B)-C(19A)-S(1B)	122.1(12)	F(2A)-C(19A)-S(1B)	100.7(14)
F(1A)-C(19A)-S(1B)	121.3(14)	F(3A)-C(19A)-S(1B)	113.6(12)
F(3)-C(19A)-S(1B)	110.3(11)	C(19B)-C(19A)-F(1)	16.3(13)
F(2)-C(19A)-F(1)	92.2(13)	F(2B)-C(19A)-F(1)	67.0(10)
F(3B)-C(19A)-F(1)	86.9(12)	F(2A)-C(19A)-F(1)	130.7(15)
F(1A)-C(19A)-F(1)	28.3(10)	F(3A)-C(19A)-F(1)	107.0(14)
F(3)-C(19A)-F(1)	81.3(11)	S(1B)-C(19A)-F(1)	100.0(9)
C(19B)-C(19A)-S(1)	84.2(15)	F(2)-C(19A)-S(1)	128.0(14)
F(2B)-C(19A)-S(1)	126.9(13)	F(3B)-C(19A)-S(1)	118.2(12)
F(2A)-C(19A)-S(1)	107.2(14)	F(1A)-C(19A)-S(1)	117.6(14)
F(3A)-C(19A)-S(1)	111.9(12)	F(3)-C(19A)-S(1)	105.8(11)
S(1B)-C(19A)-S(1)	6.6(3)	F(1)-C(19A)-S(1)	94.7(9)
C(19B)-C(19A)-S(1A)	76.5(15)	F(2)-C(19A)-S(1A)	133.1(14)
F(2B)-C(19A)-S(1A)	127.8(13)	F(3B)-C(19A)-S(1A)	113.2(12)
F(2A)-C(19A)-S(1A)	115.4(14)	F(1A)-C(19A)-S(1A)	112.3(14)
F(3A)-C(19A)-S(1A)	109.6(12)	F(3)-C(19A)-S(1A)	100.1(10)
S(1B)-C(19A)-S(1A)	14.9(4)	F(1)-C(19A)-S(1A)	87.9(9)
S(1)-C(19A)-S(1A)	8.3(4)	F(1)-F(1A)-F(2B)	153(2)
F(1)-F(1A)-C(19B)	76.6(18)	F(2B)-F(1A)-C(19B)	89.1(17)
F(1)-F(1A)-C(19)	87.8(18)	F(2B)-F(1A)-C(19)	78.5(16)
C(19B)-F(1A)-C(19)	11.3(11)	F(1)-F(1A)-F(1B)	7.1(8)
F(2B)-F(1A)-F(1B)	151.6(18)	C(19B)-F(1A)-F(1B)	70.2(16)
C(19)-F(1A)-F(1B)	81.5(16)	F(1)-F(1A)-F(2)	147.9(18)
F(2B)-F(1A)-F(2)	15.0(8)	C(19B)-F(1A)-F(2)	75.7(14)
C(19)-F(1A)-F(2)	64.7(12)	F(1B)-F(1A)-F(2)	143.6(13)
F(1)-F(1A)-C(19A)	103.3(17)	F(2B)-F(1A)-C(19A)	63.5(13)
C(19B)-F(1A)-C(19A)	26.9(12)	C(19)-F(1A)-C(19A)	15.6(11)
F(1B)-F(1A)-C(19A)	97.1(14)	F(2)-F(1A)-C(19A)	49.4(10)
F(2)-F(2A)-C(19A)	58.4(13)	F(2)-F(2A)-F(2B)	5.8(9)
C(19A)-F(2A)-F(2B)	55.5(10)	F(2)-F(2A)-C(19)	51.3(10)
C(19A)-F(2A)-C(19)	7.6(9)	F(2B)-F(2A)-C(19)	48.1(7)
F(2)-F(2A)-C(19B)	48.5(10)	C(19A)-F(2A)-C(19B)	10.9(9)
F(2B)-F(2A)-C(19B)	45.1(6)	C(19)-F(2A)-C(19B)	3.3(6)
F(3)-F(3A)-C(19A)	82.7(16)	F(3)-F(3A)-C(19)	66.7(14)
C(19A)-F(3A)-C(19)	16.1(9)	F(3)-F(3A)-C(19B)	59.7(13)
C(19A)-F(3A)-C(19B)	23.2(9)	C(19)-F(3A)-C(19B)	7.1(7)
S(1A)-O(4B)-O(4A)	79.5(11)	S(1A)-O(4B)-S(1)	11.1(6)
O(4A)-O(4B)-S(1)	90.6(11)	S(1A)-O(4B)-O(5A)	69.3(10)
O(4A)-O(4B)-O(5A)	144.4(14)	S(1)-O(4B)-O(5A)	58.7(9)
S(1A)-O(4B)-S(1B)	15.2(6)	O(4A)-O(4B)-S(1B)	93.8(10)
S(1)-O(4B)-S(1B)	5.9(4)	O(5A)-O(4B)-S(1B)	54.1(8)
O(5)-O(5B)-O(5A)	10.5(12)	O(5)-O(5B)-S(1B)	68.2(12)
O(5A)-O(5B)-S(1B)	57.8(7)	O(5)-O(5B)-S(1)	62.8(12)
O(5A)-O(5B)-S(1)	52.3(7)	S(1B)-O(5B)-S(1)	5.5(3)
O(5)-O(5B)-S(1A)	61.7(12)	O(5A)-O(5B)-S(1A)	51.2(7)
S(1B)-O(5B)-S(1A)	7.0(3)	S(1)-O(5B)-S(1A)	3.8(4)

Table B.4. Continued

O(5A)-S(1B)-O(5)	32.2(9)	O(5A)-S(1B)-O(5B)	54.5(10)
O(5)-S(1B)-O(5B)	22.3(4)	O(5A)-S(1B)-O(4B)	62.0(11)
O(5)-S(1B)-O(4B)	93.7(6)	O(5B)-S(1B)-O(4B)	115.6(6)
O(5A)-S(1B)-O(3)	128.2(9)	O(5)-S(1B)-O(3)	123.8(5)
O(5B)-S(1B)-O(3)	114.2(5)	O(4B)-S(1B)-O(3)	112.4(5)
O(5A)-S(1B)-O(4)	78.1(11)	O(5)-S(1B)-O(4)	109.9(6)
O(5B)-S(1B)-O(4)	131.7(6)	O(4B)-S(1B)-O(4)	16.2(4)
O(3)-S(1B)-O(4)	101.4(4)	O(5A)-S(1B)-C(19A)	118.1(10)
O(5)-S(1B)-C(19A)	100.6(8)	O(5B)-S(1B)-C(19A)	86.9(8)
O(4B)-S(1B)-C(19A)	115.1(8)	O(3)-S(1B)-C(19A)	110.4(7)
O(4)-S(1B)-C(19A)	110.7(8)	O(5A)-S(1B)-C(19)	125.8(10)
O(5)-S(1B)-C(19)	113.1(7)	O(5B)-S(1B)-C(19)	100.7(7)
O(4B)-S(1B)-C(19)	107.1(6)	O(3)-S(1B)-C(19)	105.5(5)
O(4)-S(1B)-C(19)	99.9(6)	C(19A)-S(1B)-C(19)	13.8(8)
O(5A)-S(1B)-C(19B)	129.5(9)	O(5)-S(1B)-C(19B)	119.7(6)
O(5B)-S(1B)-C(19B)	107.7(6)	O(4B)-S(1B)-C(19B)	103.1(5)
O(3)-S(1B)-C(19B)	102.2(4)	O(4)-S(1B)-C(19B)	94.7(5)
C(19A)-S(1B)-C(19B)	20.8(8)	C(19)-S(1B)-C(19B)	7.0(6)
O(5A)-S(1B)-O(4A)	97.1(11)	O(5)-S(1B)-O(4A)	126.6(9)
O(5B)-S(1B)-O(4A)	145.3(8)	O(4B)-S(1B)-O(4A)	36.4(8)
O(3)-S(1B)-O(4A)	99.0(7)	O(4)-S(1B)-O(4A)	22.5(6)
C(19A)-S(1B)-O(4A)	91.2(9)	C(19)-S(1B)-O(4A)	79.1(9)
C(19B)-S(1B)-O(4A)	73.2(8)	C(19A)-C(19B)-F(1A)	109(2)
C(19A)-C(19B)-F(1)	155(2)	F(1A)-C(19B)-F(1)	46.2(14)
C(19A)-C(19B)-F(2B)	67.9(18)	F(1A)-C(19B)-F(2B)	42.8(14)
F(1)-C(19B)-F(2B)	86.7(8)	C(19A)-C(19B)-F(1B)	174.3(19)
F(1A)-C(19B)-F(1B)	66.0(16)	F(1)-C(19B)-F(1B)	20.0(5)
F(2B)-C(19B)-F(1B)	106.5(9)	C(19A)-C(19B)-F(3B)	71.1(18)
F(1A)-C(19B)-F(3B)	104.7(13)	F(1)-C(19B)-F(3B)	115.6(10)
F(2B)-C(19B)-F(3B)	101.9(9)	F(1B)-C(19B)-F(3B)	112.3(9)
C(19A)-C(19B)-F(3)	81.6(18)	F(1A)-C(19B)-F(3)	112.3(14)
F(1)-C(19B)-F(3)	110.7(9)	F(2B)-C(19B)-F(3)	116.5(9)
F(1B)-C(19B)-F(3)	102.7(9)	F(3B)-C(19B)-F(3)	15.1(5)
C(19A)-C(19B)-F(2)	46.8(17)	F(1A)-C(19B)-F(2)	63.2(15)
F(1)-C(19B)-F(2)	107.8(9)	F(2B)-C(19B)-F(2)	21.1(5)
F(1B)-C(19B)-F(2)	127.6(9)	F(3B)-C(19B)-F(2)	92.2(9)
F(3)-C(19B)-F(2)	107.2(9)	C(19A)-C(19B)-F(3A)	57.3(17)
F(1A)-C(19B)-F(3A)	115.1(15)	F(1)-C(19B)-F(3A)	131.5(11)
F(2B)-C(19B)-F(3A)	101.1(10)	F(1B)-C(19B)-F(3A)	126.7(10)
F(3B)-C(19B)-F(3A)	15.8(7)	F(3)-C(19B)-F(3A)	24.4(7)
F(2)-C(19B)-F(3A)	86.7(9)	C(19A)-C(19B)-S(1A)	83.2(14)
F(1A)-C(19B)-S(1A)	142.8(14)	F(1)-C(19B)-S(1A)	113.5(9)
F(2B)-C(19B)-S(1A)	124.4(8)	F(1B)-C(19B)-S(1A)	99.3(8)
F(3B)-C(19B)-S(1A)	112.5(8)	F(3)-C(19B)-S(1A)	104.1(7)
F(2)-C(19B)-S(1A)	113.4(8)	F(3A)-C(19B)-S(1A)	101.2(8)
C(19A)-C(19B)-S(1B)	68.9(14)	F(1A)-C(19B)-S(1B)	140.5(14)
F(1)-C(19B)-S(1B)	124.5(9)	F(2B)-C(19B)-S(1B)	111.6(8)
F(1B)-C(19B)-S(1B)	112.9(7)	F(3B)-C(19B)-S(1B)	111.0(7)
F(3)-C(19B)-S(1B)	106.4(7)	F(2)-C(19B)-S(1B)	98.6(7)
F(3A)-C(19B)-S(1B)	97.2(8)	S(1A)-C(19B)-S(1B)	15.3(4)
C(19A)-C(19B)-F(2A)	22.6(17)	F(1A)-C(19B)-F(2A)	88.8(16)

Table B.4. Continued

F(1)-C(19B)-F(2A)	132.6(10)	F(2B)-C(19B)-F(2A)	46.4(8)
F(1B)-C(19B)-F(2A)	151.7(10)	F(3B)-C(19B)-F(2A)	85.5(10)
F(3)-C(19B)-F(2A)	98.6(10)	F(2)-C(19B)-F(2A)	25.6(6)
F(3A)-C(19B)-F(2A)	74.5(9)	S(1A)-C(19B)-F(2A)	93.3(8)
S(1B)-C(19B)-F(2A)	77.9(8)	F(1A)-F(1B)-C(19B)	43.8(8)
F(1A)-F(1B)-C(19)	43.2(8)	C(19B)-F(1B)-C(19)	0.6(7)
F(2)-F(2B)-F(1A)	138.8(19)	F(2)-F(2B)-C(19A)	64.8(15)
F(1A)-F(2B)-C(19A)	75.9(13)	F(2)-F(2B)-C(19)	83.9(14)
F(1A)-F(2B)-C(19)	57.3(13)	C(19A)-F(2B)-C(19)	19.1(10)
F(2)-F(2B)-C(19B)	93.5(14)	F(1A)-F(2B)-C(19B)	48.2(11)
C(19A)-F(2B)-C(19B)	28.7(11)	C(19)-F(2B)-C(19B)	9.7(9)
F(2)-F(2B)-F(2A)	9.4(14)	F(1A)-F(2B)-F(2A)	135.8(14)
C(19A)-F(2B)-F(2A)	60.1(10)	C(19)-F(2B)-F(2A)	79.0(10)
C(19B)-F(2B)-F(2A)	88.5(10)	F(2)-F(2B)-F(1)	135.7(14)
F(1A)-F(2B)-F(1)	13.2(12)	C(19A)-F(2B)-F(1)	70.9(10)
C(19)-F(2B)-F(1)	51.8(8)	C(19B)-F(2B)-F(1)	42.2(6)
F(2A)-F(2B)-F(1)	130.2(8)	C(19)-F(3B)-C(19A)	18.4(10)
C(19)-F(3B)-C(19B)	9.4(8)	C(19A)-F(3B)-C(19B)	27.8(10)

Symmetry transformations used to generate equivalent atoms: #1 -x+1,-y,-z+2 #2 -x+1,-y,-z+1

Table B.5. Experimental and statistical crystal data for 3.3

Empirical formula	C _{53.33} H _{53.33} Ag _{2.67} B _{2.67} F _{10.67} N ₈ O _{5.33} P _{2.67}
Formula weight	1493.44
Temperature	110(2) K
Wavelength	0.71073 Å
Crystal system	monoclinic
Space group	P2 ₁ /c
Unit cell dimensions	a = 15.565(2) Å α = 90 ° b = 20.999(3) Å β = 90 ° c = 28.131(4) Å γ = 90 ° 9195(2) Å ³ , 6
Volume, Z	9195(2) Å ³ , 6
Calculated density	1.618 Mg/m ³
Absorption coefficient	1.000 mm ⁻¹
F(000)	4480
Crystal size	0.17 x 0.14 x 0.04 mm
θ range for data collection	1.21 to 23.26 °
Limiting indices	-17 ≤ h ≤ 17, -23 ≤ k ≤ 23, -31 ≤ l ≤ 31
Reflections collected	67540
Independent reflections	13167 (R _{int} = 0.0836)
Completeness to θ = 23.26	99.8 %
Absorption correction	multi-scan (SADABS)
Refinement method	Full-matrix least-squares on F ²
Data / restraints / parameters	13167 / 0 / 1147
Goodness-of-fit on F ²	1.112
Final R indices [I>2σ(I)]	R1 = 0.0464, wR2 = 0.1126
R indices (all data)	R1 = 0.0543, wR2 = 0.1177
Largest diff. peak and hole	0.996 and -0.641 e ⁻ Å ⁻³

Table B.5. Continued

Bond Lengths (Å)

Ag(1)-N(1)	2.289(6)	Ag(1)-N(2)	2.296(6)
Ag(1)-P(1)	2.3363(19)	Ag(2)-N(3)	2.274(6)
Ag(2)-N(4)	2.318(7)	Ag(2)-P(2)	2.348(2)
Ag(3)-N(5)	2.265(6)	Ag(3)-N(6)	2.285(6)
Ag(3)-P(3)	2.3622(19)	Ag(4)-N(7)	2.268(6)
Ag(4)-N(8)	2.295(6)	Ag(4)-P(4)	2.352(2)
B(1)-F(2)	1.372(11)	B(1)-F(4)	1.393(12)
B(1)-F(1)	1.402(11)	B(1)-F(3)	1.410(11)
B(2)-F(8)	1.38(2)	B(2)-F(6)	1.401(15)
B(2)-F(5)	1.417(15)	B(2)-F(7)	1.429(14)
B(3)-F(9)	1.366(11)	B(3)-F(12)	1.389(11)
B(3)-F(10)	1.400(10)	B(3)-F(11)	1.410(12)
B(4)-F(15)	1.366(15)	B(4)-F(14)	1.385(15)
B(4)-F(16)	1.395(18)	B(4)-F(13)	1.443(16)
C(1)-O(1)	1.455(9)	C(1)-C(2)	1.524(11)
C(1)-H(1A)	0.9900	C(1)-H(1B)	0.9900
C(2)-C(6)	1.379(12)	C(2)-C(3)	1.387(10)
C(3)-N(1)	1.340(9)	C(3)-H(3)	0.9500
C(4)-N(1)	1.341(11)	C(4)-C(5)	1.384(12)
C(4)-H(4)	0.9500	C(5)-C(6)	1.341(13)
C(5)-H(5)	0.9500	C(6)-H(6)	0.9500
C(7)-N(2)	1.305(11)	C(7)-C(8)	1.417(12)
C(7)-H(7)	0.9500	C(8)-C(9)	1.361(13)
C(8)-H(8)	0.9500	C(9)-C(10)	1.406(12)
C(9)-H(9)	0.9500	C(10)-C(11)	1.398(11)
C(10)-C(36)#1	1.473(11)	C(11)-N(2)	1.334(10)
C(11)-H(11)	0.9500	C(12)-C(13)	1.397(11)
C(12)-C(17)	1.401(11)	C(12)-P(1)	1.813(8)
C(13)-C(14)	1.344(11)	C(13)-H(13)	0.9500
C(14)-C(15)	1.452(12)	C(14)-H(14)	0.9500
C(15)-C(16)	1.340(13)	C(15)-H(15)	0.9500
C(16)-C(17)	1.379(11)	C(16)-H(16)	0.9500
C(17)-H(17)	0.9500	C(18)-O(3)	1.468(8)
C(18)-C(64)#2	1.495(10)	C(18)-H(18A)	0.9900
C(18)-H(18B)	0.9900	C(19)-O(2)	1.456(8)
C(19)-C(20)	1.498(10)	C(19)-H(19A)	0.9900
C(19)-H(19B)	0.9900	C(20)-C(24)	1.372(12)
C(20)-C(21)	1.393(11)	C(21)-N(3)	1.345(10)
C(21)-H(21)	0.9500	C(22)-N(3)	1.359(10)
C(22)-C(23)	1.384(11)	C(22)-H(22)	0.9500
C(23)-C(24)	1.396(11)	C(23)-H(23)	0.9500
C(24)-H(24)	0.9500	C(25)-N(4)	1.304(10)
C(25)-C(26)	1.374(12)	C(25)-H(25)	0.9500
C(26)-C(27)	1.376(12)	C(26)-H(26)	0.9500
C(27)-C(28)	1.414(12)	C(27)-H(27)	0.9500
C(28)-C(29)	1.380(11)	C(28)-C(54)#2	1.503(11)
C(29)-N(4)	1.359(10)	C(29)-H(29)	0.9500
C(30)-C(35)	1.363(12)	C(30)-C(31)	1.412(12)
C(30)-P(2)	1.814(7)	C(31)-C(32)	1.374(12)
C(31)-H(31)	0.9500	C(32)-C(33)	1.353(14)
C(32)-H(32)	0.9500	C(33)-C(34)	1.396(14)
C(33)-H(33)	0.9500	C(34)-C(35)	1.403(13)

Table B.5. Continued

C(36)-H(36A)	0.9900	C(36)-H(36B)	0.9900
C(37)-O(4)	1.462(8)	C(37)-C(38)	1.520(10)
C(37)-H(37A)	0.9900	C(37)-H(37B)	0.9900
C(38)-C(39)	1.360(11)	C(38)-C(42)	1.396(11)
C(39)-N(5)	1.355(10)	C(39)-H(39)	0.9500
C(40)-N(5)	1.335(10)	C(40)-C(41)	1.394(12)
C(40)-H(40)	0.9500	C(41)-C(42)	1.379(12)
C(41)-H(41)	0.9500	C(42)-H(42)	0.9500
C(43)-N(6)	1.343(11)	C(43)-C(44)	1.357(13)
C(43)-H(43)	0.9500	C(44)-C(45)	1.368(14)
C(44)-H(44)	0.9500	C(45)-C(46)	1.392(13)
C(45)-H(45)	0.9500	C(46)-C(47)	1.365(11)
C(46)-C(72)#4	1.513(12)	C(47)-N(6)	1.350(10)
C(47)-H(47)	0.9500	C(48)-C(49)	1.397(11)
C(48)-C(53)	1.405(11)	C(48)-P(3)	1.806(7)
C(49)-C(50)	1.378(11)	C(49)-H(49)	0.9500
C(50)-C(51)	1.390(12)	C(50)-H(50)	0.9500
C(51)-C(52)	1.388(12)	C(51)-H(51)	0.9500
C(52)-C(53)	1.381(11)	C(52)-H(52)	0.9500
C(53)-H(53)	0.9500	C(54)-O(7)	1.474(9)
C(54)-C(28)#5	1.503(11)	C(54)-H(54A)	0.9900
C(54)-H(54B)	0.9900	C(55)-O(6)	1.460(8)
C(55)-C(56)	1.518(11)	C(55)-H(55A)	0.9900
C(55)-H(55B)	0.9900	C(56)-C(60)	1.370(12)
C(56)-C(57)	1.396(11)	C(57)-N(7)	1.338(10)
C(57)-H(57)	0.9500	C(58)-N(7)	1.339(10)
C(58)-C(59)	1.408(12)	C(58)-H(58)	0.9500
C(59)-C(60)	1.390(12)	C(59)-H(59)	0.9500
C(60)-H(60)	0.9500	C(61)-N(8)	1.352(10)
C(61)-C(62)	1.365(11)	C(61)-H(61)	0.9500
C(62)-C(63)	1.373(11)	C(62)-H(62)	0.9500
C(63)-C(64)	1.374(11)	C(63)-H(63)	0.9500
C(64)-C(65)	1.391(11)	C(64)-C(18)#5	1.495(10)
C(65)-N(8)	1.344(10)	C(65)-H(65)	0.9500
C(66)-C(71)	1.359(12)	C(66)-C(67)	1.369(12)
C(66)-P(4)	1.822(7)	C(67)-C(68)	1.395(13)
C(67)-H(67)	0.9500	C(68)-C(69)	1.333(13)
C(68)-H(68)	0.9500	C(69)-C(70)	1.331(13)
C(69)-H(69)	0.9500	C(70)-C(71)	1.359(12)
C(70)-H(70)	0.9500	C(71)-H(71)	0.9500
C(72)-O(8)	1.471(9)	C(72)-C(46)#6	1.513(12)
C(72)-H(72A)	0.9900	C(72)-H(72B)	0.9900
C(73)-C(74)	1.19(2)	C(73)-H(73A)	0.9800
C(73)-H(73B)	0.9800	C(73)-H(73C)	0.9800
C(74)-N(9)	1.46(2)	C(75)-C(76)	1.459(17)
C(75)-H(75A)	0.9800	C(75)-H(75B)	0.9800
C(75)-H(75C)	0.9800	C(76)-N(10)	1.110(13)
C(77)-C(78)	1.485(13)	C(77)-H(77A)	0.9800
C(77)-H(77B)	0.9800	C(77)-H(77C)	0.9800
C(78)-N(11)	1.116(11)	C(79)-C(80)	1.451(13)
C(79)-H(79A)	0.9800	C(79)-H(79B)	0.9800
C(79)-H(79C)	0.9800	C(80)-N(12)	1.145(12)
O(1)-P(4)#7	1.609(5)	O(2)-P(1)	1.626(5)
O(3)-P(1)	1.601(5)	O(4)-P(2)	1.595(6)

Table B.5. Continued

O(5)-P(2)	1.616(5)	O(6)-P(3)	1.603(5)
O(7)-P(3)	1.608(6)	O(8)-P(4)	1.609(6)
P(4)-O(1)#8	1.609(5)		
Bond Angles (°)			
N(1)-Ag(1)-P(1)	132.42(16)	N(2)-Ag(1)-P(1)	133.09(17)
N(3)-Ag(2)-N(4)	99.4(2)	N(3)-Ag(2)-P(2)	134.39(16)
N(4)-Ag(2)-P(2)	125.61(16)	N(5)-Ag(3)-N(6)	107.3(2)
N(5)-Ag(3)-P(3)	127.88(16)	N(6)-Ag(3)-P(3)	124.12(17)
N(7)-Ag(4)-N(8)	98.3(2)	N(7)-Ag(4)-P(4)	136.43(16)
N(8)-Ag(4)-P(4)	124.43(15)	N(1)-Ag(1)-N(2)	93.1(2)
F(2)-B(1)-F(1)	110.3(8)	F(4)-B(1)-F(1)	108.9(7)
F(2)-B(1)-F(3)	109.6(8)	F(4)-B(1)-F(3)	110.6(8)
F(1)-B(1)-F(3)	108.5(7)	F(8)-B(2)-F(6)	115.4(12)
F(8)-B(2)-F(5)	110.9(11)	F(6)-B(2)-F(5)	118.1(10)
F(8)-B(2)-F(7)	106.7(11)	F(6)-B(2)-F(7)	102.8(9)
F(5)-B(2)-F(7)	100.7(9)	F(9)-B(3)-F(12)	110.3(8)
F(9)-B(3)-F(10)	109.4(7)	F(12)-B(3)-F(10)	109.7(7)
F(9)-B(3)-F(11)	110.2(7)	F(12)-B(3)-F(11)	108.0(7)
F(10)-B(3)-F(11)	109.2(8)	F(15)-B(4)-F(14)	108.2(9)
F(15)-B(4)-F(16)	102.9(10)	F(14)-B(4)-F(16)	120.8(11)
F(15)-B(4)-F(13)	105.4(10)	F(14)-B(4)-F(13)	105.5(10)
F(16)-B(4)-F(13)	113.0(10)	O(1)-C(1)-C(2)	106.6(6)
O(1)-C(1)-H(1A)	110.4	C(2)-C(1)-H(1A)	110.4
O(1)-C(1)-H(1B)	110.4	C(2)-C(1)-H(1B)	110.4
H(1A)-C(1)-H(1B)	108.6	C(6)-C(2)-C(3)	117.9(8)
C(6)-C(2)-C(1)	122.7(7)	C(3)-C(2)-C(1)	119.4(8)
N(1)-C(3)-C(2)	122.2(8)	N(1)-C(3)-H(3)	118.9
C(2)-C(3)-H(3)	118.9	N(1)-C(4)-C(5)	121.9(8)
N(1)-C(4)-H(4)	119.0	C(5)-C(4)-H(4)	119.0
C(6)-C(5)-C(4)	119.1(8)	C(6)-C(5)-H(5)	120.4
C(4)-C(5)-H(5)	120.4	C(5)-C(6)-C(2)	120.5(8)
C(5)-C(6)-H(6)	119.8	C(2)-C(6)-H(6)	119.8
N(2)-C(7)-C(8)	123.3(9)	N(2)-C(7)-H(7)	118.4
C(8)-C(7)-H(7)	118.4	C(9)-C(8)-C(7)	118.2(9)
C(9)-C(8)-H(8)	120.9	C(7)-C(8)-H(8)	120.9
C(8)-C(9)-C(10)	120.0(8)	C(8)-C(9)-H(9)	120.0
C(10)-C(9)-H(9)	120.0	C(11)-C(10)-C(9)	116.1(7)
C(11)-C(10)-C(36)#1	120.9(8)	C(9)-C(10)-C(36)#1	122.4(7)
N(2)-C(11)-C(10)	124.6(8)	N(2)-C(11)-H(11)	117.7
C(10)-C(11)-H(11)	117.7	C(13)-C(12)-C(17)	119.0(7)
C(13)-C(12)-P(1)	122.8(6)	C(17)-C(12)-P(1)	118.2(6)
C(14)-C(13)-C(12)	122.2(8)	C(14)-C(13)-H(13)	118.9
C(12)-C(13)-H(13)	118.9	C(13)-C(14)-C(15)	118.2(8)
C(13)-C(14)-H(14)	120.9	C(15)-C(14)-H(14)	120.9
C(16)-C(15)-C(14)	118.9(8)	C(16)-C(15)-H(15)	120.6
C(14)-C(15)-H(15)	120.6	C(15)-C(16)-C(17)	122.9(9)
C(15)-C(16)-H(16)	118.5	C(17)-C(16)-H(16)	118.5
C(16)-C(17)-C(12)	118.5(8)	C(16)-C(17)-H(17)	120.8
C(12)-C(17)-H(17)	120.8	O(3)-C(18)-C(64)#2	106.9(6)
O(3)-C(18)-H(18A)	110.3	C(64)#2-C(18)-H(18A)	110.3
O(3)-C(18)-H(18B)	110.3	C(64)#2-C(18)-H(18B)	110.3
H(18A)-C(18)-H(18B)	108.6	O(2)-C(19)-C(20)	107.5(6)

Table B.5. Continued

O(2)-C(19)-H(19A)	110.2	C(20)-C(19)-H(19A)	110.2
O(2)-C(19)-H(19B)	110.2	C(20)-C(19)-H(19B)	110.2
H(19A)-C(19)-H(19B)	108.5	C(24)-C(20)-C(21)	118.4(7)
C(24)-C(20)-C(19)	122.1(7)	C(21)-C(20)-C(19)	119.5(8)
N(3)-C(21)-C(20)	123.5(7)	N(3)-C(21)-H(21)	118.3
C(20)-C(21)-H(21)	118.3	N(3)-C(22)-C(23)	122.2(7)
N(3)-C(22)-H(22)	118.9	C(23)-C(22)-H(22)	118.9
C(22)-C(23)-C(24)	119.1(7)	C(22)-C(23)-H(23)	120.4
C(24)-C(23)-H(23)	120.4	C(20)-C(24)-C(23)	119.3(7)
C(20)-C(24)-H(24)	120.4	C(23)-C(24)-H(24)	120.4
N(4)-C(25)-C(26)	124.6(8)	N(4)-C(25)-H(25)	117.7
C(26)-C(25)-H(25)	117.7	C(25)-C(26)-C(27)	118.5(8)
C(25)-C(26)-H(26)	120.7	C(27)-C(26)-H(26)	120.7
C(26)-C(27)-C(28)	118.6(8)	C(26)-C(27)-H(27)	120.7
C(28)-C(27)-H(27)	120.7	C(29)-C(28)-C(27)	117.9(8)
C(29)-C(28)-C(54)#2	120.3(7)	C(27)-C(28)-C(54)#2	121.8(7)
N(4)-C(29)-C(28)	122.6(8)	N(4)-C(29)-H(29)	118.7
C(28)-C(29)-H(29)	118.7	C(35)-C(30)-C(31)	119.6(7)
C(35)-C(30)-P(2)	118.2(7)	C(31)-C(30)-P(2)	122.1(6)
C(32)-C(31)-C(30)	119.9(8)	C(32)-C(31)-H(31)	120.1
C(30)-C(31)-H(31)	120.1	C(33)-C(32)-C(31)	120.7(9)
C(33)-C(32)-H(32)	119.7	C(31)-C(32)-H(32)	119.7
C(32)-C(33)-C(34)	120.4(9)	C(32)-C(33)-H(33)	119.8
C(34)-C(33)-H(33)	119.8	C(33)-C(34)-C(35)	119.3(9)
C(33)-C(34)-H(34)	120.3	C(35)-C(34)-H(34)	120.3
C(30)-C(35)-C(34)	119.9(9)	C(30)-C(35)-H(35)	120.0
C(34)-C(35)-H(35)	120.0	O(5)-C(36)-C(10)#3	108.0(6)
O(5)-C(36)-H(36A)	110.1	C(10)-#3-C(36)-H(36A)	110.1
O(5)-C(36)-H(36B)	110.1	C(10)-#3-C(36)-H(36B)	110.1
H(36A)-C(36)-H(36B)	108.4	O(4)-C(37)-C(38)	106.1(6)
O(4)-C(37)-H(37A)	110.5	C(38)-C(37)-H(37A)	110.5
O(4)-C(37)-H(37B)	110.5	C(38)-C(37)-H(37B)	110.5
H(37A)-C(37)-H(37B)	108.7	C(39)-C(38)-C(42)	118.4(7)
C(39)-C(38)-C(37)	120.7(7)	C(42)-C(38)-C(37)	120.8(7)
N(5)-C(39)-C(38)	125.0(7)	N(5)-C(39)-H(39)	117.5
C(38)-C(39)-H(39)	117.5	N(5)-C(40)-C(41)	124.3(8)
N(5)-C(40)-H(40)	117.9	C(41)-C(40)-H(40)	117.9
C(42)-C(41)-C(40)	118.4(8)	C(42)-C(41)-H(41)	120.8
C(40)-C(41)-H(41)	120.8	C(41)-C(42)-C(38)	118.5(8)
C(41)-C(42)-H(42)	120.7	C(38)-C(42)-H(42)	120.7
N(6)-C(43)-C(44)	122.8(9)	N(6)-C(43)-H(43)	118.6
C(44)-C(43)-H(43)	118.6	C(43)-C(44)-C(45)	120.1(9)
C(43)-C(44)-H(44)	119.9	C(45)-C(44)-H(44)	119.9
C(44)-C(45)-C(46)	118.8(8)	C(44)-C(45)-H(45)	120.6
C(46)-C(45)-H(45)	120.6	C(47)-C(46)-C(45)	117.4(8)
C(47)-C(46)-C(72)#4	120.9(8)	C(45)-C(46)-C(72)#4	121.5(8)
N(6)-C(47)-C(46)	124.3(8)	N(6)-C(47)-H(47)	117.8
C(46)-C(47)-H(47)	117.8	C(49)-C(48)-C(53)	118.4(7)
C(49)-C(48)-P(3)	125.0(6)	C(53)-C(48)-P(3)	116.6(6)
C(50)-C(49)-C(48)	121.0(8)	C(50)-C(49)-H(49)	119.5
C(48)-C(49)-H(49)	119.5	C(49)-C(50)-C(51)	120.5(8)
C(49)-C(50)-H(50)	119.7	C(51)-C(50)-H(50)	119.7
C(52)-C(51)-C(50)	118.7(8)	C(52)-C(51)-H(51)	120.7
C(50)-C(51)-H(51)	120.7	C(53)-C(52)-C(51)	121.4(8)

Table B.5. Continued

C(53)-C(52)-H(52)	119.3	C(51)-C(52)-H(52)	119.3
C(52)-C(53)-C(48)	119.9(8)	C(52)-C(53)-H(53)	120.1
C(48)-C(53)-H(53)	120.1	O(7)-C(54)-C(28)#5	109.6(6)
O(7)-C(54)-H(54A)	109.8	C(28)#5-C(54)-H(54A)	109.8
O(7)-C(54)-H(54B)	109.8	C(28)#5-C(54)-H(54B)	109.8
H(54A)-C(54)-H(54B)	108.2	O(6)-C(55)-C(56)	106.6(6)
O(6)-C(55)-H(55A)	110.4	C(56)-C(55)-H(55A)	110.4
O(6)-C(55)-H(55B)	110.4	C(56)-C(55)-H(55B)	110.4
H(55A)-C(55)-H(55B)	108.6	C(60)-C(56)-C(57)	119.1(7)
C(60)-C(56)-C(55)	121.9(7)	C(57)-C(56)-C(55)	118.9(7)
N(7)-C(57)-C(56)	123.0(7)	N(7)-C(57)-H(57)	118.5
C(56)-C(57)-H(57)	118.5	N(7)-C(58)-C(59)	121.9(8)
N(7)-C(58)-H(58)	119.1	C(59)-C(58)-H(58)	119.1
C(60)-C(59)-C(58)	119.0(8)	C(60)-C(59)-H(59)	120.5
C(58)-C(59)-H(59)	120.5	C(56)-C(60)-C(59)	118.7(8)
C(56)-C(60)-H(60)	120.7	C(59)-C(60)-H(60)	120.7
N(8)-C(61)-C(62)	122.1(8)	N(8)-C(61)-H(61)	118.9
C(62)-C(61)-H(61)	118.9	C(61)-C(62)-C(63)	119.7(8)
C(61)-C(62)-H(62)	120.2	C(63)-C(62)-H(62)	120.2
C(62)-C(63)-C(64)	120.0(7)	C(62)-C(63)-H(63)	120.0
C(64)-C(63)-H(63)	120.0	C(63)-C(64)-C(65)	116.9(7)
C(63)-C(64)-C(18)#5	124.0(7)	C(65)-C(64)-C(18)#5	119.0(7)
N(8)-C(65)-C(64)	123.9(7)	N(8)-C(65)-H(65)	118.0
C(64)-C(65)-H(65)	118.0	C(71)-C(66)-C(67)	117.4(7)
C(71)-C(66)-P(4)	120.6(6)	C(67)-C(66)-P(4)	121.8(6)
C(66)-C(67)-C(68)	120.9(9)	C(66)-C(67)-H(67)	119.5
C(68)-C(67)-H(67)	119.5	C(69)-C(68)-C(67)	117.9(9)
C(69)-C(68)-H(68)	121.0	C(67)-C(68)-H(68)	121.0
C(70)-C(69)-C(68)	122.6(9)	C(70)-C(69)-H(69)	118.7
C(68)-C(69)-H(69)	118.7	C(69)-C(70)-C(71)	119.1(9)
C(69)-C(70)-H(70)	120.4	C(71)-C(70)-H(70)	120.4
C(70)-C(71)-C(66)	121.8(8)	C(70)-C(71)-H(71)	119.1
C(66)-C(71)-H(71)	119.1	O(8)-C(72)-C(46)#6	108.6(6)
O(8)-C(72)-H(72A)	110.0	C(46)#6-C(72)-H(72A)	110.0
O(8)-C(72)-H(72B)	110.0	C(46)#6-C(72)-H(72B)	110.0
H(72A)-C(72)-H(72B)	108.4	C(74)-C(73)-H(73A)	109.5
C(74)-C(73)-H(73B)	109.5	H(73A)-C(73)-H(73B)	109.5
C(74)-C(73)-H(73C)	109.5	H(73A)-C(73)-H(73C)	109.5
H(73B)-C(73)-H(73C)	109.5	C(73)-C(74)-N(9)	177.5(18)
C(76)-C(75)-H(75A)	109.5	C(76)-C(75)-H(75B)	109.5
H(75A)-C(75)-H(75B)	109.5	C(76)-C(75)-H(75C)	109.5
H(75A)-C(75)-H(75C)	109.5	H(75B)-C(75)-H(75C)	109.5
N(10)-C(76)-C(75)	174.3(13)	C(78)-C(77)-H(77A)	109.5
C(78)-C(77)-H(77B)	109.5	H(77A)-C(77)-H(77B)	109.5
C(78)-C(77)-H(77C)	109.5	H(77A)-C(77)-H(77C)	109.5
H(77B)-C(77)-H(77C)	109.5	N(11)-C(78)-C(77)	176.9(11)
C(80)-C(79)-H(79A)	109.5	C(80)-C(79)-H(79B)	109.5
H(79A)-C(79)-H(79B)	109.5	C(80)-C(79)-H(79C)	109.5
H(79A)-C(79)-H(79C)	109.5	H(79B)-C(79)-H(79C)	109.5
N(12)-C(80)-C(79)	176.3(12)	C(3)-N(1)-C(4)	118.3(7)
C(3)-N(1)-Ag(1)	118.2(5)	C(4)-N(1)-Ag(1)	123.4(5)
C(7)-N(2)-C(11)	117.7(7)	C(7)-N(2)-Ag(1)	122.6(6)
C(11)-N(2)-Ag(1)	119.0(5)	C(21)-N(3)-C(22)	117.5(7)
C(21)-N(3)-Ag(2)	119.7(5)	C(22)-N(3)-Ag(2)	122.4(5)

Table B.5. Continued

C(25)-N(4)-C(29)	117.8(7)	C(25)-N(4)-Ag(2)	121.6(6)
C(29)-N(4)-Ag(2)	120.4(5)	C(40)-N(5)-C(39)	115.4(7)
C(40)-N(5)-Ag(3)	126.3(5)	C(39)-N(5)-Ag(3)	118.2(5)
C(43)-N(6)-C(47)	116.5(7)	C(43)-N(6)-Ag(3)	122.2(6)
C(47)-N(6)-Ag(3)	120.9(5)	C(57)-N(7)-C(58)	118.2(7)
C(57)-N(7)-Ag(4)	120.6(5)	C(58)-N(7)-Ag(4)	121.1(5)
C(65)-N(8)-C(61)	117.1(7)	C(65)-N(8)-Ag(4)	117.5(5)
C(61)-N(8)-Ag(4)	123.6(5)	C(1)-O(1)-P(4)#7	119.2(4)
C(19)-O(2)-P(1)	116.9(4)	C(18)-O(3)-P(1)	121.2(4)
C(37)-O(4)-P(2)	122.1(4)	C(36)-O(5)-P(2)	120.9(5)
C(55)-O(6)-P(3)	121.4(5)	C(54)-O(7)-P(3)	116.6(4)
C(72)-O(8)-P(4)	118.4(5)	O(3)-P(1)-O(2)	105.1(3)
O(3)-P(1)-C(12)	99.8(3)	O(2)-P(1)-C(12)	98.8(3)
O(3)-P(1)-Ag(1)	115.13(19)	O(2)-P(1)-Ag(1)	117.0(2)
C(12)-P(1)-Ag(1)	118.3(3)	O(4)-P(2)-O(5)	106.0(3)
O(4)-P(2)-C(30)	107.2(3)	O(5)-P(2)-C(30)	98.0(3)
O(4)-P(2)-Ag(2)	108.6(2)	O(5)-P(2)-Ag(2)	115.1(2)
C(30)-P(2)-Ag(2)	120.6(3)	O(6)-P(3)-O(7)	106.4(3)
O(6)-P(3)-C(48)	105.5(3)	O(7)-P(3)-C(48)	98.9(3)
O(6)-P(3)-Ag(3)	107.91(19)	O(7)-P(3)-Ag(3)	118.2(2)
C(48)-P(3)-Ag(3)	118.7(2)	O(8)-P(4)-O(1)#8	106.1(3)
O(8)-P(4)-C(66)	100.3(3)	O(1)#8-P(4)-C(66)	97.2(3)
O(8)-P(4)-Ag(4)	116.5(2)	O(1)#8-P(4)-Ag(4)	116.2(2)
C(66)-P(4)-Ag(4)	117.6(3)	F(2)-B(1)-F(4)	109.0(8)

Symmetry transformations used to generate equivalent atoms: #1 -x+1,y+1/2,-z+1/2 #2 -x,y+1/2,-z+1/2
#3 -x+1,y-1/2,-z+1/2 #4 -x-1,y+1/2,-z+1/2 #5 -x,y-1/2,-z+1/2 #6 -x-1,y-1/2,-z+1/2 #7 x+2,y+1,z
#8 x-2,y-1,z

Table B.6. Experimental and statistical crystal data for **3.4**

Empirical formula	C84 H78 Ag4 F12 N8 O17 P4
Formula weight	2254.93
Temperature	100(2) K
Wavelength	0.71073 Å
Crystal system, space group	Monoclinic, P2(1)/n
Unit cell dimensions	a = 9.3430(13) Å α = 90 deg. b = 31.912(5) Å β = 95.636(10) deg. c = 15.157(3) Å γ = 90 deg.
Volume	4497.2(12) Å ³
Z, Calculated density	2, 1.665 Mg/m ³
Absorption coefficient	1.024 mm ⁻¹
F(000)	2260
Crystal size	0.10 x 0.09 x 0.07 mm
θ range for data collection	2.28 to 26.00 deg.
Limiting indices	-10<=h<=11, -39<=k<=39, -18<=l<=18
Reflections collected / unique	38630 / 8838 [R(int) = 0.0809]
Completeness to θ = 26.00	99.8 %
Absorption correction	Semi-empirical from equivalents
Max. and min. transmission	0.9346 and 0.9037
Refinement method	Full-matrix least-squares on F ²
Data / restraints / parameters	8838 / 6 / 601

Table B.6. Continued

Goodness-of-fit on F^2	1.027
Final R indices [I>2σ(I)]	R1 = 0.0497, wR2 = 0.1073
R indices (all data)	R1 = 0.0797, wR2 = 0.1204
Largest diff. peak and hole	1.060 and -0.939 e.A^-3

Bond Lengths (Å)

C(21)-O(5)	1.465(6)	C(21)-C(22)	1.496(7)
C(21)-H(21A)	0.9900	C(21)-H(21B)	0.9900
Ag(1)-N(2)#1	2.297(4)	Ag(1)-P(1)	2.3576(15)
Ag(1)-O(3)	2.386(4)	Ag(1)-O(3)#2	2.509(4)
Ag(2)-N(3)#3	2.322(4)	Ag(2)-P(2)	2.3295(13)
Ag(2)-O(7)	2.344(4)	Ag(2)-N(1)	2.355(4)
N(1)-C(4)	1.329(7)	N(1)-C(3)	1.335(7)
N(2)-C(9)	1.323(7)	N(2)-C(10)	1.355(6)
N(2)-Ag(1)#1	2.297(4)	N(3)-C(24)	1.335(7)
N(3)-C(23)	1.339(6)	N(3)-Ag(2)#4	2.322(4)
N(4)-C(29)	1.337(7)	N(4)-C(30)	1.345(8)
O(1)-C(1)	1.443(6)	O(1)-P(1)	1.613(4)
O(2)-C(7)	1.449(6)	O(2)-P(1)	1.604(4)
O(3)-C(19)	1.254(7)	O(3)-Ag(1)#2	2.509(4)
O(4)-C(19)	1.229(7)	O(5)-P(2)	1.612(4)
O(6)-C(27)	1.455(6)	O(6)-P(2)	1.610(4)
O(7)-C(39)	1.240(6)	O(8)-C(39)	1.235(6)
P(1)-C(13)	1.797(6)	P(1)-C(13A)	1.835(7)
P(2)-C(33)	1.818(5)	C(1)-C(2)	1.503(8)
C(1)-H(1A)	0.9900	C(1)-H(1B)	0.9900
C(2)-C(3)	1.380(7)	C(2)-C(6)	1.386(8)
C(3)-H(3)	0.9500	C(4)-C(5)	1.393(7)
C(4)-H(4)	0.9500	C(5)-C(6)	1.376(9)
C(5)-H(5)	0.9500	C(6)-H(6)	0.9500
C(7)-C(8)	1.526(8)	C(7)-H(7A)	0.9900
C(7)-H(7B)	0.9900	C(8)-C(12)	1.380(7)
C(8)-C(9)	1.390(7)	C(9)-H(9A)	0.9500
C(10)-C(11)	1.380(8)	C(10)-H(10)	0.9500
C(11)-C(12)	1.382(8)	C(11)-H(11)	0.9500
C(12)-H(12)	0.9500	C(27)-C(28)	1.493(7)
C(27)-H(27A)	0.9900	C(27)-H(27B)	0.9900
C(28)-C(29)	1.376(8)	C(28)-C(32)	1.386(7)
C(29)-H(29)	0.9500	C(30)-C(31)	1.375(8)
C(30)-H(30)	0.9500	C(31)-C(32)	1.383(8)
C(31)-H(31)	0.9500	C(32)-H(32)	0.9500
C(33)-C(38)	1.393(7)	C(33)-C(34)	1.400(7)
C(34)-C(35)	1.378(7)	C(34)-H(34)	0.9500
C(35)-C(36)	1.377(8)	C(35)-H(35)	0.9500
C(36)-C(37)	1.385(8)	C(36)-H(36)	0.9500
C(37)-C(38)	1.373(7)	C(37)-H(37)	0.9500
C(38)-H(38)	0.9500	C(19)-C(20)	1.529(8)
C(40)-F(6)	1.324(7)	C(40)-F(4)	1.335(7)
C(40)-F(5)	1.357(7)	C(40)-C(39)	1.546(8)
C(20)-F(2)	1.268(9)	C(20)-F(1)	1.337(14)
C(20)-F(3)	1.419(11)	C(13)-C(18)	1.3900
C(13)-C(14)	1.3900	C(18)-C(17)	1.3900
C(18)-H(18)	0.9500	C(17)-C(16)	1.3900

Table B.6. Continued

C(17)-H(17)	0.9500	C(16)-C(15)	1.3900
C(16)-H(16)	0.9500	C(15)-C(14)	1.3900
C(15)-H(15)	0.9500	C(14)-H(14)	0.9500
O(9)-C(41)	1.3271	O(9)-C(43)	1.4523
C(41)-C(42)	1.4523	C(41)-H(41A)	0.9900
C(41)-H(41B)	0.9900	C(42)-H(42A)	0.9800
C(42)-H(42B)	0.9800	C(42)-H(42C)	0.9800
C(43)-C(44)	1.6254	C(43)-H(43A)	0.9900
C(43)-H(43B)	0.9900	C(44)-H(44A)	0.9800
C(44)-H(44B)	0.9800	C(44)-H(44C)	0.9800
C(13A)-C(18A)	1.3900	C(13A)-C(14A)	1.3900
C(18A)-C(17A)	1.3900	C(18A)-H(18A)	0.9500
C(17A)-C(16A)	1.3900	C(17A)-H(17A)	0.9500
C(16A)-C(15A)	1.3900	C(16A)-H(16A)	0.9500
C(15A)-C(14A)	1.3900	C(15A)-H(15A)	0.9500
C(14A)-H(14A)	0.9500	O(9A)-C(43A)	1.19(4)
O(9A)-C(41A)	1.39(5)	O(9A)-O(9A) ^{#5}	1.78(6)
C(41A)-C(42A)	1.09(4)	C(41A)-H(41C)	0.9900
C(41A)-H(41D)	0.9900	C(42A)-H(42D)	0.9800
C(42A)-H(42E)	0.9800	C(42A)-H(42F)	0.9800
C(43A)-C(44A)	1.54(5)	C(43A)-H(43C)	0.9900
C(43A)-H(43D)	0.9900	C(44A)-H(44D)	0.9800
C(44A)-H(44E)	0.9800	C(44A)-H(44F)	0.9800
C(23)-C(22)	1.389(7)	C(23)-H(23)	0.9500
C(22)-C(26)	1.389(8)	C(26)-C(25)	1.372(8)
C(26)-H(26)	0.9500	C(25)-C(24)	1.373(8)
C(25)-H(25)	0.9500	C(24)-H(24)	0.9500

Bond Angles (°)

O(5)-C(21)-C(22)	108.0(4)	O(5)-C(21)-H(21A)	110.1
C(22)-C(21)-H(21A)	110.1	O(5)-C(21)-H(21B)	110.1
C(22)-C(21)-H(21B)	110.1	H(21A)-C(21)-H(21B)	108.4
N(2) ^{#1} -Ag(1)-P(1)	132.48(11)	N(2) ^{#1} -Ag(1)-O(3)	94.10(14)
P(1)-Ag(1)-O(3)	126.83(10)	N(2) ^{#1} -Ag(1)-O(3) ^{#2}	87.96(14)
P(1)-Ag(1)-O(3) ^{#2}	122.49(10)	O(3)-Ag(1)-O(3) ^{#2}	74.39(13)
N(3) ^{#3} -Ag(2)-P(2)	125.37(11)	N(3) ^{#3} -Ag(2)-O(7)	86.81(15)
P(2)-Ag(2)-O(7)	133.28(10)	N(3) ^{#3} -Ag(2)-N(1)	98.22(14)
P(2)-Ag(2)-N(1)	116.35(11)	O(7)-Ag(2)-N(1)	86.40(14)
C(4)-N(1)-C(3)	118.0(4)	C(4)-N(1)-Ag(2)	123.0(4)
C(3)-N(1)-Ag(2)	118.7(3)	C(9)-N(2)-C(10)	117.6(4)
C(9)-N(2)-Ag(1) ^{#1}	118.7(3)	C(10)-N(2)-Ag(1) ^{#1}	123.4(4)
C(24)-N(3)-C(23)	117.1(5)	C(24)-N(3)-Ag(2) ^{#4}	122.6(3)
C(23)-N(3)-Ag(2) ^{#4}	120.3(3)	C(29)-N(4)-C(30)	115.2(5)
C(1)-O(1)-P(1)	118.3(3)	C(7)-O(2)-P(1)	118.4(3)
C(19)-O(3)-Ag(1)	112.3(4)	C(19)-O(3)-Ag(1) ^{#2}	135.1(4)
Ag(1)-O(3)-Ag(1) ^{#2}	105.61(13)	C(21)-O(5)-P(2)	117.1(3)
C(27)-O(6)-P(2)	121.6(3)	C(39)-O(7)-Ag(2)	126.9(3)
O(2)-P(1)-O(1)	105.9(2)	O(2)-P(1)-C(13)	100.0(3)
O(1)-P(1)-C(13)	101.4(3)	O(2)-P(1)-C(13A)	95.6(4)
O(1)-P(1)-C(13A)	95.1(3)	C(13)-P(1)-C(13A)	9.1(4)
O(2)-P(1)-Ag(1)	114.10(15)	O(1)-P(1)-Ag(1)	114.87(15)
C(13)-P(1)-Ag(1)	118.6(3)	C(13A)-P(1)-Ag(1)	127.6(3)
O(6)-P(2)-O(5)	105.8(2)	O(6)-P(2)-C(33)	103.4(2)

Table B.6. Continued

O(5)-P(2)-C(33)	99.1(2)	O(6)-P(2)-Ag(2)	109.30(13)
O(5)-P(2)-Ag(2)	116.58(14)	C(33)-P(2)-Ag(2)	120.94(17)
O(1)-C(1)-C(2)	109.6(5)	O(1)-C(1)-H(1A)	109.7
C(2)-C(1)-H(1A)	109.7	O(1)-C(1)-H(1B)	109.7
C(2)-C(1)-H(1B)	109.7	H(1A)-C(1)-H(1B)	108.2
C(3)-C(2)-C(6)	117.5(5)	C(3)-C(2)-C(1)	120.4(5)
C(6)-C(2)-C(1)	122.2(5)	N(1)-C(3)-C(2)	124.1(5)
N(1)-C(3)-H(3)	117.9	C(2)-C(3)-H(3)	117.9
N(1)-C(4)-C(5)	122.0(5)	N(1)-C(4)-H(4)	119.0
C(5)-C(4)-H(4)	119.0	C(6)-C(5)-C(4)	119.3(5)
C(6)-C(5)-H(5)	120.4	C(4)-C(5)-H(5)	120.4
C(5)-C(6)-C(2)	119.2(5)	C(5)-C(6)-H(6)	120.4
C(2)-C(6)-H(6)	120.4	O(2)-C(7)-C(8)	108.2(4)
O(2)-C(7)-H(7A)	110.1	C(8)-C(7)-H(7A)	110.1
O(2)-C(7)-H(7B)	110.1	C(8)-C(7)-H(7B)	110.1
H(7A)-C(7)-H(7B)	108.4	C(12)-C(8)-C(9)	116.6(5)
C(12)-C(8)-C(7)	122.6(5)	C(9)-C(8)-C(7)	120.7(5)
N(2)-C(9)-C(8)	124.9(5)	N(2)-C(9)-H(9A)	117.6
C(8)-C(9)-H(9A)	117.6	N(2)-C(10)-C(11)	121.7(5)
N(2)-C(10)-H(10)	119.2	C(11)-C(10)-H(10)	119.2
C(10)-C(11)-C(12)	119.4(5)	C(10)-C(11)-H(11)	120.3
C(12)-C(11)-H(11)	120.3	C(8)-C(12)-C(11)	119.9(5)
C(8)-C(12)-H(12)	120.1	C(11)-C(12)-H(12)	120.1
O(6)-C(27)-C(28)	108.4(4)	O(6)-C(27)-H(27A)	110.0
C(28)-C(27)-H(27A)	110.0	O(6)-C(27)-H(27B)	110.0
C(28)-C(27)-H(27B)	110.0	H(27A)-C(27)-H(27B)	108.4
C(29)-C(28)-C(32)	118.0(5)	C(29)-C(28)-C(27)	121.3(5)
C(32)-C(28)-C(27)	120.7(5)	N(4)-C(29)-C(28)	125.0(5)
N(4)-C(29)-H(29)	117.5	C(28)-C(29)-H(29)	117.5
N(4)-C(30)-C(31)	124.8(6)	N(4)-C(30)-H(30)	117.6
C(31)-C(30)-H(30)	117.6	C(30)-C(31)-C(32)	118.1(6)
C(30)-C(31)-H(31)	121.0	C(32)-C(31)-H(31)	121.0
C(31)-C(32)-C(28)	118.9(5)	C(31)-C(32)-H(32)	120.5
C(28)-C(32)-H(32)	120.5	C(38)-C(33)-C(34)	119.5(5)
C(38)-C(33)-P(2)	118.0(4)	C(34)-C(33)-P(2)	122.5(4)
C(35)-C(34)-C(33)	119.2(5)	C(35)-C(34)-H(34)	120.4
C(33)-C(34)-H(34)	120.4	C(36)-C(35)-C(34)	120.7(5)
C(36)-C(35)-H(35)	119.7	C(34)-C(35)-H(35)	119.7
C(35)-C(36)-C(37)	120.3(5)	C(35)-C(36)-H(36)	119.8
C(37)-C(36)-H(36)	119.8	C(38)-C(37)-C(36)	119.7(5)
C(38)-C(37)-H(37)	120.2	C(36)-C(37)-H(37)	120.2
C(37)-C(38)-C(33)	120.5(5)	C(37)-C(38)-H(38)	119.8
C(33)-C(38)-H(38)	119.8	O(4)-C(19)-O(3)	129.3(6)
O(4)-C(19)-C(20)	117.0(5)	O(3)-C(19)-C(20)	113.6(5)
F(6)-C(40)-F(4)	105.1(5)	F(6)-C(40)-F(5)	108.4(6)
F(4)-C(40)-F(5)	105.5(5)	F(6)-C(40)-C(39)	114.7(5)
F(4)-C(40)-C(39)	111.9(5)	F(5)-C(40)-C(39)	110.6(5)
F(2)-C(20)-F(1)	118.5(12)	F(2)-C(20)-F(3)	107.4(6)
F(1)-C(20)-F(3)	95.0(10)	F(2)-C(20)-C(19)	112.9(6)
F(1)-C(20)-C(19)	113.0(11)	F(3)-C(20)-C(19)	107.9(5)
O(8)-C(39)-O(7)	131.0(5)	O(8)-C(39)-C(40)	116.4(5)
O(7)-C(39)-C(40)	112.6(5)	C(18)-C(13)-C(14)	120.0
C(18)-C(13)-P(1)	121.1(4)	C(14)-C(13)-P(1)	118.9(4)
C(13)-C(18)-C(17)	120.0	C(13)-C(18)-H(18)	120.0

Table B.6. Continued

C(17)-C(18)-H(18)	120.0	C(16)-C(17)-C(18)	120.0
C(16)-C(17)-H(17)	120.0	C(18)-C(17)-H(17)	120.0
C(17)-C(16)-C(15)	120.0	C(17)-C(16)-H(16)	120.0
C(15)-C(16)-H(16)	120.0	C(14)-C(15)-C(16)	120.0
C(14)-C(15)-H(15)	120.0	C(16)-C(15)-H(15)	120.0
C(15)-C(14)-C(13)	120.0	C(15)-C(14)-H(14)	120.0
C(13)-C(14)-H(14)	120.0	C(41)-O(9)-C(43)	111.5
O(9)-C(41)-C(42)	111.5	O(9)-C(41)-H(41A)	109.3
C(42)-C(41)-H(41A)	109.3	O(9)-C(41)-H(41B)	109.3
C(42)-C(41)-H(41B)	109.3	H(41A)-C(41)-H(41B)	108.0
C(41)-C(42)-H(42A)	109.5	C(41)-C(42)-H(42B)	109.5
H(42A)-C(42)-H(42B)	109.5	C(41)-C(42)-H(42C)	109.5
H(42A)-C(42)-H(42C)	109.5	H(42B)-C(42)-H(42C)	109.5
O(9)-C(43)-C(44)	106.2	O(9)-C(43)-H(43A)	110.5
C(44)-C(43)-H(43A)	110.5	O(9)-C(43)-H(43B)	110.5
C(44)-C(43)-H(43B)	110.5	H(43A)-C(43)-H(43B)	108.7
C(43)-C(44)-H(44A)	109.5	C(43)-C(44)-H(44B)	109.5
H(44A)-C(44)-H(44B)	109.5	C(43)-C(44)-H(44C)	109.5
H(44A)-C(44)-H(44C)	109.5	H(44B)-C(44)-H(44C)	109.5
C(18A)-C(13A)-C(14A)	120.0	C(18A)-C(13A)-P(1)	116.2(5)
C(14A)-C(13A)-P(1)	123.8(5)	C(17A)-C(18A)-C(13A)	120.0
C(17A)-C(18A)-H(18A)	120.0	C(13A)-C(18A)-H(18A)	120.0
C(18A)-C(17A)-C(16A)	120.0	C(18A)-C(17A)-H(17A)	120.0
C(16A)-C(17A)-H(17A)	120.0	C(17A)-C(16A)-C(15A)	120.0
C(17A)-C(16A)-H(16A)	120.0	C(15A)-C(16A)-H(16A)	120.0
C(14A)-C(15A)-C(16A)	120.0	C(14A)-C(15A)-H(15A)	120.0
C(16A)-C(15A)-H(15A)	120.0	C(15A)-C(14A)-C(13A)	120.0
C(15A)-C(14A)-H(14A)	120.0	C(13A)-C(14A)-H(14A)	120.0
C(43A)-O(9A)-C(41A)	134(3)	C(43A)-O(9A)-O(9A)#5	8(3)
C(41A)-O(9A)-O(9A)#5	138(5)	C(42A)-C(41A)-O(9A)	131(4)
C(42A)-C(41A)-H(41C)	104.5	O(9A)-C(41A)-H(41C)	104.5
C(42A)-C(41A)-H(41D)	104.5	O(9A)-C(41A)-H(41D)	104.5
H(41C)-C(41A)-H(41D)	105.7	C(41A)-C(42A)-H(42D)	109.5
C(41A)-C(42A)-H(42E)	109.5	H(42D)-C(42A)-H(42E)	109.5
C(41A)-C(42A)-H(42F)	109.5	H(42D)-C(42A)-H(42F)	109.5
H(42E)-C(42A)-H(42F)	109.5	O(9A)-C(43A)-C(44A)	117(2)
O(9A)-C(43A)-H(43C)	108.1	C(44A)-C(43A)-H(43C)	108.1
O(9A)-C(43A)-H(43D)	108.1	C(44A)-C(43A)-H(43D)	108.1
H(43C)-C(43A)-H(43D)	107.3	C(43A)-C(44A)-H(44D)	109.5

Table B.6. Continued

C(43A)-C(44A)-H(44E)	109.5	H(44D)-C(44A)-H(44E)	109.5
C(43A)-C(44A)-H(44F)	109.5	H(44D)-C(44A)-H(44F)	109.5
H(44E)-C(44A)-H(44F)	109.5	N(3)-C(23)-C(22)	123.9(5)
N(3)-C(23)-H(23)	118.1	C(22)-C(23)-H(23)	118.1
C(26)-C(22)-C(23)	117.4(5)	C(26)-C(22)-C(21)	122.5(5)
C(23)-C(22)-C(21)	120.1(5)	C(25)-C(26)-C(22)	119.1(5)
C(25)-C(26)-H(26)	120.4	C(22)-C(26)-H(26)	120.4
C(26)-C(25)-C(24)	119.4(5)	C(26)-C(25)-H(25)	120.3
C(24)-C(25)-H(25)	120.3	N(3)-C(24)-C(25)	123.2(5)
N(3)-C(24)-H(24)	118.4	C(25)-C(24)-H(24)	118.4

Symmetry transformations used to generate equivalent atoms: #1 -x+1,-y+1,-z+1 #2 -x+2,-y+1,-z+1 #3 x-1/2,-y+3/2,z-1/2 #4 x+1/2,-y+3/2,z+1/2 #5 -x+2,-y+1,-z

Table B.7. Experimental and statistical crystal data for **4.1**

Empirical formula	C24 H32 Ag2 B2 F8 N8		
Formula weight	821.94		
Temperature	110(2) K		
Wavelength	0.71073 Å		
Crystal system, space group	Triclinic, P1		
Unit cell dimensions	a = 7.8817(5) Å α = 106.208(2) deg. b = 14.0058(8) Å β = 93.211(2) deg. c = 7.2894(4) Å γ = 100.710(3) deg.		
Volume	754.25(8) Å ³		
Z, Calculated density	1, 1.810 Mg/m ³		
Absorption coefficient	1.379 mm ⁻¹		
F(000)	408		
Crystal size	0.18 x 0.15 x 0.10 mm		
θ range for data collection	1.55 to 28.34 deg.		
Limiting indices	-10<=h<=10, -18<=k<=17, -9<=l<=9		
Reflections collected / unique	15414 / 6263 [R(int) = 0.0267]		
Completeness to θ = 28.34	98.9 %		
Absorption correction	Semi-empirical from equivalents		
Max. and min. transmission	0.867 and 0.765		
Refinement method	Full-matrix least-squares on F ²		
Data / restraints / parameters	6263 / 7 / 391		
Goodness-of-fit on F ²	1.028		
Final R indices [I>2σ(I)]	R1 = 0.0174, wR2 = 0.0465		
R indices (all data)	R1 = 0.0184, wR2 = 0.0472		
Absolute structure parameter	0.00		
Largest diff. peak and hole	0.323 and -0.416 e.Å ⁻³		
Bond Lengths (Å)			
Ag(1)-N(1)	2.262(6)	Ag(1)-N(3)	2.319(5)
Ag(1)-N(4)	2.336(6)	Ag(1)-N(2)	2.371(5)
Ag(2)-N(6)	2.293(6)	Ag(2)-N(7)	2.310(5)
Ag(2)-N(8)	2.322(5)	Ag(2)-N(5)	2.368(4)
F(1)-B(1)	1.363(6)	F(2)-B(1)	1.404(7)

Table B.7. Continued

F(3)-B(1)	1.367(6)	F(4)-B(1)	1.411(6)
F(5)-B(2)	1.383(8)	F(6)-B(2)	1.436(6)
F(7)-B(2)	1.361(7)	F(8)-B(2)	1.423(6)
N(1)-C(2)	1.394(7)	N(1)-C(6)	1.382(8)
N(2)-C(1)	1.406(8)	N(2)-H(2A)	0.9200
N(2)-H(2B)	0.9200	N(3)-C(8)	1.314(8)
N(3)-C(12)	1.395(7)	N(4)-C(7)	1.478(7)
N(4)-H(4A)	0.9200	N(4)-H(4B)	0.9200
N(5)-C(18)	1.302(7)	N(5)-C(14)	1.356(7)
N(6)-C(13)	1.463(8)	N(6)-H(6A)	0.9200
N(6)-H(6B)	0.9200	N(7)-C(20)	1.280(8)
N(7)-C(24)	1.327(8)	N(8)-C(19)	1.512(8)
N(8)-H(8A)	0.9200	N(8)-H(8B)	0.9200
C(1)-C(2)	1.570(8)	C(1)-H(1A)	0.9900
C(1)-H(1B)	0.9900	C(2)-C(3)	1.311(9)
C(3)-C(4)	1.445(8)	C(3)-H(3)	0.9500
C(4)-C(5)	1.337(9)	C(4)-H(4)	0.9500
C(5)-C(6)	1.358(10)	C(5)-H(5)	0.9500
C(6)-H(6)	0.9500	C(7)-C(8)	1.490(8)
C(7)-H(7A)	0.9900	C(7)-H(7B)	0.9900
C(8)-C(9)	1.367(8)	C(9)-C(10)	1.367(8)
C(9)-H(9)	0.9500	C(10)-C(11)	1.417(9)
C(10)-H(10)	0.9500	C(11)-C(12)	1.357(8)
C(11)-H(11)	0.9500	C(12)-H(12)	0.9500
C(13)-C(14)	1.542(7)	C(13)-H(13A)	0.9900
C(13)-H(13B)	0.9900	C(14)-C(15)	1.418(7)
C(15)-C(16)	1.416(8)	C(15)-H(15)	0.9500
C(16)-C(17)	1.335(10)	C(16)-H(16)	0.9500
C(17)-C(18)	1.409(6)	C(17)-H(17)	0.9500
C(18)-H(18)	0.9500	C(19)-C(20)	1.478(8)
C(19)-H(19A)	0.9900	C(19)-H(19B)	0.9900
C(20)-C(21)	1.458(8)	C(21)-C(22)	1.318(8)
C(21)-H(21)	0.9500	C(22)-C(23)	1.441(8)
C(22)-H(22)	0.9500	C(23)-C(24)	1.383(10)
C(23)-H(23)	0.9500	C(24)-H(24)	0.9500

Bond Lengths (Å)

N(1)-Ag(1)-N(3)	125.65(18)	N(1)-Ag(1)-N(4)	131.90(18)
N(3)-Ag(1)-N(4)	72.52(18)	N(1)-Ag(1)-N(2)	74.61(18)
N(3)-Ag(1)-N(2)	133.94(17)	N(4)-Ag(1)-N(2)	128.29(17)
N(6)-Ag(2)-N(7)	133.41(17)	N(6)-Ag(2)-N(8)	126.48(18)
N(7)-Ag(2)-N(8)	74.44(18)	N(6)-Ag(2)-N(5)	73.32(17)
N(7)-Ag(2)-N(5)	125.96(18)	N(8)-Ag(2)-N(5)	133.34(17)
C(2)-N(1)-C(6)	113.7(6)	C(2)-N(1)-Ag(1)	118.5(4)
C(6)-N(1)-Ag(1)	127.3(4)	C(1)-N(2)-Ag(1)	113.6(3)
C(1)-N(2)-H(2A)	108.8	Ag(1)-N(2)-H(2A)	108.8
C(1)-N(2)-H(2B)	108.8	Ag(1)-N(2)-H(2B)	108.8
H(2A)-N(2)-H(2B)	107.7	C(8)-N(3)-C(12)	115.3(5)
C(8)-N(3)-Ag(1)	116.3(4)	C(12)-N(3)-Ag(1)	128.4(4)
C(7)-N(4)-Ag(1)	106.6(3)	C(7)-N(4)-H(4A)	110.4
Ag(1)-N(4)-H(4A)	110.4	C(7)-N(4)-H(4B)	110.4
Ag(1)-N(4)-H(4B)	110.4	H(4A)-N(4)-H(4B)	108.6
C(18)-N(5)-C(14)	121.0(5)	C(18)-N(5)-Ag(2)	126.3(4)

Table B.7. Continued

C(14)-N(5)-Ag(2)	112.7(4)	C(13)-N(6)-Ag(2)	112.5(3)
C(13)-N(6)-H(6A)	109.1	Ag(2)-N(6)-H(6A)	109.1
C(13)-N(6)-H(6B)	109.1	Ag(2)-N(6)-H(6B)	109.1
H(6A)-N(6)-H(6B)	107.8	C(20)-N(7)-C(24)	121.9(5)
C(20)-N(7)-Ag(2)	116.5(4)	C(24)-N(7)-Ag(2)	121.2(4)
C(19)-N(8)-Ag(2)	111.3(4)	C(19)-N(8)-H(8A)	109.4
Ag(2)-N(8)-H(8A)	109.4	C(19)-N(8)-H(8B)	109.4
Ag(2)-N(8)-H(8B)	109.4	H(8A)-N(8)-H(8B)	108.0
N(2)-C(1)-C(2)	116.5(5)	N(2)-C(1)-H(1A)	108.2
C(2)-C(1)-H(1A)	108.2	N(2)-C(1)-H(1B)	108.2
C(2)-C(1)-H(1B)	108.2	H(1A)-C(1)-H(1B)	107.3
C(3)-C(2)-N(1)	124.3(5)	C(3)-C(2)-C(1)	120.4(5)
N(1)-C(2)-C(1)	115.3(6)	C(2)-C(3)-C(4)	119.1(6)
C(2)-C(3)-H(3)	120.4	C(4)-C(3)-H(3)	120.4
C(5)-C(4)-C(3)	118.7(6)	C(5)-C(4)-H(4)	120.7
C(3)-C(4)-H(4)	120.7	C(4)-C(5)-C(6)	119.3(6)
C(4)-C(5)-H(5)	120.4	C(6)-C(5)-H(5)	120.4
C(5)-C(6)-N(1)	124.9(6)	C(5)-C(6)-H(6)	117.6
N(1)-C(6)-H(6)	117.6	N(4)-C(7)-C(8)	114.1(5)
N(4)-C(7)-H(7A)	108.7	C(8)-C(7)-H(7A)	108.7
N(4)-C(7)-H(7B)	108.7	C(8)-C(7)-H(7B)	108.7
H(7A)-C(7)-H(7B)	107.6	N(3)-C(8)-C(9)	124.9(5)
N(3)-C(8)-C(7)	116.7(5)	C(9)-C(8)-C(7)	118.4(5)
C(8)-C(9)-C(10)	119.9(6)	C(8)-C(9)-H(9)	120.1
C(10)-C(9)-H(9)	120.1	C(9)-C(10)-C(11)	118.0(5)
C(9)-C(10)-H(10)	121.0	C(11)-C(10)-H(10)	121.0
C(12)-C(11)-C(10)	118.0(5)	C(12)-C(11)-H(11)	121.0
C(10)-C(11)-H(11)	121.0	C(11)-C(12)-N(3)	123.8(6)
C(11)-C(12)-H(12)	118.1	N(3)-C(12)-H(12)	118.1
N(6)-C(13)-C(14)	110.9(5)	N(6)-C(13)-H(13A)	109.5
C(14)-C(13)-H(13A)	109.5	N(6)-C(13)-H(13B)	109.5
C(14)-C(13)-H(13B)	109.5	H(13A)-C(13)-H(13B)	108.0
N(5)-C(14)-C(15)	119.6(5)	N(5)-C(14)-C(13)	120.0(5)
C(15)-C(14)-C(13)	120.4(5)	C(16)-C(15)-C(14)	117.8(6)
C(16)-C(15)-H(15)	121.1	C(14)-C(15)-H(15)	121.1
C(17)-C(16)-C(15)	120.3(5)	C(17)-C(16)-H(16)	119.8
C(15)-C(16)-H(16)	119.8	C(16)-C(17)-C(18)	118.9(5)
C(16)-C(17)-H(17)	120.6	C(18)-C(17)-H(17)	120.6
N(5)-C(18)-C(17)	122.3(5)	N(5)-C(18)-H(18)	118.9
C(17)-C(18)-H(18)	118.9	C(20)-C(19)-N(8)	114.0(5)
C(20)-C(19)-H(19A)	108.8	N(8)-C(19)-H(19A)	108.8
C(20)-C(19)-H(19B)	108.8	N(8)-C(19)-H(19B)	108.8
H(19A)-C(19)-H(19B)	107.7	N(7)-C(20)-C(21)	120.1(5)
N(7)-C(20)-C(19)	121.3(5)	C(21)-C(20)-C(19)	118.5(5)
C(22)-C(21)-C(20)	119.7(5)	C(22)-C(21)-H(21)	120.2
C(20)-C(21)-H(21)	120.2	C(21)-C(22)-C(23)	118.9(6)
C(21)-C(22)-H(22)	120.5	C(23)-C(22)-H(22)	120.5
C(24)-C(23)-C(22)	117.4(5)	C(24)-C(23)-H(23)	121.3
C(22)-C(23)-H(23)	121.3	N(7)-C(24)-C(23)	122.0(6)
N(7)-C(24)-H(24)	119.0	C(23)-C(24)-H(24)	119.0
F(3)-B(1)-F(1)	112.7(5)	F(3)-B(1)-F(2)	109.5(4)
F(1)-B(1)-F(2)	109.4(4)	F(3)-B(1)-F(4)	108.7(5)
F(1)-B(1)-F(4)	110.0(5)	F(2)-B(1)-F(4)	106.3(5)
F(7)-B(2)-F(5)	113.3(5)	F(7)-B(2)-F(8)	109.3(5)

Table B.7. Continued

F(5)-B(2)-F(8)	109.9(5)	F(7)-B(2)-F(6)	110.4(5)
F(5)-B(2)-F(6)	108.8(5)	F(8)-B(2)-F(6)	104.7(5)
Hydrogen bonds (\AA)			
N(2)-H(2A)...F(2)#1	3.123(7)	N(2)-H(2B)...F(3)#2	3.068(6)
N(4)-H(4A)...F(1)#1	3.049(6)	N(4)-H(4B)...F(4)#3	3.101(6)
N(6)-H(6A)...F(7)#4	3.146(6)	N(6)-H(6B)...F(8)#5	3.031(6)
N(8)-H(8A)...F(6)#6	3.070(7)	N(8)-H(8B)...F(5)#5	3.090(7)

Symmetry transformations used to generate equivalent atoms: #1 x-1,y,z+1 #2 x-1,y,z #3 x,y,z+1 #4 x,y,z-1 #5 x+1,y,z-1 #6 x+1,y,z

Table B.8. Experimental and statistical crystal data for **4.2**

Empirical formula	C56 H64 Ag4 F12 N16 O8
Formula weight	1748.71
Temperature	110(2) K
Wavelength	0.71073 Å
Crystal system, space group	Triclinic, P1
Unit cell dimensions	a = 7.4205(6) Å α = 69.342(4) deg. b = 13.2849(12) Å β = 89.255(4) deg. c = 18.0494(16) Å γ = 80.621(4) deg.
Volume	1640.8(2) Å ³
Z, Calculated density	1, 1.770 Mg/m ³
Absorption coefficient	1.275 mm ⁻¹
F(000)	872
Crystal size	0.21 x 0.15 x 0.09 mm
θ range for data collection	2.40 to 26.43 deg.
Limiting indices	-8<=h<=9, -16<=k<=16, -22<=l<=22
Reflections collected / unique	54807 / 12763 [R(int) = 0.0401]
Completeness to θ = 26.43	99.4 %
Absorption correction	multi-scan (SADABS)
Max. and min. transmission	0.8972 and 0.7792
Refinement method	Full-matrix least-squares on F ²
Data / restraints / parameters	12763 / 3 / 865
Goodness-of-fit on F ²	1.016
Final R indices [I>2σ(I)]	R1 = 0.0274, wR2 = 0.0635
R indices (all data)	R1 = 0.0364, wR2 = 0.0675
Absolute structure parameter	-0.035(14)
Largest diff. peak and hole	1.225 and -0.560 e.Å ⁻³

Bond Lengths (\AA)

Ag(1)-N(2)	2.309(3)	Ag(1)-N(4)	2.326(3)
Ag(1)-N(3)	2.402(3)	Ag(1)-N(1)	2.418(3)
Ag(1)-Ag(2)	3.0077(4)	Ag(2)-N(8)	2.265(3)
Ag(2)-N(6)	2.273(3)	Ag(2)-N(5)	2.499(3)
Ag(2)-N(7)	2.558(3)	Ag(3)-N(10)	2.298(3)
Ag(3)-N(12)	2.339(3)	Ag(3)-N(11)	2.390(3)
Ag(3)-N(9)	2.425(3)	Ag(3)-Ag(4)	3.0305(4)
Ag(4)-N(16)	2.277(3)	Ag(4)-N(14)	2.292(3)

Table B.8. Continued

Ag(4)-N(13)	2.459(3)	Ag(4)-N(15)	2.516(3)
F(1)-C(50)	1.327(5)	F(2)-C(50)	1.339(5)
F(3)-C(50)	1.330(4)	F(4)-C(52)	1.332(4)
F(5)-C(52)	1.337(4)	F(6)-C(52)	1.351(5)
F(7)-C(54)	1.332(5)	F(8)-C(54)	1.338(4)
F(9)-C(54)	1.337(5)	F(10)-C(55)	1.324(5)
F(11)-C(55)	1.328(4)	F(12)-C(55)	1.344(5)
O(1)-C(49)	1.236(4)	O(2)-C(49)	1.244(4)
O(3)-C(51)	1.248(4)	O(4)-C(51)	1.233(4)
O(5)-C(53)	1.229(4)	O(6)-C(53)	1.242(4)
O(7)-C(56)	1.242(4)	O(8)-C(56)	1.232(4)
N(1)-C(2)	1.329(4)	N(1)-C(6)	1.360(4)
N(2)-C(1)	1.477(4)	N(2)-H(2A)	0.9200
N(2)-H(2B)	0.9200	N(3)-C(8)	1.338(4)
N(3)-C(12)	1.352(4)	N(4)-C(7)	1.458(4)
N(4)-H(4A)	0.9200	N(4)-H(4B)	0.9200
N(5)-C(14)	1.336(4)	N(5)-C(18)	1.353(5)
N(6)-C(13)	1.472(4)	N(6)-H(6A)	0.9200
N(6)-H(6B)	0.9200	N(7)-C(20)	1.345(4)
N(7)-C(24)	1.347(4)	N(8)-C(19)	1.468(5)
N(8)-H(8A)	0.9200	N(8)-H(8B)	0.9200
N(9)-C(26)	1.340(4)	N(9)-C(30)	1.345(5)
N(10)-C(25)	1.474(5)	N(10)-H(10A)	0.9200
N(10)-H(10B)	0.9200	N(11)-C(32)	1.336(4)
N(11)-C(36)	1.360(4)	N(12)-C(31)	1.453(4)
N(12)-H(12A)	0.9200	N(12)-H(12B)	0.9200
N(13)-C(42)	1.337(5)	N(13)-C(38)	1.342(5)
N(14)-C(37)	1.466(5)	N(14)-H(14A)	0.9200
N(14)-H(14B)	0.9200	N(15)-C(44)	1.351(4)
N(15)-C(48)	1.352(4)	N(16)-C(43)	1.480(5)
N(16)-H(16A)	0.9200	N(16)-H(16B)	0.9200
C(1)-C(2)	1.512(5)	C(1)-H(1A)	0.9900
C(1)-H(1B)	0.9900	C(2)-C(3)	1.387(5)
C(3)-C(4)	1.389(5)	C(3)-H(3)	0.9500
C(4)-C(5)	1.380(5)	C(4)-H(4)	0.9500
C(5)-C(6)	1.381(5)	C(5)-H(5)	0.9500
C(6)-H(6)	0.9500	C(7)-C(8)	1.513(5)
C(7)-H(7A)	0.9900	C(7)-H(7B)	0.9900
C(8)-C(9)	1.378(5)	C(9)-C(10)	1.378(5)
C(9)-H(9)	0.9500	C(10)-C(11)	1.385(5)
C(10)-H(10)	0.9500	C(11)-C(12)	1.379(5)
C(11)-H(11)	0.9500	C(12)-H(12)	0.9500
C(13)-C(14)	1.520(5)	C(13)-H(13A)	0.9900
C(13)-H(13B)	0.9900	C(14)-C(15)	1.399(5)
C(15)-C(16)	1.374(5)	C(15)-H(15)	0.9500
C(16)-C(17)	1.395(6)	C(16)-H(16)	0.9500
C(17)-C(18)	1.381(5)	C(17)-H(17)	0.9500
C(18)-H(18)	0.9500	C(19)-C(20)	1.506(5)
C(19)-H(19A)	0.9900	C(19)-H(19B)	0.9900
C(20)-C(21)	1.397(5)	C(21)-C(22)	1.362(5)
C(21)-H(21)	0.9500	C(22)-C(23)	1.385(5)
C(22)-H(22)	0.9500	C(23)-C(24)	1.398(5)
C(23)-H(23)	0.9500	C(24)-H(24)	0.9500
C(25)-C(26)	1.517(5)	C(25)-H(25A)	0.9900

Table B.8. Continued

C(25)-H(25B)	0.9900	C(26)-C(27)	1.393(5)
C(27)-C(28)	1.374(5)	C(27)-H(27)	0.9500
C(28)-C(29)	1.398(5)	C(28)-H(28)	0.9500
C(29)-C(30)	1.386(5)	C(29)-H(29)	0.9500
C(30)-H(30)	0.9500	C(31)-C(32)	1.505(5)
C(31)-H(31A)	0.9900	C(31)-H(31B)	0.9900
C(32)-C(33)	1.405(5)	C(33)-C(34)	1.365(5)
C(33)-H(33)	0.9500	C(34)-C(35)	1.396(5)
C(34)-H(34)	0.9500	C(35)-C(36)	1.367(5)
C(35)-H(35)	0.9500	C(36)-H(36)	0.9500
C(37)-C(38)	1.525(5)	C(37)-H(37A)	0.9900
C(37)-H(37B)	0.9900	C(38)-C(39)	1.390(5)
C(39)-C(40)	1.373(6)	C(39)-H(39)	0.9500
C(40)-C(41)	1.391(6)	C(40)-H(40)	0.9500
C(41)-C(42)	1.375(5)	C(41)-H(41)	0.9500
C(42)-H(42)	0.9500	C(43)-C(44)	1.512(5)
C(43)-H(43A)	0.9900	C(43)-H(43B)	0.9900
C(44)-C(45)	1.389(5)	C(45)-C(46)	1.375(5)
C(45)-H(45)	0.9500	C(46)-C(47)	1.391(5)
C(46)-H(46)	0.9500	C(47)-C(48)	1.380(5)
C(47)-H(47)	0.9500	C(48)-H(48)	0.9500
C(49)-C(50)	1.551(5)	C(51)-C(52)	1.551(5)
C(53)-C(54)	1.534(5)	C(55)-C(56)	1.561(5)

Bond Angles (°)

N(2)-Ag(1)-N(4)	146.29(11)	N(2)-Ag(1)-N(3)	119.44(10)
N(4)-Ag(1)-N(3)	71.46(10)	N(2)-Ag(1)-N(1)	72.65(10)
N(4)-Ag(1)-N(1)	113.87(10)	N(3)-Ag(1)-N(1)	151.68(10)
N(2)-Ag(1)-Ag(2)	105.64(8)	N(4)-Ag(1)-Ag(2)	107.98(7)
N(3)-Ag(1)-Ag(2)	76.79(7)	N(1)-Ag(1)-Ag(2)	75.17(7)
N(8)-Ag(2)-N(6)	174.59(10)	N(8)-Ag(2)-N(5)	112.83(10)
N(6)-Ag(2)-N(5)	72.53(10)	N(8)-Ag(2)-N(7)	71.73(10)
N(6)-Ag(2)-N(7)	106.08(10)	N(5)-Ag(2)-N(7)	124.95(10)
N(8)-Ag(2)-Ag(1)	91.69(8)	N(6)-Ag(2)-Ag(1)	84.96(8)
N(5)-Ag(2)-Ag(1)	116.92(7)	N(7)-Ag(2)-Ag(1)	117.73(7)
N(10)-Ag(3)-N(12)	147.33(11)	N(10)-Ag(3)-N(11)	118.94(10)
N(12)-Ag(3)-N(11)	71.16(10)	N(10)-Ag(3)-N(9)	73.45(10)
N(12)-Ag(3)-N(9)	113.49(10)	N(11)-Ag(3)-N(9)	151.32(10)
N(10)-Ag(3)-Ag(4)	108.08(8)	N(12)-Ag(3)-Ag(4)	104.59(7)
N(11)-Ag(3)-Ag(4)	73.78(7)	N(9)-Ag(3)-Ag(4)	77.76(7)
N(16)-Ag(4)-N(14)	176.10(11)	N(16)-Ag(4)-N(13)	110.77(10)
N(14)-Ag(4)-N(13)	72.68(10)	N(16)-Ag(4)-N(15)	72.74(10)
N(14)-Ag(4)-N(15)	107.02(10)	N(13)-Ag(4)-N(15)	124.29(10)
N(16)-Ag(4)-Ag(3)	90.13(8)	N(14)-Ag(4)-Ag(3)	86.76(8)
N(13)-Ag(4)-Ag(3)	113.12(7)	N(15)-Ag(4)-Ag(3)	122.55(7)
C(2)-N(1)-C(6)	118.2(3)	C(2)-N(1)-Ag(1)	114.0(2)
C(6)-N(1)-Ag(1)	126.6(2)	C(1)-N(2)-Ag(1)	110.8(2)
C(1)-N(2)-H(2A)	109.5	Ag(1)-N(2)-H(2A)	109.5
C(1)-N(2)-H(2B)	109.5	Ag(1)-N(2)-H(2B)	109.5
H(2A)-N(2)-H(2B)	108.1	C(8)-N(3)-C(12)	118.3(3)
C(8)-N(3)-Ag(1)	115.7(2)	C(12)-N(3)-Ag(1)	126.0(2)
C(7)-N(4)-Ag(1)	113.8(2)	C(7)-N(4)-H(4A)	108.8
Ag(1)-N(4)-H(4B)	108.8	C(7)-N(4)-H(4B)	108.8

Table B.8. Continued

Ag(1)-N(4)-H(4B)	108.8	H(4A)-N(4)-H(4B)	107.7
C(14)-N(5)-C(18)	118.4(3)	C(14)-N(5)-Ag(2)	111.8(2)
C(18)-N(5)-Ag(2)	127.3(2)	C(13)-N(6)-Ag(2)	113.0(2)
C(13)-N(6)-H(6A)	109.0	Ag(2)-N(6)-H(6A)	109.0
C(13)-N(6)-H(6B)	109.0	Ag(2)-N(6)-H(6B)	109.0
H(6A)-N(6)-H(6B)	107.8	C(20)-N(7)-C(24)	118.6(3)
C(20)-N(7)-Ag(2)	109.8(2)	C(24)-N(7)-Ag(2)	129.2(2)
C(19)-N(8)-Ag(2)	111.6(2)	C(19)-N(8)-H(8A)	109.3
Ag(2)-N(8)-H(8A)	109.3	C(19)-N(8)-H(8B)	109.3
Ag(2)-N(8)-H(8B)	109.3	H(8A)-N(8)-H(8B)	108.0
C(26)-N(9)-C(30)	118.7(3)	C(26)-N(9)-Ag(3)	112.3(2)
C(30)-N(9)-Ag(3)	126.7(2)	C(25)-N(10)-Ag(3)	110.0(2)
C(25)-N(10)-H(10A)	109.7	Ag(3)-N(10)-H(10A)	109.7
C(25)-N(10)-H(10B)	109.7	Ag(3)-N(10)-H(10B)	109.7
H(10A)-N(10)-H(10B)	108.2	C(32)-N(11)-C(36)	118.5(3)
C(32)-N(11)-Ag(3)	115.7(2)	C(36)-N(11)-Ag(3)	125.5(2)
C(31)-N(12)-Ag(3)	114.3(2)	C(31)-N(12)-H(12A)	108.7
Ag(3)-N(12)-H(12A)	108.7	C(31)-N(12)-H(12B)	108.7
Ag(3)-N(12)-H(12B)	108.7	H(12A)-N(12)-H(12B)	107.6
C(42)-N(13)-C(38)	117.8(3)	C(42)-N(13)-Ag(4)	127.0(3)
C(38)-N(13)-Ag(4)	113.7(2)	C(37)-N(14)-Ag(4)	112.4(2)
C(37)-N(14)-H(14A)	109.1	Ag(4)-N(14)-H(14A)	109.1
C(37)-N(14)-H(14B)	109.1	Ag(4)-N(14)-H(14B)	109.1
H(14A)-N(14)-H(14B)	107.9	C(44)-N(15)-C(48)	117.5(3)
C(44)-N(15)-Ag(4)	110.6(2)	C(48)-N(15)-Ag(4)	129.2(2)
C(43)-N(16)-Ag(4)	110.2(2)	C(43)-N(16)-H(16A)	109.6
Ag(4)-N(16)-H(16A)	109.6	C(43)-N(16)-H(16B)	109.6
Ag(4)-N(16)-H(16B)	109.6	H(16A)-N(16)-H(16B)	108.1
N(2)-C(1)-C(2)	112.5(3)	N(2)-C(1)-H(1A)	109.1
C(2)-C(1)-H(1A)	109.1	N(2)-C(1)-H(1B)	109.1
C(2)-C(1)-H(1B)	109.1	H(1A)-C(1)-H(1B)	107.8
N(1)-C(2)-C(3)	121.8(3)	N(1)-C(2)-C(1)	117.5(3)
C(3)-C(2)-C(1)	120.7(3)	C(2)-C(3)-C(4)	120.0(3)
C(2)-C(3)-H(3)	120.0	C(4)-C(3)-H(3)	120.0
C(5)-C(4)-C(3)	118.6(3)	C(5)-C(4)-H(4)	120.7
C(3)-C(4)-H(4)	120.7	C(4)-C(5)-C(6)	118.4(3)
C(4)-C(5)-H(5)	120.8	C(6)-C(5)-H(5)	120.8
N(1)-C(6)-C(5)	123.1(3)	N(1)-C(6)-H(6)	118.4
C(5)-C(6)-H(6)	118.4	N(4)-C(7)-C(8)	113.8(3)
N(4)-C(7)-H(7A)	108.8	C(8)-C(7)-H(7A)	108.8
N(4)-C(7)-H(7B)	108.8	C(8)-C(7)-H(7B)	108.8
H(7A)-C(7)-H(7B)	107.7	N(3)-C(8)-C(9)	121.4(3)
N(3)-C(8)-C(7)	118.2(3)	C(9)-C(8)-C(7)	120.4(3)
C(10)-C(9)-C(8)	120.6(3)	C(10)-C(9)-H(9)	119.7
C(8)-C(9)-H(9)	119.7	C(9)-C(10)-C(11)	118.1(3)
C(9)-C(10)-H(10)	121.0	C(11)-C(10)-H(10)	121.0
C(12)-C(11)-C(10)	118.7(3)	C(12)-C(11)-H(11)	120.6
C(10)-C(11)-H(11)	120.6	N(3)-C(12)-C(11)	122.8(3)
N(3)-C(12)-H(12)	118.6	C(11)-C(12)-H(12)	118.6
N(6)-C(13)-C(14)	112.9(3)	N(6)-C(13)-H(13A)	109.0
C(14)-C(13)-H(13A)	109.0	N(6)-C(13)-H(13B)	109.0
C(14)-C(13)-H(13B)	109.0	H(13A)-C(13)-H(13B)	107.8
N(5)-C(14)-C(15)	122.1(3)	N(5)-C(14)-C(13)	116.8(3)
C(15)-C(14)-C(13)	121.1(3)	C(16)-C(15)-C(14)	119.2(4)

Table B.8. Continued

C(16)-C(15)-H(15)	120.4	C(14)-C(15)-H(15)	120.4
C(15)-C(16)-C(17)	119.0(4)	C(15)-C(16)-H(16)	120.5
C(17)-C(16)-H(16)	120.5	C(18)-C(17)-C(16)	118.6(4)
C(18)-C(17)-H(17)	120.7	C(16)-C(17)-H(17)	120.7
N(5)-C(18)-C(17)	122.6(4)	N(5)-C(18)-H(18)	118.7
C(17)-C(18)-H(18)	118.7	N(8)-C(19)-C(20)	112.6(3)
N(8)-C(19)-H(19A)	109.1	C(20)-C(19)-H(19A)	109.1
N(8)-C(19)-H(19B)	109.1	C(20)-C(19)-H(19B)	109.1
H(19A)-C(19)-H(19B)	107.8	N(7)-C(20)-C(21)	121.4(3)
N(7)-C(20)-C(19)	116.6(3)	C(21)-C(20)-C(19)	122.0(3)
C(22)-C(21)-C(20)	119.4(4)	C(22)-C(21)-H(21)	120.3
C(20)-C(21)-H(21)	120.3	C(21)-C(22)-C(23)	120.2(4)
C(21)-C(22)-H(22)	119.9	C(23)-C(22)-H(22)	119.9
C(22)-C(23)-C(24)	117.6(4)	C(22)-C(23)-H(23)	121.2
C(24)-C(23)-H(23)	121.2	N(7)-C(24)-C(23)	122.7(3)
N(7)-C(24)-H(24)	118.7	C(23)-C(24)-H(24)	118.7
N(10)-C(25)-C(26)	112.0(3)	N(10)-C(25)-H(25A)	109.2
C(26)-C(25)-H(25A)	109.2	N(10)-C(25)-H(25B)	109.2
C(26)-C(25)-H(25B)	109.2	H(25A)-C(25)-H(25B)	107.9
N(9)-C(26)-C(27)	121.3(3)	N(9)-C(26)-C(25)	117.3(3)
C(27)-C(26)-C(25)	121.4(3)	C(28)-C(27)-C(26)	120.0(3)
C(28)-C(27)-H(27)	120.0	C(26)-C(27)-H(27)	120.0
C(27)-C(28)-C(29)	119.1(4)	C(27)-C(28)-H(28)	120.4
C(29)-C(28)-H(28)	120.4	C(30)-C(29)-C(28)	117.6(4)
C(30)-C(29)-H(29)	121.2	C(28)-C(29)-H(29)	121.2
N(9)-C(30)-C(29)	123.4(3)	N(9)-C(30)-H(30)	118.3
C(29)-C(30)-H(30)	118.3	N(12)-C(31)-C(32)	113.7(3)
N(12)-C(31)-H(31A)	108.8	C(32)-C(31)-H(31A)	108.8
N(12)-C(31)-H(31B)	108.8	C(32)-C(31)-H(31B)	108.8
H(31A)-C(31)-H(31B)	107.7	N(11)-C(32)-C(33)	121.0(3)
N(11)-C(32)-C(31)	119.0(3)	C(33)-C(32)-C(31)	120.0(3)
C(34)-C(33)-C(32)	120.2(3)	C(34)-C(33)-H(33)	119.9
C(32)-C(33)-H(33)	119.9	C(33)-C(34)-C(35)	118.4(3)
C(33)-C(34)-H(34)	120.8	C(35)-C(34)-H(34)	120.8
C(36)-C(35)-C(34)	119.0(4)	C(36)-C(35)-H(35)	120.5
C(34)-C(35)-H(35)	120.5	N(11)-C(36)-C(35)	122.7(3)
N(11)-C(36)-H(36)	118.6	C(35)-C(36)-H(36)	118.6
N(14)-C(37)-C(38)	113.9(3)	N(14)-C(37)-H(37A)	108.8
C(38)-C(37)-H(37A)	108.8	N(14)-C(37)-H(37B)	108.8
C(38)-C(37)-H(37B)	108.8	H(37A)-C(37)-H(37B)	107.7
N(13)-C(38)-C(39)	122.6(4)	N(13)-C(38)-C(37)	116.0(3)
C(39)-C(38)-C(37)	121.4(3)	C(40)-C(39)-C(38)	118.6(4)
C(40)-C(39)-H(39)	120.7	C(38)-C(39)-H(39)	120.7
C(39)-C(40)-C(41)	119.5(4)	C(39)-C(40)-H(40)	120.3
C(41)-C(40)-H(40)	120.3	C(42)-C(41)-C(40)	118.1(4)
C(42)-C(41)-H(41)	121.0	C(40)-C(41)-H(41)	121.0
N(13)-C(42)-C(41)	123.5(4)	N(13)-C(42)-H(42)	118.3
C(41)-C(42)-H(42)	118.3	N(16)-C(43)-C(44)	112.8(3)
N(16)-C(43)-H(43A)	109.0	C(44)-C(43)-H(43A)	109.0
N(16)-C(43)-H(43B)	109.0	C(44)-C(43)-H(43B)	109.0
H(43A)-C(43)-H(43B)	107.8	N(15)-C(44)-C(45)	122.2(3)
N(15)-C(44)-C(43)	115.9(3)	C(45)-C(44)-C(43)	121.9(3)
C(46)-C(45)-C(44)	119.7(3)	C(46)-C(45)-H(45)	120.2
C(44)-C(45)-H(45)	120.2	C(45)-C(46)-C(47)	118.7(3)

Table B.8. Continued

C(45)-C(46)-H(46)	120.6	C(47)-C(46)-H(46)	120.6
C(48)-C(47)-C(46)	118.7(3)	C(48)-C(47)-H(47)	120.6
C(46)-C(47)-H(47)	120.6	N(15)-C(48)-C(47)	123.2(3)
N(15)-C(48)-H(48)	118.4	C(47)-C(48)-H(48)	118.4
O(1)-C(49)-O(2)	130.8(3)	O(1)-C(49)-C(50)	114.0(3)
O(2)-C(49)-C(50)	115.2(3)	F(1)-C(50)-F(3)	106.3(3)
F(1)-C(50)-F(2)	106.4(3)	F(3)-C(50)-F(2)	107.0(3)
F(1)-C(50)-C(49)	110.5(3)	F(3)-C(50)-C(49)	114.7(3)
F(2)-C(50)-C(49)	111.4(3)	O(4)-C(51)-O(3)	131.6(4)
O(4)-C(51)-C(52)	115.1(3)	O(3)-C(51)-C(52)	113.2(3)
F(4)-C(52)-F(5)	106.4(3)	F(4)-C(52)-F(6)	106.1(3)
F(5)-C(52)-F(6)	105.4(3)	F(4)-C(52)-C(51)	114.6(3)
F(5)-C(52)-C(51)	113.4(3)	F(6)-C(52)-C(51)	110.2(3)
O(5)-C(53)-O(6)	130.8(3)	O(5)-C(53)-C(54)	113.6(3)
O(6)-C(53)-C(54)	115.6(3)	F(7)-C(54)-F(9)	105.1(4)
F(7)-C(54)-F(8)	105.5(3)	F(9)-C(54)-F(8)	106.4(4)
F(7)-C(54)-C(53)	111.5(3)	F(9)-C(54)-C(53)	112.4(3)
F(8)-C(54)-C(53)	115.1(3)	F(10)-C(55)-F(11)	107.2(3)
F(10)-C(55)-F(12)	105.7(3)	F(11)-C(55)-F(12)	105.9(3)
F(10)-C(55)-C(56)	113.6(3)	F(11)-C(55)-C(56)	113.8(3)
F(12)-C(55)-C(56)	110.0(3)	O(8)-C(56)-O(7)	131.4(3)
O(8)-C(56)-C(55)	114.4(3)	O(7)-C(56)-C(55)	114.1(3)
Hydrogen Bonds (Å)			
N(2)-H(2A)...O(8)#1	2.993(4)	N(2)-H(2B)...O(5)#2	2.945(4)
N(4)-H(4A)...N(7)#3	3.380(4)	N(4)-H(4B)...O(2)	2.925(4)
N(6)-H(6A)...O(4)#4	2.948(4)	N(6)-H(6B)...O(2)	3.087(4)
N(8)-H(8A)...O(8)#5	2.965(4)	N(8)-H(8B)...O(5)#2	3.060(4)
N(10)-H(10A)...O(1)	2.905(4)	N(10)-H(10B)...O(3)	2.988(4)
N(12)-H(12A)...O(6)	2.949(4)	N(12)- H(12B)...N(13)#3	3.144(4)
N(14)-H(14A)...O(6)	3.076(4)	N(14)-H(14B)...O(7)#6	2.974(4)
N(16)-H(16A)...O(1)	3.049(4)	N(16)-H(16B)...O(3)#4	2.960(4)

Symmetry transformations used to generate equivalent atoms: #1 x,y,z-1 #2 x,y+1,z-1 #3 x-1,y,z #4 x+1,y,z #5 x+1,y,z-1 #6 x+1,y-1,z

Table B.9. Experimental and statistical crystal data for **4.3**

Empirical formula	C40 H48 Ag4 F12 N12 O12 S4
Formula weight	1676.62
Temperature	110(2) K
Wavelength	0.71073 Å
Crystal system, space group	Monoclinic, P2(1)/n
Unit cell dimensions	a = 8.1167(9) Å α = 90 deg. b = 22.930(4) Å β = 97.430(5) deg. c = 15.625(2) Å γ = 90 deg.
Volume	2883.7(7) Å ³
Z, Calculated density	2, 1.931 Mg/m ³
Absorption coefficient	1.588 mm ⁻¹
F(000)	1656
Crystal size	0.279 x 0.216 x 0.202 mm
θ range for data collection	2.63 to 28.30 deg.
Limiting indices	-10<=h<=10, -30<=k<=30, -20<=l<=19
Reflections collected / unique	66994 / 7095 [R(int) = 0.0308]
Completeness to θ = 28.30	99.0 %
Absorption correction	multi-scan (SADABS)
Refinement method	Full-matrix least-squares on F ²
Data / restraints / parameters	7095 / 0 / 397
Goodness-of-fit on F ²	1.416
Final R indices [I>2σ(I)]	R1 = 0.0184, wR2 = 0.0487
R indices (all data)	R1 = 0.0233, wR2 = 0.0495
Largest diff. peak and hole	0.414 and -0.391 e.Å ⁻³

Bond Lengths (Å)

Ag(1)-N(3)	2.2114(12)	Ag(1)-N(2)	2.2769(13)
Ag(1)-N(1)	2.3959(11)	Ag(1)-O(1)	2.5907(10)
Ag(1)-Ag(2)	2.9137(3)	Ag(2)-N(4)	2.1992(13)
Ag(2)-N(6)	2.2364(13)	Ag(2)-N(5)	2.4032(12)
S(1)-O(3)	1.4364(12)	S(1)-O(1)	1.4376(10)
S(1)-O(2)	1.4451(11)	S(1)-C(19)	1.8188(16)
S(2)-O(6)	1.4350(11)	S(2)-O(4)	1.4424(11)
S(2)-O(5)	1.4434(12)	S(2)-C(20)	1.8221(15)
F(1)-C(19)	1.3330(18)	F(2)-C(19)	1.3326(19)
F(3)-C(19)	1.325(2)	F(4)-C(20)	1.3278(17)
F(5)-C(20)	1.3283(17)	F(6)-C(20)	1.3252(18)
N(1)-C(2)	1.3342(18)	N(1)-C(6)	1.3429(18)
N(2)-C(1)	1.4717(18)	N(2)-H(2A)	0.931(15)
N(2)-H(2B)	0.846(17)	N(3)-C(12)	1.3422(18)
N(3)-C(8)	1.3481(18)	N(4)-C(7)	1.4905(18)
N(4)-H(4A)	0.844(16)	N(4)-H(4B)	0.889(16)
N(5)-C(14)	1.3358(18)	N(5)-C(18)	1.3409(19)
N(6)-C(13)	1.4729(19)	N(6)-H(6A)	0.826(17)
N(6)-H(6B)	0.920(16)	C(1)-C(2)	1.5112(19)
C(1)-H(1A)	0.9900	C(1)-H(1B)	0.9900
C(2)-C(3)	1.390(2)	C(3)-C(4)	1.377(2)
C(3)-H(3)	0.9500	C(4)-C(5)	1.382(2)
C(4)-H(4)	0.9500	C(5)-C(6)	1.375(2)
C(5)-H(5)	0.9500	C(6)-H(6)	0.9500
C(7)-C(8)	1.496(2)	C(7)-H(7A)	0.9900
C(7)-H(7B)	0.9900	C(8)-C(9)	1.384(2)
C(9)-C(10)	1.378(2)	C(9)-H(10)	0.9500

Table B.9. Continued

C(10)-C(11)	1.385(2)	C(10)-H(11)	0.9500
C(11)-C(12)	1.381(2)	C(11)-H(12)	0.9500
C(12)-H(13)	0.9500	C(13)-C(14)	1.507(2)
C(13)-H(13A)	0.9900	C(13)-H(13B)	0.9900
C(14)-C(15)	1.388(2)	C(15)-C(16)	1.377(2)
C(15)-H(15)	0.9500	C(16)-C(17)	1.384(2)
C(16)-H(16)	0.9500	C(17)-C(18)	1.373(2)
C(17)-H(17)	0.9500	C(18)-H(18)	0.9500
Bond Angles (°)			
N(3)-Ag(1)-N(2)	159.77(4)	N(3)-Ag(1)-N(1)	122.35(4)
N(2)-Ag(1)-N(1)	73.09(4)	N(3)-Ag(1)-O(1)	88.42(4)
N(2)-Ag(1)-O(1)	96.65(4)	N(1)-Ag(1)-O(1)	114.76(4)
N(3)-Ag(1)-Ag(2)	74.26(3)	N(2)-Ag(1)-Ag(2)	85.69(3)
N(1)-Ag(1)-Ag(2)	130.76(3)	O(1)-Ag(1)-Ag(2)	111.41(2)
N(4)-Ag(2)-N(6)	165.33(5)	N(4)-Ag(2)-N(5)	119.63(4)
N(6)-Ag(2)-N(5)	74.73(4)	N(4)-Ag(2)-Ag(1)	80.05(4)
N(6)-Ag(2)-Ag(1)	91.03(3)	N(5)-Ag(2)-Ag(1)	115.98(3)
O(3)-S(1)-O(1)	114.73(7)	O(3)-S(1)-O(2)	114.86(7)
O(1)-S(1)-O(2)	115.10(6)	O(3)-S(1)-C(19)	103.74(8)
O(1)-S(1)-C(19)	103.36(7)	O(2)-S(1)-C(19)	102.70(7)
O(6)-S(2)-O(4)	114.90(6)	O(6)-S(2)-O(5)	115.70(7)
O(4)-S(2)-O(5)	113.67(7)	O(6)-S(2)-C(20)	104.06(7)
O(4)-S(2)-C(20)	102.39(7)	O(5)-S(2)-C(20)	103.89(7)
S(1)-O(1)-Ag(1)	124.03(6)	C(2)-N(1)-C(6)	118.26(12)
C(2)-N(1)-Ag(1)	112.25(9)	C(6)-N(1)-Ag(1)	129.17(10)
C(1)-N(2)-Ag(1)	107.81(8)	C(1)-N(2)-H(2A)	107.7(9)
Ag(1)-N(2)-H(2A)	117.7(10)	C(1)-N(2)-H(2B)	105.6(11)
Ag(1)-N(2)-H(2B)	109.4(11)	H(2A)-N(2)-H(2B)	107.9(14)
C(12)-N(3)-C(8)	118.59(12)	C(12)-N(3)-Ag(1)	122.19(10)
C(8)-N(3)-Ag(1)	119.21(9)	C(7)-N(4)-Ag(2)	119.81(9)
C(7)-N(4)-H(4A)	107.9(10)	Ag(2)-N(4)-H(4A)	104.9(10)
C(7)-N(4)-H(4B)	108.1(10)	Ag(2)-N(4)-H(4B)	104.5(10)
H(4A)-N(4)-H(4B)	111.6(14)	C(14)-N(5)-C(18)	118.31(13)
C(14)-N(5)-Ag(2)	112.01(9)	C(18)-N(5)-Ag(2)	127.92(10)
C(13)-N(6)-Ag(2)	111.76(9)	C(13)-N(6)-H(6A)	108.2(11)
Ag(2)-N(6)-H(6A)	109.2(11)	C(13)-N(6)-H(6B)	107.8(9)
Ag(2)-N(6)-H(6B)	112.9(10)	H(6A)-N(6)-H(6B)	106.8(14)
N(2)-C(1)-C(2)	111.64(12)	N(2)-C(1)-H(1A)	109.3
C(2)-C(1)-H(1A)	109.3	N(2)-C(1)-H(1B)	109.3
C(2)-C(1)-H(1B)	109.3	H(1A)-C(1)-H(1B)	108.0
N(1)-C(2)-C(3)	121.95(13)	N(1)-C(2)-C(1)	117.27(12)
C(3)-C(2)-C(1)	120.77(13)	C(4)-C(3)-C(2)	119.12(14)
C(4)-C(3)-H(3)	120.4	C(2)-C(3)-H(3)	120.4
C(3)-C(4)-C(5)	119.16(14)	C(3)-C(4)-H(4)	120.4
C(5)-C(4)-H(4)	120.4	C(6)-C(5)-C(4)	118.34(13)
C(6)-C(5)-H(5)	120.8	C(4)-C(5)-H(5)	120.8
N(1)-C(6)-C(5)	123.13(14)	N(1)-C(6)-H(6)	118.4
C(5)-C(6)-H(6)	118.4	N(4)-C(7)-C(8)	112.15(11)
N(4)-C(7)-H(7A)	109.2	C(8)-C(7)-H(7A)	109.2
N(4)-C(7)-H(7B)	109.2	C(8)-C(7)-H(7B)	109.2
H(7A)-C(7)-H(7B)	107.9	N(3)-C(8)-C(9)	121.39(13)
N(3)-C(8)-C(7)	116.76(12)	C(9)-C(8)-C(7)	121.85(13)

Table B.9. Continued

C(10)-C(9)-C(8)	119.81(14)	C(10)-C(9)-H(10)	120.1
C(8)-C(9)-H(10)	120.1	C(9)-C(10)-C(11)	118.83(14)
C(9)-C(10)-H(11)	120.6	C(11)-C(10)-H(11)	120.6
C(12)-C(11)-C(10)	118.62(14)	C(12)-C(11)-H(12)	120.7
C(10)-C(11)-H(12)	120.7	N(3)-C(12)-C(11)	122.75(14)
N(3)-C(12)-H(13)	118.6	C(11)-C(12)-H(13)	118.6
N(6)-C(13)-C(14)	113.41(12)	N(6)-C(13)-H(13A)	108.9
C(14)-C(13)-H(13A)	108.9	N(6)-C(13)-H(13B)	108.9
C(14)-C(13)-H(13B)	108.9	H(13A)-C(13)-H(13B)	107.7
N(5)-C(14)-C(15)	121.83(14)	N(5)-C(14)-C(13)	117.16(13)
C(15)-C(14)-C(13)	120.92(13)	C(16)-C(15)-C(14)	119.33(14)
C(16)-C(15)-H(15)	120.3	C(14)-C(15)-H(15)	120.3
C(15)-C(16)-C(17)	118.91(14)	C(15)-C(16)-H(16)	120.5
C(17)-C(16)-H(16)	120.5	C(18)-C(17)-C(16)	118.43(15)
C(18)-C(17)-H(17)	120.8	C(16)-C(17)-H(17)	120.8
N(5)-C(18)-C(17)	123.18(15)	N(5)-C(18)-H(18)	118.4
C(17)-C(18)-H(18)	118.4	F(3)-C(19)-F(2)	108.13(14)
F(3)-C(19)-F(1)	108.10(13)	F(2)-C(19)-F(1)	107.82(13)
F(3)-C(19)-S(1)	110.84(12)	F(2)-C(19)-S(1)	111.16(11)
F(1)-C(19)-S(1)	110.67(11)	F(6)-C(20)-F(4)	108.15(12)
F(6)-C(20)-F(5)	107.23(13)	F(4)-C(20)-F(5)	107.73(12)
F(6)-C(20)-S(2)	110.36(10)	F(4)-C(20)-S(2)	111.33(10)
F(5)-C(20)-S(2)	111.86(11)		
Hydrogen Bonds (Å)			
N(2)-H(2A)...O(2)#1	3.1438(17)	N(2)-H(2B)...O(6)#2	3.1422(17)
N(4)-H(4A)...O(5)#2	2.9799(17)	N(4)-H(4B)...O(4)	2.9911(17)
N(6)-H(6A)...O(2)	3.0426(18))	N(6)-H(6B)...O(3)#1	3.0810(18)

Symmetry transformations used to generate equivalent atoms: #1 -x+1,-y,-z #2 -x+1,-y,-z+1

Table B.10. Experimental and statistical crystal data for **4.4**

Empirical formula	C18 H24 Ag2 B2 F8 N6
Formula weight	713.79
Temperature	110(2) K
Wavelength	0.71073 Å
Crystal system, space group	Triclinic, P-1
Unit cell dimensions	a = 7.1125(14) Å α = 97.23(3) deg. b = 8.3350(17) Å β = 98.51(3) deg. c = 21.471(4) Å γ = 99.10(3) deg.
Volume	1228.4(4) Å^3
Z, Calculated density	2, 1.930 Mg/m^3
Absorption coefficient	1.675 mm^-1
F(000)	700
Crystal size	0.31 x 0.27 x 0.25 mm
Θ range for data collection	1.94 to 28.39 deg.
Limiting indices	-9<=h<=9, -11<=k<=11, -28<=l<=28
Reflections collected / unique	14615 / 5935 [R(int) = 0.0226]
Completeness to θ = 25.00	97.7 %
Absorption correction	multi-scan (SADABS)

Table B.10. Continued

Max. and min. transmission	0.6776 and 0.6223		
Refinement method	Full-matrix least-squares on F ²		
Data / restraints / parameters	5935 / 10 / 341		
Goodness-of-fit on F ²	1.034		
Final R indices [I>2σ(I)]	R1 = 0.0274, wR2 = 0.0678		
R indices (all data)	R1 = 0.0317, wR2 = 0.0705		
Largest diff. peak and hole	1.216 and -0.567 e.Å ⁻³		
Bond Lengths (Å)			
Ag(1)-N(3)	2.185(2)	Ag(1)-N(2)	2.267(2)
Ag(1)-N(1)	2.355(2)	Ag(2)-N(4)	2.186(2)
Ag(2)-N(6)	2.287(2)	Ag(2)-N(5)	2.313(2)
B(1)-F(2)	1.388(3)	B(1)-F(1)	1.398(3)
B(1)-F(3)	1.400(3)	B(1)-F(4)	1.403(3)
B(2)-F(6)	1.368(4)	B(2)-F(5)	1.387(5)
B(2)-F(8)	1.403(5)	B(2)-F(7)	1.408(5)
B(2A)-F(5A)	1.352(16)	B(2A)-F(6A)	1.354(16)
B(2A)-F(7A)	1.393(16)	B(2A)-F(8A)	1.397(17)
N(1)-C(2)	1.343(3)	N(1)-C(6)	1.350(3)
N(2)-C(1)	1.466(4)	N(2)-H(2A)	0.9000
N(2)-H(2B)	0.9000	N(3)-C(12)	1.349(3)
N(3)-C(8)	1.362(3)	N(4)-C(7)	1.473(3)
N(4)-H(4A)	0.9000	N(4)-H(4B)	0.9000
N(5)-C(14)	1.339(3)	N(5)-C(18)	1.359(3)
N(6)-C(13)	1.472(3)	N(6)-H(6A)	0.9000
N(6)-H(6B)	0.9000	C(1)-C(2)	1.508(4)
C(1)-H(1A)	0.9700	C(1)-H(1B)	0.9700
C(2)-C(3)	1.411(3)	C(3)-C(4)	1.371(4)
C(3)-H(3)	0.9300	C(4)-C(5)	1.395(4)
C(4)-H(4)	0.9300	C(5)-C(6)	1.388(4)
C(5)-H(5)	0.9300	C(6)-H(6)	0.9300
C(7)-C(8)	1.517(3)	C(7)-H(7A)	0.9700
C(7)-H(7B)	0.9700	C(8)-C(9)	1.388(3)
C(9)-C(10)	1.396(3)	C(9)-H(9)	0.9300
C(10)-C(11)	1.390(4)	C(10)-H(10)	0.9300
C(11)-C(12)	1.396(4)	C(11)-H(11)	0.9300
C(12)-H(12)	0.9300	C(13)-C(14)	1.526(3)
C(13)-H(13A)	0.9700	C(13)-H(13B)	0.9700
C(14)-C(15)	1.405(3)	C(15)-C(16)	1.390(4)
C(15)-H(15)	0.9300	C(16)-C(17)	1.389(4)
C(16)-H(16)	0.9300	C(17)-C(18)	1.377(4)
C(17)-H(17)	0.9300	C(18)-H(18)	0.9300
Bond Angles (°)			
N(3)-Ag(1)-N(2)	154.73(8)	N(3)-Ag(1)-N(1)	130.16(7)
N(2)-Ag(1)-N(1)	74.86(8)	N(4)-Ag(2)-N(6)	147.26(8)
N(4)-Ag(2)-N(5)	135.55(7)	N(6)-Ag(2)-N(5)	74.97(7)
F(2)-B(1)-F(1)	109.8(2)	F(2)-B(1)-F(3)	110.0(2)
F(1)-B(1)-F(3)	109.8(2)	F(2)-B(1)-F(4)	108.0(2)
F(1)-B(1)-F(4)	109.2(2)	F(3)-B(1)-F(4)	110.1(2)
F(6)-B(2)-F(5)	112.6(4)	F(6)-B(2)-F(8)	106.3(3)
F(5)-B(2)-F(8)	107.1(3)	F(6)-B(2)-F(7)	112.4(4)

Table B.10. Continued

F(5)-B(2)-F(7)	108.7(3)	F(8)-B(2)-F(7)	109.6(4)
F(5A)-B(2A)-F(6A)	109.3(15)	F(5A)-B(2A)-F(7A)	114.9(17)
F(6A)-B(2A)-F(7A)	108.4(17)	F(5A)-B(2A)-F(8A)	111.2(14)
F(6A)-B(2A)-F(8A)	104.6(15)	F(7A)-B(2A)-F(8A)	108.0(18)
C(2)-N(1)-C(6)	118.6(2)	C(2)-N(1)-Ag(1)	114.25(17)
C(6)-N(1)-Ag(1)	126.55(17)	C(1)-N(2)-Ag(1)	114.57(17)
C(1)-N(2)-H(2A)	108.6	Ag(1)-N(2)-H(2A)	108.6
C(1)-N(2)-H(2B)	108.6	Ag(1)-N(2)-H(2B)	108.6
H(2A)-N(2)-H(2B)	107.6	C(12)-N(3)-C(8)	118.6(2)
C(12)-N(3)-Ag(1)	117.67(16)	C(8)-N(3)-Ag(1)	123.59(16)
C(7)-N(4)-Ag(2)	114.69(15)	C(7)-N(4)-H(4A)	108.6
Ag(2)-N(4)-H(4A)	108.6	C(7)-N(4)-H(4B)	108.6
Ag(2)-N(4)-H(4B)	108.6	H(4A)-N(4)-H(4B)	107.6
C(14)-N(5)-C(18)	118.4(2)	C(14)-N(5)-Ag(2)	115.54(15)
C(18)-N(5)-Ag(2)	125.88(17)	C(13)-N(6)-Ag(2)	113.57(14)
C(13)-N(6)-H(6A)	108.9	Ag(2)-N(6)-H(6A)	108.9
C(13)-N(6)-H(6B)	108.9	Ag(2)-N(6)-H(6B)	108.9
H(6A)-N(6)-H(6B)	107.7	N(2)-C(1)-C(2)	115.8(2)
N(2)-C(1)-H(1A)	108.3	C(2)-C(1)-H(1A)	108.3
N(2)-C(1)-H(1B)	108.3	C(2)-C(1)-H(1B)	108.3
H(1A)-C(1)-H(1B)	107.4	N(1)-C(2)-C(3)	121.8(3)
N(1)-C(2)-C(1)	119.4(2)	C(3)-C(2)-C(1)	118.8(2)
C(4)-C(3)-C(2)	118.8(3)	C(4)-C(3)-H(3)	120.6
C(2)-C(3)-H(3)	120.6	C(3)-C(4)-C(5)	119.7(2)
C(3)-C(4)-H(4)	120.1	C(5)-C(4)-H(4)	120.1
C(6)-C(5)-C(4)	118.3(3)	C(6)-C(5)-H(5)	120.8
C(4)-C(5)-H(5)	120.8	N(1)-C(6)-C(5)	122.7(3)
N(1)-C(6)-H(6)	118.6	C(5)-C(6)-H(6)	118.6
N(4)-C(7)-C(8)	116.36(19)	N(4)-C(7)-H(7A)	108.2
C(8)-C(7)-H(7A)	108.2	N(4)-C(7)-H(7B)	108.2
C(8)-C(7)-H(7B)	108.2	H(7A)-C(7)-H(7B)	107.4
N(3)-C(8)-C(9)	121.7(2)	N(3)-C(8)-C(7)	115.26(19)
C(9)-C(8)-C(7)	123.0(2)	C(8)-C(9)-C(10)	119.5(2)
C(8)-C(9)-H(9)	120.2	C(10)-C(9)-H(9)	120.2
C(11)-C(10)-C(9)	118.8(2)	C(11)-C(10)-H(10)	120.6
C(9)-C(10)-H(10)	120.6	C(10)-C(11)-C(12)	118.8(2)
C(10)-C(11)-H(11)	120.6	C(12)-C(11)-H(11)	120.6
N(3)-C(12)-C(11)	122.5(2)	N(3)-C(12)-H(12)	118.7
C(11)-C(12)-H(12)	118.7	N(6)-C(13)-C(14)	114.54(19)
N(6)-C(13)-H(13A)	108.6	C(14)-C(13)-H(13A)	108.6
N(6)-C(13)-H(13B)	108.6	C(14)-C(13)-H(13B)	108.6
H(13A)-C(13)-H(13B)	107.6	N(5)-C(14)-C(15)	121.4(2)
N(5)-C(14)-C(13)	119.2(2)	C(15)-C(14)-C(13)	119.4(2)
C(16)-C(15)-C(14)	119.5(2)	C(16)-C(15)-H(15)	120.3
C(14)-C(15)-H(15)	120.3	C(17)-C(16)-C(15)	118.9(2)
C(17)-C(16)-H(16)	120.5	C(15)-C(16)-H(16)	120.5
C(18)-C(17)-C(16)	118.4(2)	C(18)-C(17)-H(17)	120.8
C(16)-C(17)-H(17)	120.8	N(5)-C(18)-C(17)	123.4(2)
N(5)-C(18)-H(18)	118.3	C(17)-C(18)-H(18)	118.3

Hydrogen Bonds

N(2)-H(2A)...F(8A)#1	3.055(16)	N(2)-H(2A)...F(5)#1	3.094(3)
N(2)-H(2A)...F(8)#1	3.330(4)	N(2)-H(2B)...F(7A)	2.97(3)

Table B.10. Continued

N(2)-H(2B)...F(7)	3.211(5)	N(4)-H(4A)...F(4)	3.112(3)
N(4)-H(4B)...F(1)#1	2.982(3)	N(6)-H(6A)...F(4)#2	3.133(3)
N(6)-H(6A)...F(2)#2	3.384(3)	N(6)-H(6B)...F(2)	3.000(3)

Symmetry transformations used to generate equivalent atoms: #1 x+1,y,z #2 -x+2,-y,-z+1

Table B.11. Experimental and statistical crystal data for **4.5**

Empirical formula	C26 H24 Ag2 B2 F8 N6
Formula weight	809.87
Temperature	110(2) K
Wavelength	0.71073 Å
Crystal system, space group	Orthorhombic, P2(1)2(1)2(1)
Unit cell dimensions	a = 10.5634(6) Å α = 90 deg. b = 13.6804(9) Å β = 90 deg. c = 19.7099(11) Å γ = 90 deg.
Volume	2848.3(3) Å^3
Z, Calculated density	4, 1.889 Mg/m^3
Absorption coefficient	1.457 mm^-1
F(000)	1592
Crystal size	0.245 x 0.231 x 0.199 mm
θ range for data collection	3.15 to 28.29 deg.
Limiting indices	-14<=h<=14, -17<=k<=18, -25<=l<=25
Reflections collected / unique	33450 / 7004 [R(int) = 0.0291]
Completeness to θ = 28.29	99.3 %
Absorption correction	multi-scan (SADABS)
Refinement method	Full-matrix least-squares on F^2
Data / restraints / parameters	7004 / 0 / 397
Goodness-of-fit on F^2	1.067
Final R indices [I>2σ(I)]	R1 = 0.0174, wR2 = 0.0408
R indices (all data)	R1 = 0.0194, wR2 = 0.0412
Absolute structure parameter	-0.016(11)
Largest diff. peak and hole	0.398 and -0.255 e.Å^-3

Bond Lengths (Å)

Ag(1)-N(1)	2.1502(15)	Ag(1)-N(3)	2.2706(14)
Ag(1)-N(4)	2.2839(16)	Ag(1)-Ag(2)	2.8958(3)
Ag(2)-N(2)	2.1788(15)	Ag(2)-N(6)	2.2870(15)
Ag(2)-N(5)	2.3299(15)	F(1)-B(1)	1.393(3)
F(2)-B(1)	1.389(3)	F(3)-B(1)	1.397(3)
F(4)-B(1)	1.386(2)	F(5)-B(2)	1.413(2)
F(6)-B(2)	1.381(2)	F(7)-B(2)	1.389(2)
F(8)-B(2)	1.377(3)	N(1)-C(6)	1.337(3)
N(1)-C(2)	1.348(2)	N(2)-C(1)	1.487(2)
N(2)-H(2A)	0.9000	N(2)-H(2B)	0.9000
N(3)-C(7)	1.337(2)	N(3)-C(11)	1.344(2)
N(4)-C(16)	1.344(2)	N(4)-C(12)	1.351(2)
N(5)-C(17)	1.337(3)	N(5)-C(21)	1.341(2)
N(6)-C(26)	1.344(2)	N(6)-C(22)	1.345(2)
C(1)-C(2)	1.498(3)	C(1)-H(1A)	0.9700

Table B.11. Continued

C(1)-H(1B)	0.9700	C(2)-C(3)	1.386(3)
C(3)-C(4)	1.372(3)	C(3)-H(3)	0.9300
C(4)-C(5)	1.362(4)	C(4)-H(4)	0.9300
C(5)-C(6)	1.380(3)	C(5)-H(5)	0.9300
C(6)-H(6)	0.9300	C(7)-C(8)	1.383(3)
C(7)-H(7)	0.9300	C(8)-C(9)	1.372(3)
C(8)-H(8)	0.9300	C(9)-C(10)	1.393(3)
C(9)-H(9)	0.9300	C(10)-C(11)	1.396(2)
C(10)-H(10)	0.9300	C(11)-C(12)	1.491(3)
C(12)-C(13)	1.392(3)	C(13)-C(14)	1.388(3)
C(13)-H(13)	0.9300	C(14)-C(15)	1.383(3)
C(14)-H(14)	0.9300	C(15)-C(16)	1.376(3)
C(15)-H(15)	0.9300	C(16)-H(16)	0.9300
C(17)-C(18)	1.383(3)	C(17)-H(17)	0.9300
C(18)-C(19)	1.371(3)	C(18)-H(18)	0.9300
C(19)-C(20)	1.386(3)	C(19)-H(19)	0.9300
C(20)-C(21)	1.395(2)	C(20)-H(20)	0.9300
C(21)-C(22)	1.495(3)	C(22)-C(23)	1.388(3)
C(23)-C(24)	1.384(3)	C(23)-H(23)	0.9300
C(24)-C(25)	1.381(3)	C(24)-H(24)	0.9300
C(25)-C(26)	1.374(3)	C(25)-H(25)	0.9300
C(26)-H(26)	0.9300		

Bond Angles (°)

N(1)-Ag(1)-N(3)	136.91(6)	F(7)-B(2)-F(5)	108.22(15)
N(1)-Ag(1)-N(4)	148.32(6)	N(3)-Ag(1)-N(4)	73.34(5)
N(1)-Ag(1)-Ag(2)	82.92(4)	N(3)-Ag(1)-Ag(2)	100.56(4)
N(4)-Ag(1)-Ag(2)	81.52(4)	N(2)-Ag(2)-N(6)	142.97(6)
N(2)-Ag(2)-N(5)	145.38(6)	N(6)-Ag(2)-N(5)	71.65(5)
N(2)-Ag(2)-Ag(1)	86.46(4)	N(6)-Ag(2)-Ag(1)	85.99(4)
N(5)-Ag(2)-Ag(1)	99.82(4)	C(6)-N(1)-C(2)	118.67(17)
C(6)-N(1)-Ag(1)	119.37(13)	C(2)-N(1)-Ag(1)	121.93(13)
C(1)-N(2)-Ag(2)	120.39(12)	C(1)-N(2)-H(2A)	107.2
Ag(2)-N(2)-H(2A)	107.2	C(1)-N(2)-H(2B)	107.2
Ag(2)-N(2)-H(2B)	107.2	H(2A)-N(2)-H(2B)	106.9
C(7)-N(3)-C(11)	119.52(15)	C(7)-N(3)-Ag(1)	123.98(12)
C(11)-N(3)-Ag(1)	116.25(11)	C(16)-N(4)-C(12)	118.58(16)
C(16)-N(4)-Ag(1)	125.40(12)	C(12)-N(4)-Ag(1)	115.99(12)
C(17)-N(5)-C(21)	118.82(16)	C(17)-N(5)-Ag(2)	124.45(13)
C(21)-N(5)-Ag(2)	116.12(11)	C(26)-N(6)-C(22)	118.55(16)
C(26)-N(6)-Ag(2)	123.41(12)	C(22)-N(6)-Ag(2)	117.97(12)
N(2)-C(1)-C(2)	111.88(16)	N(2)-C(1)-H(1A)	109.2
C(2)-C(1)-H(1A)	109.2	N(2)-C(1)-H(1B)	109.2
C(2)-C(1)-H(1B)	109.2	H(1A)-C(1)-H(1B)	107.9
N(1)-C(2)-C(3)	120.93(19)	N(1)-C(2)-C(1)	117.82(16)
C(3)-C(2)-C(1)	121.25(18)	C(4)-C(3)-C(2)	119.6(2)
C(4)-C(3)-H(3)	120.2	C(2)-C(3)-H(3)	120.2
C(5)-C(4)-C(3)	119.4(2)	C(5)-C(4)-H(4)	120.3
C(3)-C(4)-H(4)	120.3	C(4)-C(5)-C(6)	118.8(2)
C(4)-C(5)-H(5)	120.6	C(6)-C(5)-H(5)	120.6
N(1)-C(6)-C(5)	122.6(2)	N(1)-C(6)-H(6)	118.7
C(5)-C(6)-H(6)	118.7	N(3)-C(7)-C(8)	122.48(17)
N(3)-C(7)-H(7)	118.8	C(8)-C(7)-H(7)	118.8

Table B.11. Continued

C(9)-C(8)-C(7)	118.75(18)	C(9)-C(8)-H(8)	120.6
C(7)-C(8)-H(8)	120.6	C(8)-C(9)-C(10)	119.36(16)
C(8)-C(9)-H(9)	120.3	C(10)-C(9)-H(9)	120.3
C(9)-C(10)-C(11)	118.94(17)	C(9)-C(10)-H(10)	120.5
C(11)-C(10)-H(10)	120.5	N(3)-C(11)-C(10)	120.95(16)
N(3)-C(11)-C(12)	117.50(14)	C(10)-C(11)-C(12)	121.54(16)
N(4)-C(12)-C(13)	121.31(17)	N(4)-C(12)-C(11)	116.74(16)
C(13)-C(12)-C(11)	121.94(15)	C(14)-C(13)-C(12)	119.33(18)
C(14)-C(13)-H(13)	120.3	C(12)-C(13)-H(13)	120.3
C(15)-C(14)-C(13)	119.00(19)	C(15)-C(14)-H(14)	120.5
C(13)-C(14)-H(14)	120.5	C(16)-C(15)-C(14)	118.75(19)
C(16)-C(15)-H(15)	120.6	C(14)-C(15)-H(15)	120.6
N(4)-C(16)-C(15)	123.02(18)	N(4)-C(16)-H(16)	118.5
C(15)-C(16)-H(16)	118.5	N(5)-C(17)-C(18)	123.1(2)
N(5)-C(17)-H(17)	118.5	C(18)-C(17)-H(17)	118.5
C(19)-C(18)-C(17)	118.5(2)	C(19)-C(18)-H(18)	120.8
C(17)-C(18)-H(18)	120.8	C(18)-C(19)-C(20)	119.16(18)
C(18)-C(19)-H(19)	120.4	C(20)-C(19)-H(19)	120.4
C(19)-C(20)-C(21)	119.33(19)	C(19)-C(20)-H(20)	120.3
C(21)-C(20)-H(20)	120.3	N(5)-C(21)-C(20)	121.13(17)
N(5)-C(21)-C(22)	116.93(15)	C(20)-C(21)-C(22)	121.95(17)
N(6)-C(22)-C(23)	121.10(17)	N(6)-C(22)-C(21)	116.40(16)
C(23)-C(22)-C(21)	122.50(16)	C(24)-C(23)-C(22)	119.67(17)
C(24)-C(23)-H(23)	120.2	C(22)-C(23)-H(23)	120.2
C(25)-C(24)-C(23)	119.10(18)	C(25)-C(24)-H(24)	120.5
C(23)-C(24)-H(24)	120.5	C(26)-C(25)-C(24)	118.27(18)
C(26)-C(25)-H(25)	120.9	C(24)-C(25)-H(25)	120.9
N(6)-C(26)-C(25)	123.30(17)	N(6)-C(26)-H(26)	118.3
C(25)-C(26)-H(26)	118.3	F(4)-B(1)-F(2)	109.60(17)
F(4)-B(1)-F(1)	109.39(17)	F(2)-B(1)-F(1)	109.92(18)
F(4)-B(1)-F(3)	110.69(18)	F(2)-B(1)-F(3)	108.11(16)
F(1)-B(1)-F(3)	109.11(17)	F(8)-B(2)-F(6)	109.87(16)
F(8)-B(2)-F(7)	110.66(18)	F(6)-B(2)-F(7)	110.30(17)
F(8)-B(2)-F(5)	108.95(16)	F(6)-B(2)-F(5)	108.80(17)

Hydrogen Bonds (Å)

N(2)-H(2A)...F(5)#1	2.977(2)	N(2)-H(2B)...F(3)#1	3.099(2)
N(2)-H(2B)...F(2)#1	3.1257(19)		

Symmetry transformations used to generate equivalent atoms: #1 x,y+1,z

Table B.12. Experimental and statistical crystal data for 4.6

Empirical formula	C7 H8 Ag F3 N2 O3 S
Formula weight	365.08
Temperature	110(2) K
Wavelength	0.71073 Å
Crystal system, space group	Monoclinic, P2(1)/c
Unit cell dimensions	a = 12.982(6) Å α = 90 deg. b = 11.458(4) Å β = 101.40(3) deg. c = 7.709(5) Å γ = 90 deg.
Volume	1124.2(10) Å ³
Z, Calculated density	4, 2.157 Mg/m ³
Absorption coefficient	2.017 mm ⁻¹
F(000)	712
Crystal size	0.167 x 0.143 x 0.094 mm
Θ range for data collection	1.60 to 28.37 deg.
Limiting indices	-17<=h<=17, -13<=k<=15, -10<=l<=10
Reflections collected / unique	39350 / 2751 [R(int) = 0.0310]
Completeness to θ = 28.37	97.5 %
Absorption correction	multi-scan (SADABS)
Refinement method	Full-matrix least-squares on F ²
Data / restraints / parameters	2751 / 0 / 154
Goodness-of-fit on F ²	1.067
Final R indices [I>2σ(I)]	R1 = 0.0194, wR2 = 0.0491
R indices (all data)	R1 = 0.0232, wR2 = 0.0502
Largest diff. peak and hole	0.562 and -0.376 e.Å ⁻³

Bond Lengths (Å)

Ag(1)-N(2)#1	2.1445(17)	Ag(1)-N(1)	2.1453(18)
S(2)-O(3)	1.4360(17)	S(2)-O(2)	1.4436(15)
S(2)-O(1)	1.4445(16)	S(2)-C(7)	1.833(2)
F(1)-C(7)	1.328(2)	F(2)-C(7)	1.335(2)
F(3)-C(7)	1.326(2)	N(1)-C(2)	1.343(3)
N(1)-C(6)	1.354(3)	N(2)-C(1)	1.468(3)
N(2)-Ag(1)#2	2.1445(17)	N(2)-H(2A)	0.9200
N(2)-H(2B)	0.9200	C(1)-C(2)	1.514(2)
C(1)-H(1C)	0.9900	C(1)-H(1D)	0.9900
C(2)-C(3)	1.388(3)	C(6)-C(5)	1.377(3)
C(6)-H(6)	0.9500	C(5)-C(4)	1.372(3)
C(5)-H(5)	0.9500	C(4)-C(3)	1.380(3)
C(4)-H(4)	0.9500	C(3)-H(3)	0.9500

Bond Angles (°)

N(2)#1-Ag(1)-N(1)	171.93(6)	O(3)-S(2)-O(2)	115.81(9)
O(3)-S(2)-O(1)	114.90(10)	O(2)-S(2)-O(1)	113.53(9)
O(3)-S(2)-C(7)	104.27(9)	O(2)-S(2)-C(7)	103.54(9)
O(1)-S(2)-C(7)	102.56(9)	C(2)-N(1)-C(6)	118.79(17)
C(2)-N(1)-Ag(1)	123.88(12)	C(6)-N(1)-Ag(1)	117.29(15)
C(1)-N(2)-Ag(1)#2	121.13(11)	C(1)-N(2)-H(2A)	107.0
Ag(1)#2-N(2)-H(2A)	107.0	C(1)-N(2)-H(2B)	107.0
Ag(1)#2-N(2)-H(2B)	107.0	H(2A)-N(2)-H(2B)	106.8
N(2)-C(1)-C(2)	114.58(15)	N(2)-C(1)-H(1C)	108.6
C(2)-C(1)-H(1C)	108.6	N(2)-C(1)-H(1D)	108.6
C(2)-C(1)-H(1D)	108.6	H(1C)-C(1)-H(1D)	107.6

Table B.12. Continued

N(1)-C(2)-C(3)	120.89(17)	N(1)-C(2)-C(1)	116.00(16)
C(3)-C(2)-C(1)	123.09(18)	N(1)-C(6)-C(5)	122.5(2)
N(1)-C(6)-H(6)	118.7	C(5)-C(6)-H(6)	118.7
C(4)-C(5)-C(6)	118.68(19)	C(4)-C(5)-H(5)	120.7
C(6)-C(5)-H(5)	120.7	C(5)-C(4)-C(3)	119.28(18)
C(5)-C(4)-H(4)	120.4	C(3)-C(4)-H(4)	120.4
C(4)-C(3)-C(2)	119.79(19)	C(4)-C(3)-H(3)	120.1
C(2)-C(3)-H(3)	120.1	F(3)-C(7)-F(1)	108.17(18)
F(3)-C(7)-F(2)	107.32(17)	F(1)-C(7)-F(2)	107.20(17)
F(3)-C(7)-S(2)	111.95(14)	F(1)-C(7)-S(2)	111.24(14)
F(2)-C(7)-S(2)	110.74(14)		
Hydrogen Bonds (Å)			
N(2)-H(2A)...O(1)#3	2.913(2)	N(2)-H(2A)...O(3)#4	2.967(3)
N(2)-H(2B)...O(1)#5	2.993(3)		

Symmetry transformations used to generate equivalent atoms: #1 -x+2,y+1/2,-z+1/2 #2 -x+2,y-1/2,-z+1/2 #3 -x+1,y-1/2,-z+1/2 #4 -x+1,-y+1,-z #5 -x+1,-y+1,-z+1

Table B.13. Experimental and statistical crystal data for **4.7**

Empirical formula	C8 H8 Ag F3 N2 O2
Formula weight	329.03
Temperature	110(2) K
Wavelength	0.71073 Å
Crystal system, space group	Orthorhombic, P2(1)2(1)2(1)
Unit cell dimensions	a = 4.7270(8) Å α = 90 deg. b = 9.8985(19) Å β = 90 deg. c = 22.111(4) Å γ = 90 deg.
Volume	1034.6(3) Å ³
Z, Calculated density	4, 2.112 Mg/m ³
Absorption coefficient	1.978 mm ⁻¹
F(000)	640
Crystal size	0.24 x 0.15 x 0.08 mm
Θ range for data collection	1.84 to 26.45 deg.
Limiting indices	-5<=h<=5, -12<=k<=12, -27<=l<=27
Reflections collected / unique	13577 / 2121 [R(int) = 0.0626]
Completeness to θ = 26.45	100.0 %
Absorption correction	multi-scan (SADABS)
Max. and min. transmission	0.8594 and 0.6461
Refinement method	Full-matrix least-squares on F ²
Data / restraints / parameters	2121 / 0 / 145
Goodness-of-fit on F ²	1.067
Final R indices [I>2σ(I)]	R1 = 0.0200, wR2 = 0.0443
R indices (all data)	R1 = 0.0229, wR2 = 0.0450
Absolute structure parameter	0.05(3)
Largest diff. peak and hole	0.621 and -0.413 e.Å ⁻³

Table B.13. Continued

Bond Lengths (Å)

Ag(1)-N(2)#1	2.186(2)	Ag(1)-N(1)	2.188(2)
Ag(1)-O(1)	2.498(2)	F(1)-C(8)	1.320(4)
F(2)-C(8)	1.322(4)	F(3)-C(8)	1.344(4)
O(1)-C(7)	1.228(3)	O(2)-C(7)	1.237(3)
N(1)-C(2)	1.343(4)	N(1)-C(6)	1.348(4)
N(2)-C(1)	1.476(3)	N(2)-Ag(1)#2	2.186(2)
N(2)-H(2A)	0.9200	N(2)-H(2B)	0.9200
C(1)-C(2)	1.508(4)	C(1)-H(1A)	0.9900
C(1)-H(1B)	0.9900	C(2)-C(3)	1.393(4)
C(3)-C(4)	1.379(4)	C(3)-H(3)	0.9500
C(4)-C(5)	1.385(4)	C(4)-H(4)	0.9500
C(5)-C(6)	1.382(4)	C(5)-H(5)	0.9500
C(6)-H(6)	0.9500	C(7)-C(8)	1.549(4)

Bond Angles (°)

N(2)#1-Ag(1)-N(1)	152.96(9)	N(2)#1-Ag(1)-O(1)	94.27(8)
N(1)-Ag(1)-O(1)	110.63(8)	C(7)-O(1)-Ag(1)	130.17(19)
C(2)-N(1)-C(6)	119.0(2)	C(2)-N(1)-Ag(1)	123.70(18)
C(6)-N(1)-Ag(1)	117.09(17)	C(1)-N(2)-Ag(1)#2	118.43(17)
C(1)-N(2)-H(2A)	107.7	Ag(1)#2-N(2)-H(2A)	107.7
C(1)-N(2)-H(2B)	107.7	Ag(1)#2-N(2)-H(2B)	107.7
H(2A)-N(2)-H(2B)	107.1	N(2)-C(1)-C(2)	112.1(2)
N(2)-C(1)-H(1A)	109.2	C(2)-C(1)-H(1A)	109.2
N(2)-C(1)-H(1B)	109.2	C(2)-C(1)-H(1B)	109.2
H(1A)-C(1)-H(1B)	107.9	N(1)-C(2)-C(3)	121.3(2)
N(1)-C(2)-C(1)	118.0(2)	C(3)-C(2)-C(1)	120.7(3)
C(4)-C(3)-C(2)	119.6(3)	C(4)-C(3)-H(3)	120.2
C(2)-C(3)-H(3)	120.2	C(3)-C(4)-C(5)	118.9(3)
C(3)-C(4)-H(4)	120.5	C(5)-C(4)-H(4)	120.5
C(6)-C(5)-C(4)	118.8(3)	C(6)-C(5)-H(5)	120.6
C(4)-C(5)-H(5)	120.6	N(1)-C(6)-C(5)	122.3(3)
N(1)-C(6)-H(6)	118.8	C(5)-C(6)-H(6)	118.8
O(1)-C(7)-O(2)	131.4(3)	O(1)-C(7)-C(8)	112.6(3)
O(2)-C(7)-C(8)	115.9(2)	F(1)-C(8)-F(2)	107.4(3)
F(1)-C(8)-F(3)	106.6(3)	F(2)-C(8)-F(3)	105.4(2)
F(1)-C(8)-C(7)	113.4(2)	F(2)-C(8)-C(7)	112.9(2)
F(3)-C(8)-C(7)	110.7(3)		

Hydrogen Bonds (Å)

N(2)-H(2A)...O(2)	2.922(3)	N(2)-H(2B)...O(1)#3	2.904(3)
-------------------	----------	---------------------	----------

Symmetry transformations used to generate equivalent atoms: #1 -x+1,y+1/2,-z+1/2 #2 -x+1,y-1/2,-z+1/2 #3 -x+2,y-1/2,-z+1/2

Table B.14. Experimental and statistical crystal data for 5.1.1

Empirical formula	C14.38 H19.50 Ag2 B2.50 F8.63 N5.13 O
Formula weight	686.74
Temperature	110(2) K
Wavelength	0.71073 Å
Crystal system, space group	Monoclinic, C2/m
Unit cell dimensions	a = 13.5924(15) Å α = 90 deg. b = 27.841(3) Å β = 113.100(2) deg. c = 13.2811(15) Å γ = 90 deg.
Volume	4623.0(9) Å ³
Z, Calculated density	8, 1.973 Mg/m ³
Absorption coefficient	1.781 mm ⁻¹
F(000)	2670
Crystal size	.128 x .091 x .062 mm
Θ range for data collection	2.85 to 25.68 deg.
Limiting indices	-16<=h<=16, -26<=k<=33, -16<=l<=16
Reflections collected / unique	12024 / 4433 [R(int) = 0.0463]
Completeness to θ = 25.00	98.8 %
Absorption correction	multi-scan (SADABS)
Refinement method	Full-matrix least-squares on F ²
Data / restraints / parameters	4433 / 10 / 378
Goodness-of-fit on F ²	1.037
Final R indices [I>2σ(I)]	R1 = 0.0679, wR2 = 0.1730
R indices (all data)	R1 = 0.0980, wR2 = 0.1959
Largest diff. peak and hole	2.259 and -1.738 e.Å ⁻³

Bond Lengths (Å)

Ag(1)-N(1)	2.181(7)	Ag(1)-N(3)	2.183(7)
Ag(1)-N(5)	2.515(9)	Ag(1)-Ag(1)#1	3.2896(14)
Ag(2)-N(2)	2.146(7)	Ag(2)-N(2)#2	2.146(7)
Ag(3)-N(4)	2.154(15)	Ag(3)-N(4)#3	2.154(15)
N(4)-C(7)	1.365(19)	N(4)-H(4A)	0.9000
N(4)-H(4B)	0.9000	C(7)-C(8)	1.480(18)
C(7)-H(7A)	0.9700	C(7)-H(7B)	0.9700
Ag(3A)-N(6A)	1.83(4)	Ag(3A)-N(4A)	2.33(3)
Ag(3A)-N(4A)#3	2.33(3)	N(4A)-H(4A1)	0.9000
N(4A)-H(4A2)	0.9000	N(6A)-C(15A)	1.12(5)
C(15A)-C(16A)	1.43(5)	C(16A)-H(16A)	0.9600
C(16A)-H(16B)	0.9600	C(16A)-H(16C)	0.9600
O(3A)-O(3A)#4	0.89(4)	B(1)-F(1)	1.33(2)
B(1)-F(4)	1.35(2)	B(1)-F(3)	1.39(3)
B(1)-F(2)	1.43(3)	B(1A)-F(1A)	1.32(2)
B(1A)-F(4A)	1.34(2)	B(1A)-F(3A)	1.39(3)
B(1A)-F(2A)	1.42(3)	B(3)-F(9)#3	1.297(16)
B(3)-F(9)	1.297(16)	B(3)-F(10)	1.32(3)
B(3)-F(8)	1.47(2)	F(8A)-F(8A)#3	1.01(6)
F(8A)-F(9A)#3	1.27(5)	F(9A)-F(8A)#3	1.27(5)
N(1)-C(4)	1.340(11)	N(1)-C(3)	1.361(11)
N(2)-C(1)	1.463(12)	N(2)-H(2A)	0.9000
N(2)-H(2B)	0.9000	N(3)-C(9)	1.317(12)
N(3)-C(10)	1.331(12)	N(5)-C(13)	1.124(13)
C(1)-C(2)	1.516(12)	C(1)-H(1A)	0.9700
C(1)-H(1B)	0.9700	C(2)-C(3)	1.383(12)
C(2)-C(6)	1.392(12)	C(3)-H(3)	0.9300

Table B.14. Continued

C(4)-C(5)	1.388(13)	C(4)-H(4)	0.9300
C(5)-C(6)	1.377(12)	C(5)-H(5)	0.9300
C(6)-H(6)	0.9300	C(8)-C(12)	1.377(16)
C(8)-C(9)	1.385(13)	C(9)-H(9)	0.9300
C(10)-C(11)	1.400(14)	C(10)-H(10)	0.9300
C(11)-C(12)	1.367(16)	C(11)-H(11)	0.9300
C(12)-H(12)	0.9300	C(13)-C(14)	1.428(16)
C(14)-H(14C)	0.9600	C(14)-H(14B)	0.9600
C(14)-H(14A)	0.9600	F(7)-B(2)#5	1.38(2)
F(7)-B(2)	1.51(3)	F(6)-B(2)#5	1.28(3)
F(6)-B(2)	1.28(3)	F(5)-B(2)	1.36(2)
B(2)-B(2)#5	0.87(4)	B(2)-F(7)#5	1.38(2)
Bond Angles (°)			
N(1)-Ag(1)-N(3)	164.3(3)	N(1)-Ag(1)-N(5)	99.9(3)
N(3)-Ag(1)-N(5)	95.8(3)	N(1)-Ag(1)-Ag(1)#1	113.25(18)
N(3)-Ag(1)-Ag(1)#1	68.27(18)	N(5)-Ag(1)-Ag(1)#1	82.5(2)
N(2)-Ag(2)-N(2)#2	172.7(4)	N(4)-Ag(3)-N(4)#3	174.9(9)
C(7)-N(4)-Ag(3)	119.9(11)	C(7)-N(4)-H(4A)	107.4
Ag(3)-N(4)-H(4A)	107.4	C(7)-N(4)-H(4B)	107.4
Ag(3)-N(4)-H(4B)	107.4	H(4A)-N(4)-H(4B)	106.9
N(4)-C(7)-C(8)	122.2(13)	N(4)-C(7)-H(7A)	106.8
C(8)-C(7)-H(7A)	106.8	N(4)-C(7)-H(7B)	106.8
C(8)-C(7)-H(7B)	106.8	H(7A)-C(7)-H(7B)	106.6
N(6A)-Ag(3A)-N(4A)	86.0(9)	N(6A)-Ag(3A)-	86.0(8)
		N(4A)#3	
N(4A)-Ag(3A)-N(4A)#3	168.0(16)	Ag(3A)-N(4A)-H(4A1)	108.9
Ag(3A)-N(4A)-H(4A2)	108.9	H(4A1)-N(4A)-H(4A2)	107.7
C(15A)-N(6A)-Ag(3A)	172(3)	N(6A)-C(15A)-C(16A)	180(4)
C(15A)-C(16A)-H(16A)	109.5	C(15A)-C(16A)-	109.5
		H(16B)	
H(16A)-C(16A)-H(16B)	109.5	C(15A)-C(16A)-	109.5
		H(16C)	
H(16A)-C(16A)-H(16C)	109.5	H(16B)-C(16A)-	109.5
		H(16C)	
F(1)-B(1)-F(4)	112.9(18)	F(1)-B(1)-F(3)	111(2)
F(4)-B(1)-F(3)	109.5(17)	F(1)-B(1)-F(2)	108.9(17)
F(4)-B(1)-F(2)	107(2)	F(3)-B(1)-F(2)	106.3(15)
F(1A)-B(1A)-F(4A)	113(2)	F(1A)-B(1A)-F(3A)	108(3)
F(4A)-B(1A)-F(3A)	113(2)	F(1A)-B(1A)-F(2A)	109(2)
F(4A)-B(1A)-F(2A)	108(3)	F(3A)-B(1A)-F(2A)	104.7(19)
F(9)#3-B(3)-F(9)	101(3)	F(9)#3-B(3)-F(10)	112(2)
F(9)-B(3)-F(10)	112(2)	F(9)#3-B(3)-F(8)	100.3(13)
F(9)-B(3)-F(8)	100.3(12)	F(10)-B(3)-F(8)	127(3)
F(8A)#3-F(8A)-F(9A)#3	129(6)	C(4)-N(1)-C(3)	117.3(7)
C(4)-N(1)-Ag(1)	122.5(6)	C(3)-N(1)-Ag(1)	120.1(6)
C(1)-N(2)-Ag(2)	113.8(6)	C(1)-N(2)-H(2A)	108.8
Ag(2)-N(2)-H(2A)	108.8	C(1)-N(2)-H(2B)	108.8
Ag(2)-N(2)-H(2B)	108.8	H(2A)-N(2)-H(2B)	107.7
C(9)-N(3)-C(10)	117.2(8)	C(9)-N(3)-Ag(1)	121.8(6)
C(10)-N(3)-Ag(1)	120.7(6)	C(13)-N(5)-Ag(1)	165.5(9)
N(2)-C(1)-C(2)	113.7(8)	N(2)-C(1)-H(1A)	108.8

Table B.14. Continued

C(2)-C(1)-H(1A)	108.8	N(2)-C(1)-H(1B)	108.8
C(2)-C(1)-H(1B)	108.8	H(1A)-C(1)-H(1B)	107.7
C(3)-C(2)-C(6)	117.4(8)	C(3)-C(2)-C(1)	120.0(8)
C(6)-C(2)-C(1)	122.6(8)	N(1)-C(3)-C(2)	123.5(8)
N(1)-C(3)-H(3)	118.3	C(2)-C(3)-H(3)	118.3
N(1)-C(4)-C(5)	123.1(8)	N(1)-C(4)-H(4)	118.5
C(5)-C(4)-H(4)	118.5	C(6)-C(5)-C(4)	118.5(8)
C(6)-C(5)-H(5)	120.8	C(4)-C(5)-H(5)	120.8
C(5)-C(6)-C(2)	120.2(8)	C(5)-C(6)-H(6)	119.9
C(2)-C(6)-H(6)	119.9	C(12)-C(8)-C(9)	117.0(10)
C(12)-C(8)-C(7)	120.6(11)	C(9)-C(8)-C(7)	122.4(12)
N(3)-C(9)-C(8)	125.4(9)	N(3)-C(9)-H(9)	117.3
C(8)-C(9)-H(9)	117.3	N(3)-C(10)-C(11)	121.7(10)
N(3)-C(10)-H(10)	119.2	C(11)-C(10)-H(10)	119.2
C(12)-C(11)-C(10)	119.7(10)	C(12)-C(11)-H(11)	120.1
C(10)-C(11)-H(11)	120.1	C(11)-C(12)-C(8)	119.0(9)
C(11)-C(12)-H(12)	120.5	C(8)-C(12)-H(12)	120.5
N(5)-C(13)-C(14)	177.9(14)	C(13)-C(14)-H(14C)	109.5
C(13)-C(14)-H(14B)	109.5	H(14C)-C(14)-H(14B)	109.5
C(13)-C(14)-H(14A)	109.5	H(14C)-C(14)-H(14A)	109.5
H(14B)-C(14)-H(14A)	109.5	B(2)#5-F(7)-B(2)	34.5(14)
B(2)#5-F(6)-B(2)	40(2)	B(2)#5-B(2)-F(6)	70.2(11)
B(2)#5-B(2)-F(5)	165(5)	F(6)-B(2)-F(5)	105(2)
B(2)#5-B(2)-F(7)#5	81(3)	F(6)-B(2)-F(7)#5	118.4(19)
F(5)-B(2)-F(7)#5	113.2(17)	B(2)#5-B(2)-F(7)	64(3)
F(6)-B(2)-F(7)	109.7(17)	F(5)-B(2)-F(7)	105.8(19)
F(7)#5-B(2)-F(7)	104(2)		

Hydrogen Bonds (Å)

N(4)-H(4A)...F(5)#3	3.00(2)	N(4)-H(4A)...F(7)#3	3.258(18)
N(4)-H(4B)...F(2)#6	2.94(2)	N(4)-H(4B)...F(3)#6	3.27(3)
N(4A)-H(4A2)...F(3A)#7	3.06(4)	N(2)-H(2A)...F(7)#8	3.054(10)
N(2)-H(2A)...F(9)#8	3.129(15)	N(2)-H(2B)...F(2A)#9	2.914(17)
N(2)-H(2B)...F(2)#9	3.063(13)	N(2)-H(2B)...F(5)#7	3.048(16)

Symmetry transformations used to generate equivalent atoms: #1 -x+2,y,-z+3 #2 x,-y+3,z #3 x,-y+2,z
#4 -x+3,-y+2,-z+4 #5 -x+2,y,-z+2 #6 -x+3/2,y+1/2,-z+2 #7 x+1/2,y+1/2,z+1 #8 -x+5/2,y+1/2,-z+3
#9 -x+2,-y+2,-z+3

Table B.15. Experimental and statistical crystal data for 5.1.2

Empirical formula	C56 H76 Ag8 B8 F32 N20
Formula weight	2586.81
Temperature	110(2) K
Wavelength	0.71073 Å
Crystal system, space group	Monoclinic, P2(1)/c
Unit cell dimensions	a = 7.8143(7) Å α = 90 deg. b = 25.736(2) Å β = 96.381(2) deg. c = 21.1937(18) Å γ = 90 deg.
Volume	4235.9(6) Å ³
Z, Calculated density	2, 2.028 Mg/m ³
Absorption coefficient	1.929 mm ⁻¹
F(000)	2512
Crystal size	0.200 × 0.210 × 0.350 mm
Θ range for data collection	1.58 to 26.35 deg.
Limiting indices	-9<=h<=8, -28<=k<=32, -26<=l<=26
Reflections collected / unique	36620 / 8655 [R(int) = 0.0436]
Completeness to θ = 26.35	100.0 %
Absorption correction	multi-scan (SADABS)
Refinement method	Full-matrix least-squares on F ²
Data / restraints / parameters	8655 / 6 / 574
Goodness-of-fit on F ²	1.128
Final R indices [I>2σ(I)]	R1 = 0.0530, wR2 = 0.1156
R indices (all data)	R1 = 0.0655, wR2 = 0.1215
Largest diff. peak and hole	2.877 and -2.169 e.Å ⁻³

Bond Lengths (Å)

Ag(1)-N(1)	2.130(5)	Ag(1)-N(3)	2.132(5)
Ag(2)-N(5)	2.111(6)	Ag(2)-N(7)	2.130(6)
Ag(3)-N(8)	2.142(5)	Ag(3)-N(4)	2.145(5)
Ag(3)-N(10)	2.609(7)	Ag(3)-Ag(4)	3.2543(8)
Ag(4)-N(2)	2.189(5)	Ag(4)-N(6)	2.195(5)
Ag(4)-N(9)	2.374(7)	F(1)-B(1)	1.398(8)
F(2)-B(1)	1.391(9)	F(3)-B(1)	1.387(8)
F(4)-B(1)	1.402(8)	F(5)-B(2)	1.405(8)
F(6)-B(2)	1.402(8)	F(7)-B(2)	1.401(8)
F(8)-B(2)	1.374(8)	F(9)-B(3)	1.378(8)
F(10)-B(3)	1.396(9)	F(11)-B(3)	1.394(8)
F(12)-B(3)	1.372(9)	F(15)-B(4)	1.370(9)
B(4)-F(14)	1.362(10)	B(4)-F(13)	1.364(9)
B(4)-F(16)	1.370(9)	N(1)-C(1)	1.479(8)
N(1)-H(1A)	0.9000	N(1)-H(1B)	0.9000
N(2)-C(4)	1.349(8)	N(2)-C(3)	1.351(8)
N(3)-C(7)	1.480(7)	N(3)-H(3A)	0.9000
N(3)-H(3B)	0.9000	N(4)-C(9)	1.348(7)
N(4)-C(10)	1.356(8)	N(5)-C(13)	1.464(9)
N(5)-H(5A)	0.9000	N(5)-H(5B)	0.9000
N(6)-C(15)	1.342(8)	N(6)-C(16)	1.349(8)
N(7)-C(19)	1.477(8)	N(7)-H(7A)	0.9000
N(7)-H(7B)	0.9000	N(8)-C(22)	1.343(8)
N(8)-C(21)	1.355(8)	N(9)-C(25)	1.132(10)
N(10)-C(27)	1.121(10)	C(1)-C(2)	1.500(8)
C(1)-H(1C)	0.9700	C(1)-H(1D)	0.9700
C(2)-C(3)	1.388(8)	C(2)-C(6)	1.398(8)

Table B.15. Continued

C(3)-H(3)	0.9300	C(4)-C(5)	1.370(9)
C(4)-H(4)	0.9300	C(5)-C(6)	1.384(9)
C(5)-H(5)	0.9300	C(6)-H(6)	0.9300
C(7)-C(8)	1.509(8)	C(7)-H(7C)	0.9700
C(7)-H(7D)	0.9700	C(8)-C(12)	1.390(8)
C(8)-C(9)	1.390(8)	C(9)-H(9)	0.9300
C(10)-C(11)	1.373(9)	C(10)-H(10)	0.9300
C(11)-C(12)	1.388(9)	C(11)-H(11)	0.9300
C(12)-H(12)	0.9300	C(13)-C(14)	1.511(9)
C(13)-H(13A)	0.9700	C(13)-H(13B)	0.9700
C(14)-C(15)	1.379(9)	C(14)-C(18)	1.395(10)
C(15)-H(15)	0.9300	C(16)-C(17)	1.370(9)
C(16)-H(16)	0.9300	C(17)-C(18)	1.383(9)
C(17)-H(17)	0.9300	C(18)-H(18)	0.9300
C(19)-C(20)	1.512(9)	C(19)-H(19A)	0.9700
C(19)-H(19B)	0.9700	C(20)-C(24)	1.380(9)
C(20)-C(21)	1.388(9)	C(21)-H(21)	0.9300
C(22)-C(23)	1.379(9)	C(22)-H(22)	0.9300
C(23)-C(24)	1.395(9)	C(23)-H(23)	0.9300
C(24)-H(24)	0.9300	C(25)-C(26)	1.468(11)
C(26)-H(26A)	0.9600	C(26)-H(26B)	0.9600
C(26)-H(26C)	0.9600	C(27)-C(28)	1.469(11)
C(28)-H(28A)	0.9600	C(28)-H(28B)	0.9600
C(28)-H(28C)	0.9600		

Bond Angles (°)

N(1)-Ag(1)-N(3)	174.4(2)	F(11)-B(3)-F(10)	108.8(6)
N(5)-Ag(2)-N(7)	174.4(2)	N(8)-Ag(3)-N(4)	163.6(2)
N(8)-Ag(3)-N(10)	94.8(2)	N(4)-Ag(3)-N(10)	101.5(2)
N(8)-Ag(3)-Ag(4)	84.16(14)	N(4)-Ag(3)-Ag(4)	104.97(14)
N(10)-Ag(3)-Ag(4)	62.6(2)	N(2)-Ag(4)-N(6)	143.53(19)
N(2)-Ag(4)-N(9)	102.7(2)	N(6)-Ag(4)-N(9)	109.5(2)
N(2)-Ag(4)-Ag(3)	74.31(13)	N(6)-Ag(4)-Ag(3)	103.89(14)
N(9)-Ag(4)-Ag(3)	118.16(18)	F(14)-B(4)-F(13)	106.8(7)
F(14)-B(4)-F(16)	109.5(8)	F(13)-B(4)-F(16)	111.3(7)
F(14)-B(4)-F(15)	107.3(7)	F(13)-B(4)-F(15)	112.5(7)
F(16)-B(4)-F(15)	109.3(6)	C(1)-N(1)-Ag(1)	112.9(4)
C(1)-N(1)-H(1A)	109.0	Ag(1)-N(1)-H(1A)	109.0
C(1)-N(1)-H(1B)	109.0	Ag(1)-N(1)-H(1B)	109.0
H(1A)-N(1)-H(1B)	107.8	C(4)-N(2)-C(3)	117.6(5)
C(4)-N(2)-Ag(4)	122.4(4)	C(3)-N(2)-Ag(4)	119.9(4)
C(7)-N(3)-Ag(1)	114.8(4)	C(7)-N(3)-H(3A)	108.6
Ag(1)-N(3)-H(3A)	108.6	C(7)-N(3)-H(3B)	108.6
Ag(1)-N(3)-H(3B)	108.6	H(3A)-N(3)-H(3B)	107.6
C(9)-N(4)-C(10)	118.3(5)	C(9)-N(4)-Ag(3)	120.3(4)
C(10)-N(4)-Ag(3)	121.3(4)	C(13)-N(5)-Ag(2)	119.3(5)
C(13)-N(5)-H(5A)	107.5	Ag(2)-N(5)-H(5A)	107.5
C(13)-N(5)-H(5B)	107.5	Ag(2)-N(5)-H(5B)	107.5
H(5A)-N(5)-H(5B)	107.0	C(15)-N(6)-C(16)	118.0(5)
C(15)-N(6)-Ag(4)	119.4(4)	C(16)-N(6)-Ag(4)	122.4(4)
C(19)-N(7)-Ag(2)	114.7(4)	C(19)-N(7)-H(7A)	108.6
Ag(2)-N(7)-H(7A)	108.6	C(19)-N(7)-H(7B)	108.6
Ag(2)-N(7)-H(7B)	108.6	H(7A)-N(7)-H(7B)	107.6

Table B.15. Continued

C(22)-N(8)-C(21)	117.8(6)	C(22)-N(8)-Ag(3)	124.2(5)
C(21)-N(8)-Ag(3)	118.0(4)	C(25)-N(9)-Ag(4)	173.3(7)
C(27)-N(10)-Ag(3)	157.5(8)	N(1)-C(1)-C(2)	112.9(5)
N(1)-C(1)-H(1C)	109.0	C(2)-C(1)-H(1C)	109.0
N(1)-C(1)-H(1D)	109.0	C(2)-C(1)-H(1D)	109.0
H(1C)-C(1)-H(1D)	107.8	C(3)-C(2)-C(6)	116.5(6)
C(3)-C(2)-C(1)	119.3(5)	C(6)-C(2)-C(1)	124.2(6)
N(2)-C(3)-C(2)	124.2(6)	N(2)-C(3)-H(3)	117.9
C(2)-C(3)-H(3)	117.9	N(2)-C(4)-C(5)	122.3(6)
N(2)-C(4)-H(4)	118.8	C(5)-C(4)-H(4)	118.8
C(4)-C(5)-C(6)	119.5(6)	C(4)-C(5)-H(5)	120.2
C(6)-C(5)-H(5)	120.2	C(5)-C(6)-C(2)	119.9(6)
C(5)-C(6)-H(6)	120.1	C(2)-C(6)-H(6)	120.1
N(3)-C(7)-C(8)	113.4(5)	N(3)-C(7)-H(7C)	108.9
C(8)-C(7)-H(7C)	108.9	N(3)-C(7)-H(7D)	108.9
C(8)-C(7)-H(7D)	108.9	H(7C)-C(7)-H(7D)	107.7
C(12)-C(8)-C(9)	117.7(5)	C(12)-C(8)-C(7)	119.9(5)
C(9)-C(8)-C(7)	122.4(5)	N(4)-C(9)-C(8)	123.0(5)
N(4)-C(9)-H(9)	118.5	C(8)-C(9)-H(9)	118.5
N(4)-C(10)-C(11)	122.0(6)	N(4)-C(10)-H(10)	119.0
C(11)-C(10)-H(10)	119.0	C(10)-C(11)-C(12)	119.3(6)
C(10)-C(11)-H(11)	120.4	C(12)-C(11)-H(11)	120.4
C(11)-C(12)-C(8)	119.7(6)	C(11)-C(12)-H(12)	120.1
C(8)-C(12)-H(12)	120.1	N(5)-C(13)-C(14)	111.9(6)
N(5)-C(13)-H(13A)	109.2	C(14)-C(13)-H(13A)	109.2
N(5)-C(13)-H(13B)	109.2	C(14)-C(13)-H(13B)	109.2
H(13A)-C(13)-H(13B)	107.9	C(15)-C(14)-C(18)	117.4(6)
C(15)-C(14)-C(13)	119.3(6)	C(18)-C(14)-C(13)	123.3(6)
N(6)-C(15)-C(14)	123.6(6)	N(6)-C(15)-H(15)	118.2
C(14)-C(15)-H(15)	118.2	N(6)-C(16)-C(17)	122.3(6)
N(6)-C(16)-H(16)	118.9	C(17)-C(16)-H(16)	118.9
C(16)-C(17)-C(18)	119.2(6)	C(16)-C(17)-H(17)	120.4
C(18)-C(17)-H(17)	120.4	C(17)-C(18)-C(14)	119.5(6)
C(17)-C(18)-H(18)	120.3	C(14)-C(18)-H(18)	120.3
N(7)-C(19)-C(20)	111.9(5)	N(7)-C(19)-H(19A)	109.2
C(20)-C(19)-H(19A)	109.2	N(7)-C(19)-H(19B)	109.2
C(20)-C(19)-H(19B)	109.2	H(19A)-C(19)-H(19B)	107.9
C(24)-C(20)-C(21)	117.6(6)	C(24)-C(20)-C(19)	125.0(6)
C(21)-C(20)-C(19)	117.4(5)	N(8)-C(21)-C(20)	123.3(6)
N(8)-C(21)-H(21)	118.3	C(20)-C(21)-H(21)	118.3
N(8)-C(22)-C(23)	122.7(6)	N(8)-C(22)-H(22)	118.6
C(23)-C(22)-H(22)	118.6	C(22)-C(23)-C(24)	118.5(6)
C(22)-C(23)-H(23)	120.7	C(24)-C(23)-H(23)	120.7
C(20)-C(24)-C(23)	120.0(6)	C(20)-C(24)-H(24)	120.0
C(23)-C(24)-H(24)	120.0	N(9)-C(25)-C(26)	179.0(8)
C(25)-C(26)-H(26A)	109.5	C(25)-C(26)-H(26B)	109.5
H(26A)-C(26)-H(26B)	109.5	C(25)-C(26)-H(26C)	109.5
H(26A)-C(26)-H(26C)	109.5	H(26B)-C(26)-H(26C)	109.5
N(10)-C(27)-C(28)	179.8(12)	C(27)-C(28)-H(28A)	109.5
C(27)-C(28)-H(28B)	109.5	H(28A)-C(28)-H(28B)	109.5
C(27)-C(28)-H(28C)	109.5	H(28A)-C(28)-H(28C)	109.5
H(28B)-C(28)-H(28C)	109.5	F(3)-B(1)-F(2)	110.2(6)
F(3)-B(1)-F(1)	109.9(5)	F(2)-B(1)-F(1)	110.4(5)
F(3)-B(1)-F(4)	108.5(5)	F(2)-B(1)-F(4)	109.1(5)

Table B.15. Continued

F(1)-B(1)-F(4)	108.7(5)	F(8)-B(2)-F(7)	109.9(5)
F(8)-B(2)-F(6)	110.5(5)	F(7)-B(2)-F(6)	109.1(5)
F(8)-B(2)-F(5)	110.0(5)	F(7)-B(2)-F(5)	108.7(5)
F(6)-B(2)-F(5)	108.6(5)	F(12)-B(3)-F(9)	111.2(6)
F(12)-B(3)-F(11)	109.3(6)	F(9)-B(3)-F(11)	108.9(6)
F(12)-B(3)-F(10)	108.6(6)	F(9)-B(3)-F(10)	110.0(6)
 Hydrogen Bonds (Å)			
N(1)-H(1A)...F(3)#1	3.051(6)	N(1)-H(1A)...F(4)#1	3.038(6)
N(1)-H(1B)...F(6)#2	3.175(6)	N(3)-H(3B)...F(2)#3	3.080(6)
N(3)-H(3A)...F(5)#3	2.961(6)	N(3)-H(3B)...F(6)#1	3.205(6)
N(5)-H(5B)...F(10)#1	3.360(7)	N(5)-H(5B)...F(11)#1	2.981(7)
N(5)-H(5A)...F(16)#4	3.060(10)	N(7)-H(7B)...F(10)#4	2.988(7)
N(7)-H(7A)...F(16)#1	2.994(9)		

Symmetry transformations used to generate equivalent atoms: #1 -x+1,y+1/2,-z+3/2 #2 -x,y+1/2,-z+3/2
#3 x,-y+3/2,z-1/2 #4 x+1,-y+3/2,z+1/2

Table B.16. Experimental and statistical crystal data for **5.2**

Empirical formula	C18 H24 Ag2 B2 F8 N6
Formula weight	713.79
Temperature	110(2) K
Wavelength	0.71073 Å
Crystal system, space group	Triclinic, P1
Unit cell dimensions	a = 6.8504(10) Å α = 110.934(6) deg. b = 8.4092(12) Å β = 97.226(6) deg. c = 11.5982(17) Å γ = 96.238(6) deg.
Volume	610.51(15) Å ³
Z, Calculated density	1, 1.941 Mg/m ³
Absorption coefficient	1.685 mm ⁻¹
F(000)	350
Crystal size	0.35 x 0.21 x 0.20 mm
θ range for data collection	1.91 to 26.53 deg.
Limiting indices	-6<=h<=8, -10<=k<=10, -14<=l<=14
Reflections collected / unique	15095 / 4220 [R(int) = 0.0259]
Completeness to θ = 26.53	97.5 %
Absorption correction	multi-scan (SADABS)
Max. and min. transmission	0.7261 and 0.5901
Refinement method	Full-matrix least-squares on F ²
Data / restraints / parameters	4220 / 3 / 325
Goodness-of-fit on F ²	1.050
Final R indices [I>2σ(I)]	R1 = 0.0199, wR2 = 0.0498
R indices (all data)	R1 = 0.0201, wR2 = 0.0500
Absolute structure parameter	0.03(2)
Largest diff. peak and hole	0.610 and -0.574 e.Å ⁻³

Table B.16. Continued

Bond Lengths (Å)

Ag(1)-N(5)	2.235(3)	Ag(1)-N(4)	2.246(3)
Ag(1)-N(6)#1	2.265(3)	Ag(2)-N(3)	2.222(4)
Ag(2)-N(1)#2	2.246(2)	Ag(2)-N(2)	2.262(3)
F(1)-B(1)	1.376(5)	F(2)-B(1)	1.378(6)
F(3)-B(1)	1.373(5)	F(4)-B(1)	1.355(7)
F(5)-B(2)	1.394(5)	F(6)-B(2)	1.387(4)
F(7)-B(2)	1.385(5)	F(8)-B(2)	1.375(5)
N(1)-C(1)	1.473(4)	N(1)-Ag(2)#3	2.246(2)
N(1)-H(1C)	0.9000	N(1)-H(1D)	0.9001
N(2)-C(4)	1.332(5)	N(2)-C(3)	1.345(4)
N(3)-C(7)	1.325(8)	N(3)-H(3A)	0.9000
N(3)-H(3B)	0.9000	N(4)-C(9)	1.328(4)
N(4)-C(10)	1.346(4)	N(5)-C(17)	1.328(5)
N(5)-C(13)	1.347(4)	N(6)-C(18)	1.468(5)
N(6)-Ag(1)#4	2.265(3)	N(6)-H(6A)	0.9000
N(6)-H(6B)	0.9000	C(1)-C(2)	1.512(4)
C(1)-H(1A)	0.9900	C(1)-H(1B)	0.9900
C(2)-C(3)	1.380(5)	C(2)-C(6)	1.384(5)
C(3)-H(3)	0.9500	C(4)-C(5)	1.378(5)
C(4)-H(4)	0.9500	C(5)-C(6)	1.380(4)
C(5)-H(5)	0.9500	C(6)-H(6)	0.9500
C(7)-C(8)	1.517(5)	C(7)-H(7A)	0.9900
C(7)-H(7B)	0.9900	C(8)-C(9)	1.382(5)
C(8)-C(12)	1.398(5)	C(9)-H(9)	0.9500
C(10)-C(11)	1.367(5)	C(10)-H(10)	0.9500
C(11)-C(12)	1.370(5)	C(11)-H(11)	0.9500
C(12)-H(12)	0.9500	C(13)-C(14)	1.378(5)
C(13)-H(13)	0.9500	C(14)-C(15)	1.371(6)
C(14)-H(14)	0.9500	C(15)-C(16)	1.394(5)
C(15)-H(15)	0.9500	C(16)-C(17)	1.391(5)
C(16)-C(18)	1.503(5)	C(17)-H(17)	0.9500
C(18)-H(18A)	0.9900	C(18)-H(18B)	0.9900

Bond Angles (°)

N(5)-Ag(1)-N(4)	121.84(10)	N(5)-Ag(1)-N(6)#1	119.78(10)
N(4)-Ag(1)-N(6)#1	117.26(10)	N(3)-Ag(2)-N(1)#2	124.0(2)
N(3)-Ag(2)-N(2)	119.5(2)	N(1)#2-Ag(2)-N(2)	116.37(10)
C(1)-N(1)-Ag(2)#3	114.85(19)	C(1)-N(1)-H(1C)	108.5
Ag(2)#3-N(1)-H(1C)	108.5	C(1)-N(1)-H(1D)	108.7
Ag(2)#3-N(1)-H(1D)	108.6	H(1C)-N(1)-H(1D)	107.6
C(4)-N(2)-C(3)	117.2(3)	C(4)-N(2)-Ag(2)	118.7(2)
C(3)-N(2)-Ag(2)	121.6(2)	C(7)-N(3)-Ag(2)	122.0(3)
C(7)-N(3)-H(3A)	106.3	Ag(2)-N(3)-H(3A)	106.4
C(7)-N(3)-H(3B)	107.4	Ag(2)-N(3)-H(3B)	107.0
H(3A)-N(3)-H(3B)	106.8	C(9)-N(4)-C(10)	118.2(3)
C(9)-N(4)-Ag(1)	119.9(2)	C(10)-N(4)-Ag(1)	121.6(2)
C(17)-N(5)-C(13)	118.0(3)	C(17)-N(5)-Ag(1)	116.5(2)
C(13)-N(5)-Ag(1)	125.5(2)	C(18)-N(6)-Ag(1)#4	112.4(2)
C(18)-N(6)-H(6A)	109.1	Ag(1)#4-N(6)-H(6A)	109.1
C(18)-N(6)-H(6B)	109.1	Ag(1)#4-N(6)-H(6B)	109.1
H(6A)-N(6)-H(6B)	107.9	N(1)-C(1)-C(2)	112.9(3)

Table B.16. Continued

N(1)-C(1)-H(1A)	109.0	C(2)-C(1)-H(1A)	109.0
N(1)-C(1)-H(1B)	109.0	C(2)-C(1)-H(1B)	109.0
H(1A)-C(1)-H(1B)	107.8	C(3)-C(2)-C(6)	118.3(3)
C(3)-C(2)-C(1)	119.9(3)	C(6)-C(2)-C(1)	121.7(3)
N(2)-C(3)-C(2)	123.5(3)	N(2)-C(3)-H(3)	118.2
C(2)-C(3)-H(3)	118.2	N(2)-C(4)-C(5)	123.1(3)
N(2)-C(4)-H(4)	118.4	C(5)-C(4)-H(4)	118.4
C(4)-C(5)-C(6)	119.2(3)	C(4)-C(5)-H(5)	120.4
C(6)-C(5)-H(5)	120.4	C(5)-C(6)-C(2)	118.7(3)
C(5)-C(6)-H(6)	120.7	C(2)-C(6)-H(6)	120.7
N(3)-C(7)-C(8)	118.7(5)	N(3)-C(7)-H(7A)	107.6
C(8)-C(7)-H(7A)	107.6	N(3)-C(7)-H(7B)	107.6
C(8)-C(7)-H(7B)	107.6	H(7A)-C(7)-H(7B)	107.1
C(9)-C(8)-C(12)	117.6(3)	C(9)-C(8)-C(7)	120.4(3)
C(12)-C(8)-C(7)	122.0(3)	N(4)-C(9)-C(8)	123.2(3)
N(4)-C(9)-H(9)	118.4	C(8)-C(9)-H(9)	118.4
N(4)-C(10)-C(11)	122.4(3)	N(4)-C(10)-H(10)	118.8
C(11)-C(10)-H(10)	118.8	C(10)-C(11)-C(12)	119.3(3)
C(10)-C(11)-H(11)	120.3	C(12)-C(11)-H(11)	120.3
C(11)-C(12)-C(8)	119.2(3)	C(11)-C(12)-H(12)	120.4
C(8)-C(12)-H(12)	120.4	N(5)-C(13)-C(14)	122.1(3)
N(5)-C(13)-H(13)	119.0	C(14)-C(13)-H(13)	119.0
C(15)-C(14)-C(13)	119.9(3)	C(15)-C(14)-H(14)	120.0
C(13)-C(14)-H(14)	120.0	C(14)-C(15)-C(16)	118.6(4)
C(14)-C(15)-H(15)	120.7	C(16)-C(15)-H(15)	120.7
C(17)-C(16)-C(15)	117.9(3)	C(17)-C(16)-C(18)	119.6(3)
C(15)-C(16)-C(18)	122.4(3)	N(5)-C(17)-C(16)	123.4(3)
N(5)-C(17)-H(17)	118.3	C(16)-C(17)-H(17)	118.3
N(6)-C(18)-C(16)	110.0(3)	N(6)-C(18)-H(18A)	109.7
C(16)-C(18)-H(18A)	109.7	N(6)-C(18)-H(18B)	109.7
C(16)-C(18)-H(18B)	109.7	H(18A)-C(18)-H(18B)	108.2
F(4)-B(1)-F(3)	112.2(4)	F(4)-B(1)-F(1)	113.0(4)
F(3)-B(1)-F(1)	110.6(4)	F(4)-B(1)-F(2)	108.1(5)
F(3)-B(1)-F(2)	106.6(4)	F(1)-B(1)-F(2)	105.9(5)
F(8)-B(2)-F(7)	111.4(3)	F(8)-B(2)-F(6)	110.1(3)
F(7)-B(2)-F(6)	111.1(3)	F(8)-B(2)-F(5)	108.0(3)
F(7)-B(2)-F(5)	108.7(3)	F(6)-B(2)-F(5)	107.4(3)

Symmetry transformations used to generate equivalent atoms: #1 x+1,y,z #2 x,y+1,z #3 x,y-1,z
#4 x-1,y,z

Table B.17. Experimental and statistical crystal data for 5.3.1

Empirical formula	C12 H16 Ag B F4 N4
Formula weight	410.97
Temperature	110(2) K
Wavelength	0.71073 Å
Crystal system, space group	Orthorhombic, Pbc _a
Unit cell dimensions	$a = 15.3184(13)$ Å $\alpha = 90$ deg. $b = 10.4897(15)$ Å $\beta = 90$ deg. $c = 18.8193(17)$ Å $\gamma = 90$ deg.
Volume	3024.0(6) Å ³
Z, Calculated density	8, 1.805 Mg/m ³
Absorption coefficient	1.375 mm ⁻¹
F(000)	1632
Crystal size	0.232 x 0.112 x 0.046 mm
θ range for data collection	3.20 to 26.45 deg.
Limiting indices	-18<=h<=18, -13<=k<=13, -23<=l<=23
Reflections collected / unique	40167 / 3087 [R(int) = 0.0391]
Completeness to θ = 26.45	99.1 %
Absorption correction	Semi-empirical from equivalents
Refinement method	Full-matrix least-squares on F ²
Data / restraints / parameters	3087 / 0 / 211
Goodness-of-fit on F ²	1.069
Final R indices [I>2σ(I)]	R1 = 0.0187, wR2 = 0.0452
R indices (all data)	R1 = 0.0274, wR2 = 0.0471
Largest diff. peak and hole	0.331 and -0.272 e.Å ⁻³

Bond Lengths (Å)

Ag(1)-N(1)	2.3057(15)	Ag(1)-N(2)#1	2.3341(16)
Ag(1)-N(4)#2	2.3572(15)	Ag(1)-N(3)	2.3776(14)
F(1)-B(1)	1.393(2)	F(2)-B(1)	1.395(2)
F(3)-B(1)	1.388(2)	F(4)-B(1)	1.398(2)
N(1)-C(1)	1.342(2)	N(1)-C(5)	1.344(2)
N(2)-C(6)	1.470(2)	N(2)-Ag(1)#1	2.3341(16)
N(2)-H(1)	0.88(2)	N(2)-H(2)	0.87(2)
N(3)-C(7)	1.332(2)	N(3)-C(11)	1.345(2)
N(4)-C(12)	1.466(2)	N(4)-Ag(1)#3	2.3572(15)
N(4)-H(3)	0.82(2)	N(4)-H(4)	0.90(2)
C(1)-C(2)	1.377(3)	C(1)-H(1A)	0.9500
C(2)-C(3)	1.378(3)	C(2)-H(2A)	0.9500
C(3)-C(4)	1.392(2)	C(3)-H(3A)	0.9500
C(4)-C(5)	1.385(2)	C(4)-C(6)	1.506(2)
C(5)-H(5A)	0.9500	C(6)-H(6A)	0.9900
C(6)-H(6B)	0.9900	C(7)-C(8)	1.381(3)
C(7)-H(7A)	0.9500	C(8)-C(9)	1.380(3)
C(8)-H(8A)	0.9500	C(9)-C(10)	1.391(2)
C(9)-H(9A)	0.9500	C(10)-C(11)	1.377(2)
C(10)-C(12)	1.510(2)	C(11)-H(11A)	0.9500
C(12)-H(12A)	0.9900	C(12)-H(12B)	0.9900

Bond Angles (°)

N(1)-Ag(1)-N(2)#1	123.50(6)	N(1)-Ag(1)-N(4)#2	100.71(6)
N(2)#1-Ag(1)-N(4)#2	112.60(6)	N(1)-Ag(1)-N(3)	115.12(5)

Table B.17. Continued

N(2)#1-Ag(1)-N(3)	95.97(5)	N(4)#2-Ag(1)-N(3)	108.90(6)
C(1)-N(1)-C(5)	117.28(16)	C(1)-N(1)-Ag(1)	123.14(12)
C(5)-N(1)-Ag(1)	119.58(11)	C(6)-N(2)-Ag(1)#1	120.86(11)
C(6)-N(2)-H(1)	109.3(13)	Ag(1)#1-N(2)-H(1)	108.1(13)
C(6)-N(2)-H(2)	105.5(13)	Ag(1)#1-N(2)-H(2)	106.7(13)
H(1)-N(2)-H(2)	105.3(18)	C(7)-N(3)-C(11)	116.95(15)
C(7)-N(3)-Ag(1)	129.02(12)	C(11)-N(3)-Ag(1)	113.98(11)
C(12)-N(4)-Ag(1)#3	118.66(11)	C(12)-N(4)-H(3)	109.1(15)
Ag(1)#3-N(4)-H(3)	101.8(14)	C(12)-N(4)-H(4)	108.4(13)
Ag(1)#3-N(4)-H(4)	107.2(12)	H(3)-N(4)-H(4)	111.5(18)
N(1)-C(1)-C(2)	122.71(17)	N(1)-C(1)-H(1A)	118.6
C(2)-C(1)-H(1A)	118.6	C(1)-C(2)-C(3)	119.24(18)
C(1)-C(2)-H(2A)	120.4	C(3)-C(2)-H(2A)	120.4
C(2)-C(3)-C(4)	119.52(17)	C(2)-C(3)-H(3A)	120.2
C(4)-C(3)-H(3A)	120.2	C(5)-C(4)-C(3)	117.15(17)
C(5)-C(4)-C(6)	123.51(16)	C(3)-C(4)-C(6)	119.35(16)
N(1)-C(5)-C(4)	124.08(17)	N(1)-C(5)-H(5A)	118.0
C(4)-C(5)-H(5A)	118.0	N(2)-C(6)-C(4)	113.86(15)
N(2)-C(6)-H(6A)	108.8	C(4)-C(6)-H(6A)	108.8
N(2)-C(6)-H(6B)	108.8	C(4)-C(6)-H(6B)	108.8
H(6A)-C(6)-H(6B)	107.7	N(3)-C(7)-C(8)	122.96(17)
N(3)-C(7)-H(7A)	118.5	C(8)-C(7)-H(7A)	118.5
C(9)-C(8)-C(7)	119.12(17)	C(9)-C(8)-H(8A)	120.4
C(7)-C(8)-H(8A)	120.4	C(8)-C(9)-C(10)	119.22(17)
C(8)-C(9)-H(9A)	120.4	C(10)-C(9)-H(9A)	120.4
C(11)-C(10)-C(9)	117.15(16)	C(11)-C(10)-C(12)	123.46(16)
C(9)-C(10)-C(12)	119.39(16)	N(3)-C(11)-C(10)	124.58(16)
N(3)-C(11)-H(11A)	117.7	C(10)-C(11)-H(11A)	117.7
N(4)-C(12)-C(10)	116.83(15)	N(4)-C(12)-H(12A)	108.1
C(10)-C(12)-H(12A)	108.1	N(4)-C(12)-H(12B)	108.1
C(10)-C(12)-H(12B)	108.1	H(12A)-C(12)-H(12B)	107.3
F(3)-B(1)-F(1)	109.62(17)	F(3)-B(1)-F(2)	109.76(16)
F(1)-B(1)-F(2)	109.35(16)	F(3)-B(1)-F(4)	109.22(16)
F(1)-B(1)-F(4)	109.80(16)	F(2)-B(1)-F(4)	109.07(16)

Symmetry transformations used to generate equivalent atoms: #1 -x,-y+2,-z+1 #2 -x,y+1/2,-z+1/2
#3 -x,y-1/2,-z+1/2

Table B.18. Experimental and statistical crystal data for 5.3.2

Empirical formula	C12 H16 Ag B F4 N4
Formula weight	410.97
Temperature	110(2) K
Wavelength	0.71073 Å
Crystal system, space group	Monoclinic, P2(1)/c
Unit cell dimensions	a = 8.6991(4) Å α = 90 deg. b = 14.1060(7) Å β = 109.607(2) deg. c = 12.9311(7) Å γ = 90 deg.
Volume	1494.76(13) Å ³
Z, Calculated density	4, 1.826 Mg/m ³
Absorption coefficient	1.391 mm ⁻¹
F(000)	816
Crystal size	0.151 x 0.222 x 0.232 mm
θ range for data collection	2.21 to 26.37 deg.
Limiting indices	-10<=h<=10, -17<=k<=17, -16<=l<=16
Reflections collected / unique	29846 / 3040 [R(int) = 0.0316]
Completeness to θ = 26.37	99.8 %
Absorption correction	Semi-empirical from equivalents
Refinement method	Full-matrix least-squares on F ²
Data / restraints / parameters	3040 / 0 / 199
Goodness-of-fit on F ²	1.080
Final R indices [I>2σ(I)]	R1 = 0.0155, wR2 = 0.0413
R indices (all data)	R1 = 0.0171, wR2 = 0.0420
Largest diff. peak and hole	0.394 and -0.313 e.Å ⁻³

Bond Lengths (Å)

Ag(1)-N(4)#1	2.3071(13)	Ag(1)-N(2)#2	2.3482(14)
Ag(1)-N(1)	2.3537(14)	Ag(1)-N(3)	2.3807(13)
F(1)-B(1)	1.382(2)	F(2)-B(1)	1.397(2)
F(3)-B(1)	1.388(2)	F(4)-B(1)	1.392(2)
N(1)-C(1)	1.475(2)	N(1)-H(1A)	0.9200
N(1)-H(1B)	0.9200	N(2)-C(4)	1.341(2)
N(2)-C(3)	1.346(2)	N(2)-Ag(1)#2	2.3482(14)
N(3)-C(11)	1.337(2)	N(3)-C(7)	1.342(2)
N(4)-C(12)	1.474(2)	N(4)-Ag(1)#3	2.3071(13)
N(4)-H(4A)	0.9200	N(4)-H(4B)	0.9200
C(1)-C(2)	1.508(2)	C(1)-H(1C)	0.9900
C(1)-H(1D)	0.9900	C(2)-C(3)	1.385(2)
C(2)-C(6)	1.391(2)	C(3)-H(3)	0.9500
C(4)-C(5)	1.379(2)	C(4)-H(4)	0.9500
C(5)-C(6)	1.382(2)	C(5)-H(5)	0.9500
C(6)-H(6)	0.9500	C(7)-C(8)	1.388(2)
C(7)-H(7)	0.9500	C(8)-C(9)	1.387(2)
C(8)-C(12)	1.510(2)	C(9)-C(10)	1.384(2)
C(9)-H(9)	0.9500	C(10)-C(11)	1.384(2)
C(10)-H(10)	0.9500	C(11)-H(11)	0.9500
C(12)-H(12A)	0.9900	C(12)-H(12B)	0.9900

Bond Angles (°)

N(4)#1-Ag(1)-N(2)#2	109.26(5)	N(4)#1-Ag(1)-N(1)	123.01(5)
N(2)#2-Ag(1)-N(1)	108.75(5)	N(4)#1-Ag(1)-N(3)	114.96(5)
N(2)#2-Ag(1)-N(3)	105.53(5)	N(1)-Ag(1)-N(3)	93.38(5)

Table B.18. Continued

C(1)-N(1)-Ag(1)	117.36(10)	C(1)-N(1)-H(1A)	108.0
Ag(1)-N(1)-H(1A)	108.0	C(1)-N(1)-H(1B)	108.0
Ag(1)-N(1)-H(1B)	108.0	H(1A)-N(1)-H(1B)	107.2
C(4)-N(2)-C(3)	117.63(14)	C(4)-N(2)-Ag(1)#2	121.52(11)
C(3)-N(2)-Ag(1)#2	120.82(10)	C(11)-N(3)-C(7)	117.38(14)
C(11)-N(3)-Ag(1)	123.23(10)	C(7)-N(3)-Ag(1)	119.32(10)
C(12)-N(4)-Ag(1)#3	111.24(9)	C(12)-N(4)-H(4A)	109.4
Ag(1)#3-N(4)-H(4A)	109.4	C(12)-N(4)-H(4B)	109.4
Ag(1)#3-N(4)-H(4B)	109.4	H(4A)-N(4)-H(4B)	108.0
N(1)-C(1)-C(2)	112.90(13)	N(1)-C(1)-H(1C)	109.0
C(2)-C(1)-H(1C)	109.0	N(1)-C(1)-H(1D)	109.0
C(2)-C(1)-H(1D)	109.0	H(1C)-C(1)-H(1D)	107.8
C(3)-C(2)-C(6)	117.53(14)	C(3)-C(2)-C(1)	123.05(14)
C(6)-C(2)-C(1)	119.40(14)	N(2)-C(3)-C(2)	123.64(15)
N(2)-C(3)-H(3)	118.2	C(2)-C(3)-H(3)	118.2
N(2)-C(4)-C(5)	122.72(15)	N(2)-C(4)-H(4)	118.6
C(5)-C(4)-H(4)	118.6	C(4)-C(5)-C(6)	119.04(15)
C(4)-C(5)-H(5)	120.5	C(6)-C(5)-H(5)	120.5
C(5)-C(6)-C(2)	119.45(15)	C(5)-C(6)-H(6)	120.3
C(2)-C(6)-H(6)	120.3	N(3)-C(7)-C(8)	124.37(15)
N(3)-C(7)-H(7)	117.8	C(8)-C(7)-H(7)	117.8
C(9)-C(8)-C(7)	117.08(14)	C(9)-C(8)-C(12)	123.11(14)
C(7)-C(8)-C(12)	119.76(14)	C(10)-C(9)-C(8)	119.37(14)
C(10)-C(9)-H(9)	120.3	C(8)-C(9)-H(9)	120.3
C(11)-C(10)-C(9)	119.21(15)	C(11)-C(10)-H(10)	120.4
C(9)-C(10)-H(10)	120.4	N(3)-C(11)-C(10)	122.56(15)
N(3)-C(11)-H(11)	118.7	C(10)-C(11)-H(11)	118.7
N(4)-C(12)-C(8)	116.20(12)	N(4)-C(12)-H(12A)	108.2
C(8)-C(12)-H(12A)	108.2	N(4)-C(12)-H(12B)	108.2
C(8)-C(12)-H(12B)	108.2	H(12A)-C(12)-H(12B)	107.4
F(1)-B(1)-F(3)	109.19(14)	F(1)-B(1)-F(4)	110.17(14)
F(3)-B(1)-F(4)	110.56(15)	F(1)-B(1)-F(2)	109.52(14)
F(3)-B(1)-F(2)	109.02(14)	F(4)-B(1)-F(2)	108.34(14)

Symmetry transformations used to generate equivalent atoms: #1 x-1,y,z #2 -x+1,-y+2,-z+2 #3 x+1,y,z

Table B.19. Experimental and statistical crystal data for **5.4**

Empirical formula	C26 H24 Ag2 B2 F8 N6
Formula weight	809.87
Temperature	110(2) K
Wavelength	0.71073 Å
Crystal system, space group	Triclinic, P-1
Unit cell dimensions	a = 7.1224(7) Å α = 92.490(5) deg. b = 10.6180(10) Å β = 96.249(5) deg. c = 19.1669(18) Å γ = 93.248(5) deg.
Volume	1436.8(2) Å ³
Z, Calculated density	2, 1.872 Mg/m ³
Absorption coefficient	1.444 mm ⁻¹
F(000)	796
Crystal size	0.177 x 0.169 x 0.062 mm
θ range for data collection	3.19 to 28.28 deg.
Limiting indices	-9<=h<=9, -13<=k<=14, -25<=l<=25
Reflections collected / unique	21440 / 6988 [R(int) = 0.0370]
Completeness to θ = 28.28	97.8 %
Absorption correction	Semi-empirical from equivalents
Refinement method	Full-matrix least-squares on F ²
Data / restraints / parameters	6988 / 10 / 443
Goodness-of-fit on F ²	1.075
Final R indices [I>2σ(I)]	R1 = 0.0291, wR2 = 0.0638
R indices (all data)	R1 = 0.0433, wR2 = 0.0663
Largest diff. peak and hole	0.716 and -0.794 e.Å ⁻³

Bond Lengths (Å)

Ag(1)-N(4)	2.1457(19)	Ag(1)-N(5)	2.286(2)
Ag(1)-N(6)	2.291(2)	Ag(1)-Ag(1)#1	2.9875(4)
Ag(2)-N(3)	2.1610(19)	Ag(2)-N(2)	2.287(2)
Ag(2)-N(1)	2.2908(19)	N(1)-C(1)	1.337(3)
N(1)-C(5)	1.346(3)	N(2)-C(10)	1.348(3)
N(2)-C(6)	1.350(3)	N(3)-C(11)	1.475(3)
N(3)-H(3A)	0.9200	N(3)-H(3B)	0.9200
N(4)-C(13)	1.342(3)	N(4)-C(14)	1.351(3)
N(5)-C(21)	1.343(3)	N(5)-C(17)	1.343(3)
N(6)-C(26)	1.331(3)	N(6)-C(22)	1.353(3)
C(1)-C(2)	1.389(3)	C(1)-H(1)	0.9500
C(2)-C(3)	1.380(4)	C(2)-H(2)	0.9500
C(3)-C(4)	1.388(3)	C(3)-H(3)	0.9500
C(4)-C(5)	1.402(3)	C(4)-H(4)	0.9500
C(5)-C(6)	1.500(3)	C(6)-C(7)	1.398(3)
C(7)-C(8)	1.387(3)	C(7)-H(7)	0.9500
C(8)-C(9)	1.374(4)	C(8)-H(8)	0.9500
C(9)-C(10)	1.381(3)	C(9)-H(9)	0.9500
C(10)-H(10)	0.9500	C(11)-C(12)	1.517(3)
C(11)-H(11A)	0.9900	C(11)-H(11B)	0.9900
C(12)-C(16)	1.390(3)	C(12)-C(13)	1.390(3)
C(13)-H(13)	0.9500	C(14)-C(15)	1.387(3)
C(14)-H(14)	0.9500	C(15)-C(16)	1.378(3)
C(15)-H(15)	0.9500	C(16)-H(16)	0.9500
C(17)-C(18)	1.389(4)	C(17)-H(17)	0.9500
C(18)-C(19)	1.372(4)	C(18)-H(18)	0.9500
C(19)-C(20)	1.379(4)	C(19)-H(19)	0.9500

Table B.19. Continued

C(20)-C(21)	1.396(3)	C(20)-H(20)	0.9500
C(21)-C(22)	1.502(3)	C(22)-C(23)	1.384(3)
C(23)-C(24)	1.390(3)	C(23)-H(23)	0.9500
C(24)-C(25)	1.387(4)	C(24)-H(24)	0.9500
C(25)-C(26)	1.389(4)	C(25)-H(25)	0.9500
C(26)-H(26)	0.9500	B(1)-F(3)	1.376(3)
B(1)-F(1)	1.395(3)	B(1)-F(4)	1.398(3)
B(1)-F(2)	1.401(3)	B(2)-F(5)	1.370(10)
B(2)-F(8)	1.373(10)	B(2)-F(7)	1.382(9)
B(2)-F(6)	1.384(11)	B(2A)-F(8A)	1.370(14)
B(2A)-F(5A)	1.371(12)	B(2A)-F(7A)	1.382(12)
B(2A)-F(6A)	1.389(14)		

Bond Angles

N(4)-Ag(1)-N(5)	145.36(8)	F(7A)-B(2A)-F(6A)	107.4(15)
N(4)-Ag(1)-N(6)	141.39(7)	N(5)-Ag(1)-N(6)	72.81(7)
N(4)-Ag(1)-Ag(1)#1	98.38(5)	N(5)-Ag(1)-Ag(1)#1	89.30(5)
N(6)-Ag(1)-Ag(1)#1	83.86(5)	N(3)-Ag(2)-N(2)	145.57(7)
N(3)-Ag(2)-N(1)	141.44(7)	N(2)-Ag(2)-N(1)	72.90(7)
C(1)-N(1)-C(5)	119.0(2)	C(1)-N(1)-Ag(2)	124.14(16)
C(5)-N(1)-Ag(2)	116.62(15)	C(10)-N(2)-C(6)	118.3(2)
C(10)-N(2)-Ag(2)	125.00(16)	C(6)-N(2)-Ag(2)	116.63(15)
C(11)-N(3)-Ag(2)	115.56(14)	C(11)-N(3)-H(3A)	108.4
Ag(2)-N(3)-H(3A)	108.4	C(11)-N(3)-H(3B)	108.4
Ag(2)-N(3)-H(3B)	108.4	H(3A)-N(3)-H(3B)	107.5
C(13)-N(4)-C(14)	118.29(19)	C(13)-N(4)-Ag(1)	119.56(15)
C(14)-N(4)-Ag(1)	122.10(16)	C(21)-N(5)-C(17)	118.6(2)
C(21)-N(5)-Ag(1)	116.74(16)	C(17)-N(5)-Ag(1)	124.50(17)
C(26)-N(6)-C(22)	118.7(2)	C(26)-N(6)-Ag(1)	124.88(16)
C(22)-N(6)-Ag(1)	116.09(15)	N(1)-C(1)-C(2)	123.0(2)
N(1)-C(1)-H(1)	118.5	C(2)-C(1)-H(1)	118.5
C(3)-C(2)-C(1)	118.0(2)	C(3)-C(2)-H(2)	121.0
C(1)-C(2)-H(2)	121.0	C(2)-C(3)-C(4)	120.0(2)
C(2)-C(3)-H(3)	120.0	C(4)-C(3)-H(3)	120.0
C(3)-C(4)-C(5)	118.5(2)	C(3)-C(4)-H(4)	120.7
C(5)-C(4)-H(4)	120.7	N(1)-C(5)-C(4)	121.4(2)
N(1)-C(5)-C(6)	116.9(2)	C(4)-C(5)-C(6)	121.7(2)
N(2)-C(6)-C(7)	121.3(2)	N(2)-C(6)-C(5)	116.9(2)
C(7)-C(6)-C(5)	121.9(2)	C(8)-C(7)-C(6)	119.1(2)
C(8)-C(7)-H(7)	120.4	C(6)-C(7)-H(7)	120.4
C(9)-C(8)-C(7)	119.6(2)	C(9)-C(8)-H(8)	120.2
C(7)-C(8)-H(8)	120.2	C(8)-C(9)-C(10)	118.4(2)
C(8)-C(9)-H(9)	120.8	C(10)-C(9)-H(9)	120.8
N(2)-C(10)-C(9)	123.3(2)	N(2)-C(10)-H(10)	118.4
C(9)-C(10)-H(10)	118.4	N(3)-C(11)-C(12)	114.35(19)
N(3)-C(11)-H(11A)	108.7	C(12)-C(11)-H(11A)	108.7
N(3)-C(11)-H(11B)	108.7	C(12)-C(11)-H(11B)	108.7
H(11A)-C(11)-H(11B)	107.6	C(16)-C(12)-C(13)	117.7(2)
C(16)-C(12)-C(11)	123.8(2)	C(13)-C(12)-C(11)	118.5(2)
N(4)-C(13)-C(12)	123.3(2)	N(4)-C(13)-H(13)	118.3
C(12)-C(13)-H(13)	118.3	N(4)-C(14)-C(15)	121.7(2)
N(4)-C(14)-H(14)	119.2	C(15)-C(14)-H(14)	119.2
C(16)-C(15)-C(14)	119.4(2)	C(16)-C(15)-H(15)	120.3

Table B.19. Continued

C(14)-C(15)-H(15)	120.3	C(15)-C(16)-C(12)	119.6(2)
C(15)-C(16)-H(16)	120.2	C(12)-C(16)-H(16)	120.2
N(5)-C(17)-C(18)	122.8(2)	N(5)-C(17)-H(17)	118.6
C(18)-C(17)-H(17)	118.6	C(19)-C(18)-C(17)	118.7(3)
C(19)-C(18)-H(18)	120.7	C(17)-C(18)-H(18)	120.7
C(18)-C(19)-C(20)	119.0(3)	C(18)-C(19)-H(19)	120.5
C(20)-C(19)-H(19)	120.5	C(19)-C(20)-C(21)	119.8(2)
C(19)-C(20)-H(20)	120.1	C(21)-C(20)-H(20)	120.1
N(5)-C(21)-C(20)	121.2(2)	N(5)-C(21)-C(22)	116.7(2)
C(20)-C(21)-C(22)	122.1(2)	N(6)-C(22)-C(23)	120.9(2)
N(6)-C(22)-C(21)	116.8(2)	C(23)-C(22)-C(21)	122.2(2)
C(22)-C(23)-C(24)	120.1(2)	C(22)-C(23)-H(23)	120.0
C(24)-C(23)-H(23)	120.0	C(25)-C(24)-C(23)	118.7(2)
C(25)-C(24)-H(24)	120.7	C(23)-C(24)-H(24)	120.7
C(24)-C(25)-C(26)	117.9(2)	C(24)-C(25)-H(25)	121.0
C(26)-C(25)-H(25)	121.0	N(6)-C(26)-C(25)	123.6(2)
N(6)-C(26)-H(26)	118.2	C(25)-C(26)-H(26)	118.2
F(3)-B(1)-F(1)	110.7(2)	F(3)-B(1)-F(4)	110.2(2)
F(1)-B(1)-F(4)	108.7(2)	F(3)-B(1)-F(2)	110.6(2)
F(1)-B(1)-F(2)	107.5(2)	F(4)-B(1)-F(2)	109.2(2)
F(5)-B(2)-F(8)	107.5(8)	F(5)-B(2)-F(7)	110.3(11)
F(8)-B(2)-F(7)	107.8(11)	F(5)-B(2)-F(6)	111.1(9)
F(8)-B(2)-F(6)	109.6(7)	F(7)-B(2)-F(6)	110.4(11)
F(8A)-B(2A)-F(5A)	113.5(13)	F(8A)-B(2A)-F(7A)	111.9(15)
F(5A)-B(2A)-F(7A)	110.6(15)	F(8A)-B(2A)-F(6A)	106.9(10)
F(5A)-B(2A)-F(6A)	106.1(12)		

Symmetry transformations used to generate equivalent atoms: #1 -x,-y+1,-z+2

Table B.20 Experimental and statistical crystal data for **6.1**

Empirical formula	C32 H32 Ag4 F12 N8 O8
Formula weight	1316.14
Temperature	110(2) K
Wavelength	0.71073 Å
Crystal system, space group	Orthorhombic, P2(1)2(1)2(1)
Unit cell dimensions	a = 10.3431(4) Å α = 90 deg. b = 17.0246(5) Å β = 90 deg. c = 23.3149(8) Å γ = 90 deg.
Volume	4105.5(2) Å ³
Z, Calculated density	4, 2.129 Mg/m ³
Absorption coefficient	1.994 mm ⁻¹
F(000)	2560
Crystal size	0.289 x 0.189 x 0.165 mm
θ range for data collection	1.48 to 26.37 deg.
Limiting indices	-12<=h<=12, -16<=k<=21, -29<=l<=29
Reflections collected / unique	51253 / 8358 [R(int) = 0.0386]
Completeness to θ = 26.37	99.8 %
Absorption correction	Semi-empirical from equivalents
Refinement method	Full-matrix least-squares on F ²
Data / restraints / parameters	8358 / 0 / 577
Goodness-of-fit on F ²	1.054

Table B.20. Continued

Final R indices [$I > 2\sigma(I)$]	R1 = 0.0209, wR2 = 0.0490		
R indices (all data)	R1 = 0.0233, wR2 = 0.0497		
Absolute structure parameter	0.00		
Largest diff. peak and hole	0.672 and -0.439 e. \AA^{-3}		
Bond Lengths (\AA)			
Ag(1)-N(4)#1	2.147(2)	Ag(1)-N(1)	2.157(2)
Ag(1)-O(1)	2.542(2)	Ag(2)-N(3)	2.165(2)
Ag(2)-N(2)	2.177(2)	Ag(2)-O(5)	2.585(2)
Ag(2)-O(3)	2.595(2)	Ag(3)-N(5)	2.158(2)
Ag(3)-N(8)	2.161(2)	Ag(3)-O(8)#2	2.549(2)
Ag(4)-N(6)	2.153(2)	Ag(4)-N(7)#1	2.164(2)
Ag(4)-O(7)	2.567(2)	F(1)-C(26)	1.332(4)
F(2)-C(26)	1.343(4)	F(3)-C(26)	1.340(4)
F(4)-C(28)	1.338(4)	F(5)-C(28)	1.325(5)
F(6)-C(28)	1.325(4)	F(7)-C(30)	1.266(4)
F(8)-C(30)	1.335(4)	F(9)-C(30)	1.315(4)
F(10)-C(32)	1.325(4)	F(11)-C(32)	1.329(4)
F(12)-C(32)	1.339(4)	O(1)-C(25)	1.234(3)
O(2)-C(25)	1.237(3)	O(3)-C(27)	1.235(4)
O(4)-C(27)	1.237(4)	O(5)-C(29)	1.230(4)
O(6)-C(29)	1.246(4)	O(7)-C(31)	1.237(4)
O(8)-C(31)	1.215(4)	O(8)-Ag(3)#3	2.549(2)
N(1)-C(1)	1.336(4)	N(1)-C(5)	1.348(4)
N(2)-C(6)	1.467(4)	N(2)-H(2A)	0.9200
N(2)-H(2B)	0.9200	N(3)-C(11)	1.344(4)
N(3)-C(7)	1.350(4)	N(4)-C(12)	1.467(4)
N(4)-Ag(1)#4	2.147(2)	N(4)-H(4A)	0.9200
N(4)-H(4B)	0.9200	N(5)-C(17)	1.346(4)
N(5)-C(13)	1.348(4)	N(6)-C(18)	1.474(4)
N(6)-H(6A)	0.9200	N(6)-H(6B)	0.9200
N(7)-C(23)	1.338(4)	N(7)-C(19)	1.339(4)
N(7)-Ag(4)#4	2.164(2)	N(8)-C(24)	1.478(4)
N(8)-H(8A)	0.9200	N(8)-H(8B)	0.9200
C(1)-C(2)	1.387(4)	C(1)-H(1)	0.9500
C(2)-C(3)	1.379(4)	C(2)-H(2)	0.9500
C(3)-C(4)	1.384(4)	C(3)-H(3)	0.9500
C(4)-C(5)	1.393(4)	C(4)-C(6)	1.521(4)
C(5)-H(5)	0.9500	C(6)-H(6C)	0.9900
C(6)-H(6D)	0.9900	C(7)-C(8)	1.383(4)
C(7)-H(7)	0.9500	C(8)-C(9)	1.390(4)
C(8)-H(8)	0.9500	C(9)-C(10)	1.393(4)
C(9)-H(9)	0.9500	C(10)-C(11)	1.389(4)
C(10)-C(12)	1.522(4)	C(11)-H(11)	0.9500
C(12)-H(12A)	0.9900	C(12)-H(12B)	0.9900
C(13)-C(14)	1.372(4)	C(13)-H(13)	0.9500
C(14)-C(15)	1.389(4)	C(14)-H(14)	0.9500
C(15)-C(16)	1.384(4)	C(15)-H(15)	0.9500
C(16)-C(17)	1.388(4)	C(16)-C(18)	1.515(4)
C(17)-H(17)	0.9500	C(18)-H(18A)	0.9900
C(18)-H(18B)	0.9900	C(19)-C(20)	1.371(4)
C(19)-H(19)	0.9500	C(20)-C(21)	1.385(4)
C(20)-H(20)	0.9500	C(21)-C(22)	1.387(4)

Table B.20. Continued

Bond Angles ($^{\circ}$)

N(4)#1-Ag(1)-N(1)	165.07(9)	N(4)#1-Ag(1)-O(1)	98.49(8)
N(1)-Ag(1)-O(1)	96.42(8)	N(3)-Ag(2)-N(2)	159.12(9)
N(3)-Ag(2)-O(5)	106.28(8)	N(2)-Ag(2)-O(5)	89.35(8)
N(3)-Ag(2)-O(3)	93.01(8)	N(2)-Ag(2)-O(3)	101.03(8)
O(5)-Ag(2)-O(3)	89.54(7)	N(5)-Ag(3)-N(8)	164.27(9)
N(5)-Ag(3)-O(8)#2	101.33(9)	N(8)-Ag(3)-O(8)#2	92.93(9)
N(6)-Ag(4)-N(7)#1	166.19(9)	N(6)-Ag(4)-O(7)	104.56(8)
N(7)#1-Ag(4)-O(7)	87.20(8)	C(25)-O(1)-Ag(1)	116.72(18)
C(27)-O(3)-Ag(2)	126.21(19)	C(29)-O(5)-Ag(2)	135.4(2)
C(31)-O(7)-Ag(4)	106.4(2)	C(31)-O(8)-Ag(3)#3	137.2(2)
C(1)-N(1)-C(5)	118.5(3)	C(1)-N(1)-Ag(1)	119.1(2)
C(5)-N(1)-Ag(1)	122.3(2)	C(6)-N(2)-Ag(2)	114.63(18)
C(6)-N(2)-H(2A)	108.6	Ag(2)-N(2)-H(2A)	108.6
C(6)-N(2)-H(2B)	108.6	Ag(2)-N(2)-H(2B)	108.6
H(2A)-N(2)-H(2B)	107.6	C(11)-N(3)-C(7)	117.3(3)
C(11)-N(3)-Ag(2)	122.76(19)	C(7)-N(3)-Ag(2)	119.9(2)
C(12)-N(4)-Ag(1)#4	116.60(18)	C(12)-N(4)-H(4A)	108.1
Ag(1)#4-N(4)-H(4A)	108.1	C(12)-N(4)-H(4B)	108.1
Ag(1)#4-N(4)-H(4B)	108.1	H(4A)-N(4)-H(4B)	107.3
C(17)-N(5)-C(13)	117.6(3)	C(17)-N(5)-Ag(3)	125.2(2)
C(13)-N(5)-Ag(3)	117.3(2)	C(18)-N(6)-Ag(4)	113.44(18)
C(18)-N(6)-H(6A)	108.9	Ag(4)-N(6)-H(6A)	108.9
C(18)-N(6)-H(6B)	108.9	Ag(4)-N(6)-H(6B)	108.9
H(6A)-N(6)-H(6B)	107.7	C(23)-N(7)-C(19)	118.2(3)
C(23)-N(7)-Ag(4)#4	124.5(2)	C(19)-N(7)-Ag(4)#4	117.2(2)
C(24)-N(8)-Ag(3)	112.66(17)	C(24)-N(8)-H(8A)	109.1
Ag(3)-N(8)-H(8A)	109.1	C(24)-N(8)-H(8B)	109.1
Ag(3)-N(8)-H(8B)	109.1	H(8A)-N(8)-H(8B)	107.8
N(1)-C(1)-C(2)	121.8(3)	N(1)-C(1)-H(1)	119.1
C(2)-C(1)-H(1)	119.1	C(3)-C(2)-C(1)	119.4(3)
C(3)-C(2)-H(2)	120.3	C(1)-C(2)-H(2)	120.3
C(2)-C(3)-C(4)	119.6(3)	C(2)-C(3)-H(3)	120.2
C(4)-C(3)-H(3)	120.2	C(3)-C(4)-C(5)	117.6(3)
C(3)-C(4)-C(6)	123.7(3)	C(5)-C(4)-C(6)	118.7(3)
N(1)-C(5)-C(4)	123.0(3)	N(1)-C(5)-H(5)	118.5
C(4)-C(5)-H(5)	118.5	N(2)-C(6)-C(4)	115.2(2)
N(2)-C(6)-H(6C)	108.5	C(4)-C(6)-H(6C)	108.5
N(2)-C(6)-H(6D)	108.5	C(4)-C(6)-H(6D)	108.5
H(6C)-C(6)-H(6D)	107.5	N(3)-C(7)-C(8)	122.3(3)
N(3)-C(7)-H(7)	118.9	C(8)-C(7)-H(7)	118.9
C(7)-C(8)-C(9)	119.6(3)	C(7)-C(8)-H(8)	120.2
C(9)-C(8)-H(8)	120.2	C(8)-C(9)-C(10)	119.2(3)
C(8)-C(9)-H(9)	120.4	C(10)-C(9)-H(9)	120.4
C(11)-C(10)-C(9)	117.2(3)	C(11)-C(10)-C(12)	119.2(3)
C(9)-C(10)-C(12)	123.7(3)	N(3)-C(11)-C(10)	124.6(3)
N(3)-C(11)-H(11)	117.7	C(10)-C(11)-H(11)	117.7
N(4)-C(12)-C(10)	114.6(2)	N(4)-C(12)-H(12A)	108.6
C(10)-C(12)-H(12A)	108.6	N(4)-C(12)-H(12B)	108.6
C(10)-C(12)-H(12B)	108.6	H(12A)-C(12)-H(12B)	107.6
N(5)-C(13)-C(14)	122.4(3)	N(5)-C(13)-H(13)	118.8
C(14)-C(13)-H(13)	118.8	C(13)-C(14)-C(15)	119.4(3)
C(13)-C(14)-H(14)	120.3	C(15)-C(14)-H(14)	120.3

Table B.20. Continued

C(16)-C(15)-C(14)	119.4(3)	C(16)-C(15)-H(15)	120.3
C(14)-C(15)-H(15)	120.3	C(15)-C(16)-C(17)	117.5(3)
C(15)-C(16)-C(18)	122.9(3)	C(17)-C(16)-C(18)	119.6(3)
N(5)-C(17)-C(16)	123.8(3)	N(5)-C(17)-H(17)	118.1
C(16)-C(17)-H(17)	118.1	N(6)-C(18)-C(16)	114.1(2)
N(6)-C(18)-H(18A)	108.7	C(16)-C(18)-H(18A)	108.7
N(6)-C(18)-H(18B)	108.7	C(16)-C(18)-H(18B)	108.7
H(18A)-C(18)-H(18B)	107.6	N(7)-C(19)-C(20)	122.3(3)
N(7)-C(19)-H(19)	118.9	C(20)-C(19)-H(19)	118.9
C(19)-C(20)-C(21)	119.6(3)	C(19)-C(20)-H(20)	120.2
C(21)-C(20)-H(20)	120.2	C(20)-C(21)-C(22)	119.1(3)
C(20)-C(21)-H(21)	120.5	C(22)-C(21)-H(21)	120.5
C(21)-C(22)-C(23)	117.5(3)	C(21)-C(22)-C(24)	122.9(3)
C(23)-C(22)-C(24)	119.6(3)	N(7)-C(23)-C(22)	123.3(3)
N(7)-C(23)-H(23)	118.4	C(22)-C(23)-H(23)	118.4
N(8)-C(24)-C(22)	113.6(2)	N(8)-C(24)-H(24A)	108.8
C(22)-C(24)-H(24A)	108.8	N(8)-C(24)-H(24B)	108.8
C(22)-C(24)-H(24B)	108.8	H(24A)-C(24)-H(24B)	107.7
O(1)-C(25)-O(2)	130.6(3)	O(1)-C(25)-C(26)	115.3(3)
O(2)-C(25)-C(26)	114.0(3)	F(1)-C(26)-F(3)	106.2(3)
F(1)-C(26)-F(2)	106.2(3)	F(3)-C(26)-F(2)	107.4(3)
F(1)-C(26)-C(25)	113.0(3)	F(3)-C(26)-C(25)	113.4(2)
F(2)-C(26)-C(25)	110.2(3)	O(3)-C(27)-O(4)	131.2(3)
O(3)-C(27)-C(28)	114.7(3)	O(4)-C(27)-C(28)	114.1(3)
F(5)-C(28)-F(6)	107.9(3)	F(5)-C(28)-F(4)	105.0(3)
F(6)-C(28)-F(4)	106.8(3)	F(5)-C(28)-C(27)	110.7(3)
F(6)-C(28)-C(27)	113.7(3)	F(4)-C(28)-C(27)	112.1(3)
O(5)-C(29)-O(6)	129.4(3)	O(5)-C(29)-C(30)	115.8(3)
O(6)-C(29)-C(30)	114.7(3)	F(7)-C(30)-F(9)	107.7(3)
F(7)-C(30)-F(8)	107.3(4)	F(9)-C(30)-F(8)	102.4(3)
F(7)-C(30)-C(29)	114.2(3)	F(9)-C(30)-C(29)	115.3(3)
F(8)-C(30)-C(29)	108.9(3)	O(8)-C(31)-O(7)	127.8(3)
O(8)-C(31)-C(32)	117.9(3)	O(7)-C(31)-C(32)	114.2(3)
F(10)-C(32)-F(11)	107.8(3)	F(10)-C(32)-F(12)	107.1(3)
F(11)-C(32)-F(12)	105.6(3)	F(10)-C(32)-C(31)	110.8(3)
F(11)-C(32)-C(31)	113.2(3)	F(12)-C(32)-C(31)	112.1(3)

Hydrogen Bonds (Å)

N(2)-H(2A)...O(1)#5	3.024(3)	N(2)-H(2A)...F(3)#5	3.290(3)
N(2)-H(2B)...O(7)	2.870(3)	N(4)-H(4A)...O(6)#6	2.914(3)
N(4)-H(4A)...O(5)#6	3.359(4)	N(4)-H(4B)...O(3)#6	3.001(3)
N(4)-H(4B)...F(6)#6	3.294(3)	N(6)-H(6A)...O(4)	2.886(3)
N(6)-H(6B)...O(2)#7	3.126(3)	N(8)-H(8A)...O(4)#3	3.109(3)
N(8)-H(8B)...O(2)#4	2.907(3)		

Symmetry transformations used to generate equivalent atoms: #1 x,y+1,z #2 x-1/2,-y+1/2,-z #3 x+1/2,-y+1/2,-z
#4 x,y-1,z #5 -x+2,y-1/2,-z+1/2 #6 -x+1,y-1/2,-z+1/2 #7 x-1/2,-y+3/2,-z

Table B.21 Experimental and statistical crystal data for **6.2**

Empirical formula	C14 H16 Ag2 F6 N4 O6 S2
Formula weight	730.17
Temperature	110(2) K
Wavelength	0.71073 Å
Crystal system, space group	Monoclinic, P2(1)/c
Unit cell dimensions	a = 10.2555(10) Å α = 90 deg. b = 23.941(2) Å β = 91.743(4) deg. c = 9.1244(8) Å γ = 90 deg.
Volume	2239.3(4) Å ³
Z, Calculated density	4, 2.166 Mg/m ³
Absorption coefficient	2.025 mm ⁻¹
F(000)	1424
Crystal size	0.14 x 0.09 x 0.06 mm
θ range for data collection	1.70 to 26.37 deg.
Limiting indices	-12<=h<=12, -29<=k<=29, -11<=l<=7
Reflections collected / unique	58756 / 4576 [R(int) = 0.0404]
Completeness to θ = 26.37	100.0 %
Absorption correction	Semi-empirical from equivalents
Max. and min. transmission	0.8881 and 0.7619
Refinement method	Full-matrix least-squares on F ²
Data / restraints / parameters	4576 / 0 / 307
Goodness-of-fit on F ²	1.061
Final R indices [I>2σ(I)]	R1 = 0.0204, wR2 = 0.0510
R indices (all data)	R1 = 0.0258, wR2 = 0.0532
Largest diff. peak and hole	0.880 and -0.583 e.Å ⁻³

Bond Lengths (Å)

Ag(1)-N(4)#1	2.1235(19)	Ag(1)-N(1)	2.1283(19)
Ag(2)-N(2)	2.1640(19)	Ag(2)-N(3)	2.1675(19)
Ag(2)-Ag(2)#2	3.1820(4)	S(1)-O(1)	1.4343(18)
S(1)-O(2)	1.4391(18)	S(1)-O(3)	1.4393(18)
S(1)-C(13)	1.820(3)	S(2)-O(5)	1.4350(19)
S(2)-O(6)	1.4369(19)	S(2)-O(4)	1.4393(18)
S(2)-C(14)	1.819(3)	F(1)-C(13)	1.321(3)
F(2)-C(13)	1.318(3)	F(3)-C(13)	1.330(3)
F(4)-C(14)	1.317(3)	F(5)-C(14)	1.322(3)
F(6)-C(14)	1.319(3)	N(1)-C(1)	1.482(3)
N(1)-H(1A)	0.9200	N(1)-H(1B)	0.9200
N(2)-C(3)	1.340(3)	N(2)-C(4)	1.347(3)
N(3)-C(7)	1.344(3)	N(3)-C(11)	1.345(3)
N(4)-C(12)	1.481(3)	N(4)-Ag(1)#3	2.1235(19)
N(4)-H(4A)	0.9200	N(4)-H(4B)	0.9200
C(1)-C(2)	1.509(3)	C(1)-H(1C)	0.9900
C(1)-H(1D)	0.9900	C(2)-C(6)	1.387(3)
C(2)-C(3)	1.391(3)	C(3)-H(3)	0.9500
C(4)-C(5)	1.363(4)	C(4)-H(4)	0.9500
C(5)-C(6)	1.382(4)	C(5)-H(5)	0.9500
C(6)-H(6)	0.9500	C(7)-C(8)	1.368(3)
C(7)-H(7)	0.9500	C(8)-C(9)	1.382(4)
C(8)-H(8)	0.9500	C(9)-C(10)	1.385(3)
C(9)-H(9)	0.9500	C(10)-C(11)	1.380(3)
C(10)-C(12)	1.508(3)	C(11)-H(11)	0.9500
C(12)-H(12A)	0.9900	C(12)-H(12B)	0.9900

Table B.21. Continued

Bond Angles ($^{\circ}$)

N(4)#1-Ag(1)-N(1)	177.85(8)	N(2)-Ag(2)-N(3)	165.38(7)
N(2)-Ag(2)-Ag(2)#2	83.98(5)	N(3)-Ag(2)-Ag(2)#2	101.56(5)
O(1)-S(1)-O(2)	114.63(12)	O(1)-S(1)-O(3)	115.85(11)
O(2)-S(1)-O(3)	113.79(11)	O(1)-S(1)-C(13)	102.74(12)
O(2)-S(1)-C(13)	104.20(12)	O(3)-S(1)-C(13)	103.44(12)
O(5)-S(2)-O(6)	114.66(12)	O(5)-S(2)-O(4)	115.60(11)
O(6)-S(2)-O(4)	113.59(11)	O(5)-S(2)-C(14)	102.12(12)
O(6)-S(2)-C(14)	104.76(12)	O(4)-S(2)-C(14)	104.06(12)
C(1)-N(1)-Ag(1)	121.71(15)	C(1)-N(1)-H(1A)	106.9
Ag(1)-N(1)-H(1A)	106.9	C(1)-N(1)-H(1B)	106.9
Ag(1)-N(1)-H(1B)	106.9	H(1A)-N(1)-H(1B)	106.7
C(3)-N(2)-C(4)	117.9(2)	C(3)-N(2)-Ag(2)	117.21(15)
C(4)-N(2)-Ag(2)	124.84(16)	C(7)-N(3)-C(11)	117.8(2)
C(7)-N(3)-Ag(2)	125.86(16)	C(11)-N(3)-Ag(2)	116.32(15)
C(12)-N(4)-Ag(1)#3	120.31(15)	C(12)-N(4)-H(4A)	107.2
Ag(1)#3-N(4)-H(4A)	107.2	C(12)-N(4)-H(4B)	107.2
Ag(1)#3-N(4)-H(4B)	107.2	H(4A)-N(4)-H(4B)	106.9
N(1)-C(1)-C(2)	111.56(19)	N(1)-C(1)-H(1C)	109.3
C(2)-C(1)-H(1C)	109.3	N(1)-C(1)-H(1D)	109.3
C(2)-C(1)-H(1D)	109.3	H(1C)-C(1)-H(1D)	108.0
C(6)-C(2)-C(3)	117.4(2)	C(6)-C(2)-C(1)	122.3(2)
C(3)-C(2)-C(1)	120.3(2)	N(2)-C(3)-C(2)	123.2(2)
N(2)-C(3)-H(3)	118.4	C(2)-C(3)-H(3)	118.4
N(2)-C(4)-C(5)	122.6(2)	N(2)-C(4)-H(4)	118.7
C(5)-C(4)-H(4)	118.7	C(4)-C(5)-C(6)	119.3(2)
C(4)-C(5)-H(5)	120.3	C(6)-C(5)-H(5)	120.3
C(5)-C(6)-C(2)	119.6(2)	C(5)-C(6)-H(6)	120.2
C(2)-C(6)-H(6)	120.2	N(3)-C(7)-C(8)	122.5(2)
N(3)-C(7)-H(7)	118.7	C(8)-C(7)-H(7)	118.7
C(7)-C(8)-C(9)	119.0(2)	C(7)-C(8)-H(8)	120.5
C(9)-C(8)-H(8)	120.5	C(8)-C(9)-C(10)	119.7(2)
C(8)-C(9)-H(9)	120.2	C(10)-C(9)-H(9)	120.2
C(11)-C(10)-C(9)	117.5(2)	C(11)-C(10)-C(12)	120.7(2)
C(9)-C(10)-C(12)	121.7(2)	N(3)-C(11)-C(10)	123.4(2)
N(3)-C(11)-H(11)	118.3	C(10)-C(11)-H(11)	118.3
N(4)-C(12)-C(10)	111.45(19)	N(4)-C(12)-H(12A)	109.3
C(10)-C(12)-H(12A)	109.3	N(4)-C(12)-H(12B)	109.3
C(10)-C(12)-H(12B)	109.3	H(12A)-C(12)-H(12B)	108.0
F(2)-C(13)-F(1)	107.6(2)	F(2)-C(13)-F(3)	109.1(2)
F(1)-C(13)-F(3)	107.2(2)	F(2)-C(13)-S(1)	110.48(19)
F(1)-C(13)-S(1)	110.86(19)	F(3)-C(13)-S(1)	111.46(18)
F(4)-C(14)-F(6)	108.0(2)	F(4)-C(14)-F(5)	108.6(2)
F(6)-C(14)-F(5)	107.2(2)	F(4)-C(14)-S(2)	110.11(19)
F(6)-C(14)-S(2)	111.08(18)	F(5)-C(14)-S(2)	111.76(18)

Table B.21. Continued

Hydrogen Bonds (Å)

N(4)-H(4A)...O(6)	3.144(3)	N(4)-H(4A)...O(4)	3.090(3)
N(4)-H(4A)...S(2)	3.650(2)	N(4)-H(4B)...O(3)	3.001(3)
N(1)-H(1A)...O(2) ^{#4}	3.022(3)	N(1)-H(1A)...S(1) ^{#4}	3.604(2)
N(1)-H(1B)...O(4) ^{#4}	3.010(3)		

Symmetry transformations used to generate equivalent atoms: #1 x-1,-y+3/2,z+1/2 #2 -x,-y+1,-z+1 #3 x+1,-y+3/2,z-1/2 #4 x-1,y,z

Table B.22 Experimental and statistical crystal data for **6.3**

Empirical formula	C14 H16 Ag F3 N4 O2
Formula weight	437.18
Temperature	110(2) K
Wavelength	0.71073 Å
Crystal system, space group	Monoclinic, P2(1)/n
Unit cell dimensions	a = 12.5447(9) Å α = 90 deg. b = 10.5573(7) Å β = 108.001(2) deg. c = 12.9994(9) Å γ = 90 deg.
Volume	1637.3(2) Å ³
Z, Calculated density	4, 1.773 Mg/m ³
Absorption coefficient	1.277 mm ⁻¹
F(000)	872
Crystal size	0.19 x 0.07 x 0.07 mm
θ range for data collection	1.97 to 28.37 deg.
Limiting indices	-16<=h<=16, -12<=k<=14, -17<=l<=17
Reflections collected / unique	60463 / 4039 [R(int) = 0.0329]
Completeness to θ = 28.37	98.5 %
Absorption correction	Semi-empirical from equivalents
Max. and min. transmission	0.9159 and 0.7906
Refinement method	Full-matrix least-squares on F ²
Data / restraints / parameters	4039 / 19 / 274
Goodness-of-fit on F ²	1.056
Final R indices [I>2σ(I)]	R1 = 0.0159, wR2 = 0.0427
R indices (all data)	R1 = 0.0185, wR2 = 0.0436
Largest diff. peak and hole	0.439 and -0.247 e.Å ⁻³

Bond Lengths (Å)

Ag(1)-N(2) ^{#1}	2.2851(10)	Ag(1)-N(4) ^{#2}	2.3028(10)
Ag(1)-N(3)	2.3765(11)	Ag(1)-N(1)	2.4460(11)
O(1)-C(13)	1.2418(15)	O(2)-C(13)	1.2409(15)
N(1)-C(5)	1.3418(18)	N(1)-C(1)	1.3422(17)
N(2)-C(6)	1.4690(15)	N(2)-Ag(1) ^{#3}	2.2851(10)
N(2)-H(2A)	0.9200	N(2)-H(2B)	0.9200
N(3)-C(7)	1.3406(17)	N(3)-C(11)	1.3415(16)
N(4)-C(12)	1.4758(16)	N(4)-Ag(1) ^{#4}	2.3028(10)
N(4)-H(4A)	0.9200	N(4)-H(4B)	0.9200
C(1)-C(2)	1.3880(18)	C(1)-H(1)	0.9500
C(2)-C(3)	1.3975(17)	C(2)-C(6)	1.5123(17)

Table B.22. Continued

C(3)-C(4)	1.3828(18)	C(3)-H(3)	0.9500
C(4)-C(5)	1.385(2)	C(4)-H(4)	0.9500
C(5)-H(5)	0.9500	C(6)-H(6A)	0.9900
C(6)-H(6B)	0.9900	C(7)-C(8)	1.3906(18)
C(7)-H(7)	0.9500	C(8)-C(9)	1.3849(18)
C(8)-C(12)	1.5118(17)	C(9)-C(10)	1.3875(19)
C(9)-H(9)	0.9500	C(10)-C(11)	1.3821(18)
C(10)-H(10)	0.9500	C(11)-H(11)	0.9500
C(12)-H(12A)	0.9900	C(12)-H(12B)	0.9900
C(13)-C(14)	1.5548(18)	C(14)-F(1)	1.315(5)
C(14)-F(3)	1.317(6)	C(14)-F(2)	1.359(7)
Bond Angles (°)			
N(2)#1-Ag(1)-N(4)#2	130.93(4)	N(2)#1-Ag(1)-N(3)	113.77(4)
N(4)#2-Ag(1)-N(3)	99.83(4)	N(2)#1-Ag(1)-N(1)	103.69(4)
N(4)#2-Ag(1)-N(1)	108.81(4)	N(3)-Ag(1)-N(1)	93.80(4)
C(5)-N(1)-C(1)	116.91(12)	C(5)-N(1)-Ag(1)	125.92(9)
C(1)-N(1)-Ag(1)	115.92(9)	C(6)-N(2)-Ag(1)#3	115.02(7)
C(6)-N(2)-H(2A)	108.5	Ag(1)#3-N(2)-H(2A)	108.5
C(6)-N(2)-H(2B)	108.5	Ag(1)#3-N(2)-H(2B)	108.5
H(2A)-N(2)-H(2B)	107.5	C(7)-N(3)-C(11)	117.44(11)
C(7)-N(3)-Ag(1)	118.26(8)	C(11)-N(3)-Ag(1)	122.62(8)
C(12)-N(4)-Ag(1)#4	116.60(8)	C(12)-N(4)-H(4A)	108.1
Ag(1)#4-N(4)-H(4A)	108.1	C(12)-N(4)-H(4B)	108.1
Ag(1)#4-N(4)-H(4B)	108.1	H(4A)-N(4)-H(4B)	107.3
N(1)-C(1)-C(2)	124.41(12)	N(1)-C(1)-H(1)	117.8
C(2)-C(1)-H(1)	117.8	C(1)-C(2)-C(3)	117.44(11)
C(1)-C(2)-C(6)	120.04(11)	C(3)-C(2)-C(6)	122.45(11)
C(4)-C(3)-C(2)	118.90(12)	C(4)-C(3)-H(3)	120.5
C(2)-C(3)-H(3)	120.5	C(3)-C(4)-C(5)	119.23(12)
C(3)-C(4)-H(4)	120.4	C(5)-C(4)-H(4)	120.4
N(1)-C(5)-C(4)	123.09(12)	N(1)-C(5)-H(5)	118.5
C(4)-C(5)-H(5)	118.5	N(2)-C(6)-C(2)	115.56(10)
N(2)-C(6)-H(6A)	108.4	C(2)-C(6)-H(6A)	108.4
N(2)-C(6)-H(6B)	108.4	C(2)-C(6)-H(6B)	108.4
H(6A)-C(6)-H(6B)	107.5	N(3)-C(7)-C(8)	123.98(12)
N(3)-C(7)-H(7)	118.0	C(8)-C(7)-H(7)	118.0
C(9)-C(8)-C(7)	117.58(12)	C(9)-C(8)-C(12)	122.85(12)
C(7)-C(8)-C(12)	119.54(12)	C(8)-C(9)-C(10)	119.17(12)
C(8)-C(9)-H(9)	120.4	C(10)-C(9)-H(9)	120.4
C(11)-C(10)-C(9)	119.17(12)	C(11)-C(10)-H(10)	120.4
C(9)-C(10)-H(10)	120.4	N(3)-C(11)-C(10)	122.65(12)
N(3)-C(11)-H(11)	118.7	C(10)-C(11)-H(11)	118.7
N(4)-C(12)-C(8)	113.66(10)	N(4)-C(12)-H(12A)	108.8
C(8)-C(12)-H(12A)	108.8	N(4)-C(12)-H(12B)	108.8
C(8)-C(12)-H(12B)	108.8	H(12A)-C(12)-H(12B)	107.7
O(2)-C(13)-O(1)	130.72(12)	O(2)-C(13)-C(14)	114.73(11)
O(1)-C(13)-C(14)	114.54(11)	F(1)-C(14)-F(3)	107.6(5)
F(1)-C(14)-F(2)	105.0(4)	F(3)-C(14)-F(2)	104.0(5)
F(1)-C(14)-C(13)	114.0(2)	F(3)-C(14)-C(13)	113.8(4)
F(2)-C(14)-C(13)	111.6(4)		

Table B.22. Continued

Hydrogen Bonds (Å)

N(2)-H(2A)...O(2)#3	3.0692(14)	N(2)-H(2B)...O(2)#5	3.0282(14)
N(4)-H(4A)...O(1)#6	3.1528(14)	N(4)-H(4A)...F(1B)#6	3.36(2)
N(4)-H(4B)...O(1)#4	3.1525(14)		

Symmetry transformations used to generate equivalent atoms: #1 -x+3/2,y-1/2,-z+1/2 #2 -x+1/2,y-1/2,-z+1/2 #3 -x+3/2,y+1/2,-z+1/2 #4 -x+1/2,y+1/2,-z+1/2 #5 x+1/2,-y+3/2,z+1/2 #6 x,y+1,z

Table B.23 Experimental and statistical crystal data for 6.4

Empirical formula	C13 H16 Ag F3 N4 O3 S
Formula weight	473.23
Temperature	110(2) K
Wavelength	0.71073 Å
Crystal system, space group	Orthorhombic, P2(1)2(1)2(1)
Unit cell dimensions	a = 7.5817(8) Å α = 90 deg. b = 10.4787(13) Å β = 90 deg. c = 21.663(2) Å γ = 90 deg.
Volume	1721.1(3) Å ³
Z, Calculated density	4, 1.826 Mg/m ³
Absorption coefficient	1.344 mm ⁻¹
F(000)	944
Crystal size	0.293 × 0.270 × 0.119 mm
θ range for data collection	3.28 to 25.75 deg.
Limiting indices	-9<=h<=8, -12<=k<=12, -26<=l<=25
Reflections collected / unique	13609 / 3284 [R(int) = 0.0252]
Completeness to θ = 25.75	99.7 %
Absorption correction	multi-scan (SADABS)
Refinement method	Full-matrix least-squares on F ²
Data / restraints / parameters	3284 / 0 / 226
Goodness-of-fit on F ²	1.061
Final R indices [I>2σ(I)]	R1 = 0.0178, wR2 = 0.0433
R indices (all data)	R1 = 0.0191, wR2 = 0.0436
Absolute structure parameter	-0.032(17)
Largest diff. peak and hole	0.681 and -0.210 e.Å ⁻³

Bond Lengths (Å)

Ag(1)-N(2)	2.3065(18)	Ag(1)-N(3)#1	2.3273(18)
Ag(1)-N(4)	2.3352(19)	Ag(1)-N(1)#2	2.3483(18)
S(1)-O(1)	1.439(2)	S(1)-O(2)	1.444(2)
S(1)-O(3)	1.445(2)	S(1)-C(13)	1.821(2)
F(1)-C(13)	1.329(3)	F(2)-C(13)	1.337(3)
F(3)-C(13)	1.344(3)	N(2)-C(4)	1.339(3)
N(2)-C(3)	1.353(3)	N(1)-C(1)	1.475(3)
N(1)-Ag(1)#3	2.3483(18)	N(1)-H(1A)	0.9200
N(1)-H(1B)	0.9200	N(4)-C(10)	1.330(3)
N(4)-C(9)	1.351(3)	N(3)-C(7)	1.481(3)
N(3)-Ag(1)#4	2.3273(18)	N(3)-H(3A)	0.9200
N(3)-H(3B)	0.9200	C(4)-C(5)	1.378(3)
C(4)-H(4)	0.9500	C(5)-C(6)	1.398(3)

Table B.23. Continued

C(5)-H(5)	0.9500	C(3)-C(2)	1.383(3)
C(3)-H(3)	0.9500	C(6)-C(2)	1.378(3)
C(6)-H(6)	0.9500	C(2)-C(1)	1.516(3)
C(7)-C(8)	1.515(3)	C(7)-H(7A)	0.9900
C(7)-H(7B)	0.9900	C(8)-C(9)	1.383(3)
C(8)-C(12)	1.385(3)	C(12)-C(11)	1.395(3)
C(12)-H(12)	0.9500	C(11)-C(10)	1.386(3)
C(11)-H(11)	0.9500	C(1)-H(1C)	0.9900
C(1)-H(1D)	0.9900	C(10)-H(10)	0.9500
C(9)-H(9)	0.9500		
Bond Angles (°)			
N(2)-Ag(1)-N(3)#1	119.86(7)	C(8)-C(9)-H(9)	118.1
N(2)-Ag(1)-N(4)	105.34(6)	N(3)#1-Ag(1)-N(4)	119.58(7)
N(2)-Ag(1)-N(1)#2	104.74(7)	N(3)#1-Ag(1)-N(1)#2	96.63(7)
N(4)-Ag(1)-N(1)#2	108.92(7)	O(1)-S(1)-O(2)	114.55(13)
O(1)-S(1)-O(3)	116.32(12)	O(2)-S(1)-O(3)	114.76(12)
O(1)-S(1)-C(13)	103.48(12)	O(2)-S(1)-C(13)	103.24(11)
O(3)-S(1)-C(13)	101.79(11)	C(4)-N(2)-C(3)	116.89(19)
C(4)-N(2)-Ag(1)	123.70(14)	C(3)-N(2)-Ag(1)	118.21(15)
C(1)-N(1)-Ag(1)#3	123.78(14)	C(1)-N(1)-H(1A)	106.4
Ag(1)#3-N(1)-H(1A)	106.4	C(1)-N(1)-H(1B)	106.4
Ag(1)#3-N(1)-H(1B)	106.4	H(1A)-N(1)-H(1B)	106.5
C(10)-N(4)-C(9)	117.4(2)	C(10)-N(4)-Ag(1)	120.06(16)
C(9)-N(4)-Ag(1)	122.28(15)	C(7)-N(3)-Ag(1)#4	118.00(13)
C(7)-N(3)-H(3A)	107.8	Ag(1)#4-N(3)-H(3A)	107.8
C(7)-N(3)-H(3B)	107.8	Ag(1)#4-N(3)-H(3B)	107.8
H(3A)-N(3)-H(3B)	107.1	F(1)-C(13)-F(2)	107.20(18)
F(1)-C(13)-F(3)	107.49(19)	F(2)-C(13)-F(3)	106.9(2)
F(1)-C(13)-S(1)	112.76(17)	F(2)-C(13)-S(1)	111.64(16)
F(3)-C(13)-S(1)	110.58(16)	N(2)-C(4)-C(5)	123.4(2)
N(2)-C(4)-H(4)	118.3	C(5)-C(4)-H(4)	118.3
C(4)-C(5)-C(6)	118.7(2)	C(4)-C(5)-H(5)	120.6
C(6)-C(5)-H(5)	120.6	N(2)-C(3)-C(2)	123.7(2)
N(2)-C(3)-H(3)	118.1	C(2)-C(3)-H(3)	118.1
C(2)-C(6)-C(5)	119.0(2)	C(2)-C(6)-H(6)	120.5
C(5)-C(6)-H(6)	120.5	C(6)-C(2)-C(3)	118.3(2)
C(6)-C(2)-C(1)	120.9(2)	C(3)-C(2)-C(1)	120.6(2)
N(3)-C(7)-C(8)	110.94(18)	N(3)-C(7)-H(7A)	109.5
C(8)-C(7)-H(7A)	109.5	N(3)-C(7)-H(7B)	109.5
C(8)-C(7)-H(7B)	109.5	H(7A)-C(7)-H(7B)	108.0
C(9)-C(8)-C(12)	118.0(2)	C(9)-C(8)-C(7)	120.9(2)
C(12)-C(8)-C(7)	121.1(2)	C(8)-C(12)-C(11)	119.0(2)
C(8)-C(12)-H(12)	120.5	C(11)-C(12)-H(12)	120.5
C(10)-C(11)-C(12)	118.7(2)	C(10)-C(11)-H(11)	120.7
C(12)-C(11)-H(11)	120.7	N(1)-C(1)-C(2)	111.91(19)
N(1)-C(1)-H(1C)	109.2	C(2)-C(1)-H(1C)	109.2
N(1)-C(1)-H(1D)	109.2	C(2)-C(1)-H(1D)	109.2
H(1C)-C(1)-H(1D)	107.9	N(4)-C(10)-C(11)	123.2(2)
N(4)-C(10)-H(10)	118.4	C(11)-C(10)-H(10)	118.4
N(4)-C(9)-C(8)	123.8(2)	N(4)-C(9)-H(9)	118.1

Table B.23. Continued

Hydrogen Bonds (Å)

N(1)-H(1A)...O(2)#5	3.076(3)	N(1)-H(1B)...O(1)#3	2.980(3)
N(3)-H(3A)...O(3)#4	3.225(3)	N(3)-H(3B)...O(2)#6	3.318(3)

Symmetry transformations used to generate equivalent atoms: #1 x-1/2,-y+3/2,-z #2 -x+2,y-1/2,-z+1/2
#3 -x+2,y+1/2,-z+1/2 #4 x+1/2,-y+3/2,-z #5 x+1,y+1,z #6 -x+3/2,-y+1,z-1/2

Table B.24 Experimental and statistical crystal data for **6.5**

Empirical formula	C32 H27 Ag2 F6 N7 O4
Formula weight	903.35
Temperature	110(2) K
Wavelength	0.71073 Å
Crystal system, space group	Triclinic, P-1
Unit cell dimensions	a = 11.6824(11) Å α = 78.317(2) deg. b = 12.2492(11) Å β = 64.335(2) deg. c = 13.2975(12) Å γ = 75.003(2) deg.
Volume	1647.8(3) Å ³
Z, Calculated density	2, 1.821 Mg/m ³
Absorption coefficient	1.272 mm ⁻¹
F(000)	896
Crystal size	0.195 × 0.172 × 0.140 mm
θ range for data collection	1.97 to 28.31 deg.
Limiting indices	-15<=h<=15, -15<=k<=16, -17<=l<=17
Reflections collected / unique	22035 / 8117 [R(int) = 0.0318]
Completeness to θ = 25.00	99.1 %
Absorption correction	multi-scan (SADABS)
Refinement method	Full-matrix least-squares on F ²
Data / restraints / parameters	8117 / 6 / 489
Goodness-of-fit on F ²	1.020
Final R indices [I>2σ(I)]	R1 = 0.0277, wR2 = 0.0608
R indices (all data)	R1 = 0.0399, wR2 = 0.0663
Largest diff. peak and hole	0.626 and -0.677 e.Å ⁻³

Bond Lengths (Å)

Ag(1)-N(1)	2.1487(18)	Ag(1)-N(4)	2.2552(19)
Ag(1)-N(3)	2.3313(19)	Ag(1)-Ag(2)#1	3.0583(3)
Ag(2)-N(2)	2.1481(19)	Ag(2)-N(6)	2.2143(19)
Ag(2)-N(5)	2.382(2)	Ag(2)-Ag(1)#1	3.0583(3)
Ag(2)-Ag(2)#2	3.1615(4)	F(4)-C(30)	1.326(3)
F(5)-C(30)	1.325(3)	F(6)-C(30)	1.332(3)
O(1)-C(27)	1.234(3)	O(2)-C(27)	1.240(3)
O(3)-C(29)	1.244(3)	O(4)-C(29)	1.234(3)
N(1)-C(1)	1.483(3)	N(1)-H(1A)	0.9000
N(1)-H(1B)	0.9000	N(2)-C(3)	1.346(3)
N(2)-C(4)	1.349(3)	N(3)-C(7)	1.342(3)
N(3)-C(11)	1.345(3)	N(4)-C(16)	1.344(3)
N(4)-C(12)	1.350(3)	N(5)-C(17)	1.336(3)
N(5)-C(21)	1.349(3)	N(6)-C(26)	1.346(3)
N(6)-C(22)	1.352(3)	N(7)-C(31)	1.137(4)

Table B.24. Continued

C(1)-C(2)	1.504(3)	C(1)-H(1C)	0.9700
C(1)-H(1D)	0.9700	C(2)-C(3)	1.385(3)
C(2)-C(6)	1.394(3)	C(3)-H(3)	0.9300
C(4)-C(5)	1.380(3)	C(4)-H(4)	0.9300
C(5)-C(6)	1.385(3)	C(5)-H(5)	0.9300
C(6)-H(6)	0.9300	C(7)-C(8)	1.386(3)
C(7)-H(7)	0.9300	C(8)-C(9)	1.377(4)
C(8)-H(8)	0.9300	C(9)-C(10)	1.388(4)
C(9)-H(9)	0.9300	C(10)-C(11)	1.393(3)
C(10)-H(10)	0.9300	C(11)-C(12)	1.496(3)
C(12)-C(13)	1.401(3)	C(13)-C(14)	1.390(3)
C(13)-H(13)	0.9300	C(14)-C(15)	1.385(4)
C(14)-H(14)	0.9300	C(15)-C(16)	1.379(3)
C(15)-H(15)	0.9300	C(16)-H(16)	0.9300
C(17)-C(18)	1.378(4)	C(17)-H(17)	0.9300
C(18)-C(19)	1.380(4)	C(18)-H(18)	0.9300
C(19)-C(20)	1.385(3)	C(19)-H(19)	0.9300
C(20)-C(21)	1.391(3)	C(20)-H(20)	0.9300
C(21)-C(22)	1.493(3)	C(22)-C(23)	1.391(3)
C(23)-C(24)	1.381(3)	C(23)-H(23)	0.9300
C(24)-C(25)	1.385(4)	C(24)-H(24)	0.9300
C(25)-C(26)	1.376(3)	C(25)-H(25)	0.9300
C(26)-H(26)	0.9300	C(27)-C(28)	1.550(3)
C(28)-F(3)	1.318(7)	C(28)-F(1)	1.339(5)
C(28)-F(2)	1.351(6)	C(29)-C(30)	1.544(3)
C(31)-C(32)	1.456(4)	C(32)-H(32A)	0.9600
C(32)-H(32B)	0.9600	C(32)-H(32C)	0.9600

Bond Angles (°)

N(1)-Ag(1)-N(4)	154.80(7)	N(1)-Ag(1)-N(3)	131.65(7)
N(4)-Ag(1)-N(3)	72.58(7)	N(1)-Ag(1)-Ag(2)#1	95.43(5)
N(4)-Ag(1)-Ag(2)#1	91.29(5)	N(3)-Ag(1)-Ag(2)#1	89.05(4)
N(2)-Ag(2)-N(6)	161.15(7)	N(2)-Ag(2)-N(5)	125.99(7)
N(6)-Ag(2)-N(5)	72.31(7)	N(2)-Ag(2)-Ag(1)#1	83.18(5)
N(6)-Ag(2)-Ag(1)#1	89.56(5)	N(5)-Ag(2)-Ag(1)#1	99.40(5)
N(2)-Ag(2)-Ag(2)#2	113.37(5)	N(6)-Ag(2)-Ag(2)#2	75.15(5)
N(5)-Ag(2)-Ag(2)#2	70.00(5)	Ag(1)#1-Ag(2)-Ag(2)#2	163.358(10)
C(1)-N(1)-Ag(1)	115.52(13)	C(1)-N(1)-H(1A)	108.4
Ag(1)-N(1)-H(1A)	108.4	C(1)-N(1)-H(1B)	108.4
Ag(1)-N(1)-H(1B)	108.4	H(1A)-N(1)-H(1B)	107.5
C(3)-N(2)-C(4)	118.07(19)	C(3)-N(2)-Ag(2)	121.26(15)
C(4)-N(2)-Ag(2)	120.42(15)	C(7)-N(3)-C(11)	118.8(2)
C(7)-N(3)-Ag(1)	125.02(16)	C(11)-N(3)-Ag(1)	115.83(14)
C(16)-N(4)-C(12)	118.5(2)	C(16)-N(4)-Ag(1)	123.67(15)
C(12)-N(4)-Ag(1)	117.59(15)	C(17)-N(5)-C(21)	118.8(2)
C(17)-N(5)-Ag(2)	125.49(16)	C(21)-N(5)-Ag(2)	113.21(15)
C(26)-N(6)-C(22)	118.7(2)	C(26)-N(6)-Ag(2)	122.06(16)
C(22)-N(6)-Ag(2)	119.26(15)	N(1)-C(1)-C(2)	113.89(18)
N(1)-C(1)-H(1C)	108.8	C(2)-C(1)-H(1C)	108.8
N(1)-C(1)-H(1D)	108.8	C(2)-C(1)-H(1D)	108.8
H(1C)-C(1)-H(1D)	107.7	C(3)-C(2)-C(6)	117.7(2)
C(3)-C(2)-C(1)	120.1(2)	C(6)-C(2)-C(1)	122.1(2)

Table B.24. Continued

N(2)-C(3)-C(2)	123.4(2)	N(2)-C(3)-H(3)	118.3
C(2)-C(3)-H(3)	118.3	N(2)-C(4)-C(5)	122.1(2)
N(2)-C(4)-H(4)	119.0	C(5)-C(4)-H(4)	119.0
C(4)-C(5)-C(6)	119.5(2)	C(4)-C(5)-H(5)	120.3
C(6)-C(5)-H(5)	120.3	C(5)-C(6)-C(2)	119.2(2)
C(5)-C(6)-H(6)	120.4	C(2)-C(6)-H(6)	120.4
N(3)-C(7)-C(8)	122.9(2)	N(3)-C(7)-H(7)	118.6
C(8)-C(7)-H(7)	118.6	C(9)-C(8)-C(7)	118.2(2)
C(9)-C(8)-H(8)	120.9	C(7)-C(8)-H(8)	120.9
C(8)-C(9)-C(10)	119.7(2)	C(8)-C(9)-H(9)	120.1
C(10)-C(9)-H(9)	120.1	C(9)-C(10)-C(11)	118.8(2)
C(9)-C(10)-H(10)	120.6	C(11)-C(10)-H(10)	120.6
N(3)-C(11)-C(10)	121.6(2)	N(3)-C(11)-C(12)	116.35(19)
C(10)-C(11)-C(12)	122.0(2)	N(4)-C(12)-C(13)	121.0(2)
N(4)-C(12)-C(11)	117.5(2)	C(13)-C(12)-C(11)	121.5(2)
C(14)-C(13)-C(12)	119.2(2)	C(14)-C(13)-H(13)	120.4
C(12)-C(13)-H(13)	120.4	C(15)-C(14)-C(13)	119.5(2)
C(15)-C(14)-H(14)	120.3	C(13)-C(14)-H(14)	120.3
C(16)-C(15)-C(14)	117.9(2)	C(16)-C(15)-H(15)	121.1
C(14)-C(15)-H(15)	121.1	N(4)-C(16)-C(15)	123.8(2)
N(4)-C(16)-H(16)	118.1	C(15)-C(16)-H(16)	118.1
N(5)-C(17)-C(18)	123.3(2)	N(5)-C(17)-H(17)	118.4
C(18)-C(17)-H(17)	118.4	C(17)-C(18)-C(19)	118.0(2)
C(17)-C(18)-H(18)	121.0	C(19)-C(18)-H(18)	121.0
C(18)-C(19)-C(20)	119.7(2)	C(18)-C(19)-H(19)	120.2
C(20)-C(19)-H(19)	120.2	C(19)-C(20)-C(21)	119.0(2)
C(19)-C(20)-H(20)	120.5	C(21)-C(20)-H(20)	120.5
N(5)-C(21)-C(20)	121.2(2)	N(5)-C(21)-C(22)	116.7(2)
C(20)-C(21)-C(22)	122.1(2)	N(6)-C(22)-C(23)	121.2(2)
N(6)-C(22)-C(21)	116.84(19)	C(23)-C(22)-C(21)	122.0(2)
C(24)-C(23)-C(22)	119.5(2)	C(24)-C(23)-H(23)	120.3
C(22)-C(23)-H(23)	120.3	C(23)-C(24)-C(25)	119.2(2)
C(23)-C(24)-H(24)	120.4	C(25)-C(24)-H(24)	120.4
C(26)-C(25)-C(24)	118.6(2)	C(26)-C(25)-H(25)	120.7
C(24)-C(25)-H(25)	120.7	N(6)-C(26)-C(25)	122.9(2)
N(6)-C(26)-H(26)	118.6	C(25)-C(26)-H(26)	118.6
O(1)-C(27)-O(2)	131.1(2)	O(1)-C(27)-C(28)	113.6(2)
O(2)-C(27)-C(28)	115.2(2)	F(3)-C(28)-F(1)	107.7(5)
F(3)-C(28)-F(2)	106.2(6)	F(1)-C(28)-F(2)	101.8(4)
F(3)-C(28)-C(27)	117.4(5)	F(1)-C(28)-C(27)	113.7(3)
F(2)-C(28)-C(27)	108.7(4)	O(4)-C(29)-O(3)	130.2(2)
O(4)-C(29)-C(30)	115.2(2)	O(3)-C(29)-C(30)	114.6(2)
F(4)-C(30)-F(5)	105.4(2)	F(4)-C(30)-F(6)	106.3(2)
F(5)-C(30)-F(6)	107.7(2)	F(4)-C(30)-C(29)	113.2(2)
F(5)-C(30)-C(29)	113.3(2)	F(6)-C(30)-C(29)	110.4(2)
N(7)-C(31)-C(32)	179.4(3)	C(31)-C(32)-H(32A)	109.5
C(31)-C(32)-H(32B)	109.5	H(32A)-C(32)-H(32B)	109.5
C(31)-C(32)-H(32C)	109.5	H(32A)-C(32)-H(32C)	109.5
H(32B)-C(32)-H(32C)	109.5		

Table B.24. Continued

Hydrogen Bonds (Å)

N(1)-H(1A)...O(3)#3	2.893(3)	N(1)-H(1B)...O(4)#4	2.868(2)
---------------------	----------	---------------------	----------

Symmetry transformations used to generate equivalent atoms: #1 -x,-y+1,-z+2 #2 -x+1,-y+1,-z+2 #3 x-1,y,z+1 #4 -x+1,-y+1,-z+1

Table B.25 Experimental and statistical crystal data for **6.6**

Empirical formula	C56 H48 Ag4 F12 N12 O12 S4
Formula weight	1868.78
Temperature	110(2) K
Wavelength	0.71073 Å
Crystal system, space group	Triclinic, P-1
Unit cell dimensions	a = 12.5520(10) Å α = 100.968(2) deg. b = 14.0365(10) Å β = 97.572(2) deg. c = 19.7135(16) Å γ = 102.963(2) deg.
Volume	3267.2(4) Å ³
Z, Calculated density	2, 1.900 Mg/m ³
Absorption coefficient	1.413 mm ⁻¹
F(000)	1848
Crystal size	0.238 x 0.187 x 0.18 mm
θ range for data collection	2.06 to 26.51 deg.
Limiting indices	-15<=h<=15, -17<=k<=17, -24<=l<=24
Reflections collected / unique	49261 / 13372 [R(int) = 0.0340]
Completeness to θ = 25.00	99.5 %
Absorption correction	multi-scan (SADABS)
Refinement method	Full-matrix least-squares on F ²
Data / restraints / parameters	13372 / 0 / 901
Goodness-of-fit on F ²	1.021
Final R indices [I>2σ(I)]	R1 = 0.0279, wR2 = 0.0679
R indices (all data)	R1 = 0.0357, wR2 = 0.0724
Largest diff. peak and hole	2.194 and -0.935 e.Å ⁻³

Bond Lengths (Å)

Ag(1)-N(1)	2.166(2)	Ag(1)-N(3)	2.260(2)
Ag(1)-N(4)	2.341(2)	Ag(1)-Ag(2)#1	3.0846(3)
Ag(2)-N(2)	2.141(2)	Ag(2)-N(6)	2.221(2)
Ag(2)-N(5)	2.357(2)	Ag(2)-Ag(1)#1	3.0846(3)
Ag(3)-N(7)	2.150(2)	Ag(3)-N(9)	2.233(2)
Ag(3)-N(10)	2.350(3)	Ag(4)-N(8)	2.139(2)
Ag(4)-N(12)	2.275(2)	Ag(4)-N(11)	2.277(2)
Ag(4)-Ag(4)#2	3.0399(4)	S(1)-O(2)	1.431(2)
S(1)-O(1)	1.444(2)	S(1)-O(3)	1.444(2)
S(1)-C(53)	1.822(3)	S(2)-O(4)	1.440(2)
S(2)-O(6)	1.445(2)	S(2)-O(5)	1.447(2)
S(2)-C(54)	1.824(3)	S(3)-O(8)	1.430(2)
S(3)-O(9)	1.433(2)	S(3)-O(7)	1.444(2)
S(3)-C(55)	1.822(4)	S(4)-O(12)	1.439(2)
S(4)-O(11)	1.440(2)	S(4)-O(10)	1.444(2)
S(4)-C(56)	1.824(3)	F(1)-C(53)	1.322(4)

Table B.25. Continued

F(2)-C(53)	1.335(4)	F(3)-C(53)	1.326(4)
F(4)-C(54)	1.333(3)	F(5)-C(54)	1.336(3)
F(6)-C(54)	1.337(3)	F(7)-C(55)	1.328(4)
F(8)-C(55)	1.331(4)	F(9)-C(55)	1.335(4)
F(10)-C(56)	1.339(3)	F(11)-C(56)	1.337(3)
F(12)-C(56)	1.340(3)	N(1)-C(1)	1.485(3)
N(1)-H(1A)	0.9000	N(1)-H(1B)	0.9000
N(2)-C(3)	1.344(3)	N(2)-C(4)	1.348(3)
N(3)-C(7)	1.347(4)	N(3)-C(11)	1.350(3)
N(4)-C(16)	1.333(4)	N(4)-C(12)	1.344(3)
N(5)-C(17)	1.338(4)	N(5)-C(21)	1.353(3)
N(6)-C(26)	1.343(4)	N(6)-C(22)	1.347(3)
N(7)-C(27)	1.476(3)	N(7)-H(7A)	0.9000
N(7)-H(7B)	0.9000	N(8)-C(29)	1.344(3)
N(8)-C(30)	1.349(3)	N(9)-C(33)	1.347(4)
N(9)-C(37)	1.347(3)	N(10)-C(42)	1.336(4)
N(10)-C(38)	1.350(4)	N(11)-C(43)	1.345(4)
N(11)-C(47)	1.348(3)	N(12)-C(52)	1.340(4)
N(12)-C(48)	1.353(3)	C(1)-C(2)	1.511(4)
C(1)-H(1C)	0.9700	C(1)-H(1D)	0.9700
C(2)-C(6)	1.383(4)	C(2)-C(3)	1.387(4)
C(3)-H(3)	0.9300	C(4)-C(5)	1.370(4)
C(4)-H(4)	0.9300	C(5)-C(6)	1.385(4)
C(5)-H(5)	0.9300	C(6)-H(6)	0.9300
C(7)-C(8)	1.374(4)	C(7)-H(7)	0.9300
C(8)-C(9)	1.379(4)	C(8)-H(8)	0.9300
C(9)-C(10)	1.384(4)	C(9)-H(9)	0.9300
C(10)-C(11)	1.388(4)	C(10)-H(10)	0.9300
C(11)-C(12)	1.496(4)	C(12)-C(13)	1.392(4)
C(13)-C(14)	1.378(4)	C(13)-H(13)	0.9300
C(14)-C(15)	1.377(4)	C(14)-H(14)	0.9300
C(15)-C(16)	1.384(4)	C(15)-H(15)	0.9300
C(16)-H(16)	0.9300	C(17)-C(18)	1.384(4)
C(17)-H(17)	0.9300	C(18)-C(19)	1.382(4)
C(18)-H(18)	0.9300	C(19)-C(20)	1.378(4)
C(19)-H(19)	0.9300	C(20)-C(21)	1.391(4)
C(20)-H(20)	0.9300	C(21)-C(22)	1.490(4)
C(22)-C(23)	1.395(4)	C(23)-C(24)	1.381(4)
C(23)-H(23)	0.9300	C(24)-C(25)	1.377(4)
C(24)-H(24)	0.9300	C(25)-C(26)	1.378(4)
C(25)-H(25)	0.9300	C(26)-H(26)	0.9300
C(27)-C(28)	1.510(4)	C(27)-H(27A)	0.9700
C(27)-H(27B)	0.9700	C(28)-C(32)	1.385(4)
C(28)-C(29)	1.387(4)	C(29)-H(29)	0.9300
C(30)-C(31)	1.375(4)	C(30)-H(30)	0.9300
C(31)-C(32)	1.377(4)	C(31)-H(31)	0.9300
C(32)-H(32)	0.9300	C(33)-C(34)	1.383(4)
C(33)-H(33)	0.9300	C(34)-C(35)	1.378(4)
C(34)-H(34)	0.9300	C(35)-C(36)	1.384(4)
C(35)-H(35)	0.9300	C(36)-C(37)	1.395(4)
C(36)-H(36)	0.9300	C(37)-C(38)	1.487(4)
C(38)-C(39)	1.379(4)	C(39)-C(40)	1.384(5)
C(39)-H(39)	0.9300	C(40)-C(41)	1.368(5)
C(40)-H(40)	0.9300	C(41)-C(42)	1.376(5)

Table B.25. Continued

C(41)-H(41)	0.9300	C(42)-H(42)	0.9300
C(43)-C(44)	1.382(4)	C(43)-H(43)	0.9300
C(44)-C(45)	1.372(4)	C(44)-H(44)	0.9300
C(45)-C(46)	1.384(4)	C(45)-H(45)	0.9300
C(46)-C(47)	1.394(4)	C(46)-H(46)	0.9300
C(47)-C(48)	1.495(4)	C(48)-C(49)	1.388(4)
C(49)-C(50)	1.381(4)	C(49)-H(49)	0.9300
C(50)-C(51)	1.385(4)	C(50)-H(50)	0.9300
C(51)-C(52)	1.381(4)	C(51)-H(51)	0.9300
C(52)-H(52)	0.9300		
Bond Angles (°)			
N(1)-Ag(1)-N(3)	155.92(8)	F(12)-C(56)-S(4)	112.24(19)
N(1)-Ag(1)-N(4)	131.85(8)	N(3)-Ag(1)-N(4)	72.14(8)
N(1)-Ag(1)-Ag(2)#1	99.96(6)	N(3)-Ag(1)-Ag(2)#1	79.60(6)
N(4)-Ag(1)-Ag(2)#1	81.63(6)	N(2)-Ag(2)-N(6)	153.20(8)
N(2)-Ag(2)-N(5)	132.81(8)	N(6)-Ag(2)-N(5)	73.00(8)
N(2)-Ag(2)-Ag(1)#1	85.77(6)	N(6)-Ag(2)-Ag(1)#1	91.92(6)
N(5)-Ag(2)-Ag(1)#1	109.17(5)	N(7)-Ag(3)-N(9)	152.96(9)
N(7)-Ag(3)-N(10)	134.85(9)	N(9)-Ag(3)-N(10)	72.15(8)
N(8)-Ag(4)-N(12)	142.39(8)	N(8)-Ag(4)-N(11)	143.89(8)
N(12)-Ag(4)-N(11)	73.10(8)	N(8)-Ag(4)-Ag(4)#2	94.98(6)
N(12)-Ag(4)-Ag(4)#2	83.48(6)	N(11)-Ag(4)-Ag(4)#2	96.34(6)
O(2)-S(1)-O(1)	115.40(14)	O(2)-S(1)-O(3)	115.47(13)
O(1)-S(1)-O(3)	113.51(12)	O(2)-S(1)-C(53)	103.00(15)
O(1)-S(1)-C(53)	104.25(14)	O(3)-S(1)-C(53)	102.98(14)
O(4)-S(2)-O(6)	115.65(12)	O(4)-S(2)-O(5)	114.95(12)
O(6)-S(2)-O(5)	114.23(12)	O(4)-S(2)-C(54)	102.78(13)
O(6)-S(2)-C(54)	102.99(13)	O(5)-S(2)-C(54)	103.86(13)
O(8)-S(3)-O(9)	115.37(15)	O(8)-S(3)-O(7)	115.24(15)
O(9)-S(3)-O(7)	114.56(13)	O(8)-S(3)-C(55)	103.12(17)
O(9)-S(3)-C(55)	103.53(16)	O(7)-S(3)-C(55)	102.50(14)
O(12)-S(4)-O(11)	115.10(13)	O(12)-S(4)-O(10)	115.24(13)
O(11)-S(4)-O(10)	115.28(13)	O(12)-S(4)-C(56)	102.26(13)
O(11)-S(4)-C(56)	102.80(13)	O(10)-S(4)-C(56)	103.47(13)
C(1)-N(1)-Ag(1)	115.33(16)	C(1)-N(1)-H(1A)	108.4
Ag(1)-N(1)-H(1A)	108.4	C(1)-N(1)-H(1B)	108.4
Ag(1)-N(1)-H(1B)	108.4	H(1A)-N(1)-H(1B)	107.5
C(3)-N(2)-C(4)	117.7(2)	C(3)-N(2)-Ag(2)	121.62(17)
C(4)-N(2)-Ag(2)	120.51(18)	C(7)-N(3)-C(11)	118.4(2)
C(7)-N(3)-Ag(1)	123.19(18)	C(11)-N(3)-Ag(1)	118.37(18)
C(16)-N(4)-C(12)	118.9(2)	C(16)-N(4)-Ag(1)	125.28(18)
C(12)-N(4)-Ag(1)	115.86(18)	C(17)-N(5)-C(21)	118.1(2)
C(17)-N(5)-Ag(2)	127.78(19)	C(21)-N(5)-Ag(2)	114.05(17)
C(26)-N(6)-C(22)	119.0(2)	C(26)-N(6)-Ag(2)	122.50(18)
C(22)-N(6)-Ag(2)	118.47(18)	C(27)-N(7)-Ag(3)	113.75(16)
C(27)-N(7)-H(7A)	108.8	Ag(3)-N(7)-H(7A)	108.8
C(27)-N(7)-H(7B)	108.8	Ag(3)-N(7)-H(7B)	108.8
H(7A)-N(7)-H(7B)	107.7	C(29)-N(8)-C(30)	118.0(2)
C(29)-N(8)-Ag(4)	120.10(18)	C(30)-N(8)-Ag(4)	121.95(18)
C(33)-N(9)-C(37)	119.3(2)	C(33)-N(9)-Ag(3)	121.85(18)
C(37)-N(9)-Ag(3)	118.75(18)	C(42)-N(10)-C(38)	118.4(3)
C(42)-N(10)-Ag(3)	126.2(2)	C(38)-N(10)-Ag(3)	115.22(19)

Table B.25. Continued

C(43)-N(11)-C(47)	118.6(2)	C(43)-N(11)-Ag(4)	124.42(19)
C(47)-N(11)-Ag(4)	116.56(18)	C(52)-N(12)-C(48)	118.4(2)
C(52)-N(12)-Ag(4)	125.12(19)	C(48)-N(12)-Ag(4)	116.46(17)
N(1)-C(1)-C(2)	114.1(2)	N(1)-C(1)-H(1C)	108.7
C(2)-C(1)-H(1C)	108.7	N(1)-C(1)-H(1D)	108.7
C(2)-C(1)-H(1D)	108.7	H(1C)-C(1)-H(1D)	107.6
C(6)-C(2)-C(3)	117.4(2)	C(6)-C(2)-C(1)	121.5(3)
C(3)-C(2)-C(1)	121.1(2)	N(2)-C(3)-C(2)	123.6(2)
N(2)-C(3)-H(3)	118.2	C(2)-C(3)-H(3)	118.2
N(2)-C(4)-C(5)	122.4(2)	N(2)-C(4)-H(4)	118.8
C(5)-C(4)-H(4)	118.8	C(4)-C(5)-C(6)	119.2(3)
C(4)-C(5)-H(5)	120.4	C(6)-C(5)-H(5)	120.4
C(2)-C(6)-C(5)	119.7(3)	C(2)-C(6)-H(6)	120.1
C(5)-C(6)-H(6)	120.1	N(3)-C(7)-C(8)	123.1(3)
N(3)-C(7)-H(7)	118.4	C(8)-C(7)-H(7)	118.4
C(7)-C(8)-C(9)	118.5(3)	C(7)-C(8)-H(8)	120.7
C(9)-C(8)-H(8)	120.7	C(8)-C(9)-C(10)	119.2(3)
C(8)-C(9)-H(9)	120.4	C(10)-C(9)-H(9)	120.4
C(9)-C(10)-C(11)	119.5(3)	C(9)-C(10)-H(10)	120.3
C(11)-C(10)-H(10)	120.3	N(3)-C(11)-C(10)	121.2(3)
N(3)-C(11)-C(12)	116.8(2)	C(10)-C(11)-C(12)	121.9(2)
N(4)-C(12)-C(13)	121.2(3)	N(4)-C(12)-C(11)	116.8(2)
C(13)-C(12)-C(11)	122.0(2)	C(14)-C(13)-C(12)	119.1(3)
C(14)-C(13)-H(13)	120.4	C(12)-C(13)-H(13)	120.4
C(15)-C(14)-C(13)	119.7(3)	C(15)-C(14)-H(14)	120.2
C(13)-C(14)-H(14)	120.2	C(14)-C(15)-C(16)	118.0(3)
C(14)-C(15)-H(15)	121.0	C(16)-C(15)-H(15)	121.0
N(4)-C(16)-C(15)	123.1(3)	N(4)-C(16)-H(16)	118.5
C(15)-C(16)-H(16)	118.5	N(5)-C(17)-C(18)	123.3(3)
N(5)-C(17)-H(17)	118.4	C(18)-C(17)-H(17)	118.4
C(19)-C(18)-C(17)	118.6(3)	C(19)-C(18)-H(18)	120.7
C(17)-C(18)-H(18)	120.7	C(20)-C(19)-C(18)	118.7(3)
C(20)-C(19)-H(19)	120.7	C(18)-C(19)-H(19)	120.7
C(19)-C(20)-C(21)	119.9(3)	C(19)-C(20)-H(20)	120.0
C(21)-C(20)-H(20)	120.0	N(5)-C(21)-C(20)	121.3(3)
N(5)-C(21)-C(22)	116.9(2)	C(20)-C(21)-C(22)	121.8(2)
N(6)-C(22)-C(23)	120.8(2)	N(6)-C(22)-C(21)	117.6(2)
C(23)-C(22)-C(21)	121.6(2)	C(24)-C(23)-C(22)	119.5(2)
C(24)-C(23)-H(23)	120.2	C(22)-C(23)-H(23)	120.2
C(25)-C(24)-C(23)	119.1(3)	C(25)-C(24)-H(24)	120.4
C(23)-C(24)-H(24)	120.4	C(24)-C(25)-C(26)	118.8(3)
C(24)-C(25)-H(25)	120.6	C(26)-C(25)-H(25)	120.6
N(6)-C(26)-C(25)	122.7(3)	N(6)-C(26)-H(26)	118.6
C(25)-C(26)-H(26)	118.6	N(7)-C(27)-C(28)	115.0(2)
N(7)-C(27)-H(27A)	108.5	C(28)-C(27)-H(27A)	108.5
N(7)-C(27)-H(27B)	108.5	C(28)-C(27)-H(27B)	108.5
H(27A)-C(27)-H(27B)	107.5	C(32)-C(28)-C(29)	117.6(2)
C(32)-C(28)-C(27)	120.7(2)	C(29)-C(28)-C(27)	121.6(2)
N(8)-C(29)-C(28)	123.1(2)	N(8)-C(29)-H(29)	118.5
C(28)-C(29)-H(29)	118.5	N(8)-C(30)-C(31)	122.4(2)
N(8)-C(30)-H(30)	118.8	C(31)-C(30)-H(30)	118.8
C(30)-C(31)-C(32)	118.9(3)	C(30)-C(31)-H(31)	120.5
C(32)-C(31)-H(31)	120.5	C(31)-C(32)-C(28)	120.0(3)
C(31)-C(32)-H(32)	120.0	C(28)-C(32)-H(32)	120.0

Table B.25. Continued

N(9)-C(33)-C(34)	122.5(3)	N(9)-C(33)-H(33)	118.8
C(34)-C(33)-H(33)	118.8	C(35)-C(34)-C(33)	118.5(3)
C(35)-C(34)-H(34)	120.7	C(33)-C(34)-H(34)	120.7
C(34)-C(35)-C(36)	119.4(3)	C(34)-C(35)-H(35)	120.3
C(36)-C(35)-H(35)	120.3	C(35)-C(36)-C(37)	119.5(3)
C(35)-C(36)-H(36)	120.3	C(37)-C(36)-H(36)	120.3
N(9)-C(37)-C(36)	120.7(3)	N(9)-C(37)-C(38)	117.3(2)
C(36)-C(37)-C(38)	122.0(3)	N(10)-C(38)-C(39)	121.2(3)
N(10)-C(38)-C(37)	116.2(2)	C(39)-C(38)-C(37)	122.6(3)
C(38)-C(39)-C(40)	119.7(3)	C(38)-C(39)-H(39)	120.1
C(40)-C(39)-H(39)	120.1	C(41)-C(40)-C(39)	118.9(3)
C(41)-C(40)-H(40)	120.6	C(39)-C(40)-H(40)	120.6
C(40)-C(41)-C(42)	118.8(3)	C(40)-C(41)-H(41)	120.6
C(42)-C(41)-H(41)	120.6	N(10)-C(42)-C(41)	123.0(3)
N(10)-C(42)-H(42)	118.5	C(41)-C(42)-H(42)	118.5
N(11)-C(43)-C(44)	123.0(3)	N(11)-C(43)-H(43)	118.5
C(44)-C(43)-H(43)	118.5	C(45)-C(44)-C(43)	118.3(3)
C(45)-C(44)-H(44)	120.9	C(43)-C(44)-H(44)	120.9
C(44)-C(45)-C(46)	119.7(3)	C(44)-C(45)-H(45)	120.1
C(46)-C(45)-H(45)	120.1	C(45)-C(46)-C(47)	119.2(3)
C(45)-C(46)-H(46)	120.4	C(47)-C(46)-H(46)	120.4
N(11)-C(47)-C(46)	121.2(3)	N(11)-C(47)-C(48)	116.6(2)
C(46)-C(47)-C(48)	122.2(2)	N(12)-C(48)-C(49)	121.3(3)
N(12)-C(48)-C(47)	116.8(2)	C(49)-C(48)-C(47)	121.8(2)
C(50)-C(49)-C(48)	119.5(3)	C(50)-C(49)-H(49)	120.2
C(48)-C(49)-H(49)	120.2	C(49)-C(50)-C(51)	119.3(3)
C(49)-C(50)-H(50)	120.4	C(51)-C(50)-H(50)	120.4
C(52)-C(51)-C(50)	118.1(3)	C(52)-C(51)-H(51)	120.9
C(50)-C(51)-H(51)	120.9	N(12)-C(52)-C(51)	123.3(3)
N(12)-C(52)-H(52)	118.3	C(51)-C(52)-H(52)	118.3
F(1)-C(53)-F(3)	107.7(3)	F(1)-C(53)-F(2)	107.3(3)
F(3)-C(53)-F(2)	107.6(3)	F(1)-C(53)-S(1)	111.8(2)
F(3)-C(53)-S(1)	111.1(2)	F(2)-C(53)-S(1)	111.1(2)
F(4)-C(54)-F(5)	107.1(2)	F(4)-C(54)-F(6)	107.9(2)
F(5)-C(54)-F(6)	108.1(2)	F(4)-C(54)-S(2)	111.7(2)
F(5)-C(54)-S(2)	110.65(19)	F(6)-C(54)-S(2)	111.2(2)
F(7)-C(55)-F(8)	108.3(3)	F(7)-C(55)-F(9)	107.5(3)
F(8)-C(55)-F(9)	106.7(3)	F(7)-C(55)-S(3)	111.1(3)
F(8)-C(55)-S(3)	112.1(2)	F(9)-C(55)-S(3)	110.9(3)
F(11)-C(56)-F(10)	107.4(2)	F(11)-C(56)-F(12)	107.1(2)
F(10)-C(56)-F(12)	107.4(2)	F(11)-C(56)-S(4)	110.77(19)
F(10)-C(56)-S(4)	111.7(2)		

Hydrogen Bonds (Å)

N(1)-H(1A)...O(3)#1	3.073(3)	N(1)-H(1B)...O(1)	3.061(3)
N(7)-H(7A)...O(5)#3	3.208(3)	N(7)-H(7B)...O(7)	3.034(3)

Symmetry transformations used to generate equivalent atoms: #1 -x+1,-y,-z+2 #2 -x+1,-y+2,-z+1 #3 x-1,y,z

Table B.26 Experimental and statistical crystal data for **7.1**

Empirical formula	C11 H14 Ag F3 N4 O3 S
Formula weight	447.19
Temperature	110(2) K
Wavelength	0.71073 Å
Crystal system, space group	Monoclinic, P2(1)/c
Unit cell dimensions	a = 6.6871(7) Å α = 90 deg. b = 25.806(2) Å β = 92.135(3) deg. c = 9.3785(8) Å γ = 90 deg.
Volume	1617.3(3) Å ³
Z, Calculated density	4, 1.837 Mg/m ³
Absorption coefficient	1.424 mm ⁻¹
F(000)	888
Crystal size	0.171 x 0.109 x 0.047 mm
θ range for data collection	2.69 to 32.15 deg.
Limiting indices	-7<=h<=9, -38<=k<=30, -12<=l<=11
Reflections collected / unique	26679 / 4711 [R(int) = 0.0318]
Completeness to θ = 25.00	99.9 %
Absorption correction	Semi-empirical from equivalents
Refinement method	Full-matrix least-squares on F ²
Data / restraints / parameters	4711 / 0 / 216
Goodness-of-fit on F ²	1.075
Final R indices [I>2σ(I)]	R1 = 0.0344, wR2 = 0.0538
R indices (all data)	R1 = 0.0493, wR2 = 0.0578
Largest diff. peak and hole	0.552 and -0.568 e.Å ⁻³

Bond Lengths (Å)

Ag(1)-N(1)	2.1583(17)	Ag(1)-N(2)#1	2.1642(18)
S(1)-O(2)	1.428(2)	S(1)-O(3)	1.4419(17)
S(1)-O(1)	1.4447(19)	S(1)-C(7)	1.814(3)
N(1)-C(6)	1.342(3)	N(1)-C(4)	1.343(3)
N(2)-C(1)	1.466(3)	N(2)-Ag(1)#2	2.1642(18)
N(2)-H(1)	0.86(3)	N(2)-H(2)	0.85(3)
N(3)-C(8)	1.139(3)	N(4)-C(10)	1.138(3)
C(1)-C(2)	1.518(3)	C(1)-H(1A)	0.9900
C(1)-H(1B)	0.9900	C(2)-C(3)	1.382(3)
C(2)-C(5)	1.392(3)	C(3)-C(4)	1.388(3)
C(3)-H(3)	0.9500	C(4)-H(4)	0.9500
C(5)-C(6)	1.383(3)	C(5)-H(5)	0.9500
C(6)-H(6)	0.9500	C(7)-F(1)	1.322(3)
C(7)-F(2)	1.332(3)	C(7)-F(3)	1.339(3)
C(8)-C(9)	1.458(4)	C(9)-H(9A)	0.9800
C(9)-H(9B)	0.9800	C(9)-H(9C)	0.9800
C(10)-C(11)	1.453(4)	C(11)-H(11A)	0.9800
C(11)-H(11B)	0.9800	C(11)-H(11C)	0.9800

Bond Angles (°)

N(1)-Ag(1)-N(2)#1	172.73(7)	O(2)-S(1)-O(3)	115.52(12)
O(2)-S(1)-O(1)	114.59(14)	O(3)-S(1)-O(1)	114.79(11)
O(2)-S(1)-C(7)	103.73(13)	O(3)-S(1)-C(7)	103.01(11)
O(1)-S(1)-C(7)	102.77(12)	C(6)-N(1)-C(4)	117.42(18)
C(6)-N(1)-Ag(1)	121.62(14)	C(4)-N(1)-Ag(1)	120.68(14)
C(1)-N(2)-Ag(1)#2	112.42(13)	C(1)-N(2)-H(1)	111.6(17)

Table B.26. Continued

Ag(1)#2-N(2)-H(1)	109.6(17)	C(1)-N(2)-H(2)	109.6(17)
Ag(1)#2-N(2)-H(2)	105.2(17)	H(1)-N(2)-H(2)	108(2)
N(2)-C(1)-C(2)	116.70(18)	N(2)-C(1)-H(1A)	108.1
C(2)-C(1)-H(1A)	108.1	N(2)-C(1)-H(1B)	108.1
C(2)-C(1)-H(1B)	108.1	H(1A)-C(1)-H(1B)	107.3
C(3)-C(2)-C(5)	117.91(19)	C(3)-C(2)-C(1)	123.63(19)
C(5)-C(2)-C(1)	118.46(19)	C(2)-C(3)-C(4)	119.1(2)
C(2)-C(3)-H(3)	120.5	C(4)-C(3)-H(3)	120.5
N(1)-C(4)-C(3)	123.2(2)	N(1)-C(4)-H(4)	118.4
C(3)-C(4)-H(4)	118.4	C(6)-C(5)-C(2)	119.6(2)
C(6)-C(5)-H(5)	120.2	C(2)-C(5)-H(5)	120.2
N(1)-C(6)-C(5)	122.8(2)	N(1)-C(6)-H(6)	118.6
C(5)-C(6)-H(6)	118.6	F(1)-C(7)-F(2)	107.2(2)
F(1)-C(7)-F(3)	107.3(2)	F(2)-C(7)-F(3)	107.9(2)
F(1)-C(7)-S(1)	112.01(18)	F(2)-C(7)-S(1)	110.86(18)
F(3)-C(7)-S(1)	111.35(17)	N(3)-C(8)-C(9)	179.6(3)
C(8)-C(9)-H(9A)	109.5	C(8)-C(9)-H(9B)	109.5
H(9A)-C(9)-H(9B)	109.5	C(8)-C(9)-H(9C)	109.5
H(9A)-C(9)-H(9C)	109.5	H(9B)-C(9)-H(9C)	109.5
N(4)-C(10)-C(11)	179.0(3)	C(10)-C(11)-H(11A)	109.5
C(10)-C(11)-H(11B)	109.5	H(11A)-C(11)-H(11B)	109.5
C(10)-C(11)-H(11C)	109.5	H(11A)-C(11)-H(11C)	109.5
H(11B)-C(11)-H(11C)	109.5		
Hydrogen Bonds (Å)			
N(2)-H(1)...O(1)#3	3.134(3)	N(2)-H(2)...O(3)#4	2.986(3)

Symmetry transformations used to generate equivalent atoms: #1 x,y,z-1 #2 x,y,z+1 #3 -x+1,-y+1,-z+2
#4 -x,-y+1,-z+2

Table B.27 Experimental and statistical crystal data for 7.2

Empirical formula	C16 H16 Ag2 F6 N4 O4
Formula weight	658.07
Temperature	110(2) K
Wavelength	0.71073 Å
Crystal system, space group	Triclinic, P-1
Unit cell dimensions	a = 9.3793(7) Å α = 95.210(2) deg. b = 10.5770(7) Å β = 91.393(2) deg. c = 11.6814(8) Å γ = 114.234(2) deg.
Volume	1049.94(13) Å ³
Z, Calculated density	2, 2.082 Mg/m ³
Absorption coefficient	1.949 mm ⁻¹
F(000)	640
Crystal size	0.11 x 0.10 x 0.07 mm
θ range for data collection	2.39 to 26.35 deg.
Limiting indices	-11<=h<=11, -13<=k<=13, -14<=l<=14
Reflections collected / unique	15985 / 4258 [R(int) = 0.0325]
Completeness to θ = 26.35	99.5 %
Absorption correction	multi-scan (SADABS)
Max. and min. transmission	0.8724 and 0.8098
Refinement method	Full-matrix least-squares on F ²
Data / restraints / parameters	4258 / 0 / 289
Goodness-of-fit on F ²	1.073
Final R indices [I>2σ(I)]	R1 = 0.0248, wR2 = 0.0585
R indices (all data)	R1 = 0.0328, wR2 = 0.0609
Largest diff. peak and hole	1.478 and -0.536 e.Å ⁻³

Bond Lengths (Å)

Ag(1)-N(2)#1	2.143(2)	Ag(1)-N(1)	2.146(2)
Ag(2)-N(3)	2.157(2)	Ag(2)-N(4)#2	2.173(2)
Ag(2)-O(1)	2.565(2)	F(1)-C(14)	1.327(4)
F(2)-C(14)	1.324(4)	F(3)-C(14)	1.322(4)
F(4)-C(16)	1.339(4)	F(5)-C(16)	1.341(3)
F(6)-C(16)	1.323(4)	O(1)-C(13)	1.232(4)
O(2)-C(13)	1.246(4)	O(3)-C(15)	1.243(3)
O(4)-C(15)	1.244(3)	N(1)-C(1)	1.332(4)
N(1)-C(5)	1.346(4)	N(2)-C(6)	1.467(4)
N(2)-Ag(1)#2	2.143(2)	N(2)-H(2A)	0.9000
N(2)-H(2B)	0.9000	N(3)-C(7)	1.337(4)
N(3)-C(11)	1.343(4)	N(4)-C(12)	1.479(4)
N(4)-Ag(2)#1	2.173(2)	N(4)-H(4A)	0.9000
N(4)-H(4B)	0.9000	C(1)-C(2)	1.382(4)
C(1)-H(1)	0.9300	C(2)-C(3)	1.392(4)
C(2)-H(2)	0.9300	C(3)-C(4)	1.384(4)
C(3)-C(6)	1.505(4)	C(4)-C(5)	1.378(4)
C(4)-H(4)	0.9300	C(5)-H(5)	0.9300
C(6)-H(6A)	0.9700	C(6)-H(6B)	0.9700
C(7)-C(8)	1.374(4)	C(7)-H(7)	0.9300
C(8)-C(9)	1.400(4)	C(8)-H(8)	0.9300
C(9)-C(10)	1.383(4)	C(9)-C(12)	1.506(4)
C(10)-C(11)	1.385(4)	C(10)-H(10)	0.9300
C(11)-H(11)	0.9300	C(12)-H(12A)	0.9700
C(12)-H(12B)	0.9700	C(13)-C(14)	1.538(5)
C(15)-C(16)	1.551(4)		

Table B.27. Continued

Bond Angles ($^{\circ}$)

N(2)#1-Ag(1)-N(1)	170.68(9)	F(5)-C(16)-C(15)	109.2(2)
N(3)-Ag(2)-N(4)#2	169.99(9)	N(3)-Ag(2)-O(1)	103.51(8)
N(4)#2-Ag(2)-O(1)	81.52(8)	C(13)-O(1)-Ag(2)	127.82(19)
C(1)-N(1)-C(5)	117.4(2)	C(1)-N(1)-Ag(1)	125.3(2)
C(5)-N(1)-Ag(1)	117.30(19)	C(6)-N(2)-Ag(1)#2	114.46(17)
C(6)-N(2)-H(2A)	108.6	Ag(1)#2-N(2)-H(2A)	108.6
C(6)-N(2)-H(2B)	108.6	Ag(1)#2-N(2)-H(2B)	108.6
H(2A)-N(2)-H(2B)	107.6	C(7)-N(3)-C(11)	117.1(2)
C(7)-N(3)-Ag(2)	124.26(19)	C(11)-N(3)-Ag(2)	118.6(2)
C(12)-N(4)-Ag(2)#1	110.83(16)	C(12)-N(4)-H(4A)	109.5
Ag(2)#1-N(4)-H(4A)	109.5	C(12)-N(4)-H(4B)	109.5
Ag(2)#1-N(4)-H(4B)	109.5	H(4A)-N(4)-H(4B)	108.1
N(1)-C(1)-C(2)	123.5(3)	N(1)-C(1)-H(1)	118.3
C(2)-C(1)-H(1)	118.3	C(1)-C(2)-C(3)	119.4(3)
C(1)-C(2)-H(2)	120.3	C(3)-C(2)-H(2)	120.3
C(4)-C(3)-C(2)	116.8(3)	C(4)-C(3)-C(6)	118.8(3)
C(2)-C(3)-C(6)	124.4(3)	C(5)-C(4)-C(3)	120.7(3)
C(5)-C(4)-H(4)	119.7	C(3)-C(4)-H(4)	119.7
N(1)-C(5)-C(4)	122.2(3)	N(1)-C(5)-H(5)	118.9
C(4)-C(5)-H(5)	118.9	N(2)-C(6)-C(3)	117.0(2)
N(2)-C(6)-H(6A)	108.0	C(3)-C(6)-H(6A)	108.0
N(2)-C(6)-H(6B)	108.0	C(3)-C(6)-H(6B)	108.0
H(6A)-C(6)-H(6B)	107.3	N(3)-C(7)-C(8)	123.8(3)
N(3)-C(7)-H(7)	118.1	C(8)-C(7)-H(7)	118.1
C(7)-C(8)-C(9)	119.5(3)	C(7)-C(8)-H(8)	120.3
C(9)-C(8)-H(8)	120.3	C(10)-C(9)-C(8)	116.7(3)
C(10)-C(9)-C(12)	119.8(3)	C(8)-C(9)-C(12)	123.4(3)
C(9)-C(10)-C(11)	120.3(3)	C(9)-C(10)-H(10)	119.8
C(11)-C(10)-H(10)	119.8	N(3)-C(11)-C(10)	122.6(3)
N(3)-C(11)-H(11)	118.7	C(10)-C(11)-H(11)	118.7
N(4)-C(12)-C(9)	115.9(2)	N(4)-C(12)-H(12A)	108.3
C(9)-C(12)-H(12A)	108.3	N(4)-C(12)-H(12B)	108.3
C(9)-C(12)-H(12B)	108.3	H(12A)-C(12)-H(12B)	107.4
O(1)-C(13)-O(2)	129.9(3)	O(1)-C(13)-C(14)	116.9(3)
O(2)-C(13)-C(14)	113.2(3)	F(3)-C(14)-F(2)	105.4(3)
F(3)-C(14)-F(1)	106.7(3)	F(2)-C(14)-F(1)	107.4(3)
F(3)-C(14)-C(13)	111.6(3)	F(2)-C(14)-C(13)	113.6(3)
F(1)-C(14)-C(13)	111.7(3)	O(3)-C(15)-O(4)	129.8(3)
O(3)-C(15)-C(16)	114.4(2)	O(4)-C(15)-C(16)	115.6(3)
F(6)-C(16)-F(4)	106.8(3)	F(6)-C(16)-F(5)	107.2(3)
F(4)-C(16)-F(5)	106.5(3)	F(6)-C(16)-C(15)	114.2(2)
F(4)-C(16)-C(15)	112.5(3)		

Hydrogen Bonds (\AA)

N(2)-H(2A)...O(3)#3	2.859(3)	N(2)-H(2B)...O(2)#4	2.837(3)
N(4)-H(4A)...O(4)#5	2.973(3)	N(4)-H(4B)...O(4)#6	2.979(3)

Symmetry transformations used to generate equivalent atoms: #1 x+1,y,z #2 x-1,y,z #3 -x,-y+1,-z+1
#4 -x,-y+2,-z+1 #5 x,y,z-1 #6 -x+1,-y+1,-z+1

Table B.28 Experimental and statistical crystal data for 7.3

Empirical formula	C14 H16 Ag F3 N4 O2
Formula weight	437.18
Temperature	110(2) K
Wavelength	0.71073 Å
Crystal system, space group	Monoclinic, C2/m
Unit cell dimensions	a = 12.4623(14) Å α = 90 deg. b = 18.273(2) Å β = 92.986(4) deg. c = 7.4106(8) Å γ = 90 deg.
Volume	1685.2(3) Å ³
Z, Calculated density	4, 1.723 Mg/m ³
Absorption coefficient	1.241 mm ⁻¹
F(000)	872
Crystal size	0.09 x 0.06 x 0.06 mm
θ range for data collection	1.98 to 25.30 deg.
Limiting indices	-14<=h<=14, -21<=k<=21, -8<=l<=8
Reflections collected / unique	7120 / 1572 [R(int) = 0.0301]
Completeness to θ = 25.30	99.2 %
Absorption correction	multi-scan (SADABS)
Max. and min. transmission	0.9349 and 0.8933
Refinement method	Full-matrix least-squares on F ²
Data / restraints / parameters	1572 / 0 / 133
Goodness-of-fit on F ²	1.012
Final R indices [I>2σ(I)]	R1 = 0.0288, wR2 = 0.0624
R indices (all data)	R1 = 0.0408, wR2 = 0.0674
Largest diff. peak and hole	0.501 and -0.853 e.Å ⁻³

Bond Lengths (Å)

Ag(1)-N(2)#1	2.321(3)	Ag(1)-N(2)#2	2.321(3)
Ag(1)-N(1)#3	2.324(3)	Ag(1)-N(1)	2.324(3)
C(8)-F(1)	1.280(5)	C(8)-F(1)#4	1.280(5)
C(8)-F(2)	1.341(6)	C(8)-C(7)	1.547(5)
O(1)-C(7)	1.232(5)	O(2)-C(7)	1.230(5)
C(1)-N(1)	1.340(4)	C(1)-C(2)	1.370(5)
C(1)-H(1)	0.9300	C(2)-C(3)	1.385(5)
C(2)-H(2)	0.9300	C(3)-C(4)	1.385(4)
C(3)-C(6)	1.495(5)	C(4)-C(5)	1.373(4)
C(4)-H(4)	0.9300	C(5)-N(1)	1.337(4)
C(5)-H(5)	0.9300	C(6)-N(2)	1.476(6)
C(6)-H(6A)	0.9700	C(6)-H(6B)	0.9700
N(2)-Ag(1)#1	2.321(3)	N(2)-H(2A)	0.9000
N(2)-H(2B)	0.9000		

Bond Angles (°)

N(2)#1-Ag(1)-N(2)#2	100.19(19)	H(2A)-N(2)-H(2B)	107.1
N(2)#1-Ag(1)-N(1)#3	101.38(10)	N(2)#2-Ag(1)-N(1)#3	121.26(9)
N(2)#1-Ag(1)-N(1)	121.26(9)	N(2)#2-Ag(1)-N(1)	101.38(10)
N(1)#3-Ag(1)-N(1)	112.13(13)	F(1)-C(8)-F(1)#4	108.6(7)
F(1)-C(8)-F(2)	104.8(4)	F(1)#4-C(8)-F(2)	104.8(4)
F(1)-C(8)-C(7)	112.5(3)	F(1)#4-C(8)-C(7)	112.5(3)
F(2)-C(8)-C(7)	113.0(4)	N(1)-C(1)-C(2)	123.6(3)
N(1)-C(1)-H(1)	118.2	C(2)-C(1)-H(1)	118.2
C(1)-C(2)-C(3)	119.7(3)	C(1)-C(2)-H(2)	120.2

Table B.28. Continued

C(3)-C(2)-H(2)	120.2	C(4)-C(3)-C(2)	117.0(3)
C(4)-C(3)-C(6)	121.7(3)	C(2)-C(3)-C(6)	121.2(3)
C(5)-C(4)-C(3)	119.7(3)	C(5)-C(4)-H(4)	120.1
C(3)-C(4)-H(4)	120.1	N(1)-C(5)-C(4)	123.5(3)
N(1)-C(5)-H(5)	118.2	C(4)-C(5)-H(5)	118.2
N(2)-C(6)-C(3)	109.1(3)	N(2)-C(6)-H(6A)	109.9
C(3)-C(6)-H(6A)	109.9	N(2)-C(6)-H(6B)	109.9
C(3)-C(6)-H(6B)	109.9	H(6A)-C(6)-H(6B)	108.3
O(1)-C(7)-O(2)	130.0(4)	O(1)-C(7)-C(8)	114.0(3)
O(2)-C(7)-C(8)	115.9(3)	C(5)-N(1)-C(1)	116.4(3)
C(5)-N(1)-Ag(1)	125.2(2)	C(1)-N(1)-Ag(1)	117.4(2)
C(6)-N(2)-Ag(1)#1	118.0(2)	C(6)-N(2)-H(2A)	107.8
Ag(1)#1-N(2)-H(2A)	107.8	C(6)-N(2)-H(2B)	107.8
Ag(1)#1-N(2)-H(2B)	107.8		

Hydrogen Bonds (Å)

N(2)-H(2B)...O(1)#1	3.008(4)	N(2)-H(2A)...O(2)#5	3.169(3)
---------------------	----------	---------------------	----------

Symmetry transformations used to generate equivalent atoms: #1 -x+1/2,-y+1/2,-z+1 #2 x-1/2,-y+1/2,z
#3 -x,y,-z+1 #4 x,-y+1,z #5 x+1/2,y-1/2,z

Table B.29 Experimental and statistical crystal data for 7.4

Empirical formula	C13 H16 Ag F3 N4 O3 S
Formula weight	473.23
Temperature	110(2) K
Wavelength	0.71073 Å
Crystal system, space group	Triclinic, P-1
Unit cell dimensions	a = 7.9279(4) Å α = 98.964(2) deg. b = 10.0058(4) Å β = 108.141(2) deg. c = 11.5642(5) Å γ = 95.402(2) deg.
Volume	851.08(7) Å^3
Z, Calculated density	2, 1.847 Mg/m^3
Absorption coefficient	1.359 mm^-1
F(000)	472
Crystal size	0.249 x 0.23 x 0.153 mm
θ range for data collection	3.18 to 28.48 deg.
Limiting indices	-10<=h<=10, -12<=k<=13, -15<=l<=15
Reflections collected / unique	29250 / 4113 [R(int) = 0.0344]
Completeness to θ = 25.00	98.3 %
Absorption correction	multi-scan (SADABS)
Refinement method	Full-matrix least-squares on F^2
Data / restraints / parameters	4113 / 0 / 226
Goodness-of-fit on F^2	1.052
Final R indices [I>2σ(I)]	R1 = 0.0187, wR2 = 0.0473
R indices (all data)	R1 = 0.0199, wR2 = 0.0477
Largest diff. peak and hole	0.847 and -0.530 e.Å^-3

Table B.29. Continued

Bond Lengths (Å)

Ag(1)-N(3)	2.2765(13)	Ag(1)-N(1)#1	2.3460(14)
Ag(1)-N(4)#2	2.3913(13)	Ag(1)-N(2)	2.4312(12)
S(1)-O(3)	1.4353(12)	S(1)-O(1)	1.4439(13)
S(1)-O(2)	1.4464(11)	S(1)-C(13)	1.8305(15)
F(1)-C(13)	1.3413(18)	F(2)-C(13)	1.3313(18)
F(3)-C(13)	1.3338(19)	N(1)-C(1)	1.474(2)
N(1)-Ag(1)#3	2.3460(14)	N(1)-H(1C)	0.9000
N(1)-H(1D)	0.9000	N(2)-C(5)	1.339(2)
N(2)-C(4)	1.343(2)	N(3)-C(7)	1.4820(19)
N(3)-H(3A)	0.9000	N(3)-H(3B)	0.9000
N(4)-C(10)	1.339(2)	N(4)-C(11)	1.340(2)
N(4)-Ag(1)#2	2.3913(13)	C(1)-C(2)	1.5089(19)
C(1)-H(1A)	0.9700	C(1)-H(1B)	0.9700
C(2)-C(6)	1.389(2)	C(2)-C(3)	1.395(2)
C(3)-C(4)	1.392(2)	C(3)-H(3)	0.9300
C(4)-H(4)	0.9300	C(5)-C(6)	1.387(2)
C(5)-H(5)	0.9300	C(6)-H(6)	0.9300
C(7)-C(8)	1.511(2)	C(7)-H(7A)	0.9700
C(7)-H(7B)	0.9700	C(8)-C(12)	1.382(2)
C(8)-C(9)	1.391(2)	C(9)-C(10)	1.386(2)
C(9)-H(9)	0.9300	C(10)-H(10)	0.9300
C(11)-C(12)	1.388(2)	C(11)-H(11)	0.9300
C(12)-H(12)	0.9300		

Bond Angles (°)

N(3)-Ag(1)-N(1)#1	119.90(5)	F(1)-C(13)-S(1)	110.53(10)
N(3)-Ag(1)-N(4)#2	117.91(5)	N(1)#1-Ag(1)-N(4)#2	109.55(5)
N(3)-Ag(1)-N(2)	118.19(5)	N(1)#1-Ag(1)-N(2)	93.50(4)
N(4)#2-Ag(1)-N(2)	92.07(4)	O(3)-S(1)-O(1)	116.00(9)
O(3)-S(1)-O(2)	114.88(8)	O(1)-S(1)-O(2)	113.97(7)
O(3)-S(1)-C(13)	103.80(7)	O(1)-S(1)-C(13)	102.72(7)
O(2)-S(1)-C(13)	103.05(7)	C(1)-N(1)-Ag(1)#3	119.88(9)
C(1)-N(1)-H(1C)	107.4	Ag(1)#3-N(1)-H(1C)	107.4
C(1)-N(1)-H(1D)	107.4	Ag(1)#3-N(1)-H(1D)	107.4
H(1C)-N(1)-H(1D)	106.9	C(5)-N(2)-C(4)	116.67(13)
C(5)-N(2)-Ag(1)	115.75(10)	C(4)-N(2)-Ag(1)	125.96(10)
C(7)-N(3)-Ag(1)	116.30(10)	C(7)-N(3)-H(3A)	108.2
Ag(1)-N(3)-H(3A)	108.2	C(7)-N(3)-H(3B)	108.2
Ag(1)-N(3)-H(3B)	108.2	H(3A)-N(3)-H(3B)	107.4
C(10)-N(4)-C(11)	116.46(13)	C(10)-N(4)-Ag(1)#2	123.28(10)
C(11)-N(4)-Ag(1)#2	120.04(11)	N(1)-C(1)-C(2)	113.18(12)
N(1)-C(1)-H(1A)	108.9	C(2)-C(1)-H(1A)	108.9
N(1)-C(1)-H(1B)	108.9	C(2)-C(1)-H(1B)	108.9
H(1A)-C(1)-H(1B)	107.8	C(6)-C(2)-C(3)	116.98(13)
C(6)-C(2)-C(1)	119.72(13)	C(3)-C(2)-C(1)	123.17(13)
C(4)-C(3)-C(2)	119.25(14)	C(4)-C(3)-H(3)	120.4
C(2)-C(3)-H(3)	120.4	N(2)-C(4)-C(3)	123.65(14)
N(2)-C(4)-H(4)	118.2	C(3)-C(4)-H(4)	118.2
N(2)-C(5)-C(6)	123.42(14)	N(2)-C(5)-H(5)	118.3
C(6)-C(5)-H(5)	118.3	C(5)-C(6)-C(2)	120.01(13)
C(5)-C(6)-H(6)	120.0	C(2)-C(6)-H(6)	120.0

Table B.29. Continued

N(3)-C(7)-C(8)	110.77(12)	N(3)-C(7)-H(7A)	109.5
C(8)-C(7)-H(7A)	109.5	N(3)-C(7)-H(7B)	109.5
C(8)-C(7)-H(7B)	109.5	H(7A)-C(7)-H(7B)	108.1
C(12)-C(8)-C(9)	117.26(14)	C(12)-C(8)-C(7)	122.19(14)
C(9)-C(8)-C(7)	120.54(14)	C(10)-C(9)-C(8)	119.20(15)
C(10)-C(9)-H(9)	120.4	C(8)-C(9)-H(9)	120.4
N(4)-C(10)-C(9)	123.86(15)	N(4)-C(10)-H(10)	118.1
C(9)-C(10)-H(10)	118.1	N(4)-C(11)-C(12)	123.44(15)
N(4)-C(11)-H(11)	118.3	C(12)-C(11)-H(11)	118.3
C(8)-C(12)-C(11)	119.76(15)	C(8)-C(12)-H(12)	120.1
C(11)-C(12)-H(12)	120.1	F(2)-C(13)-F(3)	107.75(12)
F(2)-C(13)-F(1)	107.57(13)	F(3)-C(13)-F(1)	107.19(13)
F(2)-C(13)-S(1)	112.33(10)	F(3)-C(13)-S(1)	111.26(10)
 Hydrogen Bonds (Å)			
N(1)-H(1C)...O(1)#4	3.0216(17)	N(1)-H(1D)...O(1)#5	3.2590(19)
N(3)-H(3A)...O(2)#6	3.0530(18)	N(3)-H(3B)...O(3)#7	3.0374(17)

Symmetry transformations used to generate equivalent atoms: #1 x-1,y,z #2 -x,-y+1,-z+1 #3 x+1,y,z
#4 x+1,y,z+1 #5 -x+2,-y+2,-z+1 #6 -x+1,-y+1,-z+1 #7 x,y,z+1

Table B.30 Experimental and statistical crystal data for 7.5

Empirical formula	C12 H16 Ag B F4 N4
Formula weight	410.97
Temperature	110(2) K
Wavelength	0.71073 Å
Crystal system, space group	Monoclinic, P2(1)/c
Unit cell dimensions	a = 10.2034(3) Å α = 90 deg. b = 13.3334(4) Å β = 103.690(2) deg. c = 12.3596(4) Å γ = 90 deg.
Volume	1633.70(9) Å^3
Z, Calculated density	4, 1.671 Mg/m^3
Absorption coefficient	1.273 mm^-1
F(000)	816
Crystal size	0.152 × 0.114 × 0.112 mm
θ range for data collection	3.33 to 28.27 deg.
Limiting indices	-13<=h<=13, -15<=k<=17, -16<=l<=16
Reflections collected / unique	21977 / 3961 [R(int) = 0.0299]
Completeness to θ = 28.27	97.4 %
Absorption correction	multi-scan (SADABS)
Refinement method	Full-matrix least-squares on F^2
Data / restraints / parameters	3961 / 0 / 199
Goodness-of-fit on F^2	1.042
Final R indices [I>2σ(I)]	R1 = 0.0255, wR2 = 0.0624
R indices (all data)	R1 = 0.0364, wR2 = 0.0698
Largest diff. peak and hole	0.689 and -0.375 e.Å^-3

Table B.30. Continued

Bond Lengths (Å)

Ag(1)-N(1)	2.2806(18)	Ag(1)-N(2)#1	2.327(2)
Ag(1)-N(4)#2	2.3469(18)	Ag(1)-N(3)	2.3808(18)
B(1)-F(3)	1.370(3)	B(1)-F(2)	1.373(3)
B(1)-F(1)	1.375(3)	B(1)-F(4)	1.393(3)
N(1)-C(4)	1.341(3)	N(1)-C(5)	1.343(3)
N(2)-C(1)	1.478(3)	N(2)-Ag(1)#1	2.327(2)
N(2)-H(2A)	0.9000	N(2)-H(2B)	0.9000
N(3)-C(10)	1.331(3)	N(3)-C(11)	1.345(3)
N(4)-C(7)	1.464(3)	N(4)-Ag(1)#3	2.3469(18)
N(4)-H(4A)	0.9000	N(4)-H(4B)	0.9000
C(1)-C(2)	1.507(3)	C(1)-H(1A)	0.9700
C(1)-H(1B)	0.9700	C(2)-C(3)	1.383(3)
C(2)-C(6)	1.387(3)	C(3)-C(4)	1.385(3)
C(3)-H(3)	0.9300	C(4)-H(4)	0.9300
C(5)-C(6)	1.385(3)	C(5)-H(5)	0.9300
C(6)-H(6)	0.9300	C(7)-C(8)	1.515(3)
C(7)-H(7A)	0.9700	C(7)-H(7B)	0.9700
C(8)-C(12)	1.379(3)	C(8)-C(9)	1.387(3)
C(9)-C(10)	1.386(3)	C(9)-H(9)	0.9300
C(10)-H(10)	0.9300	C(11)-C(12)	1.385(3)
C(11)-H(11)	0.9300	C(12)-H(12)	0.9300

Bond Angles (°)

N(1)-Ag(1)-N(2)#1	126.60(7)	N(1)-Ag(1)-N(4)#2	116.96(7)
N(2)#1-Ag(1)-N(4)#2	99.86(7)	N(1)-Ag(1)-N(3)	105.85(6)
N(2)#1-Ag(1)-N(3)	102.97(7)	N(4)#2-Ag(1)-N(3)	101.23(7)
F(3)-B(1)-F(2)	110.1(2)	F(3)-B(1)-F(1)	108.5(2)
F(2)-B(1)-F(1)	109.7(2)	F(3)-B(1)-F(4)	110.5(2)
F(2)-B(1)-F(4)	109.04(19)	F(1)-B(1)-F(4)	109.0(2)
C(4)-N(1)-C(5)	116.97(19)	C(4)-N(1)-Ag(1)	122.72(15)
C(5)-N(1)-Ag(1)	119.78(15)	C(1)-N(2)-Ag(1)#1	114.58(14)
C(1)-N(2)-H(2A)	108.6	Ag(1)#1-N(2)-H(2A)	108.6
C(1)-N(2)-H(2B)	108.6	Ag(1)#1-N(2)-H(2B)	108.6
H(2A)-N(2)-H(2B)	107.6	C(10)-N(3)-C(11)	117.22(19)
C(10)-N(3)-Ag(1)	120.24(14)	C(11)-N(3)-Ag(1)	122.53(15)
C(7)-N(4)-Ag(1)#3	114.13(13)	C(7)-N(4)-H(4A)	108.7
Ag(1)#3-N(4)-H(4A)	108.7	C(7)-N(4)-H(4B)	108.7
Ag(1)#3-N(4)-H(4B)	108.7	H(4A)-N(4)-H(4B)	107.6
N(2)-C(1)-C(2)	109.81(18)	N(2)-C(1)-H(1A)	109.7
C(2)-C(1)-H(1A)	109.7	N(2)-C(1)-H(1B)	109.7
C(2)-C(1)-H(1B)	109.7	H(1A)-C(1)-H(1B)	108.2
C(3)-C(2)-C(6)	117.7(2)	C(3)-C(2)-C(1)	121.2(2)
C(6)-C(2)-C(1)	121.1(2)	C(2)-C(3)-C(4)	119.5(2)
C(2)-C(3)-H(3)	120.3	C(4)-C(3)-H(3)	120.3
N(1)-C(4)-C(3)	123.2(2)	N(1)-C(4)-H(4)	118.4
C(3)-C(4)-H(4)	118.4	N(1)-C(5)-C(6)	123.2(2)
N(1)-C(5)-H(5)	118.4	C(6)-C(5)-H(5)	118.4
C(5)-C(6)-C(2)	119.3(2)	C(5)-C(6)-H(6)	120.3
C(2)-C(6)-H(6)	120.3	N(4)-C(7)-C(8)	113.17(18)
N(4)-C(7)-H(7A)	108.9	C(8)-C(7)-H(7A)	108.9
N(4)-C(7)-H(7B)	108.9	C(8)-C(7)-H(7B)	108.9

Table B.30. Continued

H(7A)-C(7)-H(7B)	107.8	C(12)-C(8)-C(9)	117.6(2)
C(12)-C(8)-C(7)	121.6(2)	C(9)-C(8)-C(7)	120.8(2)
C(10)-C(9)-C(8)	119.2(2)	C(10)-C(9)-H(9)	120.4
C(8)-C(9)-H(9)	120.4	N(3)-C(10)-C(9)	123.4(2)
N(3)-C(10)-H(10)	118.3	C(9)-C(10)-H(10)	118.3
N(3)-C(11)-C(12)	122.8(2)	N(3)-C(11)-H(11)	118.6
C(12)-C(11)-H(11)	118.6	C(8)-C(12)-C(11)	119.8(2)
C(8)-C(12)-H(12)	120.1	C(11)-C(12)-H(12)	120.1
Hydrogen Bonds (Å)			
N(2)-H(2A)...F(1)#4	3.072(3)	N(2)-H(2B)...F(4)	3.090(2)
N(4)-H(4A)...F(4)#5	3.156(2)	N(4)-H(4A)...F(2)#5	3.118(2)
N(4)-H(4B)...F(1)#6	3.282(3)		

Symmetry transformations used to generate equivalent atoms: #1 -x+1,-y+1,-z+1 #2 -x+2,y-1/2,-z+1/2
#3 -x+2,y+1/2,-z+1/2 #4 -x+1,-y+1,-z+2 #5 -x+2,-y+1,-z+1 #6 -x+2,y+1/2,-z+3/2

Table B.31 Experimental and statistical crystal data for **7.6.2**

Empirical formula	C34 H38 Ag2 B2 F8 N8		
Formula weight	948.08		
Temperature	110(2) K		
Wavelength	0.71073 Å		
Crystal system, space group	Monoclinic, P2(1)/c		
Unit cell dimensions	a = 18.763(11) Å α = 90 deg. b = 30.127(12) Å β = 91.968(17) deg. c = 6.690(3) Å γ = 90 deg.		
Volume	3779(3) Å ³		
Z, Calculated density	4, 1.666 Mg/m ³		
Absorption coefficient	1.113 mm ⁻¹		
F(000)	1896		
Crystal size	0.264 × 0.220 × 0.189 mm		
θ range for data collection	1.35 to 26.61 deg.		
Limiting indices	-23<=h<=23, -37<=k<=34, -8<=l<=8		
Reflections collected / unique	29173 / 7788 [R(int) = 0.0446]		
Completeness to θ = 25.00	99.2 %		
Absorption correction	multi-scan (SADABS)		
Refinement method	Full-matrix least-squares on F ²		
Data / restraints / parameters	7788 / 31 / 528		
Goodness-of-fit on F ²	1.078		
Final R indices [I>2σ(I)]	R1 = 0.0394, wR2 = 0.1039		
R indices (all data)	R1 = 0.0448, wR2 = 0.1072		
Largest diff. peak and hole	1.242 and -0.788 e.Å ⁻³		
Bond Lengths (Å)			
Ag(1)-N(1)	2.161(3)	Ag(1)-N(3)	2.256(3)
Ag(1)-N(4)	2.335(3)	Ag(2)-N(2)	2.138(3)
Ag(2)-N(5)	2.240(3)	Ag(2)-N(6)	2.339(3)
Ag(2)-Ag(2)#1	3.3482(12)	Ag(2)-Ag(2)#2	3.3482(13)
B(1)-F(2A)	1.365(11)	B(1)-F(3B)	1.374(7)

Table B.31. Continued

B(1)-F(4A)	1.377(10)	B(1)-F(3)	1.378(11)
B(1)-F(2B)	1.379(9)	B(1)-F(1A)	1.382(10)
B(1)-F(4)	1.384(10)	B(1)-F(2)	1.392(10)
B(1)-F(1B)	1.395(8)	B(1)-F(1)	1.400(11)
B(1)-F(3A)	1.401(9)	B(1)-F(4B)	1.408(7)
F(3)-F(3A)	0.564(16)	F(3)-F(3B)	0.575(19)
F(3)-F(4A)	1.763(17)	F(4)-F(4A)	0.58(2)
F(4)-F(4B)	0.613(15)	F(4)-F(3B)	1.758(17)
F(1A)-F(1B)	0.67(2)	F(2A)-F(2B)	0.56(4)
F(3A)-F(3B)	1.12(2)	F(4A)-F(4B)	1.17(3)
F(4A)-F(3B)	1.28(2)	F(5)-B(2)	1.390(5)
F(6)-B(2)	1.360(5)	F(7)-B(2)	1.399(5)
F(8)-B(2)	1.397(5)	N(1)-C(1)	1.464(5)
N(1)-H(1C)	0.9200	N(1)-H(1D)	0.9200
N(2)-C(4)	1.341(5)	N(2)-C(5)	1.350(4)
N(3)-C(7)	1.349(4)	N(3)-C(11)	1.349(4)
N(4)-C(17)	1.341(4)	N(4)-C(13)	1.347(4)
N(5)-C(23)	1.349(4)	N(5)-C(19)	1.351(5)
N(6)-C(29)	1.342(5)	N(6)-C(25)	1.343(4)
N(7)-C(31)	1.133(7)	N(8)-C(33)	1.141(5)
C(1)-C(2)	1.515(5)	C(1)-H(1A)	0.9900
C(1)-H(1B)	0.9900	C(2)-C(3)	1.392(5)
C(2)-C(6)	1.397(5)	C(3)-C(4)	1.389(5)
C(3)-H(3)	0.9500	C(4)-H(4)	0.9500
C(5)-C(6)	1.381(5)	C(5)-H(5)	0.9500
C(6)-H(6)	0.9500	C(7)-C(8)	1.375(5)
C(7)-H(7)	0.9500	C(8)-C(9)	1.395(5)
C(8)-C(12)	1.508(5)	C(9)-C(10)	1.392(5)
C(9)-H(9)	0.9500	C(10)-C(11)	1.400(5)
C(10)-H(10)	0.9500	C(11)-C(13)	1.497(5)
C(12)-H(12A)	0.9800	C(12)-H(12B)	0.9800
C(12)-H(12C)	0.9800	C(13)-C(14)	1.400(5)
C(14)-C(15)	1.385(5)	C(14)-H(14)	0.9500
C(15)-C(16)	1.389(5)	C(15)-H(15)	0.9500
C(16)-C(17)	1.394(5)	C(16)-C(18)	1.504(5)
C(17)-H(17)	0.9500	C(18)-H(18A)	0.9800
C(18)-H(18B)	0.9800	C(18)-H(18C)	0.9800
C(19)-C(20)	1.385(5)	C(19)-H(19)	0.9500
C(20)-C(21)	1.406(5)	C(20)-C(24)	1.498(5)
C(21)-C(22)	1.383(5)	C(21)-H(21)	0.9500
C(22)-C(23)	1.394(5)	C(22)-H(22)	0.9500
C(23)-C(25)	1.496(5)	C(24)-H(24A)	0.9800
C(24)-H(24B)	0.9800	C(24)-H(24C)	0.9800
C(25)-C(26)	1.394(5)	C(26)-C(27)	1.385(5)
C(26)-H(26)	0.9500	C(27)-C(28)	1.395(5)
C(27)-H(27)	0.9500	C(28)-C(29)	1.396(5)
C(28)-C(30)	1.506(5)	C(29)-H(29)	0.9500
C(30)-H(30A)	0.9800	C(30)-H(30B)	0.9800
C(30)-H(30C)	0.9800	C(31)-C(32)	1.459(8)
C(32)-H(32A)	0.9800	C(32)-H(32B)	0.9800
C(32)-H(32C)	0.9800	C(33)-C(34)	1.455(5)
C(34)-H(34A)	0.9800	C(34)-H(34B)	0.9800
C(34)-H(34C)	0.9800		

Table B.31. Continued

Bond Angles ($^{\circ}$)

N(1)-Ag(1)-N(3)	150.25(11)	F(6)-B(2)-F(7)	110.6(4)
N(1)-Ag(1)-N(4)	136.77(11)	N(3)-Ag(1)-N(4)	72.88(10)
N(2)-Ag(2)-N(5)	153.94(11)	N(2)-Ag(2)-N(6)	132.80(11)
N(5)-Ag(2)-N(6)	73.11(10)	N(2)-Ag(2)-Ag(2) ^{#1}	83.21(8)
N(5)-Ag(2)-Ag(2) ^{#1}	104.44(7)	N(6)-Ag(2)-Ag(2) ^{#1}	85.93(7)
N(2)-Ag(2)-Ag(2) ^{#2}	100.32(8)	N(5)-Ag(2)-Ag(2) ^{#2}	74.00(7)
N(6)-Ag(2)-Ag(2) ^{#2}	88.93(7)	Ag(2) ^{#1} -Ag(2)-Ag(2) ^{#2}	174.859(18)
F(2A)-B(1)-F(3B)	128.3(9)	F(2A)-B(1)-F(4A)	111.1(9)
F(3B)-B(1)-F(4A)	55.6(12)	F(2A)-B(1)-F(3)	121.9(11)
F(3B)-B(1)-F(3)	24.1(8)	F(4A)-B(1)-F(3)	79.6(9)
F(2A)-B(1)-F(2B)	23.4(15)	F(3B)-B(1)-F(2B)	112.7(9)
F(4A)-B(1)-F(2B)	119.5(10)	F(3)-B(1)-F(2B)	100.4(11)
F(2A)-B(1)-F(1A)	107.6(9)	F(3B)-B(1)-F(1A)	123.6(7)
F(4A)-B(1)-F(1A)	114.2(9)	F(3)-B(1)-F(1A)	119.5(9)
F(2B)-B(1)-F(1A)	117.2(10)	F(2A)-B(1)-F(4)	101.6(10)
F(3B)-B(1)-F(4)	79.2(8)	F(4A)-B(1)-F(4)	24.2(8)
F(3)-B(1)-F(4)	103.3(9)	F(2B)-B(1)-F(4)	118.6(10)
F(1A)-B(1)-F(4)	98.0(10)	F(2A)-B(1)-F(2)	14.1(8)
F(3B)-B(1)-F(2)	118.5(10)	F(4A)-B(1)-F(2)	115.7(9)
F(3)-B(1)-F(2)	108.7(11)	F(2B)-B(1)-F(2)	9.4(15)
F(1A)-B(1)-F(2)	114.7(9)	F(4)-B(1)-F(2)	111.3(9)
F(2A)-B(1)-F(1B)	115.2(10)	F(3B)-B(1)-F(1B)	107.7(7)
F(4A)-B(1)-F(1B)	127.7(8)	F(3)-B(1)-F(1B)	95.5(9)
F(2B)-B(1)-F(1B)	112.7(9)	F(1A)-B(1)-F(1B)	28.1(9)
F(4)-B(1)-F(1B)	120.1(9)	F(2)-B(1)-F(1B)	115.2(9)
F(2A)-B(1)-F(1)	108.3(11)	F(3B)-B(1)-F(1)	118.9(10)
F(4A)-B(1)-F(1)	126.1(11)	F(3)-B(1)-F(1)	108.6(11)
F(2B)-B(1)-F(1)	111.3(12)	F(1A)-B(1)-F(1)	16.0(9)
F(4)-B(1)-F(1)	113.0(11)	F(2)-B(1)-F(1)	111.5(9)
F(1B)-B(1)-F(1)	13.3(13)	F(2A)-B(1)-F(3A)	111.1(9)
F(3B)-B(1)-F(3A)	47.5(10)	F(4A)-B(1)-F(3A)	102.9(8)
F(3)-B(1)-F(3A)	23.4(6)	F(2B)-B(1)-F(3A)	87.8(11)
F(1A)-B(1)-F(3A)	109.9(7)	F(4)-B(1)-F(3A)	126.7(10)
F(2)-B(1)-F(3A)	97.1(10)	F(1B)-B(1)-F(3A)	82.3(9)
F(1)-B(1)-F(3A)	95.5(11)	F(2A)-B(1)-F(4B)	88.3(11)
F(3B)-B(1)-F(4B)	104.4(7)	F(4A)-B(1)-F(4B)	49.5(11)
F(3)-B(1)-F(4B)	128.5(9)	F(2B)-B(1)-F(4B)	110.3(9)
F(1A)-B(1)-F(4B)	81.6(9)	F(4)-B(1)-F(4B)	25.4(6)
F(2)-B(1)-F(4B)	101.2(11)	F(1B)-B(1)-F(4B)	108.6(7)
F(1)-B(1)-F(4B)	97.6(11)	F(3A)-B(1)-F(4B)	151.7(11)
F(3A)-F(3)-F(3B)	158(3)	F(3A)-F(3)-B(1)	80.7(15)
F(3B)-F(3)-B(1)	77.6(13)	F(3A)-F(3)-F(4A)	130.8(16)
F(3B)-F(3)-F(4A)	27.7(13)	B(1)-F(3)-F(4A)	50.2(6)
F(4A)-F(4)-F(4B)	156(2)	F(4A)-F(4)-B(1)	77.3(14)
F(4B)-F(4)-B(1)	79.5(11)	F(4A)-F(4)-F(3B)	28.9(13)
F(4B)-F(4)-F(3B)	129.2(13)	B(1)-F(4)-F(3B)	50.1(5)
F(1B)-F(1A)-B(1)	77.0(12)	F(2B)-F(2A)-B(1)	79.7(18)
F(3)-F(3A)-F(3B)	11.0(13)	F(3)-F(3A)-B(1)	76.0(14)
F(3B)-F(3A)-B(1)	65.0(7)	F(4)-F(4A)-F(4B)	12.2(12)
F(4)-F(4A)-F(3B)	138.6(17)	F(4B)-F(4A)-F(3B)	127.6(9)
F(4)-F(4A)-B(1)	78.6(14)	F(4B)-F(4A)-B(1)	66.6(8)

Table B.31. Continued

F(3B)-F(4A)-B(1)	62.1(8)	F(4)-F(4A)-F(3)	127.8(16)
F(4B)-F(4A)-F(3)	116.3(9)	F(3B)-F(4A)-F(3)	12.0(6)
B(1)-F(4A)-F(3)	50.2(6)	F(1A)-F(1B)-B(1)	75.0(10)
F(2A)-F(2B)-B(1)	76.9(16)	F(3)-F(3B)-F(3A)	10.8(13)
F(3)-F(3B)-F(4A)	140.3(17)	F(3A)-F(3B)-F(4A)	129.7(8)
F(3)-F(3B)-B(1)	78.3(14)	F(3A)-F(3B)-B(1)	67.6(7)
F(4A)-F(3B)-B(1)	62.3(8)	F(3)-F(3B)-F(4)	129.0(15)
F(3A)-F(3B)-F(4)	118.2(7)	F(4A)-F(3B)-F(4)	12.6(7)
B(1)-F(3B)-F(4)	50.6(5)	F(4)-F(4B)-F(4A)	11.5(12)
F(4)-F(4B)-B(1)	75.1(11)	F(4A)-F(4B)-B(1)	63.9(7)
C(1)-N(1)-Ag(1)	115.2(2)	C(1)-N(1)-H(1C)	108.5
Ag(1)-N(1)-H(1C)	108.5	C(1)-N(1)-H(1D)	108.5
Ag(1)-N(1)-H(1D)	108.5	H(1C)-N(1)-H(1D)	107.5
C(4)-N(2)-C(5)	117.2(3)	C(4)-N(2)-Ag(2)	121.2(2)
C(5)-N(2)-Ag(2)	121.6(2)	C(7)-N(3)-C(11)	118.6(3)
C(7)-N(3)-Ag(1)	123.7(2)	C(11)-N(3)-Ag(1)	117.6(2)
C(17)-N(4)-C(13)	119.1(3)	C(17)-N(4)-Ag(1)	125.8(2)
C(13)-N(4)-Ag(1)	115.2(2)	C(23)-N(5)-C(19)	119.0(3)
C(23)-N(5)-Ag(2)	117.4(2)	C(19)-N(5)-Ag(2)	122.8(2)
C(29)-N(6)-C(25)	119.2(3)	C(29)-N(6)-Ag(2)	125.6(2)
C(25)-N(6)-Ag(2)	114.6(2)	N(1)-C(1)-C(2)	116.0(3)
N(1)-C(1)-H(1A)	108.3	C(2)-C(1)-H(1A)	108.3
N(1)-C(1)-H(1B)	108.3	C(2)-C(1)-H(1B)	108.3
H(1A)-C(1)-H(1B)	107.4	C(3)-C(2)-C(6)	117.5(3)
C(3)-C(2)-C(1)	123.7(3)	C(6)-C(2)-C(1)	118.8(3)
C(4)-C(3)-C(2)	119.3(3)	C(4)-C(3)-H(3)	120.3
C(2)-C(3)-H(3)	120.3	N(2)-C(4)-C(3)	123.3(3)
N(2)-C(4)-H(4)	118.3	C(3)-C(4)-H(4)	118.3
N(2)-C(5)-C(6)	123.1(3)	N(2)-C(5)-H(5)	118.4
C(6)-C(5)-H(5)	118.4	C(5)-C(6)-C(2)	119.5(3)
C(5)-C(6)-H(6)	120.2	C(2)-C(6)-H(6)	120.2
N(3)-C(7)-C(8)	124.5(3)	N(3)-C(7)-H(7)	117.7
C(8)-C(7)-H(7)	117.7	C(7)-C(8)-C(9)	116.7(3)
C(7)-C(8)-C(12)	122.3(3)	C(9)-C(8)-C(12)	120.9(3)
C(10)-C(9)-C(8)	120.2(3)	C(10)-C(9)-H(9)	119.9
C(8)-C(9)-H(9)	119.9	C(9)-C(10)-C(11)	119.1(3)
C(9)-C(10)-H(10)	120.5	C(11)-C(10)-H(10)	120.5
N(3)-C(11)-C(10)	120.9(3)	N(3)-C(11)-C(13)	117.3(3)
C(10)-C(11)-C(13)	121.8(3)	C(8)-C(12)-H(12A)	109.5
C(8)-C(12)-H(12B)	109.5	H(12A)-C(12)-H(12B)	109.5
C(8)-C(12)-H(12C)	109.5	H(12A)-C(12)-H(12C)	109.5
H(12B)-C(12)-H(12C)	109.5	N(4)-C(13)-C(14)	121.1(3)
N(4)-C(13)-C(11)	117.0(3)	C(14)-C(13)-C(11)	121.9(3)
C(15)-C(14)-C(13)	118.8(3)	C(15)-C(14)-H(14)	120.6
C(13)-C(14)-H(14)	120.6	C(14)-C(15)-C(16)	120.7(3)
C(14)-C(15)-H(15)	119.6	C(16)-C(15)-H(15)	119.6
C(15)-C(16)-C(17)	116.7(3)	C(15)-C(16)-C(18)	122.2(4)
C(17)-C(16)-C(18)	121.2(3)	N(4)-C(17)-C(16)	123.7(3)
N(4)-C(17)-H(17)	118.2	C(16)-C(17)-H(17)	118.2
C(16)-C(18)-H(18A)	109.5	C(16)-C(18)-H(18B)	109.5
H(18A)-C(18)-H(18B)	109.5	C(16)-C(18)-H(18C)	109.5
H(18A)-C(18)-H(18C)	109.5	H(18B)-C(18)-H(18C)	109.5
N(5)-C(19)-C(20)	123.9(3)	N(5)-C(19)-H(19)	118.0
C(20)-C(19)-H(19)	118.0	C(19)-C(20)-C(21)	116.5(3)

Table B.31. Continued

C(19)-C(20)-C(24)	121.1(3)	C(21)-C(20)-C(24)	122.3(3)
C(22)-C(21)-C(20)	120.1(3)	C(22)-C(21)-H(21)	119.9
C(20)-C(21)-H(21)	119.9	C(21)-C(22)-C(23)	119.6(3)
C(21)-C(22)-H(22)	120.2	C(23)-C(22)-H(22)	120.2
N(5)-C(23)-C(22)	120.9(3)	N(5)-C(23)-C(25)	117.3(3)
C(22)-C(23)-C(25)	121.8(3)	C(20)-C(24)-H(24A)	109.5
C(20)-C(24)-H(24B)	109.5	H(24A)-C(24)-H(24B)	109.5
C(20)-C(24)-H(24C)	109.5	H(24A)-C(24)-H(24C)	109.5
H(24B)-C(24)-H(24C)	109.5	N(6)-C(25)-C(26)	121.1(3)
N(6)-C(25)-C(23)	116.7(3)	C(26)-C(25)-C(23)	122.2(3)
C(27)-C(26)-C(25)	119.2(3)	C(27)-C(26)-H(26)	120.4
C(25)-C(26)-H(26)	120.4	C(26)-C(27)-C(28)	120.4(3)
C(26)-C(27)-H(27)	119.8	C(28)-C(27)-H(27)	119.8
C(27)-C(28)-C(29)	116.5(3)	C(27)-C(28)-C(30)	122.3(3)
C(29)-C(28)-C(30)	121.2(3)	N(6)-C(29)-C(28)	123.6(3)
N(6)-C(29)-H(29)	118.2	C(28)-C(29)-H(29)	118.2
C(28)-C(30)-H(30A)	109.5	C(28)-C(30)-H(30B)	109.5
H(30A)-C(30)-H(30B)	109.5	C(28)-C(30)-H(30C)	109.5
H(30A)-C(30)-H(30C)	109.5	H(30B)-C(30)-H(30C)	109.5
N(7)-C(31)-C(32)	178.9(6)	C(31)-C(32)-H(32A)	109.5
C(31)-C(32)-H(32B)	109.5	H(32A)-C(32)-H(32B)	109.5
C(31)-C(32)-H(32C)	109.5	H(32A)-C(32)-H(32C)	109.5
H(32B)-C(32)-H(32C)	109.5	N(8)-C(33)-C(34)	178.3(4)
C(33)-C(34)-H(34A)	109.5	C(33)-C(34)-H(34B)	109.5
H(34A)-C(34)-H(34B)	109.5	C(33)-C(34)-H(34C)	109.5
H(34A)-C(34)-H(34C)	109.5	H(34B)-C(34)-H(34C)	109.5
F(6)-B(2)-F(5)	111.2(4)	F(6)-B(2)-F(8)	110.7(4)
F(5)-B(2)-F(8)	108.4(3)		

Hydrogen Bonds (\AA)

N(1)-H(1C)...F(7)#3	2.960(4)	N(1)-H(1D)...F(8)#4	2.978(4)
---------------------	----------	---------------------	----------

Symmetry transformations used to generate equivalent atoms: #1 $x, -y+3/2, z+1/2$ #2 $x, -y+3/2, z-1/2$ #3 $-x+1, -y+1, -z$ #4 $-x+1, -y+1, -z+1$

REFERENCES

1. Puddephatt, R. J. *Coord. Chem. Rev.* **2001**, *216-217*, 313-332.
2. Yaghi, O. M.; Li, H.; Davis, C.; Richardson, D.; Groy, T. L. *Acc. Chem. Res.* **1998**, *31*, 474 - 484.
3. Blake, A. J.; Champness, N. R.; Hubberstey, P.; Li, W.-S.; Withersby, M. A.; Schroder, M. *Coord. Chem. Rev.* **1999**, *183*, 117-138.
4. Khlobystov, A. N.; Blake, A. J.; Champness, N. R.; Lemenovskii, D. A.; Majouga, A. G.; Zyk, N. V.; Schröder, M. *Coord. Chem. Rev.* **2001**, *222*, 155-192.
5. Fung, E. Y.; Olmstead, M. M.; Vickery, J. C.; Balch, A. L. *Coord. Chem. Rev.* **1998**, *171*, 151-159.
6. Lees, A. J. *Chem. Rev.* **1987**, *87*, 711-743.
7. Lu, J. Y. *Coord. Chem. Rev.* **2003**, *246*, 327-347.
8. Eddaoudi, M.; Li, H.; Yaghi, O. M. *J. Am. Chem. Soc.* **2000**, *122*, 1391 - 1397.
9. Yam, V. W.-W.; Lo, W.-Y.; Lam, C.-H.; Fung, W. K.-M.; Wong, K. M.-C.; Lau, V. C.-Y.; Zhu, N. *Coord. Chem. Rev.* **2003**, *245*, 39-47.
10. Kitagawa, S.; Kitaura, R.; Noro, S.-i. *Angew. Chem., Int. Ed.* **2004**, *43*, 2334-2375.
11. Janiak, C. *J. Chem. Soc. Dalton Trans.* **2003**, *2003*, 2781-2804.
12. Hagrman, P. J.; Hagrman, D.; Zubietta, J. *Angew. Chem., Int. Ed.* **1999**, *38*, 2638-2684.
13. Park, K.-M.; Yoon, I.; Seo, J.; Lee, J.-E.; Kim, J.; Choi, K. S.; Jung, O.-S.; Lee, S. S. *Cryst. Growth Des.* **2005**, *5*, 1707 - 1709.
14. Bacchi, A.; Bosetti, E.; Carcelli, M.; Pelagatti, P.; Rogolino, D. *Eur. J. Inorg. Chem.* **2004**, 1985-1991.
15. Abbas, H.; Pickering, A. L.; Long, D.-L.; Kögerler, P.; Cronin, L. *Chem. Eur. J.* **2005**, *11*, 1071-1078.
16. Pickering, A. L.; Cooper, G. J. T.; Long, D.-L.; Cronin, L. *Polyhedron* **2004**, *23*, 2075-2079.

17. Hannon, M. J.; Painting, C. L.; Plummer, E. A.; Childs, L. J.; Alcock, N. W. *Chem. Eur. J.* **2002**, *8*, 2225-2238.
18. Zhu, H.-F.; Kong, L.-Y.; Okamura, T.-a.; Fan, J.; Sun, W.-Y.; Ueyama, N. *Eur. J. Inorg. Chem.* **2004**, *1465-1473*.
19. Yang, L.; Shan, X.; Chen, Q.; Wang, Z.; Ma, J. S. *Eur. J. Inorg. Chem.* **2004**, *1474-1477*.
20. Lu, X. L.; Leong, W. K.; Hor, T. S. A.; Goh, L. Y. *J. Organomet. Chem.* **2004**, *689*, 1746-1756.
21. Zaman, M. B.; Udachin, K.; Ripmeester, J. A.; Smith, M. D.; zur Loye, H.-C. *Inorg. Chem.* **2005**, *44*, 5047-5059.
22. Caradoc-Davies, P. L.; Hanton, L. R.; Henderson, W. *J. Chem. Soc. Dalton Trans.* **2001**, *2001*, 2749-2755.
23. Sun, D.; Cao, R.; Bi, W.; Li, X.; Wang, Y.; Hong, M. *Eur. J. Inorg. Chem.* **2004**, *2004*, 2144-2150.
24. Wei, Y.; Hou, H.; Li, L.; Fan, Y.; Zhu, Y. *Cryst. Growth. Des.* **2005**, *5*, 1405-1413.
25. Zheng, S.-L.; Tong, M.-L.; Chen, X.-M. *Coord. Chem. Rev.* **2003**, *246*, 185-202.
26. Cui, Y.; Ngo, H. L.; White, P. S.; Lin, W. *Inorg. Chem.* **2003**, *42*, 652 - 654.
27. Blondeau, P.; Lee, A. v. d.; Barboiu, M. *Inorg. Chem.* **2005**, *44*, 5649 - 5653.
28. Tabellion, F. M.; Seidel, S. R.; Arif, A. M.; Stang, P. J. *Angew. Chem. Int. Ed.* **2001**, *40*, 1529-1532.
29. Plater, M. J.; Foreman, M. R. S. J.; Gelbrich, T.; Coles, S. J.; Hursthouse, M. B. *J. Chem. Soc. Dalton Trans.* **2000**, 3065-3073.
30. Konar, S.; Zangrando, E.; Drew, M. G. B.; Ribas, J.; Chaudhuri, N. R. *J. Chem. Soc. Dalton Trans.* **2004**, *260-266*.
31. Xie, Y.-B.; Li, J.-R.; Zhang, C.; Bu, X.-H. *Cryst. Growth. Des.* **2005**, *5*, 1743-1749.
32. Liu, H.-M.; Zhang, W.; Zheng, Y.; Zhang, W.-Q. *J. Mol. Structure* **2004**, *698*, 37-40.
33. Aslanidis, P.; Cox, P. J.; Divanidis, S.; Karagiannidis, P. *Inorg. Chim. Acta*. **2004**, *357*, 2677-2686.

34. Kyono, A.; Kimata, M.; Hatta, T. *Inorg. Chim. Acta*. **2004**, *357*, 2519-2524.
35. Dong, Y.-B.; Wang, P.; Huang, R.-Q.; Smith, M. D. *Inorg. Chem.* **2004**, *43*, 4727-4739.
36. Chisholm, M. H.; Folting, K.; Kramer, K. S.; Streib, W. E. *J. Am. Chem. Soc.* **1997**, *119*, 5528-5539.
37. Chisholm, M. H.; Gallucci, J. C.; Hollandsworth, C. B. *J. Organomet. Chem.* **2003**, *684*, 269-276.
38. Clark, D. L.; Watkin, J. G. *Inorg. Chem.* **1993**, *32*, 1766-1772.
39. Crans, D. C.; Felty, R. A.; Anderson, O. P.; Miller, M. M. *Inorg. Chem.* **1993**, *32*, 247-248.
40. Moulton, B.; Zaworotko, M. J. *Chem. Rev.* **2001**, *101*, 1629-1658.
41. Adachi, K.; Kaizaki, S.; Yamada, K.; Kitagawa, S.; Kawata, S. *Chem. Letters* **2004**, *33*, 648-649.
42. Zou, Y.; Liu, W.-L.; Lu, C.-S.; Wen, L.-L.; Meng, Q.-J. *Inorg. Chem. Commun.* **2004**, *7*, 985-987.
43. Westcott, A.; Whitford, N.; Hardie, M. J. *Inorg. Chem.* **2004**, *43*, 3663-3672.
44. Cheng, J.-K.; Zhang, J.; Kang, Y.; Qin, Y.-Y.; Li, Z.-J.; Yao, Y.-G. *Polyhedron* **2004**, *23*, 2209-2215.
45. Sun, D.; Cao, R.; Bi, W.; Weng, J.; Hong, M.; Liang, Y. *Inorg. Chim. Acta*. **2004**, *357*, 991-1001.
46. Dong, Y.-B.; Jin, G.-X.; Zhao, X.; Tang, B.; Huang, R.-Q.; Smith, M. D.; Stitzer, K. E.; Loyer, Z.; Hans-Conrad *Organomet.* **2004**, *23*, 1604-1609.
47. Southward, R. E.; Thompson, D. W. *Chem. Mater.* **2004**, *16*, 1277-1284.
48. Richards, P. I.; Steiner, A. *Inorg. Chem.* **2004**, *43*, 2810-2817.
49. Eisler, D. J.; Puddephatt, R. J. *Cryst. Growth Design* **2005**, *5*, 57-59.
50. Mukherjee, P. S.; Konar, S.; Zangrand, E.; Mallah, T.; Ribas, J.; Chaudhuri, N. R. *Inorg. Chem.* **2003**, *42*, 2695 - 2703.
51. Wu, C.-D.; Lu, C.-Z.; Yang, W.-B.; Zhuang, H.-H.; Huang, J.-S. *Inorg. Chem.* **2002**, *41*, 3302 - 3307.

52. Kondo, M.; Shimamura, M.; Noro, S.-i.; Yoshitomi, T.; Minakoshi, S.; Kitagawa, S. *Chem. Letters* **1999**, 28, 285-286.
53. Fujita, M.; Sasaki, O.; Watanabe, K.-y.; Ogura, K.; Yamaguchi, K. *New J. Chem.* **1998**, 22, 189 - 191.
54. Munno, G. D.; Armentano, D.; Poerio, T.; Julve, M.; José Antonio Real *J. Chem. Soc. Dalton Trans.* **1999**, 1813 - 1818.
55. Maekawa, M.; Konaka, H.; Suenaga, Y.; Kuroda-Sowa, T.; Munakata, M. *J. Chem. Soc. Dalton Trans.* **2000**, 4160 - 4166.
56. Seward, C.; Hu, N.-X.; Wang, S. *J. Chem. Soc. Dalton Trans.* **2001**, 134 - 137.
57. Li, R.-Z.; Li, D.; Huang, X.-C.; Qi, Z.-Y.; Chen, X.-M. *Inorg. Chem. Commun.* **2003**, 6, 1017-1019.
58. Tao, J.; Yin, X.; Wei, Z.-B.; Huang, R.-B.; Zheng, L.-S. *Eur. J. Inorg. Chem.* **2004**, 125-133.
59. Wang, X.; Qin, C.; Wang, E.; Li, Y.; Hu, C.; Lin Xu *Chem. Commun.* **2004**, 378-379.
60. Seidel, S. R.; Stang, P. J. *Acc. Chem. Res.* **2002**, 35, 972-983.
61. Batten, S. R.; Robson, R. *Angew. Chem. Int. Ed.* **1998**, 37, 1460-1494.
62. Zaworotko, M. J. *Angew. Chem., Int. Ed.* **2000**, 39, 3052-3054.
63. Fujita, M.; Kwon, Y. J.; Washizu, S.; Ogura, K. *J. Am. Chem. Soc.* **1994**, 116, 1151-1152.
64. Hayashi, M.; Miyamoto, Y.; Inoue, T.; Oguni, N. *Chem. Commun.* **1991**, 1752-1753.
65. Yang, J.-H.; Zheng, S.-L.; Yu, X.-L.; Chen, X.-M. *Cryst Growth Des* **2004**, 4, 831-836.
66. Hou, L.; Li, D. *Inorg. Chem. Commun.* **2005**, 8, 128-130.
67. Sun, D.; Cao, R.; Weng, J.; Hong, M.; Liang, Y. *J. Chem. Soc. Dalton Trans.* **2002**, 3, 291-292.
68. Cotton, F. A.; Lin, C.; Murillo, C. A. *J. Chem. Soc. Dalton Trans.* **2001**, 5, 499-501.

69. Lu, J. Y.; Cabrera, B. R.; Wang, R.-J.; Li, J. *Inorg. Chem.* **1999**, *38*, 4608-4611.
70. Oh, M.; Stern, C. L.; Mirkin, C. A. *Inorg. Chem.* **2005**, *44*, 2647-2653.
71. Dong, Y.-B.; Wang, H.-Y.; Ma, J.-P.; Shen, D.-Z.; Huang, R.-Q. *Inorg. Chem.* **2005**, *44*, 4679-4692.
72. Heeger, A. J. *Angew. Chem. Int. Ed.* **2001**, *40*, 2591-2611.
73. MacDiarmid, A. G. *Angew. Chem. Int. Ed.* **2001**, *40*, 2581-2590.
74. Shirakawa, H. *Angew. Chem. Int. Ed.* **2001**, *40*, 2574-2580.
75. Chen, C.-T.; Suslick, K. S. *Coord. Chem. Rev.* **1992**, *128*, 293-322.
76. Hanack, M.; Deger, S.; Lange, A. *Coord. Chem. Rev.* **1988**, *83*, 115-136.
77. Collman, J. P.; McDevitt, J. T.; Leidner, C. R.; Yee, G. T.; Torrance, J. B.; Little, W. A. *J. Am. Chem. Soc.* **1987**, *109*, 4606 - 4614.
78. Su, W.; Hong, M.; Weng, J.; Cao, R.; Lu, S. *Angew. Chem. Int. Ed.* **2000**, *39*, 2911-2914.
79. Rao, C. N. R.; Ranganathan, A.; Pedireddi, V. R.; Raju, A. R. *Chem. Commun.* **2000**, *39*-40.
80. Cernák, J.; Orendá, M.; Potoák, I.; Chomi, J.; Orendáová, A.; Skorepa, J.; Feher, A. *Coord. Chem. Rev.* **2002**, *224*, 51-66.
81. Kahn, O.; Larionova, J.; Ouahab, L. *Chem. Commun.* **1999**, 945-952.
82. Lacroix, P. G. *Eur. J. Inorg. Chem.* **2001**, *2001*, 339-348.
83. Evans, O. R.; Lin, W. *Acc. Chem. Res.* **2002**, *35*, 511-522.
84. Horn, E.; Snow, M. R.; Tiekkink, R. T. *Aust. J. Chem.* **1987**, *40*, 761-765.
85. Bertelli, M.; Carlucci, L.; Ciani, G.; Proserpio, D. M.; Sironi, A. *J. Mater. Chem.* **1997**, *7*, 1271 - 1276.
86. Shin, D. M.; Lee, I. S.; Lee, Y.-A.; Chung, Y. K. *Inorg. Chem.* **2003**, *42*, 2977-2982.
87. Abrahams, B. F.; Batten, S. R.; Hoskins, B. F.; Robson, R. *Inorg. Chem.* **2003**, *42*, 2654-2664.
88. Sampanthar, J. T.; Vittal, J. J. *Cryst. Eng.* **2000**, *3*, 117-133.

89. Blake, A. J.; Champness, N. R.; Cooke, P. A.; Nicolson, J. E. B.; Wilson, C. *J. Chem. Soc., Dalton Trans.* **2000**, 3811-3819.
90. Brandys, M.-C.; Puddephatt, R. J. *Chem. Commun.* **2001**, 1508 - 1509.
91. Sailaja, S.; Rajasekharan, M. V. *Inorg. Chem.* **2003**, 42, 5675 - 5684.
92. Seward, C.; Chan, J.; Song, D.; Wang, S. *Inorg. Chem.* **2003**, 42, 1112 - 1120.
93. Bachechi, F.; Burini, A.; Galassi, R.; Macchioni, A.; Pietroni, B. R.; Ziarelli, F.; Zuccaccia, C. *J. Organomet. Chem.* **2000**, 593-594, 392-402.
94. Steel, P. J.; Sumby, C. *J. Chem. Commun.* **2002**, 322-323.
95. Socol, S. M.; Jacobson, R. A.; Verkade, J. G. *Inorg. Chem.* **1984**, 23, 88 - 94.
96. Affandi, D.; Berners-Price, S. J.; Effendy; Harvey, P. J.; Healy, P. C.; Ruch, B. E.; White, A. H. *J. Chem. Soc., Dalton Trans.* **1997**, 1411-1420.
97. Bowmaker, G. A.; Hanna, J. V.; Rickard, C. E. F.; Lipton, A. S. *J. Chem. Soc., Dalton Trans.* **2001**, 20-28.
98. Che, C.-M.; Tse, M.-C.; Chan, M. C. W.; Cheung, K.-K.; Phillips, D. L.; Leung, K.-H. *J. Am. Chem. Soc.* **2000**, 122, 2464-2468.
99. Deivaraj, T. C.; Vittal, J. J. *J. Chem. Soc., Dalton Trans.* **2001**, 329-335.
100. Nomiya, K.; Noguchi, R.; Shigeta, T.; Kondoh, Y.; Tsuda, K.; Ohsawa, K.; Chikaraishi-Kasuga, N.; Oda, M. *Bull. Chem. Soc. Jpn.* **2000**, 73, 1143-1152.
101. Xu, F.-B.; Weng, L.-H.; Sun, L.-J.; Zhang, Z.-Z.; Zhou, Z.-F. *Organometallics* **2000**, 19, 2658 - 2660.
102. Kitagawa, S.; Kondo, M.; Kawata, S.; Wada, S.; Maekawa, M.; Munakata, M. *Inorg. Chem.* **1995**, 34, 1455-1465.
103. Caruso, F.; Camalli, M.; Rimml, H.; Venanzi, L. M. *Inorg. Chem.* **1995**, 34, 673-679.
104. Song, H.-B.; Zhang, Z.-Z.; Mak, T. C. W. *J. Chem. Soc., Dalton Trans.* **2002**, 1336-1343.
105. Del Zotto, A.; Zangrande, E. *Inorg. Chim. Acta.* **1998**, 277, 111-117.
106. Driess, M.; Franke, F.; Merz, K. *Eur. J. Inorg. Chem.* **2001**, 10, 2661-2668.

107. Catalano, V. J.; Kar, H. M.; Bennett, B. L. *Inorg. Chem.* **2000**, 121-127.
108. Kuang, S.-M.; Zhang, L.-M.; Zhang, Z.-Z.; Wu, B.-M.; Mak, T. C. W. *Inorg. Chim. Acta.* **1999**, 284, 278-283.
109. Del Zotto, A.; Rigo, P.; Nardin, G. *Inorg. Chim. Acta.* **1996**, 247, 183-188.
110. Yam, V. W.-W.; Yu, K.-L.; Cheng, C.-C.; Yeung, P. K.-Y.; Cheung, K.-K.; Zhu, N. *Chem. Eur. J.* **2002**, 8, 4121-4128.
111. Inoguchi, Y.; Milewski-Mahrla, B.; Neugeauer, D.; Jones, P. G.; Schmidbaur, H. *Chem. Ber.* **1983**, 116, 1487-1493.
112. Yam, V. W.-W.; Yeung, P. K.-Y.; Cheung, K.-K. *Angew. Chem. Int. Ed.* **1996**, 35, 739-740.
113. Berners-Price, S. J.; Bowen, R. J.; Harvey, P. J.; Healy, P. C.; Koutsantonis, G. A. *J. Chem. Soc., Dalton Trans.* **1998**, 1743.
114. Newkome, G. R. *Chem. Rev.* **1993**, 93, 2067-2089.
115. Barloy, L.; Malaisé, G.; Ramdeehul, S.; Newton, C.; Osborn, J. A.; Kyritsakas, N. *Inorg. Chem.* **2003**, 42, 2902 - 2907.
116. Yam, V. W.-W.; Chan, L.-P.; Lai, T.-F. *J. Chem. Soc., Dalton Trans.* **1993**, 2075-2077.
117. Bowen, R. J.; Garner, A. C.; Berners-Price, S. J.; Jenkins, I. D.; Sue, R., E. *J. Organomet. Chem.* **1998**, 554, 181-184.
118. Aucott, S. M.; Slawin, A. M. Z.; Woollins, J. D. *Dalton Trans.* **2000**, 2559-2575.
119. Boggess, R. K.; Zatko, D. A. *J. Coord. Chem.* **1973**, 4, 217-224.
120. Barder, T. J.; Cotton, F. A.; Powell, G. L.; Tetrick, S. M.; Walton, R. A. *J. Am. Chem. Soc.* **1984**, 106, 1323-1332.
121. Keene, F. R.; Snow, M. R.; Stephenson, P. J.; Tiekkink, E. R. T. *Inorg. Chem.* **1988**, 27, 2040 - 2045.
122. Constable, E. C.; Housecroft, C. E.; Neuberger, M.; Schneider, A. G.; Springler, B.; Zehnder, M. *Inorg. Chim. Acta.* **2000**, 300-302, 49-55.
123. Astley, T.; Hitchman, M. A.; Keene, R.; Tiekkink, E. R. T. *J. Chem. Soc., Dalton Trans.* **1996**, 1845-1851.

124. Ke-Wu, Y.; Yuan-Qi, Y.; Zhong-Xian, H.; Yun-Hua, W. *Polyhedron* **1996**, *15*, 79-81.
125. Lastra, E.; Gamasa, M. P.; Gimeno, J.; Lanfranchi, M.; Tiripicchio, A. *J. Chem. Soc., Dalton Trans.* **1989**, 1499-1506.
126. Kodera, M.; Kajita, Y.; Tachi, Y.; JKano, K. *Inorg. Chem.* **2003**, *42*, 1193 - 1203.
127. Slagt, V. F.; Reek, J. N. H.; Kamer, P. C. J.; van Leeuwen, P. W. N. M. *Angew. Chem. Int. Ed.* **2001**, *40*, 4271-4274.
128. Cheshire, P.; Slawin, A. M. Z.; Woollins, J. D. *Inorg. Chem. Commun.* **2002**, *5*, 803-804.
129. Kurtev, K.; Ribola, D.; Jones, R. A.; Cole-Hamilton, D. J.; Wilkinson, G. *J. Chem. Soc., Dalton Trans.* **1980**, 55-58.
130. Gregorzik, R.; Wirbser, J.; Vahrenkamp, H. *Chem. Ber.* **1992**, *125*, 1575-1581.
131. Astley, T.; Headlam, H.; Hitchman, M. A.; Keene, F. R.; Pilbrow, J.; Stratemeier, H.; Tiekkink, E. R. T.; Zhong, Y. C. *J. Chem. Soc., Dalton Trans.* **1995**, 3809-3818.
132. Steiner, A.; Stalke, D. *Organomet.* **1995**, *14*, 2422-2429.
133. Shieh, S.-J.; Hong, X.; Peng, S.-M.; Che, C.-M. *J. Chem. Soc., Dalton Trans.* **1994**, 3067-3068.
134. Olmstead, M. M.; Maisondhat, A.; Farr, J. P.; Balch, A. L. *Inorg. Chem.* **1981**, *20*, 4060-4064.
135. Maisonnnet, A.; Farr, J. P.; Olmstead, M. M.; Hunt, C. T.; Balch, A. L. *Inorg. Chem.* **1982**, *21*, 3961 - 3967.
136. Keene, F. R.; Stephenson, P. J.; Tiekkink, E. R. T. *Inorg. Chim. Acta* **1991**, *187*, 217-220.
137. Bedford, R. B.; Welch, S. L. *Chem. Commun.* **2001**, *1*, 129-130.
138. Rabinowitz, R.; Pellon, J. *J. Org. Chem.* **1961**, *26*, 4623 - 4626.
139. Sheldrick, G. M.; University of Gottingen: Gottingen, Germany, 1997.
140. Sheldrick, G. M.; 6.10 ed.; Bruker AXS, Inc.: Madison, WI, 2000.
141. Erxleben, A. *Coord. Chem. Rev.* **2003**, *246*, 203-228.

142. Vetrichelvan, M.; Lai, Y.-H.; Mok, K. F. *Eur. J. Inorg. Chem.* **2004**, 2086-2095.
143. Fournier, E.; Lebrun, F.; Drouin, M.; Decken, A.; Harvey, P. D. *Inorg. Chem.* **2004**, *43*, 3127-3135.
144. Fan, J.; Sun, W.-Y.; Okamura, T.-A.; Tang, W.-X.; Ueyama, N. *Inorg. Chim. Acta.* **2004**, *357*, 2385-2389.
145. Lin, P.; Henderson, R. A.; Harrington, R. W.; Clegg, W.; Wu, C.-D.; Wu, X.-T. *Inorg. Chem.* **2004**, *43*, 181-188.
146. Dong, Y.-B.; Zhao, X.; Huang, R.-Q.; Smith, M. D.; Loya, H.-C. Z. L. *Inorg. Chem.* **2004**, *43*, 5603-5612.
147. Klausmeyer, K. K.; Feazell, R. P.; Reibenspies, J. H. *Inorg. Chem.* **2004**, *43*, 1130-1136.
148. Pickering, A. L.; Long, D.-L.; Cronin, L. *Inorg. Chem.* **2004**, *43*, 4953-4961.
149. Weisman, A.; Gozin, M.; Kraatz, H.-B.; Milstein, D. *Inorg. Chem.* **1996**, *35*, 1792-1797.
150. Bacher, A.; Erdelen, C. H.; Paulus, W.; Ringsdorf, H.; Schmidt, H.-W.; Schuhmacher, P. *Macromol.* **1999**, *32*, 4551-4557.
151. Xie, Y.-B.; Li, J.-R.; Bu, X.-H. *Polyhedron* **2005**, *24*, 413-418.
152. You, Z.-L.; Zhu, H.-L.; Liu, W.-S. *Acta Cryst. Sect. C* **2004**, *C60*, m620-m622.
153. Feazell, R. P.; Carson, C. E.; Klausmeyer, K. K. *Acta Cryst. Sect. C* **2004**, *C60*, m598-m600.
154. Goher, M. A. S.; Hafez, A. K.; Abu-Youssef, M. A. M.; Badr, A. M. A.; Gspan, C.; Mautner, F. A. *Polyhedron* **2004**, *23*, 2349-2356.
155. Sailaja, S.; Rajasekharan, M. V. *Inorg. Chem.* **2000**, *39*, 4586-4590.
156. Ok-Sang Jung, Y. J. K., Young-A Lee, Hee K. Chae, Ho G. Jang, and Jongki Hong *Inorg. Chem.* **2001**, *40*, 2105-2110.
157. Hong, M.; Su, W.; Cao, R.; Fujita, M.; Lu, J. *Chem. Eur. J.* **2000**, *6*, 427-431.
158. Zheng, S.-L.; Tong, M.-L.; Fu, R.-W.; Chen, X.-M.; Ng, S.-W. *Inorg. Chem.* **2001**, *40*, 3562-3569.
159. Feazell, R. P.; Carson, C. E.; Klausmeyer, K. K. *Inorg. Chem.* **2005**, *44*, 996-1005.

160. Kang, Y.; Lee, S. S.; Park, K.-M.; Lee, S. H.; Kang, S. O.; Ko, J. *Inorg. Chem.* **2001**, *40*, 7027-7031.
161. Reger, D. L.; Semeniuc, R. F.; Smith, M. D. *Inorg. Chem.* **2001**, *40*, 6545-6546.
162. Catalano, V. J.; Malwitz, M. A. *Inorg. Chem.* **2003**, *42*, 5483 - 5485.
163. Pykkö, P.; Runeberg, N.; Mendizabal, F. *Chem. Eur. J.* **1997**, *3*, 1451-1457.
164. Codina, A.; Fernández, E. J.; Jones, P. G.; Laguna, A.; López-de-Luzuriaga, J. M.; Monge, M.; Olmos, M. E.; Pérez, J.; Rodríguez, M. A. *J. Am. Chem. Soc.* **2002**, *124*, 6781 - 6786.
165. Fernández, E. J.; López-de-Luzuriaga, J. M.; Monge, M.; Olmos, M. E.; Pérez, J.; Laguna, A.; Mohamed, A. A.; John P. Fackler, J. *J. Am. Chem. Soc.* **2003**, *25*, 2022-2023.
166. Bachman, R. E.; Fioritto, M. S.; Fetts, S. K.; Cocker, T. M. *J. Am. Chem. Soc.* **2001**, *123*, 5376-5377.
167. Harwell, D. E.; Knobler, M. D. M. B.; Anet, F. A. L.; Hawthorne, M. F. *J. Am. Chem. Soc.* **1996**, *118*, 2679 - 2685.
168. Mohamed, A. A.; Pérez, L. M.; John P. Fackler, J. *Inorg. Chim. Acta* **2005**, *358*, 1657-1662.
169. Wang, Q.-M.; Mak, T. C. W. *J. Am. Chem. Soc.* **2001**, *123*, 7594 - 7600.
170. Omary, M. A.; Webb, T. R.; Assefa, Z.; Shankle, G. E.; Patterson, H. H. *Inorg. Chem.* **1998**, *37*, 1380-1386.
171. Pykkö, P. *Chem. Rev.* **1997**, *97*, 597-636.
172. Hermann, H. L.; Boche, G.; Schwerdtfeger, P. *Chem. Eur. J.* **2001**, *7*, 5333-5342.
173. Fernández, E. J.; López-de-Luzuriaga, J. M.; Monge, M.; Rodríguez, M. A.; Olga Crespo, M.; Gimeno, C.; Laguna, A.; Jones, P. G. *Inorg. Chem.* **1998**, *37*, 6002-6006.
174. Jiménez, J. A.; Claramunt, R. M.; Mó, O.; Yáñez, M.; Wehrmann, F.; Buntkowsky, G.; Limbach, H.-H.; Goddard, R.; Elguero, J. *Phys. Chem. Chem. Phys.* **1999**, *1*, 5113-5120.
175. Ba, Y.; Chagolla, D. *J. Phys. Chem. B* **2002**, *106*, 5250-5257.
176. Kasai, K.; Aoyagi, M.; Fujita, M. *J. Am. Chem. Soc.* **2000**, *122*, 2140-2141.

177. Feazell, R. P.; Carson, C. E.; Klausmeyer, K. K. *Eur. J. Inorg. Chem.* **2005**, 3287-3297.
178. Feazell, R. P.; Carson, C. E.; Klausmeyer, K. K. *Inorg. Chem.* **2005**, Submitted.
179. Feazell, R. P.; Carson, C. E.; Klausmeyer, K. K. *Inorg. Chem.* **2005**, Submitted Article.
180. Mascal, M.; Kerdelhué, J.-L.; Blake, A. J.; Cooke, P. A. *Angew. Chem., Int. Ed.* **1999**, 38, 1968-1971.
181. Xu, F.-B.; Li, Q.-S.; Wu, L.-Z.; Leng, X.-B.; Li, Z.-C.; Zeng, X.-S.; Chow, Y. L.; Zhang, Z.-Z. *Organometallics* **2003**, 22, 633 - 640.
182. Feazell, R. P.; Carson, C. E.; Klausmeyer, K. K. *Acta Cryst. Sect. E* **2005**, m1694-m1696.
183. Constable, E. C.; Fenske, D.; Housecroft, C. E.; Kulke, T. *Chem. Commun.* **1998**, 1998, 2659-2660.
184. Cui, G.-H.; Li, J.-R.; Tian, J.-L.; Bu, X.-H.; Batten, S. R. *Cryst. Growth. Des.* **2005**, 5, 1775-1780.
185. Batten, S. R.; Hoskins, B. F.; Moubaraki, B.; Murray, K. S.; Robson, R. *J. Chem. Soc., Dalton. Trans.* **1999**, 2977 - 2986.
186. Long, D.-L.; Blake, A. J.; Champness, N. R.; Wilson, C.; Schröder, M. *J. Am. Chem. Soc.* **2001**, 123, 3401 - 3402.
187. Masaoka, S.; Furukawa, S.; Chang, H.-C.; Mizutani, T.; Kitagawa, S. *Angew. Chem., Int. Ed.* **2001**, 40, 3817-3819.
188. Philp, D.; Stoddart, J. F. *Angew. Chem., Int. Ed. Engl.* **1996**, 35, 1154-1196.
189. Manners, I. *Angew. Chem., Int. Ed. Engl.* **1996**, 35, 1602-1621.